HAL
open science

Caractérisation de nouveaux régulateurs de la sénescence induite par un stress oncogénique dans les cellules épithéliales humaines

Clotilde Wiel

To cite this version:

Clotilde Wiel. Caractérisation de nouveaux régulateurs de la sénescence induite par un stress oncogénique dans les cellules épithéliales humaines. Biologie cellulaire. Université Claude Bernard - Lyon I, 2014. Français. NNT : 2014LYO10158 . tel-01128168

HAL Id: tel-01128168

https://theses.hal.science/tel-01128168

Submitted on 9 Mar 2015

HAL is a multi-disciplinary open access archive for the deposit and dissemination of scientific research documents, whether they are published or not. The documents may come from teaching and research institutions in France or abroad, or from public or private research centers.

L'archive ouverte pluridisciplinaire **HAL**, est destinée au dépôt et à la diffusion de documents scientifiques de niveau recherche, publiés ou non, émanant des établissements d'enseignement et de recherche français ou étrangers, des laboratoires publics ou privés.

N° d'ordre : **158-2014** **Année 2014**

THESE DE L'UNIVERSITE DE LYON

Délivrée par
L'UNIVERSITE CLAUDE BERNARD LYON I

École Doctorale
Biologie **M**oléculaire **I**ntégrative et **C**ellulaire

DIPLOME DE DOCTORAT

Soutenue publiquement

A Lyon, le 26 Septembre 2014

Par

Clotilde WIEL

CARACTÉRISATION DE NOUVEAUX RÉGULATEURS DE LA SÉNESCENCE INDUITE PAR UN STRESS ONCOGÉNIQUE DANS LES CELLULES ÉPITHÉLIALES HUMAINES

JURY

Pr Corinne ABBADIE (Rapporteur)

Pr Gerardo FERBEYRE (Rapporteur)

Dr Carl MANN (Examinateur)

Dr Caroline MOYRET-LALLE (Président du Jury)

Dr David BERNARD (Directeur de thèse)

UNIVERSITE CLAUDE BERNARD - LYON 1

Président de l'Université	**M. François-Noël GILLY**
Vice-président du Conseil d'Administration	M. le Professeur Hamda BEN HADID
Vice-président du Conseil des Etudes et de la Vie Universitaire	M. le Professeur Philippe LALLE
Vice-président du Conseil Scientifique	M. le Professeur Germain GILLET
Directeur Général des Services	M. Alain HELLEU

COMPOSANTES SANTE

Faculté de Médecine Lyon Est – Claude Bernard	Directeur : M. le Professeur J. ETIENNE
Faculté de Médecine et de Maïeutique Lyon Sud – Charles Mérieux	Directeur : Mme la Professeure C. BURILLON
	Directeur : M. le Professeur D. BOURGEOIS
Faculté d'Odontologie	Directeur : Mme la Professeure C. VINCIGUERRA
Institut des Sciences Pharmaceutiques et Biologiques	Directeur : M. le Professeur Y. MATILLON
Institut des Sciences et Techniques de la Réadaptation	Directeur : Mme. la Professeure A-M. SCHOTT
Département de formation et Centre de Recherche en Biologie Humaine	

COMPOSANTES ET DEPARTEMENTS DE SCIENCES ET TECHNOLOGIE

Faculté des Sciences et Technologies	Directeur : M. F. DE MARCHI
Département Biologie	Directeur : M. le Professeur F. FLEURY
Département Chimie Biochimie	Directeur : Mme Caroline FELIX
Département GEP	Directeur : M. Hassan HAMMOURI
Département Informatique	Directeur : M. le Professeur S. AKKOUCHE
Département Mathématiques	Directeur : M. Georges TOMANOV
Département Mécanique	Directeur : M. le Professeur H. BEN HADID
Département Physique	Directeur : M. Jean-Claude PLENET
UFR Sciences et Techniques des Activités Physiques et Sportives	Directeur : M. Y.VANPOULLE
Observatoire des Sciences de l'Univers de Lyon	Directeur : M. B. GUIDERDONI
Polytech Lyon	Directeur : M. P. FOURNIER
Ecole Supérieure de Chimie Physique Electronique	Directeur : M. G. PIGNAULT
Institut Universitaire de Technologie de Lyon 1	Directeur : M. C. VITON
Ecole Supérieure du Professorat et de l'Education	Directeur : M. A. MOUGNIOTTE
Institut de Science Financière et d'Assurances	Directeur : M. N. LEBOISNE

Thèse effectuée sous la direction du Dr David BERNARD

Centre de Recherche en Cancérologie de Lyon

INSERM 1052 – CNRS 5286

Equipe Mécanismes d'échappement à la sénescence

Centre Léon Bérard - 28 rue Laënnec

69008 LYON

Thèse financée par le Ministère de la Recherche et de l'Enseignement Supérieur (3 ans) ainsi que par les associations La Ligue Contre le Cancer et La Fondation pour la Recherche Médicale

REMERCIEMENTS

Je tiens tout d'abord à remercier les membres de mon jury pour le temps consacré à l'examination et la relecture dans les moindres détails de ce travail. Merci aux professeurs Corinne Abbadie et Gerardo Ferbeyre, mes rapporteurs, ainsi que de le docteur Carl Mann, mon examinateur. Merci également au docteur Caroline Moyret-Lalle de s'être proposé de présider ce jury de thèse.

David, merci d'avoir su me faire confiance en me proposant de réaliser ma thèse dans ton équipe. Tu m'as apporté un environnement scientifique riche, où l'investissement et l'ouverture d'esprit sont nécessaires. Durant ces années de thèse, j'ai énormément appris. Et cela m'a donné envie d'en apprendre plus encore.

Merci à tous les membres, individualités et personnalités qui composent, ou ont composé cette belle équipe. Malgré des moments difficiles, je suis toujours venue au labo avec enthousiasme, si ce n'est pour les manips, au moins pour les mots fléchés du midi ou les goûters partagés. Et c'est grâce à vous tous.

David, bon courage pour tes premières années de MCU, poste que tu as amplement mérité. Merci pour ta gentillesse, ta disponibilité et ton calme à toute épreuve (ou presque). Ton éventail de connaissances m'impressionnera toujours autant. Nadine, j'aurais aimé travailler plus longtemps avec toi. J'espère que ton avenir au sein de l'équipe sera tout aussi fructueux que les premiers mois que tu y as passés. Audrey, tu es dans l'équipe depuis peu aussi, mais tu y as déjà toute ta place, et pas seulement parce que tu travailles sur les ¾ des projets de l'équipe ! N'oublie pas de garder un peu de ton énergie. Je te souhaite de découvrir d'autres manips que le cryostat ou le cryobroyeur ! Mylène, nouveau lab manager de l'équipe. Tu grimpes, tu grimpes ! Et j'espère que ce sera durable. Sans toi, l'équipe ne tournerait pas aussi bien. Tu as supporté mes plaintes répétées, mes crises de nerfs, mes pétages de câble. Et merci pour les (nombreuses) extractions d'ARNs ! Ton rire, que je pouvais entendre depuis mon bureau, va me manquer. Benjamin, espèce d'enc….. Je ne te remercie pas pour les multiples surnoms dont tu m'as affublé, et dont toi seul as le don. Mais merci, entre autres, pour nos échanges scientifiques toujours enrichissants. Merci d'avoir été là, d'être là, scientifiquement et humainement. Une pensée pour toutes les autres personnes passées dans l'équipe, notamment Hélène (LD), Hélène (S), tous les stagiaires dont Marine, JC, Lauriane... Vous étiez top. Avant tout, merci pour tous les moments de pure rigolade. Sans ça, la thèse aurait eu beaucoup moins de saveur. Et surtout, perpétuez ce bel esprit d'équipe. Il est précieux.

Je n'oublie pas ma deuxième équipe non plus, les Bartho. Merci à vous tous, notamment Johann, Lindsay, David Pikachu, Roxane, Nico (et Bastien, même si tu ne fais plus partie officiellement de l'équipe) pour vos « cafés cafés », vos délires, et votre soutien indéfectible.

Je remercie aussi toutes les personnes du 2ème étage du Cheney D, Freddy, Mme Agnès toujours disponible, les nombreuses personnes que j'ai côtoyées durant ces quatre ans et demi au centre : Justine, Sylvaine, Marine, Rana… et tous ceux que j'oublie… Un grand merci Christophe pour ton aide précieuse au confocal, ta gentillesse et ta disponibilité.

Les filles du miam miam du mercredi midi : Lindsay, Roxane (encore vous), Doriane et Mélanie. Petite bouffée d'air frais hors du labo tous les mercredis. Bon courage pour la suite et fin de vos thèses respectives !! Ebticem, pour avoir partagé sans te plaindre (et contre ta volonté) un bout de ton bureau… Nicolas, pour les post-it laissés sur le PSM le week-end. Laurent et Geoffrey, pour vos blagues débiles plus que limites, vos nombreux coups foireux, mais qui, j'avoue, m'ont bien faite rire. Geoffrey, pour les bons moments passés autour d'une bière, ou à discuter science, ou GOT. Promis, j'aurai (presque ?) fini le 5ème livre avant de partir.

Mélanie, le calme du 6ème étage n'est pas la seule raison de mes nombreuses visites. Merci infiniment de m'avoir écouté si patiemment, et de me comprendre. Merci aussi pour les échanges scientifiques. Charlotte, mon petit chou à la crème. Les discussions avec toi prenaient parfois l'air d'un salon de thé… mille mercis. La thèse apporte aussi son lot de belles rencontres !

Merci à ma poulette Clara. 12 ans que tu me soutiens dans toutes les épreuves. Et tu auras été présente dans les moments faciles et moins faciles de cette thèse.

Enfin, je pense à mes frères, et à ma famille, que j'ai trop peu vus durant ces années de thèse. Veuillez m'excuser pour les anniversaires manqués, les rares apparitions ou les moments trop furtifs passés en votre compagnie. Après ces nombreuses années d'étude, je tiens surtout à remercier mes parents, qui m'ont toujours soutenue, sans condition, sans jamais me mettre la pression (je sais le faire toute seule ça). C'est grâce à vous que j'en suis là aujourd'hui, et je ne pourrai jamais vous remercier suffisamment.

RESUME DE LA THESE

La sénescence est un arrêt stable de prolifération mis en place en réponse à différents stress cellulaires, comme le raccourcissement des télomères (sénescence réplicative) ou le stress oncogénique (sénescence induite par un oncogène, OIS) et constitue un processus s'opposant à la prolifération des cellules tumorales. La plupart des études menées dans des fibroblastes ont permis d'identifier p53 et pRb comme acteurs majeurs de la sénescence. Toutefois, l'étude de l'OIS dans les mélanocytes ou les cellules épithéliales a révélé de nouveaux mécanismes, n'impliquant pas obligatoirement ces deux voies canoniques. L'objectif de ma thèse est de caractériser de nouveaux régulateurs de l'OIS dans les cellules épithéliales. Pour cela deux approches différentes ont été utilisées.

Dans une première partie, je me suis intéressée aux effets de l'activité portée par les lysyl oxydases (LOX), famille d'enzyme connue pour favoriser le processus métastatique, sur l'échappement à l'OIS. L'inhibition de LOX et LOXL2 stabilise l'OIS dans les cellules épithéliales mammaires humaines et dans un modèle murin d'adénocarcinomes du pancréas. Ce travail a permis de montrer que l'activité Lox est impliquée dans l'initiation tumorale.

Dans un deuxième temps, en utilisant un criblage perte de fonction nous avons isolé plusieurs gènes dont l'inhibition stable d'expression permet un échappement à l'OIS dans les cellules épithéliales mammaire humaines. Parmi eux, j'ai caractérisé l'implication de deux canaux calciques, ITPR2 et MCU, dans l'échappement à la sénescence. ITPR2, qui permet la sortie de calcium du réticulum endoplasmique, et MCU, qui permet l'entrée de calcium dans la matrice de la mitochondrie, s'avèrent être deux acteurs nécessaires à la signalisation calcique lors de l'OIS. De manière importante, les mouvements calciques sont associés à une chute du potentiel de membrane mitochondrial, et à la génération d'espèces réactives de l'oxygène. Ce travail montre que les mouvements calciques semblent également être impliqués dans le processus de sénescence réplicative.

Mots clés: sénescence; cancer; lysysl oxydase; ITPR2; MCU; calcium

ABSTRACT

CHARACTERIZATION OF NEW ONCOGENE-INDUCED SENESCENCE REGULATORS IN HUMAN EPITHELIAL CELLS

Senescence is a stable proliferation arrest triggered by several cellular stresses such as telomeres shortening (replicative senescence) or oncogenic activation (oncogene-induced senescence, OIS). Senescence counteracts proliferation of malignant cells, and as such, constitutes a failsafe program. Senescence was first evidenced in fibroblasts, and most of the following studies were conducted in human or murine fibroblasts, allowing the identification of p53 and pRb pathways as strong regulators of senescence. However the few studies investigating senescence pathways involved in other cell types, such as melanocytes or epithelial cells unveiled new p53/pRB-independent mechanisms. The aim of my thesis was then to characterize new senescence regulators in human epithelial cells.

We were first interested in characterizing lysyl oxidase activity (Lox) on OIS escape. LOX enzymes are mainly known to favor metastatic processes. Lox activity inhibition stabilized OIS in vitro, but also senescence in a transgenic murine model of pancreatic ductal adenocarcinoma. This work demonstrated that Lox activity is involved in tumoral initiation by promoting senescence escape.

Using a loss-of-function screen, we identified several genes whose down-regulation allowed OIS escape of human mammary epithelial cells. Among them I have characterized ITPR2 and MCU, two calcium-related channels. Loss of ITPR2, known to mediate endoplasmic reticulum (ER) calcium release, as well as loss of MCU, necessary for mitochondrial calcium uptake, enable escape from OIS. During OIS, ITPR2 triggers calcium release from the ER, followed by mitochondrial calcium accumulation through MCU channels. Mitochondrial calcium accumulation leads to a subsequent decrease in mitochondrial membrane potential, reactive oxygen species accumulation and senescence. This ER-mitochondria calcium transport is not restricted to OIS, but is also involved in replicative senescence. Our results show a functional role of calcium release by the ITPR2 channel and its subsequent accumulation in the mitochondria.

Keywords: senescence; cancer; lysysl oxidase; ITPR2; MCU; calcium

SOMMAIRE

RESUME DE LA THESE ---------- *6*

ABSTRACT ---------- *7*

SOMMAIRE ---------- *8*

LISTE DES FIGURES ---------- *11*

LISTE DES TABLEAUX ---------- *12*

LISTE DES ABREVIATIONS ---------- *13*

INTRODUCTION GENERALE ---------- *17*

Chapitre I : La sénescence ---------- **17**

1.1 Caractéristiques des cellules sénescentes ---------- **17**

1.1.1 Arrêt de prolifération ---------- 17

1.1.2 Morphologie ---------- 21

1.1.3 Activité β-galactosidase Associée à la Sénescence (SA-β-gal) ---------- 21

1.1.4 Phénotype Sécrétoire Associé à la Sénescence (SASP) ---------- 22

1.1.5 Induction de $p16^{INK4A}$ ---------- 22

1.1.6 Foyers d'Hétérochromatine Associés à la Sénescence (SAHF) ---------- 23

1.1.7 Résistance à l'apoptose ---------- 24

1.1.8 Altération de l'expression génique ---------- 24

1.1.9 Autres marqueurs ---------- 26

1.2 Inducteurs de sénescence ---------- **27**

1.2.1 Sénescence réplicative ---------- 27

1.2.2 Sénescence Induite par un Oncogène (OIS) ---------- 28

1.2.3 Sénescence Induite par Invalidation d'Oncogène (OIIS) ---------- 29

1.2.4 Stress oxydant ---------- 30

1.2.5 Autres types de stress ---------- 30

1.3 Les voies de signalisation canoniques de la sénescence ---------- **33**

1.3.1 La voie p53 dans la sénescence ---------- 33

1.3.1.1 Les dommages à l'ADN et p53 ---------- 33

1.3.1.2 $p14^{ARF}$ et p53 ---------- 34

1.3.2 La voie $p16^{INK4A}$/Rb dans la sénescence ---------- 34

1.3.3 Acteurs clés de la stabilité de la sénescence ---------- 36

1.4 Rôles de la sénescence dans différentes réponses physiopathologiques ---------- **37**

1.4.1 La sénescence est impliquée dans le vieillissement ---------- 37

1.4.2 La sénescence participe à la réparation de tissus ---------- 38

1.4.3 La sénescence dans le développement ---------- 39

1.5 La sénescence est un mécanisme anti-tumoral ---------- 40
1.5.1 Sénescence réplicative, barrière à la progression tumorale ---------- 40
1.5.2 La sénescence induite par un stress oncogénique, barrière à la progression tumorale -- 40
1.5.3 Sénescence induite par la thérapie (TIS ---------- 44

Chapitre II : L'OIS dans les cellules épithéliales ---------- 45
2.1 Rôle controversé de p53 dans l'OIS ---------- 45
2.2 Implication relative des DDR ---------- 46
2.3 Implication relative de p16^{INK4A} ---------- 48
2.4 L'OIS dans les cellules épithéliales ---------- 50
2.5 Objectifs de la thèse ---------- 52

RESULTATS ---------- 55

Chapitre I : Rôle de l'activité lysyl oxydase dans l'échappement à l'OIS ---------- 55
1.1 Introduction ---------- 55
1.1.1 Famille des lysyl oxidases ---------- 55
1.1.2 Rôle anti-tumoral de Lox ---------- 57
1.1.3 Rôles de Lox dans la progression tumorale ---------- 57
1.1.4 Rôles émergents de Lox dans l'initiation tumorale ---------- 61
1.2 Article 1 : Lysyl oxidase activity regulates oncogenic stress response and tumorigenesis ---------- 62
1.3 Résultats supplémentaires ---------- 82
1.4 Revue : Lysyl oxidases: emerging promoters of senescence escape, tumor initiation and progression ---------- 87

Chapitre II : Caractérisation du rôle de canaux calciques dans l'OIS ---------- 94
2.1 Introduction ---------- 94
2.1.1 Description du criblage dans les hMECs ---------- 94
2.1.2 Identification de MCU et ITPR2 ---------- 97
2.1.2.1 Inositol Tri-Phosphate Receptor 2 ---------- 99
2.1.2.2 Mitochondrial Calcium Uniporter ---------- 102
2.1.2.3 Mesure du calcium mitochondrial ---------- 104
2.1.3 Signalisation calcique entre réticulum et mitochondrie ---------- 105
2.1.3.1 Le réticulum endoplasmique ---------- 105
2.1.3.2 La mitochondrie ---------- 106
2.1.3.3 Les structures de Membranes Associées aux Mitochondries (MAMs) ---------- 106
2.2 Article 2 : Endoplasmic reticulum calcium release through ITPR2 channels leads to mitochondrial calcium accumulation and senescence ---------- 109

DISCUSSION GENERALE ET PERSPECTIVES ---------- 134

1 Un modèle cellulaire original ---------- 134
1.1 Sénescence sans induction de p16^{INK4A} ? ---------- 134
1.2 Réversibilité de la sénescence ---------- 135
2 Mécanismes par lesquels Lox déstabilise la sénescence ---------- 137
3 Criblage génétique ---------- 141
3.1 Isolation des canaux calciques ITPR2 et MCU, deux nouveaux régulateurs de la sénescence 141

3.1.1 Comment sont régulés les ITPR pendant la sénescence ? ---------- 141
3.1.2 Régulation de MCU ---------- 143
3.2 Identification d'ABCC3, régulateur indirect des canaux calciques pendant l'OIS ? --------- 145
3.3 Identification du canal potassique KCNA1 comme régulateur de l'OIS ---------- 146
4 L'échange de calcium entre RE et mitochondrie est un processus pro-apoptotique, et pro-sénescent ---------- 146
4.1 Le calcium : un messager de mort et de sénescence ---------- 146
4.2 Bcl-2 au carrefour de l'apoptose et de la sénescence ? ---------- 147
5 Des perturbations de la mitochondrie et du RE peuvent affecter le contrôle qualité des protéines ---------- 148
5.1 L'OIS dans les cellules épithéliales est-elle associée à un stress du RE ? ---------- 148
5.2 La sénescence et les processus autophagiques ---------- 149
6 La mitochondrie : au cœur de nombreux processus fondamentaux cellulaires ---------- 150
6.1 Dynamisme de la mitochondrie durant la sénescence ---------- 150
6.2 Mitochondrie et métabolisme pendant la sénescence ---------- 154
6.3 Dysfonctionnements mitochondriaux à la source des ROS pendant la sénescence ? ----- 155
7 Est-ce que le calcium cytosolique est aussi un messager de la sénescence ? ---------- 156

BIBLIOGRAPHIE ---------- 158

ANNEXES ---------- 188

Article 3 : Potassium Channel KCNA1 Modulates Oncogene-Induced Senescence and Transformation ---------- 189

Article 4 : Glucose metabolism and hexosamine pathway regulate oncogene-induced senescence ---------- 220

Article 5 : PLA2R1 mediates tumor suppression by activating JAK2 ---------- 238

LISTE DES FIGURES

Figure 1 : Les complexes cyclines-CDK régulent l'activation de la protéine Rb 18

Figure 2 : Morphologie de cellules épithéliales lors de la sénescence 20

Figure 3 : Voie de signalisation d'une réponse aux dommages à l'ADN 32

Figure 4 : Les voies de signalisation de la sénescence 35

Figure 5 : Rôles de la sénescence 43

Figure 6 : Représentation schématique d'une courbe de croissance de cellules épithéliales..... 49

Figure 7 : Structures de LOX et LOXL2 56

Figure 8 : LOX est impliqué dans différents processus favorisant le développement tumoral 60

Figure 9 : L'expression de LOX et LOXL2 augmente dans les parties tumorales des souris KIA. 83

Figure 10 : L'expression de LOX, LOXL1 et LOXL2 augmente dans les PDAC humains..... 85

Figure 11 : L'Inhibition de la voie PI3K stabilise la sénescence induite par MEK. 86

Figure 12 : Criblage génétique 96

Figure 13 : Structure des ITPR 98

Figure 14 : Voie de l'IP_3..... 100

Figure 15 : Représentation schématique du complexe MCU et de ses régulateurs 101

Figure 16 : Représentation de la protéine de fusion mito-GCaMP2 utilisée pour mesurer le calcium mitochondrial 103

Figure 17 : Représentation schématique du RE, de la mitochondrie et des MAMs 107

Figure 18 : Mécanisme(s) par lesquels l'activité Lox pourrait déstabiliser la sénescence induite par un stress oncogénique..... 138

Figure 19 : Mécanismes non exhaustifs de la régulation des ITPR 142

Figure 20 : Hypothèse de travail concernant le mécanisme par lequel ABCC3 régule l'OIS..... 144

Figure 21 : Perturbations du dynamisme de la mitochondrie pendant la sénescence..... 152

LISTE DES TABLEAUX

Tableau 1 : Tableau récapitulatif des caractéristiques des cellules sénescentes 25

Tableau 2 voies de signalisation impliquées dans la sénescence des fibroblastes et des cellules épithéliales 47

Tableau 3 : sénescence dans les fibroblastes et les cellules épithéliales..... 49

Tableau 4 : Gènes identifiés lors du criblage génétique 97

LISTE DES ABREVIATIONS

4-OHT : 4-Hydroxy-Tamoxifène
53 BP1 : p53-binding protein 1

ABC : ATP-binding Cassette
ABCC3 : ABC transporter, family B, member 3
ADN : Acide Désoxyribonucléique
ALT : Alternative Lengthening of Telomeres
AMPK : AMP-Activated Protein kinase
ARN : Acide RiboNucléique
ARNm : ARN messager
ARK5 : AMPK-related protein 5 (NUAK1)
ATM : Ataxia Telangiectasia mutated
ATR : ATM and RAD3-related

BAPN : β-aminopropionitrile
BMDC : Bone Marrow-Derived Cells
BMP-1 : Bone Morphogenetic Protein-1

CDK : Cyclin-Dependent Kinase
CKI : Cyclin-Dependent Kinase inhibitor
CHK : Checkpoint Kinase
CIP1 : CDK-interacting protein 1
CXCR2 : Chemokine, CXC motif, Receptor 2

DAPI : 4',6-diamidino-2-phenylindole
DDR : DNA-Damage Response
DEC-1 : Deleted in Oesophageal Cancer-1
DcR2 : Decoy Receptor-2
DMBA : 7,12-dimethylbenz(a)anthracene

E2F : E2 Factor
ECM : Extra-Cellular Matrix (Matrice Extra-cellulaire)
EMT : Epithelial-Mesenchymal Transition (Transition Epithelio-Mésenchymateuse)
ERK: Extracellular signal-Regulated Kinase

FGF-2 : Fibroblast Growth Factor-2

HIF1 : Hypoxia-inducible factor 1
HIRA : Histone cell cycle defective A
HP1 : Heterochromatin Protein 1
hMEC : Human Mammary Epithelial Cell
hTERC : Human telomerase RNA component
hTERT : Human Telomerase Reverse Transcriptase

IL : Interleukine

IMM : Inner Mitochondrial Membrane (Membrane Mitochondriale Interne)
INK4 : Inhibitor of CDK4
IP3 : Inositol TriPhosphate
ITPR2 : Inositol-TriPhosphate Receptor 2 (aussi IP_3R2 pour Inositol Phosphate 3 Receptor2)

KIA : Pdx1-Cre, LSL-$Kras^{G12D/+}$, INK4a/$Arf^{lox/lox}$ mice

Lox Activité lysyl oxydase
LOX : Lysyl Oxydase (protéine)
LOXL 1-4 : Lysyl Oxydase-Like (1-4) (protéines)

MAM : Mitochondria-Associated Membranes
MAPK : Mitogen Activated Protein Kinase
MCU : Mitochondrial Calcium Uniporter
MCUR1 : Mitochondrial Calcium Uniporter Regulator 1
MDM2 : Mouse Double Minute 2
MEF : Mouse Embryonic Fibroblast
MICU1 : Mitochondrial Calcium Uptake 1
MEK : MAK/ERK kinase
MMP : Matrix Metalloproteinase
MRP : Multidrug resistant Protein
MRN : MRE 11-RAD50-NBS1
MFN : Mitofusin (1 et 2)
mTOR : Mammalian Target of Rapamycin

NF1 : NeuroFibromin 1
NFκB : Nuclear Factor of kappa light chain gene enhancer in B cells

OIS : Oncogene-Induced Senescence
OMM : Outer Mitochondrial Membrane

PDAC : Pancreatic Ductal AdenoCarcinoma
PAI-1 : Plasminogen Activator Inhibitor-1
PDH : Pyruvate DésHydrogénase
PDP2 : Pyruvate DésHydrogénase Phosphatase-2
PI3K : PhosphatidylInositol-3 Pinase
PICS : Pten-loss-Induced Cellular Senescence
PIN : Prostate Intraepithelial Neoplasia
PKA : Protein Kinase A
PKB/AKT : Protein Kinase B
PKC : Protein Kinase C
PLC : Phospholipase C
PML : PromyeLocytic Leukemia nuclear
PRC : Polycomb Repressive Complex
PTEN : Phosphatase and Tensin Homologue

RAF : Rat Fibrosarcoma (BRAF)

Ras :	Rat Sarcoma (H-Ras, Harvey ; K-Ras, Kristen ; N-Ras : Neuroblastoma)
RE :	Réticulum Endoplasmique (REL : Lisse ; REG : granuleux)
Rb :	RetinoBlastoma protein
ROS :	Reactive Oxygen Species
SA-β-gal :	Senescence-Associated-β-galactosidase
SAHF :	Senescence-Associated Heterochromatin Foci
SASP :	Senescence-Associated Secretory Phenotype
shRNA :	short hairpin RNA
siRNA :	small interfering RNA
SKP2 :	S-phase-associated protein-2
SUV39H1 :	Suppressor of Variegation 3-9 homologue 1
TERC :	Telomerase RNA component
TOP1 :	Topoisomerase 1
TPA :	12-O-tetradecanoylphorbol-13-acetate
UPR :	Unfolded Protein Response
VDAC :	Voltage Dependent Anion Channel
VEGF :	Vascular Endothelial Growth Factor
WNT :	Wingless-type MMTV integration site
WT :	Wild Type

INTRODUCTION GÉNÉRALE

INTRODUCTION GENERALE

Chapitre I : La sénescence

La sénescence est un arrêt de prolifération cellulaire irréversible induit par différents types de stress. Les cellules sénescentes, comme nous allons le voir dans les paragraphes suivants, présentent de nombreuses caractéristiques phénotypiques. Ce programme cellulaire a été décrit pour la première fois par Hayflick et Moorhead en 1961. En cultivant des fibroblastes primaires, ils ont observé que ceux-ci ne pouvaient pas proliférer indéfiniment (à l'inverse des cellules tumorales couramment utilisées à l'époque) mais qu'après un certain nombre de divisions cellulaires, ils rencontrent une limite réplicative. Rapidement, Hayflick a proposé que la sénescence puisse limiter le cancer et favoriser le vieillissement. L'utilisation de modèles murins a permis de confirmer que les cellules sénescentes s'accumulent dans l'organisme au fils des années, et que la sénescence peut jouer un rôle important dans le processus de tumorigénèse. Après avoir décrit les caractéristiques des cellules sénescentes, je présenterai les différents inducteurs de la sénescence, les voies de signalisation impliquées, et les rôles physiopathologiques associés. Je présenterai notamment pourquoi la sénescence constitue une barrière importante au développement tumoral.

1.1 Caractéristiques des cellules sénescentes

Les cellules sénescentes, quel que soit le stimulus activateur, présentent de nombreux changements phénotypiques et moléculaires qui permettent de les identifier *in vitro* et *in vivo*. Ces marqueurs sont soit des acteurs de l'établissement de la sénescence soit un reflet des changements phénotypiques associés à la sénescence. L'identification des cellules sénescentes est complexe puisque chaque biomarqueur, pris individuellement, n'est pas suffisant pour caractériser une cellule sénescente. Il est donc nécessaire d'en combiner plusieurs. La plupart des cellules sénescentes sont définies par un arrêt de prolifération irréversible, une morphologie spécifique, une augmentation de l'activité β-galactosidase, et un phénotype sécrétoire particulier.

1.1.1 Arrêt de prolifération

L'élément majeur, indispensable mais non suffisant à l'identification de la sénescence cellulaire, est l'arrêt de prolifération. Le cycle cellulaire est composé de quatre phases successives : la phase S (synthèse de l'ADN), la phase G1, la phase G2, et enfin la phase M (mitose).

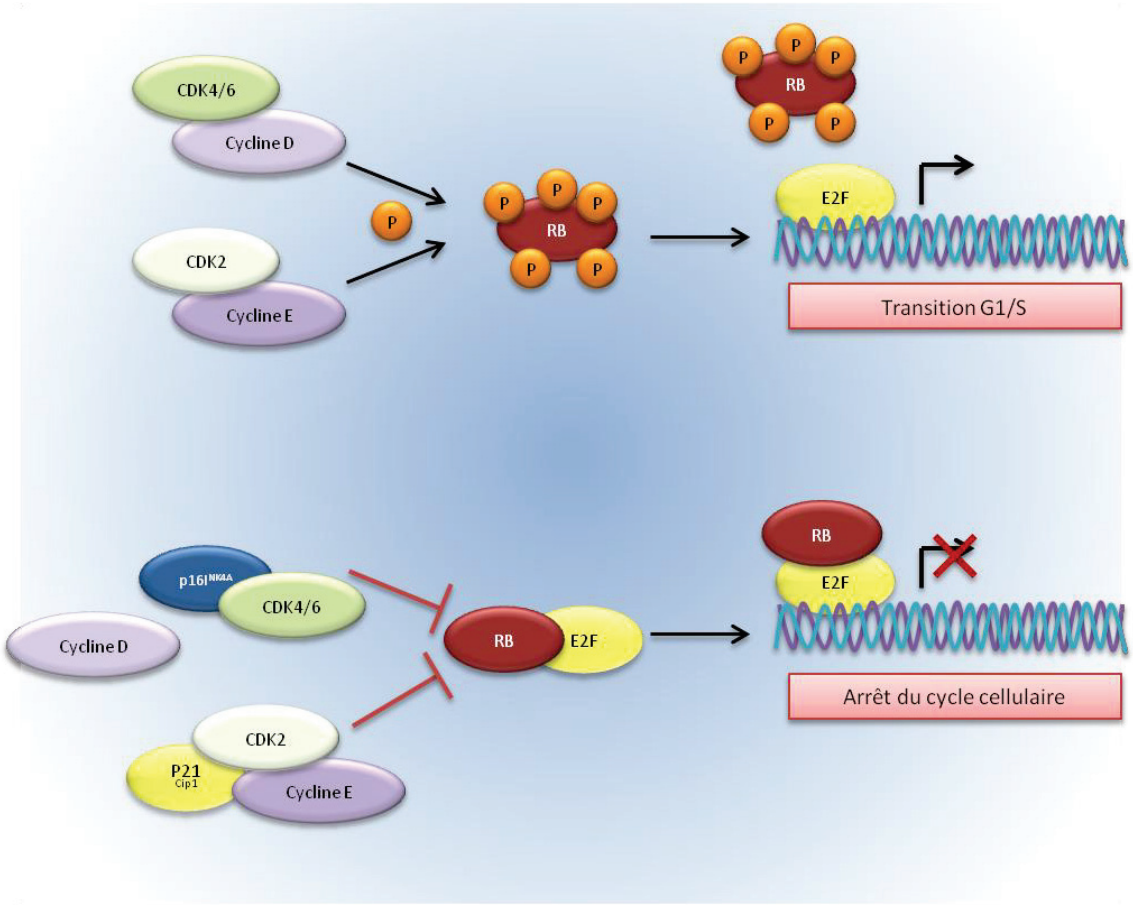

Figure 1 : Les complexes cyclines-CDK régulent l'activation de la protéine Rb

a) Les complexes CDK-cyclines phosporylent la protéine Rb, l'empêchant de se lier à E2F. Suite à cette étape initiatrice, les cyclines E-CDK phosphorylent à leur tour Rb.

b) Pendant la sénescence, $p16^{INK4A,}$ dont l'expression augmente inhibe CDK4/6 en se liant à CDK4/6 et empêche leur liaison avec la cycline D. L'induction de $p21^{Cip1}$ inhibe l'activité kinase de la CDK2. Rb se retrouve dans un état d'hypophosphorylation où il peut se lier et inhiber E2F.

Une cinquième phase, la phase G0, correspond à un état de quiescence. La transition d'une phase à la suivante est contrôlée par les complexes cycline/kinases dépendantes des cyclines (*Cyclin-Dependant Kinases*, CDK). Les complexes cyclines/CDK sont inactivés par deux familles principales de protéines inhibitrices de CDK (CKI) : la famille INK4 et la famille CIP/KIP.

La famille INK4 composée des protéines $p16^{INK4A}$, $p15^{INK4B}$, $p18^{INK4C}$, et $p14^{ARF}$ ($P19^{ARF}$ chez la souris) inhibe spécifiquement la liaison de la cycline D aux CDK4 et CDK6. Les complexes cyclines-CDK4/6, en hyperphosphorylant la protéine Rb, permettent l'activation du facteur de transcription E2F, et ainsi favorisent la transcription des gènes impliqués dans la progression du cycle cellulaire *(figure 1)*. La famille Cip/Kip est composée des membres $p21^{CIP1}$, $p27^{Kip1}$ et $p57^{Kip2}$ et inhibe l'activité kinase des cyclines (Sherr and Roberts, 1999). Les principaux CKI surexprimés lors de la sénescence sont $p16^{INK4A}$, $p14^{ARF}$, $p21^{Cip1}$. L'implication de $p27^{Kip1}$ et de $p57^{Kip2}$ dans l'arrêt du cycle dans un contexte de sénescence n'a été que très peu étudiée, mais il semblerait que $p27^{Kip1}$ puisse jouer un rôle (Lin *et al.*, 2010; Cao *et al.*, 2011).

Généralement, les cellules sénescentes sont arrêtées en phase G1 (Di Leonardo *et al.*, 1994; Herbig *et al.*, 2004; Ogryzko *et al.*, 1996; Serrano *et al.*, 1997) mais il a été reporté que certains oncogènes, en fonction du contexte cellulaire, peuvent induire un arrêt du cycle en phase G2 (Di Micco *et al.*, 2006; Olsen *et al.*, 2002; Zhu *et al.*, 1998). Enfin, en réponse à des agents chimiothérapeutiques, les cellules cancéreuses peuvent être arrêtées en phase G2 ou S (Shay and Roninson, 2004).

Bien que métaboliquement actives, les cellules sénescentes sont incapables de reprendre leur croissance, malgré des conditions de prolifération adéquates, contrairement aux cellules quiescentes. L'arrêt dans le cycle cellulaire ne se produit pas seulement dans les cellules sénescentes, mais aussi dans les cellules en différentiation terminale. L'observation de l'arrêt de prolifération et de sa stabilité est donc nécessaire mais pas suffisante pour identifier une cellule sénescente.

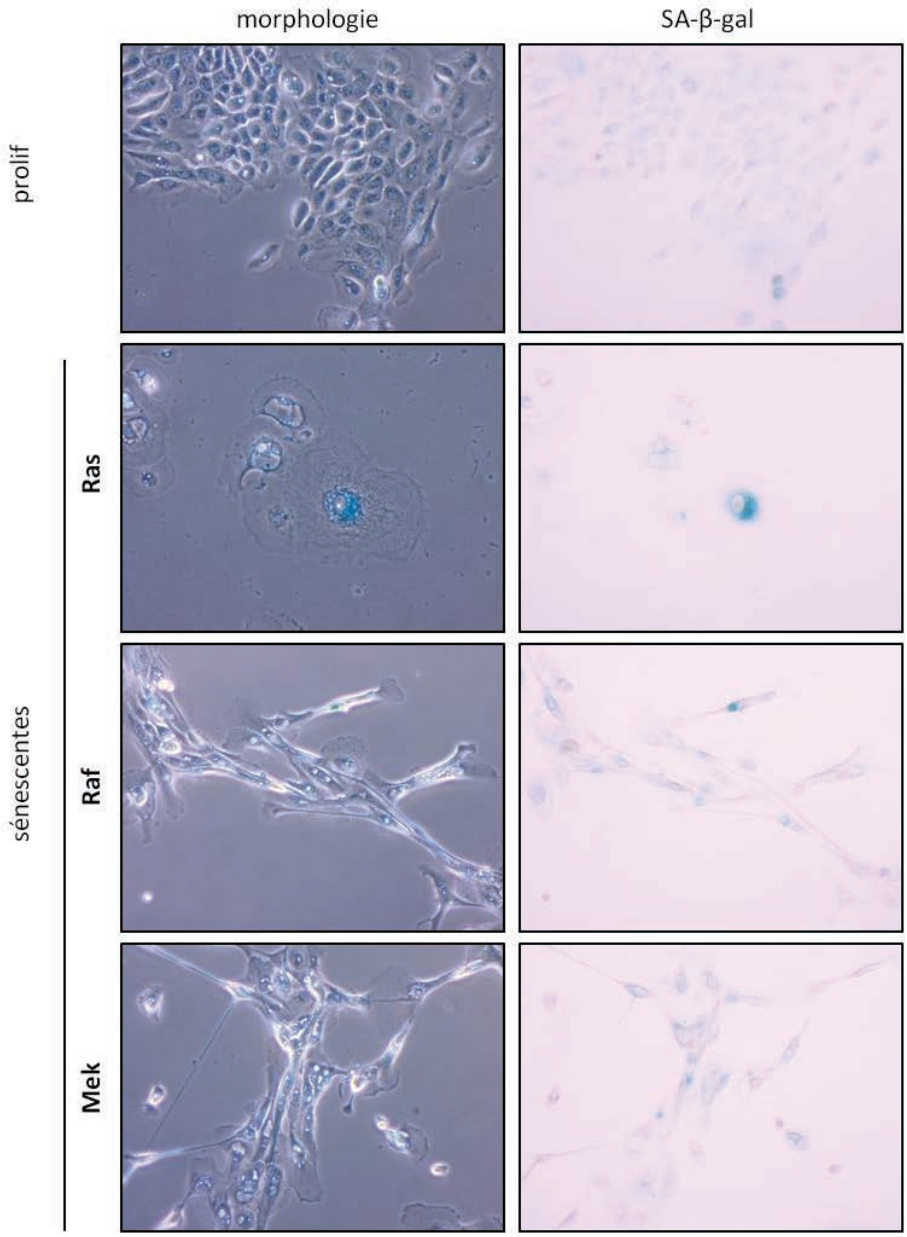

Figure 2 : Morphologie de cellules épithéliales lors de la sénescence

Morphologie de cellules épithéliales mammaires humaines (hMECs) qui prolifèrent (prolif) ou sénescentes après activation de versions mutées de de Ras, Raf ou Mek (sénescentes).

L'activité SA-β-gal est également montrée.

1.1.2 Morphologie

Les cellules sénescentes en culture sont larges et aplaties, avec un compartiment cytoplasmique étendu et un noyau plus gros, parfois multi-nucléé. Toutefois les causes et surtout les conséquences de cette morphologie particulière ne sont pas connues. Il est intéressant de noter que selon le type et le stress cellulaire la morphologie acquise par la cellule sénescente peut être différente. Par exemple l'activation de l'oncogène Ras se traduit par une morphologie très plate et très ronde (Serrano *et al.*, 1997). L'activation des oncogènes Raf et Mek, en aval de Ras, se manifeste par une morphologie très allongée, accompagnée de longs prolongements cytoplasmiques (Zhu *et al.*, 1998) *(figure 2)*. Une vacuolisation du cytoplasme (Denoyelle *et al.*, 2006) et une augmentation de la masse lysosomale sont également observées.

1.1.3 Activité β-galactosidase Associée à la Sénescence (SA-β-gal)

L'équipe de Campisi a identifié en 1995 une enzyme, la β-galactosidase, dont l'activité peut être détectée à pH 6 dans les cellules sénescentes, *in vitro* et *in vivo* (Dimri *et al.*, 1995). La détection de l'activité enzymatique à ce pH sous-optimal est due à une augmentation de la masse lysosomale et donc de l'enzyme pendant la sénescence (Kurz *et al.*, 2000). Pour autant, l'activité de la β-galactosidase, codée par le gène *GLB1*, n'est pas nécessaire à la mise en place du phénotype sénescent (Lee *et al.*, 2006 a). A l'heure actuelle le test d'activité SA-β-galactosidase est le marqueur le plus couramment utilisé, à la fois *in vitro et in vivo* et reste indispensable à l'identification de cellules sénescentes *(figure 2)*.

1.1.4 Phénotype Sécrétoire Associé à la Sénescence (SASP)

Il a été observé dans le surnageant de cellules sénescentes une augmentation de protéines impliquées dans la dégradation de la matrice extra-cellulaire (*Extra-Cellular Matrix*, ECM) comme le tissue-type plasminogen activator (t-PA) (West *et al.*, 1996), ou des métalloprotéinases (MMP) (Millis *et al.*, 1992; West *et al.*, 1989). Par la suite, il a été montré que la sénescence, quelle que soit l'origine du stress, est caractérisée par une augmentation accrue de l'expression de gènes impliqués notamment dans l'inflammation (Coppé *et al.*, 2006; Krtolica *et al.*, 2001; Parrinello *et al.*, 2005). Ce phénotype particulier porte le nom de Phénotype Sécrétoire Associé à la Sénescence (*Senescence-Associated Secreted Phenotype*, SASP) et marque un profond remaniement dans la sécrétion des protéines (Campisi and d'Adda di Fagagna, 2007). Toutes les études montrent clairement que le SASP, composé de protéases, de cytokines, et d'autres facteurs sécrétés encore non identifiés, constitue un réseau de signalisation complexe pouvant affecter non seulement les cellules sénescentes (effet intracrine et autocrine renforçant la sénescence) mais aussi leur micro-environnement (cellules avoisinantes normales, pré-tumorales ou tumorales) par un effet paracrine (Kuilman *et al.*, 2008; Acosta *et al.*, 2008, 2013; Coppé *et al.*, 2008; Krtolica *et al.*, 2001). Il apparaît alors que la sénescence n'est pas un simple arrêt de prolifération (Campisi, 2005). Les rôles bivalents du SASP, pro et anti tumoraux, seront abordés avec les rôles de la sénescence *(voir paragraphes 1.4 et 1.5)*. Bien que les facteurs de transcription C/EPBβ et NFκB aient déjà été identifiés comme régulateurs du SASP (Chien *et al.*, 2011; Jing *et al.*, 2011), ce dernier constitue un processus complexe qui nécessite encore des études approfondies.

1.1.5 Induction de $p16^{INK4A}$

Les cellules sénescentes sont marquées par un profond remaniement de l'expression des gènes, notamment pour établir le programme de sénescence (Mason *et al.*, 2004; Shelton *et al.*, 1999; Yoon *et al.*, 2004). On observe notamment une expression des CKI $p16^{INK4A}$, $p21^{cip1}$ et/ou $p15^{INK4B}$. *In vitro* mais aussi *in vivo* les cellules sénescentes présentent généralement une forte expression de $p16^{INK4A}$ (Collado *et al.*, 2005; Serrano *et al.*, 1997; Baker *et al.*, 2011 b; Krishnamurthy *et al.*, 2004; Melk *et al.*, 2004; Waaijer *et al.*, 2012).

Des souris exprimant le promoteur de $p16^{INK4A}$ couplé à la luciférase ont permis de suivre *in vivo* l'expression de ce régulateur du cycle dans des modèles de vieillissement ou des modèles de papillomes induit par un protocole DMBA-TPA (Yamakoshi *et al.*, 2009). L'utilisation de souris knock-in exprimant la luciférase sous le contrôle du promoteur de $p16^{INK4A}$ a notamment confirmé que l'expression de $p16^{INK4A}$ est fortement activée dans les tissus néoplasiques, permettant ainsi de détecter très rapidement l'émergence de tumeurs *in vivo*. Ces données confirment que $p16^{INK4A}$ est

un marqueur sensible et fiable de la transformation néoplasique (Burd *et al.*, 2013). Comme je le développerai plus tard dans ce chapitre, p16^{INK4A} joue un rôle important dans la sénescence en bloquant le cycle cellulaire. Toutefois nous verrons dans le chapitre suivant que son implication n'est pas toujours obligatoire.

1.1.6 Foyers d'Hétérochromatine Associés à la Sénescence (SAHF)

La coloration de l'ADN de cellules normales fait apparaître une distribution diffuse et homogène de l'ADN dans le noyau. Dans le cas de cellules sénescentes, cette coloration peut faire apparaître des foyers de chromatine condensée, appelés Foyers d'hétérochromatine Associées à la Sénescence (*Senescence-Associated Heterochromatin Foci*, SAHF) (Narita *et al.*, 2003). Les SAHF sont constitués de plusieurs couches distinctes d'hétérochromatine prouvant une organisation complexe (Chandra and Narita, 2012).

Les SAHF sont enrichis en protéines typiques de l'hétérochromatine comme la HP1 *(Heterochromatin Protein 1*) ou le variant d'histone macroH2A. La formation des SAHF est notamment régulée par la protéine HIRA (*Histone cell cycle regulation defective A*) et nécessite la présence de corps nucléaires incluant la protéine PML (*ProMyelocytic Leukemia*) (Ferbeyre *et al.*, 2000; Pearson *et al.*, 2000; Vernier *et al.*, 2011; Zhang *et al.*, 2005).

Fonctionnellement, les SAHF semblent être dépendants d'une activation de la voie p16^{INK4A}/Rb, et les foyers d'hétérochromatine semblent réprimer les gènes cibles de E2F impliqués dans la prolifération (Narita *et al.*, 2003). Il en a alors été déduit que la formation de SAHF au cours de la sénescence participait à l'arrêt du cycle, et était responsable de la stabilité de la sénescence : une fois les SAHF formés, la présence de dommages à l'ADN et des inhibiteurs du cycle ne sont plus nécessaire pour maintenir la sénescence (Bakkenist *et al.*, 2004). Il a toutefois été montré que les SAHF peuvent persister après l'inactivation de points de contrôle du cycle et l'échappement à la sénescence qui en découle, suggérant que les gènes nécessaires à la progression tumorale ne sont pas réprimés par les SAHF dans ces conditions. De plus, l'analyse d'échantillons tumoraux a révélé que les SAHF y sont également maintenus. Les SAHF, en protégeant l'ADN et en diminuant les réponses aux dommages à l'ADN permettraient la survie des cellules (Di Micco *et al.*, 2011). De plus, on peut observer de la sénescence sans pour autant observer de SAHF révélant que l'importance des SAHF pour l'établissement de la sénescence varie en fonction du type cellulaire et de la source de stress (Kosar *et al.*, 2011). Ces données remettent en question d'une part la fonction des SAHF dans la sénescence et d'autre part l'importance fonctionnelle des SAHF dans l'arrêt du cycle.

1.1.7 Résistance à l'apoptose

L'apoptose est un processus de mort cellulaire qui permet d'éliminer rapidement les cellules stressées ou endommagées. Les cellules sénescentes sont pour la plupart résistantes à l'apoptose contrairement aux cellules jeunes (Wang, 1995; Gansauge *et al.*, 1997; Seluanov *et al.*, 2001). Cela peut être dû à une absence de stabilisation de p53 dans les cellules sénescentes (Seluanov *et al.*, 2001). Il a été montré que la caspase-3 (Rebbaa *et al.*, 2003; Marcotte *et al.*, 2004) ainsi que la protéine anti-apoptotique Bcl-2 (Wang, 1995; Crescenzi *et al.*, 2003; Ryu *et al.*, 2007) participent à cette résistance à l'apoptose de fibroblastes sénescents. Il apparaît alors évident qu'apoptose et sénescence sont interconnectés, puisque la modulation de protéines pro- ou anti-apoptotiques a un effet sur la sénescence.

Les mécanismes selon lesquels la sénescence rend les cellules résistantes à l'apoptose ne sont toutefois pas clairement identifiés. De même les raisons pour lesquelles les cellules entrent préférentiellement en apoptose ou en sénescence en réponse à un stress ne sont pas comprises. Il a été montré que les cellules épithéliales et les fibroblastes activent plutôt un programme de sénescence alors que les lymphocytes auront une réponse apoptotique, soulignant ainsi un lien avec le type cellulaire. Certains suggèrent que toutes les cellules sont capables d'activer ces deux voies, et que la nature et/ou l'intensité du signal de stress pourrait être la cause d'une réponse différente (Rodier *et al.*, 2007).

1.1.8 Altération de l'expression génique

De nombreuses études ont montré que le profil d'expression génique des cellules sénescentes est très différent de celui des cellules normales. L'expression de nombreux régulateurs du cycle cellulaire, activateurs ou inhibiteurs, est largement modifiée. Outre l'induction des CKI $p16^{INK4A}$ et $p21^{Cip1}$, l'expression de gènes codant pour de nombreuses protéines qui favorisent la progression dans le cycle cellulaire (cyclines A et B, PCNA, c-Fos…) est réprimé (Mason *et al.*, 2004). Néanmoins, beaucoup de gènes dont l'expression change ne semblent pas être reliés au cycle cellulaire, notamment les facteurs du SASP (Trougakos *et al.*, 2006).

Le remaniement de l'expression génique se traduit également par un profond changement de l'expression de microARNs (Gorospe and Abdelmohsen, 2011). Il a été reporté que la surexpression de microARNs peut influencer plusieurs mécanismes impliqués dans la sénescence comme la régulation du cycle cellulaire, l'expression d'IL-6 et d'IL-8 ou la formation de l'hétérochromatine (Hermeking, 2010; Bhaumik *et al.*, 2009; Li *et al.*, 2010; Benhamed *et al.*, 2012).

marqueurs phénotypiques	marqueurs moléculaires
absence de prolifération	CKI
absence de réponse aux facteurs de croissance	p53 /ARF
morphologie élargie et aplatie	Dommages à l'ADN
SA-β-gal	SASP
SASP	DcR2/Dec1/Sprouty2
SAHF/ corps nucléaires PML	DDR
DNA Scars	HMGA
augmentation de la masse lysosomale/autophagie	marqueurs d'hétérochromatine
	diminution de la lamine B

Tableau 1 : Tableau récapitulatif des caractéristiques des cellules sénescentes

Adapté de (Salama *et al.*, 2014)

L'altération de l'expression génique est un trait commun aux cellules sénescentes, mais les profils des changements d'expression dépendent du type cellulaire et du stress. La sénescence n'est donc pas une réponse unique, mais propre à chaque cellule (Nelson *et al.*, 2014).

1.1.9 Autres marqueurs

D'autres marqueurs de sénescence ont été identifiés : l'induction de Dec1 (*Deleted in oesophageal Cancer 1*) et DcR2 (*Decoy Receptor 2*) sont des marques de sénescence *in vitro* et *in vivo* (Collado *et al.*, 2005). Il a également été reporté que WNT16B, un facteur sécrété de la famille Wnt, est surexprimé lors de la sénescence réplicative et de la sénescence induite par Ras, constituant lui aussi un nouvel outil pour détecter de la sénescence (Binet *et al.*, 2009). L'augmentation d'expression de Sprouty2 a également été impliquée dans la mise en place de la sénescence (Courtois-Cox *et al.*, 2006).

Les cellules sénescentes sont aussi caractérisées par une augmentation de l'activité autophagique (Narita and Young, 2009; Narita *et al.*, 2011). Les agrégats de lipofuscine connus pour s'accumuler avec l'âge s'avèrent être utiles pour détecter les tissus sénescents dans lesquels il est parfois techniquement difficile de détecter l'activité SA-β-gal (Georgakopoulou *et al.*, 2013). Plusieurs études rapportent également une réduction de l'expression de la lamine B1 durant la sénescence (Freund *et al.*, 2012; Sadaie *et al.*, 2013; Shah *et al.*, 2013).

Le terme de SAPD (*Senescence-Associated Protein Degradation*) a récemment été introduit (Deschênes-Simard *et al.*, 2013). L'activation aberrante des kinases ERK 1 et 2 induite par l'activation de Ras aboutit à la dégradation par le protéasome de protéines phosphorylées qui semblent nécessaires à la croissance et la prolifération des cellules, au fonctionnement normal des mitochondries, ou au métabolisme des ARN. Il est suggéré que la dégradation importante de ces protéines engendre un stress contribuant à la sénescence. Ces observations ne sont pas restreintes à la sénescence induite par un stress oncogénique (*Oncogene-Induced Senscence*, OIS) puisque le raccourcissement des télomères semble être associé au même profil (Deschênes-Simard *et al.*, 2013).

L'établissement de la sénescence est un processus qui peut être séparé en plusieurs étapes : évènements déclencheurs, initiation d'une réponse de sénescence, entrée en sénescence, et enfin mise en place progressive d'un phénotype sénescent, révélant que la sénescence n'est pas un processus figé mais dynamique. Les marques caractérisant la sénescence *(tableau 1)* n'apparaissent donc pas toutes en même temps, et dépendent du contexte cellulaire.

1.2 Inducteurs de sénescence

La sénescence est un programme déclenché par les stress cellulaires. Nous verrons dans les paragraphes suivants que nous pouvons différencier divers stress, qui aboutissent donc potentiellement à plusieurs types de sénescence.

1.2.1 Sénescence réplicative

A chaque division cellulaire les cellules perdent entre 50 et 200 pb aux extrémités de leurs chromosomes, les télomères, composés d'une répétition du tandem TTAAGGG, et de protéines. Ces structures, longues de 10-15 kb chez les humains, forment une structure en boucle T qui permet de protéger les extrémités des chromosomes d'une potentielle dégradation. Cependant, après un nombre non défini de divisions, les télomères atteignent une taille critique et ne peuvent plus former cette boucle T. Les extrémités simple-brins ainsi mises à nues activent une réponse aux dommages à l'ADN (*DNA-Damage Response*, DDR), via p53, aboutissant à un arrêt du cycle, à l'apoptose ou à la sénescence.

La réintroduction de la sous unité catalytique de la télomérase (hTERT) dans des cellules primaires humaines permet d'allonger les télomères, d'augmenter la durée de vie des cellules, et donc d'éviter la sénescence réplicative, prouvant que celle-ci est due au raccourcissement des télomères (Bodnar, 1998). L'expression de la hTERT est devenue par la suite une méthode couramment utilisée pour immortaliser les cellules primaires. Les cellules cancéreuses expriment pour la plupart hTERT (Shay, 1997), ou rallongent leurs télomères utilisant un procédé appelé Alternative Lengthening of Telomeres (ALT) (Muntoni and Reddel, 2005), leur conférant un potentiel réplicatif illimité. Il est clairement établi que les dommages à l'ADN, notamment les cassures double-brins, peuvent contribuer à une induction de sénescence (Gire *et al.*, 2004). Bien que le signal exact d'entrée en sénescence ne soit pas identifié, dès qu'un télomère dans une cellule atteint une taille trop courte ou qu'un télomère est dysfonctionnel, une réponse aux dommages à l'ADN est activée (Hemann *et al.*, 2001).

Une réponse aux dommages à l'ADN aboutit généralement à un arrêt du cycle cellulaire permettant de réparer les cassures d'ADN avant que la cellule ne se divise. Or, dans le cas de la sénescence réplicative, les cellules ne reprennent pas leur division, suggérant que les cassures d'ADN détectées ne sont pas complètement réparées. Les cellules qui sénescent avec une DDR persistante ont des foyers nucléaires appelés DNA-SCARS (*DNA segments with Chromatin Alterations Reinforcing Senescence*) contenant des protéines des DDR activées (d'Adda di Fagagna *et al.*, 2003; Herbig *et al.*,

2004; Rodier *et al.*, 2009). L'équipe de d'Adda di Fagagna a récemment montré que lors de la sénescence réplicative la voie des dommages à l'ADN reste activée car subsistent des séquences télomériques mises à nues qui ne peuvent pas être réparées. Ce mécanisme permettrait d'éviter que les chromosomes ne fusionnent entre eux et d'assurer ainsi à la fois leur l'intégrité et celle de la cellule (Fumagalli *et al.*, 2012).

Outre la sénescence réplicative, d'autres causes peuvent induire une sénescence dite prématurée, qui apparaît avant que le raccourcissement des télomères n'ait lieu, comme la sénescence induite par un stress oncogénique ou par un stress oxydant.

1.2.2 Sénescence Induite par un Oncogène (OIS)

En 1997 Serrano *et al* ont montré que l'expression ectopique d'une version mutée de Ras, H-Ras^{G12V}, dans des fibroblastes primaires aboutit à un arrêt de prolifération qui comporte les caractéristiques de la sénescence : augmentation de l'activité β-galactosidase, induction de p16^{INK4A} et de p53 (Serrano *et al.*, 1997). Il s'agit de la sénescence induite par un oncogène, autrement appelée OIS pour *Oncogene-Induced Senescence*. Cette réponse cellulaire ne se produit pas seulement après activation de Ras puisque la surexpression ou l'expression de versions mutées d'autres oncogènes de la voie MAPK (MAP kinase), tels que Raf ou Mek permet également d'induire cette sénescence prématurée (Lin *et al.*, 1998; Michaloglou *et al.*, 2005; Campaner *et al.*, 2010; Bartkova *et al.*, 2006; Zhu *et al.*, 1998). Par la suite, cette réponse à été généralisée à d'autres types d'oncogènes (Denchi *et al.*, 2005; Xu *et al.*, 2008; Gorgoulis and Halazonetis, 2010). L'OIS peut également être induite par la perte d'un gène suppresseur de tumeur qui va engendrer l'activation d'un oncogène. Par exemple, la perte de PTEN (*Phosphatase and Tensin homolog*), inhibiteur de la voie PI3K/Akt, induit un arrêt de prolifération dépendant de p53 (Chen *et al.*, 2005 b; Kim *et al.*, 2007). La perte d'autres suppresseurs de tumeurs, tels que NeuroFibromin 1 (NF1) (Courtois-Cox *et al.*, 2006) ou von Hippel-Lindau (VHL) (Young *et al.*, 2008) aboutit également à une sénescence prématurée, considérée comme de l'OIS.

L'expression de la télomérase dans ces cellules ne permet pas d'échapper à l'OIS démontrant que ce mécanisme est indépendant du raccourcissement des télomères (Wei and Sedivy, 1999). Néanmoins, les causes moléculaires de l'OIS ne semblent pas être totalement différentes de celles causant la sénescence réplicative : la réplication aberrante de l'ADN causée par l'oncogène est à la source d'un stress réplicatif, d'une réponse aux dommages à l'ADN, et de la sénescence. En effet, l'inhibition de la réponse aux dommages à l'ADN empêche les fibroblastes d'entrer en sénescence prématurée, favorise leur prolifération, et les prédispose à la transformation maligne (Bartkova *et al.*, 2006; Mallette *et al.*, 2007; Di Micco *et al.*, 2006). De manière intéressante, l'activation d'un

oncogène, en causant un stress réplicatif, peut également altérer la structure et la fonction des télomères dans les cellules qui n'ont pas d'activité télomérase (Suram *et al.*, 2012). L'activation de Ras peut également engendrer des hauts niveaux d'espèces réactives de l'oxygène (*Reactive Oxygen Species*, ROS) dans la cellule. Ces derniers causent alors des dommages à l'ADN dits « oxydatifs » (Lee *et al.*, 1999).

En 2005, plusieurs groupes ont indépendamment montré que l'activation de différents oncogènes induit la sénescence *in vivo*. L'équipe de Manuel Serrano a rapporté que l'induction de K-Ras^{G12V} dans un modèle murin est associé à de la sénescence dans les tissus bénins (augmentation de l'activité β-galactosidase, arrêt de prolifération, induction de p16^{INKA} mais aussi de p15^{INK4B}, Dec1, et DcR2) alors que toutes les marques de sénescence ont disparu dans les tissus malins. Dans une autre étude, Braig et ses collègues ont pu démontrer que l'OIS retarde le développement des lymphomes induits par N-Ras^{G12D} (Braig *et al.*, 2005). Les naevi (lésions bénignes de la peau autrement appelées grains de beauté) qui expriment B-Raf^{V600E} sont aussi très riches en cellules sénescentes (Michaloglou *et al.*, 2005). Enfin, l'équipe de Pandolfi a utilisé pour la première fois un modèle murin où la déplétion de PTEN induit de la sénescence dans les tissus néoplasiques de la prostate (*Prostate Intraepithelial Neoplasia*, PIN). Ces premières études ont été suivies par de nombreuses autres, impliquant d'autres oncogènes et d'autres tissus, soulignant l'importance de l'OIS *in vivo*.

Bien que la sénescence réplicative ait facilement été mise en évidence dans des souris âgées, la relevance de l'OIS *in vivo* a été remise en cause pendant plusieurs années. En effet, les études faites *in vivo* sur la conséquence de l'expression de Ras divergent : l'activation de K-Ras dans différents contextes induit de la prolifération sans sénescence (Lee and Bar-Sagi, 2010; Tuveson *et al.*, 2004; Guerra *et al.*, 2003). Il a été proposé que des faibles niveaux d'activation de Ras aboutissent à une stimulation de la prolifération cellulaire, alors que des niveaux plus élevés induisent un arrêt de croissance de type sénescence (Sarkisian *et al.*, 2007). Il apparaît clairement qu'outre les niveaux de Ras, les boucles de régulation mises en jeu sont importantes dans l'établissement de la sénescence (Courtois-Cox *et al.*, 2006; Kennedy *et al.*, 2011; Vredeveld *et al.*, 2012).

1.2.3 Sénescence Induite par Invalidation d'Oncogène (OIIS)

La sénescence induite par invalidation d'oncogène (*Oncogene InvalidationInduced Senescence*, OIIS) est un processus qui a majoritairement lieu dans les cellules cancéreuses, et repose sur le fait que les cellules sont dépendantes de leur oncogène pour proliférer (Weinstein, 2000). Après inactivation d'un oncogène, les cellules tumorales peuvent s'arrêter de proliférer, entrer en apoptose ou en sénescence. Ainsi, l'inactivation de MYC, ou de K-Ras peut engendrer une régression de la tumeur (Jain *et al.*, 2002; Felsher and Bishop, 1999; Pelengaris *et al.*, 1999). Aussi étonnant que cela

puisse être, les cellules cancéreuses qui ont la plupart du temps des voies de signalisation p53 et Rb altérées peuvent induire une réponse de type sénescence, soit parce que ces voies peuvent être réactivées, soit parce que des voies alternatives peuvent être induites (Nardella *et al.*, 2011). Cette découverte a immédiatement suscité un grand intérêt. Actuellement plusieurs groupes essaient désormais d'identifier les mécanismes pour réactiver ces systèmes de sauvegarde dans les tumeurs, et ainsi développer des outils thérapeutiques *(voir le paragraphe 1.5.3, Sénescence induite par la thérapie)*.

1.2.4 Stress oxydant

D'autres facteurs sont également connus pour induire un stress engendrant la sénescence tel que le stress oxydatif par l'intermédiaire des ROS produits par les mitochondries (Lu and Finkel, 2008; Moiseeva *et al.*, 2009). L'exposition des cellules à des faibles doses de ROS telles que l'H_2O_2 induit un arrêt de croissance similaire à la sénescence (Dumont *et al.*, 2000; Chen and Ames, 1994) et les niveaux de ROS augmentent pendant la sénescence réplicative (Furumoto *et al.*, 1998), et l'OIS (Lee *et al.*, 1999). De plus, le traitement des cellules avec des antioxydants permet de retarder l'entrée en sénescence réplicative (Chen and Ames, 1994). Une étude récente a suggéré que les ROS induisent la sénescence via des dommages à l'ADN et une activation de $p21^{CIP1}$ (Passos *et al.*, 2010). D'autres études relient les ROS à l'activation des voies p53 – Rb (Itahana *et al.*, 2003; Iwasa *et al.*, 2003). La génération de ROS a également été impliquée dans l'oxydation du pool de nucléotides qui, si ceux-ci ne sont pas éliminés, induit de la sénescence prématurée (Rai *et al.*, 2009).

Le potentiel réplicatif des cellules est également influencé par les niveaux d'oxygène dans lesquels les cellules sont cultivées, preuve que le stress oxydatif joue un rôle dans l'établissement de la sénescence. La culture de fibroblastes avec un taux d'oxygène physiologique - 3% d'O_2 au lieu de 20% - permet de retarder la sénescence réplicative (Parrinello *et al.*, 2003). De même, les cellules murines qui ont pourtant de longs télomères et qui expriment pour la plupart la télomérase sénescent dans des conditions de culture classiques. Les fort taux d'O_2, auxquels les cellules murines sont plus sensibles que les cellules humaines, induisent des cassures dans l'ADN et activent une réponse de dommages à l'ADN (Parrinello *et al.*, 2003).

Bien qu'il soit désormais établi que les ROS jouent un rôle important dans la sénescence, leur mécanisme de génération, la nature de cette implication ainsi que leurs fonctions exactes restent encore à être déterminés.

1.2.5 Autres types de stress

D'autres sources de stress, très variées, peuvent induire la sénescence. Par exemple, une activation chronique de certaines cytokines type interféron-β est à la source d'un arrêt de prolifération type sénescence suite à une augmentation des radicaux d'oxygène (Moiseeva *et al.*, 2006). De même, la sénescence peut être induite par une activation chronique du TGF-β par la formation de SAHF au travers l'activation de la voie $p16^{INK4A}$-Rb (Vijayachandra *et al.*, 2003; Zhang and Cohen, 2004). Des modificateurs de la chromatine, tels que des inhibiteurs des histones desacétylases peuvent également, sans endommager l'ADN, activer les protéines ATM et p53 (Bakkenist and Kastan, 2003), et induire ainsi une réponse de sénescence (Ogryzko *et al.*, 1996; Munro *et al.*, 2004). Enfin, Mannava et ses collègues ont récemment montré qu'une réduction du pool de nucléotides peut induire la sénescence dépendante des dommages à l'ADN (Mannava *et al.*, 2013). Dans le cas des cellules épithéliales et des mélanocytes, un milieu de culture inadapté, ou l'absence de composants et/ou de cellules de la matrice extracellulaire engendre un stress associé à de la sénescence (Ramirez *et al.*, 2001).

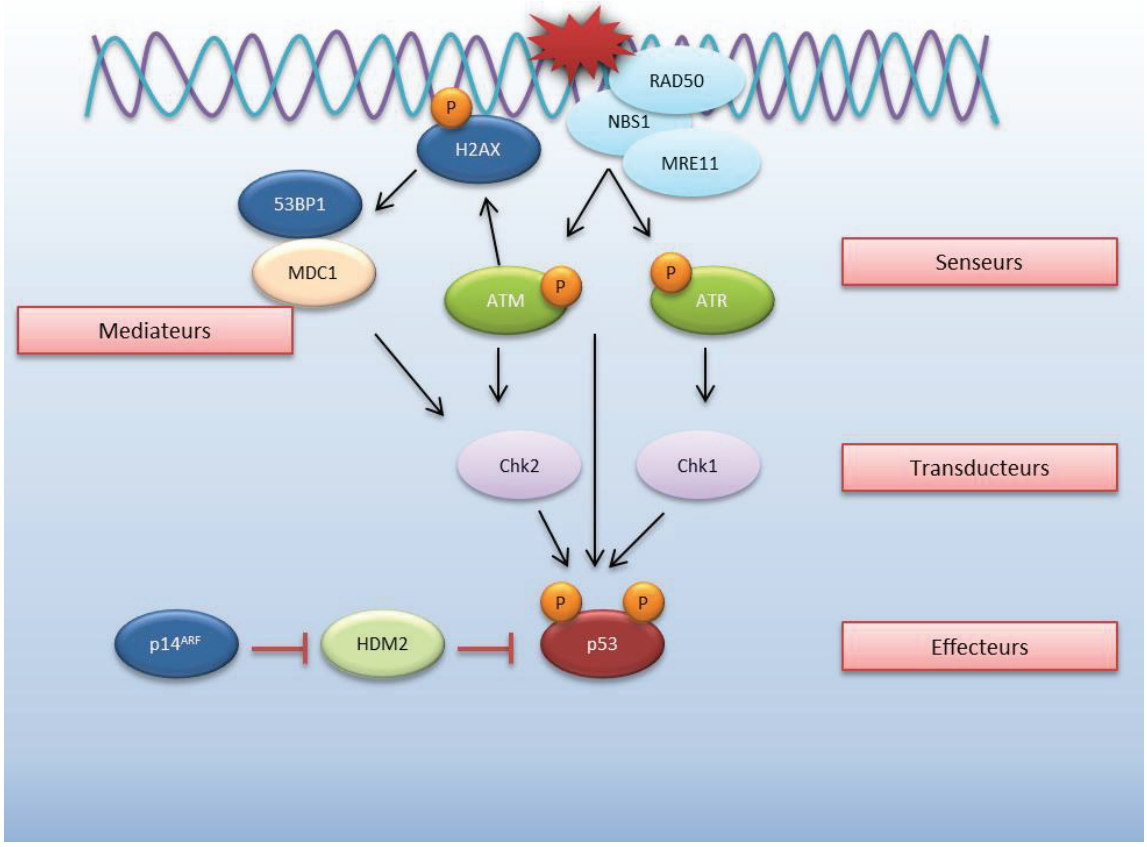

Figure 3 : Voie de signalisation d'une réponse aux dommages à l'ADN

Les cassures double-brins sont reconnues par le complexe MRN (MRE11-RAD50-NBS1) et aboutissent à la phosphorylation et l'activation d'ATM. Cela permet la phosphorylation de H2AX qui entraine le recrutement de médiateurs, et permet ainsi d'amplifier le signal. L'activation d'ATM et ATR permet la phosphorylation des transducteurs Chk1 et Chk2, et de l'effecteur p53.

53BP1 : p53-binding protein ; MDC1, mediator of DNA damage checkpoint 1 ; P : Phosphate

Adapté de (Meek, 2009)

1.3 Les voies de signalisation canoniques de la sénescence

Les deux voies de signalisation de p53 et de Rb sont largement décrites dans la littérature comme étant primordiales dans la mise en place de la sénescence. Ces deux voies interagissent entres elles, mais peuvent également stopper le cycle cellulaire de manière indépendante, selon le type cellulaire.

1.3.1 La voie p53 dans la sénescence

1.3.1.1 Les dommages à l'ADN et p53

P53, autrement appelé « gardien du génome », est le suppresseur de tumeur le mieux décrit, et le plus étudié, notamment à cause de son importance dans les cancers sporadiques. En effet, près de la moitié des cancers ont des mutations dans ce gène (Levine, 1997). En réponse à différents stress, la protéine p53 est stabilisée et active alors la transcription de ses gènes cibles, impliqués notamment dans l'arrêt du cycle transitoire nécessaire à la réparation des dommages à l'ADN. Cependant, s'i ces derniers sont trop nombreux ou irréparables la cellule engage un processus d'apoptose ou de sénescence, selon le contexte cellulaire.

Pendant la sénescence, une réponse de dommages à l'ADN est initiée par le recrutement au niveau des cassures de l'ADN des protéines nécessaires à la reconnaissance, la signalisation et la réparation des cassures double-brin. Les protéines impliquées dans ce processus, comme ATM, ATR, Chk1 et Chk2 activent directement p53 par phosphorylation ce qui engendre la transcription du CKI $p21^{Cip1}$ *(Figure 3)*. Ce dernier interagit préférentiellement avec CDK2 bloquant la formation du complexe cyclineE-CDK2 (Harper *et al.*, 1993) et entrainant l'arrêt du cycle cellulaire en G1-S. $P21^{Cip1}$ est également connu pour interagir avec la voie Rb en inhibant le facteur de transcription E2F, faisant de lui un acteur essentiel dans l'arrêt du cycle cellulaire.

L'importance des DDR dans la sénescence a été révélée expérimentalement par l'inhibition de p53, $p21^{Cip1}$ ou de différentes protéines des voies ATM/ATR. L'absence d'un de ces acteurs fait disparaitre l'arrêt de prolifération normalement observé lors de la sénescence (Herbig *et al.*, 2004; Brown, 1997; d'Adda di Fagagna *et al.*, 2003; Gire *et al.*, 2004; Di Micco *et al.*, 2006).

Bien que les DDR soient une voie de signalisation qui parait importante dans l'établissement de l'arrêt du cycle cellulaire, certaines études montrent que l'OIS peut être induite sans activation de DDR (Efeyan *et al.*, 2009; Alimonti *et al.*, 2010) et sans l'implication de p53. Ce sujet sera plus amplement discuté dans le chapitre II de cette introduction.

1.3.1.2 $p14^{ARF}$ et p53

$P14^{ARF}$ (ARF, *Alternative Reading Frame*, $p19^{ARF}$ chez la souris) est une protéine capable d'interagir avec la ligase HDM2 (MDM2 chez la souris) et de lever l'inhibition de p53 sur cette dernière (Weber *et al.*, 1999; Kamijo *et al.*, 1998) *(figure 4)*. HDM2 interfère avec la capacité de p53 à transactiver ses gènes cibles, et le délocalise dans le cytoplasme où la protéine est dégradée (Haupt *et al.*, 1997). $P14^{ARF}$ est codée pour sa plus grande partie par le même gène que $p16^{INK4A}$, mais sa traduction ne suit pas le même cadre de lecture. Des souris qui n'expriment pas $p19^{ARF}$ développent plus de tumeurs, suggérant que $p14^{ARF}$ est un suppresseur de tumeurs, tout comme $p16^{INK4A}$ (Serrano *et al.*, 1996). La voie $p19^{ARF}$-p53 est une des voies principales, mais non exclusive, pour induire la sénescence chez la souris (Lowe and Sherr, 2003; Sharpless, 2005). L'importance de cette voie chez l'humain est toutefois loin d'être aussi claire (Kamijo *et al.*, 1997; Wei *et al.*, 2001; Dimri *et al.*, 2000). Dans des MEFs, l'activation de Ras peut induire $p14^{ARF}$ mais cela ne semble pas être le cas dans les cellules humaines (Gil and Peters, 2006; Brookes *et al.*, 2002; Wei *et al.*, 2001).

1.3.2 La voie $p16^{INK4A}$/Rb dans la sénescence

Un autre CKI important dans la sénescence est $p16^{INK4a}$ (Stein *et al.*, 1999; Itahana *et al.*, 2003). Ce suppresseur de tumeur, ainsi que $p15^{INKB}$ et $p14^{ARF}$, sont codés par le locus INK4B/ARF/INK4A. Il a été montré que $p16^{INK4A}$ peut être inactivé dans les cancers par délétion, mutation, ou méthylation de son promoteur. Toutefois, l'inactivation seule de $p16^{INk4A}$ n'est pas suffisante pour induire de la tumorigénèse.

$p16^{INK4A}$, par sa spécificité d'interaction avec les complexes cycline-CDK4/6, permet un enrichissement de Rb sous une forme hypophosphorylée, favorisant ainsi la formation du complexe répresseur Rb-E2F (Lukas *et al.*, 1995) *(figure 4)*, aboutissant à la répression des gènes cibles de E2F impliqués dans la progression du cycle cellulaire (Ohtani *et al.*, 1995) L'expression de $p16^{INK4A}$, contrairement à $p21^{cip1}$, n'est pas régulée par p53, mais par la voie Ras-Raf-Mek dans les fibroblastes humains et murins (Lin *et al.*, 1998; Serrano *et al.*, 1997) ainsi que dans les mélanocytes humains et murins.

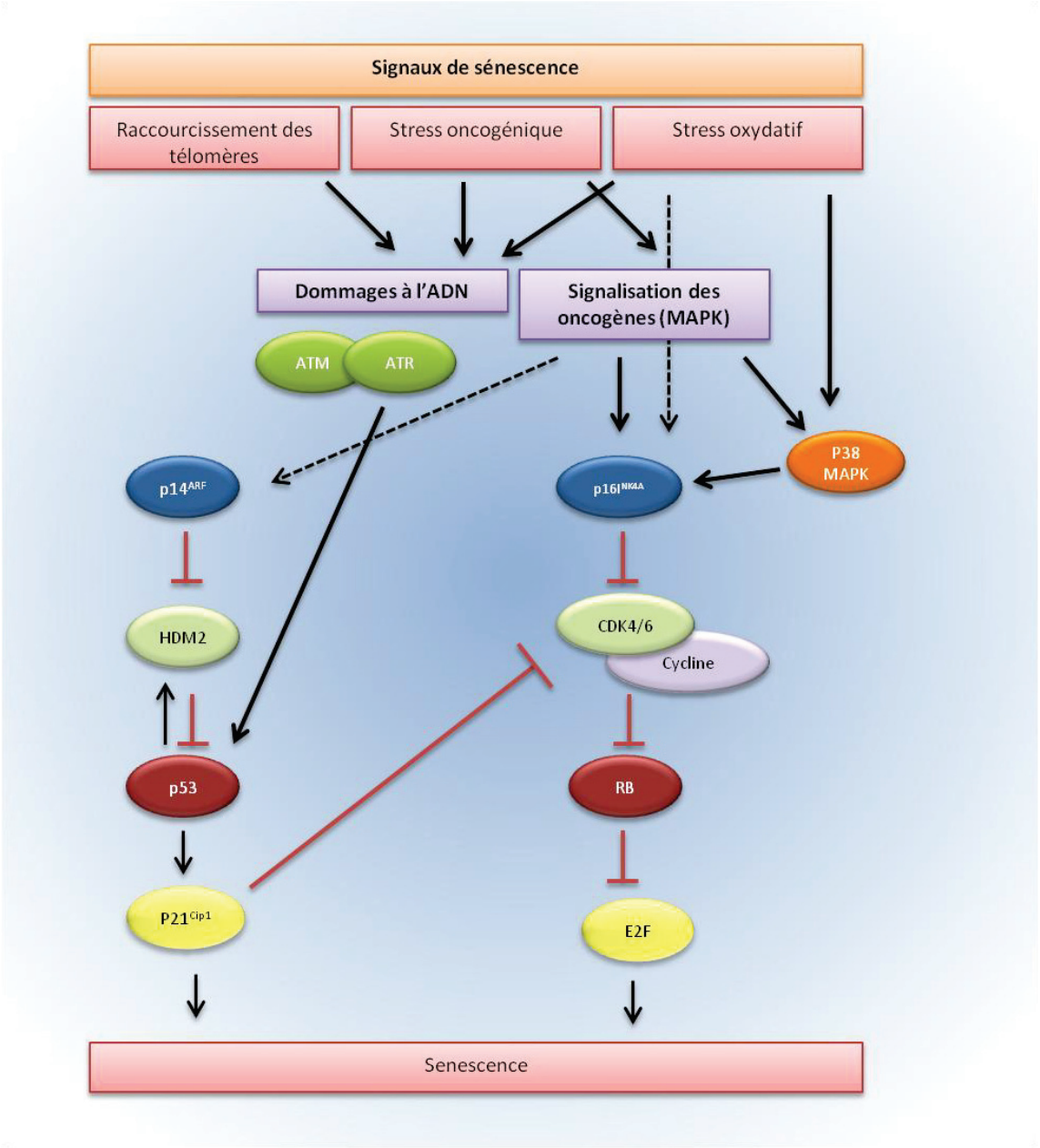

Figure 4 : Les voies de signalisation de la sénescence

Différents stress comme le stress oncogénique ou l'attrition des télomères peut induire une réponse de dommages à l'ADN via la voie ATM/ATR et activer p53. P53 peut aussi être activé par $p14^{ARF}$ qui inactive l'ubiquitine ligase HDM2, empêchant ainsi sa dégradation. HDM2, qui fait partie des gènes cible de p53, peut aussi directement se lier à p53 et inhiber sa fonction transcriptionnelle. La stabilisation et l'accumulation de p53 permet l'activation de gènes cibles comme p21Cip1.

L'activation d'un oncogène fait intervenir la voie $p16^{INK4A}$/Rb.

$P16^{INK4A}$ inhibe les complexes cycline-CDK4/6, empêchant la phosphorylation de pRb, qui peut alors lier et inhiber E2F.

La régulation transcriptionnelle de p16^{INK4A} fait intervenir le facteur de transcription Ets2, lui-même activé par phosphorylation via ERK et p38MAPKinase, en réponse à une activation de Ras. A l'inverse, la transcription de p16^{INK4A} est réprimée par les complexes polycombes (PRC) (Jacobs *et al.*, 1999; Gil *et al.*, 2004). Après l'entrée en sénescence, l'expression de p21^{cip1} diminue rapidement (Stein *et al.*, 1999), mais l'arrêt de prolifération est maintenu par celle de p16^{INK4A} (Serrano *et al.*, 1993).

1.3.3 Acteurs clés de la stabilité de la sénescence

Pendant la sénescence cellulaire, les activités de la famille Rb et de p53 augmentent drastiquement. L'inactivation d'une de ces deux protéines dans des MEFs sénescents permet la réversion du phénotype et la reprise de la division cellulaire (Sage *et al.*, 2003; Dirac and Bernards, 2003; Sage, 2000; Dannenberg, 2000). Ces données suggèrent que Rb et p53 sont nécessaires non seulement à l'induction de la sénescence dans les cellules murines mais aussi à sa stabilité.

Il a été décrit dans les cellules humaines, une fois la voie Rb pleinement engagée notamment par l'expression de p16^{INK4A}, que l'arrêt de prolifération devient irréversible et n'est plus abrogé par l'inactivation de Rb et p53 (Dai and Enders, 2000; Sharpless and DePinho, 2005). En contradiction avec ces résultats, il a été rapporté que l'inactivation de p53 est suffisante pour rendre la sénescence réplicative de fibroblastes BJ réversible, mais pas celle de Wi-38. Et l'inactivation de p53 et Rb dans les Wi-38 ne leur permet pas de reprendre leur prolifération. Les niveaux de p16^{INK4A} semblent être impliqués dans ces différences, puisque les BJ sont connus pour exprimer faiblement p16^{INK4A} contrairement aux Wi-38. (Beauséjour *et al.*, 2003). De même, l'inactivation de la sécrétion de certaines interleukines du SASP engendre une réversibilité de la sénescence (Kuilman *et al.*, 2008). L'inactivation de certains CKI permet également de réverser en partie l'OIS induite par Raf dans des Wi-38 (Jeanblanc *et al.*, 2012)

Les mécanismes permettant d'expliquer l'arrêt de prolifération irréversible, ou non, des cellules sénescentes restent largement méconnus, et de nombreux éléments, allant du contexte cellulaire, au micro-environnement sont à prendre en compte. La stabilité de la sénescence, mécanisme s'opposant essentiellement au développement tumoral semble déterminante dans l'évolution de la lésion bénigne.

1.4 Rôles de la sénescence dans différentes réponses physiopathologiques

La caractéristique première de la sénescence est l'arrêt de prolifération stable. Celui-ci a longtemps été considéré comme étant l'élément clé dans l'implication de la sénescence dans les différents processus physio-pathologiques. Toutefois, l'étude du SASP a révélé son implication dans tous ces processus, suggérant que la sénescence est un programme cellulaire ne se limitant pas à un arrêt de prolifération. Dans les sections suivantes, les différents contextes physiologiques associés à la sénescence seront développés. Nous verrons alors que les cellules sénescentes peuvent favoriser le développement de nombreuses maladies, cancer et autres pathologies liées à l'âge.

1.4.1 La sénescence est impliquée dans le vieillissement

Le vieillissement est défini par une altération de fonctions biologiques, aboutissant au développement de pathologies liées à l'âge et à la mort (Kirkwood and Austad, 2000). Hayflick avait énoncé très tôt l'hypothèse selon laquelle la sénescence cellulaire pouvait être reliée au vieillissement des organismes (Hayflick and Moorhead, 1961). On peut en effet observer une accumulation de cellules sénescentes avec l'âge (Dimri *et al.*, 1995; Ressler *et al.*, 2006). De nombreuses pathologies chroniques liées au vieillissement sont aussi marquées par un enrichissement en cellules sénescentes, comme la bronchopneumopathie chronique obstructive (Zhou *et al.*, 2011; Bartling, 2013) ou l'hypertension pulmonaire (Noureddine *et al.*, 2011). Dans un modèle murin où l'activité du suppresseur de tumeur p53 est accrue, les souris présentent des tissus enrichis en cellules sénescentes et montrent de nombreux signes de vieillissement prématuré (Tyner *et al.*, 2002; Maier *et al.*, 2004). A l'inverse, l'élimination des cellules sénescentes dans un modèle murin diminue la présence de maladies liées à l'âge mais ne modifient pas pour autant la durée de vie de ces souris (Baker *et al.*, 2011 b).

Fonctionnellement, il a été proposé que la sénescence, en limitant le potentiel réplicatif des cellules, pourrait diminuer le nombre de cellules progénitrices compromettant la régénération des tissus (Liu *et al.*, 2007). En outre, une inflammation chronique est une marque caractéristique du vieillissement, qui peut contribuer à de nombreuses maladies liées à l'âge (Franceschi, 2007; Chung *et al.*, 2009; Brennan *et al.*, 1995; Brod, 2000). Le SASP, contenant de nombreuses cytokines pro-inflammatoires, secrété par les cellules sénescentes accumulées dans un organisme vieillissant peut être à l'origine de cette inflammation chronique (Rodier and Campisi, 2011). La corrélation entre sénescence, inflammation et vieillissement suggère un rôle de la sénescence cellulaire dans le vieillissement des organismes.

Le cancer, comme les pathologies dégénératives, est une maladie liée à l'âge, où les fonctions des tissus sont altérées (Balducci and Ershler, 2005). L'accumulation de cellules sénescentes dans les tissus âgés peut avoir des effets délétères. Les facteurs du SASP notamment sont connus pour favoriser le processus de transformation (Davalos *et al.*, 2010). Les cytokines pro-inflammatoires, quand elles sont présentes de manière chronique, peuvent engendrer des effets pro-oncogéniques comme l'invasion, la migration, et la prolifération des cellules pré-malignes (Coppé *et al.*, 2008; Krtolica *et al.*, 2001; Bavik *et al.*, 2006; Coppé *et al.*, 2010 b, 2006; Ksiazek *et al.*, 2008; Millis *et al.*, 1992; Kang *et al.*, 2003; Coppé *et al.*, 2010 a; Laberge *et al.*, 2011; Parrinello *et al.*, 2005). Les effets pro-tumoraux du SASP sont soulignés par le fait que les cellules ayant échappé à la sénescence par inactivation d'acteurs clé maintiennent ce phénotype sécrétoire. Les cytokines perdent leur effet sur le maintien et le renforcement de la sénescence car les voies de signalisation en aval sont inactivées, mais leur effet pro-tumoral perdure, favorisant ainsi la prolifération des cellules (Coppé *et al.*, 2008; Rodier *et al.*, 2009).

In vivo, plusieurs études utilisant des xénogreffes ont montré que les cellules sénescentes peuvent promouvoir la progression tumorale de lésions cancéreuses et pré-cancéreuses (Krtolica *et al.*, 2001; Liu and Hornsby, 2007; Bartholomew *et al.*, 2009; Coppé *et al.*, 2010 b; Bhatia *et al.*, 2008). Ces expériences soulignent l'importance du stroma tumoral, et des fibroblastes sénescents dans la progression tumorale. L'utilisation de souris transgéniques ayant un système immunitaire fonctionnel a confirmé l'implication directe du SASP et de l'inflammation sur les processus de croissance et d'invasion cellulaire (Pribluda *et al.*, 2013; Yoshimoto *et al.*, 2013).

Les effets délétères de la sénescence proviennent finalement majoritairement de la sécrétion chronique des facteurs du SASP par les cellules sénescentes accumulées dans les organismes vieillissants. Cette accumulation avec l'âge des cellules sénescentes peut être due à une augmentation de la production de celles-ci et/ou à une diminution de leur élimination, potentiellement suite à une réponse immunitaire affaiblie. Cette sénescence chronique s'oppose à la sénescence « aigue », réponse biologique contrôlée mise en place en réponse à des processus précis, tels que la réparation tissulaire, le développement *(figure 5)*.

1.4.2 La sénescence participe à la réparation de tissus

Les effets du SASP semblent être beaucoup plus larges que ce qui a été initialement envisagé. Le SASP, par sa composition, pourrait être impliqué dans la réparation de tissus : les facteurs de croissance et les protéases pour la réparation, les facteurs qui recrutent les cellules du système immunitaire pour éliminer les pathogènes et les protéines qui mobilisent les cellules souches forment un ensemble tout à fait adapté à la réparation de tissus. Il a d'ailleurs été montré que des

facteurs de la matrice extra-cellulaire (MMPs, CCN1) sécrétés par les cellules sénescentes lors de la cicatrisation favorisent la réparation de tissus hépatiques ou cutanés et limitent l'apparition de fibroses (Krizhanovsky *et al.*, 2008; Jun and Lau, 2010).

1.4.3 La sénescence dans le développement

La sénescence a largement été considérée comme une réponse à divers stress dans les tissus adultes. En novembre 2013, deux études ont montré un nouveau rôle de la sénescence dans le développement embryologique de la souris. Cette sénescence est caractérisée notamment par un arrêt de prolifération, une augmentation de l'activité SA-β-galactosidase, et du CKI $p15^{INKB}$ ainsi que l'apparition d'un SASP (Muñoz-Espín *et al.*, 2013; Storer *et al.*, 2013).

1.5 La sénescence est un mécanisme anti-tumoral

Comme décrit précédemment, la sénescence chronique pourrait favoriser le développement tumoral. Néanmoins, la sénescence reste principalement considérée comme une réponse s'y opposant en empêchant la prolifération de cellules tumorales ou en cours de transformation. De plus, de nombreux stress favorisant l'initiation et la progression tumorale déclenchent la sénescence : stress oxydant, instabilité génomique (dommages à l'ADN) et surtout l'activation oncogénique.

1.5.1 Sénescence réplicative, barrière à la progression tumorale

Alors que les cellules tumorales sont immortelles, les cellules primaires somatiques ont un potentiel de réplication limité par la sénescence réplicative. Les cellules tumorales, durant leur processus de transformation, contournent cette limite de réplication. En effet, comme cela a été mentionné auparavant, les tumeurs humaines adoptent des programmes pour maintenir leurs télomères. De manière intéressante, l'inhibition de l'activité télomérase *in vitro* dans les cellules tumorales limite leur croissance, et induit l'apoptose (Hahn *et al.*, 1999; Zhang *et al.*, 1999; Zumstein and Lundblad, 1999). La génération de souris TERC$^{-/-}$ (*Telomerase RNA Component*) a montré que des télomères dysfonctionnels limitent l'initiation et la progression tumorale (Deng *et al.*, 2008). Toutefois, la réponse exacte d'un dysfonctionnement des télomères sur la progression tumorale était compliquée à identifier puisque les modèles murins utilisés exprimaient un p53 fonctionnel capable d'induire à la fois l'apoptose et la sénescence (Deng *et al.*, 2008). Des modèles de souris présentant un dysfonctionnement des télomères (souris TERC$^{-/-}$), associé à une inhibition de l'apoptose induite par p53, montrent que les dysfonctionnements des télomères peuvent inhiber la formation de tumeurs sans induction d'apoptose. La suppression tumorale s'avère être dépendante de l'induction de la sénescence réplicative dépendante de p53-p21^{Cip1} (Feldser and Greider, 2007; Cosme-Blanco *et al.*, 2007).

1.5.2 La sénescence induite par un stress oncogénique, barrière à la progression tumorale

Etant donné que les premières études effectuées *in vitro* sur l'OIS utilisaient des surexpressions de H-ras^{V12G}, la communauté scientifique a longtemps été partagée sur la pertinence de ces études et sur le rôle physiologique de l'OIS *in vivo*. En 2005, plusieurs études ont montré que, contrairement aux lésions malignes, les lésions pré-néoplasiques sont riches en cellules sénescentes (Chen *et al.*, 2005 b; Michaloglou *et al.*, 2005; Collado *et al.*, 2005; Braig *et al.*, 2005) apportant ainsi les premières preuves que l'OIS peut avoir un rôle anti-tumoral *in vivo*. De manière intéressante, ces expériences ont été conduites dans différents types de tumeurs : lymphomes, mélanomes,

adénocarcinomes de la prostate et des poumons. L'activation oncogénique associée à l'absence de régulateurs de la sénescence tels que p53 ou SUV39H1 conduit au développement de tumeurs agressives. Cette absence de sénescence dans ces tumeurs démontre ainsi le rôle fonctionnel de l'OIS en tant que barrière physiologique au développement tumoral (Chen *et al.*, 2005 b; Braig *et al.*, 2005). D'autres études sont venues compléter ces informations (Dankort *et al.*, 2007; Bennecke *et al.*, 2010; Dhomen *et al.*, 2009). Cela suggère que l'inactivation de la sénescence par des mutations peut contrecarrer les effets de l'OIS favorisant ainsi le développement tumoral. De plus, dans les tumeurs qui ont contourné la sénescence pour se développer, différents suppresseurs de tumeurs sont inactivés (Chen *et al.*, 2005 b; Collado *et al.*, 2005; Lazzerini Denchi *et al.*, 2005; Acosta *et al.*, 2008). Ces observations soulignent qu'il est nécessaire d'inactiver les voies qui régulent la sénescence pour permettre le développement tumoral mettant ainsi en avant le rôle anti-tumoral de l'OIS.

L'accumulation de cellules sénescentes dans les lésions bénignes n'a pas seulement été démontrée dans les modèles murins. En effet, l'équipe de Daniel Peeper a montré que les naevi humains, exprimant B-Raf^{V600E} sont riches en cellules sénescentes (Michaloglou *et al.*, 2005). De même, l'analyse de PIN humains a révélé la présence de cellules sénescentes (Chen *et al.*, 2005 b; Acosta *et al.*, 2008). De nombreuses autres études ont montré dans des tissus humains que la sénescence cellulaire est associée aux étapes précoces du développement tumoral, mais est perdue dans les étapes tardives (Bartkova *et al.*, 2006; Courtois-Cox *et al.*, 2006; Kuilman *et al.*, 2008; Acosta *et al.*, 2013; Fujita *et al.*, 2009).

Les analyses du SASP ont également apporté des preuves que la sénescence est un processus anti-tumoral. Les chimiokines, les interleukines, ou PAI-1 (*Plasminogen Activator Inhibitor 1*) peuvent renforcer la sénescence *in vivo* (Acosta *et al.*, 2008; Kuilman *et al.*, 2008; Kortlever *et al.*, 2006). Par exemple, il a été montré que le récepteur à l'IL-8 et GROα, CXCR2, est surexprimé dans des lésions bénignes de type PIN ou dans des papillomes induits par un traitement DMBA-TPA. De plus des niveaux faibles de CXCR2 ou de ses ligands ont été rapportés dans les stades malins de cancers (Ginos, 2004; Toruner *et al.*, 2004). De manière intéressante, une mutation inactivatrice de CXCR2 atténue l'OIS de cellules d'adénocarcinomes du poumon, soulignant le rôle du SASP dans la sénescence *in vivo* (Acosta *et al.*, 2008).

En 2007, deux études originales utilisant des modèles murins dans lesquels p53 peut être activé ou inactivé ont évalué l'effet de la réactivation de p53 dans différents types de tumeurs (Xue *et al.*, 2007; Ventura *et al.*, 2007). L'absence de p53 a permis le développement de lymphomes, sarcomes ou encore de carcinomes du foie qui ont spontanément régressé après la réactivation de

p53. Il est à noter que dans le cas des lymphomes cette régression est associée à une induction de l'apoptose et dans le cas des sarcomes et carcinomes à une forte réponse de type sénescence. L'équipe de Scott Lowe a montré que l'induction de la sénescence et des cytokines inflammatoires est associée à un recrutement du système immunitaire inné (neutrophiles, macrophages, et cellules Natural Killer (NK)), conduisant à l'élimination des cellules sénescentes. Dans ces modèles la réexpression de p53 induit une réponse seulement dans les cellules tumorales. Ces données suggèrent que la restauration de p53 dans les tumeurs pourrait être un moyen efficace de limiter la croissance tumorale. Une nouvelle fois, le SASP joue un rôle important dans le devenir des cellules sénescentes. Ces facteurs inflammatoires sécrétés par les cellules sénescentes peuvent recruter le système immunitaire, afin d'éliminer les tumeurs lors des thérapies pro-sénescence, mais peuvent également initier une surveillance immunitaire adaptative (impliquant des macrophages, et des lymphocytes T $CD4^+$) des cellules sénescentes pré-malignes. En effet, l'élimination de cellules pré-malignes sénescentes est nécessaire pour empêcher leur évolution en carcinome (Kang *et al.*, 2011).

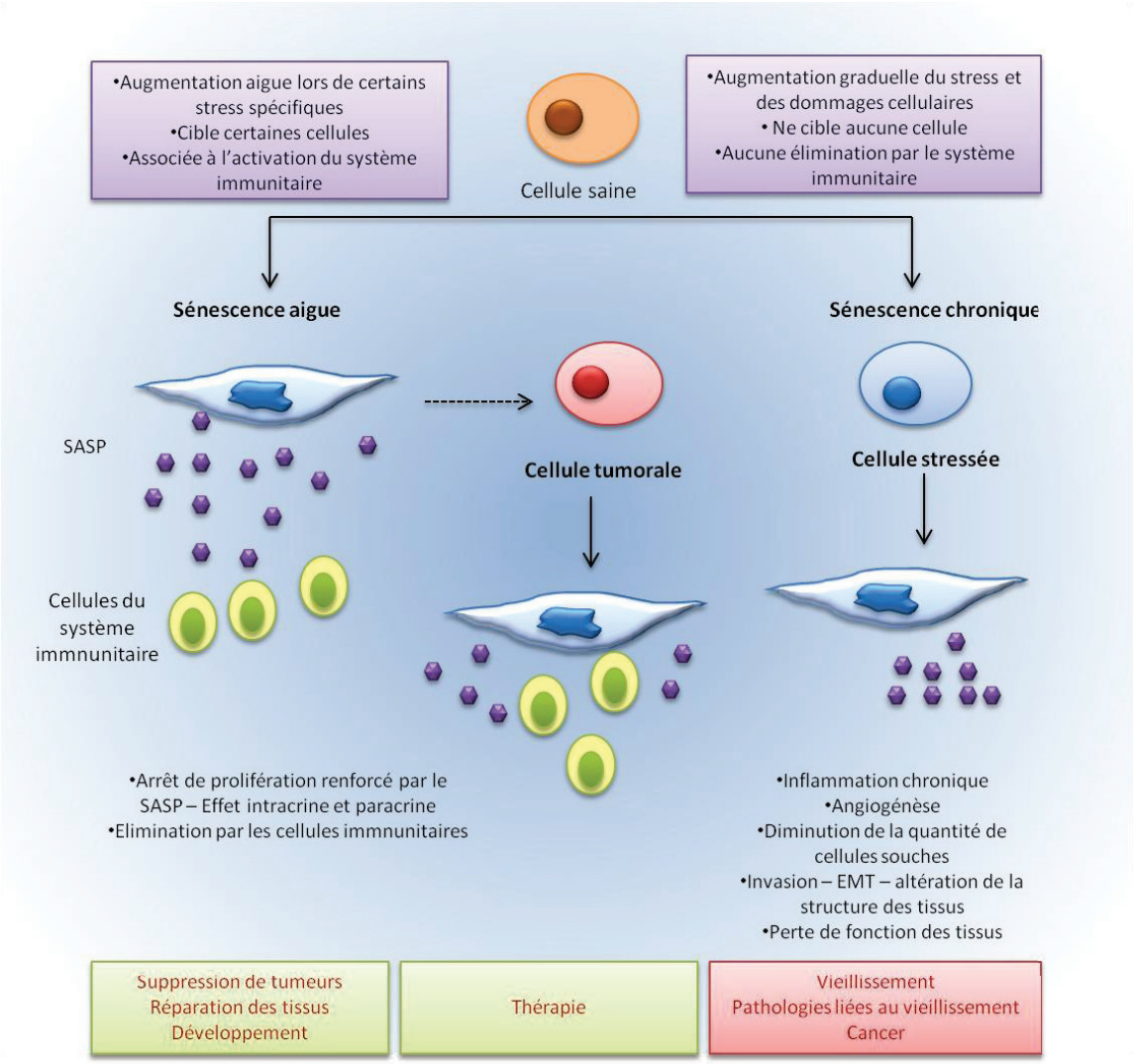

Figure 5 : Rôles de la sénescence

La sénescence aigue est un processus contrôlé mis en place lors du développement, de la réparation des tissus, ou lors de l'OIS, permettant l'arrêt de prolifération de certaines cellules, et la sécrétion d'un SASP ayant des fonctions autocrines et paracrines. Dans ce cas, la sénescence est associée à un recrutement du système immunitaire permettant l'élimination des cellules sénescentes.

Une sénescence chronique se met en place suite à des dommages cellulaires progressifs. Cette sénescence ne semble pas cibler des cellules spécifiques, et n'est pas associée à une élimination par le système immunitaire, potentiellement parce que celui-ci est déficient. Le SASP, dans ces conditions peut engendrer une inflammation chronique, induire l'angiogénèse, ou l'EMT. Cette sénescence chronique contribue à une perte de régénération des cellules, et une perte de fonction des tissus.

La sénescence peut également être induite ou ré-induite dans les cellules tumorales.

Adapté de (van Deursen, 2014)

1.5.3 Sénescence induite par la thérapie (TIS)

De manière insoupçonnée, la réponse aux agents habituels de chimiothérapies ou à la radiation qui causent des dommages à l'ADN dans les cellules qui se divisent, et donc principalement dans les cellules cancéreuses, est souvent accompagnée d'une induction de sénescence (Gewirtz *et al.*, 2008; Poele *et al.*, 2002). Cette sénescence induite par la thérapie (*Therapy-Induced Senescence*) repose en partie sur la réactivation des voies $p16^{INK4A}$ ou p53. En effet, des modèles génétiques où l'une de ces deux voies est inactivée montrent des résistances aux traitements (Chang *et al.*, 2002; Roberson *et al.*, 2005; Chang *et al.*, 1999).

D'autres approches émergent pour induire la sénescence, autrement que via les drogues chimiothérapeutiques. En activant p53, ou modulant des activateurs du cycle cellulaire, il est possible d'induire de la sénescence dans les tumeurs (Nardella *et al.*, 2011). Une autre manière d'induire de la sénescence dans les tumeurs serait d'exploiter l'addiction aux oncogènes dont font preuve la plupart des tumeurs *(voir paragraphe 1.2.3 Sénescence Induite par invalidation d'un oncogène)*. L'inhibition de la transcription de *c-MYC* dans un modèle de myélome multiple a pu induire un arrêt du cycle des cellules tumorales, ainsi que de la sénescence (Delmore *et al.*, 2011). Toutefois, le défi dans cette approche est d'élaborer des inhibiteurs exploitables en clinique et de s'assurer que le système immunitaire est fonctionnel afin d'éliminer des cellules nouvellement sénescentes et d'éviter leur présence chronique qui peut avoir des effets délétères.

Chapitre II : L'OIS dans les cellules épithéliales

Dans le chapitre précédent, j'ai décrit les caractéristiques générales de la sénescence. Or, que ce soit pour l'étude de la sénescence réplicative ou celle de l'OIS, les modèles cellulaires très largement utilisés *in vitro* sont les fibroblastes. Les mécanismes identifiés dans ces modèles ont souvent été extrapolés aux cellules épithéliales et aux carcinomes. Comme cela a été décrit précédemment, l'OIS constitue une barrière importante au développement tumoral, y compris dans les carcinomes. Pour autant, peu de données sur l'OIS ont été obtenues dans des modèles épithéliaux. Comme nous allons le voir par la suite, les mécanismes survenant dans les cellules épithéliales lors de l'OIS peuvent être en partie différents de ceux survenant dans les fibroblastes.

2.1 Rôle controversé de p53 dans l'OIS

L'implication de p53, principalement via la réponse aux dommages à l'ADN a été clairement démontrée dans l'établissement et le maintien de la sénescence dans les fibroblastes humains. De nombreuses études ont ainsi montré que la déplétion de p53, seule ou associée à l'inactivation de la voie Rb, permet aux fibroblastes exprimant H-Ras de reprendre leur prolifération (Gorgoulis and Halazonetis, 2010; Bartkova *et al.*, 2006; Serrano *et al.*, 1997; Di Micco *et al.*, 2006). Cette dépendance à p53 a été largement généralisée, et apparaît souvent comme nécessaire.

Toutefois, l'activation de p53 par la nutlin-3, ou la surexpression de p53 dans des cellules dérivées de fibrosarcomes (HT1080), induit une conversion de la sénescence induite par une surexpression de $p21^{Cip1}$ en quiescence, via l'inhibition de mTOR (*Mammalian Target Of Rapamycin*). La suppression de la sénescence par p53 a également été confirmée dans des WI38-tert traités avec de l'H_2O_2 (Demidenko *et al.*, 2010). A l'inverse, l'activation de la voie mTOR, utilisant un shRNA ciblant l'expression de son régulateur négatif TSC2, empêche p53 d'induire la conversion sénescence/quiescence (Korotchkina *et al.*, 2010; Schug, 2010). Ces données mettent en évidence l'implication de la voie mTOR dans l'établissement de la sénescence, et révèlent des nouveaux mécanismes jusque là inconnus.

De plus, l'étude de l'OIS dans des modèles épithéliaux a révélé que p53 n'est pas obligatoirement impliqué. Par exemple, en utilisant des kératinocytes primaires, ou immortalisés (cellules EPC2) Takaoka et ses collègues ont montré que $H\text{-}Ras^{G12V}$ induit de la sénescence dans ces cellules, sans aucune induction de p53. Aussi, l'expression ectopique d'un mutant de p53 dominant

négatif n'a aucune influence sur la réponse de sénescence montrant que dans ce modèle de kératinocytes, p53 n'est pas nécessaire à la mise en place de la sénescence (Takaoka *et al.*, 2004).

Dans un autre modèle cellulaire, les mélanocytes, p53 et $p16^{INK4A}$ ne semblent pas non plus indispensables aux cellules pour la mise en place de l'OIS. La déplétion de *c-MYC*, dans les cellules de mélanomes induit de la sénescence. L'inhibition de p53 et de $p16^{INK4A}$ par shRNA dans ces lignées cellulaires de mélanomes n'a aucune incidence sur la sénescence induite par $B\text{-}Raf^{V600E}$ ou $N\text{-}Ras^{Q61R}$. Surtout, ces observations ont été confirmées dans un modèle de mélanocytes humains normaux (Zhuang *et al.*, 2008). Toujours dans les mélanocytes primaires humains, $H\text{-}Ras^{G12V}$ induit une sénescence indépendante de p53 et de $p16^{INK4A}$. L'OIS induite dans ces cellules pourrait être dépendante d'une activation d'une réponse au stress du réticulum endoplasmique, associée à une accumulation de protéines mal conformées dans cet organite aboutissant à une réponse de type UPR *(Unfolded Protein Response*). De manière surprenante, l'OIS induite par $B\text{-}Raf^{V600E}$ dans les mêmes cellules n'engage pas une réponse de type UPR, soulignant l'importance du contexte génétique, et de l'oncogène (Denoyelle *et al.*, 2006). Aussi, l'inhibition pharmacologique des dommages à l'ADN (développé dans le point suivant) ou l'extinction de p53 par shRNA n'a aucun impact sur la sénescence des mélanocytes induite par $N\text{-}Ras^{Q61K}$ (Haferkamp *et al.*, 2009 b). Enfin, l'OIS dans les mélanocytes murins ou les cellules épithéliales mammaires humaines n'est pas non plus toujours dépendante de p53 (Ha *et al.*, 2007; Cipriano *et al.*, 2011).

Ces différentes études mettent en avant le fait que les mécanismes sous-jacents de l'OIS sont très différents entre les fibroblastes d'une part et les mélanocytes et les cellules épithéliales d'autre part. A la suite de ces observations, il est facilement envisageable de penser que ces mécanismes peuvent également être différents dans d'autres types cellulaires et sont loin d'être exclusifs.

2.2 Implication relative des DDR

L'activation de la voie des DDR semblait être la cause majeure de l'OIS. Deux voies peuvent intervenir soit par l'hyper réplication induite par l'activation d'un oncogène, engendrant des cassures simples et doubles brins (au niveau de la fourche de réplication), ou via l'induction de cassures simple et double brins à cause des ROS générés par l'oncogène. En effet, la déplétion de ATM associée à l'inactivation de la voie Rb, ou de Chk2, entre autres, est associée à une résistance à la sénescence induite par Ras^{G12V} démontrant le rôle de l'activation d'une réponse aux dommages à l'ADN pour l'établissement de l'OIS (Mallette *et al.*, 2007; Di Micco *et al.*, 2006).

	cellules humaines				cellules murines
	fibroblastes IMR90	fibroblastes BJ	mélanocytes	cellules épithéliales	MEFs
	voie p53				
ATM	Requis/non requis	requis	non requis	non requis	non requis
Chk2	non étudié	requis	non requis	non requis	non requis
p53	partiellement requis/ non requis	partiellement requis/ requis	requis	non requis	requis
$p14^{ARF}$	non requis	non requis	non requis	non requis	requis
$p21^{cip1}$	non requis	non étudié	non requis	Requis/ non requis	non requis
voie pRb					
Rb	partiellement requis/ non requis	partiellement requis/ non requis	partiellement requis		non requis
$p16^{INK4A}$	partiellement requis/ non requis	partiellement requis/ non requis	requis/non requis	non requis	requis/non requis
indépendant de p53 et pRb					
	IL-6	non étudié	IGFBP7 stress du RE	TGFβ	non étudié

Tableau 2 voies de signalisation impliquées dans la sénescence des fibroblastes et des cellules épithéliales

Implication des différentes voies dans l'induction de la sénéscence dans des fibroblastes murins (MEFs), ou des fibroblastes mélanocytes humains ou cellules épithéliales humaines. Adapté de (Haferkamp *et al.*, 2009 b)

Toutefois, l'inhibition par la caféine de l'activité des kinases ATM et ATR, résultant en une diminution de la phosphorylation de Chk2 et p53, n'a aucun impact perceptible sur l'entrée en sénescence des mélanocytes (Haferkamp *et al.*, 2009 b). De même, l'équipe de Pandolfi a montré que l'inactivation de PTEN dans un modèle de cancer de la prostate induit de la sénescence, appelée PICS (Chen *et al.*, 2005 b). La caractérisation de cette sénescence a révélé que celle-ci se produit en l'absence de dommages à l'ADN car aucune phosphorylation de ATM, de p53, de Chk1 ou de Chk2 n'est observée (Alimonti *et al.*, 2010). Cipriano et ses collègues ont également remis en question les observations habituellement faites dans les fibroblastes. Ils ont étudié l'OIS dans des cellules épithéliales mammaires humaines, et ont observé que Ras est capable d'induire un arrêt de prolifération de manière indépendante de p53 et de $p16^{INK4A}$, mais aussi des dommages à l'ADN. En effet, l'inhibition génétique (par shRNA) de ATM ou de Chk2 n'a aucun impact sur la sénescence induite par Ras (Cipriano *et al.*, 2011).

2.3 Implication relative de $p16^{INK4A}$

L'importance de $p16^{INK4A}$ dans l'induction de l'OIS a souvent été montrée. Par exemple, des fibroblastes humains déficients en $p16^{INK4A}$ sont résistants à la sénescence induite par H-Ras (Drayton *et al.*, 2003). De même, dans des fibroblastes humains fraîchement isolés qui n'expriment que de très faibles niveaux de $p16^{INK4A}$, H-Ras n'est qu'un faible inducteur de sénescence (Benanti and Galloway, 2004). De plus, les niveaux de $p16^{INK4A}$ dans les BJ et MEFs sénescents sont faibles, contrairement à ceux d'IMR90 et de WI-38. De manière surprenante, Michaloglou et ses collègues ont pourtant observé que dans des fibroblastes BJ immortalisés qui expriment un shRNA ciblant $p16^{INK4A}$, l'expression de $B\text{-}Raf^{V600E}$ est toujours capable d'induire la sénescence. Cette découverte remet en question l'importance de $p16^{INK4A}$ ou en tout cas la généralisation de son rôle dans l'OIS dans les fibroblastes. Elle pose également la question de la situation dans les autres types cellulaires.

Les expériences de Zhuang et ses collègues mentionnées dans le paragraphe précédent montrent que l'inhibition de $p16^{INK4A}$ (et de p53) dans des mélanocytes normaux n'a pas de conséquence sur la réponse de sénescence induite par $B\text{-}Raf^{V600E}$ ou $N\text{-}Ras^{Q61R}$. Les expériences effectuées par Sebastian Haferkamp corroborent ces observations et les complètent puisqu'il a été montré que ni $p16^{INK4A}$, ni $p14^{ARF}$ ne sont indispensables pour induire l'entrée en sénescence induite par $N\text{-}Ras^{Q61K}$ (Haferkamp *et al.*, 2009 a). L'ensemble de ces données est récapitulé sous forme de tableau. Il montre d'une part que les études sont parfois divergentes *(Tableau 2)* et d'autre part que notamment dans les cellules épithéliales les différents types de stress oncogéniques peuvent induire une sénescence qui ne va activer ni la voie p53, ni la voie des dommages à l'ADN, ni $p16^{INK4A}$.

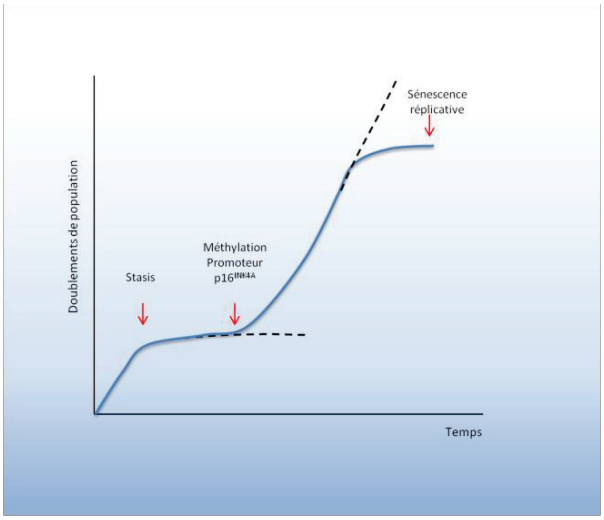

Figure 6 : Représentation schématique d'une courbe de croissance de cellules épithéliales

Les cellules épithéliales rencontrent un premier arrêt de prolifération, appelé stasis (1er plateau). Quelques cellules de la population vont pouvoir émerger en réprimant l'expression de $p16^{INK4A}$ par méthylation du promoteur. Les cellules rencontrent ensuite un autre arrêt de prolifération, la sénescence réplicative, qui peut être évitée par l'expression de la sous-unité catalytique de la télomérase.

	fibroblastes	cellules épithéliales mammaires	
caractéristique	sénescence	1er plateau	2ème plateau
absence de croissance	+	+	+
SA-β-gal	+	+	+
expansion de la population au-delà du plateau d'arrêt de croissance	-	+	-
nomenclature	limite d'Hayflick, sénescence, sénescence réplicative irréversible, M1	sélection, sénescence, arrêt terminal, M0	sénescence, sénescence réplicative, agonescence
nomenclatures actuelle	**sénescence réplicative**	**stasis**	**sénescence réplicative**

Tableau 3 : sénescence dans les fibroblastes et les cellules épithéliales

adapté de (Romanov *et al.*, 2001)

2.4 L'OIS dans les cellules épithéliales

Les mécanismes impliqués dans le processus de sénescence, et surtout l'OIS, sont donc dépendants du contexte cellulaire. Les études de l'OIS dans des modèles cellulaires plus pertinents que dans les fibroblastes ont révélé la complexité des mécanismes mis en jeu. En effet, les voies p53 et $p16^{INK4A}$, habituellement reconnues comme étant les éléments majeurs indispensables à l'établissement de la sénescence n'apparaissent plus comme étant les seules impliquées dans ces processus. Outre la sénescence des fibroblastes, celle des mélanocytes primaires et de cellules de mélanomes ont été très étudiées. A l'inverse, les mécanismes mis en jeu dans l'OIS dans les cellules épithéliales primaires restent très flous. Les rares études menées sur ce sujet dévoilent des mécanismes nouveaux en contraste avec les voies canoniques (Cipriano *et al.*, 2011; Takaoka *et al.*, 2004)

De plus, la culture de cellules épithéliales primaires humaines fait apparaître des différences importantes avec la culture des fibroblastes. Je ne développerai que le cas des cellules épithéliales mammaires humaines dans la section qui suit, bien que ces observations soient valables dans d'autres types de cellules épithéliales comme les kératinocytes.

Les cellules épithéliales primaires mammaires humaines, une fois mises en culture, se répliquent pendant une dizaine de doublement de populations avant de rencontrer une barrière à leur prolifération (1er plateau, statis). En effet, les cellules entrent en sénescence, arrêt de croissance qui peut s'apparenter à la sénescence réplicative de fibroblastes. Cet arrêt de prolifération, parfois appelé M_0, ou sélection, est désormais connu sous le nom de stasis, puisqu'il ne s'agit pas de sénescence réplicative mais d'une sénescence associée à un stress caractérisée par une forte expression de $p16^{INK4A}$. Toutefois, une sous-population de cellules parviennent à reprendre leur prolifération (Romanov *et al.*, 2001). Plusieurs études ont montré que la reprise de la prolifération est due à l'extinction de l'expression de $p16^{INK4A}$ par méthylation de son promoteur (Brenner *et al.*, 1998; Foster *et al.*, 1998; Huschtscha *et al.*, 1998; Wong *et al.*, 1999) (*figure 6).* Les cellules entrent par la suite en sénescence réplicative (deuxième plateau), dépendant du raccourcissement des télomères.

Il est important de noter que Raf est capable d'induire un arrêt de prolifération dans les hMECs post-stasiques, et ce de manière indépendante de p53 et de la voie p16^{INK4A}-Rb. De plus, l'OIS liée à Raf dans des cellules pré-stasiques qui peuvent donc encore exprimer p16^{INK4A}, ne montre aucune induction de p16 ^{INK4A}. La sénescence dans les hMECS, pré- ou post-stasiques, peut donc être indépendante de p16^{INK4A} (Olsen *et al.*, 2002). La méthylation spontanée du promoteur de p16^{INK4A} est aussi observée dans des cellules épithéliales mammaires humaines, *in vivo*, et de manière comparable aux conditions de culture n'exprime pas obligatoirement p16^{INK4A} (Holst et al., 2003). L'ensemble de ces données montre que même si p16^{INK4A} est inactivée l'OIS peut encore être induite.

Au regard des études menées sur la culture des cellules épithéliales humaines, il apparaît nettement des différences fondamentales avec la culture des fibroblastes *(Tableau 3)*. Ces différences peuvent potentiellement expliquer pourquoi les voies de signalisation activées lors de l'OIS dans les fibroblastes et les cellules épithéliales s'avèrent être parfois divergentes.

2.5 Objectifs de la thèse

Comme je viens de le discuter, l'OIS dans les cellules épithéliales est très mal caractérisée. Potentiellement, de nombreux nouveaux régulateurs de la sénescence dans ces cellules restent à être découverts. Pour caractériser de nouveaux mécanismes impliqués dans l'échappement à l'OIS des cellules épithéliales et le développement des carcinomes, j'ai utilisé deux approches différentes : l'une ciblée, étudiant l'effet de l'activité lysysl oxidase sur la réversion de l'OIS, et l'autre globale, utilisant un criblage perte de fonction.

Afin de caractériser de nouveaux régulateurs de la sénescence dans les cellules épithéliales humaines, j'ai utilisé un modèle cellulaire original : des cellules épithéliales mammaires humaines post-stasiques qui n'expriment pas $p16^{INK4}$ suite à la méthylation du promoteur. Ces cellules sont également immortalisées par l'expression ectopique de la sous-unité catalytique hTERT empêchant ainsi la sénescence réplicative. Enfin, ces cellules expriment également une forme conditionnellement active d'un oncogène muté (Mek ou Raf) généré par la fusion des séquences codant pour l'oncogène et le domaine de liaison muté du récepteur aux œstrogènes (Collado *et al.*, 2005; Woods *et al.*, 1997; Blalock *et al.*, 2000). L'activation de Mek ou de Raf aboutit après ajout de 4-hydroxytamoxifène (4-OHT) à de l'OIS comparable à celle obtenue par l'expression continue d'oncogènes actifs. Ce système d'oncogène fusionné a été utilisé *in vitro* et *in vivo* notamment pour étudier la réponse au stress oncogénique (Narita *et al.*, 2011; Vredeveld *et al.*, 2012; Zhu *et al.*, 1998).

L'intérêt de ce modèle, en plus de récapituler l'OIS, permet de contrôler le niveau d'activation de l'oncogène. Nous avons aussi observé que quelques jours après l'arrêt de l'activation de l'oncogène, les cellules reprennent leur prolifération et perdent leurs marqueurs de sénescence. L'instabilité de la sénescence dans ce modèle peut être due à l'absence d'expression de $p16^{INK4A}$ connu pour verrouiller l'arrêt de prolifération. En modulant la sénescence dans ce modèle original, de nouveaux mécanismes influençant la réversibilité de l'OIS peuvent alors être étudiés. Cela fera l'objet de ma première partie des résultats dans laquelle je présenterai les effets de l'activité lysyl oxidase sur le processus de réversion de la sénescence.

Dans une deuxième partie, je présenterai une seconde approche, plus globale cette fois-ci, pour identifier des nouveaux régulateurs de l'OIS dans les cellules épithéliales humaines, en utilisant le modèle décrit précédemment. En réalisant un criblage génétique perte de fonction, à l'aide d'une banque de shRNA, le laboratoire a pu identifier 61 gènes dont l'extinction peut potentiellement permettre aux cellules d'échapper à la sénescence maintenue par une activation constante de

l'oncogène. Au cours de ma thèse, j'ai participé à l'étude du transporteur ABCC3, et à celle du canal potassique KCNA1 *(voir annexe)*, deux gènes identifiés lors du criblage. Mais je me suis plus particulièrement intéressée à deux canaux impliqués dans le transport du calcium entre le réticulum endoplasmique et la mitochondrie : ITPR2 et MCU.

RESULTATS

RESULTATS

Chapitre I : Rôle de l'activité lysyl oxydase dans l'échappement à l'OIS

Dans cette première partie, je me suis intéressée à l'effet de l'activité lysyl oxydase sur la stabilité de l'OIS.

1.1 Introduction

1.1.1 Famille des lysyl oxidases

La famille des lysyl oxidases (LOX) est composée de 5 membres : LOX, et LOX-like 1 à 4 (LOXL1 – LOXL4). Ces enzymes sécrétées font partie de la famille des amines oxydases. La fonction la plus connue et la mieux caractérisée est la réticulation du collagène et de l'élastine de la matrice extra-cellulaire (ECM), qui induit une tension nécessaire à l'intégrité de nombreux tissus. Parmi ces 5 protéines, LOX et LOXL1 sont sécrétées sous une forme immature, les formes Pro-LOX et pro-LOXL1. L'enzyme devient mature après clivage par la Bone Morphogenetic Protein 1 (BMP-1). Deux éléments distincts sont crées : pour LOX, le pro-peptide de 18 kDa, qui ne porte aucune activité enzymatique, et l'enzyme LOX active, d'une taille de 30 kDa *(figure 7).*

Une expression et/ou une activité aberrantes des LOXs sont reportées dans différentes pathologies et de manière peu surprenante beaucoup d'entre elles sont liées à une altération de l'ECM ou à des cancers (Barker *et al.*, 2012). Il a été reporté que les membres de la famille LOX peuvent être sur- ou sous-exprimés dans les cancers. De même, il apparaît que les LOXs peuvent avoir des fonctions extracellulaires mais aussi intracellulaires. Ces données suggèrent que les LOXs pourraient avoir des rôles opposés dans le développement des cancers et des métastases. Toutefois, les fonctions de LOXL, LOXL3 et LOXL4 sont très peu étudiées, c'est pourquoi dans les paragraphes suivants je présenterai l'implication de LOX et LOXL2 uniquement dans les différents processus tumoraux.

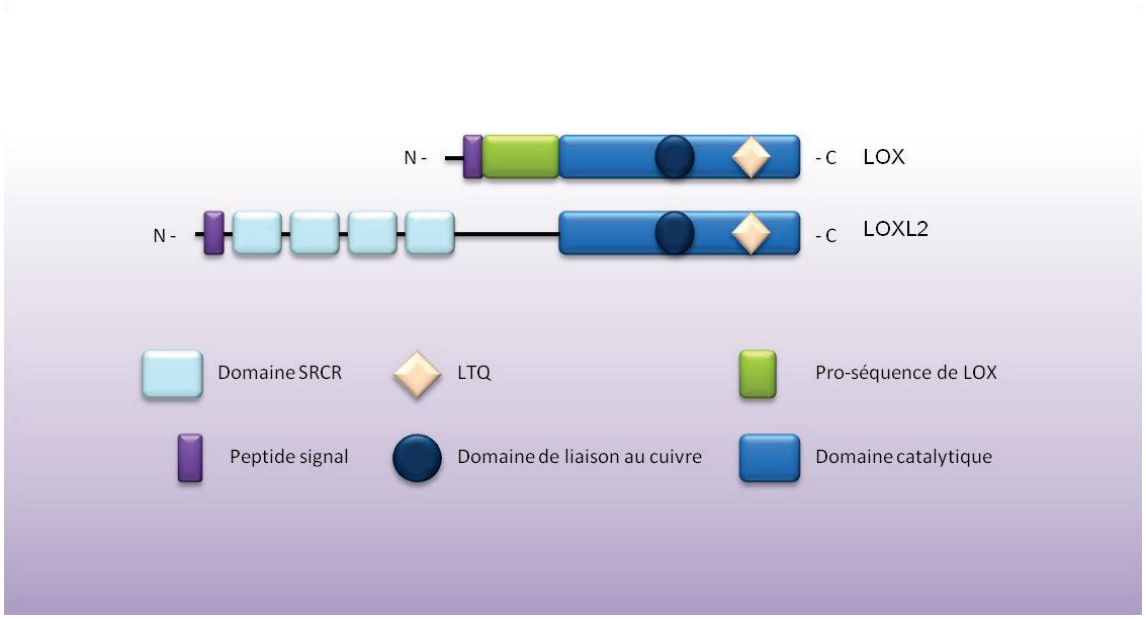

Figure 7 : Structures de LOX et LOXL2

La famille des lysyl oxydases contiennent une région C-Terminale hautement conservée. Celle-ci contient un motif de liaison au cuivre, et un co-facteur de type lysyl-tyrosyl quinone (LTQ), qui sont respectivement nécessaires au repliement conformationnel de la protéine, et à son activité.

LOX contient une pro-séquence qui est clivée pour permettre l'activation de la pro-enzyme.

LOXL2 contient 4 domaines de type scavenger receptor cystéine-rich (SRCR) dans sa region N-Terminale.

1.1.2 Rôle anti-tumoral de Lox

L'une des premières fonctions connues de LOX a été son effet inhibiteur sur la transformation induite par H-Ras ce qui lui a valu d'être appelé Ras recision gene (*Rrg*) (Kenyon *et al.*, 1991; Contente *et al.*, 1990). Il est désormais prouvé que les activités suppressives de transformations néoplasiques sont dues au pro-peptide de LOX (LOX-PP). Ce pro-peptide peut inhiber la voie de signalisation qui mène à l'activation de NFκB dans des cellules (en culture et en xénogreffes) où H-Ras ou HER2 (connu également sous le nom de *ERBB2* ou *neu*) sont surexprimés (Palamakumbura *et al.*, 2004; Min *et al.*, 2007; Sánchez-Morgan *et al.*, 2011; Wu *et al.*, 2007). Il a également été montré que LOX-PP module la voie de signalisation du Fibroblast Growth Factor-2 (FGF-2) dans certaines lignées cancéreuses prostatiques (Palamakumbura *et al.*, 2009). Enfin, LOX-PP pourrait avoir une activité inhibitrice sur la croissance de tumeurs en induisant de l'apoptose (Bais *et al.*, 2012). Seule LOX, et potentiellement LOXL-1 qui peut aussi être clivé, semblent avoir des rôles anti-tumoraux via le pro-peptide. Cependant, aucune donnée *in vivo* n'est venue confirmer ces observations. L'importance du pro-peptide dans la régression tumorale apparaît très relative, comparée à l'implication largement démontrée de l'activité lysyl oxydase dans la progression tumorale.

1.1.3 Rôles de Lox dans la progression tumorale

L'implication de la famille LOXs dans le développement tumoral a été amplement étudiée. De multiples études montrent que l'ARNm ainsi que la protéine LOX sont surexprimés dans de nombreux types de cancers : cancer de sein, colorectal et de la prostate (Erler *et al.*, 2006; Kirschmann *et al.*, 2002; Baker *et al.*, 2011 a, 2012; Lapointe *et al.*, 2004). De même, il a été démontré une corrélation entre l'augmentation de l'expression de LOX et de LOXL2 et une diminution de la survie (Peinado *et al.*, 2008; Barry-Hamilton *et al.*, 2010; Barker *et al.*, 2011; Moreno-Bueno *et al.*, 2011; Offenberg *et al.*, 2008; Ahn *et al.*, 2013). Comme je le détaillerai dans les paragraphes suivants, l'activité lysyl oxydase favorise la progression tumorale ainsi que le processus métastatique *(figure 8)*.

Bien que l'effet de l'activité Lox sur l'invasion cellulaire soit majoritairement décrit via une augmentation de la rigidité de la matrice extracellulaire, Lox peut avoir des cibles intra-cellulaires. LOXL2 peut en effet interagir avec le facteur de transcription embryonnaire Snail, un inducteur fort de la transition epithélio-mésenchymateuse (TEM, ou EMT pour *Epithelial-Mesenchymal Transition*) (Peinado *et al.*, 2005), un processus impliqué dans les étapes d'invasion des cellules cancéreuses en permettant la conversion des cellules épithéliales polarisées et jointives, en cellules mésenchymateuses isolées à fort pouvoir métatstatique. Nicolas Herranz et ses collègues confirment que la localisation nucléaire de LOXL2 puisse être impliquée dans la répression d'expression de la

cadhérine-E. Ils démontrent aussi que l'activité Lox de LOXL2 est impliquée dans la désamination de la lysine 4 de l'histone 3. Ils proposent que LOXL2, en modifiant les histones, puisse participer à la régulation de gènes impliqués dans la tumorigénèse (Herranz *et al.*, 2012). Ces observations sont en accord avec le fait que LOX et LOXL2 peuvent catalyser l'oxydation de protéines avec un point isoélectrique basique (pI > 8) telles que les histones (Kagan *et al.*, 1983; Giampuzzi *et al.*, 2003). Il a aussi été montré que LOXL2 régule l'expression de composants des jonctions serrées, et des complexes de la polarité cellulaire (Moreno-Bueno *et al.*, 2011), indépendamment de l'activité Lox (Cuevas *et al.*, 2014). Ces données suggèrent que les LOXs pourraient altérer l'expression de gènes impliqués dans la progression tumorale, soit par l'intermédiaire de l'activité Lox soit de façon indépendante de cette dernière (Oleggini and Donato, 2011)

Les promoteurs de LOX et LOXL2 comportent des éléments de réponse à HIF1 (*Hypoxia Inducible Factor-1*, HIF1) permettant l'expression de LOX et LOXL2 en conditions d'hypoxie (Erler *et al.*, 2006). L'hypoxie est un phénomène caractérisé par une réduction sévère de la pression partielle en oxygène dans une région donnée ou dans un tissu pouvant mener à la mort des cellules en cas d'exposition prolongée. Les cellules cancéreuses sont capables de s'adapter notamment en modifiant leur métabolisme (effet Warburg) et peuvent survivre dans ces conditions dépourvues en oxygène (Harris, 2002; Bertout *et al.*, 2008).

En réponse à l'hypoxie, plusieurs phénomènes se mettent en place. L'angiogénèse, qui en est un des plus importants est mis en place. L'angiogénèse est un processus complexe qui nécessite la prolifération ainsi que la migration des cellules endothéliales, et la dégradation de la membrane basale des vaisseaux sanguins et de la matrice associée. L'angiogénèse nécessite donc un profond remaniement de l'ECM (Sottile, 2004). L'activité Lox peut participer à ce mécanisme en remodelant la matrice extra-cellulaire par l'augmentation du dépôt de fibres élastiques dans les parois des vaisseaux sanguins (Lelièvre *et al.*, 2008). LOXL2 est aussi impliquée dans la formation des nouveaux vaisseaux par la réticulation du collagène IV de la membrane basale des cellules endothéliales (Bignon *et al.*, 2011) favorisant la migration des cellules endothéliales et l'angiogénèse dans des modèles de xénogreffes (Zaffryar-Eilot *et al.*, 2013).

Kirschmann et son équipe ont montré que LOX est responsable, au moins en partie, des capacités invasives et migratoires de lignées cellulaires cancéreuses (Kirschmann *et al.*, 1999, 2002). L'inhibition de LOX et de LOXL2 permet également de bloquer le processus métastatique dans des modèles de xénogreffes (Peng *et al.*, 2009; Bondareva *et al.*, 2009). Fonctionnellement, l'activité Lox pourrait promouvoir l'invasion en réticulant le collagène, en modulant la voie FAK-Src ((Peng *et al.*, 2009) ou par l'intermédiaire d'une EMT, (Barry-Hamilton *et al.*, 2010).

Il a également été montré que LOX et LOXL2 sécrétés par les cellules hypoxiques s'accumulent aux futures sites de métastases pour remodeler la matrice-extracellulaire en recrutant et en favorisant l'adhésion des cellules dérivées de la moelle épinière (*Bone Marrow-Derived Cell,* BMDCs) (Erler *et al.*, 2009; Wong *et al.*, 2011). Ces niches métastatiques sont composées de protéines et de BMDCs qui forment un environnement adéquat dans lequel les cellules disséminées peuvent proliférer et former des métastases dans l'organe envahi. Ces observations sont en accord avec les hypothèses selon lesquelles les phénomènes de migration et d'invasion (comme l'EMT) ne sont pas obligatoirement des éléments tardifs de la progression tumorale mais peuvent aussi se produire en parallèle du le développement de la tumeur primaire.

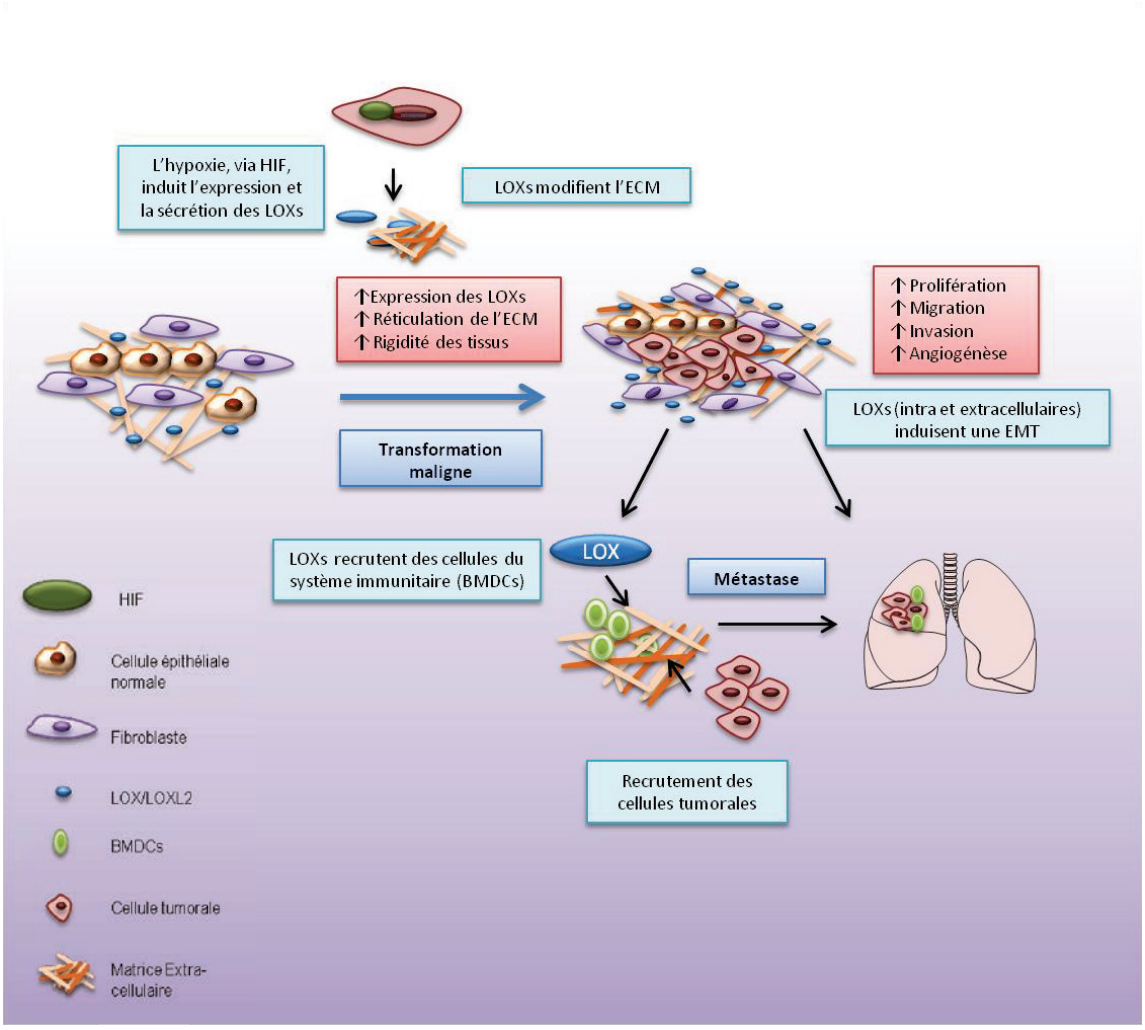

Figure 8 : LOX est impliqué dans différents processus favorisant le développement tumoral

L'augmentation d'expression des LOXs notamment en réponse à l'hypoxie augmente le remodelage de l'ECM et sa réticulation, permettant d'augmenter la prolifération, l'invasion et la migration des cellules tumorales, en régulant des processus comme l'EMT et l'angiogénèse. LOX et LOXL2 sécrétés par les cellules hypoxiques s'accumulent aux futures sites de métastases pour remodeler la matrice-extracellulaire en recrutant et en favorisant l'adhésion des BMDCs.

HIF : Hypoxia-Inducible Factor ; BMDC : Bone-Marrow Derived Cells; ECM : Matrice-Extra-Cellulaire.

Adapté de (Barker *et al.*, 2012)

1.1.4 Rôles émergents de Lox dans l'initiation tumorale

La composition de la matrice change durant le développement d'un cancer. En réponse à des stress, les cellules stromales, peuvent sécréter de manière aberrante des composants de la matrice ou en induire une organisation dysfonctionnelle. Ce phénomène peut moduler le comportement des cellules épithéliales. L'évolution des carcinomes est largement influencée par les altérations du micro-environnement, et plus particulièrement par le remodelage de la matrice (Erler and Weaver, 2009). Par exemple, une augmentation des dépôts de collagène et de la réticulation de fibres de la matrice contribuent à rigidifier l'ECM. Ces deux facteurs combinés vont promouvoir la transformation maligne en activant la signalisation de facteurs de croissance ou en déstabilisant l'intégrité des tissus (Paszek *et al.*, 2005). Il a d'abord été pensé que l'activité lysyl oxidase n'avait d'impact uniquement au sein des foyers métastatiques (Erler *et al.*, 2006; Kirschmann *et al.*, 1999; Bondareva *et al.*, 2009). Mais plus récemment, plusieurs articles ont démontré l'inverse avec l'implication de l'activité Lox au sein des foyers primaires (Baker *et al.*, 2012, 2011 a; Peng *et al.*, 2009).

En 2009, le groupe de Weaver a publié que l'activité Lox pouvait directement coopérer avec l'oncogène Neu (HER2/ERBb2) pour favoriser la formation de tumeurs primaires (Levental *et al.*, 2009). En effet, la rigidité accrue de la matrice induite par LOX active les adhésions focales, augmente l'activité de la PI3K, et induit la formation de tumeurs.

Au vu des ces résultats, nous nous sommes demandé si l'activité Lox pouvait promouvoir l'initiation tumorale en permettant l'échappement à la sénescence induite par le stress oncogénique.

1.2 Article 1 : Lysyl oxidase activity regulates oncogenic stress response and tumorigenesis

Lysyl oxidase activity regulates oncogenic stress response and tumorigenesis

Clotilde Wiel, Arnaud Augert, David F Vincent, Delphine Gitenay, David Vindrieux, Benjamin Le Calvé, Vanessa Arfi, Hélène Lallet-Daher, Caroline Reynaud, Isabelle Treilleux, Laurent Bartholin, Etienne Lelièvre et David Bernard

Publié en septembre 2013 dans le journal *Cell Death & Disease*

Afin d'étudier la réversibilité de l'OIS dans les cellules épithéliales mammaires humaines, nous avons utilisé un modèle cellulaire dans lequel l'arrêt de prolifération induit par l'oncogène Mek est instable *(figure 1)*. Dans ce modèle, nous avons étudié l'impact de l'activité lysyl oxydase sur la stabilité de la sénescence. Nous avons observé que la surexpression des enzymes LOX et LOXL2 favorise l'échappement à l'OIS *(figure 2)*. L'ajout de surnageants provenant de culture de cellules surexprimant LOX ou LOXL2 permet également d'induire un échappement à l'OIS *(figure 3)*. A l'inverse, l'inhibition de l'activité Lox par la molécule BAPN (β-aminopropionitrile) permet de stabiliser l'OIS des hMECs *(figure 4)*.

Pour étudier l'effet de l'activité Lox sur le développement tumoral, nous avons utilisé un modèle murin d'adénocarcinomes du pancréas (PDAC) induits par K-Ras^{G12D} et où p16^{INK4A} n'est pas exprimé. Ce modèle agressif, où la médiane de survie est d'environ 6 à 7 semaines, est pourtant associé à un phénotype de sénescence *(figure supplémentaire 4)*. Après l'injection quotidienne de surnageants concentrés contenant LOX, nous avons analysé les pancréas des souris et nous avons noté une diminution des marqueurs de sénescence associée à une augmentation de la prolifération des cellules. L'analyse du collagène nous a permis de confirmer une augmentation de la réticulation du collagène chez les souris injectées avec LOX confirmant que l'enzyme injectée est fonctionnelle *(figure 5)*. Pour valider l'effet de l'activité Lox sur l'échappement à l'OIS nous avons également traité les souris avec l'inhibiteur des LOXs, le BAPN. Celui-ci, en plus de stabiliser la sénescence dans les lésions pancréatiques, permet d'augmenter la survie des souris de 20% *(figure 6)*.

In vitro, et *in vivo*, l'activité Lox régule la stabilité de l'OIS par l'intermédiaire de la kinase FAK *(figure 7)*. L'inhibition de cette dernière permet en effet de stabiliser l'OIS in vitro, alors que sa surexpression permet un échappement à l'OIS stabilisée par le BAPN *(figure 8)*.

Ces résultats montrent pour la première fois que moduler l'activité Lox peut permettre de stabiliser l'OIS, ou permettre son échappement, et décrivent un nouveau rôle pour ces enzymes dans l'initiation tumorale.

OPEN

Citation: Cell Death and Disease (2013) 4, e855; doi:10.1038/cddis.2013.382
© 2013 Macmillan Publishers Limited All rights reserved 2041-4889/13
www.nature.com/cddis

Lysyl oxidase activity regulates oncogenic stress response and tumorigenesis

C Wiel[1,2,3,4], A Augert[1,2,3,4], DF Vincent[1,2,3,4], D Gitenay[1,2,3,4], D Vindrieux[1,2,3,4], B Le Calvé[1,2,3,4], V Arfi[1,2,3,4], H Lallet-Daher[1,2,3,4], C Reynaud[4,5], I Treilleux[3], L Bartholin[1,2,3,4], E Lelievre[6,7] and D Bernard*[,1,2,3,4,7]

Cellular senescence, a stable proliferation arrest, is induced in response to various stresses. Oncogenic stress-induced senescence (OIS) results in blocked proliferation and constitutes a fail-safe program counteracting tumorigenesis. The events that enable a tumor in a benign senescent state to escape from OIS and become malignant are largely unknown. We show that lysyl oxidase activity contributes to the decision to maintain senescence. Indeed, in human epithelial cell the constitutive expression of the LOX or LOXL2 protein favored OIS escape, whereas inhibition of lysyl oxidase activity was found to stabilize OIS. The relevance of these *in vitro* observations is supported by *in vivo* findings: in a transgenic mouse model of aggressive pancreatic ductal adenocarcinoma (PDAC), increasing lysyl oxidase activity accelerates senescence escape, whereas inhibition of lysyl oxidase activity was found to stabilize senescence, delay tumorigenesis, and increase survival. Mechanistically, we show that lysyl oxidase activity favors the escape of senescence by regulating the focal-adhesion kinase. Altogether, our results demonstrate that lysyl oxidase activity participates in primary tumor growth by directly impacting the senescence stability.
Cell Death and Disease (2013) **4,** e855; doi:10.1038/cddis.2013.382; published online 10 October 2013
Subject Category: Cancer

Oncogene-induced senescence (OIS) drives cells into a stable cell cycle arrest, causing them to acquire specific markers (morphology, senescence-associated β-galactosidase activity (SA-β-Gal), for example) in response to aberrant oncogenic signals.[1] In responsive cells, the stress generated by oncogene activation counterbalances the proliferation-stimulating potential of this activation by triggering senescence. Various benign tumors (melanoma nevi, prostatic intraepithelial neoplasias, lung adenomas) caused by oncogene activation accumulate senescent cells. The tumors remain in a benign state as long as senescence is sustained. Conversion to malignancy of senescing benign lesions thus involves escape from senescence.[2–4]

The p16-Rb and p53 pathways are key pathways in the regulation of OIS and senescence in general,[1,5–8] but mounting evidence shows that senescence can occur without any involvement of either of these pathways. To date, little is known about these mechanisms.[9–15] Most of the data demonstrating a central role of p53, its upstream activators, (DNA damage, $p14^{ARF}$) and the p16-Rb pathway have been obtained with fibroblasts. Similar data generated in human epithelial cells (HECs) or other lineages are quite rare, and suggest a more complex picture of the genetic events involved in escape from senescence.[15] Among primary HECs, primary human mammary epithelial cells probably constitute the best-characterized cell model. Post-stasis human mammary epithelial cells are unable to express $p16^{INK4a}$,[16] but they can still enter senescence, in a p53-independent manner in response to oncogenic stress.[14] We have thus chosen this model to investigate alternative pathways involved in escape from OIS.

Lysyl oxidase activity (LOX), exerted by the LOX, LOXL1, LOXL2, LOXL3, and LOXL4 proteins,[17,18] regulates cell behavior by oxidizing lysine residues of their substrates and H_2O_2 production. LOX-family members are reported to exert both intracellular and extracellular effects, and to share or display specific activities.[19–23] For example, LOX, LOXL1, and LOXL2 share the ability to promote migration, invasion, and metastasis and to regulate extracellular matrix organization.[20,24–30] How LOX activity affects cancer cell growth is still a matter of debate, as in some cases it is reported to have no effect[24,25] and in other cases to favor cancer cell growth[19,27,28] *in vitro* or *in vivo*. Although both LOXL2 and LOXL3 seem to exert some specific effects on cancer by targeting the embryonic transcription factor Snail,[22] some of the effects shared by LOXL2 and LOX are exerted via activation of the focal-adhesion kinase (FAK).[19,24,27,31–33]

In the context of neu-induced breast tumorigenesis, importantly, LOX activity appears to favor tumorigenesis by regulating FAK.[31] The oncogenic potential of neu, a tyrosine

[1]Inserm U1052, Centre de Recherche en Cancérologie de Lyon; [2]CNRS UMR5286, Centre de Recherche en Cancérologie de Lyon; [3]Centre Léon Bérard; [4]Université de Lyon, Lyon, France; [5]Inserm U1033, Lyon, France and [6]UMR8161, Institut de Biologie de Lille, CNRS/Universités de Lille 1 et 2, Lille, France
*Corresponding author: D Bernard, Centre de Recherche en Cancérologie de Lyon, 28, rue Laënnec, Centre Léon Bérard, Lyon 69373, France. Tel: +33 4 26 55 67 92; Fax: +33 4 78 78 27 20; E-mail: david.bernard@lyon.unicancer.fr
[7]These authors contributed equally to this work.
Keywords: senescence; lysyl oxidase; oncogenic stress; FAK
Abbreviations: 4-OHT, 4-hydroxytamoxifen; BAPN, β-aminopropionitrile; HEC, human epithelial cells; HEC-TM, HEC–hTert–MEK:ER; HEC-TR, HEC–hTert–RAF:ER; FAK, focal-adhesion kinase; LOX, lysyl oxidase; LOXL -1 -2 -3 -4, LOX-Like (-1 -2 -3 -4); OIS, oncogene-induced senescence; PDAC, pancreatic ductal adenocarcinoma; SA-β-Gal, senescence-associated β-galactosidase; WT, wild-type mice; KIA, Pdx1-Cre, LSL-KrasG12D/+, INK4a/Arflox/lox mice
Received 31.7.13; revised 03.9.13; accepted 03.9.13; Edited by A Finazzi-Agró

kinase receptor, can be limited by activation of the OIS fail-safe program.[34] We thus hypothesized that LOX activity might affect oncogene-induced tumorigenesis by impacting the OIS fail-safe program triggered by oncogenic activation. We show that LOX activity is indeed a key regulator of OIS, thereby affecting tumorigenesis.

Results

An unstable OIS model based on HECs. To study OIS in HECs, we used post-stasis mammary HECs, which do not express p16^{INK4a}.[16] We reasoned that this extinction of p16^{INK4a} would favor senescence instability, as demonstrated by other studies.[35,36] The cells were next immortalized by forced hTert expression (sustaining telomere integrity and thus avoiding replicative senescence[16]) and stably infected to express an inducible oncogene: MEK:ER (HEC-TM cells) or, in some experiments, RAF:ER (HEC-TR cells). In HEC-TM cells, where MEK was activated by a 3-day treatment with 4-hydroxytamoxifen (4-OHT) (Figure 1a), as indicated by increased phosphorylation of its substrate ERK (Figure 1b), we first checked that OIS was induced on d0. OIS induction by 4-OHT was demonstrated by loss of the two proliferation markers examined (cyclin A, a cyclin accumulated in the S to early M phases and PhosphoH3Ser10, a marker of late mitosis) (Figure 1b), growth arrest (Figure 1c), the appearance of the SA-β-Gal marker (Figure 1d) and an increase of the senescence markers IL8[5] and Sprouty2[37] (Figure 1e). As hypothesized, HEC-TM cells monitored after entry into senescence proved able to resume growth (Figure 1c) and to lose SA-β-Gal activity (Figure 1d) and other senescence markers (Figure 1e). This model is thus a suitable model for uncovering new mechanisms accelerating or inhibiting escape from OIS in HECs.

LOX activity regulates escape from OIS in HECs. To investigate the possible role of LOX activity in regulating senescence, we first used RT–qPCR to measure levels of transcripts corresponding to Lox-family proteins in HECs. LOX, LOXL1, and LOXL2 mRNAs were detected in these cells but LOXL3 and LOXL4 transcripts were not (Supplementary Figure 1). Cells were then infected with LOX- or LOXL2-encoding vectors, two main LOX-family members expressed in HEC, and their expression was checked by immunoblotting (Figure 2a). Cells constitutively expressing LOX, LOXL2, or neither of these were treated with 4-OHT to trigger senescence (d0), released from oncogenic stress for 3 days (d3), and then examined for escape from senescence (Figure 1a). On d3, although the initial growth arrest (d0) was similar in control, LOX-expressing, and LOXL2-expressing cells (Figure 2b), the LOX- and LOXL2-expressing cells displayed escape from OIS in contrast to control cells, that is, they were growing (Figure 2b), fewer of them were SA-β-Gal-positive (Figure 2c), and they displayed a decrease of senescence markers (Figure 2d). Thus, LOX and LOXL2 promote escape from OIS and this effect is not due to a simple growth advantage, as their constitutive expression does not affect cell growth in the absence of oncogenic stress induction (Figure 2e).

Secreted LOX favors escape from OIS in HECs. As LOX proteins are secreted, their production by various cells of the tumor microenvironment (such as fibroblasts or endothelial cells) might contribute, along with synthesis by the epithelial cells, to affecting the response to oncogenic stress. We thus examined whether extracellular LOX might impact OIS. We first measured LOX protein levels in the supernatants of constitutively expressing cells. As expected, LOX and LOXL2 were found in the supernatants (Figure 3a), LOX in its 30-kD mature form lacking the pro-domain and LOXL2 displaying the same size as in the lysate, as this protein contains no pro-domain.[17,18] Accordingly, the LOX and LOXL2 supernatants displayed increased LOX activity (Figure 3b). The results of colony assays (Figure 3c) and SA-β-Gal staining (Figure 3d) showed that adding LOX or LOXL2 supernatant to HEC-TM cells is sufficient to trigger escape from senescence. Importantly, LOX catalytic activity was found to be responsible for LOX-triggered escape from senescence: this escape was completely blocked upon addition of 3-aminopropionitrile (BAPN), an inhibitor of the catalytic activity of all the LOX proteins[38–40] (Figures 3c and d), and a catalytically inactive LOX form proved unable to induce senescence reversal (Supplementary Figure 2).

Inhibiting LOX catalytic activity stabilizes OIS in HECs. Interestingly, HEC-TM cells displayed spontaneous escape from senescence after oncogenic stress and OIS induction (Figures 1 and 4a–b). As increasing LOX activity favors senescence escape, we next investigated whether this spontaneous escape might be inhibited by inhibiting any endogenous LOX activity due to LOX, LOXL1, and/or LOXL2 (Supplementary Figure 1). During oncogenic stress, LOX activity inhibition by BAPN treatment did not significantly affect entry into OIS (Figures 4b–d), but it did, strikingly, completely block spontaneous escape from OIS, as shown by (i) the inability of treated cells to grow, in contrast to control cells (Figure 4b), (ii) their ability to maintain SA-β-Gal activity (Figure 4c) and other senescence markers (Figure 4d) under conditions where untreated cells lost these markers. These effects were not due to direct inhibition of cell growth by LOX, as BAPN treatment alone did not modify HEC-TM cell growth (Figure 4e). This set of data was obtained by inhibiting LOX activity during oncogenic stress induction. Interestingly, inhibiting LOX activity when the cells were already senescent (d0) also stabilized senescence (Supplementary Figure 3), supporting the idea that LOX activity modifies escape from senescence but not entry into senescence.

LOX activity regulates OIS stability *in vivo*. To address the relevance of these interesting *in vitro* observations on HECs, we sought an appropriate mouse model that would be relevant to human cancer biology. We decided to focus on pancreatic ductal adenocarcinoma (PDAC), because (i) p16 is generally lost in human PDAC,[41] and (ii) we observed LOX and LOXL2 induction (Supplementary Figure 4a) as well as some senescence (Supplementary Figure 4b) in a mouse model developing aggressive PDAC at the frequency of 100% by the age of 6–7 weeks as a result of pancreatic expression of an oncogenic Ras in a p16-null background

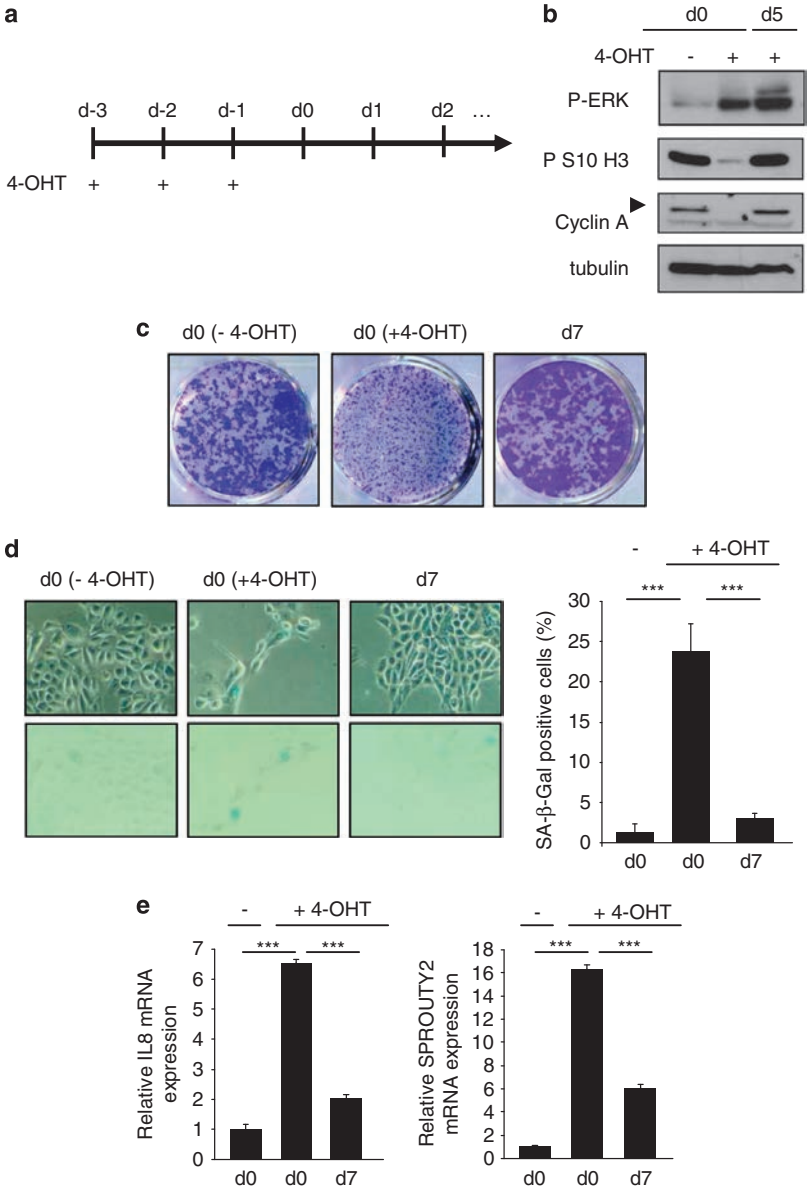

Figure 1 HEC-TM cells enter senescence after MEK activation. (**a**) HEC-TM cells were treated for 3 days with 4-OHT to activate MEK and were monitored the following days. (**b**) Cell extracts were prepared and analyzed by immunoblotting with the indicated antibodies at d0 or at d5. Tubulin was used as a loading control. (**c**) Cells were PFA-fixed and crystal violet-stained. (**d**) Cells were fixed and assayed for SA-β-Gal activity. (**e**) RNAs were prepared and RT-qPCRs were performed against the indicated genes. Expression was normalized against the level of actin mRNA. The experiments shown in this figure are representative of at least 3 independent experiments

(Pdx1-Cre, LSL-Kras$^{G12D/+}$, INK4a/Arf$^{lox/lox}$[42,43]). Wild-type (WT) and Pdx1-Cre, LSL-Kras$^{G12D/+}$, INK4a/Arf$^{lox/lox}$ (KIA) mice were killed 45 days after birth. The pancreases of KIA and WT animals were dissected and the normal zone was separated from the tumoral zone. In the KIA mice, the normal part (confirmed by hematoxylin-phloxine-saffron (HPS) staining) showed senescence (as indicated by the presence of SA-β-Gal activity) and tested negative for the proliferation marker Ki67 (Supplementary Figure 4b). In contrast, the tumoral part (confirmed by HPS staining) no longer displayed any SA-β-Gal activity and was Ki67-positive (Supplementary Figure 4b). The pancreases of WT animals displayed no SA-β-Gal activity and no Ki67 staining (Supplementary Figure 4b). KIA mice thus constitute an attractive model for testing OIS stability, and more specifically, the ability of LOX activity to regulate OIS *in vivo*.

To examine whether increased LOX activity might accelerate senescence, we first injected concentrated LOX protein supernatants (Figure 3) in mice. The LOX activity increase was observed in pancreatic extract for at least 4 h after intraperitoneal injection (Supplementary Figure 5). We then injected LOX protein supernatants into KIA mice, every day

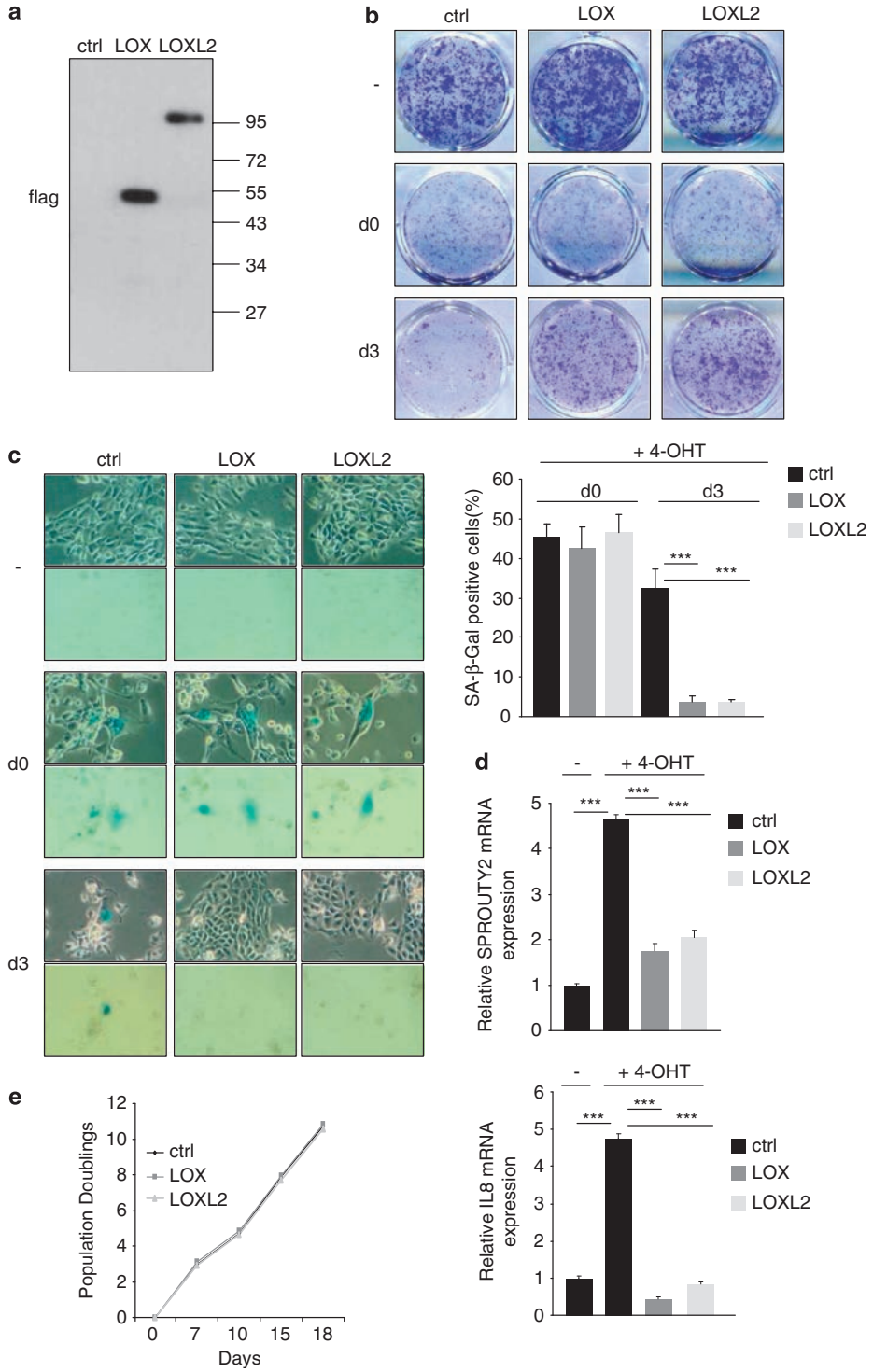

Figure 2 LOX expression and LOXL2 expression favor escape from OIS. HEC-TM cells were infected with an empty control or a LOX- or LOXL2-encoding vector and puromycin selected. (**a**) Cell lysates were prepared and analyzed by immunobloting with an anti-flag antibody. (**b**) HEC-TM cells were treated or not for 3 days with 4-OHT (d0), PFA-fixed and crystal violet-stained to measure cell growth at the indicated time points. (**c**) Cells were treated as in (**b**), fixed, and assayed for SA-β-Gal activity. (**d**) RNAs were prepared at d3 and RT-qPCRs were performed against the indicated senescence markers. Expression was normalized against the level of actin mRNA. (**e**) HEC-TM cells expressing a LOX-encoding, a LOXL-encoding or an empty control vector were counted after each passage and seeded at the same density. Population doublings are presented. The experiments shown in this figure are representative of at least three independent experiments

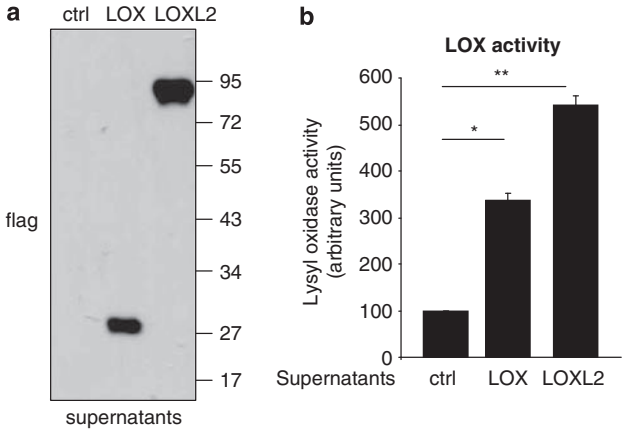
a
ctrl LOX LOXL2
flag
95
72
55
43
34
27
17
supernatants
b
LOX activity
Lysyl oxidase activity (arbitrary units)
600
500
400
300
200
100
0
**
*
Supernatants ctrl LOX LOXL2

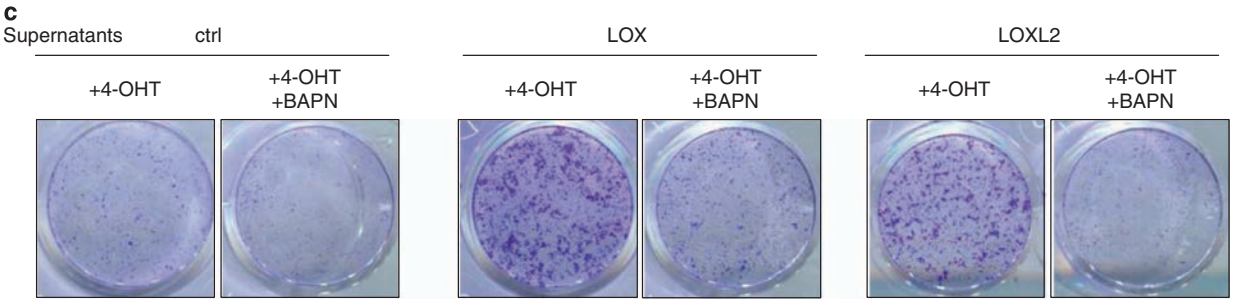
c
Supernatants ctrl
LOX
LOXL2
+4-OHT
+4-OHT +BAPN
+4-OHT
+4-OHT +BAPN
+4-OHT
+4-OHT +BAPN

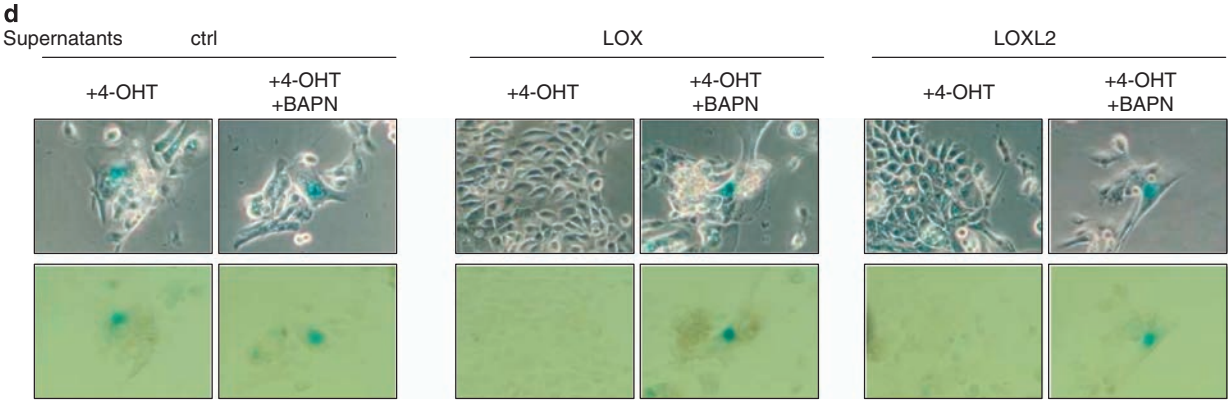
d
Supernatants ctrl
LOX
LOXL2
+4-OHT
+4-OHT +BAPN
+4-OHT
+4-OHT +BAPN
+4-OHT
+4-OHT +BAPN

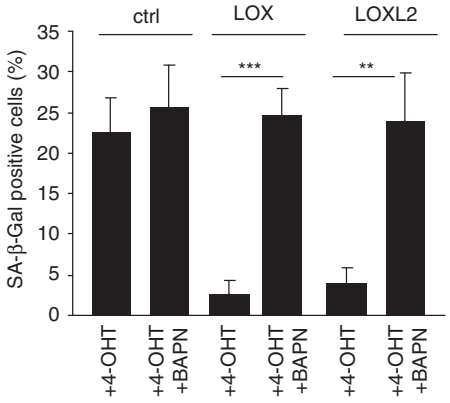
ctrl
LOX
LOXL2
SA-β-Gal positive cells (%)
35
30
25
20
15
10
5
0
***
**
+4-OHT
+4-OHT +BAPN
+4-OHT
+4-OHT +BAPN
+4-OHT
+4-OHT +BAPN

from days 23 to 38 after birth, and confirmed the LOX activity increase on the basis of better collagen fiber organization in the pancreatic tumor microenvironment 39 days after birth (Figure 5a). The SA-β-Gal (Figure 5b), Dec1 (Figure 5c) and Wnt16B (Figure 5d) senescence markers were all found to be lower and the Ki67 proliferation marker higher (Figure 5e) in mice injected with LOX supernatants than in mice injected with control supernatants. Hence, in agreement with the *in vitro* results, LOX activity can also accelerate escape from senescence *in vivo* in an aggressive model of PDAC.

We next examined whether LOX activity inhibition by BAPN might prevent the spontaneous escape from senescence observed 45 days after birth. The pancreases of BAPN-treated WT animals displayed no SA-β-Gal activity and no Ki67 staining (Supplementary Figure 4b), in agreement with the *in vitro* observation that BAPN cannot induce senescence in the absence of oncogenic stress (Figure 4e). BAPN injection into KIA mice resulted in the inhibition of pancreatic LOX catalytic activity, as measured by collagen fiber organization (Figure 6a). The pancreases of untreated mice were found to be SA-β-Gal-negative, whereas those of the BAPN-treated mice were SA-β-Gal-positive (Figure 6b) and displayed increased levels of the Dec1 and Wnt16B senescence markers (Figures 6c and d) and a decreased level of the Ki67 proliferation marker (Figure 6e). Importantly, LOX-inhibition-induced stabilization of senescence led to a significant increase in mouse survival (Figure 6f). Altogether, these results tally with our *in vitro* results and strongly support an involvement of LOX in regulating senescence stability, *in vivo* tumorigenesis, and survival.

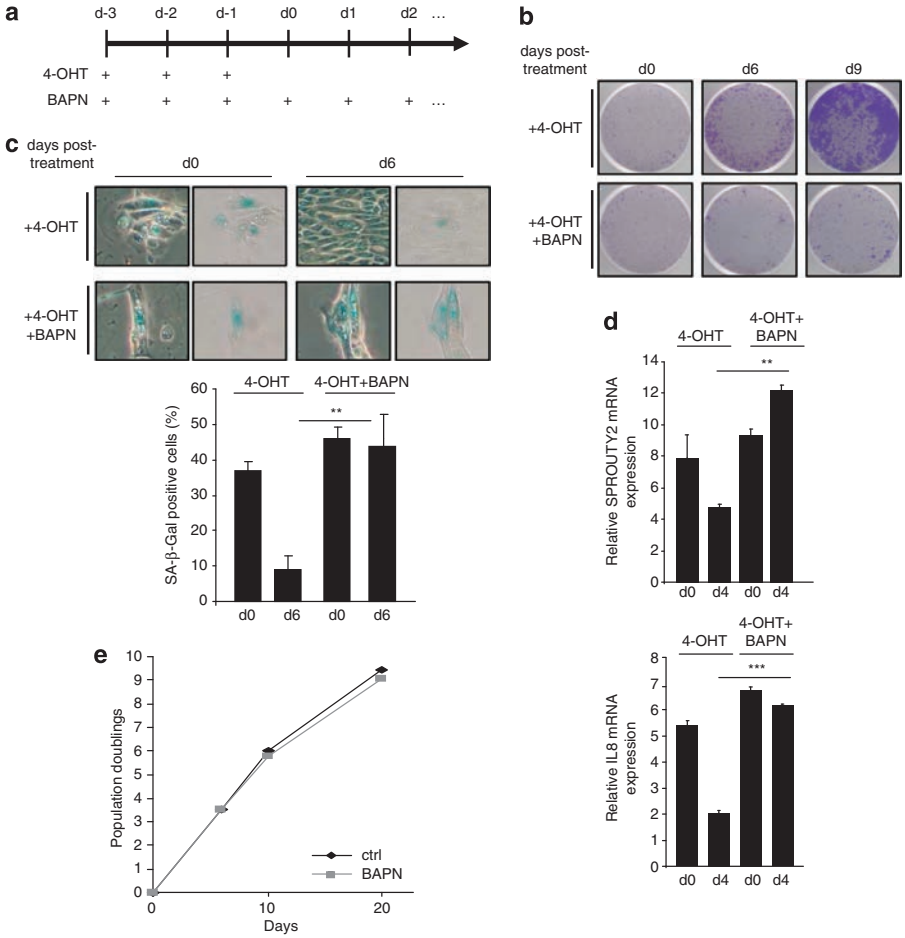

Figure 4 LOX activity inhibition blocks spontaneous escape from OIS. (**a**) Protocol of treatment to induce senescence and inhibition of its reversal in HEC-TM cells. (**b**) HEC-TM cells were treated for 3 days with 4-OHT, with or without BAPN. Cells were PFA-fixed and crystal violet-stained to measure cell growth at various time points. (**c**) Cells were treated as in (**b**), fixed and assayed for SA-β-Gal activity or (**d**) RNA were prepared and analyzed by RT-qPCR against the indicated genes and normalized with respect to actin. (**e**) HEC-TM cells were treated or not with BAPN every day. After each passage, cells were counted and seeded at the same density. Population doublings are presented. The experiments shown in this figure are representative of at least three independent experiments

Figure 3 Activity of secreted LOX or LOXL2 favors escape from OIS. (**a**) Supernatants of LOX- or LOXL2-expressing HEC-TM cells or of ones containing the empty control vector were concentrated and analyzed by immunoblotting with an anti-flag antibody. (**b**) LOX activity was measured in concentrated supernatants and normalized to 100% for the ctrl cells ($\pm$ S.E.M.). (**c**) HEC-TM cells were treated for 3 days with 4-OHT $+/-$ BAPN together with the indicated supernatant, PFA-fixed and crystal violet-stained to measure cell growth on d3, and (**d**) assayed for SA-β-Gal activity on d3. The experiments shown in this figure are representative of at least three independent experiments

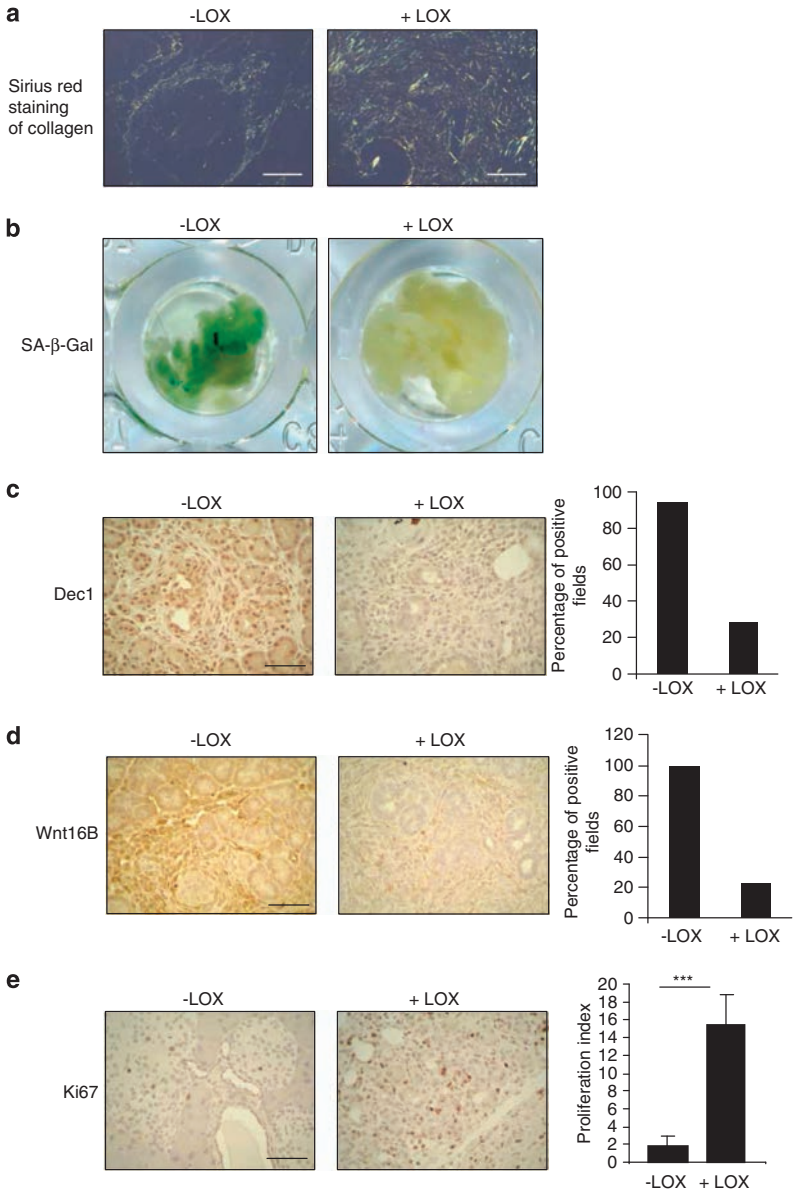

Figure 5 LOX activity favors escape from senescence *in vivo* in a model of PDAC. Pdx1-Cre;LSL-Kras$^{G12D/+}$; Ink4a/Arf$^{lox/lox}$ (KIA) mice were injected with concentrated LOX or control supernatant every day from day 23 after birth. Mice were killed 39 days after birth and their pancreases fixed before analysis. (**a**) A Sirius red staining of collagen was performed at the indicated times. Collagen fiber organization is illustrated by pictures made by polarized light microscopy (scale bar: 200 μm). (**b**) SA-β-Gal assays were performed on pancreas samples at the indicated times. (**c**) IHC performed against the Dec1 senescence marker. (**d**) IHC against the Wnt16B senescence marker. (**e**) IHC against the Ki67 proliferation marker. For (**c**–**e**) Scale bar: 50 μm

LOX activity impacts OIS by modulating FAK activity. LOX activity is reported in various contexts to impact FAK activity.[19,24,27,31–33] We thus investigated *in vitro* and *in vivo* whether FAK might have a role in regulating senescence. *In vitro*, the level of P-FAK (FAK^{Y397}) was found to decrease during OIS (Figure 7a), and this decrease was sustained by LOX activity inhibition (Figure 7b). *In vivo*, the level of P-FAK was found to increase in the pancreases of LOX-injected KIA mice (Figure 7c) and to decrease in those of KIA mice when LOX activity was inhibited by BAPN treatment (Figure 7d).

That FAK signaling affects OIS stability is further supported by the observation that sub-cytostatic doses of two FAK inhibitors (FAK Inhibitor 14 and PF 573228) inhibited growth resumption (Figure 8a) and sustained senescence markers (Figures 8b and c). To determine whether FAK activation might allow cells to escape from 4-OHT/BAPN-induced irreversible senescence, we used HEC-TR cells expressing a constitutively active form of FAK (Figure 8d). After 4-OHT/BAPN treatment, the ability of these cells to form colonies (Figure 8e) and their decreased levels of senescence markers

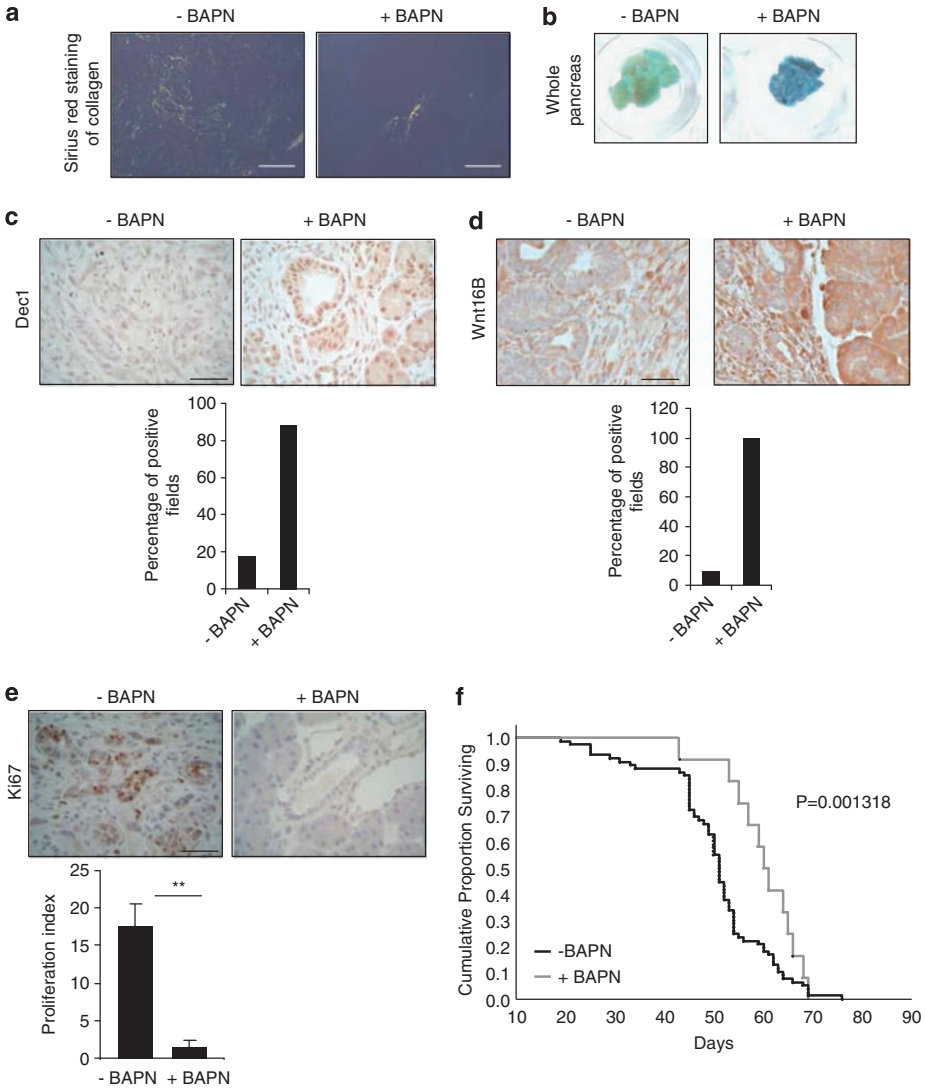

Figure 6 LOX inhibition stabilizes senescence and delays carcinogenesis *in vivo*. Pdx1-Cre;LSL-Kras$^{G12D/+}$;Ink4a/Arf$^{lox/lox}$ (KIA) mice were injected or not with BAPN, three times a week from day 25 after birth. Mice were killed 45 days after birth and their pancreases fixed before analysis. (**a**) Sirius red staining of collagen was performed and representative photographs obtained by polarized light microscopy are displayed (scale bar: 200 μm). (**b**) SA-β-Gal assays were performed on pancreas samples at the indicated times. (**c**) IHC against the Dec1 senescence marker. (**d**) IHC against the Wnt16B senescence marker. (**e**) IHC against the Ki67 proliferation marker. For (**c**–**e**) scale bar: 50 μm. (**f**) KIA mice were injected ($n = 12$) or not ($n = 75$) with the LOX inhibitor BAPN. Kaplan–Meier analyses of the probability to survive were performed. *P*-values were calculated using a log rank test

(Figures 8f and g) showed that they could escape from treatment-induced irreversible senescence even when LOX activity was inhibited. These data constitute compelling evidence that LOX activity influences OIS by regulating FAK signaling.

Discussion

Little is known about pathways, other than the p16-Rb and the p53 pathways, that might participate in controlling OIS. Here we show that LOX activity has a role in regulating escape from OIS, as this escape is triggered when LOX activity is increased by constitutive LOX or LOXL2 expression or by treating cells with secreted LOX or LOXL2.

Interestingly, HEC-TM cells show spontaneous escape from OIS. This instability of senescence might be due to loss of p16^{INK4a} resulting from methylation of its promoter,[16] as a decreased p16 level is reported to possibly favor escape from senescence.[35,36] This raises the question of whether the phenomenon we observed is really senescence. We think it is, because (i) the level of SA-β-Gal senescence marker increases, (ii) the levels of other independent senescence markers increase, and (iii) proliferation is blocked as long as the oncogenic stress is sustained. Interestingly, blocking LOX activity in this situation is sufficient to stabilize the growth

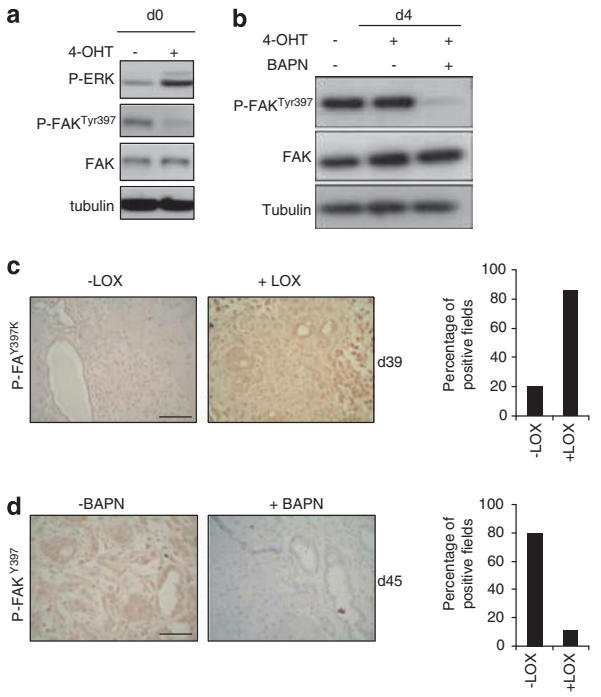

Figure 7 FAK is modulated by LOX activity. (**a**) HEC-TM wells were treated for 3 days with 4-OHT. Cell extracts were prepared and analyzed by immunoblotting with antibodies directed against P-ERK, P-FAK, FAK, and tubulin. (**b**) HEC-TM cells were treated for 3 days with 4-OHT, with or without BAPN. BAPN treatment was carried out for 4 days. Cell extracts were prepared and analyzed by immunoblotting with antibodies directed against P-FAK, FAK, and tubulin. (**c**) Pancreases of mice, 39 days after birth, treated or not with LOX supernatants, were analyzed by IHC with an antibody targeting P-FAK. (**d**) Pancreases of mice, 45 days after birth, treated or not with BAPN, were analyzed by IHC with an antibody targeting P-FAK

arrest and the senescence markers and thus to maintain the senescent phenotype. Importantly, raising or lowering the LOX activity does not affect the proliferation of HEC cells. The growth-promoting effect of LOX activity is observed only in the context of OIS. In our *in vivo* model we have also observed a transient senescent phenotype, possibly due to the lack of p16^{INK4a} expression, and again this phenotype is regulated by LOX activity.

LOX and LOXL2 are reported to be expressed both by epithelial cells and by cells of the tumor microenvironment.[20,31,44] This means that these proteins, although expressed by different cells of different lineages, might impact epithelial cell behavior. To recapitulate the production of LOX and LOXL2 by tumor cells as well as cells of the tumor microenvironment, we have manipulated extracellular LOX and LOXL2 and described their impact on the epithelial cells response to the oncogenic stress.

Like other groups in the context of metastasis, primary tumor growth, or tumorigenesis, we observe an influence of FAK on biological responses to LOX activity.[19,24,27,31–33] We might speculate that the PI3K pathway is a downstream effector of the action of FAK on senescence, as it is known to be regulated by FAK[45] and as it has recently been reported to inhibit senescence induction by activated RAS or RAF in mouse models of melanoma or pancreatic cancer.[46,47] How LOX activity activates FAK remains unclear. Some suggest that activation might be due to ECM stiffening, while others propose that it might be due to the hydrogen peroxide released by intrinsic LOX activity.[19,24,27,31–33]

Altogether, our results support the view that the LOX activity, in addition to the p16^{INK4a} pathway, regulates OIS and might thus affect tumorigenesis.

Materials and Methods

Cell culture. Mammary HECs (Lonza, Barcelona, Spain) were cultured in MEBM (Promocell, Heidelberg, Germany) and penicillin/streptomycin (Life Technologies, Saint Aubin, France). Virus-producing GP293 cells (Clontech, Saint-Germain-en-Laye, France) were cultured in DMEM (Life Technologies) supplemented with 10% FBS (Thermo Fisher Scientific, Waltham, MA, USA) and penicillin/streptomycin. Infected cells were selected, as appropriate, with neomycin (100 μg/ml), puromycin (500 ng/ml), or both.

Reagents and plasmids. Four-hydroxytamoxifen (4-OHT) (Sigma, Lyon, France) was used daily for 3 days at 250 nM final concentration. 3-Aminopropionitrile (fumarate salt) (A3134, Sigma) was used daily at 350 μM final concentration for *in vitro* analysis. FAK inhibitor 14 (3414, Tocris Bioscience, Bristol, UK) and PF 573228 (3239, Tocris Bioscience) were used daily at the following respective final concentrations: 250 nM and 500 nM.

The following plasmids were used: pWZL-Neo-Myr-Flag-FAK (Addgene plasmid 20610, Cambridge, MA, USA),[48] pBabe-hygro-hTert (Addgene plasmid 1773),[49] pBAbe-puro-Raf:ER,[50] pNLP-Neo-Mek:ER.[3] For LOX and LOXL2 cloning, the C-terminally FLAG-tagged mouse LOX and LOXL2 cassettes were amplified by PCR with PFU (Agilent Technologies, Les Ulis, France)[44] and introduced into the pLPCX vector (Clontech) between the *Not*I and *Cla*I sites. Catalytically inactive LOX was created by PCR site-directed mutagenesis to introduce the inactive mutations K314A and Y349F, as previously described[51] and cloned into pLPCX vector as indicated above.

Transfection and infection. GP293 cells were transfected with PEI reagent according to the manufacturer's recommendations (Euromedex, Souffelweyersheim, France). Two days after transfection, target HECs were infected with viral supernatant mixed with fresh medium (1/2) and polybrene (final concentration: 8 μg/ml).

Antibodies. The antibodies used were: anti-phosphoERK (9101, Cell Signaling, Danvers, MA, USA), anti-phosphoFAKTyr397 (3283, Cell Signaling, 44624G, Life Technologies), anti-FAK (3285, Cell Signaling), anti-flag (200472, Agilent Technologies), anti-phosphohistone3Ser10 (ab14955, Abcam, Paris, France), anti-cyclinA (H432, sc-751, Santa Cruz Biotechnology, Heidelberg, Germany), anti-Ki67 (clone Tec-3, M7249, DAKO, Les Ulis, France), and anti-tubulin (T6199, Sigma), WNT16B (LS-A9630, MBL, Nanterre, France).

Cell growth assays. Fifteen thousand cells were seeded into six-well plates and treated or not with the indicated compound(s). At the end of the experiments, cells were fixed with 4% PFA for 15 min, washed with water, and stained with a crystal violet solution (Sigma).

LOX activity assays. Activity assays for detection of BAPN-inhibitable LOX enzyme activity were performed with the Amplex Red Monoamine Oxidase Assay Kit (A12214, Molecular Probes, Life Technologies, Saint Aubin, France). Briefly, conditioned cell medium was concentrated with Amicon 10-kDa cutoff filters (Millipore, Darmstadt, Germany). Aliquots were added to the final reaction mix containing 100 μM Amplex Red, 0.5 U/ml horseradish peroxidase, 2 mM benzylamine substrate and incubated for 1 h. The fluorescent product was excited at 560 nm and the emission was read at 590 nm. Parallel assays were prepared with 500 μM BAPN to completely inhibit the activity of LOX, and the difference in emission intensity was recorded. Assays were run in quintuplicate and specific activity is reported as a mean of all assays.

RT-qPCR. Cells were lysed in TriReagent (Sigma) and total RNAs were isolated via an acidphenol extraction procedure using Phase Lock gel tubes (5′). RNA (2 μg) was reverse-transcribed with the First-Strand cDNA Synthesis Kit (GE Healthcare, Velizy-Villacoublay, France) according to the manufacturer's

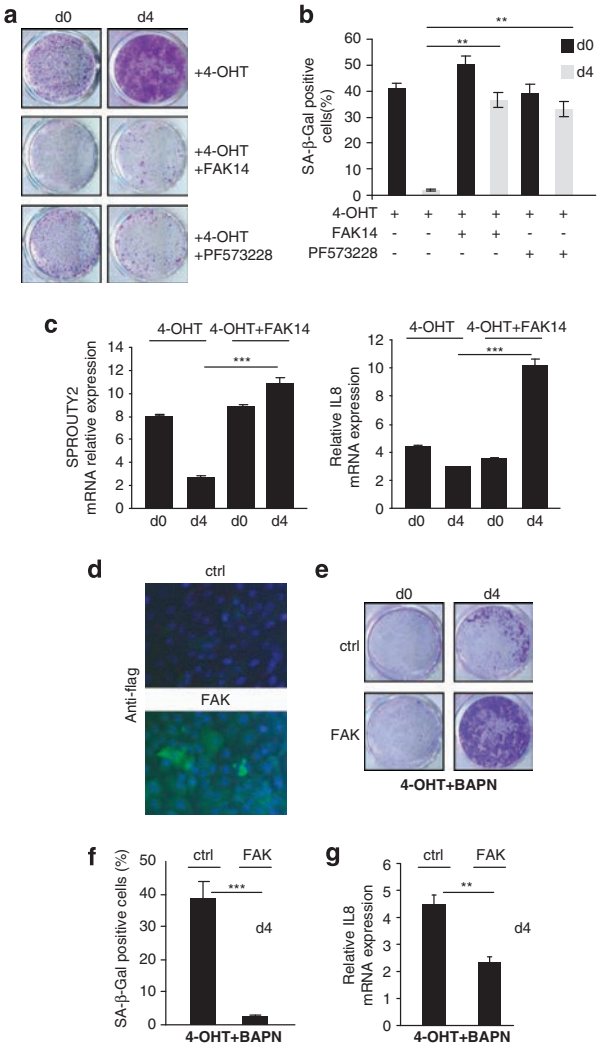

Figure 8 FAK activity participates in senescence modulation by LOX activity. (**a**) HEC-TM cells were treated with 4-OHT, with or without FAK inhibitors, for 3 days and then cultured for an additional 4 days with or without the indicated FAK inhibitors (d4), fixed, and crystal violet-stained. (**b**) Cells were fixed and their SA-β-Gal activity assayed on d0 and d4. (**c**) RNA was prepared and RT-qPCR was performed against senescence markers. (**d**) HEC-TR cells were infected with a FAK-encoding or an empty control retroviral vector and neomycin-selected. Immunofluorescence against the Flag tag was performed. (**e**) Selected cells were treated with 4-OHT + BAPN for 3 days (d0) and with BAPN for 4 additional days (d4). Cells were next fixed, crystal violet-stained, and (**f**) assayed for SA-β-Gal activity, or (**g**) RNAs were prepared and RT-qPCR performed on a senescence marker

directions. Q-PCR experiments were carried out in a Light Cycler 2.0 instrument, in Light Cycler Taqman Master Mix (Roche, Meylan, France) and with the Universal Probe Library (Roche Diagnostics, Meylan, France). The following primers were used: IL-8 5′-AGACAGCAGAGCACACAAGC-3′ and 5′-ATGGTTCCTTCC GGTGGT-3′, SPROUTY2 5′-TTTGCACATCGCAGAAAGAA-3′ and 5′-TCA GGTCTTGGAAGTGTGGTC-3′, LOX 5′-GGATACGGCACTGGCTACTT-3′ and 5′-GACGCCTGGATGTAGTAGGG-3′, LOXL1 5′-GCATGCACCTCTCATACCC-3′ and 5′-CAGTCGATGTCCGCATTGTA-3′, LOXL2 5′-TGACCTGCTGAACCT CAATG-3′ and 5′-TGGCACACTCGTAATTCTTCTG-3′. The actin gene was used as a normalizer, with the 5′-ATTGGCAATGAGCGGTTC-3′ and 5′-GGATGCCAC AGGACTCCAT-3′ primers.

Mouse engineering and treatment. By crossing Pdx1-Cre;Ink4a/Arf$^{lox/lox}$ (no phenotype) with LSL-Kras$^{G12D/+}$; Ink4a/Arf$^{lox/lox}$ (no phenotype) individuals, we 'routinely' generate Pdx1-Cre;LSL-Kras$^{G12D/+}$; Ink4a/Arf$^{lox/lox}$ animals (representing 25% of the total progeny according to the expected Mendelian inheritance) developing macroscopic pancreatic cancer at the frequency of 100% by the age of 6–7 weeks. Mice were treated by intraperitoneal injection of BAPN (100 mg/kg, dissolved in saline) or vehicle three times a week (half) or every day (half). Conditioned cell media from ctrl, LOX-expressing, or LOXL2-expressing cells were concentrated as described, and 100 μl of either ctrl supernatant or of a mix of 50 μl LOX supernatant and 50 μl LOXL2 supernatant was injected intraperitoneally every day for the indicated time. The experiments were performed in accordance with the animal care guidelines of the European Union and French laws and were validated by the local Animal Ethic Evaluation Committee (CECCAPP).

SA-β-Gal analysis. Senescence-associated β-galactosidase activity was assayed in HECs and on pancreatic sections fixed and stained with the Senescence Beta-galactosidase Kit (Cell Signaling) as recommended by the manufacturer.

Histology and sirius red staining. Pancreatic sections (4–5 μm) were stained with HPS. For immunohistochemical analysis, paraffin-embedded murine pancreatic tumor tissues were used. Slides were serially sectioned at 4-μm thickness. After deparaffinization and rehydration, the slides were incubated in 5% hydrogen peroxide in sterile water to block endogenous peroxidases. For heat-induced antigen retrieval, tissue sections were boiled in 10 mmol/l citrate buffer pH6 in a microwave oven for 20 min. The slides were then incubated at room temperature for 1 hour with the primary antibody diluted in 'low-background' antibody diluent (DAKO Real). After rinsing in PBS, the slides were incubated with a biotinylated secondary antibody bound to a streptavidin peroxidase conjugate (Dako E0468) for 1 hour at room temperature. Bound antibody was revealed and sections were finally counterstained with hematoxylin.

Paraffin-treated sections of pancreas were stained for 1 hour in 0.1% picrosirius red solution (Direct Red 80, 365548, Sigma) in picric acid solution (P6744, Sigma), washed twice with acidified water, and then mounted in Eukitt quick-hardening mounting medium (03989, Sigma). Samples were analyzed upon polarized light microscopy.

Statistical analysis. The values are presented as mean ± S.D. unless stated otherwise. Statistical analysis were performed using the Student's *t*-test (*$P<0.05$, **<0.01, ***<0.001). The number of independent replicates for each experiment was indicated in the figure legends. Survival of the mice was analyzed using a Kaplan–Meier method. *P*-values were calculated using a log-rank test.

Conflict of Interest

The authors declare no conflict of interest.

Acknowledgements. We thank members of the laboratory I Puisieux and P Sommer for helpful discussions, and we also thank S Léon, B Kaniewski, S Martel, and M Ferrand for technical assistance. This work was carried out with the support of the 'RTRS Fondation Synergie Lyon Cancer', the 'Association pour la Recherche sur le Cancer', the 'Fondation de France', and the 'Institut National du Cancer'.

1. Serrano M, Lin AW, McCurrach ME, Beach D, Lowe SW. Oncogenic ras provokes premature cell senescence associated with accumulation of p53 and p16INK4a. *Cell* 1997; **88**: 593–602.
2. Chen Z, Trotman LC, Shaffer D, Lin HK, Dotan ZA, Niki M *et al.* Crucial role of p53-dependent cellular senescence in suppression of Pten-deficient tumorigenesis. *Nature* 2005; **436**: 725–730.
3. Collado M, Gil J, Efeyan A, Guerra C, Schuhmacher AJ, Barradas M *et al.* Tumour biology: Senescence in premalignant tumours. *Nature* 2005; **436**: 642.
4. Michaloglou C, Vredeveld LC, Soengas MS, Denoyelle C, Kuilman T, van der Horst CM *et al.* BRAFE600-associated senescence-like cell cycle arrest of human naevi. *Nature* 2005; **436**: 720–724.
5. Acosta JC, O'Loghlen A, Banito A, Guijarro MV, Augert A, Raguz S *et al.* Chemokine Signaling via the CXCR2 Receptor Reinforces Senescence. *Cell* 2008; **133**: 1006–1018.
6. Kuilman T, Michaloglou C, Vredeveld LCW, Douma S, van Doorn R, Desmet CJ *et al.* Oncogene-induced senescence relayed by an interleukin-dependent inflammatory network. *Cell* 2008; **133**: 1019–1031.

7. Sun P, Yoshizuka N, New L, Moser BA, Li Y, Liao R *et al.* PRAK is essential for ras-induced senescence and tumor suppression. *Cell* 2007; **128**: 295–308.
8. Wajapeyee N, Serra RW, Zhu X, Mahalingam M, Green MR. Oncogenic BRAF induces senescence and apoptosis through pathways mediated by the secreted protein IGFBP7. *Cell* 2008; **132**: 363–374.
9. Christoffersen NR, Shalgi R, Frankel LB, Leucci E, Lees M, Klausen M *et al.* p53-independent upregulation of miR-34a during oncogene-induced senescence represses MYC. *Cell Death Differ* 2010; **17**: 236–245.
10. Ewald JA, Desotelle JA, Wilding G, Jarrard DF. Therapy-induced senescence in cancer. *J Natl Cancer Inst* 2010; **102**: 1536–1546.
11. Humbert N, Navaratnam N, Augert A, Da Costa M, Martien S, Wang J *et al.* Regulation of ploidy and senescence by the AMPK-related kinase NUAK1. *EMBO J* 2010; **29**: 376–386.
12. Lin HK, Chen Z, Wang G, Nardella C, Lee SW, Chan CH *et al.* Skp2 targeting suppresses tumorigenesis by Arf-p53-independent cellular senescence. *Nature* 2010; **464**: 374–379.
13. Scurr LL, Pupo GM, Becker TM, Lai K, Schrama D, Haferkamp S *et al.* IGFBP7 is not required for B-RAF-induced melanocyte senescence. *Cell* 2010; **141**: 717–727.
14. Cipriano R, Kan CE, Graham J, Danielpour D, Stampfer M, Jackson MW. TGF-beta signaling engages an ATM-CHK2-p53-independent RAS-induced senescence and prevents malignant transformation in human mammary epithelial cells. *Proc Natl Acad Sci USA* 2011; **10**: 8668–8673.
15. Bianchi-Smiraglia A, Nikiforov MA. Controversial aspects of oncogene-induced senescence. *Cell Cycle* 2012; **11**: 4147–4151.
16. Kiyono T, Foster SA, Koop JI, McDougall JK, Galloway DA, Klingelhutz AJ. Both Rb/p16INK4a inactivation and telomerase activity are required to immortalize human epithelial cells. *Nature* 1998; **396**: 84–88.
17. Csiszar K. Lysyl oxidases: a novel multifunctional amine oxidase family. *Prog Nucleic Acid Res Mol Biol* 2001; **70**: 1–32.
18. Lucero HA, Kagan HM. Lysyl oxidase: an oxidative enzyme and effector of cell function. *Cell Mol Life Sci* 2006; **63**: 2304–2316.
19. Baker AM, Bird D, Lang G, Cox TR, Erler JT. Lysyl oxidase enzymatic function increases stiffness to drive colorectal cancer progression through FAK. *Oncogene* 2013; **32**: 1863–1868.
20. Barker HE, Chang J, Cox TR, Lang G, Bird D, Nicolau M *et al.* LOXL2-mediated matrix remodeling in metastasis and mammary gland involution. *Cancer Res* 2011; **71**: 1561–1572.
21. Herranz N, Dave N, Millanes-Romero A, Morey L, Diaz VM, Lorenz-Fonfria V *et al.* Lysyl oxidase-like 2 deaminates lysine 4 in histone H3. *Mol Cell* 2012; **46**: 369–376.
22. Peinado H, Del Carmen Iglesias-de la Cruz M, Olmeda D, Csiszar K, Fong KS, Vega S *et al.* A molecular role for lysyl oxidase-like 2 enzyme in snail regulation and tumor progression. *EMBO J* 2005; **24**: 3446–3458.
23. Vadasz Z, Kessler O, Akiri G, Gengrinovitch S, Kagan HM, Baruch Y *et al.* Abnormal deposition of collagen around hepatocytes in Wilson's disease is associated with hepatocyte specific expression of lysyl oxidase and lysyl oxidase like protein-2. *J Hepatol* 2005; **43**: 499–507.
24. Erler JT, Bennewith KL, Nicolau M, Dornhofer N, Kong C, Le QT *et al.* Lysyl oxidase is essential for hypoxia-induced metastasis. *Nature* 2006; **440**: 1222–1226.
25. Erler JT, Bennewith KL, Cox TR, Lang G, Bird D, Koong A *et al.* Hypoxia-induced lysyl oxidase is a critical mediator of bone marrow cell recruitment to form the premetastatic niche. *Cancer Cell* 2009; **15**: 35–44.
26. Bondareva A, Downey CM, Ayres F, Liu W, Boyd SK, Hallgrimsson B *et al.* The lysyl oxidase inhibitor, beta-aminopropionitrile, diminishes the metastatic colonization potential of circulating breast cancer cells. *PLoS One* 2009; **4**: e5620.
27. Baker AM, Cox TR, Bird D, Lang G, Murray GI, Sun XF *et al.* The role of lysyl oxidase in SRC-dependent proliferation and metastasis of colorectal cancer. *J Natl Cancer Inst* 2011; **103**: 407–424.
28. Barry-Hamilton V, Spangler R, Marshall D, McCauley S, Rodriguez HM, Oyasu M *et al.* Allosteric inhibition of lysyl oxidase-like-2 impedes the development of a pathologic microenvironment. *Nat Med* 2010; **16**: 1009–1017.
29. Pez F, Dayan F, Durivault J, Kaniewski B, Aimond G, Le Provost GS *et al.* The HIF-1-inducible lysyl oxidase activates HIF-1 via the Akt pathway in a positive regulation loop and synergizes with HIF-1 in promoting tumor cell growth. *Cancer Res* 2011; **71**: 1647–1657.
30. Lee GH, Kim DS, Chung MJ, Chae SW, Kim HR, Chae HJ *et al.* Lysyl oxidase-like-1 enhances lung metastasis when lactate accumulation and monocarboxylate transporter expression are involved. *Oncol Lett* 2011; **2**: 831–838.
31. Levental KR, Yu H, Kass L, Lakins JN, Egeblad M, Erler JT *et al.* Matrix crosslinking forces tumor progression by enhancing integrin signaling. *Cell* 2009; **139**: 891–906.
32. Payne SL, Fogelgren B, Hess AR, Seftor EA, Wiley EL, Fong SF *et al.* Lysyl oxidase regulates breast cancer cell migration and adhesion through a hydrogen peroxide-mediated mechanism. *Cancer Res* 2005; **65**: 11429–11436.
33. Peng L, Ran YL, Hu H, Yu L, Liu Q, Zhou Z *et al.* Secreted LOXL2 is a novel therapeutic target that promotes gastric cancer metastasis via the Src/FAK pathway. *Carcinogenesis* 2009; **30**: 1660–1669.
34. Trost TM, Lausch EU, Fees SA, Schmitt S, Enklaar T, Reutzel D *et al.* Premature senescence is a primary fail-safe mechanism of ERBB2-driven tumorigenesis in breast carcinoma cells. *Cancer Res* 2005; **65**: 840–849.
35. Beausejour CM, Krtolica A, Galimi F, Narita M, Lowe SW, Yaswen P *et al.* Reversal of human cellular senescence: roles of the p53 and p16 pathways. *EMBO J* 2003; **22**: 4212–4222.
36. Takahashi A, Ohtani N, Yamakoshi K, Iida S, Tahara H, Nakayama K *et al.* Mitogenic signalling and the p16INK4a-Rb pathway cooperate to enforce irreversible cellular senescence. *Nat Cell Biol* 2006; **8**: 1291–1297.
37. Courtois-Cox S, Genther Williams SM, Reczek EE, Johnson BW, McGillicuddy LT, Johannessen CM *et al.* A negative feedback signaling network underlies oncogene-induced senescence. *Cancer Cell* 2006; **10**: 459–472.
38. Tang SS, Trackman PC, Kagan HM. Reaction of aortic lysyl oxidase with beta-aminopropionitrile. *J Biol Chem* 1983; **258**: 4331–4338.
39. Tang SS, Chichester CO, Kagan HM. Comparative sensitivities of purified preparations of lysyl oxidase and other amine oxidases to active site-directed enzyme inhibitors. *Connect Tissue Res* 1989; **19**: 93–103.
40. Wilmarth KR, Froines JR. In vitro and in vivo inhibition of lysyl oxidase by aminopropionitriles. *J Toxicol Environ Health* 1992; **37**: 411–423.
41. Welsch T, Kleeff J, Friess H. Molecular pathogenesis of pancreatic cancer: advances and challenges. *Curr Mol Med* 2007; **7**: 504–521.
42. Bardeesy N, Sharpless NE, DePinho RA, Merlino G. The genetics of pancreatic adenocarcinoma: a roadmap for a mouse model. *Semin Cancer Biol* 2001; **11**: 201–218.
43. Hingorani SR, Petricoin EF, Maitra A, Rajapakse V, King C, Jacobetz MA *et al.* Preinvasive and invasive ductal pancreatic cancer and its early detection in the mouse. *Cancer Cell* 2003; **4**: 437–450.
44. Lelievre E, Hinek A, Lupu F, Buquet C, Soncin F, Mattot V. VE-statin/egfl7 regulates vascular elastogenesis by interacting with lysyl oxidases. *EMBO J* 2008; **27**: 1658–1670.
45. Hanks SK, Ryzhova L, Shin NY, Brabek J. Focal adhesion kinase signaling activities and their implications in the control of cell survival and motility. *Front Biosci* 2003; **8**: d982–d996.
46. Kennedy AL, Morton JP, Manoharan I, Nelson DM, Jamieson NB, Pawlikowski JS *et al.* Activation of the PIK3CA/AKT pathway suppresses senescence induced by an activated RAS oncogene to promote tumorigenesis. *Mol Cell* 2011; **42**: 36–49.
47. Vredeveld LC, Possik PA, Smit MA, Meissl K, Michaloglou C, Horlings HM *et al.* Abrogation of BRAFV600E-induced senescence by PI3K pathway activation contributes to melanomagenesis. *Genes Dev* 2012; **26**: 1055–1069.
48. Boehm JS, Zhao JJ, Yao J, Kim SY, Firestein R, Dunn IF *et al.* Integrative genomic approaches identify IKBKE as a breast cancer oncogene. *Cell* 2007; **129**: 1065–1079.
49. Counter CM, Hahn WC, Wei W, Caddle SD, Beijersbergen RL, Lansdorp PM *et al.* Dissociation among in vitro telomerase activity, telomere maintenance, and cellular immortalization. *Proc Natl Acad Sci USA* 1998; **95**: 14723–14728.
50. Woods D, Parry D, Cherwinski H, Bosch E, Lees E, McMahon M. Raf-induced proliferation or cell cycle arrest is determined by the level of Raf activity with arrest mediated by p21Cip1. *Mol Cell Biol* 1997; **17**: 5598–5611.
51. Wang SX, Mure M, Medzihradszky KF, Burlingame AL, Brown DE, Dooley DM *et al.* A crosslinked cofactor in lysyl oxidase: redox function for amino acid side chains. *Science* 1996; **273**: 1078–1084.

Cell Death and Disease **is an open-access journal published by** ***Nature Publishing Group*****. This work is licensed under a Creative Commons Attribution-NonCommercial-ShareAlike 3.0 Unported License. To view a copy of this license, visit http://creativecommons.org/licenses/by-nc-sa/3.0/**

Supplementary Information accompanies this paper on Cell Death and Disease website (http://www.nature.com/cddis)

Supplementary Figure Legends

Supplementary Figure 1 Lox expression in HEC-TM cells. HEC-TM RNAs were prepared and transcript-level expression of the various LOX genes was analyzed by RTqPCR.

Supplementary Figure 2 A catalytically inactive mutant of Lox loses its ability to induce escape from OIS. Supernatants of empty ctrl, Lox, and Lox Y349F-K314A HEC-TM cells were concentrated and analyzed (**a**) by immunoblotting with an anti-flag antibody, (**b**) by measuring the LOX activity. (**c**) HEC-TM cells were treated for 3 days with 4-OHT together with the indicated supernatant, PFA fixed, and crystal violet stained to measure cell growth on d0 and d5. Experiments were performed at least 3 times.

Supplementary Figure 3 LOX activity inhibition blocks escape from OIS. (**a**) Schematic representation of the protocol of treatment with 4-OHT with or without BAPN. (**b**) HEC-TM cells were treated as indicated. Cells were fixed and crystal violet stained or (**c**) their SA-β-Gal activity was assayed.

Supplementary Figure 4 A transgenic mouse model of Kras-induced PDAC displays some senescence. Pdx1-Cre; LSL-Kras$^{G12D/+}$; INK4a/Arf$^{lox/lox}$ (KIA) and control Pdx1-Cre; INK4a/Arf$^{lox/lox}$ (WT) mice were used. (**a**) Pancreatic RNA was prepared and expression of the various Lox proteins was analyzed by RTqPCR using the following primers; Lox Fwd 5'-CAGGCTGCACAATTTCACC-3', Rev 5'-CAAACACCAGGTACGGCTTT-3'; LoxL1 Fwd 5'-TATGCCTGCACCTCTCACAC-3', Rev 5'-TGTCCGCATTGTATGTGTCAT-3'; LoxL2 Fwd 5'-GGCGCTTCCAGACAGAGT-3', Rev 5'-CTCCATCCTTGTCCTGTGCT-3', LoxL3 Fwd 5'-GTGGACCCATAGTGCCAAAT-3', Rev 5'-CAGCTCAGATTGTCCAACCA-3', LoxL4 Fwd 5'-

GGCGTTGCCTGTATGAACA-3', Rev 5'- CCAAGTACGCCGTCTCTTGTA-3'. (**b**) Mice were sacrificed 45 days after birth and macrodissected. Normal and tumoral zones in the KIA mice were extracted. Pancreas samples (WT, WT+BAPN, KIA normal, KIA tumoral) were fixed and their normal/tumoral status was histologically determined by HPS staining. An SA-β-Gal activity assay was used to detect senescence, Ki67 staining to determine the proliferative status, and Sirius staining to visualize collagen organization (scale bar: 200 μm).

Supplementary Figure 5 LOX supernatants were injected by IP into 3 mice per experimental point. At the indicated times, mice were euthanized and their pancreases were extracted and frozen. The pancreases were next ground with a cryogenic mill (Cryotec) and powders were homogenized in RIPA buffer. LOX activity assays were performed with 10 μg protein per sample in duplicate.

Supplementary Figure 1

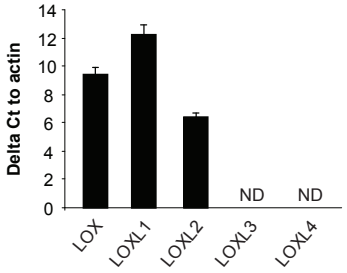

Supplementary Figure 2

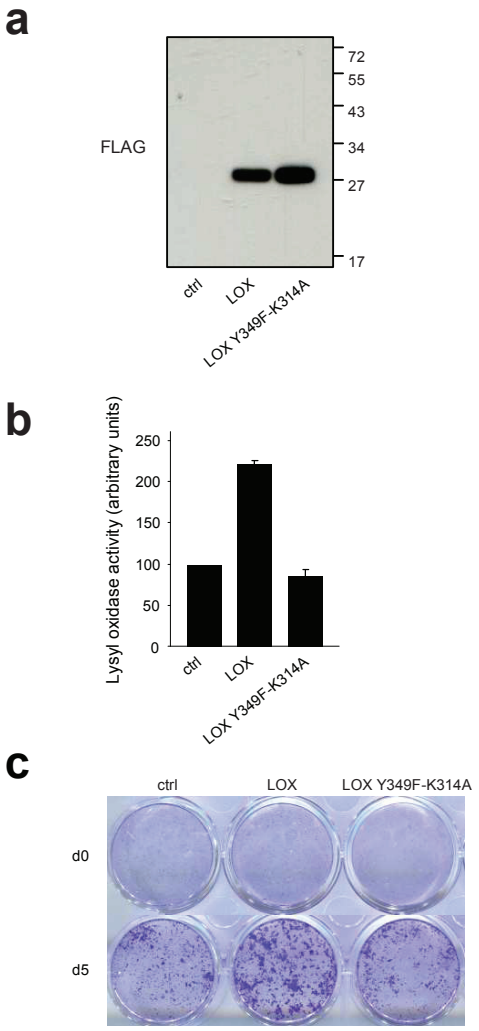

Supplementary Figure 3

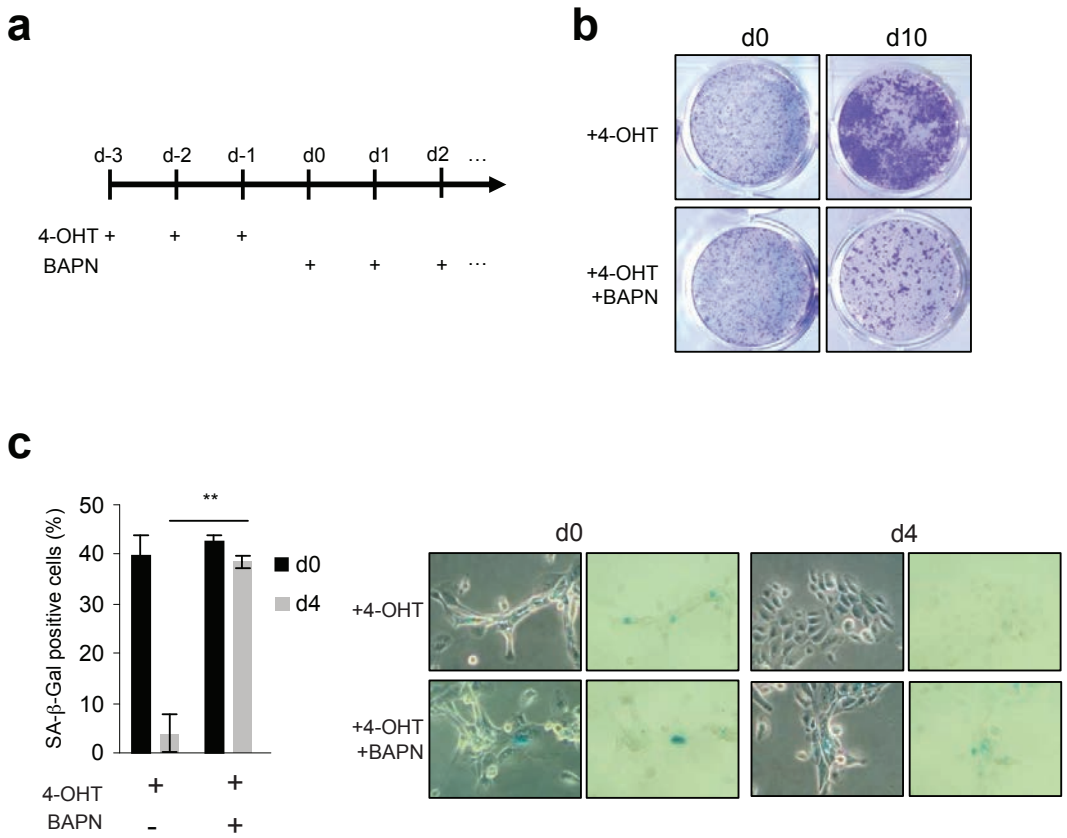

Supplementary Figure 4

a

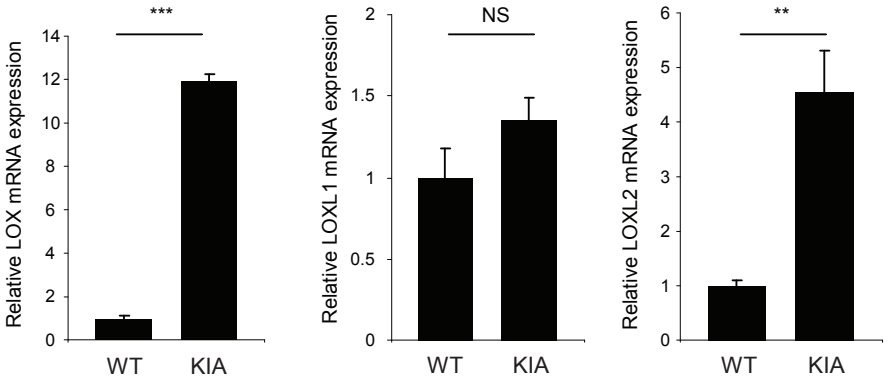

b

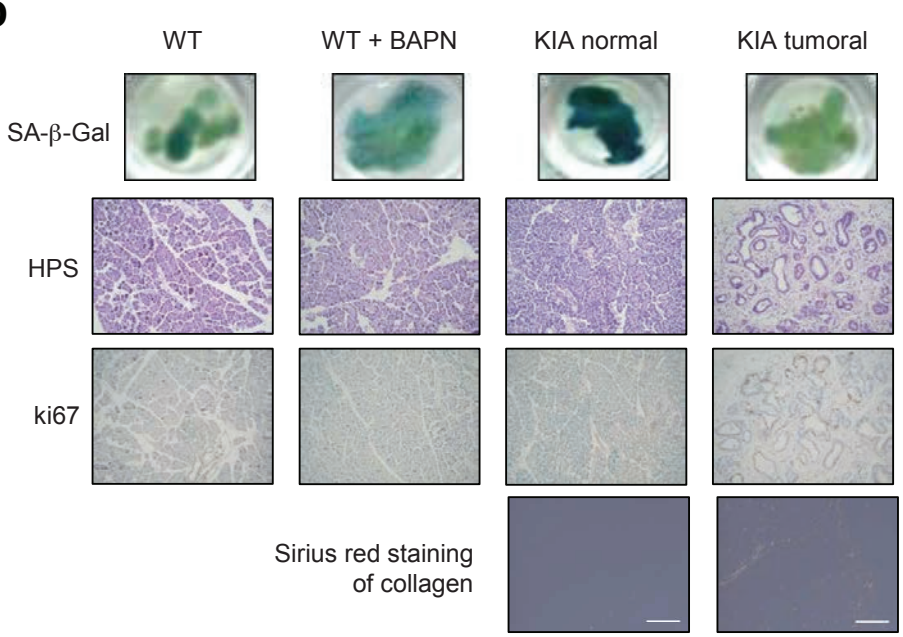

Supplementary Figure 5

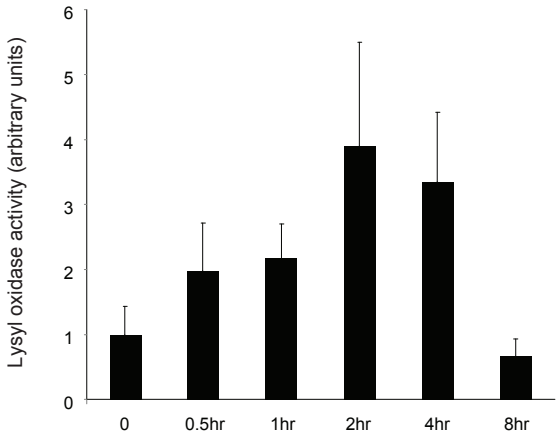

1.3 Résultats supplémentaires

Alors que les études de l'activité lysyl oxydase ne concernaient que des modèles d'invasion et de migration cellulaires, nos résultats, ajoutés aux récents travaux de quelques groupes (Pez *et al.*, 2011; Levental *et al.*, 2009; Barry-Hamilton *et al.*, 2010), renforcent l'idée nouvelle que l'activité Lox peut promouvoir l'initiation tumorale. Ils montrent que les formes secrétées de LOX et LOXL2 peuvent promouvoir l'instabilité de la sénescence favorisant ainsi le développement tumoral.

Nous n'avons pas détecté de variations de l'expression des LOXs mais plutôt une augmentation de leurs activités dans les hMECS soumis à un stress oncogénique. Il serait donc intéressant d'étudier l'impact de cette activité sur l'établissement de la sénescence et plus spécifiquement sur l'échappement à l'OIS observé 6 jours après son induction. Par ailleurs, l'inhibition de l'activité Lox par le BAPN dès l'activation du stress oncogénique ne semble renforcer que légèrement l'entrée en sénescence *(article1, figure 4b, d, jour 0)*. Pour autant, l'inhibition de l'activité Lox une fois une fois la sénescence établie (à partir du jour 0) permet de la stabiliser *(article 1, supplementary figure 3)* suggérant que l'activité Lox modifie l'échappement à la sénescence et non son induction

Bien que les premières données investiguant les niveaux d'expression de LOX ont montré une baisse du taux d'ARNm dans les cancers (Hämäläinen *et al.*, 1995; Parker *et al.*, 2004; Kaneda *et al.*, 2004), il a pourtant été récemment admis que de nombreux cancers sont associés à une augmentation de l'expression de LOX (cancer de sein, pancréas)(Barker *et al.*, 2012). Dans le cas des souris KIA que nous avons utilisées dans notre étude, nous avons pu montrer une augmentation de l'ARNm de LOX et de LOXL2, en comparaison avec des pancréas murins normaux *(article 1, figure supplémentaire 4a)*. Nous retrouvons cette augmentation d'expression au niveau protéique dans les parties tumorales de pancréas des souris KIA *(figure 9)*. De manière très intéressante, l'analyse de pancréas normaux et tumoraux humains a révélé que LOX et LOXL2 sont également surexprimés dans les parties tumorales *(figure 10)*.

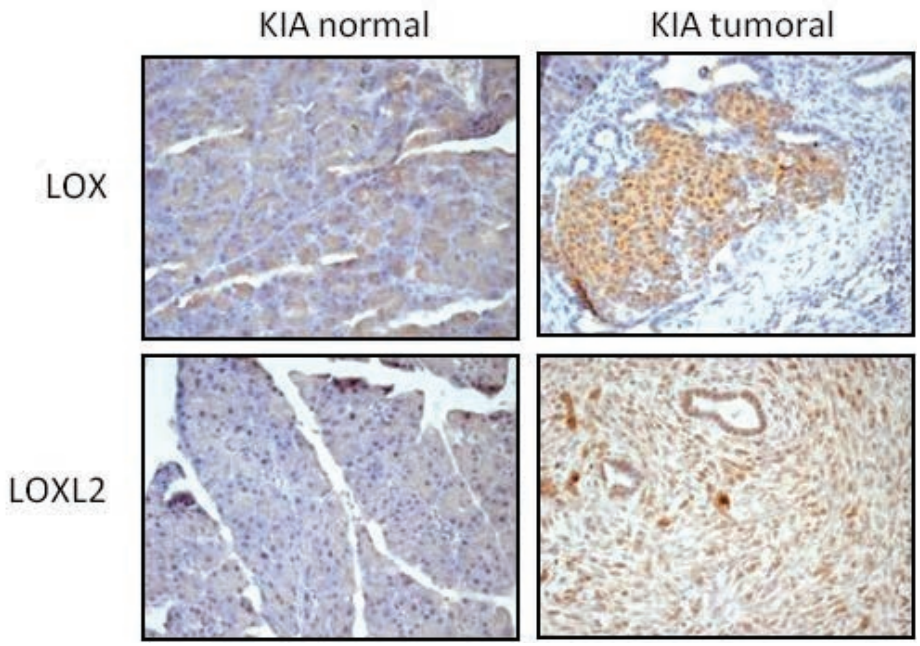

Figure 9 : L'expression de LOX et LOXL2 augmente dans les parties tumorales des souris KIA.

Des IHC contre LOX et LOXL2 ont été faites sur des coupes de pancréas de souris KIA. Des parties représentatives normales et tumorales sont montrées.

KIA : Pdx1-Cre, LSL-Kras$^{G12D/+}$, INK4A/Arf$^{lox/lox}$ mice

Ces informations soulignent l'importance que peut avoir l'activité Lox dans la progression tumorale par l'échappement à la sénescence. L'augmentation de l'expression de LOX et LOXL2 dans le développement des adénocarcinomes du pancréas est corrélée au fait que les PDAC sont l'un des cancers les plus riches en stroma. Le micro-environnement de ces tumeurs comprend des fibroblastes, des cellules stellaires pancréatiques, des cellules immunitaires, des vaisseaux sanguins et des composants de l'ECM tels que le collagène, la fibronectine, des protéoglycannes, l'acide hyaluronique, des enzymes (comme LOX et LOXL2) ainsi que des protéases. Ce micro-environnement est d'autant plus important que sa composition évolue avec la progression tumorale (Feig *et al.*, 2012). Le nombre élevé de fibroblastes peut en partie expliquer la forte expression de LOX et de LOXL2 puisque ces cellules sécrètent en grande quantité ces enzymes. De plus, plusieurs études indiquent que les tumeurs pancréatiques sont très hypoxiques (Shibaji *et al.*, 2003; Kitada *et al.*, 2003; Hiraoka *et al.*, 2010). La pression partielle en oxygène dans différentes parties de pancréas issues de sept patients atteints de PDAC (normales ou tumorales) a été mesurée. Leurs résultats montrent une forte diminution du pourcentage d'oxygène dans les tissus tumoraux (Koong *et al.*, 2000) par rapport aux tissus sains adjacents. Etant donné que LOX et LOXL2 sont des cibles du facteur de transcription HIF1, leur surexpression est directement liée à la présence d'hypoxie.

Nous avons également montré que l'inhibition de la voie PI3K-AKT permet de stabiliser l'OIS dans les cellules épithéliales mammaires humaines *(figure 11)*. Ce point sera discuté plus longuement dans la partie discussion.

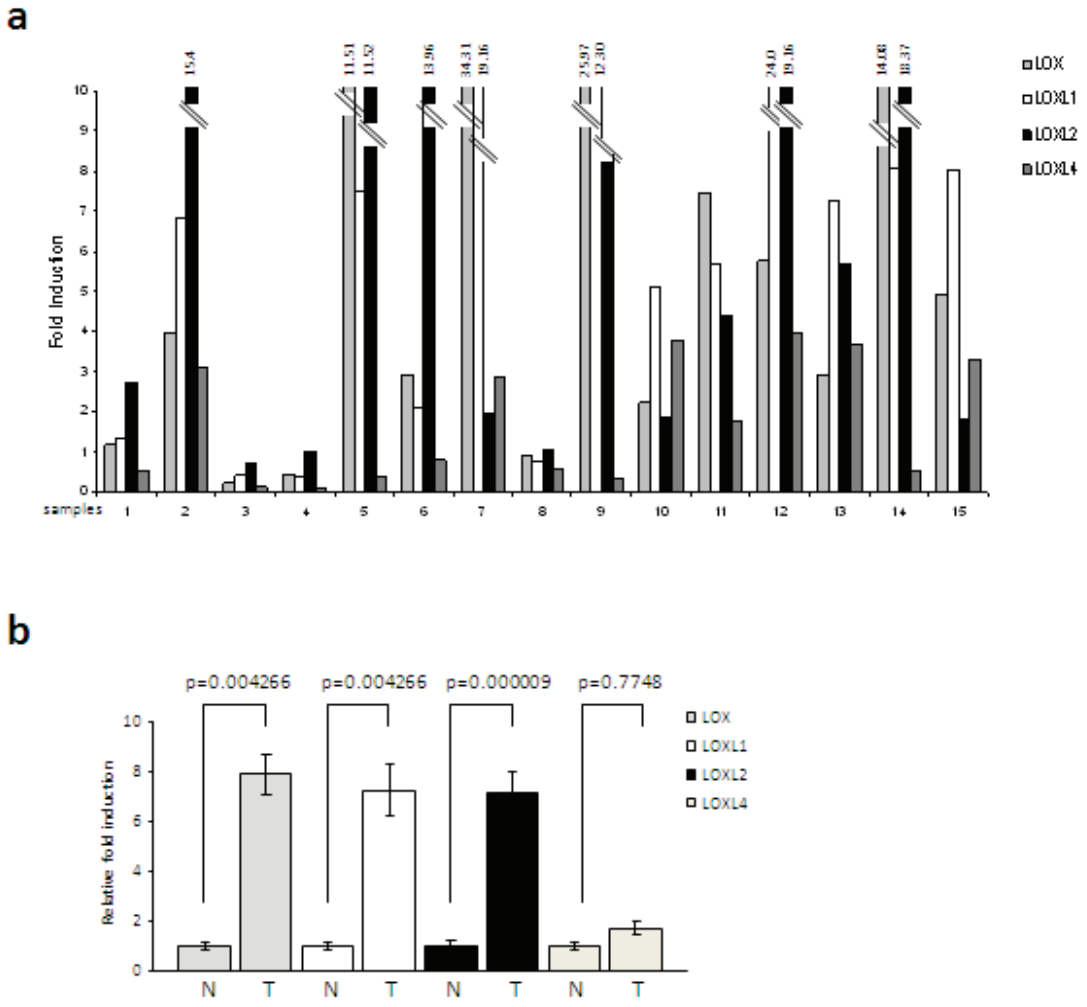

Figure 10 : L'expression de LOX, LOXL1 et LOXL2 augmente dans les PDAC humains.

(a) Les ARNs de PDAC et de tissus pancréatiques adjacents normaux ont été extraits chez 15 patients (fournis par le centre de ressources biologiques de l'Hôpital Edouard Herriot de Lyon). Les ARNs ont ensuite été rétro-transcrits et une PCR quantitative a permis de déterminer les taux d'expression relatifs de LOX, LOXL1, LOXL2, LOXL3 et LOXL4. LOXL3 n'a pas été détecté.

(b) Moyennes d'induction de LOX, LOXL1, LOXL2 et LOXL4 sont représentées ± SEM. Les P-values ont été déterminées en utilisant un test de Mann-Whitney.

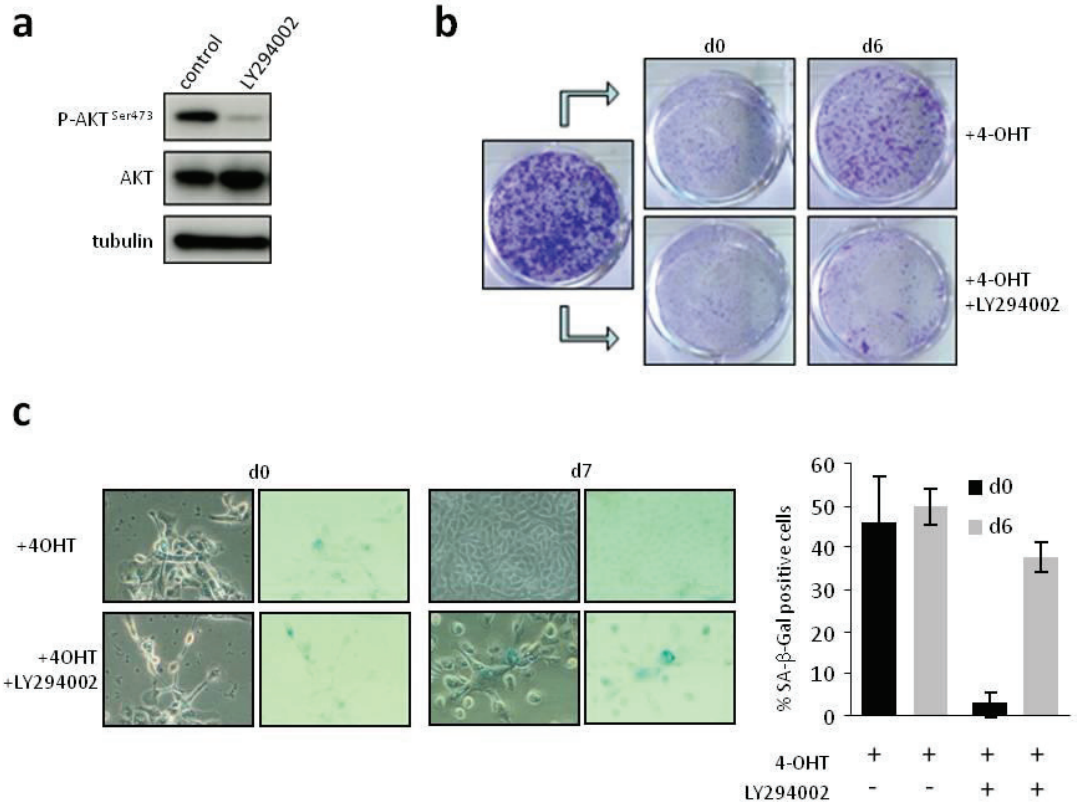

Figure 11 : L'Inhibition de la voie PI3K stabilise la sénescence induite par MEK.

a) Les cellules HEC-TM ont été traitées avec un inhibiteur de PI3K (LY294002).Les extraits cellulaires ont été préprarés et un western blot a été fait contre p-AKT afin de vérifier l'efficacité de l'inhibiteur.

b) Les cellules HEC-TM one été traitées avec du 4-OHT avec ou sans l'inhibiteur de PI3K pendant 3 jours (d0) puis traitées uniquement avec le LY294002 pendant 7 jours supplémentaires (d7). Les cellules ont ensuite été fixées, et colorées au crystal violet, ou c) leur activité SA-β-Gal a été analysée.

1.4 Revue : Lysyl oxidases: emerging promoters of senescence escape, tumor initiation and progression

Cancer Cell & Microenvironment 2014; 1: 51-56.

http://www.smartscitech.com/index.php/ccm

REVIEW

Lysyl oxidases: emerging promoters of senescence escape, tumor initiation and progression

David Bernard[1, 2, 3, 4,*], Clotilde Wiel[1, 2, 3, 4,*]

[1]*INSERM U1052, Centre de Recherche en Cancérologie de Lyon, Lyon, F-69373, France*
[2]*CNRS UMR5286, Lyon, F-69373, France*
[3]*Centre Léon Bérard, Lyon, F-69373, France*
[4]*Université de Lyon, Lyon, F-69373, France*

*These authors contributed equally to this work.
Correspondence: David Bernard
E-mail: david.bernard@lyon.unicancer.fr
Received: March 12, 2014
Published online: July 02, 2014

Lysyl oxidase activity, exhibited by five lox members, has been extensively associated with tumor progression and metastasis. Notably, it is well documented that lox factors, mainly LOX and LOXL2 proteins, are implicated in invasion, cell migration, and angiogenesis in response to tumor-associated hypoxia. In the clinic, their expression correlates with bad prognosis for cancer progression and patient survival. Recently, lox factors have been observed to promote senescence escape, a critical event in tumorigenesis. In two mouse cancer susceptibility models for breast and pancreatic cancer, LOX and/or LOXL2 were found to promote tumorigenesis in cooperation with an oncogenic signal. Mechanistically, lox factors might mediate their effects via several mechanisms; from reorganizing the extracellular matrix and tumor microenvironment, promoting activation of specific pathways such as FAK and Akt pathways, to regulating gene expression by modifying the histone tails on specific target genes such as E-cadherin. This modification impacts the epithelial-mesenchymal transition, a process involved in senescence escape, tumor initiation and progression. The recent literature highlights an important role of lox factors in cancer, and an antibody directed against LOXL2 is already undergoing clinical trials. A better understanding of the biology of these factors will help the design and application of new lox-derived therapeutic tools.

Keywords: LOX; LOXL2; lysyl oxidase; cancer; senescence; metastasis

Cancer Cell & Microenvironment 2014; 1:51-56. doi: 10.14800/ccm.120; © 2014 by Smart Science & Technology, LLC.

Introduction

Aspects of the tumor microenvironment, such as the extracellular matrix (ECM) composition and stiffness, are known to influence tumor progression, yet the ECM can be considerably altered during tumor progression [1]. Lysyl oxidase (lox) activity is a major regulator of ECM stiffness and its enzymatic activity mediates crosslinking of matrix components such as collagen and elastin [2]. The Lox family is composed of 5 members: LOX, LOXL1, LOXL2, LOXL3 and LOXL4, with the five members sharing a strongly conserved C-terminal part, containing the catalytic domain. In contrast, the N-terminal domain is more divergent, suggesting both redundant and different biological functions of these proteins. LOX and LOXL1 are secreted as pro-enzymes, so require cleavage to become fully active, whilst the other members are secreted as active enzymes. Once secreted, they modify ECM structure and stiffness by crosslinking their substrates. In recent years, several studies have been published reporting an intracellular role for LOX and LOXL2 [3–8].

LOX protein was first described, more than 30 years

ago, as a tumor suppressive gene. Indeed, it was first named *the ras recision gene* (*rrg*) because of its ability to counteract RAS-induced transformation. It has since been demonstrated that the propeptide, possessing no enzymatic activity, is responsible for this anti-tumoral property [9,10], due to its pro-apoptotic effect [11]. It is less clear if other LOX members share those, or other, anti-tumoral properties. In the last ten years, some lox family members, including LOX, have emerged as pro-tumoral factors. This review will highlight recent major findings concerning a pro-tumoral activity of lox family members.

Role of lox factors on tumor progression

Local tumor hypoxia occurs in most human tumors [12]. Hypoxia results in an adaptive tumor response in an attempt to overcome the immediate local lack of oxygen and longer term lack of nutrients. This response is mainly induced by the Hypoxia Inducible Factor alpha (HIF) transcription program that provokes changes in tumor metabolism and angiogenesis, as well as an increase in tumor cell migration, invasion and metastasis [13–15]. A major breakthrough in lox cancer biology came from the initial discovery that the LOX protein is directly up-regulated by HIF transcription factors [16]. Besides LOX protein, at least LOXL2 and LOXL4 are also up-regulated during hypoxia, in various biological conditions and sample types [16–18].

Prior to the discovery of a link between hypoxia and lox factors, the Hendrix laboratory had observed that LOX is up-regulated in invasive breast cancer cells [19]. The same laboratory then extended their initial observations by finding highest LOXL1, LOXL2, LOXL3 and LOXL4 levels in breast cancer cells with strong invasive properties. Functionally, constitutive LOX expression results in increased invasive properties, which was reversed by inhibiting lox activity [20]. The increased invasive phenotype induced by LOX was then correlated to hypoxia, hypoxia being a well-known promoter of cell invasion and metastasis [16]. Since then, LOX and LOXL2 have been experimentally shown to promote cell invasion and metastasis in various contexts, including, but not limited to, breast cancers [21,22], gastric cancers [23] and colorectal cancers [24].

Mechanistically, it was demonstrated by Erler and colleagues that LOX secreted by hypoxic cells plays an important function in the formation of pre-metastatic niches. Those niches, composed of proteins and of Bone Marrow-Derived Cells (BMDCs), constitute the perfect environment in which disseminated cells can proliferate and form metastases. Secreted LOX proteins accumulate at distant sites, modify the ECM, and can attract and recruit BMDCs, notably myeloid CD11+b cells [25]. Similarly to LOX in breast cancer models, LOXL2, induced by HIF1alpha, is also able to alter the ECM in lungs, even before the recruitment of BMDCs [26].

Promotion of cancer cell dissemination by lox factors might rely on their ability to promote tumor angiogenesis. Tumor angiogenesis is mainly driven by hypoxic conditions, which boosts the expression of lox factors, and is required to solve oxygen and nutrient shortage in the hypoxic tumor. This complex mechanism involves proliferation and migration of endothelial cells and remodeling of the basal membrane of blood vessels [27] and is coordinated by LOX and LOXL2. This has been reported in various models including using a zebrafish model during capillary formation [28] and in various tumor xenograft models in mice [29,30]. LOX and LOXL2 might impact angiogenesis by regulating endothelial cell proliferation and migration by collagen assembly and scaffolding [28] and by impacting the production of VEGF [30].

The relevance of these functional *in vitro* and *in vivo* experiments in the clinic are strongly supported by numerous independent studies showing a strong link between increased LOX expression/activity with a decrease in both overall and metastasis-free survival [16,20,24,31,32]. Similar observations have been made for LOXL2 [4,22,33–36].

Together, the abundant data produced so far demonstrate an important role of at least LOX and LOXL2 in promoting metastasis formation, with subsequent poor prognosis for cancer evolution and patient survival. This also suggests strong redundancy of at least LOX and LOXL2 proteins in cancer progression.

Role of lox members in tumor initiation

During malignant transformation, ECM composition and structure change significantly, due to abnormal secretion of ECM components by stromal cells and cancer cells, leading to dysfunctional organization. The behavior of normal cells, and evolution of the carcinoma, are affected by these alterations [37]. It is known that increased collagen deposition and enhanced matrix cross-linking stiffen the ECM. The stiffened matrix might promote transformation by activating growth factor pathways or by perturbing tissue integrity [38]. However, the impact of LOX and LOXL proteins on primary tumor growth is contentious, with some reports showing no impact on growth [16,19–21], whilst more recent studies suggested otherwise [39,40]. For example, recent observations demonstrate that lox factors increase the proliferation of colorectal cancer cells *in vitro* and *in vivo* [24,31,39]. Besides the ability of lox factors to promote primary tumor growth, a new concept has emerged: the

involvement of lox factors in cooperating with an oncogenic signal to promote tumor initiation and formation.

Tumor initiation and formation require an oncogenic signal in conjunction with the disabling of intrinsic safeguard mechanisms. Safeguard mechanisms are activated by oncogenic signals and normally result in proliferation arrest and/or cell death. Senescence is activated by the oncogenic signals occurring during tumor initiation and its activation results in proliferation arrest and elimination of these defective cells by the immune system [41–44]. Our recent work shows that lox factors, at least LOX and LOXL2, promote oncogene-induced senescence (OIS) escape in a model of human epithelial cells, suggesting that lox factors cooperate with an oncogenic signal to promote tumorigenesis [45]. In a genetic mouse model of aggressive pancreatic ductal adenocarcinoma (PDAC), we showed that increasing LOX and LOXL2 proteins promote senescence escape, whereas decreasing lox activity stabilizes senescence, delays tumorigenesis and increases mice survival [45]. Previously, the Weaver laboratory observed that the LOX protein cooperates with the Erbb2 oncogene to induce breast tumorigenesis [46], supporting the view that lox factors are able to cooperate with oncogenic signals to promote senescence escape and tumorigenesis.

Together the recent data summarized in this paragraph emphasizes a role of lox factors in the tumorigenesis process, together with its well-known role in tumor progression.

Molecular mechanisms regulated by lox factors and impacting tumor initiation and progression

The well-described role of lox factors in ECM reorganization has now been described to impact the activity of other cellular pathways. ECM stiffness and, in particular, collagen organization has been shown to increase the Src/FAK pathway, possibly through an integrin-dependent manner [16,24,45–47]. Byproducts of lox activity, ie H2O2, might also participate in FAK activation [16,23]. Further studies report an involvement of the PI3K/Akt pathway, possibly in a FAK-dependent manner, in lox factor-mediated promotion of tumor initiation and progression [39,46]. Our unpublished results also suggest that FAK activation by LOX or LOXL2 activates the PI3K /Akt pathway, which can be involved in OIS bypass [48,49]. In addition, the PI3K/Akt pathway is known to promote tumor progression [50,51].

The epithelial-mesenchymal transition (EMT), a process converting epithelial cells into mesenchymal ones, promotes migration and metastasis [52,53] and promotes senescence escape [54]. Importantly, EMT has been linked to PI3K/Akt pathway activation [55] suggesting a link between lox factors, PI3K/Akt pathway and EMT. However, whilst EMT has been shown to be induced by lox factors [4,6,17,40,56], it has not been linked, so far, to the PI3K/Akt pathway. Barry-Hamilton and colleagues reported an activity-dependent effect of LOXL2 on EMT, as extracellular LOXL2 from conditioned media induces an EMT in MCF-7 cells whereas a catalytically-inactive LOXL2 mutant did not. The involvement of the PI3K/Akt pathway in EMT in this study was not investigated [40].

Surprisingly, the intra-cellular lox factors were reported to have most effect on EMT. Notably, several studies have implicated intra-cellular LOXL2 in promoting EMT. It was first shown that LOXL2 was able to interact and stabilize Snail, an embryonic transcription factor activated during EMT. The interaction between Snail and LOXL2 cooperates to repress E-cadherin expression as well as other genes, whose loss is necessary to fully engage an EMT [4,6]. Cano and colleagues subsequently showed that a catalytically inactive LOXL2 mutant was still able to cooperate with Snail to repress E-cadherin expression, and to activate the FAK/Src pathway, both leading to EMT induction [56]. These provocative results challenged the compelling evidence describing lox factors acting through its activity to exert their pro-tumoral activities (see for example [16,24,45–47]).

Emphasizing a role of lox factors as putative transcriptional regulators, earlier studies demonstrated an interaction with, and oxidation of, some histones by lox factors [57,58]. Herranz and colleagues have confirmed that LOXL2 can be located in the nucleus, where it acts as a repressor of E-cadherin expression, although in this case, the repression of E-cadherin was lox activity-dependent. Indeed, they demonstrate that LOXL2 catalytic activity is involved in H3K4 deamination [5]. To date, the numerous available data have led to the conclusion that lox factors mediate pro-tumoral effects through their enzymatic activities. Still, compelling evidence points towards enzyme-independent effects of lox factors on cancer; LOX might mediate an anti-tumoral action through its pro-domain [9,10], whereas the activity-independent activity of LOXL2 retains pro-tumoral action, possibly through the 4 scavenger domains of its N-terminus [4,6,56,59].

Knowledge of the role and mechanism of action of lox factors in cancer is increasing, however we still need to characterize them further, particularly the redundancy and specificity between lox factors, as well as the contribution of the catalytic dependent and independent effects of lox proteins. This is particularly important as a

clinical tool; an mAb directed against LOXL2, is currently undergoing clinical trials for aggressive colon and pancreatic cancers and it could be envisioned that other family members could be targeted for various other forms of cancer.

Acknowledgements

Our work was supported by grants of the Fondation de France, the Fondation ARC and the "Institut National du Cancer" (Transla13-049). CW is supported by the "Ligue national contre le Cancer" and the "Fondation pour la Recherche Médicale"

References

1. Lu P, Weaver VM, Werb Z. The extracellular matrix: a dynamic niche in cancer progression. J Cell Biol 2012; 196:395–406. http://dx.doi.org/10.1083/jcb.201102147 PMid:22351925 PMCid:PMC3283993
2. Lucero H a, Kagan HM. Lysyl oxidase: an oxidative enzyme and effector of cell function. Cell Mol Life Sci 2006; 63:2304–16. http://dx.doi.org/10.1007/s00018-006-6149-9 PMid:16909208
3. Kagan HM, Li W. Lysyl oxidase: properties, specificity, and biological roles inside and outside of the cell. J Cell Biochem 2003; 88:660–72. http://dx.doi.org/10.1002/jcb.10413 PMid:12577300
4. Moreno-Bueno G, Salvador F, Martín A, Floristán A, Cuevas EP, Santos V, et al. Lysyl oxidase-like 2 (LOXL2), a new regulator of cell polarity required for metastatic dissemination of basal-like breast carcinomas. EMBO Mol Med 2011; 3:528–44. http://dx.doi.org/10.1002/emmm.201100156 PMid:21732535 PMCid:PMC3377095
5. Herranz N, Dave N, Millanes-Romero A, Morey L, Díaz VM, Lórenz-Fonfría V, et al. Lysyl Oxidase-like 2 Deaminates Lysine 4 in Histone H3. Mol Cell 2012; 4:1–8.
6. Peinado H, Del Carmen Iglesias-de la Cruz M, Olmeda D, Csiszar K, Fong KSK, Vega S, et al. A molecular role for lysyl oxidase-like 2 enzyme in snail regulation and tumor progression. EMBO J 2005; 24:3446–58. http://dx.doi.org/10.1038/sj.emboj.7600781 PMid:16096638 PMCid:PMC1276164
7. Li W, Nellaiappan K, Strassmaier T, Graham L, Thomas KM, Kagan HM. Localization and activity of lysyl oxidase within nuclei of fibrogenic cells. Proc Natl Acad Sci U S A 1997; 94:12817–22. http://dx.doi.org/10.1073/pnas.94.24.12817 PMid:9371758 PMCid:PMC24221
8. Jansen MK, Csiszar K. Intracellular localization of the matrix enzyme lysyl oxidase in polarized epithelial cells. Matrix Biol 2007; 26:136–9. http://dx.doi.org/10.1016/j.matbio.2006.09.004 PMid:17074474 PMCid:PMC1851931
9. Palamakumbura AH, Jeay S, Guo Y, Pischon N, Sommer P, Sonenshein GE, et al. The propeptide domain of lysyl oxidase induces phenotypic reversion of ras-transformed cells. J Biol Chem 2004; 279:40593–600. http://dx.doi.org/10.1074/jbc.M406639200 PMid:15277520
10. Contente S, Kenyon K, Rimoldi D, Friedman RM. Expression of gene rrg is associated with reversion of NIH 3T3 transformed by LTR-c-H-ras. Science 1990; 249:796–8. http://dx.doi.org/10.1126/science.1697103 PMid:1697103
11. Bais M V, Nugent MA, Stephens DN, Sume SS, Kirsch KH, Sonenshein GE, et al. Recombinant lysyl oxidase propeptide protein inhibits growth and promotes apoptosis of pre-existing murine breast cancer xenografts. PLoS One 2012; 7:e31188. http://dx.doi.org/10.1371/journal.pone.0031188 PMid:22363577 PMCid:PMC3280126
12. Vaupel P, Mayer A. Hypoxia in cancer: significance and impact on clinical outcome. Cancer Metastasis Rev 2007; 26:225–39. http://dx.doi.org/10.1007/s10555-007-9055-1 PMid:17440684
13. Semenza GL. Molecular mechanisms mediating metastasis of hypoxic breast cancer cells. Trends Mol Med 2012; 18:534–43. http://dx.doi.org/10.1016/j.molmed.2012.08.001 PMid:22921864 PMCid:PMC3449282
14. Semenza GL. Hypoxia-inducible factors: mediators of cancer progression and targets for cancer therapy. Trends Pharmacol Sci 2012; 33:207–14. http://dx.doi.org/10.1016/j.tips.2012.01.005 PMid:22398146 PMCid:PMC3437546
15. Lu X, Kang Y. Hypoxia and hypoxia-inducible factors: master regulators of metastasis. Clin Cancer Res 2010; 16:5928–35. http://dx.doi.org/10.1158/1078-0432.CCR-10-1360 PMid:20962028 PMCid:PMC3005023
16. Erler JT, Bennewith KL, Nicolau M, Dornhöfer N, Kong C, Le Q-T, et al. Lysyl oxidase is essential for hypoxia-induced metastasis. Nature 2006; 440:1222–6. http://dx.doi.org/10.1038/nature04695 PMid:16642001
17. Schietke R, Warnecke C, Wacker I, Schödel J, Mole DR, Campean V, et al. The lysyl oxidases LOX and LOXL2 are necessary and sufficient to repress E-cadherin in hypoxia: insights into cellular transformation processes mediated by HIF-1. J Biol Chem 2010; 285:6658–69. http://dx.doi.org/10.1074/jbc.M109.042424 PMid:20026874 PMCid:PMC2825461
18. Wong CC-L, Zhang H, Gilkes DM, Chen J, Wei H, Chaturvedi P, et al. Inhibitors of hypoxia-inducible factor 1 block breast cancer metastatic niche formation and lung metastasis. J Mol Med (Berl) 2012; 90:803–15. http://dx.doi.org/10.1007/s00109-011-0855-y PMid:22231744 PMCid:PMC3437551
19. Kirschmann DA, Seftor EA, Nieva DR, Mariano EA, Hendrix MJ. Differentially expressed genes associated with the metastatic phenotype in breast cancer. Breast Cancer Res Treat 1999; 55:127–36.

http://dx.doi.org/10.1023/A:1006188129423
PMid:10481940

20. Kirschmann D a, Seftor E a, Fong SFT, Nieva DRC, Sullivan CM, Edwards EM, et al. A molecular role for lysyl oxidase in breast cancer invasion. Cancer Res 2002; 62:4478–83. PMid:12154058
21. Bondareva A, Downey CM, Ayres F, Liu W, Boyd SK, Hallgrimsson B, et al. The Lysyl Oxidase Inhibitor, β-Aminopropionitrile, Diminishes the Metastatic Colonization Potential of Circulating Breast Cancer Cells. Westermark P, editor. PLoS One 2009; 4:e5620.
22. Barker HE, Chang J, Cox TR, Lang G, Bird D, Nicolau M, et al. LOXL2-mediated matrix remodeling in metastasis and mammary gland involution. Cancer Res 2011; 71:1561–72. http://dx.doi.org/10.1158/0008-5472.CAN-10-2868 PMid:21233336 PMCid:PMC3842018
23. Peng L, Ran Y-L, Hu H, Yu L, Liu Q, Zhou Z, et al. Secreted LOXL2 is a novel therapeutic target that promotes gastric cancer metastasis via the Src/FAK pathway. Carcinogenesis 2009; 30:1660–9. http://dx.doi.org/10.1093/carcin/bgp178 PMid:19625348
24. Baker A-M, Cox TR, Bird D, Lang G, Murray GI, Sun X-F, et al. The role of lysyl oxidase in SRC-dependent proliferation and metastasis of colorectal cancer. J Natl Cancer Inst 2011; 103:407–24. http://dx.doi.org/10.1093/jnci/djq569 PMid:21282564
25. Erler JT, Bennewith KL, Cox TR, Lang G, Bird D, Koong A, et al. Hypoxia-induced lysyl oxidase is a critical mediator of bone marrow cell recruitment to form the premetastatic niche. Cancer Cell 2009; 15:35–44. http://dx.doi.org/10.1016/j.ccr.2008.11.012 PMid:19111879 PMCid:PMC3050620
26. Wong C-MCC-L, Gilkes DM, Zhang H, Chen J, Wei H, Chaturvedi P, et al. Hypoxia-inducible factor 1 is a master regulator of breast cancer metastatic niche formation. Proc Natl Acad Sci U S A 2011435:16369–74.
27. Campbell NE, Kellenberger L, Greenaway J, Moorehead RA, Linnerth-Petrik NM, Petrik J. Extracellular matrix proteins and tumor angiogenesis. J Oncol 2010; 2010:586905. http://dx.doi.org/10.1155/2010/586905 PMid:20671917 PMCid:PMC2910498
28. Bignon M, Pichol-Thievend C, Hardouin J, Malbouyres M, Bréchot N, Nasciutti L, et al. Lysyl oxidase-like protein-2 regulates sprouting angiogenesis and type IV collagen assembly in the endothelial basement membrane. Blood 2011; 118:3979–89. http://dx.doi.org/10.1182/blood-2010-10-313296 PMid:21835952
29. Zaffryar-Eilot S, Marshall D, Voloshin T, Bar-Zion A, Spangler R, Kessler O, et al. Lysyl Oxidase-Like-2 Promotes Tumour Angiogenesis and is a Potential Therapeutic Target in Angiogenic Tumours. Carcinogenesis 2013; bgt241. http://dx.doi.org/10.1093/carcin/bgt241 PMid:23828904
30. Baker A-M, Bird D, Welti JC, Gourlaouen M, Lang G, Murray GI, et al. Lysyl oxidase plays a critical role in endothelial cell stimulation to drive tumor angiogenesis. Cancer Res 2013; 73:583–94. http://dx.doi.org/10.1158/0008-5472.CAN-12-2447 PMid:23188504 PMCid:PMC3548904
31. Baker A-M, Bird D, Lang G, Cox TR, Erler JT. Lysyl oxidase enzymatic function increases stiffness to drive colorectal cancer progression through FAK. Oncogene 2012; 32:1863–8. http://dx.doi.org/10.1038/onc.2012.202 PMid:22641216
32. Lapointe J, Li C, Higgins JP, van de Rijn M, Bair E, Montgomery K, et al. Gene expression profiling identifies clinically relevant subtypes of prostate cancer. Proc Natl Acad Sci U S A 2004; 101:811–6. http://dx.doi.org/10.1073/pnas.0304146101 PMid:14711987 PMCid:PMC321763
33. Peinado H, Moreno-Bueno G, Hardisson D, Pérez-Gómez E, Santos V, Mendiola M, et al. Lysyl oxidase-like 2 as a new poor prognosis marker of squamous cell carcinomas. Cancer Res 2008; 68:4541–50. http://dx.doi.org/10.1158/0008-5472.CAN-07-6345 PMid:18559498
34. Barry-Hamilton V, Spangler R, Marshall D, McCauley S, Rodriguez HM, Oyasu M, et al. Allosteric inhibition of lysyl oxidase-like-2 impedes the development of a pathologic microenvironment. Nat Med 2010; 16:1009–17. http://dx.doi.org/10.1038/nm.2208 PMid:20818376
35. Offenberg H, Brünner N, Mansilla F, Orntoft Torben F, Birkenkamp-Demtroder K. TIMP-1 expression in human colorectal cancer is associated with TGF-B1, LOXL2, INHBA1, TNF-AIP6 and TIMP-2 transcript profiles. Mol Oncol 2008; 2:233–40. http://dx.doi.org/10.1016/j.molonc.2008.06.003 PMid:19383344
36. Ahn SG, Dong SM, Oshima A, Kim WH, Lee HM, Lee SA, et al. LOXL2 expression is associated with invasiveness and negatively influences survival in breast cancer patients. Breast Cancer Res Treat 2013; 141:89-99 http://dx.doi.org/10.1007/s10549-013-2662-3 PMid:23933800
37. Erler JT, Weaver VM. Three-dimensional context regulation of metastasis. Clin Exp Metastasis 2009; 26:35–49. http://dx.doi.org/10.1007/s10585-008-9209-8 PMid:18814043 PMCid:PMC2648515
38. Paszek MJ, Zahir N, Johnson KR, Lakins JN, Rozenberg GI, Gefen A, et al. Tensional homeostasis and the malignant phenotype. Cancer Cell 2005; 8:241–54. http://dx.doi.org/10.1016/j.ccr.2005.08.010 PMid:16169468
39. Pez F, Dayan F, Durivault J, Kaniewski B, Aimond G, Le Provost GS, et al. The HIF-1-inducible lysyl oxidase activates HIF-1 via the Akt pathway in a positive regulation loop and synergizes with HIF-1 in promoting tumor cell growth. Cancer Res 2011; 71:1647–57. http://dx.doi.org/10.1158/0008-5472.CAN-10-1516 PMid:21239473
40. Barry-Hamilton V, Spangler R, Marshall D, McCauley S, Rodriguez HM, Oyasu M, et al. Allosteric inhibition of lysyl oxidase-like-2 impedes the development of a pathologic microenvironment. Nat Med 2010; 16:1009–17.

http://dx.doi.org/10.1038/nm.2208
PMid:20818376

41. Hanahan D, Weinberg RA. Hallmarks of cancer: the next generation. Cell 2011; 144:646–74.
http://dx.doi.org/10.1016/j.cell.2011.02.013
PMid:21376230

42. Ben-porath I, Weinberg RA. When cells get stressed : an integrative view of cellular senescence. J Clin Invest 2004; 113:8–13.
http://dx.doi.org/10.1172/JCI200420663
http://dx.doi.org/10.1172/JCI20663
PMid:14702100

43. Collado M, Serrano M. Senescence in tumours: evidence from mice and humans. Nat Rev Cancer 2010; 10:51–7.
http://dx.doi.org/10.1038/nrc2772
PMid:20029423 PMCid:PMC3672965

44. Kang T-W, Yevsa T, Woller N, Hoenicke L, Wuestefeld T, Dauch D, et al. Senescence surveillance of pre-malignant hepatocytes limits liver cancer development. Nature 2011; 479:547–51.
http://dx.doi.org/10.1038/nature10599
PMid:22080947

45. Wiel C, Augert A, Vincent DF, Gitenay D, Vindrieux D, Le Calvé B, et al. Lysyl oxidase activity regulates oncogenic stress response and tumorigenesis. Cell Death Dis 2013; 4:e855.
http://dx.doi.org/10.1038/cddis.2013.382
PMid:24113189 PMCid:PMC3824691

46. Levental KR, Yu H, Kass L, Lakins JN, Egeblad M, Erler JT, et al. Matrix crosslinking forces tumor progression by enhancing integrin signaling. Cell 2009; 139:891–906.
http://dx.doi.org/10.1016/j.cell.2009.10.027
PMid:19931152 PMCid:PMC2788004

47. Payne SL, Fogelgren B, Hess AR, Seftor E a, Wiley EL, Fong SFT, et al. Lysyl oxidase regulates breast cancer cell migration and adhesion through a hydrogen peroxide-mediated mechanism. Cancer Res 2005; 65:11429–36.
http://dx.doi.org/10.1158/0008-5472.CAN-05-1274
PMid:16357151

48. Kennedy AL, Morton JP, Manoharan I, Nelson DM, Jamieson NB, Pawlikowski JS, et al. Activation of the PIK3CA/AKT pathway suppresses senescence induced by an activated RAS oncogene to promote tumorigenesis. Mol Cell 2011; 42:36–49.
http://dx.doi.org/10.1016/j.molcel.2011.02.020
PMid:21474066 PMCid:PMC3145340

49. Vredeveld LCW, Possik PA, Smit MA, Meissl K, Michaloglou C, Horlings HM, et al. Abrogation of BRAFV600E-induced senescence by PI3K pathway activation contributes to melanomagenesis. Genes Dev 2012; 26:1055–69.
http://dx.doi.org/10.1101/gad.187252.112
PMid:22549727 PMCid:PMC3360561

50. Samuels Y, Ericson K. Oncogenic PI3K and its role in cancer. Curr Opin Oncol 2006; 18:77–82.
http://dx.doi.org/10.1097/01.cco.0000198021.99347.b9

51. Qiao M, Sheng S, Pardee AB. Metastasis and AKT activation. Cell Cycle 2008; 2991–6.
http://dx.doi.org/10.4161/cc.7.19.6784
PMid:18818526

52. Tsuji T, Ibaragi S, Hu G. Epithelial-mesenchymal transition and cell cooperativity in metastasis. Cancer Res 2009; 69:7135–9.
http://dx.doi.org/10.1158/0008-5472.CAN-09-1618
PMid:19738043 PMCid:PMC2760965

53. Yao D, Dai C, Peng S. Mechanism of the mesenchymal-epithelial transition and its relationship with metastatic tumor formation. Mol Cancer Res 2011; 9:1608–20.
http://dx.doi.org/10.1158/1541-7786.MCR-10-0568
PMid:21840933

54. Ansieau S, Courtois-Cox S, Morel A-P, Puisieux A. Failsafe program escape and EMT: a deleterious partnership. Semin Cancer Biol 2011; 21:392–6.
PMid:21986518

55. Larue L, Bellacosa A. Epithelial-mesenchymal transition in development and cancer: role of phosphatidylinositol 3' kinase/AKT pathways. Oncogene 2005; 24:7443–54.
http://dx.doi.org/10.1038/sj.onc.1209091
PMid:16288291

56. Cuevas EP, Moreno-Bueno G, Canesin G, Santos V, Portillo F, Cano A. LOXL2 catalytically inactive mutants mediate epithelial-to-mesenchymal transition. Biol Open 2014; 3:129-37
http://dx.doi.org/10.1242/bio.20146841
PMid:24414204 PMCid:PMC3925316

57. Giampuzzi M, Oleggini R, Di Donato A. Demonstration of in vitro interaction between tumor suppressor lysyl oxidase and histones H1 and H2: definition of the regions involved. Biochim Biophys Acta 2003; 1647:245–51.
http://dx.doi.org/10.1016/S1570-9639(03)00059-1

58. Kagan HM, Williams MA, Calaman SD, Berkowitz EM. Histone H1 is a substrate for lysyl oxidase and contains endogenous sodium borotritide-reducible residues. Biochem Biophys Res Commun 1983; 115:186–92.
http://dx.doi.org/10.1016/0006-291X(83)90987-7

59. Lugassy J, Zaffryar-Eilot S, Soueid S, Mordoviz A, Smith V, Kessler O, et al. The enzymatic activity of lysyl oxidas-like-2 (LOXL2) is not required for LOXL2-induced inhibition of keratinocyte differentiation. J Biol Chem 2012; 287:3541–9.
http://dx.doi.org/10.1074/jbc.M111.261016
PMid:22157764 PMCid:PMC3271007

To cite this article: David Bernard, et al. Lysyl oxidases: emerging promoters of senescence escape, tumor initiation and progression. *Can Cell Microenviron* 2014; 1:51-56. doi: 10.14800/ccm.120.

Chapitre II : Caractérisation du rôle de canaux calciques dans l'OIS

2.1 Introduction

2.1.1 Description du criblage dans les hMECs

De nombreux groupes ont utilisé des banques de shRNA pour approfondir les connaissances en matière de processus tumoraux (Firestein *et al.*, 2008; Silva *et al.*, 2008; Schlabach *et al.*, 2008; Ngo *et al.*, 2006; Westbrook *et al.*, 2005; Gazin *et al.*, 2007). C'est en effet une approche puissante, permettant d'identifier de nouveaux rôles pour certains gènes. Dans le domaine de la sénescence, c'est également un criblage perte de fonction qui a permis à l'équipe de Jesus Gil, par exemple, d'identifier CXCR2 comme acteur dans la sénescence (Acosta *et al.*, 2008). Au sein de notre équipe, la technique de criblage dans des fibroblastes a déjà permis d'identifier PLA2R1 (Augert *et al.*, 2009), l'AMPK-related protein kianse 5 (ARK5 /NUAK1) (Humbert *et al.*, 2010) et la topoisomérase 1 (TOP1) (Humbert *et al.*, 2009).

Nous avons effectué le criblage dans les hMECs-TM grâce à la banque « Decode RNAi viral screening pools » commercialisée par Open Biosystems. Cette banque est basée sur la construction d'un vecteur lentiviral (pGIPZ) qui contient un promoteur de type CMV régulant la transcription du shRNA inséré *(figure 12a)*. La banque code pour 70000 shRNA, divisés en 7 pools de 10000 shRNA ciblant l'ensemble des gènes du génome. Une fois inséré dans le génome de la cellule, le shRNA est continuellement transcrit menant à l'extinction totale ou partielle du gène ciblé.

Les cellules hMECS-TM, ensemencées en boites de 10 cm, ont été infectées avec un pool de shRNA. Deux jours après l'infection, l'activation de l'oncogène Mek est induite par addition de 4-OHT. L'activité de Mek est maintenue par un traitement au 4-OHT tous les 2 jours pendant 30 jours. Les cellules infectées par un vecteur contrôle entrent de manière stable en sénescence. Parmi les cellules, celles infectées avec les pools 3 et 7 présentent un échappement à la sénescence, puisqu'elles sont capables de proliférer *(figure 12b)*. L'ADN génomique des cellules ayant échappé à la sénescence est récupéré et analysé afin d'identifier les shRNA présents responsables de ce phénotype.

a

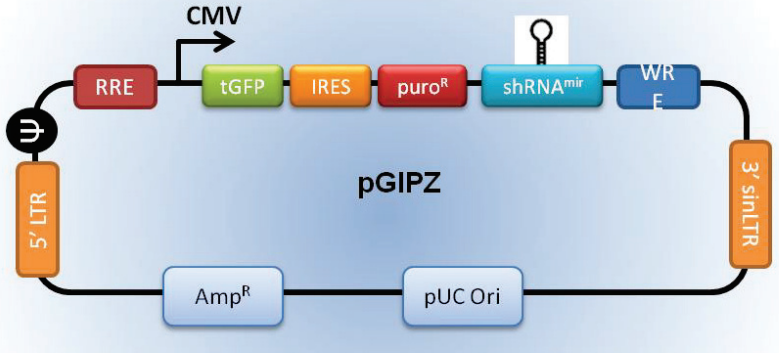

Elément	utilité
Promoteur CMV	promoteur du cytomegalovirus humain qui permet une forte expression du transgène (type RNA polymerase II)
tGFP	rapporteur TurboGFP qui permet de suivre la transduction et l'expression
Puro^R	résistance à la puromycine
IRES	les gènes *tGFP* et *puro^R* sont exprimés en un seul transcrit
shRNA	shRNA induisant l'extinction du gène d'intérêt
5' LTR	5' Long Terminal Repeat
3' SIN-LTR	3' self-inactivating Long Terminal Repeat pour augmenter la sécurité d'utilisation du lentivirus
ψ	Psi packaging sequence, permet au génome viral d'utiliser les systèmes d'encapsidation du lentivirus
RRE	Rev Response Element, améliore le titre viral en augmentant l'efficacité de l'encapsidation
WRE	Woodchuck hepatitis post-transcriptional regulatory element, améliore l'epression du transgène dans les cellules cibles

b

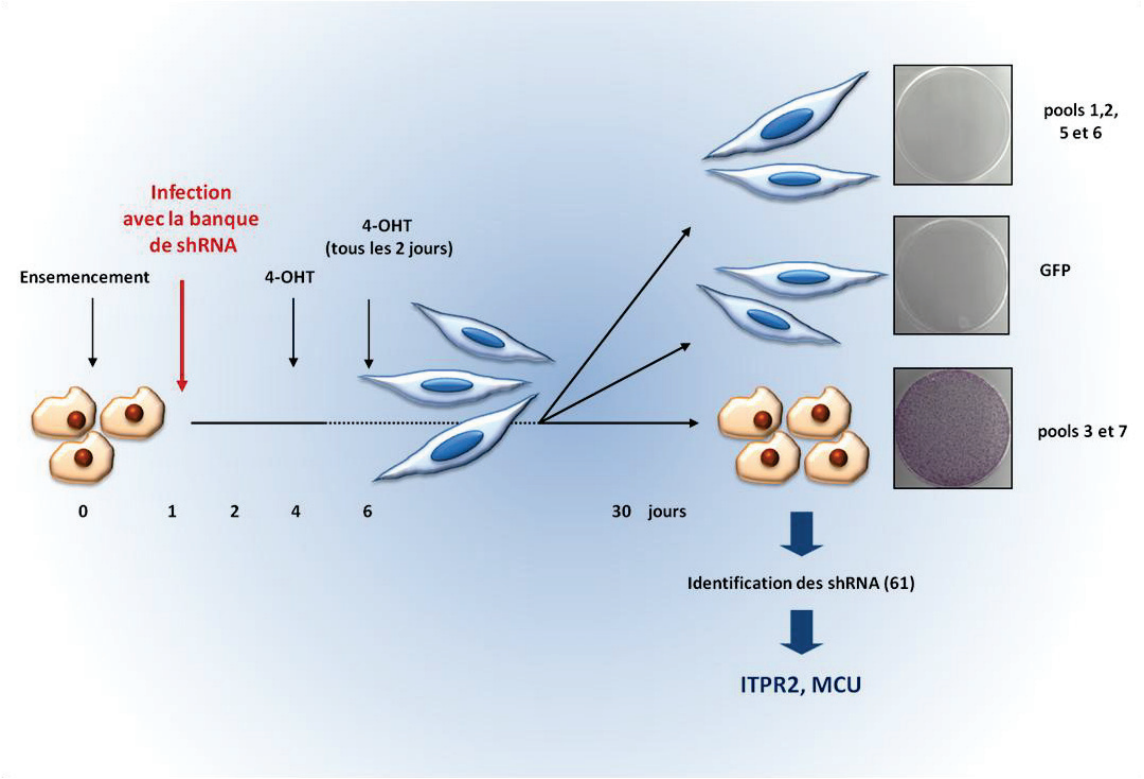

Figure 12 : Criblage génétique

a) réprésentation schématique du vecteur pGIPZ utilisé lors du criblage génétique.

b) Le criblage génétique a été effectué dans les cellules hMEC-TM. Les cellules ont été ensemencées, infectées le jour suivant avec 7 pools de shRNA. Au 4ème jour, le traitement 4-OHT (100nM) a débuté, et est renouvelé tous les 2 jours. Au 30ème jour, des clones émergeants ont été observés parmi les cellules infectées avec les pools 3 et 7, correspondant à un échappement à l'OIS. Les cellules infectées avec un vecteur ne contenant pas de shRNA sont utilisées comme contrôle. Pour identifier les shRNA permettant un échappement à l'OIS, l'ADN génomique de ces cellules a été extrait, amplifié par PCR en suivant le protocole du fabricant. L'ADNg a ensuite été cloné, amplifié, et séquencé. Les séquences obtenues ont par la suite été blastées afin d'identifier l'ARNm ciblé par le shRNA.

2.1.2 Identification de MCU et ITPR2

Parmi les gènes identifiés par le criblage perte de fonction, nous nous sommes intéressés à deux gènes : *ITPR2* et *MCU* (*CCDC109A)*, codant respectivement pour le récepteur à l'inositol tri-phosphate de type 2 (ITPR2 ou plus communément appelé IP_3R2), et le Mitochondrial Calcium Uniporter (MCU). Ce point sera développé par la suite, mais il est important de souligner que ces deux canaux sont liés à l'échange de calcium entre le réticulum endoplasmique (RE) et la mitochondrie. Il est donc probable qu'ils appartiennent à la même voie de signalisation.

ABCC3	*BNIP3L*	*ESSRB*	*IL17A*	*MYADML*	*PLXND1*	*SNORB-2*
ACACB	*BRAP*	*FBXO9*	***ITPR2***	*MYOM3*	*POLM*	*TRAT1*
ACVR2A	*CASP2*	*FSHR*	***KCNA1***	*NDRG3*	*PPP1R8*	*UBQLN1*
ACSBG2	*CNIH4*	*G6PC*	*KCTD7*	*NRK*	*RAB9A*	***WASL***
ADAM12	*COPS2*	*GHRH*	*KIF11*	*OSBPL2*	*RAB14*	*ZBTB9*
ADAM15	*DAD1*	*GLT8D3*	*LHX8*	*PBX3*	*RNF111*	*ZCWPW2*
ALX1	*DDX10*	*GNRHR*	*LRRTM1*	*PDXP*	*RNF150*	***ZNF133***
AP4M1	*EGLN1*	*HAT1*	***MAP4***	*PDXDC2*	*SDF2L1*	
ARMCX2	*ELF5*	*IGF1*	***MCU***	*PFTK1*	*SNORA65*	

Tableau 4 : Gènes identifiés lors du criblage génétique

Liste des 61 gènes identifiés par le criblage perte de fonction illustré dans la figure 12.

En gras apparaissent les gènes pour lesquels j'ai participé à la caractérisation. En rouge : travail présenté dans ce manuscrit. En bleu : travail présenté en annexe, ou en cours de réalisation. En noir : autres gènes que j'ai testé.

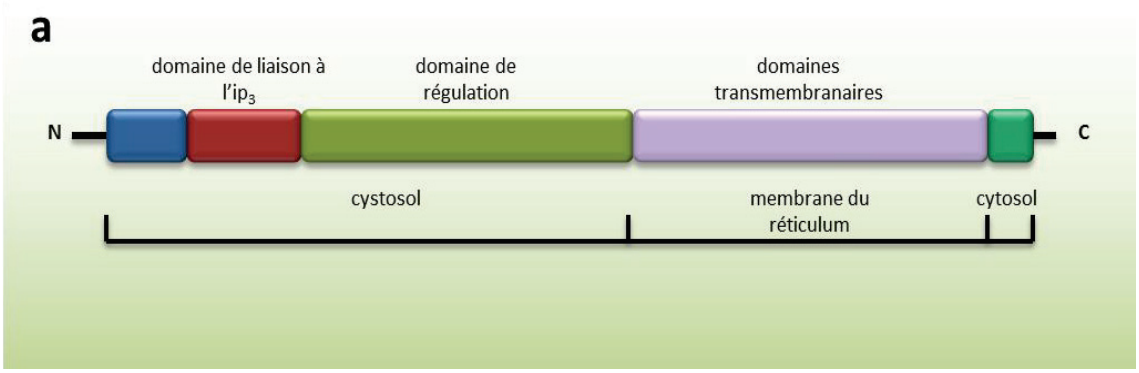

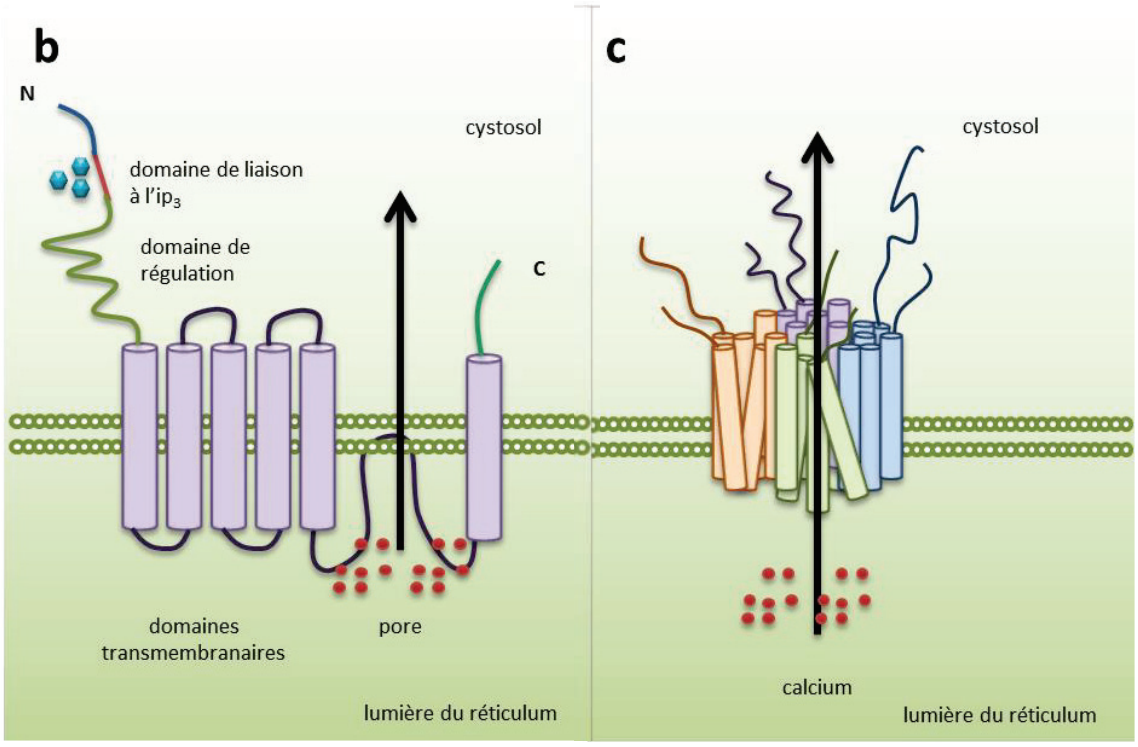

Figure 13 : Structure des ITPR

a) Représentation schématique des différents domaines d'une sous-unité d'un récepteurs ITPR, avec en partie N-terminale le domaine de liaison à l'IP_3. Le domaine de régulation contient plusieurs sites consensus de phosphorylation.

b) Représentation d'une sous-unité d'un récepteur, avec les 6 domaines transmembranaires.

c) Structure quaternaire des ITPR

2.1.2.1 Inositol Tri-Phosphate Receptor 2

Les Récepteurs à l'IP_3 sont les principaux canaux par lesquels le calcium sort du RE. Il en existe 3 isoformes : ITPR1, 2 et 3. Ces protéines ont une structure quaternaire composée de l'assemblage 4 sous-unités de 130 kDa chacune. La partie N-terminale des sous-unités contient une séquence de liaison à l'Inositol 1,4,5-TriPhosphate (IP_3). L'ouverture de ces récepteurs est principalement régulée par l'IP_3 et le calcium lui-même. Toutefois, leur activité peut aussi être régulée par phosphorylation, puisqu'ils contiennent des sites consensus de phosphorylation et plusieurs sites de fixation des kinases (Vanderheyden *et al.*, 2009) *(Figure 14)*.

Voie de l'IP_3

De nombreux stimuli peuvent induire la production d'IP_3, via l'activation de récepteurs couplés aux protéines G ou des récepteurs de type tyrosine kinase. Une fois qu'ils sont activés, la phospholipase C associée à la membrane plasmique (PLC) catalyse la production de deux second messagers par hydrolyse du phosphatidylinositol 4,5-biphosphate (PIP_2) ancré dans la membrane plasmique. Le diacylglyécerol (DAG) et l'inositol-1,4,5-triphosphate (IP_3) se retrouvent ainsi libérés. L'IP_3, composé soluble, diffuse depuis la membrane plasmique jusqu'au RE où il peut se fixer aux ITPRs et induire leur ouverture *(Figure 14)*. Le calcium séquestré dans le RE est alors déchargé dans le cytosol où il peut être capté par la mitochondrie. Cet aspect sera spécifiquement détaillé dans les paragraphes suivants.

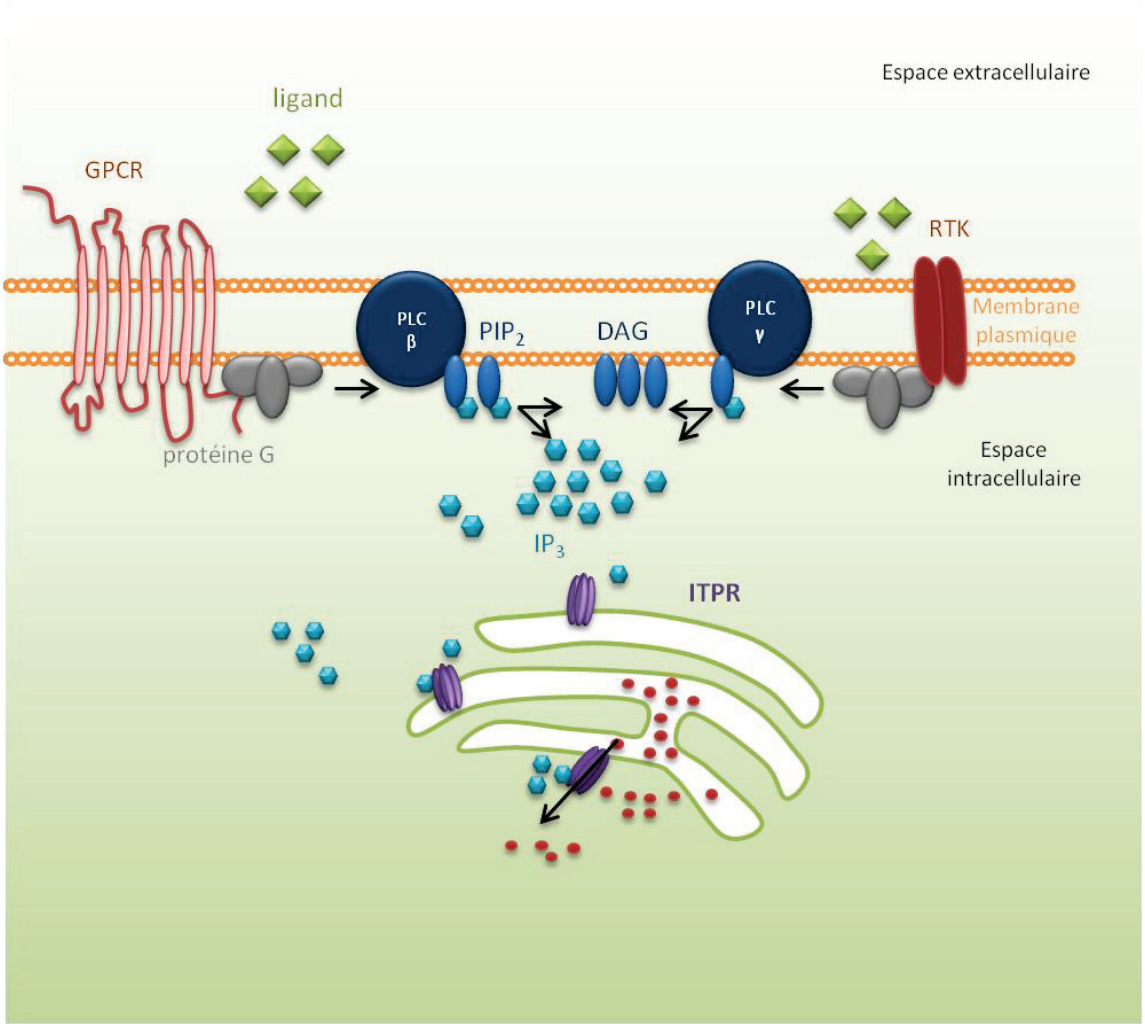

Figure 14 : Voie de l'IP_3

L'activation des récepteurs de type GPCR ou RTK induit la génération DAG et d'IP_3 via les PLCβ et γ. L'IP_3 soluble diffuse dans le cytoplasme où il peut se lier et activer ses récepteurs. L'activation des ITPR (ou IP_3R) induit leur ouverture et la libération du calcium depuis le RE jusque dans le cytoplasme.

DAG : DiAcylGlycérol ; GPCR: Récepteur couplé aux protéines G ; IP_3 : Inositol-TriPhosphate ; ITPR : Récepteur à l'InositolTriPhosphate ; PLC : PhosphoLipase C ; RTK : Récepteur Tyrosine Kinase

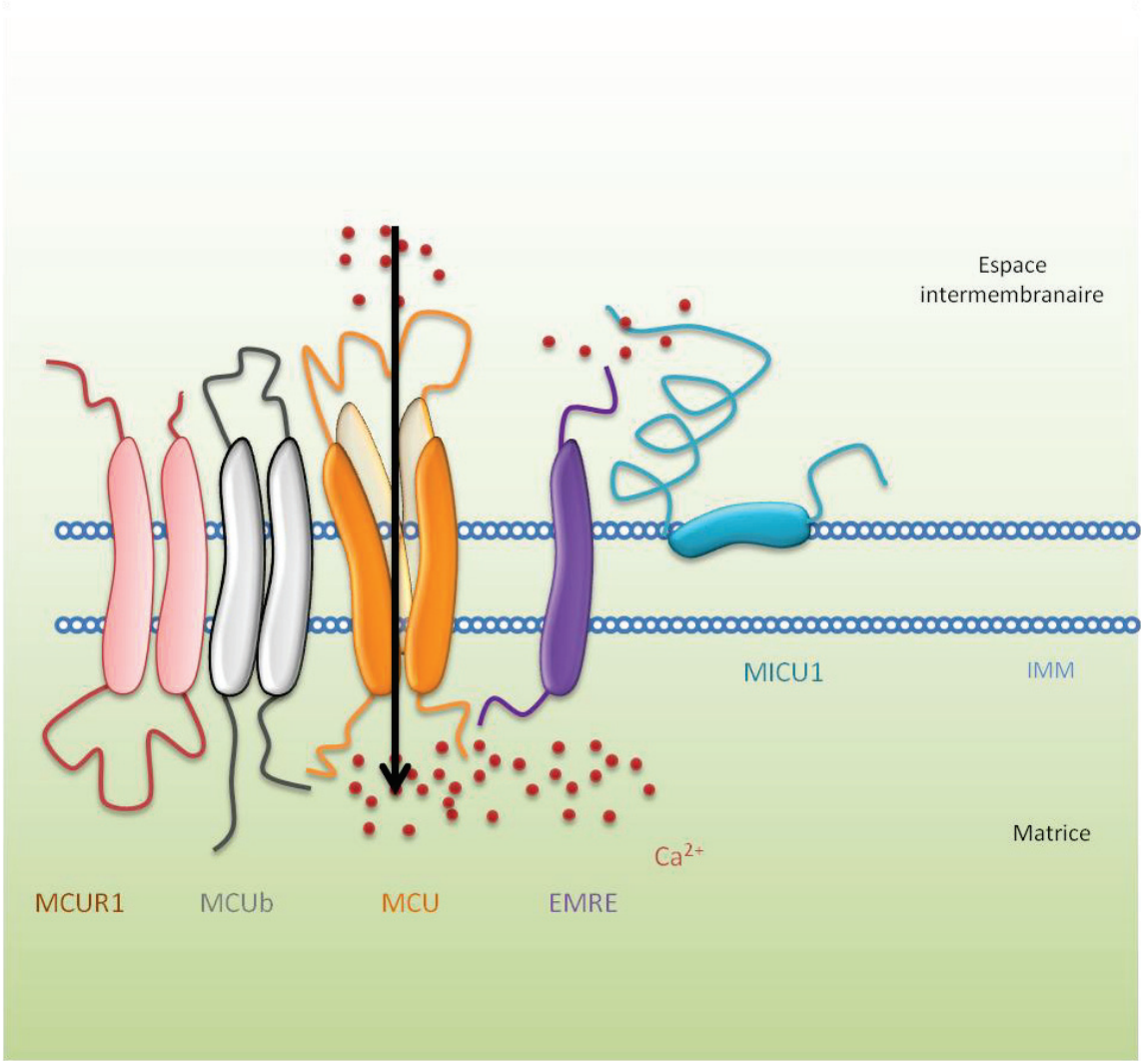

Figure 15 : Représentation schématique du complexe MCU et de ses régulateurs

Le MCU est régulé par MCUR1 et EMRE nécessaires pour son activité, MICU1 qui module son activité, et MCUb qui l'inhibe.

MCU :Mitochondrial Calcium Unipoter, MCUR : Mitochondrial Calcium Uniporter Regulator 1, EMRE : Essential MCU Regulator, MICU1 :Mitochondrial Calcium Uptake 1, IMM : Membrane mitochondriale Interne.

Adapté de (Marchi and Pinton, 2013)

2.1.2.2 Mitochondrial Calcium Uniporter

Depuis plus de 40 ans, de nombreux laboratoires ont essayé d'identifier le MCU, mais toutes ces recherches ont été infructueuses. De nouvelles approches pour l'identifier ont alors été mises en place. En 2008, Mootha et ses collègues ont généré une « génothèque » spécifique de la mitochondrie (MitoCarta) en réalisant des analyses par spectrométrie de masse sur des mitochondries hautement purifiées ou des préparations mitochondriales brutes extraites à partir de 14 tissus murins différents. Utilisant cette base de données, l'équipe de Rizzuto, tout comme celle de Mootha la même année, ont pu identifier la protéine qui jouait le rôle de MCU (De Stefani *et al.*, 2011; Baughman *et al.*, 2011). Cette découverte récente de l'identité exacte du MCU laisse la porte ouverte à de nombreuses recherches, notamment par la génération de souris KO ou de souris transgéniques afin d'étudier le rôle de ce transporteur (Pan *et al.*, 2013 b), et d'étudier l'implication potentielle du calcium mitochondrial dans de nombreuses pathologies et processus biologiques. Plusieurs régulateurs essentiels de MCU ont également été identifiés comme le Mitochondrial Calcium Uptake 1 et 2 (MICU1 et MICU2), le Mitochondrial Calcium Uniporter Regulator 1 (MCUR1), MCUb (isogène de MCU) agissant comme un dominant négatif et l'Essential MCU Regulator (EMRE) (Sancak *et al.*, 2013) qui forment tous un complexe avec MCU (Marchi and Pinton, 2013) *(figure 15)*.

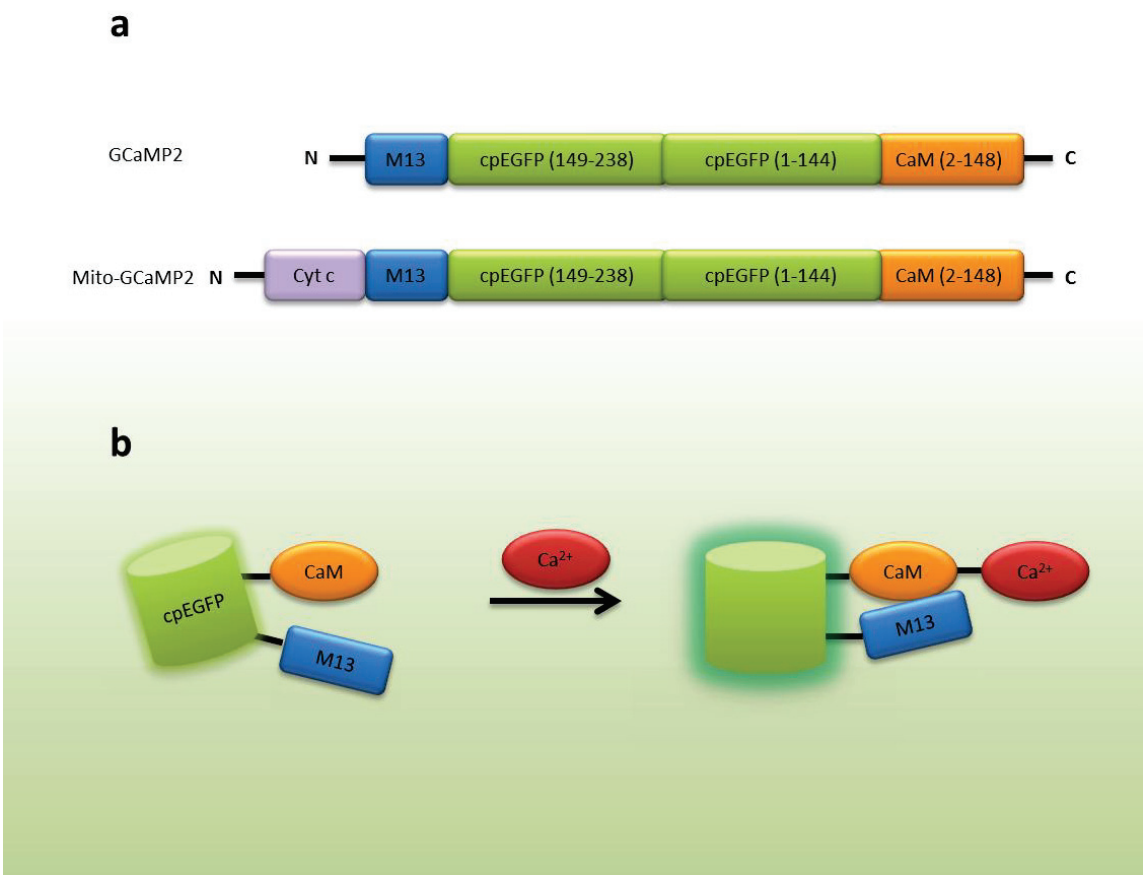

Figure 16 : Représentation de la protéine de fusion mito-GCaMP2 utilisée pour mesurer le calcium mitochondrial

a) Séquence simplifiée de la forme permutée de la cpEGFP (GFP permutée de façon circulaire) liée à une séquence de la calmoduline (CaM), à un peptide de la chaine légère de la myosine kinase (M13). L'ajout de la séquence codant les 12 premiers acides aminés de la sous-unité IV de la cytohrome c oxidase permet de localiser la protéine de fusion dans la mitochondrie.

b) L'intensité de fluorescence émise par GCaMP2 change grâce à un changement conformationnel de la protéine cpEGFP qui a lieu après fixation du calcium à la calmoduline, qui se lie alors à son peptide cible M13.

Inspiré de (Chen *et al.*, 2011; Iguchi *et al.*, 2012).

2.1.2.3 Mesure du calcium mitochondrial

Pour mesurer le calcium cellulaire et ses flux au sein de la cellule, plusieurs techniques existent. Les plus anciennes sont les sondes fluorescentes comme le Fura-2 ou l'Indo-1 (Grynkiewicz *et al.*, 1985). Par la suite, de nouveaux outils ont été développés : les indicateurs de calcium génétiques (*Genetically Encoded Calcium Indicator*, GECI). Deux types de GECIs existent, ceux basés sur la technique de FRET (*Förster Resonance Energy Transfer*) et ceux basés sur une construction type eGFP (*enhanced Green Fluorescent Protein*) appelés GCaMP (Kotlikoff, 2007). Dans ce cas là, la GFP permutée est fusionnée à la calmoduline et à un peptide cible de la calmoduline (M13). La liaison de calcium à la calmoduline permet l'interaction entre la calmoduline et le peptide M13 altère la conformation de la protéine GFP induisant ainsi une augmentation de la fluorescence. L'intensité de fluorescence émise est directement corrélée à la concentration en calcium (Nakai *et al.*, 2001; Nagai *et al.*, 2001; Souslova *et al.*, 2007). L'intérêt de cette approche est de pouvoir cibler des localisations spécifiques de la cellule, comme le cytosol, le RE, le noyau ou encore la mitochondrie en ajoutant à la construction une séquence spécifique ciblant un compartiment cellulaire (Miyawaki *et al.*, 1997; Trenker *et al.*, 2007; Iguchi *et al.*, 2012; Poburko *et al.*, 2009; Lee *et al.*, 2006 b; Parkinson *et al.*, 2014; Simonetti *et al.*, 2013). Nous avons utilisé une construction de type GCaMP2, dérivée de GCaMP1 où la fluorescence émise est plus intense (Tallini *et al.*, 2006). Une séquence peptidique composée des 12 premiers acides aminés issus de la sous-unité IV de la cytochrome c oxydase a été ajoutée permettant d'adresser la protéine de fusion exprimée dans la mitochondrie (Chen *et al.*, 2011) *(figure 16)*. Nous avons ensuite cloné cette séquence dans un vecteur rétroviral de type pLNCX2 afin de pouvoir exprimer stablement la protéine de fusion dans les cellules épithéliales par un mécanisme de transduction virale. Une partie des résultats présentés dans l'article suivant utilisent cette technique pour mesurer les changements de concentrations calciques au sein des mitochondries.

2.1.3 Signalisation calcique entre réticulum et mitochondrie

Le calcium participe à de nombreux mécanismes physiologiques fondamentaux comme le contrôle du cycle cellulaire, la survie, l'apoptose, la migration ou l'expression de gènes (Berridge *et al.*, 2003). Etant donné que le calcium est un second messager très important dans la régulation de fonctions physiologiques fondamentales, ses concentrations intracellulaires sont très finement régulées (Berridge *et al.*, 2003). Le maintien de cette homéostasie implique l'entrée de calcium depuis le compartiment extracellulaire, mais aussi l'entrée ou la sortie de calcium depuis des organelles de stockage comme le réticulum endoplasmique ou les mitochondries (Carafoli, 2003). Des altérations dans les voie de signalisation du calcium sont impliquées dans la progression tumorale, comme la prolifération, la migration, l'invasion et la formation de métastases (Monteith *et al.*, 2012, 2007). Par la suite, j'ai volontairement axé les informations qui vont suivre sur le calcium mitochondrial et du RE.

2.1.3.1 Le réticulum endoplasmique

Le réticulum endoplasmique, lisse (REL) ou granuleux (REG), est considéré comme l'organelle intracellulaire le plus important en volume de la cellule. Les activités principales du RE sont la synthèse, la maturation et l'acheminement des protéines vers l'appareil de Golgi (Chevet *et al.*, 2001). Le RE constitue un réservoir de calcium indispensable où sa concentration peut atteindre 500µM contre seulement 10-100 nM dans le cytosol. La libération de calcium peut être activée par des stimulations électriques ou chimiques (Bootman *et al.*, 2002; Verkhratsky, 2002). Pour fonctionner comme une organelle de stockage de calcium, le réticulum doit exprimer au moins trois types de protéines : (1) des pompes à calcium ATP-dépendantes afin de transporter le calcium du cytosol au RE (types SERCA) (2) des protéines luminales chaperonnes qui fixent et stockent le calcium et (3) des canaux calciques qui permettent la libération contrôlée de calcium hors du réticulum selon un gradient électrochimique. Les protéines chaperonnes qui fixent le calcium dans le RE sont également capables de réguler l'activité d'autres éléments comme les pompes ou les canaux, soulignant ainsi une étroite relation entre calcium et fonction du RE.

2.1.3.2 La mitochondrie

Les mitochondries sont des organelles très dynamiques dotées d'une plasticité importante et soumises à un remodelage constant. Elles sont impliquées principalement dans des mécanismes énergétiques tels que la génération d'ATP ou la β-oxydation des acides gras. Elles possèdent deux membranes, interne (IMM) et externe (OMM), séparant 3 compartiments : la face cytosolique de l'OMM, l'espace inter-membranaire, et la matrice. L'IMM porte notamment les complexes de la chaine respiratoire et l'ATP synthase. L'OMM, grâce à la présence de nombreuses porines peut laisser circuler librement des petites molécules (< 5-10kDa) entre le cytoplasme et l'espace inter-membranaire. A l'inverse, l'IMM est complètement imperméable à toutes les molécules y compris les protons. Cette particularité permet à la chaine respiratoire de produire un gradient de proton nécessaire à la phosphorylation oxydative (Giorgi *et al.*, 2009). Ce gradient électrochimique, à la source du potentiel de membrane mitochondrial $\Delta\psi_m$ constitue la force motrice de l'entrée de calcium dans la matrice. Le calcium peut librement traverser l'OMM, grâce à l'expression abondante de canaux VDACs (*Voltage-Dependent Anion Channels*) mais nécessite d'être pris en charge par le MCU localisé dans l'IMM pour atteindre la matrice (Patron *et al.*, 2013).

2.1.3.3 Les structures de Membranes Associées aux Mitochondries (MAMs)

Les premières observations selon lesquelles le RE et la mitochondrie pouvaient s'associer remontent à plus de 50 ans (Copeland and Dalton, 1959). Puis, dans les années 1970, plusieurs groupes ont visualisé les contacts entre ces deux organelles (Lewis and Tata, 1973; Morré *et al.*, 1971). Par la suite, des analyses tridimensionnelles sont venues confirmer ces observations (de Brito and Scorrano, 2008; Rizzuto *et al.*, 1998; Csordás *et al.*, 2006). Il s'est révélé que les interactions entre ces deux organelles sont si fortes que le fractionnement cellulaire a permis d'isoler des « membranes associées aux mitochondries » (*Mitochondria-Associated Membranes*, MAM) (Vance *et al.*, 1997; Wieckowski *et al.*, 2009) *(figure 17)*

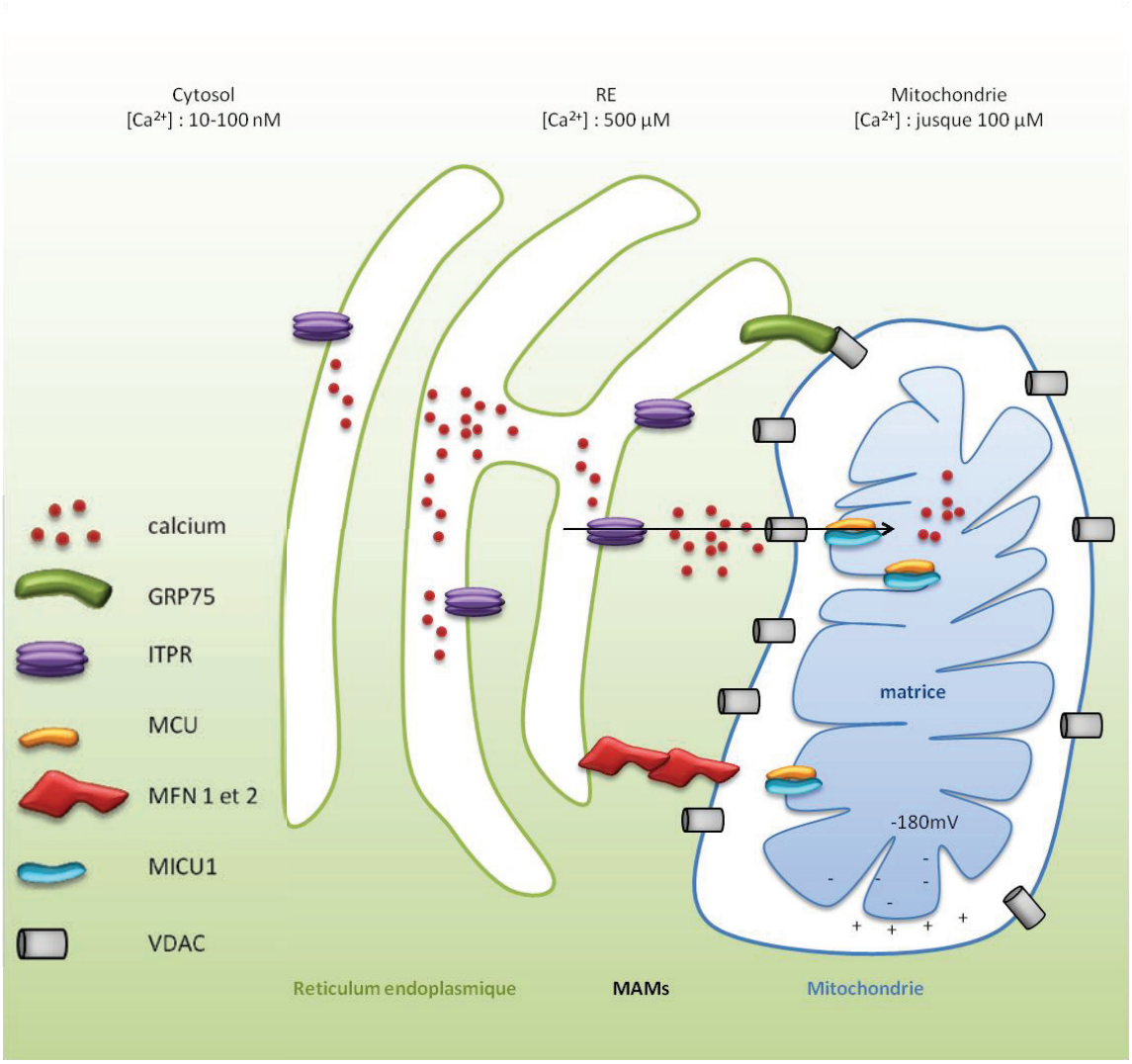

Figure 17 : Représentation schématique du RE, de la mitochondrie et des MAMs

Les structures de type MAMs (Membranes Associées aux Mitochondries) sont dues aux fortes interactions entre le RE et les mitochondries. Ces interactions sont notamment médiées par les protéines Mfn1 et 2, GRP75 et VDAC. Les ITPR activés libèrent le calcium qui peut librement entrer dans l'espace intermédiaire de la mitochondrie par les VDAC. Le calcium fortement concentré grâce à ces structures est ensuite transporté par le MCU jusque dans la matrice mitochondriale. La formation de ces structures permet d'assurer un transfert efficace de calcium entre les 2 organelles et d'assurer les processus biologiques nécessitant le calcium mitochondrial.

ITPR : InositolTriPhosphate Receptor ; GRP75 : Glucose Related Protein 75 ; MCU : Mitochondrial Calcium Uniporter ; MICU1 : Mitochondrial Calcium Uptake 1 ; VDAC : Voltage Dependent Anion Channel.

Récemment, il a été montré que ces structures jouent un rôle crucial dans les voies de signalisation calciques. En effet, la proximité physique entre le RE et les mitochondries permet une transmission directe et sélective des signaux de calcium (Giorgi *et al.*, 2009). Après stimulation de la cellule, les mitochondries sont capables d'incorporer directement le calcium relargué par le RE (Kirichok *et al.*, 2004; Rizzuto *et al.*, 1993; Csordás *et al.*, 1999). Les interactions entre ces organelles sont modulées notamment par les protéines mitofusin -1 et -2 (MFN-1 et MFN-2) qui permettent de réguler la morphologie du RE et stabiliser les interactions entre RE et mitochondrie assurant ainsi un transfert efficace de calcium (de Brito and Scorrano, 2008). Il a également été observé que les canaux VDAC puissent interagir avec les ITPR via la protéine chaperonne Glucose-Regulated Protein (GRP75) (Szabadkai *et al.*, 2006). Ces interactions sont d'autant plus importantes qu'elles forment des micro-domaines qui permettent de concentrer en certains points le calcium cytosolique libéré par le RE. Le MCU, bien qu'hautement sélectif pour le calcium a une affinité faible pour celui-ci, nécessitant une concentration en calcium dans l'environnement direct de la mitochondrie suffisamment élevée pour être actif. La présence de MAMS permet d'atteindre ces hautes concentrations détectées par le senseur MICU1 (Csordás *et al.*, 2013).

Les MAMs sont enrichies en de nombreuses protéines régulatrices de l'autophagie (Beclin-1) ou de l'apoptose (Bcl-2, Bad), soulignant un rôle fondamental de ces jonctions dans ces processus cellulaires. On y trouve aussi des protéines PML, habituellement nucléaires, qui semblent réguler l'état de phosphorylation et d'activation des récepteurs IPTRs (Giorgi *et al.*, 2010).

La libération de calcium dans les mitochondries est un processus cellulaire essentiel qui est requis pour une respiration mitochondriale efficace, le maintien du rendement énergétique et la suppression de l'autophagie. Les récepteurs à l'IP_3 sont des centres d'échanges de calcium qui régulent également finement la survie ainsi que les processus de mort par l'intermédiaire de nombreux oncogènes ou de gènes suppresseurs de tumeurs (Akl and Bultynck, 2013). L'ensemble de ces données nous a permis de sélectionner parmi les gènes identifiés *ITPR2* et *MCU* afin d'évaluer leur implication dans l'OIS.

2.2 Article 2 : Endoplasmic reticulum calcium release through ITPR2 channels leads to mitochondrial calcium accumulation and senescence

Endoplasmic reticulum calcium release through ITPR2 channels leads to mitochondrial calcium accumulation and senescence

Clotilde Wiel*, Hélène Lallet-Daher*, Delphine Gitenay, Baptiste Gras, Benjamin Le Calvé, Arnaud Augert, Mylène Ferrand, Natalia Prevarskaya, David Vindrieux et David Bernard

* ces auteurs ont contribué de manière équivalente à ce travail

Publié en Mai 2014 dans le journal *Nature Communications*

Le criblage perte de fonction dans les hMECs-TM nous a permis d'identifier ITPR2 (IP_3R2) comme régulateur de la sénescence. Nous avons confirmé que l'extinction d'expression d'ITPR2 grâce à 2 shRNA permet un échappement à l'OIS *(figure 1)*, alors que l'activation directe des ITPR par l'IP_3 induit une sénescence prématurée *(figure 2).* Etant donné que les ITPR sont des canaux permettant la sortie de calcium du RE vers le cytosol, nous avons suivi les flux de calcium pendant la sénescence. Nous avons observé lors de l'OIS une redistribution du calcium *(figure 3)* spécifiquement dans les mitochondries *(figure 4)*, qui est abolie dans les cellules exprimant un shRNA ciblant ITPR2 *(figures 3 et 4)*.

Or, MCU, le canal permettant cette assimilation de calcium dans les mitochondries est également un gène identifié lors de ce criblage. Nous avons donc analysé par la suite l'implication de MCU dans l'OIS et nous avons montré qu'empêcher la relocalisation du calcium dans les mitochondries lors de la sénescence via 3 shRNA ciblant MCU favorise l'échappement à la sénescence *(figure 5)*.

Nous nous sommes ensuite demandé quelles étaient les conséquences de cette accumulation de calcium mitochondrial et par quels mécanismes la sénescence est induite. Nous avons pour cela analysé le potentiel de membrane mitochondrial $\Delta\psi_m$. Il s'avère que celui-ci est fortement altéré lors de la sénescence *(figure 6)* et que la chute de ce potentiel de membrane induit une sénescence prématurée *(figure 7)*. L'inhibition de la relocalisation du calcium dans les mitochondries par l'extinction d'ITPR2 et de MCU permet de restaurer le $\Delta\psi_m$ *(figure 6)*. De plus, lors de la sénescence, on observe une augmentation de la production de ROS due au calcium mitochondrial *(figure 8)*.

La relocalisation du calcium dans les mitochondries, dépendante d'ITPR2 et de MCU, est suivie par une chute du $\Delta_{\psi m}$ et est associée à une production de ROS, médiateur connu de la sénescence. L'ensemble de ces données révèlent une nouvelle voie de signalisation que l'on retrouve durant l'OIS ainsi que la sénescence réplicative *(figure supplémentaire 9).*

nature COMMUNICATIONS

ARTICLE

Received 26 Nov 2013 | Accepted 3 Apr 2014 | Published 6 May 2014

DOI: 10.1038/ncomms4792

Endoplasmic reticulum calcium release through ITPR2 channels leads to mitochondrial calcium accumulation and senescence

Clotilde Wiel[1,2,3,4,*], Hélène Lallet-Daher[1,2,3,4,*], Delphine Gitenay[1,2,3,4], Baptiste Gras[1,2,3,4], Benjamin Le Calvé[1,2,3,4], Arnaud Augert[1,2,3,4], Mylène Ferrand[1,2,3,4], Natalia Prevarskaya[5], Hélène Simonnet[1,2,3,4], David Vindrieux[1,2,3,4] & David Bernard[1,2,3,4]

Senescence is involved in various pathophysiological conditions. Besides loss of retinoblastoma and p53 pathways, little is known about other pathways involved in senescence. Here we identify two calcium channels; inositol 1,4,5-trisphosphate receptor, type 2 (ITPR2) (also known as inositol 1,4,5-triphosphate receptor 2 (IP3R2)) and mitochondrial calcium uniporter (MCU) as new senescence regulators in a loss-of-function genetic screen. We show that loss of ITPR2, known to mediate endoplasmic reticulum (ER) calcium release, as well as loss of MCU, necessary for mitochondrial calcium uptake, enable escape from oncogene-induced senescence (OIS). During OIS, ITPR2 triggers calcium release from the ER, followed by mitochondrial calcium accumulation through MCU channels. Mitochondrial calcium accumulation leads to a subsequent decrease in mitochondrial membrane potential, reactive oxygen species accumulation and senescence. This ER-mitochondria calcium transport is not restricted to OIS, but is also involved in replicative senescence. Our results show a functional role of calcium release by the ITPR2 channel and its subsequent accumulation in the mitochondria.

[1] Inserm U1052, Centre de Recherche en Cancérologie de Lyon, Senescence escape mechanisms lab, F-69000 Lyon, France. [2] CNRS UMR5286, F-69000 Lyon, France. [3] Centre Léon Bérard, F-69000 Lyon, France. [4] Université de Lyon, F-69000 Lyon, France. [5] Inserm U1003, Equipe labellisée par la Ligue Nationale contre le cancer, Laboratory of Excellence, Ion Channels Science and Therapeutics, Université Lille I Sciences et Technologies, F-59655 Villeneuve d'Ascq, France. * These authors contributed equally to this work. Correspondence and requests for materials should be addressed to D.B. (email: david.bernard@lyon.unicancer.fr).

© 2014 Macmillan Publishers Limited. All rights reserved.

Senescence is characterized by a stable proliferation arrest accompanied by the acquisition of several specific features. It is activated by numerous cellular stresses, such as replicative exhaustion, oncogenic signals or oxidative stress[1]. It is now accepted that senescence induction acts as a protective mechanism against oncogenic events, tumour initiation and progression[2–5]. Besides the cancer-regulated role of senescence, it is also known to be involved in an increasing number of other processes, such as wound healing and various aging-related diseases[6,7]. Most of the pathways known to regulate senescence and, in particular, senescence escape, point to a central role of the p53 as well as the p16–retinoblastoma pathways[8]. Nevertheless, emerging evidences support the existence of other mechanisms regulating senescence escape, although, to date, little is known about these mechanisms[9–15]. Most of the data demonstrating a central role of the p53 and its upstream activators (DNA damage, $p14^{ARF}$) and $p16^{INK4A}$–retinoblastoma pathways were performed in fibroblasts. Similar data generated in human epithelial cells or in other lineages are rather rare, and display a more complex picture of the genetic events involved in senescence escape[15]. For example, human mammary epithelial cells (HECS), which are known to not express $p16^{INK4A}$ (ref. 16), enter senescence in response to oncogenic stress in a DNA damage/p53-independent manner[14,15].

Here, we identify inositol 1,4,5-trisphosphate receptor, type 2 (ITPR2) and mitochondrial calcium uniporter (MCU) as two new actors of senescence, whose knockdown results in senescence escape. Their identification sheds light on the role of calcium movement, and in particular, mitochondrial calcium accumulation in senescence induction.

Results

Identification of calcium channels as senescence modulators. To isolate new senescence regulators, we have performed a loss-of-function genetic screen covering the entire genome to isolate specific small-hairpin RNAs (shRNAs) allowing oncogene-induced senescence (OIS) escape in immortalized HECs. We used post-stasis HECs, which do not express $p16^{INK4A}$ (ref. 16), immortalized by stable expression of hTert (HEC–telomerase reverse transcriptase (Tert)). Cells were infected to stably express MAPK/ERK kinase (MEK):endoplasmic reticulum (ER), a 4-hydroxytamoxifen (4OHT) inducible MEK oncogene, to induce oncogenic stress (HEC–TM). HEC–TM cells were treated with 4OHT at doses not affecting HEC-Tert cell growth. HEC–TM were infected with an shRNA library covering the whole genome and treated every 2 days with 4OHT to induce senescence. Cells having escaped senescence were amplified and their shRNA identified. We have identified multiple potential shRNA-targeted genes. Details of the screening strategy, methods and results were previously described in Lallet-Daher *et al.*[17] We were particularly interested in focusing our work on the ITPR2 calcium channel. This channel is a member of the inosotol 1,4,5-triphosphate (IP3) receptor (ITPR) family, composed of two other members: ITPR1 and ITPR3, the most ubiquitously expressed family of calcium-released channel of the ER. A search in the Oncomine database, a cancer microarray database allowing differential expression analyses between the most major types of cancer and normal tissues, showed a general decrease of ITPR2 mRNA in numerous cancer types (Supplementary Table 1) although an increase in ITPR2 mRNA was also observed in other cancer types (Supplementary Table 1). Interestingly, in the majority of cases, this increase was detected in benign tumours such as oncocytoma (Supplementary Fig. 1a) and prostatic intraepithelial neoplasia (Supplementary Fig. 1b), benign tissues being known to accumulate senescent cells[3]. Finally, ITPR2 levels were found to be significantly lower in primary breast tumours in a cohort of patients displaying metastasis versus the metastasis-free group (Supplementary Fig. 1c). Together, these observations prompted us to study the role of ITPR2 in oncogene-induced senescence escape, a key step required for tumour initiation and progression.

ITPR2 knockdown promotes OIS escape. To validate the role of ITPR2 in OIS, we generated two different ITPR2-targeting shRNAs. As expected, these shRNA strongly decreased ITPR2 mRNA levels (Fig. 1a) without impacting ITPR1 and ITPR3 mRNA levels (Supplementary Fig. 2a). Functionally, ITPR2 depletion by these two shRNAs overcame the growth arrest induced by oncogenic stress (+4OHT), as measured by the ability of the cells to maintain their growth (Fig. 1b,c). Knockdown also resulted in a decrease of two independent senescence markers; senescence-associated beta-galactosidase (SA-β-Gal) activity (Fig. 1d) and interleukin 8 expression (Fig. 1e), further confirming a role of ITPR2 in OIS escape. By performing quantitative reverse transcriptase-PCR (qRT–PCR), we found that ITPR1, 2 and 3 were all expressed in HEC–TM cells (Supplementary Fig. 2b). Interestingly, ITPR1 (Supplementary Fig. 2c) and ITPR3 knockdown (Supplementary Fig. 2d), also promoted OIS escape (Supplementary Fig. 2e). Of note, expression of ITPR1, 2 and 3 were only slightly altered during senescence, suggesting their role during senescence might be owing to alterations of their activities rather than alteration of their expression (Supplementary Fig. 2f).

IP3-induced ITPR activation induces premature senescence. We next wanted to know whether a gain-of-function of ITPR activity affected senescence. To this end, the ITPR ligand, IP3 (membrane-permeant), was used to activate ITPR. Interestingly, ITPR activation blocked cell growth (Fig. 2a,b), induced SA-β-Gal activity (Fig. 2c) and the interleukin 8 senescence marker expression (Fig. 2d). Together, the data show that ITPR loss-of-function promotes OIS escape, whereas ITPR activation by IP3 induces a premature senescence.

Oncogene stress provokes mitochondrial calcium relocation. As ITPR2 and the other members of ITPR family are calcium channels involved in regulating the exit of calcium from the ER[18], we examined calcium changes during OIS using the Oregon Green calcium probe. We tracked calcium in live proliferating cells (−4OHT) and in cells in OIS (+4OHT). We observed a strong change in calcium localization and pattern as it accumulated in dots in the cytoplasm of senescent cells (Fig. 3a,b). Interestingly, a change in calcium pattern was not found in ITPR2-knockdown cells (Fig. 3a,b). We conclude that senescent cells, at least in response to oncogenic stress, display an altered calcium homoeostasis and this phenomena involves the ITPR2 channel.

Oncogene stress lead to mitochondrial calcium accumulation. We next wanted to determine the altered localization of calcium in senescent cells. We hypothesized that the mitochondria would be involved in this redistribution, since calcium release by the ER can be transferred to mitochondria[19], and also because the MCU[20,21], a key component in mitochondrial calcium uptake, was identified in the genetic screen[17]. To examine the localization of calcium dots in senescent cells, we used an red fluorescent protein (RFP)-tagged mitochondrial protein which showed that the calcium dots co-localize with the mitochondria during OIS (Fig. 4a, yellow dots). To further confirm mitochondrial calcium accumulation in senescent cells, we introduced a genetically encoded, mitochondrially targeted calcium indicator

© 2014 Macmillan Publishers Limited. All rights reserved.

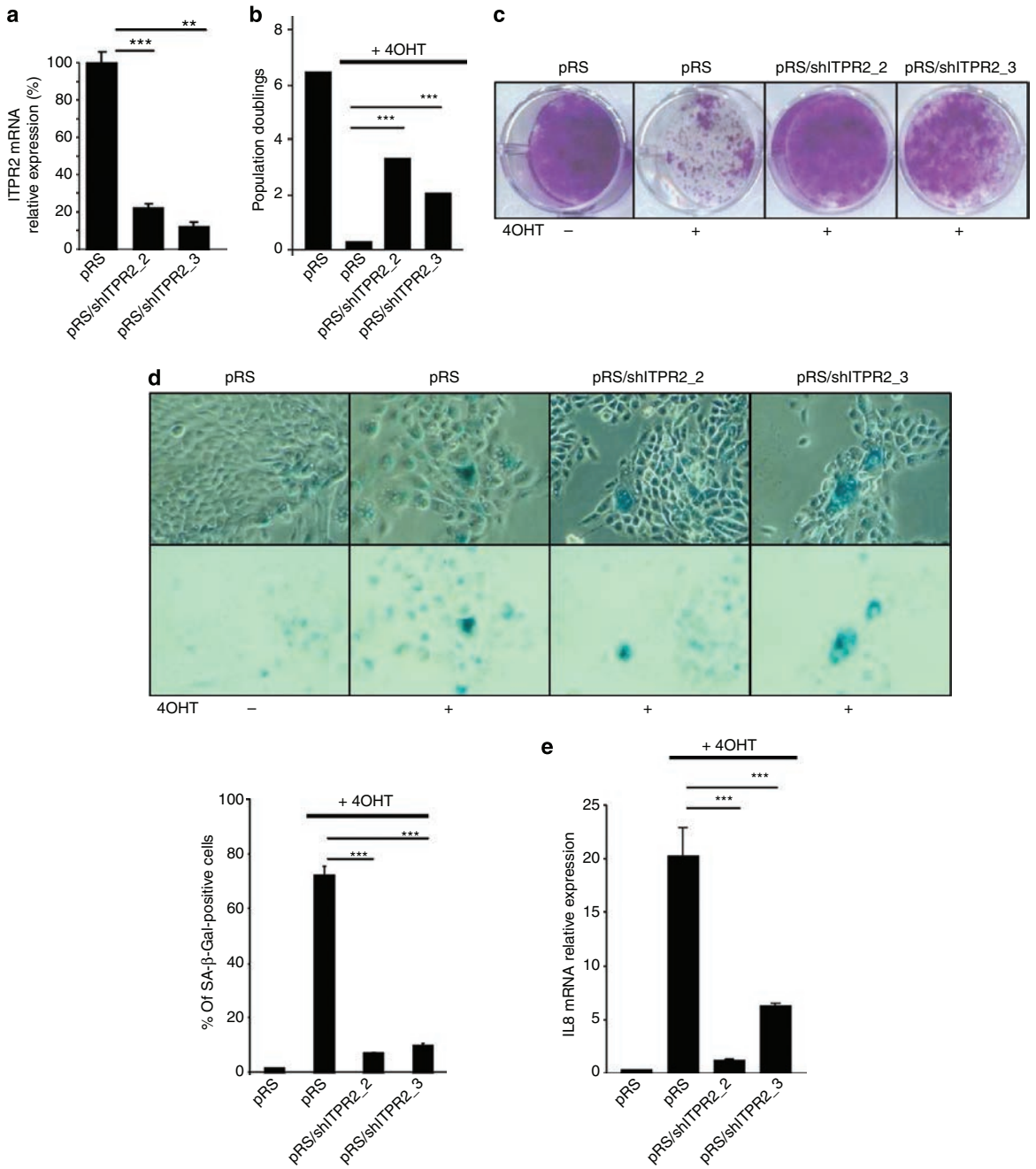

Figure 1 | ITPR2 knockdown promotes escape from OIS. HEC-TM cells were infected with a control empty vector (pRS) or with two independent ITPR2-targeting shRNA (shITRP2_2 and 3) retroviral vectors and then the selected puromycin. (**a**) RNAs were extracted, retro-transcribed and ITPR2 mRNA levels analyzed by quantitative PCR. ITPR2 mRNA expression was normalized to β-actin mRNA expression. (**b**) Cells were treated daily with 4OHT for 3 days to induce senescence. Six days after the 4OHT treatment, cells were counted and the number of population doublings was calculated. (**c**) After seeding, cells were treated daily with 4OHT for 3 days. After 10 days, cells were paraformaldehyde fixed and crystal violet stained to monitor cell growth. (**d**) Cells were seeded and 4OHT treated. Six days later, cells were fixed and SA-β-Gal activity was assayed (mean ± s.d. are shown). (**e**) Cells were seeded and 4OHT treated. RNAs were extracted and expression of the IL8 senescence marker analyzed by RT-qPCR. IL8 mRNAs were normalized against β-actin levels. Images shown are representative of experiments performed at least three times. Graphs are presented with s.e.m. as errors bars, except for panel (**d**), and the student *t*-test was used to determine the *P*-value. $^{**}P<0.01$; $^{***}P<0.001$.

'mito-GCaMP2' (ref. 22). The specificity of this mitochondrial calcium reporter was demonstrated as its fluorescence increased following IP3 treatment, which was inhibited when the cells were pre-treated with an inhibitor of MCU (Ru360) (Fig. 4b). Importantly, we observed a fluorescence increase in senescent cells, absent in ITPR2-knockdown cells (Fig. 4c). Inversely, ITPR activation by IP3 treatment, which induced senescence (Fig. 2), also resulted in mitochondrial calcium accumulation (Fig. 4d).

© 2014 Macmillan Publishers Limited. All rights reserved.

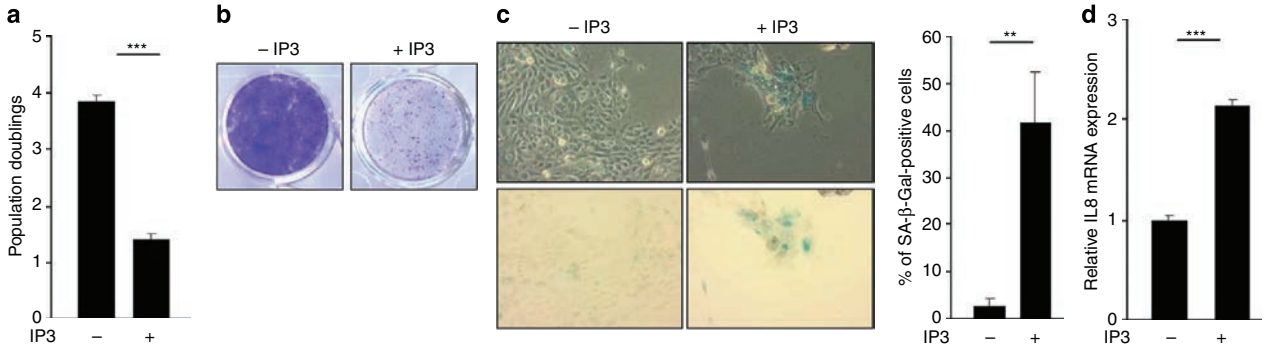

Figure 2 | ITPR activation induces premature senescence. HEC-TM cells were seeded at the same density and treated or not every day for 5 days with 5 μM IP3. The following day, various assays were performed. (**a**) Cells were counted and the number of population doublings was calculated. (**b**) Cells were paraformaldehyde fixed and crystal violet stained to monitor cell growth. (**c**) Cells were fixed and SA-β-Gal activity was assayed. Means ± s.d. are presented in the graph. (**d**) RNAs were extracted and expression of the IL8 senescence marker analyzed by RT-qPCR. IL8 mRNAs were normalized to β-actin levels. Images shown are representative of experiments performed at least twice. Graphs are presented with s.e.m. as errors bars, except for panel (**c**), and the student *t*-test was used to determine the *P*-value. $^{**}P<0.01$; $^{***}P<0.001$.

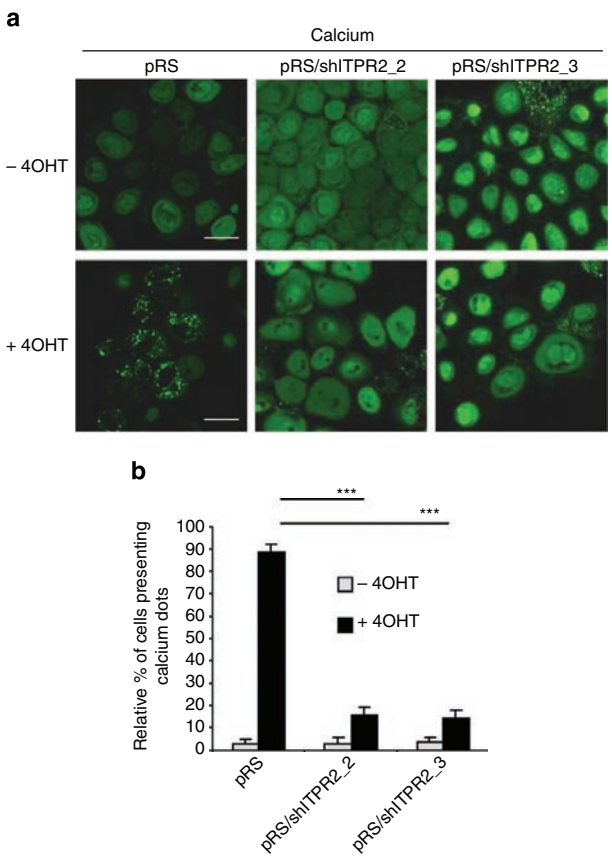

Figure 3 | ITPR2 participates in calcium movement during OIS. (**a**) HEC-TM cells expressing or not an shRNA directed against ITPR2 were seeded at the same density. The following day, they were treated daily with 4OHT for 3 days and the next day, living cells were incubated with the calcium probe (Oregon green) and their fluorescence analyzed by confocal microscopy. (**b**) Percentage of cells displaying calcium dots was calculated for each condition. Scale bar, 50 μM. Graphs are presented with s.e.m. as errors bars, and the student *t*-test was used to determine the *P*-value. $^{***}P<0.001$.

Overall, this demonstrates that senescent cells accumulate calcium in mitochondria, with calcium accumulation and OIS being abolished in ITPR2-knockdown cells.

Mitochondrial calcium accumulation mediates OIS. To functionally demonstrate that calcium entry is a key event in ITPR-mediating OIS, we performed knockdown against MCU. As expected, MCU-knockdown cells (Fig. 5a) displayed a strong decrease in mitochondrial calcium accumulation following oncogenic stress induction (Fig. 5b). This decreased mitochondrial calcium level allowed cells to escape OIS, as measured by their ability to proliferate (Fig. 5c,d) and the absence of senescence markers (Fig. 5e,f). In addition, knockdown of MICU1 (Supplementary Fig. 3a), an interactor and modulator of MCU[23,24], potentiated low oncogenic stress to induce OIS (Supplementary Fig. 3b,c) with concomitant mitochondrial calcium accumulation (Supplementary Fig. 3d).

Our results support the findings that, during OIS, calcium released from the ER through ITPR channels accumulates in the mitochondria, resulting in senescence. An ER/mitochondria liaison can facilitate calcium exchange between both organelles[19]. We then examined ER/mitochondria contact sites by co-labelling both organelles and counting co-localized signals to examine whether there was any change during OIS. No changes in the number of contact sites were observed during OIS or in ITPR2-knockdown cells (Supplementary Fig. 4).

Mitochondrial calcium leads to mitochondrial potential drop. The next question we wanted to address was how mitochondrial calcium overload leads to OIS. Abnormal levels of calcium in the mitochondria are known to result in a decrease of the mitochondrial potential ($\Delta\psi(m)$)[25,26]. We observed a drop in the $\Delta\psi(m)$ during OIS, as assayed by the fluorescence intensity drop of the Rhodamine 123 (Supplementary Fig. 5) and by the ratiometric change of JC-1 fluorescence (Fig. 6a,b). Oncogenic stress-induced mitochondrial depolarization was not observed in ITPR2- or MCU-knockdown cells (Fig. 6a,b and Supplementary Fig. 5), suggesting that mitochondrial calcium overload during OIS triggers the $\Delta\psi(m)$ drop. This was largely supported by the observation that, following oncogenic stress induction, mitochondrial calcium accumulation occurred before the $\Delta\psi(m)$ drop (Supplementary Fig. 6). While our results suggest

© 2014 Macmillan Publishers Limited. All rights reserved.

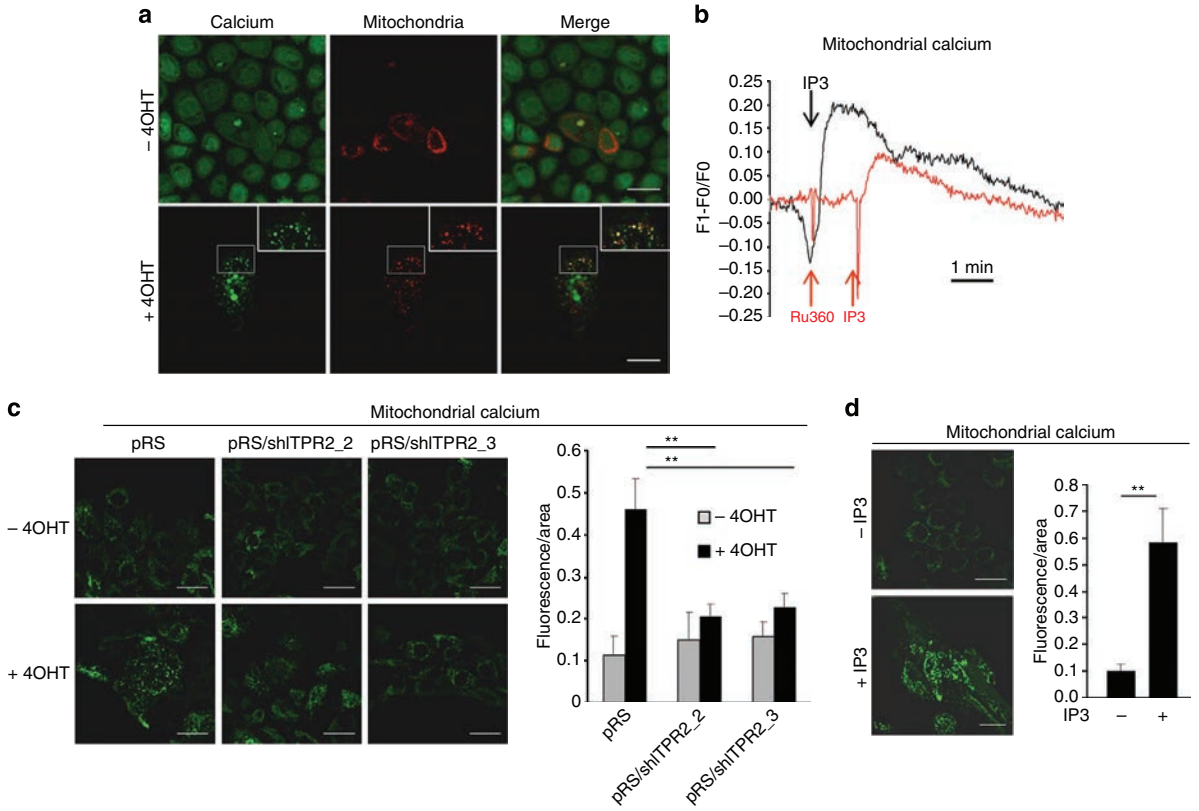

Figure 4 | Oncogenic stress induces mitochondrial calcium uptake during OIS. (**a**) HEC-TM cells were seeded at the same density, treated or not with 4OHT, transduced to express an RFP-coupled mitochondrial protein and a day later labelled by the calcium probe. Live cells fluorescence was examined using confocal microscopy. (**b**) HEC-TM cells were infected with a retroviral vector encoding the mitochondrial calcium genetic reporter (mito-GCaMP2). Cells were treated with 5 μM IP3, with or without 10 μM Ru360 MCU inhibitor. Fluorescence intensities in at least five ROI were recorded and results displayed. (**c**) Senescence was induced by 4OHT treatment for 3 days. Three days after the end of this treatment, mitochondrial calcium reporter fluorescence intensity was recorded and quantified for each condition ($n>5$ fields for nontreated cells, $n>10$ fields for treated cells). Quantification is representative of experiments performed at least three times. (**d**) Cells were treated or not with 5 μM IP3 for 5 days. The following day, mitochondrial calcium reporter fluorescence intensity was recorded and quantified for each condition ($n>15$ fields). Scale bar, 50 μM. Graphs are presented with s.e.m. as errors bars, and the student *t*-test was used to determine the *P*-value. $^{**}P<0.01$.

that mitochondrial calcium accumulation is the initiating event and that it precedes depolarization, it is also probable that depolarization further amplifies mitochondrial calcium accumulation as previously described[27]. To assess the role of Δψ(m) drop during senescence, we treated cells with the carbonyl cyanide 4-(trifluoromethoxy)phenylhydrazone (FCCP) uncoupler to force mitochondrial depolarization (Fig. 7a). Mitochondrial depolarization was found to block cell growth (Fig. 7b,c) and to induce senescence markers (Fig. 7d,e) supporting a key role of a Δψ(m) drop in OIS. In all the above experiments, we verified that immortalized HEC, not expressing the MEK:ER oncogene, did not display any alterations in senescence, mitochondrial calcium levels and Δψ(m) in response to 4OHT treatment (Supplementary Fig. 7).

Mitochondrial potential drop leads to ROS production. Mitochondrial calcium accumulation and mitochondrial depolarization are known to generate ROS, which are OIS mediators[28,29]. First we analyzed whether senescence was induced by oncogenic stress through ITPR2 involved ROS production. We observed an ROS increase in response to oncogenic stress in an ITPR2-dependent manner (Fig. 8a). Accordingly, we also observed a rise in ROS production during IP_3- or FCCP-induced premature senescence (Supplementary Fig. 8). Further supporting a role of ROS in mediating oncogenic stress/mitochondrial calcium accumulation-induced senescence, treatment with the antioxidant GSH resulted in OIS escape (Fig. 8b).

Mitochondrial calcium participates in replicative senescence. The above results were generated in the context of OIS, we next wanted to assess whether similar redistribution of calcium occurs during replicative senescence, a senescence induced by short telomeres and a DNA damage-like response, and not based on oncogenic stress. To this end, we used WI38 human fibroblasts[30] (Supplementary Fig. 8a,b). In accordance with OIS, replicative senescent fibroblasts were also found to display mitochondrial calcium accumulation (Supplementary Fig. 9c,d) and a Δψ(m) drop (Supplementary Fig. 9e,f). Importantly, MCU and ITPR2 knockdown inhibited these alterations during replicative senescence (Supplementary Fig. 9g) and delayed senescence (Supplementary Fig. 9h,i). Together, these data support a major role of calcium signalling and mitochondrial activity alterations during replicative senescence, suggesting that calcium displacement and ensuing consequences are general markers and actors of senescence.

© 2014 Macmillan Publishers Limited. All rights reserved.

Discussion

Using a loss-of-function genetic screen, we identified ITPR2 and MCU, two calcium channels whose depletion allowed OIS bypass. This identification has revealed a major role of calcium movement and mitochondrial calcium accumulation in the regulation of OIS. Importantly, the participation of these channels and mitochondrial calcium accumulation was also observed during replicative senescence. Overall, our results unveil a novel signalling pathway involving increased mitochondrial calcium uptake inducing OIS.

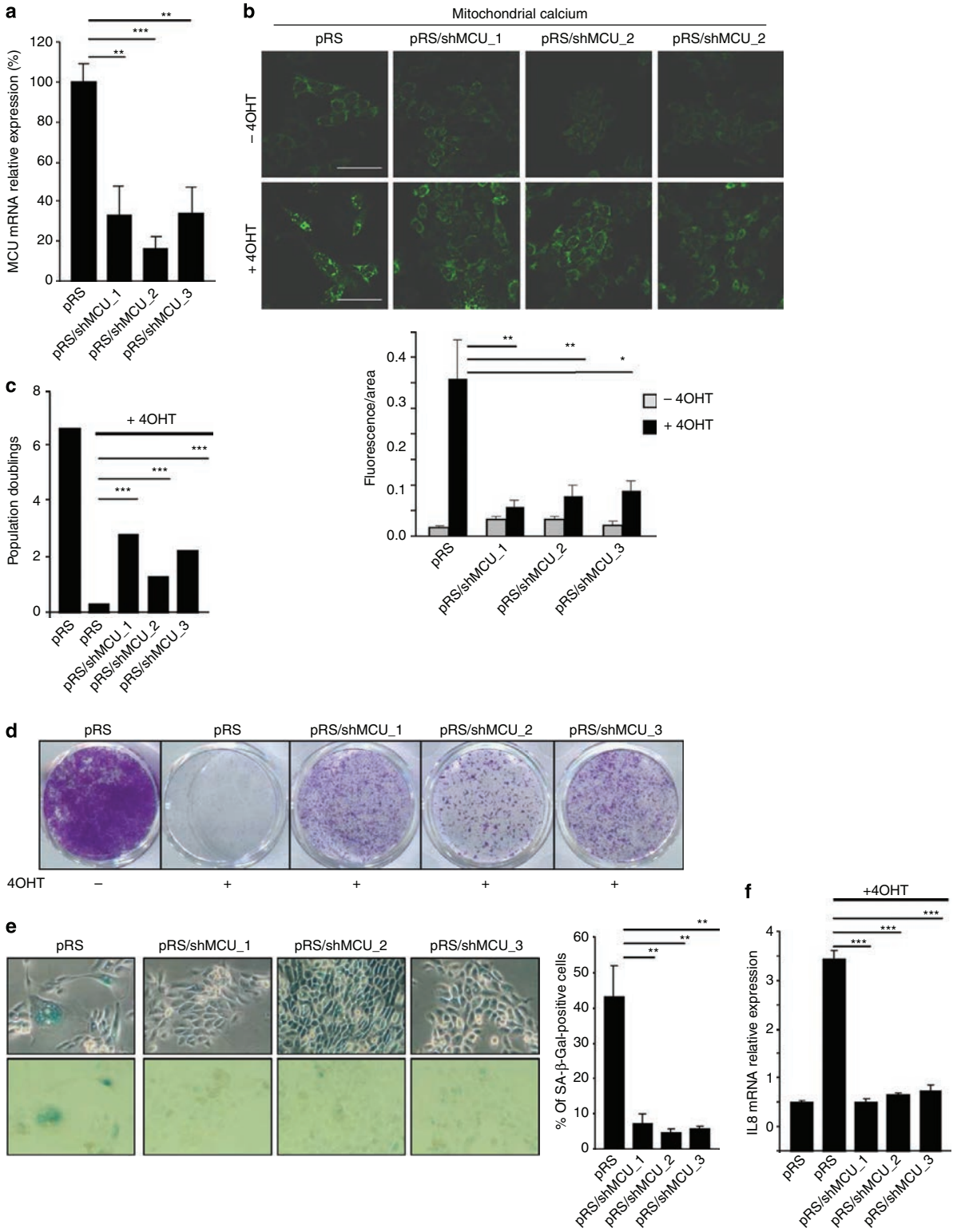

© 2014 Macmillan Publishers Limited. All rights reserved.

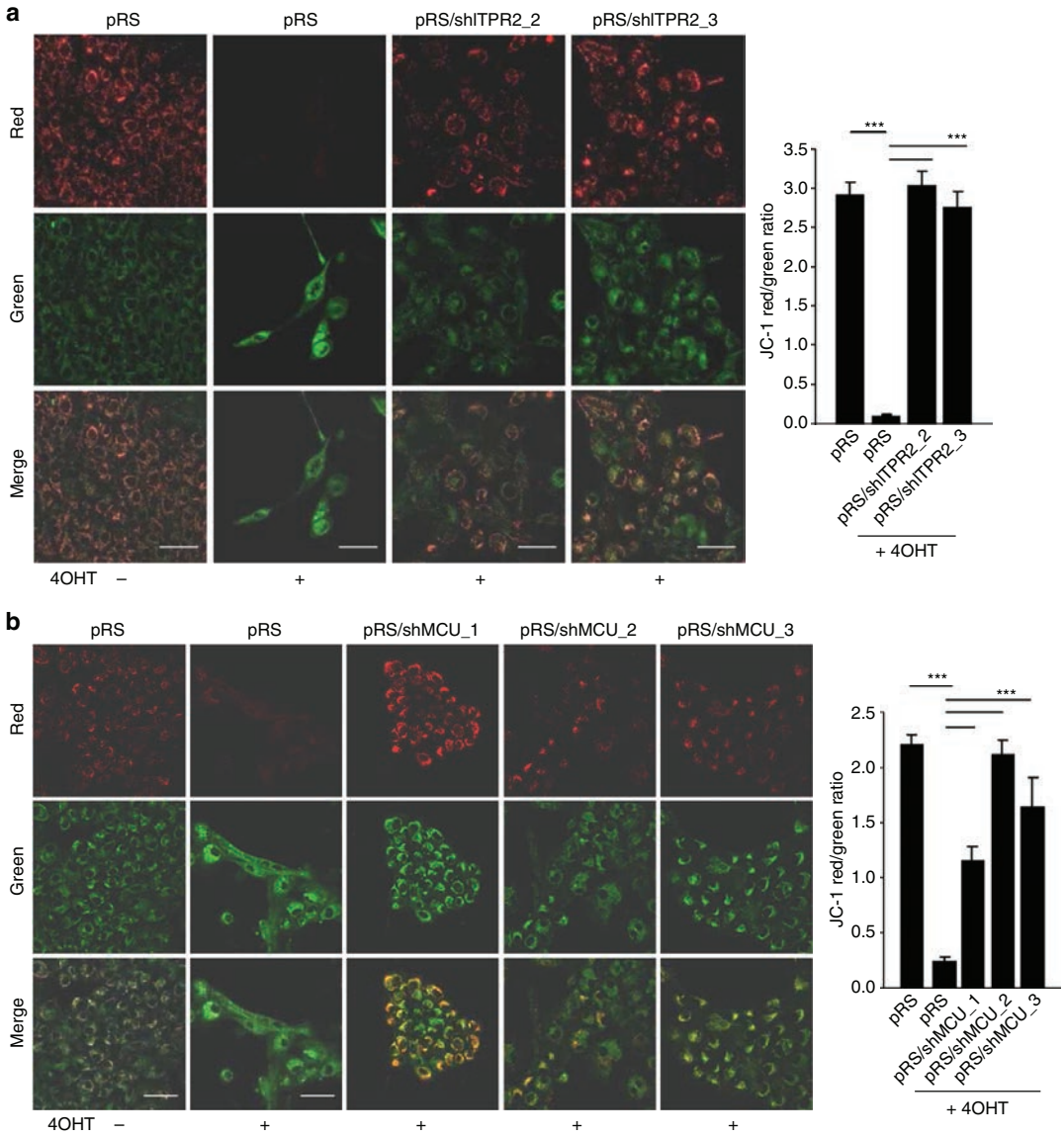

Figure 6 | Mitochondrial calcium accumulation during OIS provokes a drop in the mitochondrial potential. (**a**) HEC–TM cells were infected with a control empty vector (pRS) or with ITPR2-targeting shRNA retroviral vectors. After seeding they were treated for 3 days with 4OHT. Four days later, JC-1 probe was added and live fluorescence recorded and quantified. JC-1 red/green ratio was calculated to follow $\Delta\psi(m)$ (**b**) HEC–TM cells were infected with a control (ctrl) or with ITPR2-targeting shRNA retroviral vectors. They were next processed as described in (**a**) to measure $\Delta\psi(m)$ in the various conditions. Six to 12 fields were analyzed for each condition. Scale bar, 50 μM. Images shown are representative of experiments performed at least twice. Graphs are presented with s.e.m. as errors bars. *P*-values were determined using the student *t*-test. $^{*}P<0.05$; $^{**}P<0.01$; $^{***}P<0.001$.

Figure 5 | MCU knockdown blocks mitochondrial calcium accumulation and induces OIS escape. HEC–TM cells were infected with a control empty vector (pRS) or independent MCU-targeting shRNA retroviral vectors and then puromycin selected. (**a**) RNA were prepared and retro-transcribed. Quantitative PCR against MCU was performed and the results were normalized to β-actin mRNA levels. (**b**) Cells transduced with a mitochondrial calcium genetic reporter were seeded at the same density, treated with 4OHT for 3 days. Four days later, fluorescence intensities were recorded and results displayed ($n>5$ fields for nontreated cells, $n>10$ fields for treated cells). (**c**) After seeding the same amount of cells, they were treated daily with 4OHT for 3 days to induce senescence. Six days after the 4OHT treatment, cells were counted and the number of population doublings was calculated. (**d**) Empty pRS or shRNA-MCU expressing cells were seeded at the same density, treated for 3 days with 4OHT. Ten days later, cells were paraformaldehyde fixed and crystal violet stained to monitor cell growth. (**e**) Cells were seeded, and treated for the next 3 days with 4OHT. Six days later, cells were fixed and an SA-β-Gal assay performed. SA-β-Gal-positive cells were counted and representative photographs are shown (Mean ± s.d.) (**f**) The day after seeding, cells were 4OHT treated for 3 days. Two days later, RNAs were prepared, retro-transcribed and analyzed by quantitative PCR against IL8 and normalized to β-actin levels. Scale bar, 50 μM. Graphs are presented with s.e.m. as errors bars, except for panel (**e**), and the student *t*-test was used to determine the *P*-value. $^{*}P<0.05$; $^{**}P<0.01$; $^{***}P<0.001$.

© 2014 Macmillan Publishers Limited. All rights reserved.

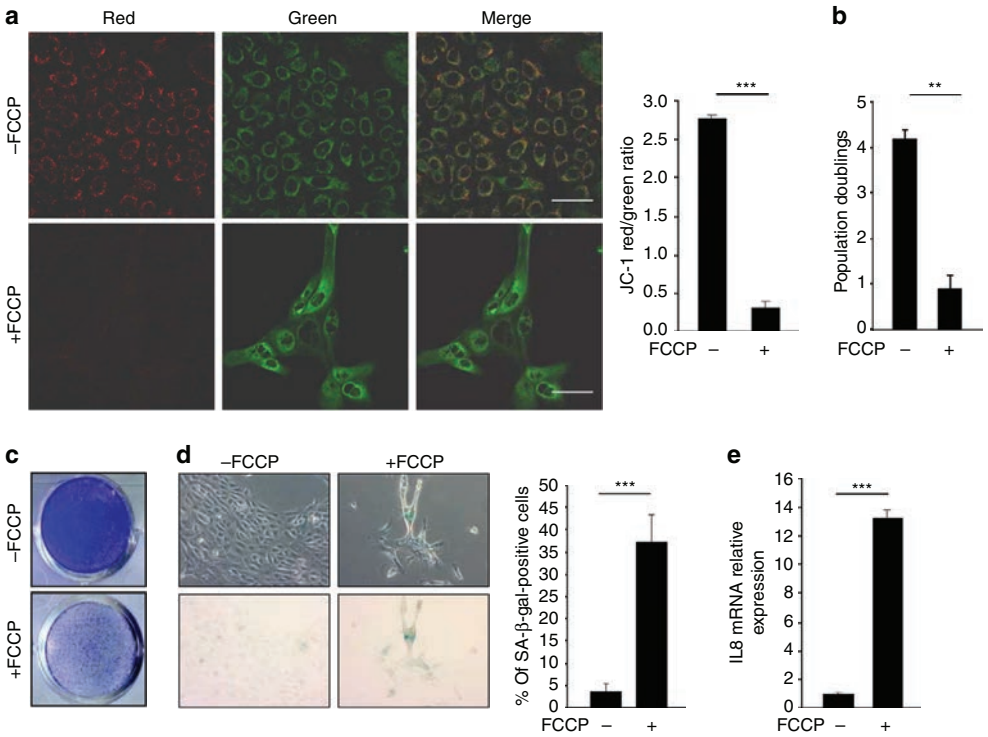

Figure 7 | Mitochondrial depolarization induces premature senescence. HEC-TM cells were seeded at the same density and treated or not with 300 nM FCCP for 4 days. The following day, cells were analyzed. (**a**) Cells were incubated with JC-1 probe and live fluorescence (Em 500–560 nm = green, and Em 590–650 nm = red) was recorded and quantified. JC-1 red/green ratio was calculated to evaluate $\Delta\psi(m)$ ($n > 10$ fields). (**b**) Cells were counted and the number of population doublings was calculated. (**c**) Cells were paraformaldehyde fixed and crystal violet stained to monitor cell growth. (**d**) Cells were fixed and SA-β-Gal staining performed. Mean ± s.d. shown. (**e**) RNA were extracted and RT-qPCR against IL8 senescence marker performed. Results are normalized to β-actin levels. Experiments were performed in triplicate, and results displayed are representative of experiments performed at least twice. Scale bar, 50 μM. Graphs are presented with s.e.m. as errors bars, and the student *t*-test was used to determine the *P*-value. $^{**}P < 0.01$; $^{***}P < 0.001$.

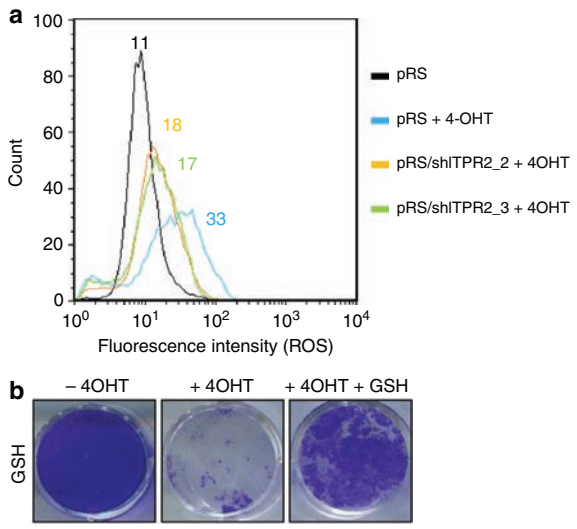

Figure 8 | ITPR2 activity regulates OIS through ROS production. (**a**) HEC-TM cells expressing or not ITPR2-directed shRNA were treated with 4OHT for 3 days. Two days later, cells were incubated with H2DCF-DA (30 min; 3 μM) and their ROS contents analyzed by FACS. (**b**) HEC-TM cells were treated with 4OHT for 3 days and GSH at 0.05 mM for 3 days.

In this study, we mainly investigated the role of mitochondrial calcium accumulation on senescence, following its release from the ER through ITPR2. The rationale for studying this was—calcium release by the ER can be transferred to the mitochondria[19] where calcium might exert deleterious effects (that is, apoptosis)[25,26]— and an shRNA directed against MCU, a transporter allowing mitochondrial calcium entry, was isolated during the genetic screen as potentially allowing OIS escape. The data accumulated confirm a prosenescent role of mitochondrial calcium accumulation. Indeed, the calcium accumulated in senescent cells (OIS, replicative senescence, induced by IP3) and its decrease by MCU knockdown results in senescence escape.

ITPR channels are known regulators of other responses such as ER stress, autophagy and apoptosis[31–37]. The effect of ITPR2 on senescence did not appear to be linked to its role in ER stress (Supplementary Fig. 10a) or apoptosis (Supplementary Fig. 10b), as both of these remained unchanged during OIS. Autophagy, as described by others[38], is modified during OIS, and this is partly reverted in ITPR2-knockdown cells (Supplementary Fig. 10c). Further studies will be required to determine a link between ITPR2, calcium and autophagy during senescence.

The mitochondrial calcium accumulation observed during OIS or replicative senescence resulted in a decrease of the $\Delta\psi(m)$ and subsequent ROS production. Interestingly, decrease of the $\Delta\psi(m)$ is observed in senescent cells, in aging and in response to oncogenic stress[39–42]. Nevertheless, the mechanisms responsible

© 2014 Macmillan Publishers Limited. All rights reserved.

for the deregulation of mitochondrial activity in stress-induced senescent cells are not known. Our data support the view that accumulation of mitochondrial calcium is responsible for the $\Delta\psi(m)$ drop induced during replicative or oncogene-induced senescence. In addition, we observe that decreased $\Delta\psi(m)$ leads to ROS production that according to our results, has an impact on senescence. It is also possible that other processes affected by mitochondrial activity alterations, such as decreased ATP production during senescence, participate in senescence regulation[30,41,43–45]. We have recently reported that the decreased ATP levels during OIS in the same model correlated with decreased glucose entry and metabolism[46]. In light of our results, we speculate that the mitochondrial alterations we observed also contribute to decrease ATP levels.

In conclusion, our results outline a new pathway, controlled by ITPR2, but also by other ITPR and MCU calcium channels causing mitochondrial calcium accumulation, which decreases mitochondrial activity, and induces ROS accumulation and senescence. Our results offer new perspectives for understanding and developing new tools to manipulate senescence and its related disorders.

Methods

Cell culture. HECs (Lonza) were cultured in mammary epithelial cell growth medium (Promocell) supplemented with penicillin/streptomycin 100 U ml^{-1} (Life Technologies). Virus-packaging GP293 cells (Clontech) and human fibroblasts WI38 cells (ATCC) were cultured in Dulbecco's modified Eagle's medium (DMEM, Life Technologies) supplemented with 10% foetal bovine serum (Life Technologies) and penicillin/streptomycin 100 U ml^{-1} (Life Technologies). The cells were maintained at 37 °C under a 5% CO_2 atmosphere.

Vectors and gene transfer. Retrovirus pRetroSuperpuro (pRS) encoding shRNAs directed against ITPR2 and MCU were constructed by subcloning oligonucleotides targeting the following sequences: sh2 ITPR2 5′-GAGAAATGTTAGAGAAGAA-3′, sh3 ITPR2 5′-CAGAAAACTACTAGAGAAA-3′, sh1 MCU 5′-CGGCTTACCT GGTGGGAAT-3′, sh2 MCU 5′-AGGCAGAAATGGACCTTAA-3′, sh3 MCU 5′- GTTTTGACCTAGAGAAATA as described in Brummelkamp *et al.*[47] Mitochondrial calcium fluorescent genetic reporter 'mito-GCaMP2' was extracted by digestion with StuI-HindIII from pCDN3.1 vector[22] and cloned EcoRV-HindIII into pLNCX2 retroviral vector (Clontech). The plasmid pNLCΔMEK1 (ΔN3, S218E, S222D):ER was used to transfer the MEK oncogene. PEI reagent (Euromedex) was used according to the manufacturer's recommendations to transfect GP293 cells with the indicated vector. Two days after transfection, the virus-containing supernatant was mixed with fresh medium (1/2) and hexadimethrine bromide at 8 μg ml^{-1} (Sigma) and used to infect target cells. Infected HECs were selected with G418 (Life Technologies) at 100 μg ml^{-1} and/or puromycin (InvivoGen) at 500 ng ml^{-1}. Knockdown of ITPR1 or ITPR3 was performed using Mission Lentiviral Transduction particles targeting ITPR1 (NM_002222) or ITPR3 (NM_002224) (or Green Fluroscent Protein as control) purchased from Sigma-Aldrich (clone ID TRCN0000061244 and TRCN0000061326).

Chemicals. 4OHT (Sigma) was used daily for 3 days at 250 nM. FCCP (sc-203578, Santa Cruz) was used daily at 300 nM, 236-Tri-O-Butyryl-myo-Inositol-145-Trisphosphate-Hexakis(acetoxymethyl) Ester, IP_3-AM (Sichem) was used at a final concentration of 5 μM. 10 mM Ru360 (Sigma) was used to inhibit MCU. Reduced glutathione (GSH) (Sigma) was used at a concentration of 0.05 mM.

ROS quantification. Cellular ROS contents were measured by incubating cells with 3 μM H_2DCF-DA probe for 30 min. The cells were washed in phosphate-buffered saline (PBS) (1 ×) buffer, trypsinised, washed again and resuspended in 500 μl PBS. ROS levels were analyzed by Fluorescence Activated Cell Sorting on a FACSCalibur flow cytometer, with 10,000 events recorded. The final data were analyzed using the Flow Jo 7.5.5 software.

SA-β-Gal analysis and growth assays. Cells were seeded into six-well plates. Briefly, for growth assays, cells were washed in PBS, fixed for 15 min in 3% formaldehyde and then coloured with a crystal violet solution. For SA-β-gal assay, cells were washed twice in PBS, fixed for 5 min (room temperature) in 2%formaldehyde/0.2% glutaraldehyde, washed twice in PBS, and incubated overnight at 37 °C (no CO2) with a fresh SA-β-Gal stain solution as previously described in Augert *et al.*[30]

Immunoblotting. Protein extracts were resolved by SDS-polyacrylamide gel electrophoresis and transferred to 0.45 μm nitrocellulose membrane (BioRad). Membranes were blocked in PBS containing 5% nonfat milk, 0.05% Tween 20. They were then probed overnight at 4 °C with the appropriate antibodies and dilutions. The secondary antibodies were either a peroxidase-conjugated donkey antirabbit immunoglobulin G or a peroxidase-conjugated goat antimouse immunoglobulin G (Jackson ImmunoResearch Laboratories, 1:5,000). Peroxidase activity was revealed using an enhanced chemiluminescence kit (GE healthcare). The primary antibodies used were: anti-phosphoERK (1:1,000, 9101, Cell Signalling), anti-phospho-histone3Ser10 (1:1,000, ab14955, Abcam), anti-active caspase 3 (1:250, ab 32042, Abcam), anti-LC3 (1:7,500, PM036, MBL) and anti-tubulin (1:5,000, T6199, Sigma).

Reverse transcription and real-time quantitative PCR. Total RNA were extracted based on a phenol-chloroform protocol, using TriReagent (Sigma-Aldrich) and PhaseLockGel tubes (Eppendorf). 2 μg of total RNA was retro-transcribed into complementary DNA (cDNA) using The First-Strand cDNA Synthesis Kit (GE Healthcare, Chalfont St Giles, UK) according to the manufacturer's instructions. A 1:60 dilution of this RT reaction mixture was used as the cDNA template for qPCR. TaqMan qPCR was carried out on a LightCycler 2.0 System (Roche Applied Science). The final qPCR mixture was composed of the LightCycler TaqMan mix (dilution 1:5) (Roche), 200 nM of primers, the Universal Probe Library probe (100 nM) for the gene of interest (TaqMan Gene Expression Assays (primers/probe), Life Technologies) added up with 1.67 μl of cDNA template. All reactions were performed in triplicate. The relative amount of mRNA was calculated by the comparative Cp method following normalization against β-actin. The primers and probes used are listed in the Supplementary Table 2.

Confocal microscopy. Samples were analyzed with a Zeiss LSM 780 NLO confocal microscope using a × 63 oil or a × 40 oil objective. During imaging, live cells were maintained at 37 °C in the microscope's environmental chamber. Image acquisition was carried out with the same gain, amplification, and exposure time between each experimental condition and the corresponding control. Images were captured using the Zen software and were then processed (cropping, addition of scale bars) using NIH ImageJ. Fluorescence intensity was measured with the ImageJ software. In each 8 bit image, fluorescence intensity above an automatic threshold was measured and if necessary, the corresponding area was also recorded.

Calcium imaging and mitochondrial labelling. Cells were plated in glass-bottom dishes (ThermoScientific-Nunc). Cells were transduced with a modified baculovirus coding a mitochondrial protein fused to a RFP according to the manufacturer's recommendations (CellLight Mitochondria-RFP, BacMam 2.0, C10505, Life Technologies). Sixteen hours post-transduction, Oregon Green488 dye (O-6147, Molecular Probes) was used to visualize any change in calcium localization in the cytoplasmic compartment. Cells were washed three times with 1 ml of HBSS without calcium (Life Technologies), treated with Oregon Green488 dye at 2 nM for 30 min at 37 °C and washed twice with HBSS without calcium. Live cells were analyzed using confocal microscopy (Ex 561 nm/Em535–690 m).

Alternatively, cells were transduced with a genetically encoded mitochondrially targeted calcium indicator. Following selection with G418, cells were seeded in glass-bottom dishes and treated with 4OHT, IP_3-AM or FCCP as indicated. Fluorescence (Ex 488 nm/Em 500–570 nm) was investigated in live cells using Zeiss LSM 780 confocal microscope. Fluorescence intensity was quantified (ImageJ). Results were calculated by dividing the mean pixel intensity by the area of the measured spot. In short-term analysis, fluorescence was recorded every 1.5 s using a Zeiss LSM 780 confocal microscope. The duration of the change in mitochondrial calcium change at a region-of-interest (ROI) was calculated as the average of each ROI. Permeant-IP_3 was injected after 1 min of measurement at a final concentration of 5 μM. Results are shown as (F1-F0)/F0, where F0 is the mean of the intensities from 10 s to 50 s.

Mitochondrial membrane potential. Cells were plated in glass-bottom dishes (ThermoScientific-Nunc). To measure $\Delta\psi(m)$, cells were washed three times with 1 ml of HBSS without calcium, incubated with 10 μM Rhodamine 123 (R-302, Life Technologies) for 30 min, and washed again extensively before analysis by confocal microscopy (Ex 514 nm/Em520–660 nm).

Alternatively, a ratiometric JC-1 probe (M34152, Life technologies) was used to discriminate energized and de-energized mitochondria. Fluorescence emission shift from green (530 nm) to red (590 nm) occurs when the dye is concentrated. As red fluorescent aggregates in areas with high potential membrane, mitochondrial depolarization is indicated by decreased red/green fluorescence intensity ratio. Cells were washed, incubated 10 min at 37 °C with 2 μM JC-1, washed extensively and fluorescence emission was recorded using an LSM 780 Zeiss confocal microscope (Ex 488 nm/Em 500–560 nm/590–650 nm).

ER-mito contact sites. A Z-stack of optical sections was captured using a Zeiss LSM 780 confocal microscope with an Apochromat 63 × /1.40 oil objective (0.720 μM slice thickness, 30 Z sections collected at 0.360 μM intervals). Nuclei

© 2014 Macmillan Publishers Limited. All rights reserved.

were labelled with Hoechst, ER were labelled with anti-calnexin (C5C9, 2679, Cell Signalling), and MitoProfile Total OXPHOS Human Antibody Cocktail (ab110411, Abcam) was used to label mitochondria. Colocalisation between ER and mitochondria was quantified using Manders' overlap coefficient.

Statistics. Graphs are presented with s.e.m. as errors bars, unless stated otherwise, and the student *t*-test was used to determine the *P*-value. $^{*}P<0.05$; $^{**}P<0.01$; $^{***}P<0.001$ unless specified otherwise in the figure legends.

References

1. Kuilman, T., Michaloglou, C., Mooi, W. J. & Peeper, D. S. The essence of senescence. *Genes Dev.* **24,** 2463–2479 (2010).
2. Ben Porath, I. & Weinberg, R. A. When cells get stressed: an integrative view of cellular senescence. *J. Clin. Invest.* **113,** 8–13 (2004).
3. Collado, M. & Serrano, M. Senescence in tumours: evidence from mice and humans. *Nat. Rev. Cancer* **10,** 51–57 (2010).
4. Hanahan, D. & Weinberg, R. A. Hallmarks of cancer: the next generation. *Cell* **144,** 646–674 (2011).
5. Kang, T. W. *et al.* Senescence surveillance of pre-malignant hepatocytes limits liver cancer development. *Nature* **479,** 547–551 (2011).
6. Campisi, J. Cellular senescence: putting the paradoxes in perspective. *Curr. Opin. Genet. Dev.* **21,** 107–112 (2011).
7. Jun, J. I. & Lau, L. F. The matricellular protein CCN1 induces fibroblast senescence and restricts fibrosis in cutaneous wound healing. *Nat. Cell Biol.* **12,** 676–685 (2010).
8. Itahana, K., Campisi, J. & Dimri, G. Mechanisms of cellular senescence in human and mouse cells. *Biogerontology* **5,** 1–10 (2004).
9. Christoffersen, N. R. *et al.* p53-independent upregulation of miR-34a during oncogene-induced senescence represses MYC. *Cell Death Differ.* **17,** 236–245 (2010).
10. Ewald, J. A., Desotelle, J. A., Wilding, G. & Jarrard, D. F. Therapy-induced senescence in cancer. *J. Natl Cancer Inst.* **102,** 1536–1546 (2010).
11. Humbert, N. *et al.* Regulation of ploidy and senescence by the AMPK-related kinase NUAK1. *EMBO J.* **29,** 376–386 (2010).
12. Lin, H. K. *et al.* Skp2 targeting suppresses tumorigenesis by Arf-p53-independent cellular senescence. *Nature* **464,** 374–379 (2010).
13. Scurr, L. L. *et al.* IGFBP7 is not required for B-RAF-induced melanocyte senescence. *Cell* **141,** 717–727 (2010).
14. Cipriano, R. *et al.* TGF-beta signalling engages an ATM-CHK2-p53-independent RAS-induced senescence and prevents malignant transformation in human mammary epithelial cells. *Proc. Natl Acad. Sci. USA* **108,** 8668–8673 (2011).
15. Bianchi-Smiraglia, A. & Nikiforov, M. A. Controversial aspects of oncogene-induced senescence. *Cell Cycle* **11,** 4147–4151 (2012).
16. Kiyono, T. *et al.* Both Rb/p16INK4a inactivation and telomerase activity are required to immortalize human epithelial cells. *Nature* **396,** 84–88 (1998).
17. Lallet-Daher, H. *et al.* Potassium channel KCNA1 modulates oncogene-induced senescence and transformation. *Cancer Res.* **73,** 5253–5265 (2013).
18. Yamamoto-Hino, M. *et al.* Cloning and characterization of human type 2 and type 3 inositol 1,4,5-trisphosphate receptors. *Receptors Channels* **2,** 9–22 (1994).
19. de Brito, O. M. & Scorrano, L. An intimate liaison: spatial organization of the endoplasmic reticulum-mitochondria relationship. *EMBO J.* **29,** 2715–2723 (2010).
20. Baughman, J. M. *et al.* Integrative genomics identifies MCU as an essential component of the mitochondrial calcium uniporter. *Nature* **476,** 341–345 (2011).
21. Csordas, G., Varnai, P., Golenar, T., Sheu, S. S. & Hajnoczky, G. Calcium transport across the inner mitochondrial membrane: molecular mechanisms and pharmacology. *Mol. Cell Endocrinol.* **353,** 109–113 (2012).
22. Chen, M. *et al.* Differential mitochondrial calcium responses in different cell types detected with a mitochondrial calcium fluorescent indicator, mito-GCaMP2. *Acta Biochim. Biophys. Sin. (Shanghai)* **43,** 822–830 (2011).
23. Csordas, G. *et al.* MICU1 controls both the threshold and cooperative activation of the mitochondrial Ca(2)(+) uniporter. *Cell. Metab.* **17,** 976–987 (2013).
24. Mallilankaraman, K. *et al.* MICU1 is an essential gatekeeper for MCU-mediated mitochondrial Ca(2+) uptake that regulates cell survival. *Cell* **151,** 630–644 (2012).
25. Duchen, M. R. Mitochondria and calcium: from cell signalling to cell death. *J. Physiol* **529**(Pt 1): 57–68 (2000).
26. Huser, C. A. & Davies, M. E. Calcium signalling leads to mitochondrial depolarization in impact-induced chondrocyte death in equine articular cartilage explants. *Arthritis Rheum.* **56,** 2322–2334 (2007).
27. Bernardi, P. & Rasola, A. Calcium and cell death: the mitochondrial connection. *Subcell. Biochem.* **45,** 481–506 (2007).
28. Leikam, C., Hufnagel, A., Schartl, M. & Meierjohann, S. Oncogene activation in melanocytes links reactive oxygen to multinucleated phenotype and senescence. *Oncogene* **27,** 7070–7082 (2008).
29. Rai, P. *et al.* Continuous elimination of oxidized nucleotides is necessary to prevent rapid onset of cellular senescence. *Proc. Natl Acad. Sci. USA* **106,** 169–174 (2009).
30. Augert, A. *et al.* The M-type receptor PLA2R regulates senescence through the p53 pathway. *EMBO Rep.* **10,** 271–277 (2009).
31. Boehning, D., Patterson, R. L. & Snyder, S. H. Apoptosis and calcium: new roles for cytochrome c and inositol 1,4,5-trisphosphate. *Cell Cycle* **3,** 252–254 (2004).
32. Decuypere, J. P., Bultynck, G. & Parys, J. B. A dual role for Ca(2+) in autophagy regulation. *Cell Calcium* **50,** 242–250 (2011).
33. Decuypere, J. P. *et al.* The IP(3) receptor-mitochondria connection in apoptosis and autophagy. *Biochim. Biophys. Acta* **1813,** 1003–1013 (2011).
34. Khan, A. A. *et al.* Lymphocyte apoptosis: mediation by increased type 3 inositol 1,4,5-trisphosphate receptor. *Science* **273,** 503–507 (1996).
35. Lam, D., Kosta, A., Luciani, M. F. & Golstein, P. The inositol 1,4,5-trisphosphate receptor is required to signal autophagic cell death. *Mol. Biol. Cell* **19,** 691–700 (2008).
36. Li, G. *et al.* Role of ERO1-alpha-mediated stimulation of inositol 1,4,5-triphosphate receptor activity in endoplasmic reticulum stress-induced apoptosis. *J. Cell Biol.* **186,** 783–792 (2009).
37. Luciani, D. S. *et al.* Roles of IP3R and RyR Ca2+ channels in endoplasmic reticulum stress and beta-cell death. *Diabetes* **58,** 422–432 (2009).
38. Young, A. R. *et al.* Autophagy mediates the mitotic senescence transition. *Genes Dev.* **23,** 798–803 (2009).
39. Hutter, E. *et al.* Senescence-associated changes in respiration and oxidative phosphorylation in primary human fibroblasts. *Biochem. J.* **380,** 919–928 (2004).
40. Hagen, T. M. *et al.* Mitochondrial decay in hepatocytes from old rats: membrane potential declines, heterogeneity and oxidants increase. *Proc. Natl Acad. Sci. USA* **94,** 3064–3069 (1997).
41. Moiseeva, O., Bourdeau, V., Roux, A., Deschenes-Simard, X. & Ferbeyre, G. Mitochondrial dysfunction contributes to oncogene-induced senescence. *Mol. Cell Biol.* **29,** 4495–4507 (2009).
42. Rottenberg, H. & Wu, S. Mitochondrial dysfunction in lymphocytes from old mice: enhanced activation of the permeability transition. *Biochem. Biophys. Res. Commun.* **240,** 68–74 (1997).
43. Passos, J. F. *et al.* Mitochondrial dysfunction accounts for the stochastic heterogeneity in telomere-dependent senescence. *PLoS Biol.* **5,** e110 (2007).
44. Acosta, J. C. *et al.* Chemokine signalling via the CXCR2 receptor reinforces senescence. *Cell* **133,** 1006–1018 (2008).
45. Passos, J. F. & Von Zglinicki, T. Oxygen free radicals in cell senescence: are they signal transducers? *Free Radic. Res.* **40,** 1277–1283 (2006).
46. Gitenay, D. *et al.* Glucose metabolism and hexosamine pathway regulate oncogene-induced senescence. *Cell Death Dis.* **5,** e1089 (2014).
47. Brummelkamp, T. R., Bernards, R. & Agami, R. A system for stable expression of short interfering RNAs in mammalian cells. *Science* **296,** 550–553 (2002).

Acknowledgements

We thank Stéphanie Courtois-Cox and Sarah Kabani for critical reading of the manuscript, Christophe Vanbelle, from the SFR Lyon-EST CeCILE platform, for expertise in confocal microscopy, Professor Xianhua Wang for the kind gift of plasmid pcDNA3.1 mitochondrial GCaMP2 and Professor Jan Parys and laboratory members for helpful discussions. This work was carried out with the support of the 'Institut National du Cancer', the 'Ligue Nationale contre le cancer, comité de la Savoie', the 'Fondation ARC', the 'Fondation de France' and the 'RTRS Fondation Synergie Lyon Cancer'. C.W. is supported by the 'Ligue national contre le Cancer' and the 'Fondation pour la Recherche Médicale'.

Author contributions

C.W., H.L.-D., D.G., B.G., A.A., M.F. and D.V. performed experiments; C.W., H.L.-D., B.L.C., N.P., H.S. and D.B. Analyzed data; C.W., H.L.D. and D.B. designed experiments; C.W. and D.B. wrote the paper.

Additional information

Supplementary Information accompanies this paper at http://www.nature.com/naturecommunications

Competing financial interests: The authors declare no competing financial interests.

Reprints and permission information is available online at http://npg.nature.com/reprintsandpermissions/

How to cite this article: Wiel, C. *et al.* Endoplasmic reticulum calcium release though ITPR2 channels leads to mitochondrial calcium accumulation and senescence. *Nat. Commun.* 5:3792 doi: 10.1038/ncomms4792 (2014).

© 2014 Macmillan Publishers Limited. All rights reserved.

Supplementary Figure 1, Wiel *et al*

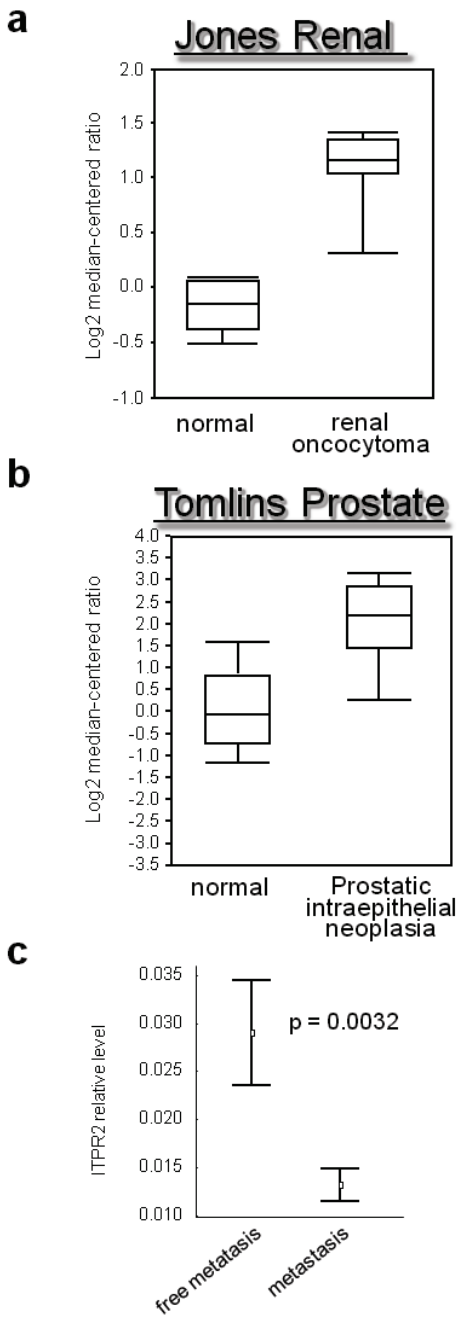

Supplementary Figure 1 ITPR2 increases in benign tumors and decreases in aggressive ones (a-b) According to the Oncomine database, expression of ITPR2 increases in renal oncocytoma (a) and prostatic intraepithelial neoplasia (b) that are benign tumors. (c) RNA from human primary breast cancer samples were analysed for ITPR2 mRNA expression by RTqPCR and normalised against actin mRNA. Metastasis status was 3 years after surgery.

Supplementary Figure 2, Wiel *et al*

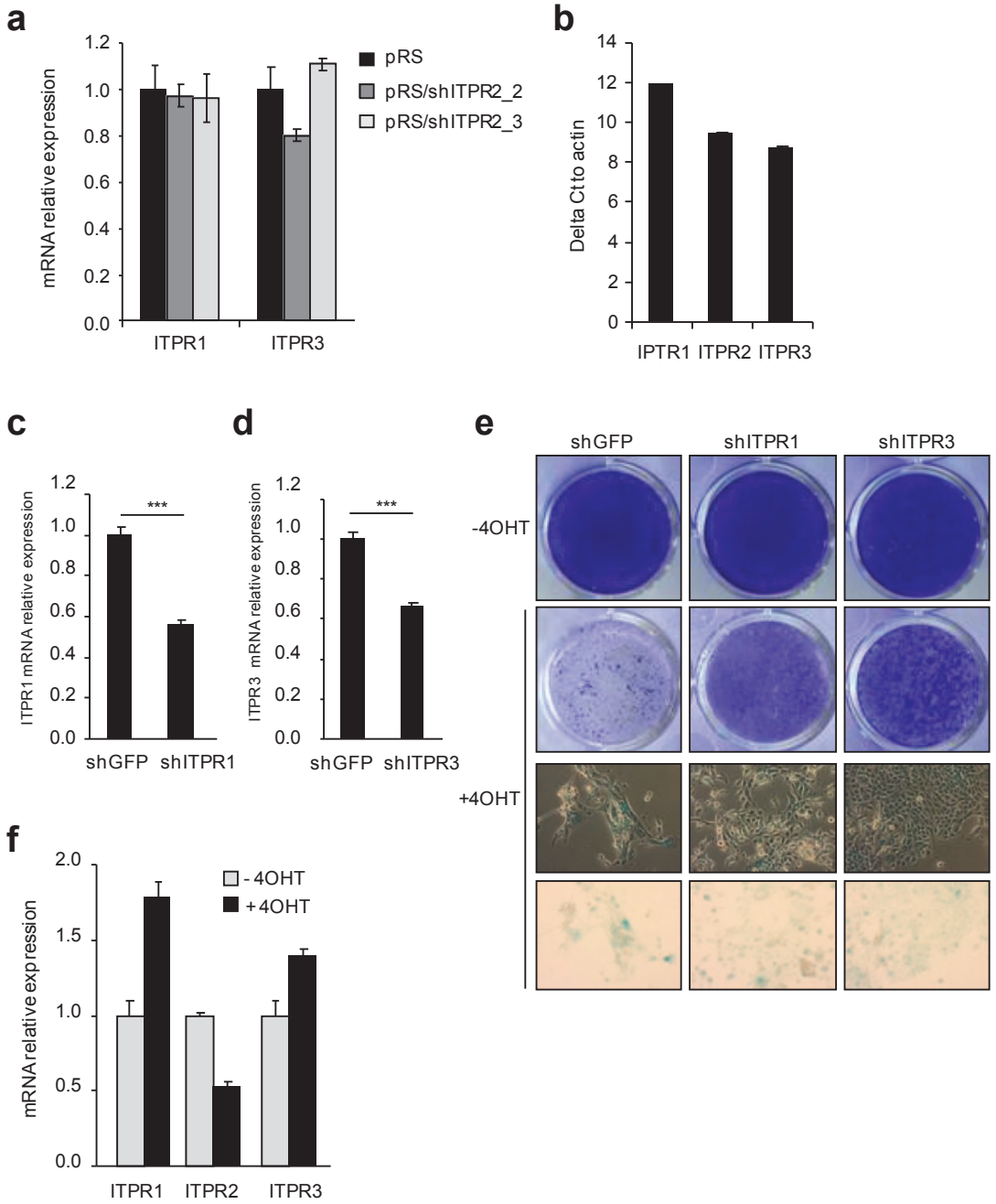

Supplementary Figure 2 Role of ITPR1 and ITPR3 during OIS. (a) RNA from ctrl, shITPR2_2 and ITPR2_3 cells were extracted, and mRNA levels of ITPR1 and ITPR3 were assessed by qRT-PCR. (b) Levels of ITPR1, ITPR2 and ITPR3 in HECs cells were evaluated by qRT-PCR. (c) and (d) ITPR1 and ITPR3 mRNA levels were assessed in shITPR1 and shITPR3 cells, respectively. (e) The day after seeding, cells were treated with 4OHT. Ten days after treatment, HEC-TM cells were fixed, stained with crystal violet, or assessed for their SA-b-gal activity. Data are representative of 3 experiments. (f) HEC-TM cells were treated with 4OHT or not. After treatment, RNA was extracted, and expression of ITPR1, ITPR2 and ITPR3 was investigated by qRT-PCR**.** Experiments were performed twice. S.e.m are shown as errors bars, p values were determined using student t test. ***p< 0.001

Supplementary Figure 3, Wiel *et al*

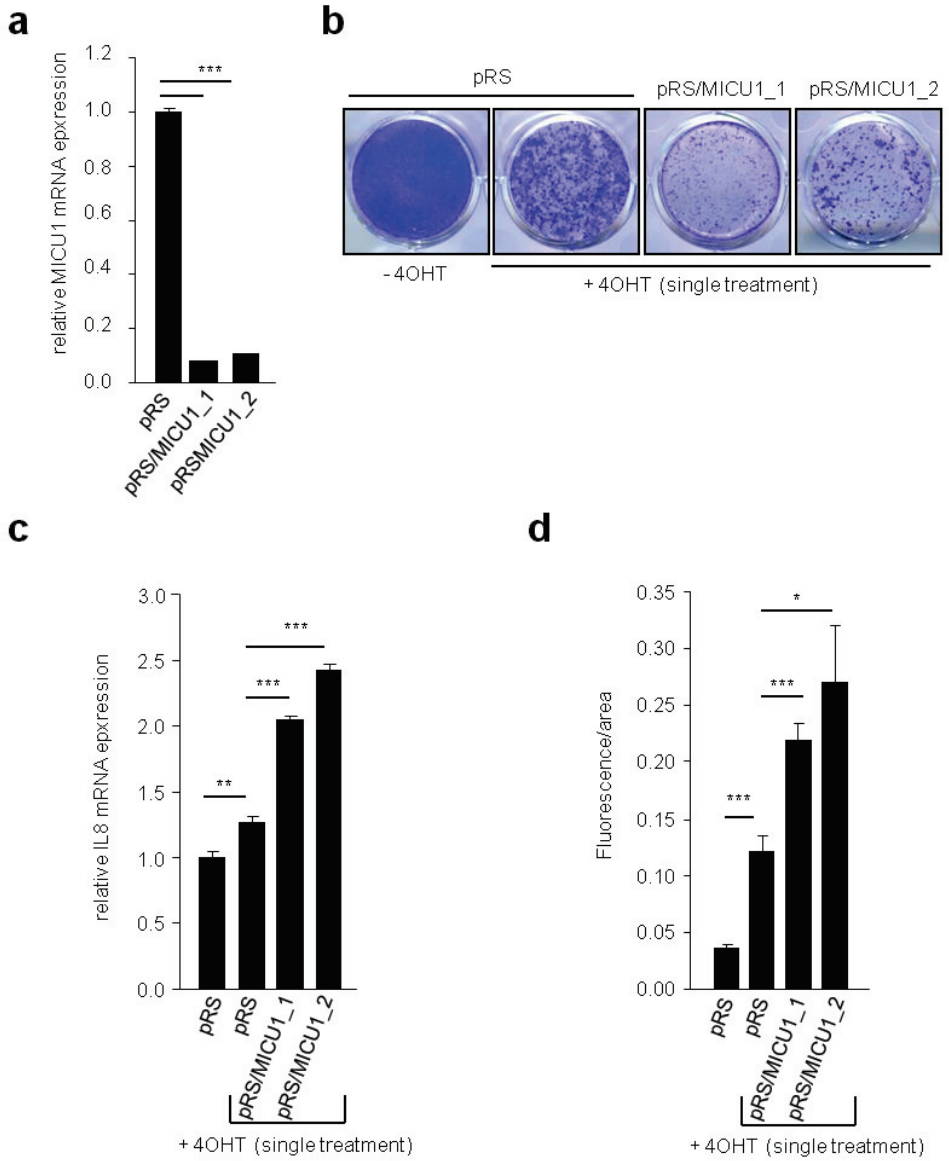

Supplementary Figure 3 MICU1 knockdown potentiates OIS. (a) pRetroSuperpuro (pRS) encoding shRNAs directed against MICU1 were constructed by subcloning oligonucleotides targeting the following sequences: sh1 5'- GAGCTGATCTGAAGGGAAA-3', sh2 5'-GAATGGAGATGGAGAAGTA 3'. HMEC-TM cells were infected by the indicated retroviral vectors and puromycin selected. RNA were prepared, and retro-transcription quantitative PCR were performed using the following primers for MICU1 analysis 5' -tgatgtggacactgcattgag-3' and 5' -cctgctgcatggtcacttt-3', with the Taqman UPL probe #19 (Roche). (b-d) Cells were treated or not with a single dose of 4-OHT. Six days later, cells were fixed and crystal violet stained. Representative images are displayed. (c) or RNA were prepared and level of IL8 mRNA determined by retro-transcription quantitative PCR. (d) Mitochondrial calcium reporter fluorescence intensity was recorded and quantified for each condition (n>10 fields). Mean (±s.e.m) of two experiments are shown. p values were determined using student t test.*p< 0.05; **p<0.01; ***p< 0.001.

Supplementary Figure 4, Wiel *et al*

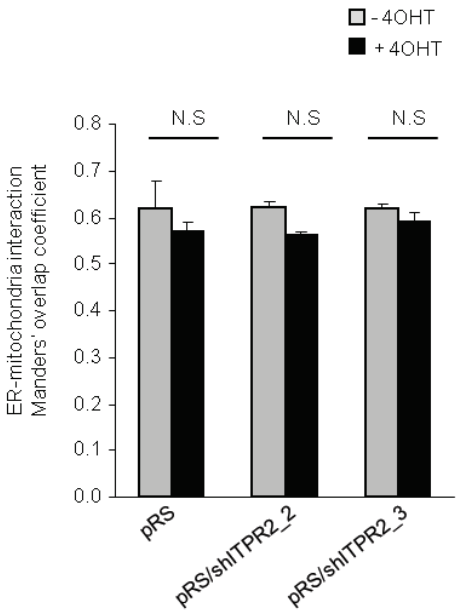

Supplementary Figure 4 Senescence or knock-down of ITPR2 does not impair ER-mitochondria contacts. Ctrl or shITPR2 cells were seeded on glass dishes, treated or not with 4OHT and fixed with methanol. Immunofluorescence was performed to label mitochondria and ER. MitoProfile® Total OXPHOS Human Antibody Cocktail (Abcam) and anti-calnexin (C5C9, 2679, Cell Signaling) were used. A Z-stack of optical sections was captured using a Zeiss LSM 780 confocal microscope. To analyze colocalization of ER and mitochondria, the Manders' overlap coefficient (varying between 0 and 1, with 0 for no overlap, and +1 for perfect overlap) was calculated. Mean ± s.d. NS: not significant

Supplementary Figure 5, Wiel *et al*

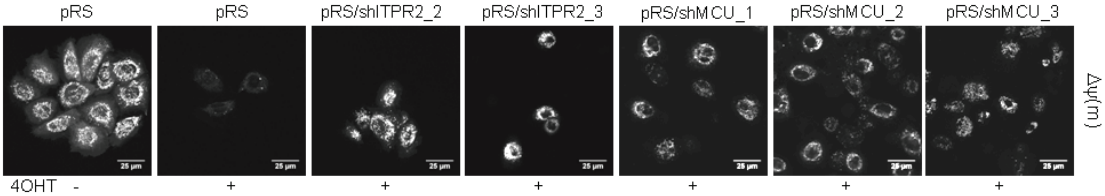

Supplementary Figure 5 Knockdown of ITPR2 and MCU sustain ΔΨ(m). Cells were seeded at the same density, treated by 4OHT for 3 days and living cells were next incubated with a ΔΨ(m) marker (Rhodamine 123). Cell fluorescence was analysed by confocal microscopy (Ex 514 nm/Em520-660 nm). Scale bar: 25µM

Supplementary Figure 6, Wiel *et al*

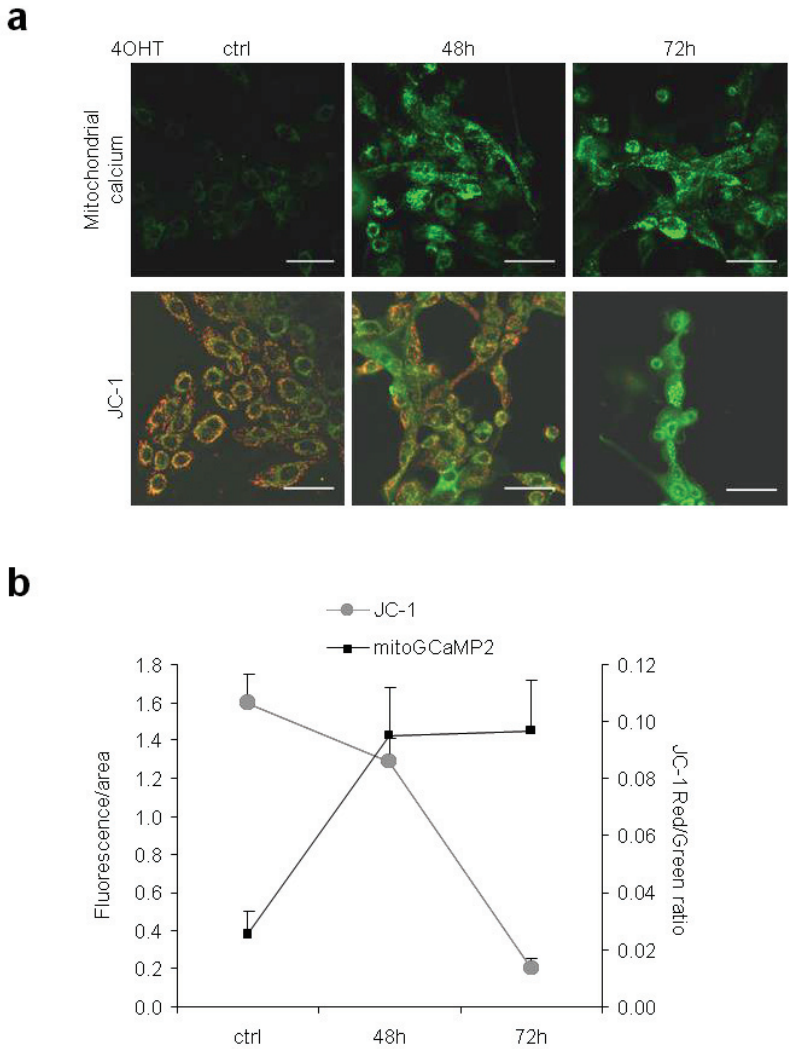

Supplementary Figure 6 Mitochondrial calcium accumulation occurs before ΔΨ(m). (a) HEC-TM cells, transduced with or without the mitonchondrial calcium indicator, were seeded and treated with 4OHT daily for 48h. Fluorescence emitted in live cells by the calcium indicator (upperpanel), or by the JC-1 dye (lower panel) was analysed by confocal microscopy at 48h (end of treatment) or 72h. (b) Fluorescence was quantified, in each condition (n>10 fields), and displayed. Representative quantification and images are shown. Experiments were performed twice. Scale bar: 50 μM

Supplementary Figure 7, Wiel *et al*

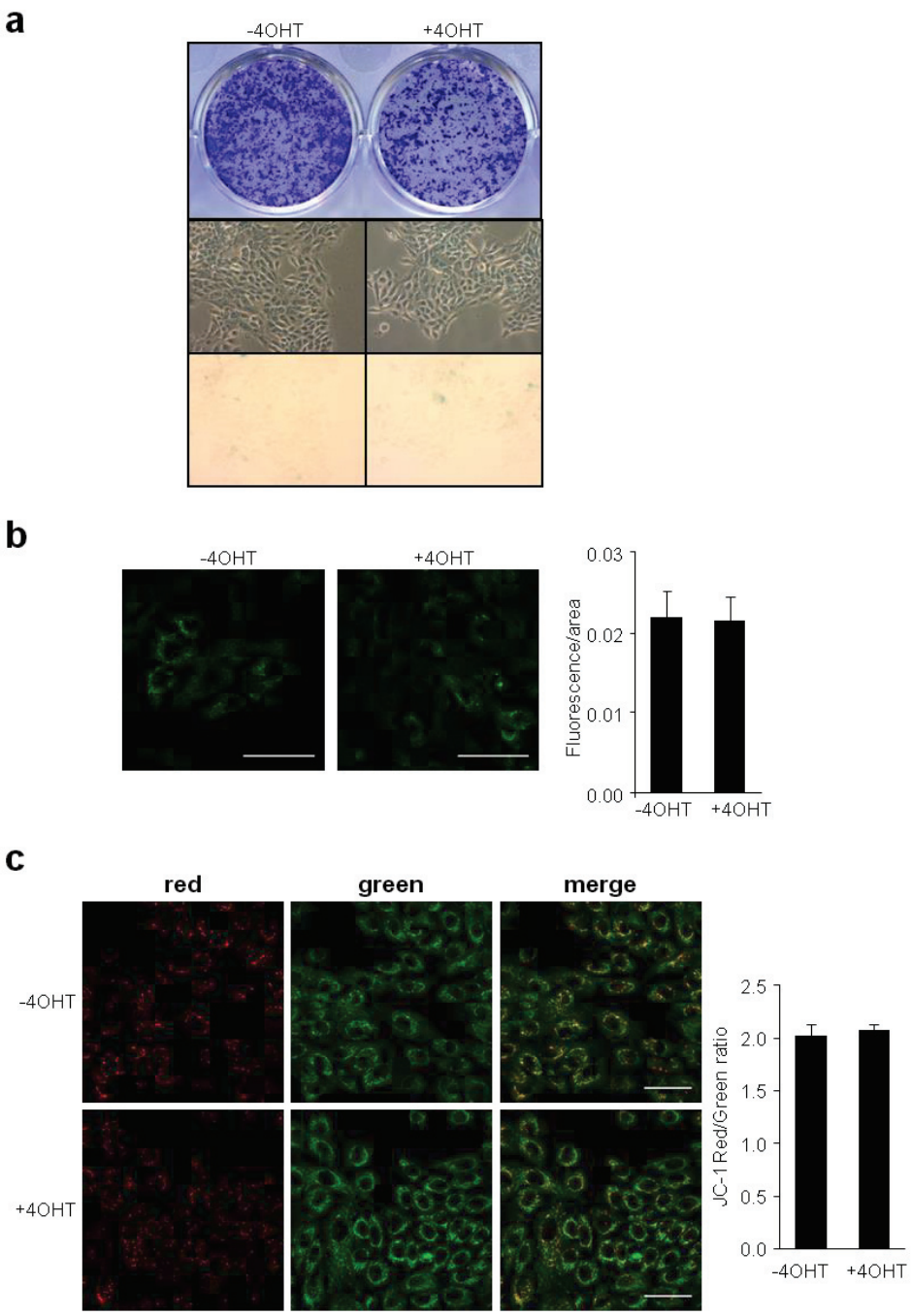

Supplementary Figure 7 4OHT treatment in immortalized HEC (without MEK:ER) does not impact proliferation, mitochondrial calcium or Δψ(m). (a) HEC-Tert cells were seeded, treated for 3 days with 4OHT or not, and fixed. Cells were stained with crystal violet (upper panel) or assessed for their SA-beta-gal activity (lower panel). (b) HEC-Tert cells were transduced with the mitochondrial calcium indicator, selected, and seeded in glass-bottom dishes. After 4OHT treatment, fluorescence was investigated by confocal microscopy, and then quantified. (c) HEC-Tert cells were seeded in glass-bottom dishes, treated with 4OHT, and incubated for 10 min with the JC-1 dye. Fluorescence was recorded using a LSM 780 confocal microscope, and ratio of fluorescence intensity (emission 590-650 nm / emission 500-560 nm) was calculated. n=10 fields for each condition. Scale bar: 50 µM

Supplementary Figure 8, Wiel *et al*

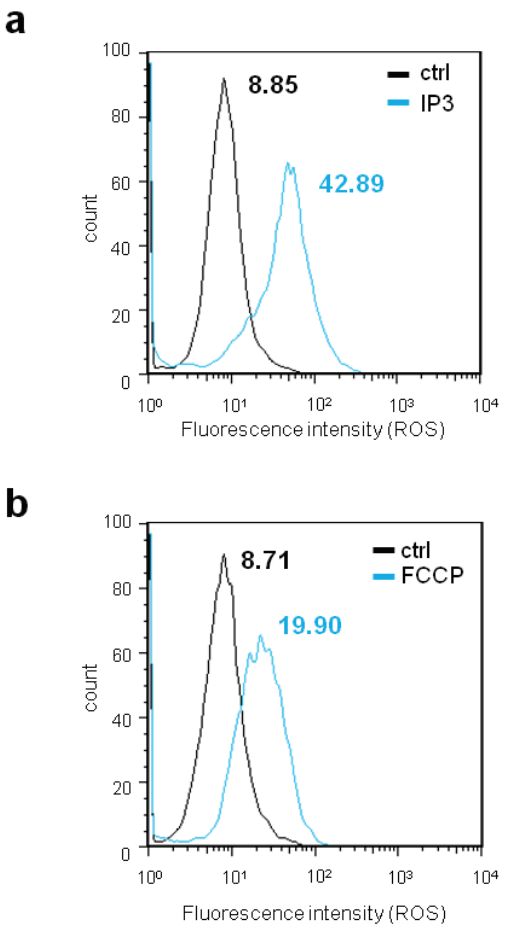

Supplementary Figure 8 Premature senescence induced by IP3 or FCCP results in ROS production. After daily treatment with IP3 pr FCCP, cells were incubated 30 min with the H_2DCF-DA probe, trypsinized, washed with PBS and ROS levels in 10,000 events were assessed by flow cytometry using a FACSCalibur. Data were analysed with Flow Jo software. Experiments were performed twice.

Supplementary Figure 9, Wiel *et al*

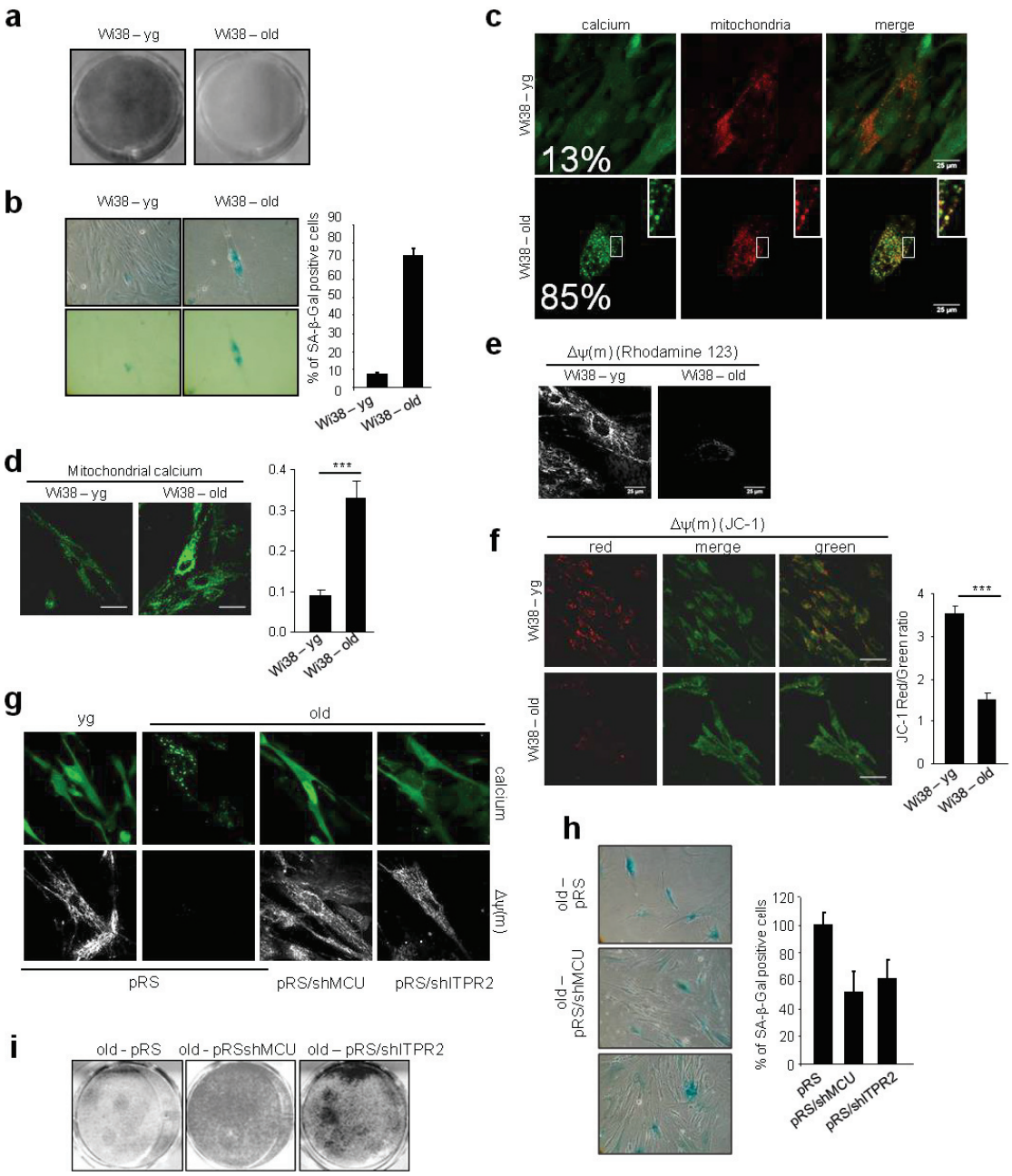

Supplementary Figure 9 Knock-down of ITPR2 and MCU delays replicative senescence by preventing calcium relocalization and mitochondrial depolazization. Young (<p23) and old (>p26) Wi38 cells were used. (a) cells were seeded at the same density, fixed 2 weeks later and crystal violet stained. (b) SA-β-gal activity was checked. (c) Cells were transduced with a RFP-coupled mitochondrial protein and incubated with oregeon green to visualise calcium. Fluorescence was recorded using a LSM 780 confocal microscope in live cells. Scale bar: 25μM. (d) Cells were transduced with the mitochondrial calcium indicator mito-GCaMP2, and fluorescence in young and old cells was analysed with a confocal microscope. (e) Mitochondrial membrane potential was assessed with Rhodamine 123 or (f) with the JC-1 probe. N=5 fields (young cells), n=15 fields (old cells). (g) to (i) young Wi38 cells were transduced with an shRNA targeting MCU or ITPR2, or with an empty vector (ctrl), and were split every week. (g) Cells were incubated with Oregon Green or Rhodamine 123, and analysed by confocal microscopy. (h) SA-β-gal activity was assessed, and (i) proliferation was assayed by a crystal violet staining. Scale bar: 50 μM. .*p< 0.05; **p<0.01; ***p< 0.001

Supplementary Figure 10, Wiel *et al*

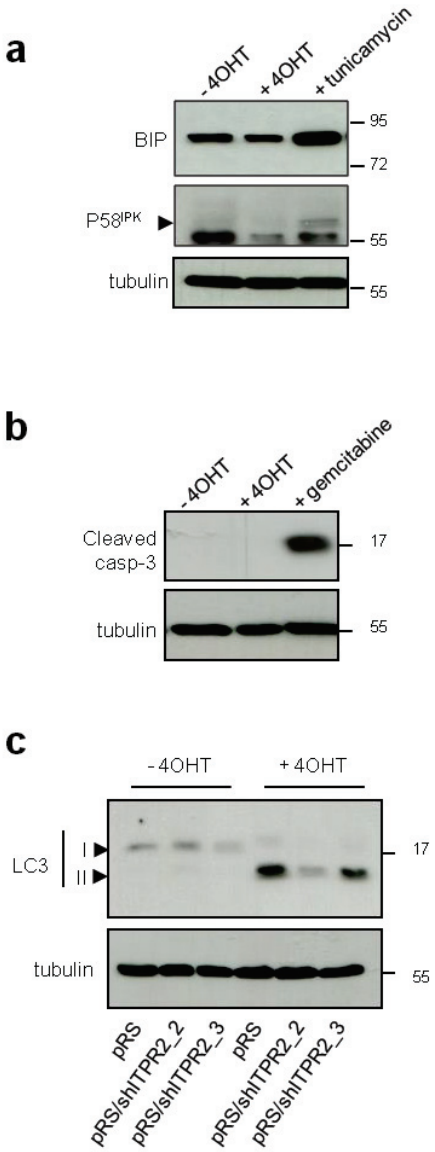

Supplementary Figure 10 Apoptosis, autophagy and ER stress during OIS. (a) HMEC-TM cells were treated or not with 4OHT or tunicamycine, as a positive control to induce an ER stress. Protein extracts were prepared and immunoblot performed using antibodies directed against the indicated ER stress markers. (b) HMEC-TM cells were treated or not with 4OHT or gemcitabine, as a positive control to induce apoptosis. Protein extracts were prepared and immunoblot performed using an antibody directed against the active cleaved caspase-3. (c) HMEC-TM cells were treated or not with 4OHT. Protein extracts were prepared and immunoblot performed using an antibody directed against LC3. LC3 form II appeared when autophagy is induced.

Supplementary Table 1, Wiel *et al*

Supplementary Table 1 ITPR2 expression decreases in various cancers

Cancer	number of analyses with altered ITPR2 expression	Decrease (D) or Increase (I) in cancer
Bladder	1	D
Brain and CNS	4	I
Cervical	3	D
Esophageal	3	D
Head and Neck	3	D
Kidney	3+2	D+I
Melanoma	2	D
Other	3	D
Ovarian	1	D
Pancreatic	1	D
Prostate	4	I
Sarcoma	1	D

Supplementary Table 1 The Oncomine database was interrogated for expression of ITPR2 in cancer with the following threshold: p-value <0.001, fold change >2, gene rank of 10%.

Supplementary Table 2, Wiel *et al*

Supplementary Table 2 List of primers used for quantitative PCR

Gene Name	NCBI reference sequence	Primers	UPL probe
ACTB	NM_001101.3	Right 5'-attggcaatgagcggttc-3' Left 5'-cgtggatgccacaggact-3'	11
ITPR1	NM_002222.5	Right 5'-tgcaaatcctgctcctctgt-3' Left 5'-tacccagcggctgctaac-3'	17
ITPR2	NM_002223.2	Right 5'-aaagcctcagtggaatcctgt-3' Left 5'-atggcaattccacgattttt-3'	41
ITPR3	NM_002224.3	Right 5'-ggagcaagatcgtccatca-3' Left 5'-ctgctgtagccagtgcagac-3'	1
MCU	NM_138357.1	Right 5'-ctggctcccctggaaaag-3' Left 5'-ccaccccatagcaccaaa-3'	35
MICU1	NM_006077.3	Right 5' -tgatgtggacactgcattgag-3' Left 5'- cctgctgcatggtcacttt-3'	19
IL8	NM_000584.3	Right 5'-agacagcagagcacacaagc-3' Left 5'-atggttccttccggtggt-3'	72

Supplementary Table 2 List of primers, their sequences and UPL probes used for quantitative PCR.

DISCUSSION GENERALE ET PERSPECTIVES

DISCUSSION GENERALE ET PERSPECTIVES

Mon travail de thèse a pour objectif d'identifier de nouveaux mécanismes régulant l'OIS dans les cellules épithéliales. En effet, près de 85% des cancers humains sont des carcinomes, des tumeurs d'origine épithéliale. Pourtant, la majorité des résultats publiés sur les mécanismes de régulation de l'OIS sont basés sur l'utilisation de fibroblastes rendant l'extrapolation de ces résultats aux carcinomes difficile. Bien qu'il soit cependant évident qu'il existe des mécanismes communs entre l'OIS mise en place dans les fibroblastes et les cellules épithéliales, il est nécessaire de mieux caractériser ceux mis en jeu dans ces dernières.

Au cours de ma thèse, je me suis donc principalement intéressée à identifier de nouveaux acteurs de l'OIS dans les cellules épithéliales humaines en utilisant un modèle cellulaire original. J'ai d'une part pu identifier un nouvel acteur de la stabilité de l'OIS dans les cellules épithéliales, et pu d'autre part caractériser une nouvelle voie de signalisation impliquée dans la sénescence.

J'ai en effet décrit un nouveau rôle pour les enzymes LOX et LOXL2 dans l'initiation tumorale, puisque ces enzymes participent au développement tumoral en favorisant l'échappement à la sénescence *in vitro* et *in vivo*. En utilisant une approche de criblage génétique, j'ai également pu caractériser le rôle d'ITPR2 et de MCU, deux canaux qui permettent la relocalisation du calcium depuis le RE jusque dans les mitochondries. Ce travail a révélé une nouvelle voie de signalisation dans la sénescence impliquant pour la première fois le calcium mitochondrial dans l'OIS.

1 Un modèle cellulaire original

1.1 Sénescence sans induction de $p16^{INK4A}$?

Le rôle de $p16^{INK4A}$ dans la sénescence a largement été démontré dans les fibroblastes humains. L'importance de ce CKI dans l'établissement de la sénescence des cellules épithéliales est largement plus discutée (Takaoka *et al.*, 2004; Cipriano *et al.*, 2011). Une caractéristique du modèle cellulaire utilisé pour mes travaux de thèse est l'absence d'expression de $p16^{INK4A}$. Il est alors possible d'étudier d'autres voies impliquées dans la régulation de la sénescence qui n'auraient pas pu être détectées dans d'autres modèles exprimant $p16^{INK4A}$. Nous avons pu ainsi identifier l'importance des mouvements calciques dans l'OIS des cellules épithéliales. Ces observations ont par la suite été étendues à la sénescence réplicative de WI-38 dont la sénescence dépend fortement de $p16^{INK4A}$.

Les hMECs post-stasiques présentent les marqueurs essentiels à l'identification du phénotype de sénescence, c'est-à-dire l'arrêt de prolifération, une activité SA-β-galactosidase et la mise en place d'un SASP, montrant que les cellules épithéliales peuvent entrer en sénescence malgré l'absence d'expression de $p16^{INK4A}$.

In vivo nous avons montré que l'activation de $K\text{-}Ras^{G12D}$ dans le pancréas de souris qui n'expriment pas $p16^{INKA}$ aboutit au développement rapide de PDAC. L'analyse des lésions montre toutefois que celles-ci sont associées à de la sénescence. Il a également été rapporté que l'activation de K-Ras dans le pancréas, couplée à la perte d'expression de Rb induit une sénescence instable (Carrière *et al.*, 2011). Nous pouvons donc en conclure que l'inactivation de la voie $p16^{INK4A}$-Rb n'abroge pas la sénescence induite par K-Ras mais semble diminuer fortement sa stabilité.

1.2 Réversibilité de la sénescence

Nous avons observé que l'OIS induite par Mek ou Raf dans les cellules hMECs immortalisées est réversible puisque les cellules sont capables de spontanément reprendre leur prolifération. Cette caractéristique nous a permis dans un premier temps d'identifier un nouveau mécanisme impliqué dans la stabilité de la sénescence. Le fait que $p16^{INK4A}$ semble participer au maintien de l'arrêt de prolifération par l'induction des SHAF souligne son implication dans la stabilité de la sénescence. Il a également été décrit que $p16^{INK4A}$ peut être induit après l'arrêt du cycle cellulaire qui est dans ce cas dépendant de $p21^{Cip1}$ suggérant que son expression est surtout nécessaire pour maintenir l'arrêt de prolifération (Serrano *et al.*, 1993). Ces éléments nous amènent à penser que dans les hMECs post-stasiques l'absence de $p16^{INK4A}$ pourrait être responsable de la réversibilité de l'OIS. L'utilisation de cellules pré-stasiques pourrait déterminer si la présence de $p16^{INK4A}$ peut empêcher la réversion spontanée de la sénescence induite par des versions activées de Mek ou de Raf.

Il est également possible que l'immortalisation induite par la transduction de l'hTERT contribue au manque de stabilité de l'OIS des hMECs. En effet, d'après les travaux conduits par Julia Yaglom les cellules épithéliales immortalisées MCF10A, en réponse à un oncogène, présentent des marqueurs de sénescence mais ne montrent pas d'arrêt stable de prolifération malgré l'expression ectopique de $p16^{INK4A}$ (Sherman *et al.*, 2011). Ils en concluent que l'immortalisation des cellules est responsable de la reprise rapide de prolifération. L'utilisation de la lignée cellulaire MCF10A qui exprime une télomérase endogène diffère toutefois de l'utilisation de cellules épithéliales primaires immortalisées au sein de notre équipe, et peut expliquer la différence ente leurs conclusions et les nôtres.

L'utilisation de cellules primaires non immortalisées hMECs Mek :ER ou Raf :ER a nous permis de démontrer que ces cellules sont en effet plus sensibles au stress oncogénique (1 traitement 4-OHT 100 nM pour induire de la sénescence, contre 2 ou 3 traitements 4-OHT dans des cellules immortalisées). Toutefois, la surexpression de protéines permettant l'échappement à la sénescence de cellules immortalisées, comme les sous-unités catalytiques β ou γ de la PKA, aboutit également à une reprise de la prolifération de cellules primaires (Lallet-Daher *et al.*, 2013) avec cependant un délai plus important (20 jours contre moins de 7 jours dans les cellules immortalisées). La sénescence des hMECS est donc réversible que les cellules soient immortalisées ou non. Néanmoins, ces observations ne nous permettent pas d'expliquer la différence de délai observé dans la reprise de prolifération. Il a été récemment montré que lors de l'OIS, les dommages à l'ADN peuvent affecter de manière stochastique toutes les toutes les séquences chromosomiques y compris les télomères (Suram *et al.*, 2012). Les cellules non immortalisées peuvent donc être endommagées au niveau des télomères contrairement aux cellules ayant une activité télomérase. Cette observation pourrait expliquer pourquoi la sénescence parait plus stable dans les cellules primaires.

Les cellules murines se différencient des cellules humaines somatiques par le fait qu'elles expriment la télomérase (Prowse and Greider, 1995; Blasco *et al.*, 1997; Kipling and Cooke, HJ, 1990). Pour autant ces cellules entrent parfaitement en sénescence en réponse a des oncogènes (Serrano *et al.*, 1997). Le nombre toujours croissant de modèles murins utilisés pour démontrer l'occurrence de l'OIS *in vivo*, et identifier ses régulateurs est la preuve que l'immortalisation n'empêche pas sénescence induite par un stress oncogénique.

Il a également été suggéré que la stabilité de la sénescence provient de l'extinction de gènes pro-prolifératifs grâce à la formation de SAHF (*voir intro, paragraphe 1.1.6*) Une étude récente dans des MEFs a montré que l'hétérochromatisation induite par Rb est dépendante de sa liaison aux protéines PML, déjà connues pour leur rôle dans la sénescence (Talluri and Dick, 2014). Or la présence de PML dans les tissus néoplasiques est corrélée à l'évolution de la lésion et à la stabilité de la sénescence. Ainsi, les hyperplasies de la prostate, enrichies en PML restent à un stade bénin, alors que les PIN, pauvres en corps nucléaires PML, peuvent potentiellement évoluer en lésions cancéreuses (Vernier *et al.*, 2011). Il a été proposé que plusieurs types de sénescence, complète et incomplète, pourraient expliquer ces différences de stabilité (Vernier and Ferbeyre, 2014).

L'essence même de la sénescence est d'être irréversible. L'apparition dans la littérature de termes pour caractériser les niveaux de sénescence est nouvelle, et ouvre la voie à de nouvelles études permettant de mieux discriminer les types et niveaux de sénescence, non plus seulement en fonction de l'inducteur mais aussi en fonction des différentes marques de sénescence. Cette vision

est renforcée par le fait que les marqueurs de sénescence apparaissent de manière graduelle après l'induction du stress. La voie est désormais ouverte pour découvrir les acteurs empêchant la sénescence d'être complète/irréversible, et d'opter pour une nouvelle nomenclature.

2 Mécanismes par lesquels Lox déstabilise la sénescence

En utilisant un modèle d'OIS dans des cellules épithéliales mammaires humaines, nous avons montré que la surexpression de LOX et LOXL2 induit un échappement à la sénescence induite par Mek alors que l'inhibition de l'activité Lox stabilise l'OIS. L'inhibition de Lox dans un modèle de PDAC induit par K-Ras^{G12D} stabilise la sénescence et augmente significativement la survie des souris. L'inhibition de la kinase FAK permet également de stabiliser l'OIS.

Aussi, nous avons observé qu'une inhibition pharmacologique d'Akt par le composé chimique LY294002 permet de stabiliser la sénescence induite par Raf ou Mek *(figure 7, page des résultats supplémentaires)*. Deux groupes ont récemment montré que l'activation de la voie PI3K/Akt, conjointement avec celle de Raf-Mek, n'a pas d'effet cumulatif mais permet un échappement à la sénescence (Kennedy *et al.*, 2011; Vredeveld *et al.*, 2012). En effet, l'ablation d'un allèle de *Pten* dans un modèle murin de souris Pdx1-Cre K-Ras^{G12D} induit un échappement à la sénescence induite par K-Ras dans les lésions néoplasiques PanIN (Kennedy *et al.*, 2011). L'activation de la voie PI3K induit également une inhibition de la sénescence dépendante de B-Raf^{V600E} dans le mélanome (Vredeveld *et al.*, 2012). Dans les poumons, il a été montré que le développement des lésions cancéreuses induites par K-Ras, positives pour certains marqueurs de sénescence, est accélérée par l'inactivation de Pten (Iwanaga *et al.*, 2008). Ces données confortent le fait que la voie PI3K interfère avec la voie Raf-Mek, en aval de Ras.

Il a de plus été rapporté que FAK peut réguler la voie PI3K (Xia *et al.*, 2004). Nous pouvons supposer que dans les hMECs l'activité Lox déstabilise la sénescence induite par Mek via la phosphorylation de FAK et l'activation de la voie PI3K en aval. L'ensemble de ces données soutient l'idée que dans notre modèle murin de PDAC, Lox pourrait favoriser l'échappement à la sénescence en activant cette voie *(figure 18).*

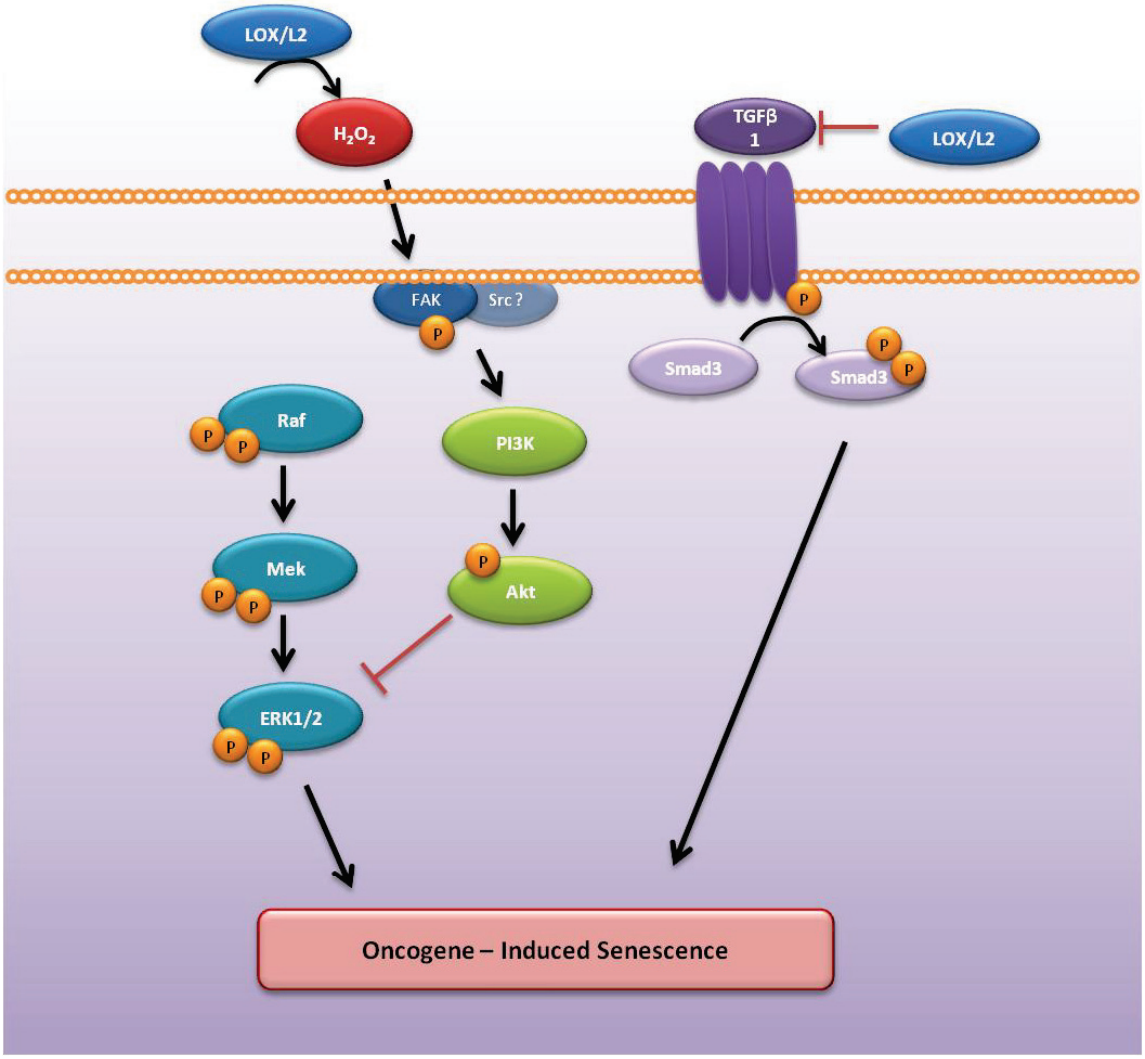

Figure 18 : Mécanisme(s) par lesquels l'activité Lox pourrait déstabiliser la sénescence induite par un stress oncogénique

L'activité Lox, en produisant de l'H_2O_2 comme sous-produit de la réaction d'oxydation, pourrait activer les kinases FAK, et la v oie PI3K/Akt en aval. L'activation de cette voie est connue pour déstabiliser la sénescence induite par la voie Ras/Raf/Mek.

Alternativement, LOX pourrait interagir avec le TGFβ-1 et inhiber la voie de signalaisation en aval, dépendante de Smad3, aboutissant à un échappement à la sénescence.

Les niveaux d'activation des oncogènes pourraient expliquer les différences dans les variations des réponses cellulaires : absence ou présence de sénescence (Sarkisian *et al.*, 2007; Ferbeyre, 2007). Récemment, il a été proposé que les niveaux d'activation de ERK1 et 2 étaient déterminants dans l'établissement de la sénescence. En effet, les hauts niveaux d'activation de ERK augmenteraient les taux de phosphorylation et de dégradation des protéines. La dégradation aberrante de ces pools de protéines impliquées dans le cycle cellulaire notamment induirait un stress participant à l'établissement de la sénescence L'activation de la voie PI3K/Akt pourrait, en inhibant l'activité des kinases ERK, diminuer ce stress et favoriser l'échappement à la sénescence (Deschênes-Simard *et al.*, 2013).

Toutefois, plusieurs questions restent pour le moment sans réponse. Le mécanisme exact de l'activation de FAK par Lox permettant l'échappement à la sénescence reste méconnu. LOX et LOXL2 ont comme activité principale l'oxydation des résidus lysyl du collagène. Afin d'étudier l'effet du collagène sur l'échappement à la sénescence, les cellules sur-exprimant ou non LOX et LOXL2 ont été cultivées en présence de collagène fibrillaire. Aucune différence dans l'entrée ou l'échappement à la sénescence n'a pu être observée en comparaison avec les expériences menées sur boites de cultures sans collagène. Ces résultats suggèrent que le collagène n'est pas le substrat par lequel sont médiés les effets de Lox sur la sénescence.

Il a été montré que FAK peut être activée par le peroxyde d'hydrogène (Vepa *et al.*, 1999; Basuroy *et al.*, 2010; Yang *et al.*, 2004) et que LOX en génrant de l'H_2O_2 comme sous-produit de la réaction d'oxydation, peut également activer FAK (Payne *et al.*, 2005). Nous pouvons donc supposer que l'activation de FAK et de la voie PI3K/Akt en aval pourrait se faire au travers de ce sous produit *(figure 18)*. Paradoxalement, il est connu que l'H_2O_2 engendre un stress oxydant menant à l'induction de la sénescence (Lu and Finkel, 2008). Ces deux idées paraissent contradictoires. Toutefois, la surexpression de LOX ou LOXL2 dans notre modèle n'a d'influence (positive) sur la prolifération que dans le cas où le stress oncogénique est présent. Nous pouvons en déduire que la production d'H_2O_2 par Lox, qui ne ralentit pas la croissance des cellules, reste très faible, et n'est pas comparable avec les doses utilisées expérimentalement pour induire un stress oxydatif (de l'ordre de 100µM). Il est aussi possible que l'H_2O_2 extracellulaire produit par LOX ou LOXL2 qui agissent principalement en extracellulaire soit moins toxique que s'il était produit directement en intra-cellulaire.

Une autre hypothèse pour expliquer le mécanisme par lequel Lox déstabilise la sénescence réside dans l'interaction entre LOX et TGFβ1. Il a en effet été montré que l'activité Lox est capable d'inhiber la voie de signalisation en aval des récepteurs au TGFβ, c'est-à-dire la phosphorylation de Smad3 (Atsawasuwan *et al.*, 2008). Or, le TGFβ est pro-sénescent (Cipriano *et al.*, 2011; Acosta *et al.*,

2013). Ces données pourraient constituer une autre piste d'investigation pour comprendre l'effet de Lox sur l'OIS *(figure 18)*.

Enfin, il a en plus été démontré que les facteurs embryonnaires induisant une EMT, tels que Twist, coopèrent avec un oncogène et permettent l'échappement à l'OIS (Ansieau *et al.*, 2008). L'activité Lox, capable de réguler le processus d'EMT (Peinado *et al.*, 2005; Barry-Hamilton *et al.*, 2010) pourrait contribuer à l'échappement à l'OIS par ce mécanisme.

3 Criblage génétique

La méthode de criblage a permis à l'équipe d'identifier plus de 60 gènes comme potentiellement impliqués dans l'échappement à l'OIS. Une grande partie d'entre eux n'ont pas pu être validés par la suite (test avec 3 shRNA différents qui doivent induire une bonne extinction du gène ciblé et permettre la réversion du phénotype), et d'autres n'ont pas encore été investigués. Cette technique a permis à notre équipe de caractériser des gènes impliqués dans la régulation de l'OIS et dans la transformation maligne qui paraissent à première vue surprenants (Lallet-Daher *et al.*, 2013).

3.1 Isolation des canaux calciques ITPR2 et MCU, deux nouveaux régulateurs de la sénescence

Grâce à ce criblage perte de fonction, nous avons identifié *ITPR2* et *MCU* impliqués dans l'échange de calcium entre le RE et la mitochondrie comme régulateurs de la sénescence. Cependant, bien que nous ayons pu identifier une nouvelle voie impliquée dans la sénescence, les mécanismes en amont de la libération de calcium par les ITPR reste à être élucidés.

3.1.1 Comment sont régulés les ITPR pendant la sénescence ?

Nos données ne semblent pas indiquer d'augmentation significative des niveaux d'ARNm des ITPR pendant l'OIS dans le modèle hMEC. Il est donc possible que les échanges de calcium soient plutôt favorisés par une augmentation de l'activité des ITPR. Etant donné que ces récepteurs sont majoritairement activés par l'IP_3, nous pouvons nous demander si le stress oncogénique est associé à une augmentation de production de ce messager. Il est prévu de doser l'IP_3 pendant le stress oncogénique. Si la production d'IP_3 augmente durant la sénescence, il resterait ensuite à déterminer les signaux qui induisent sa production. L'IP_3 est en effet un second messager produit après activation des récepteurs couplés aux protéines G ou des récepteurs types tyrosine kinase (Berridge, 1993) famille importante de récepteurs, comprenant notamment des récepteurs de protéines du SASP.

Il est intéressant de souligner que la signalisation du calcium provenant du RE est modulée par de nombreux oncogènes ou suppresseurs de tumeurs. Bcl-2 par exemple régule le flux calcique provenant du réticulum en inhibant les ITPR.

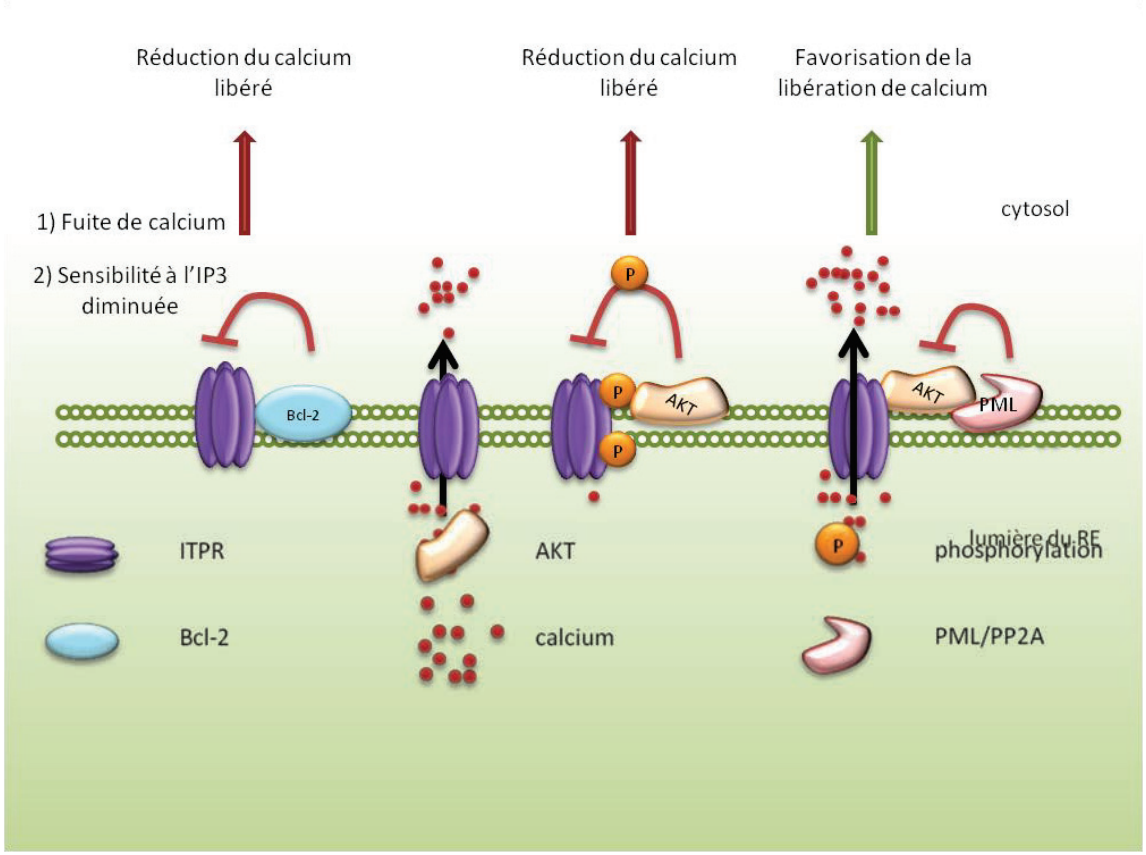

Figure 19 : Mécanismes non exhaustifs de la régulation des ITPR

Bcl-2 peut réduire la quantité de calcium libéré par les ITPR : 1) en induisant une fuite de calcium du RE, diminuant alors la quantité de calcium libéré par les ITPR lorsque ceux-ci sont stimulés, ou 2) en diminuant la sensibilité de Bcl-2 à l'IP_3.

Akt, en phosphorlyant les ITPR, inhibe leur activité. PML, via PP2A, déphosphoryle Akt et favorise la libération de calcium par les ITPR.

RE : Reticulum Endoplasmique

Cette inhibition empêche ainsi la surcharge de calcium dans la mitochondrie menant à l'apoptose – et potentiellement à la sénescence (Szado *et al.*, 2008; Pinton and Rizzuto, 2006) *(figure 19)*. De manière intéressante, Akt pourrait une nouvelle fois être impliqué dans l'échappement à la sénescence puisque celui-ci, en phosphorylant les récepteurs ITPR, inhibe leur activité. A l'inverse, le gène suppresseur de tumeur *PML* favorise l'accumulation de calcium dans la mitochondrie en inhibant Akt (Giorgi *et al.*, 2010) *(figure 19)*. La protéine PML connue pour son rôle dans la régulation de la transcription augmente pendant la sénescence réplicative et prématurée sous forme de corps nucléaires(Ferbeyre *et al.*, 2000; Pearson *et al.*, 2000; Bischof *et al.*, 2002). Elle participe activement par son interaction avec Rb à la répression de gènes cibles de E2F (Vernier *et al.*, 2011; Talluri and Dick, 2014). On peut légitimement se demander si pendant la sénescence les flux calciques entre le RE et mitochondries sont favorisés par un enrichissement des MAMs en PML. La régulation du complexe ITPR/AKT/PML pendant la sénescence serait donc un axe d'étude pertinent à développer.

3.1.2 Régulation de MCU

Suite à la découverte du MCU, de nombreuses études visant à caractériser ce transporteur ainsi que ses sous unités régulatrices (MCUR1 (Mallilankaraman et al., 2012), MICU1 (Perocchi et al., 2010) et EMRE (Sancak et al., 2013)) ont été publiées (Curry *et al.*, 2013; Prudent *et al.*, 2013; Raffaello *et al.*, 2013; Qiu *et al.*, 2013; Fieni *et al.*, 2012). Ces travaux ont ouvert une nouvelle voie dans l'étude de la régulation du calcium mitochondrial et son implication dans des processus biologiques comme la mort cellulaire, ou comme nous l'avons montré, dans la sénescence. Pour autant, le rôle de MCU dans la tumorigénèse n'a pas encore été démontré. Récemment, il a été publié que le miR-25, qui est surexprimé dans de nombreux cancers, affecte *MCU,* induisant une forte diminution de l'accumulation de calcium dans la mitochondrie, et générant des cellules résistantes à l'apoptose dans des modèles de tumeurs du colon et de la prostate (Marchi *et al.*, 2013).

La régulation du MCU est toutefois mal connue et complexe vu le nombre de sous-unités régulatrices qui interagissent avec ce canal. Nous avons montré que la diminution d'expression de MCU permet un échappement à l'OIS, en inhibant la relocalisation du calcium dans les mitochondries. La perte d'expression de MICU1, le senseur de calcium (Csordás *et al.*, 2013; Perocchi *et al.*, 2010; de la Fuente *et al.*, 2014; Mallilankaraman *et al.*, 2012) potentialise le stress oncogénique, probablement parce que son absence aboutit à une entrée non contrôlée de calcium lors de l'OIS . Notre travail contribue donc à montrer l'importance du MCU et de sa régulation dans les mécanismes de sauvegarde – telles que l'apoptose et la sénescence.

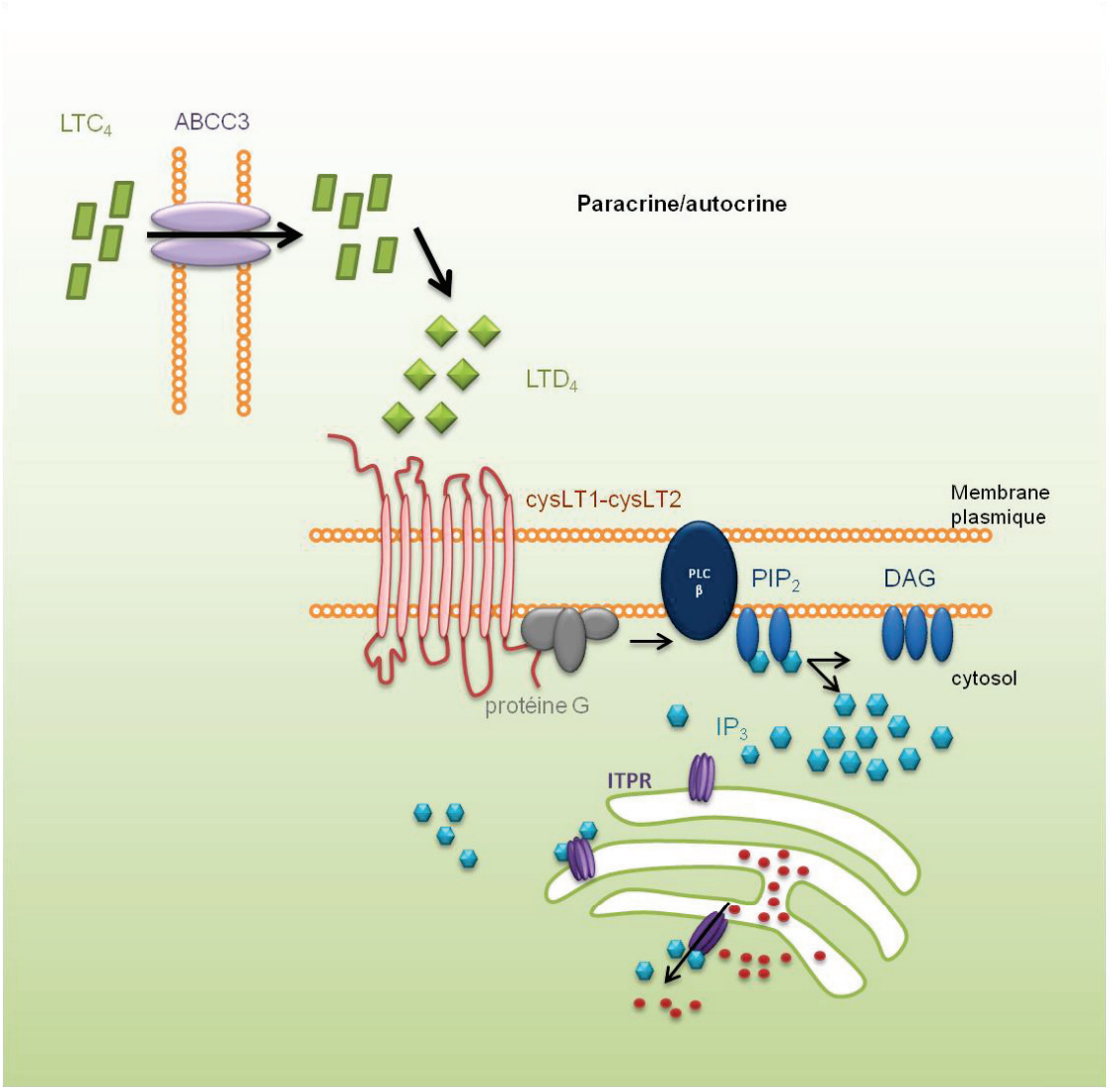

Figure 20 : Hypothèse de travail concernant le mécanisme par lequel ABCC3 régule l'OIS

ABCC3 transporte le LTC_4 en dehors de la cellule. Celui-ci est métabolisé en LTD_4, et peut se fixer sur ses récepteurs couplés au protéines G, les cysLT1 et cysLT2. Cela activerait alors la production de l'IP_3 par l'intermédiaire des phosholipases C. L'étude du calcium mitochondrial lors de la sénescence, en présence ou absence d'ABCC3 permettra de valider cette hypothèse.

DAG : DiAcylGlycérol ; IP_3 : Inositol-TriPhosphate ; ITPR : Récepteur à l'InositolTriPhosphate ; PIP2 : PhosphatidylInositol 4,5-biPhosphate ; LT : Leukotriène ; PLC : PhosphoLipase C

3.2 Identification d'ABCC3, régulateur indirect des canaux calciques pendant l'OIS ?

Parmi les gènes identifiés lors du criblage, nous avons étudié le gène *ABCC3* (précédemment dénommé MRP3 pour *Multidrug Resistant Protein*) codant pour un transporteur membranaire de la famille des ABC (*ATP-Binding Cassette*).

Nous avons confirmé, après avoir isolé un shRNA contre ABBC3 dans le criblage que l'extinction d'ABCC3 permet un échappement à l'OIS *in vitro*, mais également *in vivo* dans un modèle murin de carcinogénèse de la peau induite par Ras (Abel *et al.*, 2009) favorisant ainsi la formation de carcinomes. La surexpression d'ABCC3 agit en synergie avec une faible activation oncogénique pour induire l'OIS. La fonction de transporteur semble être impliquée dans ces observations. En effet, la surexpression d'une version mutée d'ABBC3 qui abolit sa capacité à transporter ses substrats ne coopère plus avec un faible stress oncogénique pour induire la sénescence. Parmi les substrats d'ABCC3 se trouve le médiateur lipidique leukotriène C4 (LTC_4). Une fois transporté hors de la cellule, celui-ci est métabolisé en LTD_4 et LTE_4 (Fletcher *et al.*, 2010). L'hypothèse sur laquelle nous travaillons actuellement est de savoir si le LTD_4, en se liant à ses récepteurs couplés aux protéines G, les cysLT1 et cyLT2, pourrait activer la voie de l'IP_3 et participer à l'OIS *(figure 20)*.

3.3 Identification du canal potassique KCNA1 comme régulateur de l'OIS

Le criblage dans les hMECs a également permis d'identifier le canal potassique KCNA1 comme régulateur de l'OIS (Lallet-Daher *et al.*, 2013). En effet, celui-ci est relocalisé au niveau de la membrane plasmique lors du stress oncogénique, aboutissant à une dépolarisation du potentiel de membrane $\Delta V_{(m)}$. Cette relocalisation est dépendante de la protéine kinase A (PKA) dont l'activité diminue fortement durant le stress oncogénique. L'inhibition de cette relocalisation permet un échappement à l'OIS. L'ensemble des données suggèrent fortement que KCNA1 régule l'OIS en régulant la concentration en potassium du milieu extra-cellulaire, et l'état de polarisation de la membrane plasmique. Ces changements de polarisation peuvent affecter différentes voies intracellulaires, notamment la libération de calcium du RE via les ITPR (Liu *et al.*, 2009).

L'ensemble des résultats du laboratoire montre que les canaux ioniques, potassique ou calciques, jouent un rôle prépondérant jusque là inconnu dans la régulation de la sénescence. Il serait alors intéressant d'étudier dans son ensemble la régulation des flux ioniques lors de la sénescence. Cet axe est actuellement en développement dans le laboratoire.

4 L'échange de calcium entre RE et mitochondrie est un processus pro-apoptotique, et pro-sénescent

4.1 Le calcium : un messager de mort et de sénescence

La connexion entre surcharge calcique dans la mitochondrie et mort cellulaire est largement démontrée. Une surcharge trop importante de calcium est néfaste puisque cela altère la respiration mitochondriale et mène à la chute du potentiel de membrane, au gonflement de la mitochondrie, à la perméabilisation de l'OMM et finalement à la libération de cytochrome c menant à l'apoptose (Hajnóczky *et al.*, 2006). La quantité de calcium absorbée par la mitochondrie dépend notamment des pulses de calcium libéré par les ITPR (Csordás and Hajnóczky, 2001; Csordás *et al.*, 1999). La mitochondrie est aussi un organite qui a des capacités de réguler sa concentration calcique, soit en pompant le calcium vers le cytosol soit via le PTP (*Permeability Transition Pore*) (Duchen, 1999; Bernardi *et al.*, 1999).

Notre travail nous a permis d'observer la dissipation du potentiel de membrane mitochondrial suite à la prise de calcium. Détecter par immunofluorescence du cytochrome c dans le cytosol des cellules sénescentes permettrait de savoir si une rupture de la membrane mitochondriale a lieu. Pour autant, nous avons observé lors de la sénescence, OIS ou réplicative, une augmentation

de calcium dans la mitochondrie dépendante d'ITPR2 et MCU sans observer de mort cellulaire. Comment pourrait-on alors expliquer lors de la sénescence une activation d'une voie impliquée dans l'induction de l'apoptose ? Il est clair que les réponses de sénescence et d'apoptose impliquent des voies de signalisation communes, et la relocalisation du calcium mitochondrial pourrait en faire partie. L'analyse du calcium mitochondrial pendant le stress oncogénique montre une augmentation dans les premières 24h, qui est ensuite soutenue dans les 48h suivantes. Pendant la sénescence on observerait une accumulation graduelle et chronique de calcium dans la mitochondrie. L'accumulation graduelle de calcium aboutirait finalement à un dysfonctionnement marqué (fission, perte du $\Delta\Psi_m$, altérations métaboliques) de la mitochondrie mais n'induisant pas des signaux de mort cellulaire. A l'inverse, une surcharge calcique mitochondriale soudaine et rapide aboutirait à l'apoptose.

L'analyse des oscillations de calcium pendant le stress oncogénique permettrait de répondre à ces questions et notamment de définir les réponses mises en place par les mitochondries pour gérer un afflux massif de calcium.

4.2 Bcl-2 au carrefour de l'apoptose et de la sénescence ?

Bcl-2 est largement connu pour ses fonctions anti-apoptotiques. Il a par ailleurs déjà été démontré que cette protéine est associée à la résistance à l'apoptose des cellules sénescentes (Wang, 1995; Crescenzi *et al.*, 2003; Ryu *et al.*, 2007). Il a également été montré que Bcl-2 est capable de promouvoir une sénescence induite par p53 quand l'apoptose est inhibée (Schmitt *et al.*, 2002; Rincheval *et al.*, 2002) ou que Bcl-2 permet de renforcer la sénescence induite par Ras dans les fibroblastes (Tombor *et al.*, 2003). Les effets de Bcl-2 sur le cycle cellulaire sont souvent associés à une induction de $p27^{Kip1}$ et une inhibition de CDK requis pour la progression dans la phase G1 du cycle (Greider *et al.*, 2002; Linette *et al.*, 1996; Crescenzi *et al.*, 2003). Une nouvelle fois, les données obtenues dans des cellules épithéliales sont très rares.

Les rôles de Bcl-2 semblent être toutefois au moins en partie dépendants du calcium. En effet, Bcl-2 pourrait diminuer l'impact du calcium libéré par les ITPR soit en interagissant directement avec les ITPR et inhiber la sortie de calcium par ces récepteurs (Chen *et al.*, 2004; Rong *et al.*, 2009, 2008) soit en abaissant le taux de calcium dans le RE (Pinton *et al.*, 2000; Foyouzi-Youssefi *et al.*, 2000) *(figure 19 p149)*. Plusieurs études ont également impliqué Bcl-2 dans l'homéostasie du calcium mitochondrial bien que les mécanismes ne soient toujours pas clairs (Bonneau *et al.*, 2013). La surexpression de Bcl-2 dans des cellules neurales permettrait aux mitochondries d'absorber plus de calcium sans effet délétère sur la respiration (Murphy *et al.*, 1996). Deux autres groupes ont confirmé

que Bcl-2 permettrait d'augmenter les capacités de stockage en calcium des mitochondries (Zhu *et al.*, 1999; Hirata *et al.*, 2012). On peut alors se demander si Bcl-2 dont l'augmentation d'expression est souvent rapportée pendant la sénescence pourrait également influencer le transfert de calcium entre le RE et la mitochondrie, et être en partie responsable de la résistance des mitochondries à l'afflux de calcium, et de la résistance à l'apoptose.

Il avait déjà été proposé, pour induire la mort cellulaire de cellules cancéreuses, d'activer spécifiquement la transmission de calcium entre le réticulum et la mitochondrie. La possibilité que cette activation puisse également engendrer de la sénescence renforce l'intérêt de cette approche thérapeutique.

5 Des perturbations de la mitochondrie et du RE peuvent affecter le contrôle qualité des protéines

Le RE est un organite siège de nombreux processus cellulaires liés à la maturation des protéines, la synthèse de phospholipides, de cholestérol, de stéroïdes et à l'homéostasie du calcium intracellulaire. De nombreuses fonctions du RE dont les fonctions des protéines chaperonnes sont couplées aux niveaux en Ca^{2+}. Une diminution de la concentration calcique engendre alors une accumulation de protéines mal conformées et aboutit au stress du RE. De nombreuses études montrent que le RE est également impliqué dans l'autophagie ou l'apoptose (Decuypere *et al.*, 2011 a; Parys *et al.*, 2012; Harr and Distelhorst, 2010)

5.1 L'OIS dans les cellules épithéliales est-elle associée à un stress du RE ?

Ce stress du RE, réponse qui bloque la traduction de manière globale, induit des gènes impliqués dans une réponse apoptotique via différents senseurs. La liaison de la protéine chaperonne Grp78-BIP (*Glucose-Related Protein 78 – immunoglobin-Binding Protein*) aux protéines mal repliées libère et active PERK, IRE1α, ATF6. L'UPR (*unfolded protein response*) est initiée pour rétablir une fonction normale du RE et rétablir l'homéostasie calcique. Cela se traduit par l'augmentation de la dégradation des protéines non repliées via le protéasome et l'autophagie. Cependant, en cas de stress trop sévère ou prolongé l'UPR ne peut pas être efficace et un programme de mort cellulaire est enclenché afin d'éliminer la cellule défectueuse (Szegezdi *et al.*, 2006; Schrçder and Schröder, 2008)

Dans les hMECs, l'activation oncogénique est associée à une fuite du calcium depuis le réticulum. Pour autant, nous n'avons observé aucune induction d'un stress du RE *(article 2, figure*

supplémentaire 10). Des données préliminaires semblent toutefois indiquer une diminution globale des N-glycosylations lors de l'OIS des cellules épithéliales *(données non montrées)*. Or, il est connu que des agents bloquant le processus de la glycosylation comme la tunicamycine induisent l'accumulation de protéines mal conformées, créant alors un stress du RE prolongé suivi d'une UPR. Pendant le stress oncogénique dans le modèle hMEC on observe donc une diminution de la concentration de calcium du RE (hypothèse à vérifier) et une diminution globale des glycosylations des protéines, deux mécanismes pouvant mener à un stress du RE. Aucune réponse de type UPR ne semble pourtant être induite. Une étude a toutefois rapporté qu'une réponse de type UPR participe activement à la mise en place de la sénescence induite par H-Ras^{G12V} dans des mélanocytes (Denoyelle *et al.*, 2006). Il serait donc intéressant d'étudier plus en profondeur cet aspect pour déterminer les facteurs induisant ou non une UPR lors de la sénescence.

5.2 La sénescence et les processus autophagiques

L'autophagie est un processus catabolique mis en place en période de stress où les cellules digèrent leurs propres composants pour générer de l'énergie et des précurseurs métaboliques (Yang and Klionsky, 2010; Kimmelman, 2011). En plus de réguler l'homéostasie énergétique, l'autophagie joue un rôle important dans le contrôle qualité des protéines (Hoare *et al.*, 2011). Plusieurs données semblent indiquer une dérégulation des signaux autophagiques lors de la sénescence. En effet, des marqueurs de l'autophagie sont induits pendant le stress oncogénique montrant une perturbation du flux autophagique dans les hMECs (augmentation de LC3 membranaire, structures de doubles membranes spécifiques à l'autophagosome visibles au microscope électronique, *données non montrées*). Il est aussi montré que les signaux calciques sont fortement liés à l'autophagie et que les ITPR sont connus pour réguler l'autophagie (Decuypere *et al.*, 2011 b).

On aurait pu s'attendre à des perturbations de l'autophagie dans les cellules exprimant un shITPR2. En effet, les ITPR sont notamment connus pour séquestrer, par l'intermédiaire de Bcl-2 la protéine pro-autophagique Beclin-1 (Vicencio *et al.*, 2009). Il a aussi été montré que la suppression des ITPR est associée à une augmentation de l'autophagie dépendante de la voie AMPK, enclenchée en tant que processus de survie (Cárdenas *et al.*, 2010). AMPK est un indicateur du statut énergétique de la cellule dont l'activité augmente dans des conditions de stress métabolique qui aboutissent à l'augmentation du ratio cytosolique AMP /ATP (Hardie, 2007). Le transfert de calcium entre RE et mitochondries est en effet un processus cellulaire nécessaire pour la respiration mitochondriale et le maintien du statut bioénergétique de la cellule (Cárdenas *et al.*, 2010). L'inhibition d'ITPR2 n'induit pourtant pas d'autophagie dans les hMECs sûrement parce que les flux calciques de base ne sont pas perturbés grâce à la présence des autres ITPR (1 et 3).

Par contre, durant le stress oncogénique des cellules épithéliales, le marqueur autophagique LC3 membranaire augmente *(figure supplémentaire 10c)*, mais l'AMPK est faiblement activée *(article 4, annexe 2 figure supplémentaire 5)* malgré la diminution d'ATP observée dans les cellules sénescentes *(article 4, annexe 2, figure 1)*. Cet élément, associé à l'augmentation de LC3 membranaire, suggère que le flux autophagique est bloqué dans les cellules sénescentes plutôt que d'être induit. Il serait intéressant d'investiguer plus en détail l'effet de l'extinction partielle d'ITPR2, permettant l'échappement à la sénescence, sur l'autophagie.

D'autres études ont pourtant associé l'autophagie à la sénescence (Gamerdinger *et al.*, 2009; Capparelli *et al.*, 2012; Gerland *et al.*, 2003). Il a en effet été proposé que l'autophagie participe à la biogénèse des protéines du SASP permettant de renforcer la sénescence (Young *et al.*, 2009; Narita *et al.*, 2011). L'autophagie pourrait également permettre une dégradation des protéines endommagées (Gamerdinger *et al.*, 2009). Récemment, l'équipe de Peter Adams a proposé un mécanisme selon lequel des fragments de chromatine rejetés dans le cytoplasme pourraient être dégradés par un processus autophagique (Ivanov *et al.*, 2013).

Toutefois, le rôle de l'autophagie dans la sénescence reste débattu. Ras pourrait également induire de l'autophagie favorisant la transformation cellulaire. Dans ce contexte, l'inactivation de l'autophagie rend les cellules plus sensibles à la sénescence (Wang *et al.*, 2012). Enfin, il a été montré que des kératinocytes sénescents, bien que résistants à l'apoptose, pouvaient mourir via un mécanisme autophagique (Gosselin *et al.*, 2009). Le rôle de l'autophagie a toujours été difficile à déterminer, notamment dans les divers processus de tumorigenèse. Par son rôle contrôle-qualité, en éliminant les tissus endommagés, l'inflammation ou l'instabilité génomique, l'autophagie peut supprimer l'initiation tumorale. Mais en recyclant les nutriments, l'autophagie maintient le métabolisme, la croissance et la survie des cellules cancéreuses (White, 2012).

Il apparaît donc que le processus autophagique est modifié pendant la sénescence. L'ensemble de ces données, associée aux nôtres, montre que l'autophagie, la sénescence, et les signaux calciques sont interconnectés, bien qu'il soit difficile à l'heure actuelle d'identifier les événements causals des conséquences.

6 La mitochondrie : au cœur de nombreux processus fondamentaux cellulaires

6.1 Dynamisme de la mitochondrie durant la sénescence

Les mitochondries sont dotées d'un réseau tubulaire dynamique, subissant constamment des fissions et fusions, potentiellement afin d'assurer une répartition mitochondriale homogène dans la cellule, et d'apporter de l'ATP dans toutes les régions cytosoliques de la cellule. Il apparaît désormais clairement que maintenir le dynamisme mitochondrial est crucial pour le bon fonctionnement cellulaire (Scorrano, 2013).

J'ai pu observer, outre les changements dans leur charge calcique et leur dépolarisation, que les mitochondries étaient également altérées morphologiquement. En effet la forme des mitochondries évolue énormément suite à l'activation du stress oncogénique, en passant d'abord par une phase d'élongation importante et aberrante, avant que les mitochondries ne deviennent très rondes *(figure 21a)*. Les variations de structure suggèrent une altération des processus de fusion/fission des mitochondries médiés habituellement par les protéines Mfn 1 et 2 et OPA1 (*Optic Atrophy gene 1*) et par les protéines Drp1 (*Dynamin-Related Protein 1*) et Fis1 respectivement (Scorrano, 2013). Des anomalies dans ces processus de fusion et fission sont associés à un arrêt de croissance, à chute du $\Delta\Psi_m$ et à une respiration défectueuse (Chen *et al.*, 2005 a; Parone *et al.*, 2008). De manière intéressante, quelques études impliquent ces anomalies dans la sénescence. En effet, une inhibition de la fission mitochondriale engendre de la sénescence associée à une génération de ROS et à la perte du $\Delta\Psi_m$ (Lee *et al.*, 2007). Les cellules endothéliales en sénescence réplicative présentent un déficit de la fission mitochondriale. De manière assez surprenante, cela les rend plus résistantes aux ROS (Mai *et al.*, 2010). Le potentiel de membrane est également nécessaire aux processus de fusion (Legros *et al.*, 2002). L'ensemble de ces données suggère fortement des perturbations dans ces processus lors de la sénescence *(figure 21b)*. L'autophagie est également associée à une élongation des mitochondries probablement nécessaire pour maintenir la production d'ATP et l'intégrité cellulaire (Gomes *et al.*, 2011). L'élongation des mitochondries pourrait donc constituer une première réponse adaptative de la cellule face au stress oncogénique.

De plus, le RE semble également jouer un rôle dans la fission des mitochondries. Il a en effet été montré que les fissions mitochondriales ont lieu aux sites de contacts entre les deux organelles où les tubules du RE peuvent engendrer une constriction de la mitochondrie (Friedman *et al.*, 2011; Korobova *et al.*, 2013). Bien que les contacts entre le RE et les mitochondries ne semblent pas être significativement perturbés pendant la sénescence (*article 2, figure supplémentaire 4*) cela n'exclue

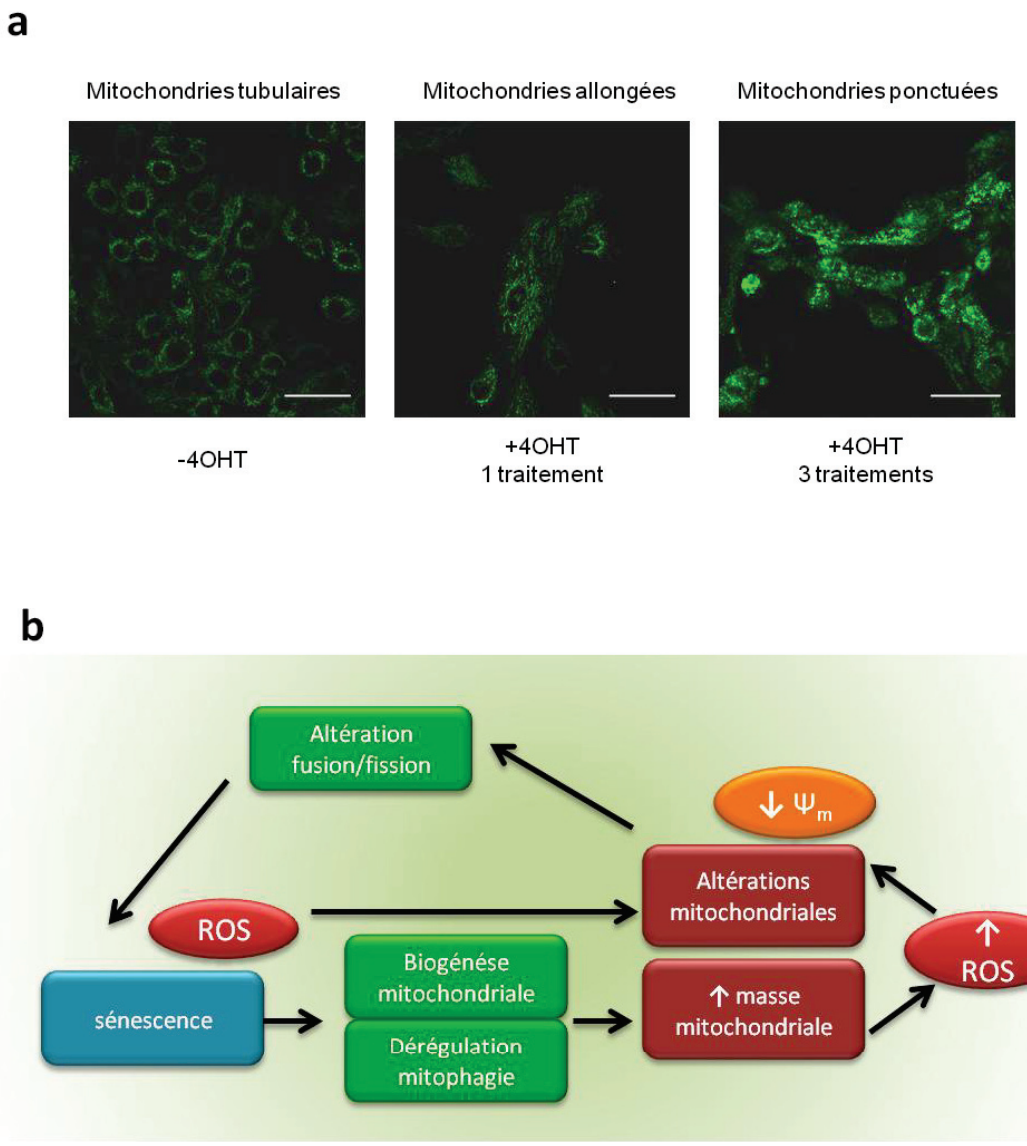

Figure 21 : Perturbations du dynamisme de la mitochondrie pendant la sénescence

pas que des dysfonctionnements du RE en conditions de stress puissent aboutir à des perturbations dans les processus de fission/fusion.

La réponse au stress oncogénique dans les cellules épithéliales est associée à une augmentation de la masse mitochondriale mesurée par le MitoTracker non dépendant du potentiel de membrane (*données non montrées et figure 21b)*. Il a également été rapporté une augmentation de la masse mitochondriale dans des fibroblastes après activation de Ras et ce, associée à une production de ROS plus importante (Moiseeva *et al.*, 2009). Cette biogénèse des mitochondries serait favorisée afin de remplacer celles défectueuses. Les mitochondries nouvellement formées, également exposées au stress oncogénique et aux ROS pourraient cependant aussi être altérées. La méthode utilisée pour évaluer la masse mitochondriale - MitoFluo Green qui s'incorpore dans les membranes lipidiques des mitochondries - ne permet pas de déterminer si les mitochondries sont plus nombreuses ou plus grosses.

Alternativement, l'augmentation de la masse mitochondriale lors de la sénescence pourrait provenir d'une altération de la dégradation des mitochondries. Quand les mitochondries sont sévèrement endommagées et perdent leur potentiel de membrane, celles-ci sont spécifiquement éliminées par un processus de macroautophagie appelé mitophagie (Zhang, 2013; Ashrafi and Schwarz, 2013). L'élimination des mitochondries est essentielle dans le contrôle qualité de ces organites, notamment parce que l'altération des mitochondries peut résulter en une augmentation du stress oxydatif. La dégradation des mitochondries défectueuses supprime donc le stress oxydatif et préserve les fonctions mitochondriales. La chute du $\Delta\Psi_m$ et les ROS font partie des éléments déclencheurs de la mitophagie (Rimessi *et al.*, 2013). Or, la sénescence est associée à une perturbation du flux autophagique dont le rôle est mal déterminé. Cette dérégulation de l'autophagie pourrait se traduire par une dérégulation du processus mitophagique lors du stress oncogénique aboutissant ainsi à une accumulation de mitochondries défectueuses génératrices de ROS *(figure 21)*. D'ailleurs, il a été montré que les MEFs en sénescence réplicative sont marquées par une réduction de la mitophagie mise en place pour éliminer les mitochondries dépolarisées et endommagées par du CCCP (Hoshino *et al.*, 2013). Tellement ces processus, autophagie, mitophagie, stress du réticulum endoplasmique sont en lien direct avec la sénescence, il devient nécessaire d'élucider l'impact de l'autophagie et potentiellement de la mitophagie dans la sénescence – cause ou conséquence - et d'éclaircir la fonction et la contribution de ces réponses cellulaires.

6.2 Mitochondrie et métabolisme pendant la sénescence

Nous avons montré qu'une dépolarisation des mitochondries aboutit à un arrêt de croissance associé à de la sénescence *(article 2, figure 7)*. Nos données et celles de la littérature indiquent qu'interférer avec les fonctions mitochondriales est suffisant pour induire de la sénescence. En effet, une dépolarisation mitochondriale faible mais prolongée est un stress suffisant pour induire de la sénescence et la production de ROS dans les hMECS *(article 2, figure 7 et figure supplémentaire 8b)*. Il a aussi été montré qu'il était possible d'induire de la sénescence en réprimant l'expression de RISP (*Rieske Iron Sulfur Protein*) qui permet le transfert d'électrons nécessaires à la phosphorylation oxydative (Moiseeva *et al.*, 2009) ou en utilisant des inhibiteurs de la phosphorylation oxydative (Moiseeva *et al.*, 2009; Stöckl *et al.*, 2006). La perte du potentiel de membrane ou tout autre évènement affectant la phosphorylation oxydative risque d'aboutir à une diminution de la production d'ATP. Les dysfonctionnements mitochondriaux que nous avons rapportés peuvent expliquer, du moins en partie, la diminution diminution d'ATP observée dans les cellules sénescentes (*article 4, annexe 2* (Gitenay *et al.*, 2014)).

D'autres mécanismes affectant la mitochondrie peuvent également altérer la production d'ATP et le métabolisme d'une manière plus générale. En effet, le calcium régule l'activité de 3 déshydrogénases de la matrice mitochondriale : la pyruvate déshydrogénase (PDH) est régulée par une phosphatase dépendante du calcium. L'α-cetoglutarate et l'isocitrate-déshydrogénase sont régulées par liaison directe au calcium. L'augmentation de l'activité de ces déshydrogénases augmente la quantité de NADH disponible et donc le flux d'électrons dans la chaine respiratoire. Le rôle premier du calcium est donc de stimuler la phosphorylation oxydative, en régulant ces enzymes du cycle de Krebs ou l'ATP synthase du complexe V de la chaine respiratoire. Quand la fonction mitochondriale est altérée, la chaine respiratoire défectueuse réduit la force motrice nécessaire à l'entrée de calcium nécessaire aux enzymes du cycle de Krebs et donc la synthèse d'ATP (Gunter *et al.*, 2000).

Durant la sénescence induite par B-Raf^{V600E}, l'équipe de Daniel Peeper a observé une augmentation de l'activité de la PDH suite notamment à l'activation de la pyruvate déshydrogénase phosphatase (PDP2, sensible au calcium) induisant une augmentation de l'utilisation du pyruvate dans le cycle de Krebs. Cela favorise la respiration cellulaire en augmentant l'activité de la chaine respiratoire, mais augmente également le stress redox en favorisant la production de ROS (Kaplon *et al.*, 2013). D'autres études impliquent également une dérégulation du cycle de Krebs durant la sénescence avec des résultats opposés (Jiang *et al.*, 2013).

Malgré des données contradictoires et complexes dans la littérature, une perturbation du métabolisme mitochondrial et du métabolisme d'une manière générale (Jiang *et al.*, 2013; Gitenay *et al.*, 2014; Favaro *et al.*, 2012) semble réguler la sénescence. Nos résultats sur l'effet du calcium sur la physiologie de la mitochondrie appuient ces conclusions.

6.3 Dysfonctionnements mitochondriaux à la source des ROS pendant la sénescence ?

Les ROS sont des sous-produits générés par différents processus physiologiques. Différentes sources cellulaires de ROS ont été identifiées mais il est généralement admis que la principale source de ROS est la respiration mitochondriale. Plus de 90% de l'O_2 consommé est transformé en H_2O par une réaction catalysée par la cytochrome oxydase. Cependant, les transporteurs d'électrons de la chaine mitochondriale peuvent transférer un électron à de l'O_2, générant ainsi l'anion superoxide ($O_2\bullet^-$). La dismutation spontanée ou enzymatique de ce radical aboutit à la génération de péroxyde d'hydrogène H_2O_2, qui a son tour peut produire le radical hydroxyl •OH. Il a été établi que les niveaux de ROS augmentent pendant la sénescence réplicative ainsi que pendant l'OIS (Passos *et al.*, 2007 a; Ramsey and Sharpless, 2006; Lu and Finkel, 2008; Lee *et al.*, 1999), *voir introduction, paragraphe 1.2.4)*. Dans la plupart des cas, le traitement des cellules avec des antioxydants permet l'échappement à la sénescence suggérant un rôle fonctionnel des ROS dans la sénescence, notamment en activant une DDR. Pour autant, les mécanismes moléculaires par lesquels les ROS engendrent de la sénescence sont mal connus.

Il a été montré que les ROS participent à la sénescence réplicative en raccourcissant les télomères (von Zglinicki, 2000). De plus, le raccourcissement des télomères dans une population cellulaire se produit à des vitesses différentes. Par contre, les cellules qui sénescent le plus tôt sont celles qui ont les des télomères les plus courts, et qui ont surtout des niveaux de ROS intracellulaires les plus élevés (Passos *et al.*, 2007 a).

Plusieurs études montrent donc que les ROS sont nécessaires à l'établissement de la sénescence. Pour autant, d'où proviennent ces ROS exactement ? Par quels mécanismes sont il générés ? Ces questions restent encore à l'heure actuelle très peu investiguées (Passos *et al.*, 2007 b). Une faible proportion de ces ROS semblent être non mitochondriaux (Catalano *et al.*, 2005) (Takahashi *et al.*, 2006). L'augmentation de la respiration suite à l'activation de la PDH pendant la sénescence induite par B-Raf est associée à une augmentation de la production de ROS (Kaplon *et al.*, 2013). Nos données montrent également un dysfonctionnement de la physiologie de la mitochondrie qui est associée à la génération de ROS. L'augmentation de la masse mitochondriale est également rapportée dans des fibroblastes sénescents (Lee *et al.*, 2002; Passos *et al.*, 2007 b; Moiseeva *et al.*, 2009) et dans les hMECs sénescentes *(données non montrées)*. L'augmentation totale de ROS

intracellulaires pourrait donc en plus provenir d'une augmentation de la biogénèse/absence de dégradation des mitochondries. On peut donc supposer que les dysfonctionnements mitochondriaux observés pendant la sénescence peuvent être à la source de ROS.

Nos résultats indiquent pour la première fois que les dynamiques de calcium sont perturbées pendant le stress oncogénique et la sénescence réplicative, et résultent en une altération de la physiologie de la mitochondrie associée à la production de ROS.

7 Est-ce que le calcium cytosolique est aussi un messager de la sénescence ?

Les mitochondries en absorbant le calcium jouent un rôle primordial dans la régulation du calcium cytosolique. On peut supposer que le calcium libéré par les ITPR ne soit pas totalement assimilé par les mitochondries, ou que certaines mitochondries trop altérées libèrent du calcium aboutissant ainsi à une augmentation prolongée du calcium cytosolique, impactant certaines voies de signalisation en aval. Le calcium cytosolique libéré suite aux dysfonctionnements mitochondriaux résulte en une activation des facteurs de transcription CREB et NFκB (Arnould *et al.*, 2002; Biswas *et al.*, 1999). Ces forts taux de calcium cytosolique prolongés peuvent également induire l'activation des facteurs de transcription NFAT (*Nuclear Factor of Activated T cell*), famille composée de 5 isoformes exprimés de manière ubiquitaire, dont 4 indirectement régulés par le calcium. Bien que NFAT 1 semble avoir un rôle pro-tumoral, il semblerait que NFAT2 et NFAT3 aient à l'inverse un rôle anti-tumoral (Pan *et al.*, 2013 a).

En plus de mesurer les oscillations du calcium cytosolique pendant la sénescence, il est prévu d'étudier la localisation - cytosolique ou nucléaire - et donc l'activation de NFAT1 et 2. Pour cela, des protéines fusionnées à la GFP seront surexprimées dans les cellules. En fonction du résultat, il sera possible d'étudier quels sont les gènes régulés par ces facteurs de transcription lors de la sénescence. Il est intéressant de souligner que les facteurs NFAT et NFκB sont proches, par leur structure et leurs fonctions. NFκB a été largement impliqué dans l'expression des facteurs du SASP (Jing *et al.*, 2011; Chien *et al.*, 2011). On peut spéculer sur le rôle de NFAT dans la sénescence, et imaginer que ces facteurs induisent également l'expression de gènes impliqués dans la réponse inflammatoire notamment.

BIBLIOGRAPHIE

BIBLIOGRAPHIE

-A-

Abel EL, Angel JM, Kiguchi K, and DiGiovanni J. (2009). Multi-stage chemical carcinogenesis in mouse skin: fundamentals and applications. *Nat. Protoc.* **4**: 1350–62.

Acosta JC, Banito A, Wuestefeld T, Georgilis A, Janich P, Morton JP, *et al.* (2013). A complex secretory program orchestrated by the inflammasome controls paracrine senescence. *Nat. Cell Biol.* **15**: 1–15.

Acosta JC, O'Loghlen A, Banito A, Guijarro M V, Augert A, Raguz S, *et al.* (2008). Chemokine signaling via the CXCR2 receptor reinforces senescence. *Cell* **133**: 1006–18.

Ahn SG, Dong SM, Oshima A, Kim WH, Lee HM, Lee SA, *et al.* (2013). LOXL2 expression is associated with invasiveness and negatively influences survival in breast cancer patients. *Breast Cancer Res. Treat.*

Akl H, and Bultynck G. (2013). Altered Ca(2+) signaling in cancer cells: proto-oncogenes and tumor suppressors targeting IP3 receptors. *Biochim. Biophys. Acta* **1835**: 180–93.

Alimonti A, Nardella C, Chen Z, Clohessy JG, Carracedo A, Trotman LC, *et al.* (2010). A novel type of cellular senescence that can be enhanced in mouse models and human tumor xenografts to suppress prostate tumorigenesis. *J. Clin. Invest.* **120**: 681–93.

Ansieau S, Bastid J, Doreau A, Morel A, Bouchet BP, Thomas C, *et al.* (2008). Induction of EMT by twist proteins as a collateral effect of tumor-promoting inactivation of premature senescence. *Cancer Cell* **14**: 79–89.

Arnould T, Vankoningsloo S, Renard P, Houbion a, Ninane N, Demazy C, *et al.* (2002). CREB activation induced by mitochondrial dysfunction is a new signaling pathway that impairs cell proliferation. *EMBO J.* **21**: 53–63.

Ashrafi G, and Schwarz TL. (2013). The pathways of mitophagy for quality control and clearance of mitochondria. *Cell Death Differ.* **20**: 31–42.

Atsawasuwan P, Mochida Y, Katafuchi M, Kaku M, Fong KSK, Csiszar K, *et al.* (2008). Lysyl oxidase binds transforming growth factor-beta and regulates its signaling via amine oxidase activity. *J. Biol. Chem.* **283**: 34229–40.

Augert A, Payré C, de Launoit Y, Gil J, Lambeau G, and Bernard D. (2009). The M-type receptor PLA2R regulates senescence through the p53 pathway. *EMBO Rep.* **10**: 271–7.

-B-

Bais M V, Nugent MA, Stephens DN, Sume SS, Kirsch KH, Sonenshein GE, *et al.* (2012). Recombinant lysyl oxidase propeptide protein inhibits growth and promotes apoptosis of pre-existing murine breast cancer xenografts. *PLoS One* **7**: e31188.

Baker A-M, Bird D, Lang G, Cox TR, and Erler JT. (2012). Lysyl oxidase enzymatic function increases stiffness to drive colorectal cancer progression through FAK. *Oncogene* **32**: 1863–68.

Baker A-M, Cox TR, Bird D, Lang G, Murray GI, Sun X-F, *et al.* (2011).(a). The role of lysyl oxidase in SRC-dependent proliferation and metastasis of colorectal cancer. *J. Natl. Cancer Inst.* **103**: 407–24.

Baker DJ, Wijshake T, Tchkonia T, LeBrasseur NK, Childs BG, van de Sluis B, *et al.* (2011).(b). Clearance of p16Ink4a-positive senescent cells delays ageing-associated disorders. *Nature* **479**: 232–6.

Bakkenist CJ, Drissi R, Wu J, Kastan MB, and Dome JS. (2004). Disappearance of the telomere dysfunction-induced stress response in fully senescent cells. *Cancer Res.* **64**: 3748–52.

Bakkenist CJ, and Kastan MB. (2003). DNA damage activates ATM through intermolecular autophosphorylation and dimer dissociation. *Nature* **421**: 499–506.

Balducci L, and Ershler WB. (2005). Cancer and ageing: a nexus at several levels. *Nat. Rev. Cancer* **5**: 655–62.

Barker HE, Chang J, Cox TR, Lang G, Bird D, Nicolau M, *et al.* (2011). LOXL2-mediated matrix remodeling in metastasis and mammary gland involution. *Cancer Res.* **71**: 1561–72.

Barker HE, Cox TR, and Erler JT. (2012). The rationale for targeting the LOX family in cancer. *Nat. Rev. Cancer* **12**: 540–52.

Barry-Hamilton V, Spangler R, Marshall D, McCauley S, Rodriguez HM, Oyasu M, *et al.* (2010). Allosteric inhibition of lysyl oxidase-like-2 impedes the development of a pathologic microenvironment. *Nat. Med.* **16**: 1009–17.

Bartholomew JN, Volonte D, and Galbiati F. (2009). Caveolin-1 regulates the antagonistic pleiotropic properties of cellular senescence through a novel Mdm2/p53-mediated pathway. *Cancer Res.* **69**: 2878–86.

Bartkova J, Rezaei N, Liontos M, Karakaidos P, Kletsas D, Issaeva N, *et al.* (2006). Oncogene-induced senescence is part of the tumorigenesis barrier imposed by DNA damage checkpoints. *Nature* **444**: 633–7.

Bartling B. (2013). Cellular senescence in normal and premature lung aging. *Z. Gerontol. Geriatr.* **46**: 613–22.

Basuroy S, Dunagan M, Sheth P, Seth A, and Rao RK. (2010). Hydrogen peroxide activates focal adhesion kinase and c-Src by a phosphatidylinositol 3 kinase-dependent mechanism and promotes cell migration in Caco-2 cell monolayers. *Am. J. Physiol. Gastrointest. Liver Physiol.* **299**: G186–95.

Baughman JM, Perocchi F, Girgis HS, Plovanich M, Belcher-Timme CA, Sancak Y, *et al.* (2011). Integrative genomics identifies MCU as an essential component of the mitochondrial calcium uniporter. *Nature* **476**: 341–5.

Bavik C, Coleman I, Dean JP, Knudsen B, Plymate S, and Nelson PS. (2006). The gene expression program of prostate fibroblast senescence modulates neoplastic epithelial cell proliferation through paracrine mechanisms. *Cancer Res.* **66**: 794–802.

Beauséjour CM, Krtolica A, Galimi F, Narita M, Lowe SW, Yaswen P, *et al.* (2003). Reversal of human cellular senescence: roles of the p53 and p16 pathways. *EMBO J.* **22**: 4212–22.

Benanti JA, and Galloway DA. (2004). Normal human fibroblasts are resistant to RAS-induced senescence. *Mol. Cell. Biol.* **24**: 2842–52.

Benhamed M, Herbig U, Ye T, Dejean A, and Bischof O. (2012). Senescence is an endogenous trigger for microRNA-directed transcriptional gene silencing in human cells. *Nat. Cell Biol.* **14**: 266–75.

Bennecke M, Kriegl L, Bajbouj M, Retzlaff K, Robine S, Jung A, *et al.* (2010). Ink4a/Arf and oncogene-induced senescence prevent tumor progression during alternative colorectal tumorigenesis. *Cancer Cell* **18**: 135–46.

Bernardi P, Scorrano L, Colonna R, Petronilli V, and Di Lisa F. (1999). Mitochondria and cell death. Mechanistic aspects and methodological issues. *Eur. J. Biochem.* **264**: 687–701.

Berridge MJ, Bootman MD, and Roderick HL. (2003). Calcium signalling: dynamics, homeostasis and remodelling. *Nat. Rev. Mol. Cell Biol.* **4**: 517–29.

Berridge MJ. (1993). Inositol trisphosphate and calcium signalling. *Nature* **361**: 315–25.

Bertout J a, Patel S a, and Simon MC. (2008). The impact of O2 availability on human cancer. *Nat. Rev. Cancer* **8**: 967–75.

Bhatia B, Multani AS, Patrawala L, Chen X, Calhoun-Davis T, Zhou J, *et al.* (2008). Evidence that senescent human prostate epithelial cells enhance tumorigenicity: cell fusion as a potential mechanism and inhibition by p16INK4a and hTERT. *Int. J. Cancer* **122**: 1483–95.

Bhaumik D, Scott GK, Schokrpur S, Patil CK, Orjalo A V, Rodier F, *et al.* (2009). MicroRNAs miR-146a/b negatively modulate the senescence-associated inflammatory mediators IL-6 and IL-8. *Aging (Albany. NY).* **1**: 402–11.

Bignon M, Pichol-Thievend C, Hardouin J, Malbouyres M, Bréchot N, Nasciutti L, *et al.* (2011). Lysyl oxidase-like protein-2 regulates sprouting angiogenesis and type IV collagen assembly in the endothelial basement membrane. *Blood* **118**: 3979–89.

Binet R, Ythier D, Robles AI, Collado M, Larrieu D, Fonti C, *et al.* (2009). WNT16B is a new marker of cellular senescence that regulates p53 activity and the phosphoinositide 3-kinase/AKT pathway. *Cancer Res.* **69**: 9183–91.

Bischof O, Kirsh O, Pearson M, Itahana K, Pelicci PG, and Dejean A. (2002). Deconstructing PML-induced premature senescence. *EMBO J.* **21**: 3358–69.

Biswas G, Adebanjo O a, Freedman BD, Anandatheerthavarada HK, Vijayasarathy C, Zaidi M, *et al.* (1999). Retrograde Ca2+ signaling in C2C12 skeletal myocytes in response to mitochondrial genetic and metabolic stress: a novel mode of inter-organelle crosstalk. *EMBO J.* **18**: 522–33.

Blalock WL, Pearce M, Steelman LS, Franklin RA, McCarthy SA, Cherwinski H, *et al.* (2000). A conditionally-active form of MEK1 results in autocrine tranformation of human and mouse hematopoietic cells. *Oncogene* **19**: 526–36.

Blasco M a, Lee HW, Hande MP, Samper E, Lansdorp PM, DePinho R a, *et al.* (1997). Telomere shortening and tumor formation by mouse cells lacking telomerase RNA. *Cell* **91**: 25–34.

Bodnar a. G. (1998). Extension of Life-Span by Introduction of Telomerase into Normal Human Cells. *Science (80-.).* **279**: 349–352.

Bondareva A, Downey CM, Ayres F, Liu W, Boyd SK, Hallgrimsson B, *et al.* (2009). The Lysyl Oxidase Inhibitor, β-Aminopropionitrile, Diminishes the Metastatic Colonization Potential of Circulating Breast Cancer Cells. *PLoS One* **4**: e5620.

Bonneau B, Prudent J, Popgeorgiev N, and Gillet G. (2013). Non-apoptotic roles of Bcl-2 family: the calcium connection. *Biochim. Biophys. Acta* **1833**: 1755–65.

Bootman MD, Petersen OH, and Verkhratsky A. (2002). The endoplasmic reticulum is a focal point for co-ordination of cellular activity. *Cell Calcium* **32**: 231–4.

Braig M, Lee S, Loddenkemper C, Rudolph C, Peters AHFM, Schlegelberger B, *et al.* (2005). Oncogene-induced senescence as an initial barrier in lymphoma development. *Nature* **436**: 660–5.

Brennan FM, Maini RN, and Feldmann M. (1995). Cytokine expression in chronic inflammatory disease. *Br. Med. Bull.* **51**: 368–84.

Brenner a J, Stampfer MR, and Aldaz CM. (1998). Increased p16 expression with first senescence arrest in human mammary epithelial cells and extended growth capacity with p16 inactivation. *Oncogene* **17**: 199–205.

De Brito OM, and Scorrano L. (2008). Mitofusin 2 tethers endoplasmic reticulum to mitochondria. *Nature* **456**: 605–10.

Brod SA. (2000). Unregulated inflammation shortens human functional longevity. *Inflamm. Res.* **49**: 561–70.

Brookes S, Rowe J, Ruas M, Llanos S, Clark PA, Lomax M, *et al.* (2002). INK4a-deficient human diploid fibroblasts are resistant to RAS-induced senescence. *EMBO J.* **21**: 2936–45.

Brown JP. (1997). Bypass of Senescence After Disruption of p21CIP1/WAF1 Gene in Normal Diploid Human Fibroblasts. *Science (80-.).* **277**: 831–834.

Burd CE, Sorrentino JA, Clark KS, Darr DB, Krishnamurthy J, Deal AM, *et al.* (2013). Monitoring tumorigenesis and senescence in vivo with a p16(INK4a)-luciferase model. *Cell* **152**: 340–51.

-C-

Campaner S, Doni M, Hydbring P, Verrecchia A, Bianchi L, Sardella D, *et al.* (2010). Cdk2 suppresses cellular senescence induced by the c-myc oncogene. *Nat. Cell Biol.* **12**: 54–9; sup pp 1–14.

Campisi J, and d'Adda di Fagagna F. (2007). Cellular senescence: when bad things happen to good cells. *Nat. Rev. Mol. Cell Biol.* **8**: 729–40.

Campisi J. (2005). Senescent cells, tumor suppression, and organismal aging: good citizens, bad neighbors. *Cell* **120**: 513–22.

Cao X, Xue L, Han L, Ma L, Chen T, and Tong T. (2011). WW domain-containing E3 ubiquitin protein ligase 1 (WWP1) delays cellular senescence by promoting p27(Kip1) degradation in human diploid fibroblasts. *J. Biol. Chem.* **286**: 33447–56.

Capparelli C, Chiavarina B, Whitaker-menezes D, Pestell TG, Pestell RG, Hulit J, *et al.* (2012). and autophagy in cancer-associated fibroblasts , " fueling " tumor growth via paracrine interactions , without an increase in neo-angiogenesis. : 3599–3610.

Carafoli E. (2003). The calcium-signalling saga: tap water and protein crystals. *Nat. Rev. Mol. Cell Biol.* **4**: 326–32.

Cárdenas C, Miller RA, Smith I, Bui T, Molgó J, Müller M, *et al.* (2010). Essential regulation of cell bioenergetics by constitutive InsP3 receptor Ca2+ transfer to mitochondria. *Cell* **142**: 270–83.

Carrière C, Gore AJ, Norris AM, Gunn JR, Young AL, Longnecker DS, *et al.* (2011). Deletion of Rb Accelerates Pancreatic Carcinogenesis by Oncogenic Kras and Impairs Senescence in Premalignant Lesions. *Gastroenterology* **141**: 1091–101.

Catalano A, Rodilossi S, Caprari P, Coppola V, and Procopio A. (2005). 5-Lipoxygenase regulates senescence-like growth arrest by promoting ROS-dependent p53 activation. *EMBO J.* **24**: 170–9.

Chandra T, and Narita M. (2012). High-order chromatin structure and the epigenome in SAHFs. *Nucleus* **4**: 23–8.

Chang B-D, Swift ME, Shen M, Fang J, Broude E V, and Roninson IB. (2002). Molecular determinants of terminal growth arrest induced in tumor cells by a chemotherapeutic agent. *Proc. Natl. Acad. Sci. U. S. A.* **99**: 389–94.

Chang BD, Xuan Y, Broude E V, Zhu H, Schott B, Fang J, *et al.* (1999). Role of p53 and p21waf1/cip1 in senescence-like terminal proliferation arrest induced in human tumor cells by chemotherapeutic drugs. *Oncogene* **18**: 4808–18.

Chen H, Chomyn A, and Chan DC. (2005).(a). Disruption of fusion results in mitochondrial heterogeneity and dysfunction. *J. Biol. Chem.* **280**: 26185–92.

Chen M, Wang Y, Hou T, Zhang H, Qu A, and Wang X. (2011). Differential mitochondrial calcium responses in different cell types detected with a mitochondrial calcium fluorescent indicator , mito-GCaMP2. *Acta Biochim Biophys Sin* **43**: 822–830.

Chen Q, and Ames BN. (1994). Senescence-like growth arrest induced by hydrogen peroxide in human diploid fibroblast F65 cells. *Proc. Natl. Acad. Sci. U. S. A.* **91**: 4130–4.

Chen R, Valencia I, Zhong F, McColl KS, Roderick HL, Bootman MD, *et al.* (2004). Bcl-2 functionally interacts with inositol 1,4,5-trisphosphate receptors to regulate calcium release from the ER in response to inositol 1,4,5-trisphosphate. *J. Cell Biol.* **166**: 193–203.

Chen Z, Trotman LC, Shaffer D, Lin H-K, Dotan Z a, Niki M, *et al.* (2005).(b). Crucial role of p53-dependent cellular senescence in suppression of Pten-deficient tumorigenesis. *Nature* **436**: 725–30.

Chevet E, Cameron PH, Pelletier MF, Thomas DY, and Bergeron JJM. (2001). The endoplasmic reticulum: integration of protein folding , quality control , signaling and degradation. : 120–124.

Chien Y, Scuoppo C, Wang X, Fang X, Balgley B, Bolden JE, *et al.* (2011). Control of the senescence-associated secretory phenotype by NF-κB promotes senescence and enhances chemosensitivity. *Genes Dev.* **25**: 2125–36.

Chung HY, Cesari M, Anton S, Marzetti E, Giovannini S, Seo AY, *et al.* (2009). Molecular inflammation: underpinnings of aging and age-related diseases. *Ageing Res. Rev.* **8**: 18–30.

Cipriano R, Kan CE, Graham J, Danielpour D, Stampfer M, and Jackson MW. (2011). TGF-beta signaling engages an ATM-CHK2-p53-independent RAS-induced senescence and prevents malignant transformation in human mammary epithelial cells. *Proc. Natl. Acad. Sci. U. S. A.* **108**: 8668–73.

Collado M, Gil J, Efeyan A, Guerra C, Schuhmacher AJ, Barradas M, *et al.* (2005). Tumour biology: senescence in premalignant tumours. *Nature* **436**: 642.

Contente S, Kenyon K, Rimoldi D, and Friedman RM. (1990). Expression of gene rrg is associated with reversion of NIH 3T3 transformed by LTR-c-H-ras. *Science* **249**: 796–8.

Copeland DE, and Dalton AJ. (1959). An association between mitochondria and the endoplasmic reticulum in cells of the pseudobranch gland of a teleost. *J. Biophys. Biochem. Cytol.* **5**: 393–6.

Coppé J-P, Desprez P-Y, Krtolica A, and Campisi J. (2010).(a). The senescence-associated secretory phenotype: the dark side of tumor suppression. *Annu. Rev. Pathol.* **5**: 99–118.

Coppé J-P, Kauser K, Campisi J, and Beauséjour CM. (2006). Secretion of vascular endothelial growth factor by primary human fibroblasts at senescence. *J. Biol. Chem.* **281**: 29568–74.

Coppé J-P, Patil CK, Rodier F, Krtolica A, Beauséjour CM, Parrinello S, *et al.* (2010).(b). A human-like senescence-associated secretory phenotype is conserved in mouse cells dependent on physiological oxygen. *PLoS One* **5**: e9188.

Coppé J-P, Patil CK, Rodier F, Sun Y, Muñoz DP, Goldstein J, *et al.* (2008). Senescence-associated secretory phenotypes reveal cell-nonautonomous functions of oncogenic RAS and the p53 tumor suppressor. *PLoS Biol.* **6**: 2853–68.

Cosme-Blanco W, Shen M-F, Lazar AJF, Pathak S, Lozano G, Multani AS, *et al.* (2007). Telomere dysfunction suppresses spontaneous tumorigenesis in vivo by initiating p53-dependent cellular senescence. *EMBO Rep.* **8**: 497–503.

Courtois-Cox S, Williams SMG, Reczek EE, Johnson BW, McGillicuddy LT, Johannessen CM, *et al.* (2006). A negative feedback signaling network underlies oncogene-induced senescence. *Cancer Cell* **10**: 459–72.

Crescenzi E, Palumbo G, and Brady HJM. (2003). Bcl-2 activates a programme of premature senescence in human carcinoma cells. *Biochem. J.* **375**: 263–74.

Csordás G, Golenár T, Seifert ELL, Kamer KJJ, Sancak Y, Perocchi F, *et al.* (2013). MICU1 Controls Both the Threshold and Cooperative Activation of the Mitochondrial Ca2+ Uniporter. *Cell Metab.* **17**: 976–987.

Csordás G, and Hajnóczky G. (2001). Sorting of calcium signals at the junctions of endoplasmic reticulum and mitochondria. *Cell Calcium* **29**: 249–62.

Csordás G, Renken C, Várnai P, Walter L, Weaver D, Buttle KF, *et al.* (2006). Structural and functional features and significance of the physical linkage between ER and mitochondria. *J. Cell Biol.* **174**: 915–21.

Csordás G, Thomas a P, and Hajnóczky G. (1999). Quasi-synaptic calcium signal transmission between endoplasmic reticulum and mitochondria. *EMBO J.* **18**: 96–108.

Cuevas EP, Moreno-Bueno G, Canesin G, Santos V, Portillo F, and Cano A. (2014). LOXL2 catalytically inactive mutants mediate epithelial-to-mesenchymal transition. *Biol. Open*.

Curry MC, Peters A a, Kenny P a, Roberts-Thomson SJ, and Monteith GR. (2013). Mitochondrial calcium uniporter silencing potentiates caspase-independent cell death in MDA-MB-231 breast cancer cells. *Biochem. Biophys. Res. Commun.* **434**: 695–700.

-D-

d'Adda di Fagagna F, Reaper PM, Clay-Farrace L, Fiegler H, Carr P, Von Zglinicki T, *et al.* (2003). A DNA damage checkpoint response in telomere-initiated senescence. *Nature* **426**: 194–8.

Dai CY, and Enders GH. (2000). p16 INK4a can initiate an autonomous senescence program. *Oncogene* **19**: 1613–22.

Dankort D, Filenova E, Collado M, Serrano M, Jones K, and McMahon M. (2007). A new mouse model to explore the initiation, progression, and therapy of BRAFV600E-induced lung tumors. *Genes Dev.* **21**: 379–84.

Dannenberg J-H. (2000). Ablation of the Retinoblastoma gene family deregulates G1 control causing immortalization and increased cell turnover under growth-restricting conditions. *Genes Dev.* **14**: 3051–3064.

Davalos AR, Coppe J-P, Campisi J, and Desprez P-Y. (2010). Senescent cells as a source of inflammatory factors for tumor progression. *Cancer Metastasis Rev.* **29**: 273–83.

Decuypere J-P, Bultynck G, and Parys JB. (2011).(a). A dual role for Ca(2+) in autophagy regulation. *Cell Calcium* **50**: 242–50.

Decuypere J-P, Monaco G, Bultynck G, Missiaen L, De Smedt H, and Parys JB. (2011).(b). The IP(3) receptor-mitochondria connection in apoptosis and autophagy. *Biochim. Biophys. Acta* **1813**: 1003–13.

Delmore JE, Issa GC, Lemieux ME, Rahl PB, Shi J, Jacobs HM, *et al.* (2011). BET bromodomain inhibition as a therapeutic strategy to target c-Myc. *Cell* **146**: 904–17.

Demidenko ZN, Korotchkina LG, Gudkov A V, and Blagosklonny M V. (2010). Paradoxical suppression of cellular senescence by p53. *Proc. Natl. Acad. Sci. U. S. A.* **107**: 9660–4.

Denchi EL, Attwooll C, Pasini D, and Helin K. (2005). Deregulated E2F Activity Induces Hyperplasia and Senescence-Like Features in the Mouse Pituitary Gland Deregulated E2F Activity Induces Hyperplasia and Senescence-Like Features in the Mouse Pituitary Gland †.

Deng Y, Chan SS, and Chang S. (2008). Telomere dysfunction and tumour suppression: the senescence connection. *Nat. Rev. Cancer* **8**: 450–8.

Denoyelle C, Abou-Rjaily G, Bezrookove V, Verhaegen M, Johnson TM, Fullen DR, *et al.* (2006). Anti-oncogenic role of the endoplasmic reticulum differentially activated by mutations in the MAPK pathway. *Nat. Cell Biol.* **8**: 1053–63.

Deschênes-Simard X, Gaumont-Leclerc M-F, Bourdeau V, Lessard F, Moiseeva O, Forest V, *et al.* (2013). Tumor suppressor activity of the ERK/MAPK pathway by promoting selective protein degradation. *Genes Dev.* **27**: 900–15.

Van Deursen JM. (2014). The role of senescent cells in ageing. *Nature* **509**: 439–46.

Dhomen N, Reis-filho JS, da Rocha Dias S, Hayward R, Savage K, Delmas V, *et al.* (2009). Oncogenic Braf induces melanocyte senescence and melanoma in mice. *Cancer Cell* **15**: 294–303.

Dimri GP, Itahana K, Acosta M, and Campisi J. (2000). Regulation of a Senescence Checkpoint Response by the E2F1 Transcription Factor and p14 ARF Tumor Suppressor Regulation of a Senescence Checkpoint Response by the E2F1 Transcription Factor and p14 ARF Tumor Suppressor.

Dimri GP, Lee X, Basile G, Acosta M, Scott G, Roskelley C, *et al.* (1995). A biomarker that identifies senescent human cells in culture and in aging skin in vivo. *Proc. Natl. Acad. Sci. U. S. A.* **92**: 9363–7.

Dirac AMG, and Bernards R. (2003). Reversal of senescence in mouse fibroblasts through lentiviral suppression of p53. *J. Biol. Chem.* **278**: 11731–4.

Drayton S, Rowe J, Jones R, Vatcheva R, Cuthbert-heavens D, Marshall J, *et al.* (2003). Tumor suppressor p16 INK4a determines sensitivity of human cells to transformation by cooperating cellular oncogenes. **4**: 301–310.

Duchen MR. (1999). Topical Review Contributions of mitochondria to animal physiology: from homeostatic sensor to calcium signalling and cell death. : 1–17.

Dumont P, Burton M, Chen QM, Gonos ES, Frippiat C, Mazarati JB, *et al.* (2000). Induction of replicative senescence biomarkers by sublethal oxidative stresses in normal human fibroblast. *Free Radic. Biol. Med.* **28**: 361–73.

-E-

Efeyan A, Murga M, Martinez-Pastor B, Ortega-Molina A, Soria R, Collado M, *et al.* (2009). Limited role of murine ATM in oncogene-induced senescence and p53-dependent tumor suppression. *PLoS One* **4**: e5475.

Erler JT, Bennewith KL, Cox TR, Lang G, Bird D, Koong A, *et al.* (2009). Hypoxia-induced lysyl oxidase is a critical mediator of bone marrow cell recruitment to form the premetastatic niche. *Cancer Cell* **15**: 35–44.

Erler JT, Bennewith KL, Nicolau M, Dornhöfer N, Kong C, Le Q-T, *et al.* (2006). Lysyl oxidase is essential for hypoxia-induced metastasis. *Nature* **440**: 1222–6.

Erler JT, and Weaver VM. (2009). Three-dimensional context regulation of metastasis. *Clin. Exp. Metastasis* **26**: 35–49.

-F-

Favaro E, Bensaad K, Chong MG, Tennant D a, Ferguson DJP, Snell C, *et al.* (2012). Glucose utilization via glycogen phosphorylase sustains proliferation and prevents premature senescence in cancer cells. *Cell Metab.* **16**: 751–64.

Feig C, Gopinathan A, Neesse A, Chan DS, Cook N, and Tuveson DA. (2012). The pancreas cancer microenvironment. *Clin. Cancer Res.* **18**: 4266–76.

Feldser DM, and Greider CW. (2007). Short telomeres limit tumor progression in vivo by inducing senescence. *Cancer Cell* **11**: 461–9.

Felsher DW, and Bishop JM. (1999). Reversible Tumorigenesis by MYC in Hematopoietic Lineages. *Mol. Cell* **4**: 199–207.

Ferbeyre G, de Stanchina E, Querido E, Baptiste N, Prives C, and Lowe SW. (2000). PML is induced by oncogenic ras and promotes premature senescence. *Genes Dev.* **14**: 2015–27.

Ferbeyre G. (2007). Barriers to Ras transformation. *Nat. Cell Biol.* **9**: 483–5.

Fieni F, Lee SB, Jan YN, and Kirichok Y. (2012). Activity of the mitochondrial calcium uniporter varies greatly between tissues. *Nat. Commun.* **3**: 1317.

Firestein R, Bass AJ, Kim SY, Dunn IF, Silver SJ, Guney I, *et al.* (2008). CDK8 is a colorectal cancer oncogene that regulates beta-catenin activity. *Nature* **455**: 547–51.

Fletcher JI, Haber M, Henderson MJ, and Norris MD. (2010). ABC transporters in cancer: more than just drug efflux pumps. *Nat. Rev. Cancer* **10**: 147–56.

Foster SA, Wong DJ, Barrett MT, and Galloway DA. (1998). Inactivation of p16 in human mammary epithelial cells by CpG island methylation. *Mol. Cell. Biol.* **18**: 1793–801.

Foyouzi-Youssefi R, Arnaudeau S, Borner C, Kelley WL, Tschopp J, Lew DP, *et al.* (2000). Bcl-2 decreases the free Ca2+ concentration within the endoplasmic reticulum. *Proc. Natl. Acad. Sci. U. S. A.* **97**: 5723–8.

Franceschi C. (2007). Inflammaging as a major characteristic of old people: can it be prevented or cured? *Nutr. Rev.* **65**: S173–6.

Freund A, Laberge R-M, Demaria M, and Campisi J. (2012). Lamin B1 loss is a senescence-associated biomarker. *Mol. Biol. Cell* **23**: 2066–75.

Friedman JR, Lackner LL, West M, DiBenedetto JR, Nunnari J, and Voeltz GK. (2011). ER tubules mark sites of mitochondrial division. *Science* **334**: 358–62.

Fujita K, Mondal AM, Horikawa I, Nguyen GH, Kumamoto K, Sohn JJ, *et al.* (2009). p53 isoforms Delta133p53 and p53beta are endogenous regulators of replicative cellular senescence. *Nat. Cell Biol.* **11**: 1135–42.

Fumagalli M, Rossiello F, Clerici M, Barozzi S, Cittaro D, Kaplunov JM, *et al.* (2012). Telomeric DNA damage is irreparable and causes persistent DNA-damage-response activation. *Nat. Cell Biol.* **14**: 355–65.

Furumoto K, Inoue E, Nagao N, Hiyama E, and Miwa N. (1998). Age-dependent telomere shortening is slowed down by enrichment of intracellular vitamin C via suppression of oxidative stress. *Life Sci.* **63**: 935–48.

-G-

Gamerdinger M, Hajieva P, Kaya AM, Wolfrum U, Hartl FU, and Behl C. (2009). Protein quality control during aging involves recruitment of the macroautophagy pathway by BAG3. *EMBO J.* **28**: 889–901.

Gansauge S, Gansauge F, Gause H, Poch B, Schoenberg MH, and Beger HG. (1997). The induction of apoptosis in proliferating human fibroblasts by oxygen radicals is associated with a p53- and p21WAF1CIP1 induction. *FEBS Lett.* **404**: 6–10.

Gazin C, Wajapeyee N, Gobeil S, Virbasius C-M, and Green MR. (2007). An elaborate pathway required for Ras-mediated epigenetic silencing. *Nature* **449**: 1073–7.

Georgakopoulou E a, Tsimaratou K, Evangelou K, Fernandez Marcos PJ, Zoumpourlis V, Trougakos IP, *et al.* (2013). Specific lipofuscin staining as a novel biomarker to detect replicative and stress-induced senescence. A method applicable in cryo-preserved and archival tissues. *Aging (Albany. NY).* **5**: 37–50.

Gerland L-M, Peyrol S, Lallemand C, Branche R, Magaud J-P, and Ffrench M. (2003). Association of increased autophagic inclusions labeled for β-galactosidase with fibroblastic aging. *Exp. Gerontol.* **38**: 887–895.

Gewirtz D a, Holt SE, and Elmore LW. (2008). Accelerated senescence: an emerging role in tumor cell response to chemotherapy and radiation. *Biochem. Pharmacol.* **76**: 947–57.

Giampuzzi M, Oleggini R, and Di Donato A. (2003). Demonstration of in vitro interaction between tumor suppressor lysyl oxidase and histones H1 and H2: definition of the regions involved. *Biochim. Biophys. Acta - Proteins Proteomics* **1647**: 245–251.

Gil J, Bernard D, Martínez D, and Beach D. (2004). Polycomb CBX7 has a unifying role in cellular lifespan. *Nat. Cell Biol.* **6**.

Gil J, and Peters G. (2006). Regulation of the INK4b-ARF-INK4a tumour suppressor locus: all for one or one for all. *Nat. Rev. Mol. Cell Biol.* **7**: 667–77.

Ginos MA. (2004). Identification of a Gene Expression Signature Associated with Recurrent Disease in Squamous Cell Carcinoma of the Head and Neck. *Cancer Res.* **64**: 55–63.

Giorgi C, Ito K, Lin H-K, Santangelo C, Wieckowski MR, Lebiedzinska M, *et al.* (2010). PML regulates apoptosis at endoplasmic reticulum by modulating calcium release. *Science* **330**: 1247–51.

Giorgi C, De Stefani D, Bononi A, Rizzuto R, and Pinton P. (2009). Structural and functional link between the mitochondrial network and the endoplasmic reticulum. *Int. J. Biochem. Cell Biol.* **41**: 1817–27.

Gire V, Roux P, Wynford-Thomas D, Brondello J-M, and Dulic V. (2004). DNA damage checkpoint kinase Chk2 triggers replicative senescence. *EMBO J.* **23**: 2554–63.

Gitenay D, Wiel C, Lallet-Daher H, Vindrieux D, Aubert S, Payen L, *et al.* (2014). Glucose metabolism and hexosamine pathway regulate oncogene-induced senescence. *Cell Death Dis.* **5**: e1089.

Gomes LC, Benedetto G Di, Scorrano L, and Di Benedetto G. (2011). During autophagy mitochondria elongate, are spared from degradation and sustain cell viability. *Nat. Cell Biol.* **13**: 589–98.

Gorgoulis VG, and Halazonetis TD. (2010). Oncogene-induced senescence: the bright and dark side of the response. *Curr. Opin. Cell Biol.* **22**: 816–27.

Gorospe M, and Abdelmohsen K. (2011). MicroRegulators come of age in senescence. *Trends Genet.* **27**: 233–41.

Gosselin K, Deruy E, Martien S, Vercamer C, Bouali F, Dujardin T, *et al.* (2009). Senescent Keratinocytes Die by Autophagic Programmed Cell Death. *Am. J. Pathol.* **174**: 423–35.

Greider C, Chattopadhyay A, Parkhurst C, and Yang E. (2002). BCL-x(L) and BCL2 delay Myc-induced cell cycle entry through elevation of p27 and inhibition of G1 cyclin-dependent kinases. *Oncogene* **21**: 7765–75.

Grynkiewicz G, Poenie M, and Tsien RY. (1985). A new generation of Ca2+ indicators with greatly improved fluorescence properties. *J. Biol. Chem.* **260**: 3440–50.

Guerra C, Mijimolle N, Dhawahir A, Dubus P, Barradas M, Serrano M, *et al.* (2003). Tumor induction by an endogenous K-ras oncogene is highly dependent on cellular context. *Cancer Cell* **4**: 111–20.

Gunter TE, Buntinas L, Sparagna G, Eliseev R, and Gunter K. (2000). Mitochondrial calcium transport: mechanisms and functions. *Cell Calcium* **28**: 285–96.

-H-

Ha L, Ichikawa T, Anver M, Dickins R, Lowe S, Sharpless NE, *et al.* (2007). ARF functions as a melanoma tumor suppressor by inducing p53-independent senescence. *Proc. Natl. Acad. Sci. U. S. A.* **104**: 10968–73.

Haferkamp S, Scurr LL, Becker TM, Frausto M, Kefford RF, and Rizos H. (2009).(a). Oncogene-induced senescence does not require the p16(INK4a) or p14ARF melanoma tumor suppressors. *J. Invest. Dermatol.* **129**: 1983–91.

Haferkamp S, Tran SL, Becker TM, Scurr LL, Kefford RF, and Rizos H. (2009).(b). The relative contributions of the p53 and pRb pathways in oncogene-induced melanocyte senescence. *Aging (Albany. NY).* **1**: 542–56.

Hahn WC, Stewart SA, Brooks MW, York SG, Eaton E, Kurachi A, *et al.* (1999). Inhibition of telomerase limits the growth of human cancer cells. *Nat. Med.* **5**: 1164–70.

Hajnóczky G, Csordás G, Das S, Garcia-Perez C, Saotome M, Sinha Roy S, *et al.* (2006). Mitochondrial calcium signalling and cell death: approaches for assessing the role of mitochondrial Ca2+ uptake in apoptosis. *Cell Calcium* **40**: 553–60.

Hämäläinen ER, Kemppainen R, Kuivaniemi H, Tromp G, Vaheri A, Pihlajaniemi T, *et al.* (1995). Quantitative polymerase chain reaction of lysyl oxidase mRNA in malignantly transformed human cell lines demonstrates that their low lysyl oxidase activity is due to low quantities of its mRNA and low levels of transcription of the respective gene. *J. Biol. Chem.* **270**: 21590–3.

Hardie DG. (2007). AMP-activated/SNF1 protein kinases: conserved guardians of cellular energy. *Nat. Rev. Mol. Cell Biol.* **8**: 774–85.

Harper JW, Adami GR, Wei N, Keyomarsi K, and Elledge SJ. (1993). The p21 Cdk-interacting protein Cip1 is a potent inhibitor of G1 cyclin-dependent kinases. *Cell* **75**: 805–16.

Harr MW, and Distelhorst CW. (2010). Apoptosis and autophagy: decoding calcium signals that mediate life or death. *Cold Spring Harb. Perspect. Biol.* **2**: a005579.

Harris AL. (2002). Hypoxia--a key regulatory factor in tumour growth. *Nat. Rev. Cancer* **2**: 38–47.

Haupt Y, Maya R, Kazaz A, and Oren M. (1997). Mdm2 promotes the rapid degradation of p53. *Nature* **387**: 296–9.

Hayflick L, and Moorhead PS. (1961). The serial cultivation of human diploid cell strains. *Exp. Cell Res.* **25**: 585–621.

Hemann MT, Strong MA, Hao LY, and Greider CW. (2001). The shortest telomere, not average telomere length, is critical for cell viability and chromosome stability. *Cell* **107**: 67–77.

Herbig U, Jobling WA, Chen BPC, Chen DJ, and Sedivy JM. (2004). Telomere shortening triggers senescence of human cells through a pathway involving ATM, p53, and p21(CIP1), but not p16(INK4a). *Mol. Cell* **14**: 501–13.

Hermeking H. (2010). The miR-34 family in cancer and apoptosis. *Cell Death Differ.* **17**: 193–9.

Herranz N, Dave N, Millanes-Romero A, Morey L, Díaz VM, Lórenz-Fonfría V, *et al.* (2012). Lysyl Oxidase-like 2 Deaminates Lysine 4 in Histone H3. *Mol. Cell* **4**: 1–8.

Hiraoka N, Ino Y, Sekine S, Tsuda H, Shimada K, Kosuge T, *et al.* (2010). Tumour necrosis is a postoperative prognostic marker for pancreatic cancer patients with a high interobserver reproducibility in histological evaluation. *Br. J. Cancer* **103**: 1057–65.

Hirata H, Lopes GS, Jurkiewicz A, Garcez-do-Carmo L, and Smaili SSb-2 modulates endoplasmic reticulum and mitochondrial calcium stores in P cells. (2012). Bcl-2 modulates endoplasmic reticulum and mitochondrial calcium stores in PC12 cells. *Neurochem. Res.* **37**: 238–43.

Hoare M, Young ARJ, and Narita M. (2011). Autophagy in cancer: having your cake and eating it. *Semin. Cancer Biol.* **21**: 397–404.

Holst CR, Nuovo GJ, Esteller M, Chew K, Baylin SB, Herman JG, *et al.* (2003). Methylation of p16INK4a Promoters Occurs in Vivo in Histologically Normal Human Mammary Epithelia. *Cancer Res.* **63**: 1596–601.

Hoshino A, Mita Y, Okawa Y, Ariyoshi M, Iwai-Kanai E, Ueyama T, *et al.* (2013). Cytosolic p53 inhibits Parkin-mediated mitophagy and promotes mitochondrial dysfunction in the mouse heart. *Nat. Commun.* **4**: 2308.

Humbert N, Martien S, Augert A, Da Costa M, Mauen S, Abbadie C, *et al.* (2009). A Genetic Screen Identifies Topoisomerase 1 as a Regulator of Senescence. *Cancer Res.* **69**: 4101–4106.

Humbert N, Navaratnam N, Augert A, Da Costa M, Martien S, Wang J, *et al.* (2010). Regulation of ploidy and senescence by the AMPK-related kinase NUAK1. *EMBO J.* **29**: 376–86.

Huschtscha LI, Noble JR, Neumann AA, Moy EL, Barry P, Melki JR, *et al.* (1998). Loss of p16INK4 expression by methylation is associated with lifespan extension of human mammary epithelial cells. *Cancer Res.* **58**: 3508–12.

-I-

Iguchi M, Kato M, Nakai J, Takeda T, Matsumoto-Ida M, Kita T, *et al.* (2012). Direct monitoring of mitochondrial calcium levels in cultured cardiac myocytes using a novel fluorescent indicator protein, GCaMP2-mt. *Int. J. Cardiol.* **158**: 225–34.

Itahana K, Zou Y, Itahana Y, Martinez J, Beausejour C, Jacobs JJL, *et al.* (2003). Control of the Replicative Life Span of Human Fibroblasts by p16 and the Polycomb Protein Bmi-1. *Mol. Cell. Biol.* **23**: 389–401.

Ivanov A, Pawlikowski J, Manoharan I, van Tuyn J, Nelson DM, Rai TS, *et al.* (2013). Lysosome-mediated processing of chromatin in senescence. *J. Cell Biol.* **202**: 129–43.

Iwanaga K, Yang Y, Raso MG, Ma L, Hanna AE, Thilaganathan N, *et al.* (2008). Pten inactivation accelerates oncogenic K-ras-initiated tumorigenesis in a mouse model of lung cancer. *Cancer Res.* **68**: 1119–27.

Iwasa H, Han J, and Ishikawa F. (2003). Mitogen-activated protein kinase p38 defines the common senescence-signalling pathway. *Genes Cells* **8**: 131–44.

-J-

Jacobs JJ, Kieboom K, Marino S, DePinho R a, and van Lohuizen M. (1999). The oncogene and Polycomb-group gene bmi-1 regulates cell proliferation and senescence through the ink4a locus. *Nature* **397**: 164–8.

Jain M, Arvanitis C, Chu K, Dewey W, Leonhardt E, Trinh M, *et al.* (2002). Sustained loss of a neoplastic phenotype by brief inactivation of MYC. *Science* **297**: 102–4.

Jeanblanc M, Ragu S, Gey C, Contrepois K, Courbeyrette R, Thuret J-Y, *et al.* (2012). Parallel pathways in RAF-induced senescence and conditions for its reversion. *Oncogene* **31**: 3072–85.

Jiang P, Du W, Mancuso A, Wellen KE, and Yang X. (2013). Reciprocal regulation of p53 and malic enzymes modulates metabolism and senescence. *Nature* **493**: 689–93.

Jing H, Kase J, Dörr JR, Milanovic M, Lenze D, Grau M, *et al.* (2011). Opposing roles of NF-κB in anti-cancer treatment outcome unveiled by cross-species investigations. *Genes Dev.* **25**: 2137–46.

Jun J-I, and Lau LF. (2010). The matricellular protein CCN1 induces fibroblast senescence and restricts fibrosis in cutaneous wound healing. *Nat. Cell Biol.* **12**: 676–85.

-K-

Kagan HM, Williams MA, Calaman SD, and Berkowitz EM. (1983). Histone H1 is a substrate for lysyl oxidase and contains endogenous sodium borotritide-reducible residues. *Biochem. Biophys. Res. Commun.* **115**: 186–92.

Kamijo T, Weber JD, Zambetti G, Zindy F, Roussel MF, and Sherr CJ. (1998). Functional and physical interactions of the ARF tumor suppressor with p53 and Mdm2. *Proc. Natl. Acad. Sci. U. S. A.* **95**: 8292–7.

Kamijo T, Zindy F, Roussel MF, Quelle DE, Downing JR, Ashmun RA, *et al.* (1997). Tumor suppression at the mouse INK4a locus mediated by the alternative reading frame product p19ARF. *Cell* **91**: 649–59.

Kaneda A, Wakazono K, Tsukamoto T, Watanabe N, Yagi Y, Tatematsu M, *et al.* (2004). Lysyl oxidase is a tumor suppressor gene inactivated by methylation and loss of heterozygosity in human gastric cancers. *Cancer Res.* **64**: 6410–5.

Kang MK, Kameta A, Shin K-H, Baluda MA, Kim H-R, and Park N-H. (2003). Senescence-associated genes in normal human oral keratinocytes. *Exp. Cell Res.* **287**: 272–81.

Kang T-W, Yevsa T, Woller N, Hoenicke L, Wuestefeld T, Dauch D, *et al.* (2011). Senescence surveillance of pre-malignant hepatocytes limits liver cancer development. *Nature* **479**: 547–51.

Kaplon J, Zheng L, Meissl K, Chaneton B, Selivanov VA, Mackay G, *et al.* (2013). A key role for mitochondrial gatekeeper pyruvate dehydrogenase in oncogene-induced senescence. *Nature* **498**: 109–12.

Kennedy AL, Morton JP, Manoharan I, Nelson DM, Jamieson NB, Pawlikowski JS, *et al.* (2011). Activation of the PIK3CA/AKT pathway suppresses senescence induced by an activated RAS oncogene to promote tumorigenesis. *Mol. Cell* **42**: 36–49.

Kenyon K, Contente S, Trackman PC, Tang J, Kagan HM, and Friedman RM. (1991). Lysyl oxidase and rrg messenger RNA. *Science* **253**: 802.

Kim J-S, Lee C, Bonifant CL, Ressom H, and Waldman T. (2007). Activation of p53-dependent growth suppression in human cells by mutations in PTEN or PIK3CA. *Mol. Cell. Biol.* **27**: 662–77.

Kimmelman AC. (2011). The dynamic nature of autophagy in cancer. *Genes Dev.* **25**: 1999–2010.

Kipling D, and Cooke, HJ. (1990). Hypervariable ultra-long telomeres in mice. *Nature* **347**.

Kirichok Y, Krapivinsky G, and Clapham DE. (2004). The mitochondrial calcium uniporter is a highly selective ion channel. *Nature* **427**: 360–4.

Kirkwood TBL, and Austad SN. (2000). Why do we age? **408**: 233–238.

Kirschmann D a, Seftor E a, Fong SFT, Nieva DRC, Sullivan CM, Edwards EM, *et al.* (2002). A molecular role for lysyl oxidase in breast cancer invasion. *Cancer Res.* **62**: 4478–83.

Kirschmann DA, Seftor EA, Nieva DR, Mariano EA, and Hendrix MJ. (1999). Differentially expressed genes associated with the metastatic phenotype in breast cancer. *Breast Cancer Res. Treat.* **55**: 127–36.

Kitada T, Seki S, Sakaguchi H, Sawada T, Hirakawa K, and Wakasa K. (2003). Clinicopathological significance of hypoxia-inducible factor-1alpha expression in human pancreatic carcinoma. *Histopathology* **43**: 550–5.

Koong AC, Mehta VK, Le QT, Fisher GA, Terris DJ, Brown JM, *et al.* (2000). Pancreatic tumors show high levels of hypoxia. *Int. J. Radiat. Oncol. Biol. Phys.* **48**: 919–22.

Korobova F, Ramabhadran V, and Higgs HN. (2013). An actin-dependent step in mitochondrial fission mediated by the ER-associated formin INF2. *Science* **339**: 464–7.

Korotchkina LG, Leontieva O V, Bukreeva EI, Demidenko ZN, Gudkov A V, and Blagosklonny M V. (2010). The choice between p53-induced senescence and quiescence is determined in part by the mTOR pathway. *Aging (Albany. NY).* **2**: 344–52.

Kortlever RM, Higgins PJ, and Bernards R. (2006). Plasminogen activator inhibitor-1 is a critical downstream target of p53 in the induction of replicative senescence. *Nat. Cell Biol.* **8**: 877–84.

Kosar M, Bartkova J, Hubackova S, Hodny Z, Lukas J, and Bartek J. (2011). Senescence-associated heterochromatin foci are dispensable for cellular senescence, occur in a cell type- and insult-dependent manner and follow expression of p16 ink4a. *Cell Cycle* **10**: 457–468.

Kotlikoff MI. (2007). Genetically encoded Ca2+ indicators: using genetics and molecular design to understand complex physiology. *J. Physiol.* **578**: 55–67.

Krishnamurthy J, Torrice C, Ramsey MR, Kovalev GI, Al-regaiey K, Su L, *et al.* (2004). Ink4a/Arf expression is a biomarker of aging. *J. Clin. Invest.* **114**: 1299–307.

Krizhanovsky V, Yon M, Dickins R a, Hearn S, Simon J, Miething C, *et al.* (2008). Senescence of activated stellate cells limits liver fibrosis. *Cell* **134**: 657–67.

Krtolica A, Parrinello S, Lockett S, Desprez PY, and Campisi J. (2001). Senescent fibroblasts promote epithelial cell growth and tumorigenesis: a link between cancer and aging. *Proc. Natl. Acad. Sci. U. S. A.* **98**: 12072–7.

Ksiazek K, Jörres A, and Witowski J. (2008). Senescence induces a proangiogenic switch in human peritoneal mesothelial cells. *Rejuvenation Res.* **11**: 681–3.

Kuilman T, Michaloglou C, Vredeveld LCW, Douma S, van Doorn R, Desmet CJ, *et al.* (2008). Oncogene-induced senescence relayed by an interleukin-dependent inflammatory network. *Cell* **133**: 1019–31.

Kurz DJ, Decary S, Hong Y, and Erusalimsky JD. (2000). Senescence-associated (beta)-galactosidase reflects an increase in lysosomal mass during replicative ageing of human endothelial cells. *J. Cell Sci.* **113 (Pt 2**: 3613–22.

-L-

De la Fuente S, Matesanz-Isabel J, Fonteriz RI, Montero M, and Alvarez J. (2014). Dynamics of mitochondrial Ca2+ uptake in MICU1-knockdown cells. *Biochem. J.* **458**: 33–40.

Laberge R-M, Awad P, Campisi J, and Desprez P-Y. (2011). Epithelial-Mesenchymal Transition Induced by Senescent Fibroblasts. *Cancer Microenviron.* **5**: 39–44.

Lallet-Daher H, Wiel C, Gitenay D, Navaratnam N, Augert A, Le Calvé B, *et al.* (2013). Potassium Channel KCNA1 Modulates Oncogene-Induced Senescence and Transformation. *Cancer Res.* **73**: 5253–5265.

Lapointe J, Li C, Higgins JP, van de Rijn M, Bair E, Montgomery K, *et al.* (2004). Gene expression profiling identifies clinically relevant subtypes of prostate cancer. *Proc. Natl. Acad. Sci. U. S. A.* **101**: 811–6.

Lazzerini Denchi E, Attwooll C, Pasini D, Helin K, and Denchi EL. (2005). Deregulated E2F activity induces hyperplasia and senescence-like features in the mouse pituitary gland. *Mol. Cell. Biol.* **25**: 2660–72.

Lee AC, Fenster BE, Ito H, Takeda K, Bae NS, Hirai T, *et al.* (1999). Ras proteins induce senescence by altering the intracellular levels of reactive oxygen species. *J. Biol. Chem.* **274**: 7936–40.

Lee BY, Han J a, Im JS, Morrone A, Johung K, Goodwin EC, *et al.* (2006).(a). Senescence-associated beta-galactosidase is lysosomal beta-galactosidase. *Aging Cell* **5**: 187–95.

Lee H-C, Yin P-H, Chi C-W, and Wei Y-H. (2002). Increase in mitochondrial mass in human fibroblasts under oxidative stress and during replicative cell senescence. *J. Biomed. Sci.* **9**: 517–26.

Lee KE, and Bar-Sagi D. (2010). Oncogenic KRas Suppresses Inflammation-Associated Senescence of Pancreatic Ductal Cells. *Cancer Cell* **18**: 448–58.

Lee MY, Song H, Nakai J, Ohkura M, Kotlikoff MI, Kinsey SP, *et al.* (2006).(b). Local subplasma membrane Ca2+ signals detected by a tethered Ca2+ sensor. *Proc. Natl. Acad. Sci. U. S. A.* **103**: 13232–7.

Lee S, Jeong S-Y, Lim W-C, Kim S, Park Y-Y, Sun X, *et al.* (2007). Mitochondrial fission and fusion mediators, hFis1 and OPA1, modulate cellular senescence. *J. Biol. Chem.* **282**: 22977–83.

Legros F, Lombe A, Frachon P, and Rojo M. (2002). Mitochondrial Fusion in Human Cells Is Efficient , Requires the Inner Membrane Potential , and Is Mediated by Mitofusins □. *Mol. Biol. Cell* **13**: 4343–4354.

Lelièvre E, Hinek A, Lupu F, Buquet C, Soncin F, and Mattot V. (2008). VE-statin/egfl7 regulates vascular elastogenesis by interacting with lysyl oxidases. *EMBO J.* **27**: 1658–70.

Di Leonardo a, Linke SP, Clarkin K, and Wahl GM. (1994). DNA damage triggers a prolonged p53-dependent G1 arrest and long-term induction of Cip1 in normal human fibroblasts. *Genes Dev.* **8**: 2540–2551.

Levental KR, Yu H, Kass L, Lakins JN, Egeblad M, Erler JT, *et al.* (2009). Matrix crosslinking forces tumor progression by enhancing integrin signaling. *Cell* **139**: 891–906.

Levine AJ. (1997). P53, the Cellular Gatekeeper for Growth and Division. *Cell* **88**: 323–31.

Lewis JA, and Tata JR. (1973). A rapidly sedimenting fraction of rat liver endoplasmic reticulum. *J. Cell Sci.* **13**: 447–59.

Li G, Luna C, Qiu J, Epstein DL, and Gonzalez P. (2010). Modulation of inflammatory markers by miR-146a during replicative senescence in trabecular meshwork cells. *Invest. Ophthalmol. Vis. Sci.* **51**: 2976–85.

Lin a. W, Barradas M, Stone JC, van Aelst L, Serrano M, and Lowe SW. (1998). Premature senescence involving p53 and p16 is activated in response to constitutive MEK/MAPK mitogenic signaling. *Genes Dev.* **12**: 3008–19.

Lin H-K, Chen Z, Wang G, Nardella C, Lee S-W, Chan C-HC-HC-HC-H, *et al.* (2010). Skp2 targeting suppresses tumorigenesis by Arf-p53-independent cellular senescence. *Nature* **464**: 374–9.

Linette GP, Li Y, Roth K, and Korsmeyer SJ. (1996). Cross talk between cell death and cell cycle progression: BCL-2 regulates NFAT-mediated activation. *Proc. Natl. Acad. Sci. U. S. A.* **93**: 9545–52.

Liu D, and Hornsby PJ. (2007). Senescent human fibroblasts increase the early growth of xenograft tumors via matrix metalloproteinase secretion. *Cancer Res.* **67**: 3117–26.

Liu H, Fergusson MM, Castilho RM, Liu J, Cao L, Chen J, *et al.* (2007). Augmented Wnt signaling in a mammalian model of accelerated aging. *Science* **317**: 803–6.

Liu Q-H, Zheng Y-M, Korde AS, Yadav VR, Rathore R, Wess J, *et al.* (2009). Membrane depolarization causes a direct activation of G protein-coupled receptors leading to local Ca2+ release in smooth muscle. *Proc. Natl. Acad. Sci. U. S. A.* **106**: 11418–23.

Lowe SW, and Sherr CJ. (2003). Tumor suppression by Ink4a-Arf: progress and puzzles. *Curr. Opin. Genet. Dev.* **13**: 77–83.

Lu T, and Finkel T. (2008). Free radicals and senescence. *Exp. Cell Res.* **314**: 1918–22.

Lukas J, Parry D, Aagaard L, Mann DJ, Bartkova J, Strauss M, *et al.* (1995). Retinoblastoma-protein-dependent cell-cycle inhibition by the tumour suppressor p16. *Nature* **375**: 503–6.

-M-

Mai S, Klinkenberg M, Auburger G, Bereiter-Hahn J, and Jendrach M. (2010). Decreased expression of Drp1 and Fis1 mediates mitochondrial elongation in senescent cells and enhances resistance to oxidative stress through PINK1. *J. Cell Sci.* **123**: 917–26.

Maier B, Gluba W, Bernier B, Turner T, Mohammad K, Guise T, *et al.* (2004). Modulation of mammalian life span by the short isoform of p53. *Genes Dev.* **18**: 306–19.

Mallette FA, Gaumont-Leclerc M-F, and Ferbeyre G. (2007). The DNA damage signaling pathway is a critical mediator of oncogene-induced senescence. *Genes Dev.* **21**: 43–8.

Mallilankaraman K, Doonan P, Cárdenas C, Chandramoorthy HC, Müller M, Miller R, *et al.* (2012). MICU1 is an essential gatekeeper for MCU-mediated mitochondrial Ca(2+) uptake that regulates cell survival. *Cell* **151**: 630–44.

Mannava S, Moparthy KC, Wheeler LJ, Natarajan V, Zucker SN, Fink EE, *et al.* (2013). Depletion of deoxyribonucleotide pools is an endogenous source of DNA damage in cells undergoing oncogene-induced senescence. *Am. J. Pathol.* **182**: 142–51.

Marchi S, Lupini L, Patergnani S, Rimessi A, Missiroli S, Bonora M, *et al.* (2013). Downregulation of the mitochondrial calcium uniporter by cancer-related miR-25. *Curr. Biol.* **23**: 58–63.

Marchi S, and Pinton P. (2013). The mitochondrial calcium uniporter complex: molecular components, structure and physiopathological implications. *J. Physiol.* **00**: 1–11.

Marcotte R, Lacelle C, and Wang E. (2004). Senescent fibroblasts resist apoptosis by downregulating caspase-3. *Mech. Ageing Dev.* **125**: 777–83.

Mason DX, Jackson TJ, and Lin AW. (2004). Molecular signature of oncogenic ras-induced senescence. *Oncogene* **23**: 9238–46.

Meek DW. (2009). Tumour suppression by p53: a role for the DNA damage response? *Nat. Rev. Cancer* **9**: 714–23.

Melk A, Schmidt BMW, Takeuchi O, Sawitzki B, Rayner DC, and Halloran PF. (2004). Expression of p16INK4a and other cell cycle regulator and senescence associated genes in aging human kidney. *Kidney Int.* **65**: 510–20.

Di Micco R, Fumagalli M, Cicalese A, Piccinin S, Gasparini P, Luise C, *et al.* (2006). Oncogene-induced senescence is a DNA damage response triggered by DNA hyper-replication. *Nature* **444**: 638–42.

Di Micco R, Sulli G, Dobreva M, Liontos M, Botrugno O a, Gargiulo G, *et al.* (2011). Interplay between oncogene-induced DNA damage response and heterochromatin in senescence and cancer. *Nat. Cell Biol.* **13**: 292–302.

Michaloglou C, Vredeveld LCW, Soengas MS, Denoyelle C, Kuilman T, van der Horst CM a M, *et al.* (2005). BRAFE600-associated senescence-like cell cycle arrest of human naevi. *Nature* **436**: 720–4.

Millis AJ, Hoyle M, McCue HM, and Martini H. (1992). Differential expression of metalloproteinase and tissue inhibitor of metalloproteinase genes in aged human fibroblasts. *Exp. Cell Res.* **201**: 373–9.

Min C, Kirsch KH, Zhao Y, Jeay S, Palamakumbura AH, Trackman PC, *et al.* (2007). The tumor suppressor activity of the lysyl oxidase propeptide reverses the invasive phenotype of Her-2/neu-driven breast cancer. *Cancer Res.* **67**: 1105–12.

Miyawaki A, Llopis J, Heim R, Mccaffery JM, Adams JA, Ikura M, *et al.* (1997). Fluorescent indicators for Ca 2 + based on green fluorescent proteins and calmodulin. **388**: 882–887.

Moiseeva O, Bourdeau V, Roux A, Deschênes-Simard X, and Ferbeyre G. (2009). Mitochondrial dysfunction contributes to oncogene-induced senescence. *Mol. Cell. Biol.* **29**: 4495–507.

Moiseeva O, Mallette FA, Mukhopadhyay UK, Moores A, and Ferbeyre G. (2006). DNA damage signaling and p53-dependent senescence after prolonged beta-interferon stimulation. *Mol. Biol. Cell* **17**: 1583–92.

Monteith GR, Davis FM, and Roberts-Thomson SJ. (2012). Calcium channels and pumps in cancer: changes and consequences. *J. Biol. Chem.* **287**: 31666–73.

Monteith GR, McAndrew D, Faddy HM, and Roberts-Thomson SJ. (2007). Calcium and cancer: targeting Ca2+ transport. *Nat. Rev. Cancer* **7**: 519–30.

Moreno-Bueno G, Salvador F, Martín A, Floristán A, Cuevas EP, Santos V, *et al.* (2011). Lysyl oxidase-like 2 (LOXL2), a new regulator of cell polarity required for metastatic dissemination of basal-like breast carcinomas. *EMBO Mol. Med.* **3**: 528–44.

Morré DJ, Merritt WD, and Lembi CA. (1971). Connections between mitochondria and endoplasmic reticulum in rat liver and onion stem. *Protoplasma* **73**: 43–9.

Muñoz-Espín D, Cañamero M, Maraver A, Gómez-López G, Contreras J, Murillo-Cuesta S, *et al.* (2013). Programmed cell senescence during mammalian embryonic development. *Cell* **155**: 1104–18.

Munro J, Barr NI, Ireland H, Morrison V, and Parkinson EK. (2004). Histone deacetylase inhibitors induce a senescence-like state in human cells by a p16-dependent mechanism that is independent of a mitotic clock. *Exp. Cell Res.* **295**: 525–38.

Muntoni A, and Reddel RR. (2005). The first molecular details of ALT in human tumor cells. *Hum. Mol. Genet.* **14 Spec No**: R191–6.

Murphy a N, Bredesen DE, Cortopassi G, Wang E, and Fiskum G. (1996). Bcl-2 potentiates the maximal calcium uptake capacity of neural cell mitochondria. *Proc. Natl. Acad. Sci. U. S. A.* **93**: 9893–8.

-N-

Nagai T, Sawano a, Park ES, and Miyawaki a. (2001). Circularly permuted green fluorescent proteins engineered to sense Ca2+. *Proc. Natl. Acad. Sci. U. S. A.* **98**: 3197–202.

Nakai J, Ohkura M, and Imoto K. (2001). A high signal-to-noise Ca(2+) probe composed of a single green fluorescent protein. *Nat. Biotechnol.* **19**: 137–41.

Nardella C, Clohessy JG, Alimonti A, and Pandolfi PP. (2011). Pro-senescence therapy for cancer treatment. *Nat. Rev. Cancer* **11**: 503–11.

Narita MM, Nun S, Heard E, Lin AW, Hearn S a., Spector DL, *et al.* (2003). Rb-Mediated Heterochromatin Formation and Silencing of E2F Target Genes during Cellular Senescence State. *Cell* **113**: 703–716.

Narita MM, Young ARJ, Arakawa S, Samarajiwa S a, Nakashima T, Yoshida S, *et al.* (2011). Spatial coupling of mTOR and autophagy augments secretory phenotypes. *Science* **332**: 966–70.

Narita MM, and Young ARJ. (2009). Autophagy facilitates oncogene-induced senescence. *Cancer Res.* **5**: 1046–1047.

Nelson DM, McBryan T, Jeyapalan JC, Sedivy JM, and Adams PD. (2014). A comparison of oncogene-induced senescence and replicative senescence: implications for tumor suppression and aging. *Age (Dordr).*

Ngo VN, Davis RE, Lamy L, Yu X, Zhao H, Lenz G, *et al.* (2006). A loss-of-function RNA interference screen for molecular targets in cancer. *Nature* **441**: 106–10.

Noureddine H, Gary-Bobo G, Alifano M, Marcos E, Saker M, Vienney N, *et al.* (2011). Pulmonary artery smooth muscle cell senescence is a pathogenic mechanism for pulmonary hypertension in chronic lung disease. *Circ. Res.* **109**: 543–53.

-O-

Offenberg H, Brünner N, Mansilla F, Orntoft Torben F, and Birkenkamp-Demtroder K. (2008). TIMP-1 expression in human colorectal cancer is associated with TGF-B1, LOXL2, INHBA1, TNF-AIP6 and TIMP-2 transcript profiles. *Mol. Oncol.* **2**: 233–40.

Ogryzko V V, Hirai TH, Russanova VR, Barbie DA, and Howard BH. (1996). Human fibroblast commitment to a senescence-like state in response to histone deacetylase inhibitors is cell cycle dependent. *Mol. Cell. Biol.* **16**: 5210–8.

Ohtani K, DeGregori J, and Nevins JR. (1995). Regulation of the cyclin E gene by transcription factor E2F1. *Proc. Natl. Acad. Sci. U. S. A.* **92**: 12146–50.

Oleggini R, and Donato A Di. (2011). Lysyl oxidase regulates MMTV promoter: indirect evidence of histone H1 involvement. **532**: 522–532.

Olsen CL, Gardie B, Yaswen P, and Stampfer MR. (2002). Raf-1-induced growth arrest in human mammary epithelial cells is p16-independent and is overcome in immortal cells during conversion. *Oncogene* **21**: 6328–39.

-P-

Palamakumbura a H, Vora SR, Nugent M a, Kirsch KH, Sonenshein GE, and Trackman PC. (2009). Lysyl oxidase propeptide inhibits prostate cancer cell growth by mechanisms that target FGF-2-cell binding and signaling. *Oncogene* **28**: 3390–400.

Palamakumbura AH, Jeay S, Guo Y, Pischon N, Sommer P, Sonenshein GE, *et al.* (2004). The propeptide domain of lysyl oxidase induces phenotypic reversion of ras-transformed cells. *J. Biol. Chem.* **279**: 40593–600.

Pan M-G, Xiong Y, and Chen F. (2013).(a). NFAT gene family in inflammation and cancer. *Curr. Mol. Med.* **13**: 543–54.

Pan X, Liu J, Nguyen T, Liu C, Sun J, Teng Y, *et al.* (2013).(b). The physiological role of mitochondrial calcium revealed by mice lacking the mitochondrial calcium uniporter. *Nat. Cell Biol.* **15**: 1464–72.

Parker BS, Argani P, Cook BP, Liangfeng H, Chartrand SD, Zhang M, *et al.* (2004). Alterations in vascular gene expression in invasive breast carcinoma. *Cancer Res.* **64**: 7857–66.

Parkinson K, Baines AE, Keller T, Gruenheit N, Bragg L, North RA, *et al.* (2014). Calcium-dependent regulation of Rab activation and vesicle fusion by an intracellular P2X ion channel. *Nat. Cell Biol.* **16**: 87–98.

Parone P a, Da Cruz S, Tondera D, Mattenberger Y, James DI, Maechler P, *et al.* (2008). Preventing mitochondrial fission impairs mitochondrial function and leads to loss of mitochondrial DNA. *PLoS One* **3**: e3257.

Parrinello S, Coppe J-P, Krtolica A, and Campisi J. (2005). Stromal-epithelial interactions in aging and cancer: senescent fibroblasts alter epithelial cell differentiation. *J. Cell Sci.* **118**: 485–96.

Parrinello S, Samper E, Krtolica A, Goldstein J, Melov S, and Campisi J. (2003). Oxygen sensitivity severely limits the replicative lifespan of murine fibroblasts. *Nat. Cell Biol.* **5**: 741–7.

Parys JB, Decuypere J-P, and Bultynck G. (2012). Role of the inositol 1,4,5-trisphosphate receptor/Ca2+-release channel in autophagy. *Cell Commun. Signal.* **10**: 17.

Passos JF, Nelson G, Wang C, Richter T, Simillion C, Proctor CJ, *et al.* (2010). Feedback between p21 and reactive oxygen production is necessary for cell senescence. *Mol. Syst. Biol.* **6**: 347.

Passos JF, Saretzki G, Ahmed S, Nelson G, Richter T, Peters H, *et al.* (2007).(a). Mitochondrial dysfunction accounts for the stochastic heterogeneity in telomere-dependent senescence. *PLoS Biol.* **5**: e110.

Passos JF, Saretzki G, and von Zglinicki T. (2007).(b). DNA damage in telomeres and mitochondria during cellular senescence: is there a connection? *Nucleic Acids Res.* **35**: 7505–13.

Paszek MJ, Zahir N, Johnson KR, Lakins JN, Rozenberg GI, Gefen A, *et al.* (2005). Tensional homeostasis and the malignant phenotype. *Cancer Cell* **8**: 241–54.

Patron M, Raffaello A, Granatiero V, Tosatto A, Merli G, De Stefani D, *et al.* (2013). The mitochondrial calcium uniporter (MCU): molecular identity and physiological roles. *J. Biol. Chem.* **288**: 10750–8.

Payne SL, Fogelgren B, Hess AR, Seftor E a, Wiley EL, Fong SFT, *et al.* (2005). Lysyl oxidase regulates breast cancer cell migration and adhesion through a hydrogen peroxide-mediated mechanism. *Cancer Res.* **65**: 11429–36.

Pearson M, Carbone R, Sebastiani C, Cioce M, Fagioli M, Saito S, *et al.* (2000). PML regulates p53 acetylation and premature senescence induced by oncogenic Ras. *Nature* **406**: 207–10.

Peinado H, Del Carmen Iglesias-de la Cruz M, Olmeda D, Csiszar K, Fong KSK, Vega S, *et al.* (2005). A molecular role for lysyl oxidase-like 2 enzyme in snail regulation and tumor progression. *EMBO J.* **24**: 3446–58.

Peinado H, Moreno-Bueno G, Hardisson D, Pérez-Gómez E, Santos V, Mendiola M, *et al.* (2008). Lysyl oxidase-like 2 as a new poor prognosis marker of squamous cell carcinomas. *Cancer Res.* **68**: 4541–50.

Pelengaris S, Littlewood T, Khan M, Elia G, and Evan G. (1999). Reversible activation of c-Myc in skin: induction of a complex neoplastic phenotype by a single oncogenic lesion. *Mol. Cell* **3**: 565–77.

Peng L, Ran Y-L, Hu H, Yu L, Liu Q, Zhou Z, *et al.* (2009). Secreted LOXL2 is a novel therapeutic target that promotes gastric cancer metastasis via the Src/FAK pathway. *Carcinogenesis* **30**: 1660–9.

Perocchi F, Gohil VM, Girgis HS, Bao XR, McCombs JE, Palmer AE, *et al.* (2010). MICU1 encodes a mitochondrial EF hand protein required for Ca(2+) uptake. *Nature* **467**: 291–6.

Pez F, Dayan F, Durivault J, Kaniewski B, Aimond G, Le Provost GS, *et al.* (2011). The HIF-1-inducible lysyl oxidase activates HIF-1 via the Akt pathway in a positive regulation loop and synergizes with HIF-1 in promoting tumor cell growth. *Cancer Res.* **71**: 1647–57.

Pinton P, Ferrari D, Magalhães P, Schulze-Osthoff K, Di Virgilio F, Pozzan T, *et al.* (2000). Reduced loading of intracellular Ca(2+) stores and downregulation of capacitative Ca(2+) influx in Bcl-2-overexpressing cells. *J. Cell Biol.* **148**: 857–62.

Pinton P, and Rizzuto R. (2006). Bcl-2 and Ca2+ homeostasis in the endoplasmic reticulum. *Cell Death Differ.* **13**: 1409–18.

Poburko D, Liao C-H, van Breemen C, and Demaurex N. (2009). Mitochondrial regulation of sarcoplasmic reticulum Ca2+ content in vascular smooth muscle cells. *Circ. Res.* **104**: 104–12.

Poele RH, Okorokov AL, Jardine L, Cummings J, and Joel SP. (2002). DNA Damage Is Able to Induce Senescence in Tumor Cells in Vitro and in Vivo DNA Damage Is Able to Induce Senescence in Tumor Cells in Vitro and in Vivo 1. : 1876–1883.

Pribluda A, Elyada E, Wiener Z, Hamza H, Goldstein RE, Biton M, *et al.* (2013). A Senescence-Inflammatory Switch from Cancer-Inhibitory to Cancer-Promoting Mechanism. *Cancer Cell*.

Prowse KR, and Greider CW. (1995). Developmental and tissue-specific regulation of mouse telomerase and telomere length. *Proc. Natl. Acad. Sci. U. S. A.* **92**: 4818–22.

Prudent J, Popgeorgiev N, Bonneau B, Thibaut J, Gadet R, Lopez J, *et al.* (2013). Bcl-wav and the mitochondrial calcium uniporter drive gastrula morphogenesis in zebrafish. *Nat. Commun.* **4**: 2330.

-Q-

Qiu J, Tan Y-W, Hagenston AM, Martel M-A, Kneisel N, Skehel P a, *et al.* (2013). Mitochondrial calcium uniporter Mcu controls excitotoxicity and is transcriptionally repressed by neuroprotective nuclear calcium signals. *Nat. Commun.* **4**: 2034.

-R-

Raffaello A, De Stefani D, Sabbadin D, Teardo E, Merli G, Picard A, *et al.* (2013). The mitochondrial calcium uniporter is a multimer that can include a dominant-negative pore-forming subunit. *EMBO J.* **32**: 2362–76.

Rai P, Onder TT, Young JJ, McFaline JL, Pang B, Dedon PC, *et al.* (2009). Continuous elimination of oxidized nucleotides is necessary to prevent rapid onset of cellular senescence. *Proc. Natl. Acad. Sci. U. S. A.* **106**: 169–74.

Ramirez RD, Morales CP, Herbert BS, Rohde JM, Passons C, Shay JW, *et al.* (2001). Putative telomere-independent mechanisms of replicative aging reflect inadequate growth conditions. *Genes Dev.* **15**: 398–403.

Ramsey MR, and Sharpless NE. (2006). NEWS AND VIEWS ROS as a tumour suppressor? **8**: 1213–1215.

Rebbaa A, Zheng X, Chou PM, and Mirkin BL. (2003). Caspase inhibition switches doxorubicin-induced apoptosis to senescence. *Oncogene* **22**: 2805–11.

Ressler S, Bartkova J, Niederegger H, Bartek J, Scharffetter-Kochanek K, Jansen-Dürr P, *et al.* (2006). p16INK4A is a robust in vivo biomarker of cellular aging in human skin. *Aging Cell* **5**: 379–89.

Rimessi A, Bonora M, Marchi S, Patergnani S, Marobbio CMT, Lasorsa FM, *et al.* (2013). Perturbed mitochondrial Ca2+ signals as causes or consequences of mitophagy induction. *Autophagy* **9**: 1677–86.

Rincheval V, Renaud F, Lemaire C, Godefroy N, Trotot P, Boulo V, *et al.* (2002). Bcl-2 can promote p53-dependent senescence versus apoptosis without affecting the G1/S transition. *Biochem. Biophys. Res. Commun.* **298**: 282–8.

Rizzuto R, Brini M, Murgia M, and Pozzan T. (1993). Microdomains with high Ca2+ close to IP3-sensitive channels that are sensed by neighboring mitochondria. *Science* **262**: 744–7.

Rizzuto R, Pinton P, Carrington W, Fay FS, Fogarty KE, Lifshitz LM, *et al.* (1998). Close Contacts with the Endoplasmic Reticulum as Determinants of Mitochondrial Ca2+ Responses. *Science (80-.).* **280**: 1763–1766.

Roberson RS, Kussick SJ, Vallieres E, Chen S-YJ, and Wu DY. (2005). Escape from therapy-induced accelerated cellular senescence in p53-null lung cancer cells and in human lung cancers. *Cancer Res.* **65**: 2795–803.

Rodier F, Campisi J, and Bhaumik D. (2007). Two faces of p53: aging and tumor suppression. *Nucleic Acids Res.* **35**: 7475–84.

Rodier F, and Campisi J. (2011). Four faces of cellular senescence. *J. Cell Biol.* **192**: 547–56.

Rodier F, Coppé J-P, Patil CK, Hoeijmakers W a M, Muñoz DP, Raza SR, *et al.* (2009). Persistent DNA damage signalling triggers senescence-associated inflammatory cytokine secretion. *Nat. Cell Biol.* **11**: 973–9.

Romanov SR, Kozakiewicz BK, Holst CR, Stampfer MR, Haupt LM, and Tlsty TD. (2001). Normal human mammary epithelial cells spontaneously escape senescence and acquire genomic changes. *Nature* **409**: 633–7.

Rong Y-P, Aromolaran AS, Bultynck G, Zhong F, Li X, McColl K, *et al.* (2008). Targeting Bcl-2-IP3 receptor interaction to reverse Bcl-2's inhibition of apoptotic calcium signals. *Mol. Cell* **31**: 255–65.

Rong Y-P, Barr P, Yee VC, and Distelhorst CW. (2009). Targeting Bcl-2 based on the interaction of its BH4 domain with the inositol 1,4,5-trisphosphate receptor. *Biochim. Biophys. Acta* **1793**: 971–8.

Ryu SJ, Oh YS, and Park SC. (2007). Failure of stress-induced downregulation of Bcl-2 contributes to apoptosis resistance in senescent human diploid fibroblasts. *Cell Death Differ.* **14**: 1020–8.

-S-

Sadaie M, Salama R, Carroll T, Tomimatsu K, Chandra T, Young ARJ, *et al.* (2013). Redistribution of the Lamin B1 genomic binding profile affects rearrangement of heterochromatic domains and SAHF formation during senescence. *Genes Dev.* **27**: 1800–8.

Sage J, Miller AL, Pérez-Mancera PA, Wysocki JM, and Jacks T. (2003). Acute mutation of retinoblastoma gene function is sufficient for cell cycle re-entry. *Nature* **424**: 223–8.

Sage J. (2000). Targeted disruption of the three Rb-related genes leads to loss of G1 control and immortalization. *Genes Dev.* **14**: 3037–3050.

Salama R, Sadaie M, Hoare M, and Narita M. (2014). Cellular senescence and its effector programs. *Genes Dev.* **28**: 99–114.

Sancak Y, Markhard AL, Kitami T, Kovács-Bogdán E, Kamer KJ, Udeshi ND, *et al.* (2013). EMRE is an essential component of the mitochondrial calcium uniporter complex. *Science* **342**: 1379–82.

Sánchez-Morgan N, Kirsch KH, Trackman PC, and Sonenshein GE. (2011). The lysyl oxidase propeptide interacts with the receptor-type protein tyrosine phosphatase kappa and inhibits β-catenin transcriptional activity in lung cancer cells. *Mol. Cell. Biol.* **31**: 3286–97.

Sarkisian CJ, Keister B a, Stairs DB, Boxer RB, Moody SE, and Chodosh LA. (2007). Dose-dependent oncogene-induced senescence in vivo and its evasion during mammary tumorigenesis. *Nat. Cell Biol.* **9**: 493–505.

Schlabach MR, Luo J, Solimini NL, Hu G, Xu Q, Li MZ, *et al.* (2008). Cancer proliferation gene discovery through functional genomics. *Science* **319**: 620–4.

Schmitt CA, Fridman JS, Yang M, Lee S, Baranov E, Hoffman RM, *et al.* (2002). A Senescence Program Controlled by p53 and p16 INK4a Contributes to the Outcome of Cancer Therapy. **109**: 335–346.

Schrçder M, and Schröder M. (2008). Endoplasmic reticulum stress responses.

Schug TT. (2010). mTOR favors senescence over quiescence in p53-arrested cells. *Aging (Albany. NY).* **2**: 327–8.

Scorrano L. (2013). Keeping mitochondria in shape: a matter of life and death. *Eur. J. Clin. Invest.* **43**: 886–93.

Seluanov A, Gorbunova V, Falcovitz A, Sigal A, Milyavsky M, Zurer I, *et al.* (2001). Change of the death pathway in senescent human fibroblasts in response to DNA damage is caused by an inability to stabilize p53. *Mol. Cell. Biol.* **21**: 1552–64.

Serrano M, Hannon GJ, and Beach D. (1993). A new regulatory motif in cell-cycle control causing specific inhibition of cyclin D/CDK4. *Nature* **366**: 704–7.

Serrano M, Lee H, Chin L, Cordon-Cardo C, Beach D, and DePinho RA. (1996). Role of the INK4a locus in tumor suppression and cell mortality. *Cell* **85**: 27–37.

Serrano M, Lin AW, Mccurrach ME, Beach D, and Lowe SW. (1997). Oncogenic ras provokes premature cell senescence associated with accumulation of p53 and p16INK4a. *Cell* **88**: 593–602.

Shah PP, Donahue G, Otte GL, Capell BC, Nelson DM, Cao K, *et al.* (2013). Lamin B1 depletion in senescent cells triggers large-scale changes in gene expression and the chromatin landscape. *Genes Dev.* **27**: 1787–99.

Sharpless NE, and DePinho RA. (2005). Cancer: crime and punishment. *Nature* **436**: 636–7.

Sharpless NE. (2005). INK4a/ARF: a multifunctional tumor suppressor locus. *Mutat. Res.* **576**: 22–38.

Shay JW, and Roninson IB. (2004). Hallmarks of senescence in carcinogenesis and cancer therapy. *Oncogene* **23**: 2919–33.

Shay JW. (1997). Telomerase in human development and cancer. *J. Cell. Physiol.* **173**: 266–70.

Shelton DN, Chang E, Whittier PS, Choi D, and Funk WD. (1999). Microarray analysis of replicative senescence. *Curr. Biol.* **9**: 939–45.

Sherman MY, Meng L, Stampfer M, Gabai VL, and Yaglom JA. (2011). Oncogenes induce senescence with incomplete growth arrest and suppress the DNA damage response in immortalized cells. *Aging Cell* **10**: 949–61.

Sherr CJ, and Roberts JM. (1999). CDK inhibitors: positive and negative regulators of G1-phase progression. *Genes Dev.* **13**: 1501–1512.

Shibaji T, Nagao M, Ikeda N, Kanehiro H, Hisanaga M, Ko S, *et al.* (2003). Prognostic significance of HIF-1 alpha overexpression in human pancreatic cancer. *Anticancer Res.* **23**: 4721–7.

Silva JM, Marran K, Parker JS, Silva J, Golding M, Schlabach MR, *et al.* (2008). Profiling essential genes in human mammary cells by multiplex RNAi screening. *Science* **319**: 617–20.

Simonetti M, Hagenston AM, Vardeh D, Freitag HE, Mauceri D, Lu J, *et al.* (2013). Nuclear calcium signaling in spinal neurons drives a genomic program required for persistent inflammatory pain. *Neuron* **77**: 43–57.

Sottile J. (2004). Regulation of angiogenesis by extracellular matrix. *Biochim. Biophys. Acta* **1654**: 13–22.

Souslova E a, Belousov V V, Lock JG, Strömblad S, Kasparov S, Bolshakov AP, *et al.* (2007). Single fluorescent protein-based Ca2+ sensors with increased dynamic range. *BMC Biotechnol.* **7**: 37.

De Stefani D, Raffaello A, Teardo E, Szabò I, and Rizzuto R. (2011). A forty-kilodalton protein of the inner membrane is the mitochondrial calcium uniporter. *Nature* **476**: 336–40.

Stein GH, Drullinger LF, Soulard A, and Dulić V. (1999). Differential roles for cyclin-dependent kinase inhibitors p21 and p16 in the mechanisms of senescence and differentiation in human fibroblasts. *Mol. Cell. Biol.* **19**: 2109–17.

Stöckl P, Hütter E, Zwerschke W, and Jansen-Dürr P. (2006). Sustained inhibition of oxidative phosphorylation impairs cell proliferation and induces premature senescence in human fibroblasts. *Exp. Gerontol.* **41**: 674–82.

Storer M, Mas A, Robert-Moreno A, Pecoraro M, Ortells MC, Di Giacomo V, *et al.* (2013). Senescence is a developmental mechanism that contributes to embryonic growth and patterning. *Cell* **155**: 1119–30.

Suram A, Kaplunov J, Patel PL, Ruan H, Cerutti A, Boccardi V, *et al.* (2012). Oncogene-induced telomere dysfunction enforces cellular senescence in human cancer precursor lesions. *EMBO J.* **31**: 2839–51.

Szabadkai G, Bianchi K, Várnai P, De Stefani D, Wieckowski MR, Cavagna D, *et al.* (2006). Chaperone-mediated coupling of endoplasmic reticulum and mitochondrial Ca2+ channels. *J. Cell Biol.* **175**: 901–11.

Szado T, Vanderheyden V, Parys JB, Smedt H De, Rietdorf K, Kotelevets L, *et al.* (2008). receptors by protein kinase B / Akt inhibits Ca 2 ⍰ release and apoptosis. **105**.

Szegezdi E, Logue SE, Gorman AM, and Samali A. (2006). Mediators of endoplasmic reticulum stress-induced apoptosis. *EMBO Rep.* **7**: 880–5.

-T-

Takahashi A, Ohtani N, Yamakoshi K, Iida S, Tahara H, Nakayama KKI, *et al.* (2006). Mitogenic signalling and the p16INK4a-Rb pathway cooperate to enforce irreversible cellular senescence. *Nat. Cell Biol.* **8**: 1291–7.

Takaoka M, Harada H, Deramaudt TB, Oyama K, Andl CD, Johnstone CN, *et al.* (2004). Ha-Ras(G12V) induces senescence in primary and immortalized human esophageal keratinocytes with p53 dysfunction. *Oncogene* **23**: 6760–8.

Tallini YN, Ohkura M, Choi B-R, Ji G, Imoto K, Doran R, *et al.* (2006). Imaging cellular signals in the heart in vivo: Cardiac expression of the high-signal Ca2+ indicator GCaMP2. *Proc. Natl. Acad. Sci. U. S. A.* **103**: 4753–8.

Talluri S, and Dick F a. (2014). The retinoblastoma protein and PML collaborate to organize heterochromatin and silence E2F-responsive genes during senescence. *Cell Cycle* **13**: 641–51.

Tombor B, Rundell K, and Oltvai ZN. (2003). Bcl-2 promotes premature senescence induced by oncogenic Ras. *Biochem. Biophys. Res. Commun.* **303**: 800–807.

Toruner GA, Ulger C, Alkan M, Galante AT, Rinaggio J, Wilk R, *et al.* (2004). Association between gene expression profile and tumor invasion in oral squamous cell carcinoma. *Cancer Genet. Cytogenet.* **154**: 27–35.

Trenker M, Malli R, Fertschai I, Levak-Frank S, and Graier WF. (2007). Uncoupling proteins 2 and 3 are fundamental for mitochondrial Ca2+ uniport. *Nat. Cell Biol.* **9**: 445–52.

Trougakos IP, Saridaki A, Panayotou G, and Gonos ES. (2006). Identification of differentially expressed proteins in senescent human embryonic fibroblasts. *Mech. Ageing Dev.* **127**: 88–92.

Tuveson DA, Shaw AT, Willis NA, Silver DP, Jackson EL, Chang S, *et al.* (2004). Endogenous oncogenic K-ras(G12D) stimulates proliferation and widespread neoplastic and developmental defects. *Cancer Cell* **5**: 375–87.

Tyner SD, Venkatachalam S, Choi J, Jones S, Ghebranious N, Igelmann H, *et al.* (2002). p53 mutant mice that display early ageing-associated phenotypes. *Nature* **415**: 45–53.

-V-

Vance JE, Stone SJ, and Faust JR. (1997). Abnormalities in mitochondria-associated membranes and phospholipid biosynthetic enzymes in the mnd/mnd mouse model of neuronal ceroid lipofuscinosis. *Biochim. Biophys. Acta* **1344**: 286–99.

Vanderheyden V, Devogelaere B, Missiaen L, De Smedt H, Bultynck G, and Parys JB. (2009). Regulation of inositol 1,4,5-trisphosphate-induced Ca2+ release by reversible phosphorylation and dephosphorylation. *Biochim. Biophys. Acta* **1793**: 959–70.

Ventura A, Kirsch DG, McLaughlin ME, Tuveson D a, Grimm J, Lintault L, *et al.* (2007). Restoration of p53 function leads to tumour regression in vivo. *Nature* **445**: 661–5.

Vepa S, Scribner WM, Parinandi NL, English D, Garcia JG, and Natarajan V. (1999). Hydrogen peroxide stimulates tyrosine phosphorylation of focal adhesion kinase in vascular endothelial cells. *Am. J. Physiol.* **277**: L150–8.

Verkhratsky A. (2002). The endoplasmic reticulum and neuronal calcium signalling. **32**: 393–404.

Vernier M, Bourdeau V, Gaumont-Leclerc M-F, Moiseeva O, Bégin V, Saad F, *et al.* (2011). Regulation of E2Fs and senescence by PML nuclear bodies. *Genes Dev.* **25**: 41–50.

Vernier M, and Ferbeyre G. (2014). Complete senescence: RB and PML share the task. *Cell Cycle* **13**: 24351540.

Vicencio JM, Ortiz C, Criollo a, Jones a WE, Kepp O, Galluzzi L, *et al.* (2009). The inositol 1,4,5-trisphosphate receptor regulates autophagy through its interaction with Beclin 1. *Cell Death Differ.* **16**: 1006–17.

Vijayachandra K, Lee J, and Glick AB. (2003). Smad3 regulates senescence and malignant conversion in a mouse multistage skin carcinogenesis model. *Cancer Res.* **63**: 3447–52.

Vredeveld LCW, Possik PA, Smit MA, Meissl K, Michaloglou C, Horlings HM, *et al.* (2012). Abrogation of BRAFV600E-induced senescence by PI3K pathway activation contributes to melanomagenesis. *Genes Dev.* **26**: 1055–1069.

-W-

Waaijer MEC, Parish WE, Strongitharm BH, van Heemst D, Slagboom PE, de Craen AJM, *et al.* (2012). The number of p16INK4a positive cells in human skin reflects biological age. *Aging Cell* **11**: 722–5.

Wang E. (1995). Senescent Human Fibroblasts Resist Programmed Cell Death , and Failure to Suppress bcl2 Is Involved. *Cancer Res.* **55**: 2284–2292.

Wang Y, Wang XD, Lapi E, Sullivan A, Jia W, He Y-W, *et al.* (2012). Autophagic activity dictates the cellular response to oncogenic RAS. *Proc. Natl. Acad. Sci. U. S. A.* **109**: 13325–30.

Weber JD, Taylor LJ, Roussel MF, Sherr CJ, and Bar-Sagi D. (1999). Nucleolar Arf sequesters Mdm2 and activates p53. *Nat. Cell Biol.* **1**: 20–6.

Wei S, and Sedivy JM. (1999). Expression of catalytically active telomerase does not prevent premature senescence caused by overexpression of oncogenic Ha-Ras in normal human fibroblasts. *Cancer Res.* **59**: 1539–43.

Wei W, Hemmer RM, and Sedivy JM. (2001). Role of p14(ARF) in replicative and induced senescence of human fibroblasts. *Mol. Cell. Biol.* **21**: 6748–57.

Weinstein IB. (2000). Disorders in cell circuitry during multistage carcinogenesis: the role of homeostasis. *Carcinogenesis* **21**: 857–64.

West MD, Pereira-Smith OM, and Smith JR. (1989). Replicative senescence of human skin fibroblasts correlates with a loss of regulation and overexpression of collagenase activity. *Exp. Cell Res.* **184**: 138–47.

West MD, Shay JW, Wright WE, and Linskens MH. (1996). Altered expression of plasminogen activator and plasminogen activator inhibitor during cellular senescence. *Exp. Gerontol.* **31**: 175–93.

Westbrook TF, Martin ES, Schlabach MR, Leng Y, Liang AC, Feng B, *et al.* (2005). A genetic screen for candidate tumor suppressors identifies REST. *Cell* **121**: 837–48.

White E. (2012). Deconvoluting the context-dependent role for autophagy in cancer. *Nat. Rev. Cancer* **12**: 401–10.

Wieckowski MR, Giorgi C, Lebiedzinska M, Duszynski J, and Pinton P. (2009). Isolation of mitochondria-associated membranes and mitochondria from animal tissues and cells. *Nat. Protoc.* **4**: 1582–90.

Wong C-MCC-L, Gilkes DM, Zhang H, Chen J, Wei H, Chaturvedi P, *et al.* (2011). Hypoxia-inducible factor 1 is a master regulator of breast cancer metastatic niche formation. *Proc. Natl. Acad. Sci. U. S. A.* **435**: 16369–74.

Wong DJ, Foster SA, Galloway DA, and Reid BJ. (1999). Progressive region-specific de novo methylation of the p16 CpG island in primary human mammary epithelial cell strains during escape from M(0) growth arrest. *Mol. Cell. Biol.* **19**: 5642–51.

Woods D, Parry D, Cherwinski H, Bosch E, Lees E, and McMahon M. (1997). Raf-induced proliferation or cell cycle arrest is determined by the level of Raf activity with arrest mediated by p21Cip1. *Mol. Cell. Biol.* **17**: 5598–611.

Wu M, Min C, Wang X, Yu Z, Kirsch KH, Trackman PC, *et al.* (2007). Repression of BCL2 by the tumor suppressor activity of the lysyl oxidase propeptide inhibits transformed phenotype of lung and pancreatic cancer cells. *Cancer Res.* **67**: 6278–85.

-X-

Xia H, Nho RS, Kahm J, Kleidon J, and Henke C a. (2004). Focal adhesion kinase is upstream of phosphatidylinositol 3-kinase/Akt in regulating fibroblast survival in response to contraction of type I collagen matrices via a beta 1 integrin viability signaling pathway. *J. Biol. Chem.* **279**: 33024–34.

Xu M, Yu Q, Subrahmanyam R, Difilippantonio MJ, Ried T, and Sen JM. (2008). Beta-catenin expression results in p53-independent DNA damage and oncogene-induced senescence in prelymphomagenic thymocytes in vivo. *Mol. Cell. Biol.* **28**: 1713–23.

Xue W, Zender L, Miething C, Dickins R a, Hernando E, Krizhanovsky V, *et al.* (2007). Senescence and tumour clearance is triggered by p53 restoration in murine liver carcinomas. *Nature* **445**: 656–60.

-Y-

Yamakoshi K, Takahashi A, Hirota F, Nakayama R, Ishimaru N, Kubo Y, *et al.* (2009). Real-time in vivo imaging of p16Ink4a reveals cross talk with p53. *J. Cell Biol.* **186**: 393–407.

Yang S, Yip R, Polena S, Sharma M, Rao S, Griciene P, *et al.* (2004). Reactive oxygen species increased focal adhesion kinase production in pulmonary microvascular endothelial cells. *Proc. West. Pharmacol. Soc.* **47**: 54–6.

Yang Z, and Klionsky DJ. (2010). Eaten alive: a history of macroautophagy. *Nat. Cell Biol.* **12**: 814–22.

Yoon IK, Kim HK, Kim YK, Song I, Kim W, Kim S, *et al.* (2004). Exploration of replicative senescence-associated genes in human dermal fibroblasts by cDNA microarray technology. *Exp. Gerontol.* **39**: 1369–78.

Yoshimoto S, Loo TM, Atarashi K, Kanda H, Sato S, Oyadomari S, *et al.* (2013). Obesity-induced gut microbial metabolite promotes liver cancer through senescence secretome. *Nature* **499**: 97–101.

Young AP, Schlisio S, Minamishima YA, Zhang Q, Li L, Grisanzio C, *et al.* (2008). VHL loss actuates a HIF-independent senescence programme mediated by Rb and p400. *Nat. Cell Biol.* **10**: 361–9.

Young ARJ, Narita M, Ferreira M, Kirschner K, Sadaie M, Darot JFJ, *et al.* (2009). Autophagy mediates the mitotic senescence transition. *Genes Dev.*: 798–803.

Zaffryar-Eilot S, Marshall D, Voloshin T, Bar-Zion A, Spangler R, Kessler O, *et al.* (2013). Lysyl Oxidase-Like-2 Promotes Tumour Angiogenesis and is a Potential Therapeutic Target in Angiogenic Tumours. *Carcinogenesis*: bgt241–.

Von Zglinicki T. (2000). Role of oxidative stress in telomere length regulation and replicative senescence. *Ann. N. Y. Acad. Sci.* **908**: 99–110.

-Z-

Zhang H, and Cohen SN. (2004). Smurf2 up-regulation activates telomere-dependent senescence. *Genes Dev.* **18**: 3028–40.

Zhang J, Pickering CR, Holst CR, Gauthier ML, and Tlsty TD. (2006). p16INK4a modulates p53 in primary human mammary epithelial cells. *Cancer Res.* **66**: 10325–31.

Zhang J. (2013). Autophagy and Mitophagy in Cellular Damage Control. *Redox Biol.* **1**: 19–23.

Zhang R, Poustovoitov M V, Ye X, Santos HA, Chen W, Daganzo SM, *et al.* (2005). Formation of MacroH2A-containing senescence-associated heterochromatin foci and senescence driven by ASF1a and HIRA. *Dev. Cell* **8**: 19–30.

Zhang X, Mar V, Zhou W, Harrington L, and Robinson MO. (1999). Telomere shortening and apoptosis in telomerase-inhibited human tumor cells. *Genes Dev.* **13**: 2388–99.

Zhou F, Onizawa S, Nagai A, and Aoshiba K. (2011). Epithelial cell senescence impairs repair process and exacerbates inflammation after airway injury. *Respir. Res.* **12**: 78.

Zhu J, Woods D, McMahon M, and Bishop JM. (1998). Senescence of human fibroblasts induced by oncogenic Raf. *Genes Dev.* **12**: 2997–3007.

Zhu L, Ling S, Yu X, Venkatesh L, Subramanian T, Chinnadurai G, *et al.* (1999). Modulation of Mitochondrial Ca2+ Homeostasis by Bcl-2. *J. Biol. Chem.* **274**: 33267–33273.

Zhuang D, Mannava S, Grachtchouk V, Tang W-H, Patil S, Wawrzyniak J a, *et al.* (2008). C-MYC overexpression is required for continuous suppression of oncogene-induced senescence in melanoma cells. *Oncogene* **27**: 6623–34.

Zumstein LA, and Lundblad V. (1999). Telomeres: has cancer's Achilles' heel been exposed? *Nat. Med.* **5**: 1129–30.

ANNEXES

Article 3 : Potassium Channel KCNA1 Modulates Oncogene-Induced Senescence and Transformation

Published OnlineFirst June 17, 2013; DOI: 10.1158/0008-5472.CAN-12-3690

Tumor and Stem Cell Biology

Cancer Research

Potassium Channel KCNA1 Modulates Oncogene-Induced Senescence and Transformation

Hélène Lallet-Daher[1,2,3,4], Clotilde Wiel[1,2,3,4], Delphine Gitenay[1,2,3,4], Naveenan Navaratnam[5], Arnaud Augert[1,2,3,4], Benjamin Le Calvé[1,2,3,4], Stéphanie Verbeke[6], David Carling[5], Sébastien Aubert[7,8], David Vindrieux[1,2,3,4], and David Bernard[1,2,3,4]

Abstract

Oncogene-induced senescence (OIS) constitutes a failsafe program that restricts tumor development. However, the mechanisms that link oncogenesis to senescence are not completely understood. We carried out a loss-of-function genetic screen that identified the potassium channel KCNA1 as a determinant of OIS escape that can license tumor growth. Oncogenic stress triggers an increase in KCNA1 expression and its relocation from the cytoplasm to the membrane. Mechanistically, this relocation is due to a loss of protein kinase A (PKA)-induced phosphorylation at residue S446 of KCNA1. Accordingly, sustaining PKA activity or expressing a KCNA1 phosphomimetic mutant maintained KCNA1 in the cytoplasm and caused escape from OIS. KCNA1 relocation to the membrane induced a change in membrane potential that invariably resulted in cellular senescence. Restoring KCNA1 expression in transformation-competent cells triggered variation in membrane potential and blocked RAS-induced transformation, and PKA activation suppressed both effects. Furthermore, KCNA1 expression was reduced in human cancers, and this decrease correlated with an increase in breast cancer aggressiveness. Taken together, our results identify a novel pathway that restricts oncogenesis through a potassium channel-dependent senescence pathway. *Cancer Res; 73(16); 5253–65. ©2013 AACR.*

Introduction

Cellular senescence is induced by various cellular stresses such as telomere shortening or oncogenic stress and it results in a stable form of cell-cycle arrest and the appearance of new cellular features such as in morphology or senescence-associated β-galactosidase activity (SA-β-Gal). Senescence by its antigrowth signal is considered as a barrier against tumor development (1–4).

The concept of oncogene-induced senescence (OIS) as a tumor-suppressive mechanism emerged in the late 90s, with the observation that activated oncogenes cause senescence of normal cells in culture (5). After years of debate about the relevance of this observation, a set of *in vivo* studies revealed the presence of senescence in premalignant tumors and its absence in malignant tumors (4). In addition to confirmation of the relevance of oncogene-induced senescence, molecular insights into its regulation have emerged. Key cell-cycle regulators such as those directly regulating the p16-pRb and p53 pathways are reported to affect oncogene-induced senescence (6). Recently, some unexpected mechanisms impacting these pathways have been shown to regulate senescence, for example, regulation by DNA damage, by secreted factors such as cytokines, and by autophagy (7–10).

Most of these pathways involved a central role of the p53 as well as of the p16–Rb pathways in human cells (11), but the experimental evidence were mainly obtained using only human fibroblasts. Emerging evidences support the existence of other mechanisms regulating senescence escape. To date, little is known about these mechanisms (12–18). Similar data generated in human epithelial cells or in other lineages are rather rare and seem to display a more complex picture of the genetic events involved in senescence escape (18). As an example, poststasis human mammary epithelial cells (HMEC), which are not expressing the p16INK4A (19), enter in senescence in response to an oncogenic stress in a DNA damage-p53–independent pathway (17, 18).

In this study, we have carried out a functional loss-of-function short hairpin RNA (shRNA) genetic screen to identify senescence regulators displaying tumor-suppressive activity involved in OIS-escape in human epithelial cells. By this means, we have identified the importance of a potassium channel KCNA1 as a regulator of OIS. In particular, we observed a fine regulation of the localization of this channel to the cell membrane controlled by the protein kinase A (PKA). In addition, we

Authors' Affiliations: [1]Inserm U1052, Centre de Recherche en Cancérologie de Lyon, [2]CNRS UMR5286, [3]Centre Léon Bérard, [4]Université de Lyon, Lyon; [5]Cellular Stress Group, MRC Clinical Sciences Centre, Faculty of Medicine, Imperial College, Hammersmith Campus, London, United Kingdom; [6]INSERM U916, Bergonié Cancer Institute, Université Bordeaux, Bordeaux; [7]Institut de Pathologie, CHRU, Faculté de Médecine, Université de Lille; and [8]Inserm U837, Jean-Pierre Aubert Research Center, Lille, France

Note: Supplementary data for this article are available at Cancer Research Online (http://cancerres.aacrjournals.org/).

Corresponding Author: David Bernard, CRCL, UMR INSERM U1052/CNRS 5286, Centre Léon Bérard, 28, rue Laënnec, 69373 LYON Cedex 08, France. Phone: 334-2655-6792; Fax: 334-7878-2720; E-mail: david.bernard@lyon.unicancer.fr

doi: 10.1158/0008-5472.CAN-12-3690

©2013 American Association for Cancer Research.

Downloaded from cancerres.aacrjournals.org on May 19, 2014. © 2013 American Association for Cancer Research.

Published OnlineFirst June 17, 2013; DOI: 10.1158/0008-5472.CAN-12-3690

provide evidence that change in KCNA1 localization impacts on membrane potential, cellular senescence, and transformation processes.

Materials and Methods

Cell culture

HMECs (Lonza) were cultured in mammary epithelial cell growth medium (Promocell) and penicillin/streptomycin 100 U/mL (Invitrogen). Virus-packaging GP293 cells (Clontech), PlatE (20) cells, and NIH3T3 cells (American Type Culture Collection) were cultured in Dulbecco's Modified Eagle Medium (DMEM; Invitrogen) supplemented with 10% FBS (Hyclone Perbio) and gentamycin (Invitrogen) at 80 μg/mL.

Genetic screening

One hundred thousand HMEC-TM cells were seeded into 10 cm dishes. The following day, each dish was infected with a pool of the short hairpin RNA (shRNA) library (10,000 shRNAs per pool and in 7 pools; Decode RNAi viral screening pools, Thermo Scientific) and treated every 2 days with 400 nmol/L 4-OHT, a concentration that did not impact HMEC-T proliferation (data not shown). Thirty days later, gDNA was prepared from 2 pools out of 7 with clones that escaped senescence. PCR was used to amplify shRNA-coding DNA according to the manufacturer's recommendations for the two conditions. They were next cloned into the pGEMTeasy vector (Promega). One hundred clones were sequenced and shRNA in each clone were identified.

Vectors

KCNA1–shRNA-encoding retroviral vectors were used to knock down KCNA1 (SourceBioScience LifeSciences, NKI_p3205F1410Q, NKI_p3205J1710Q). KCNA1 cDNA [Open Biosystems (MHS1010-98052646)] was excised by EcoRI and cloned into the pLPCX (Clontech) retroviral vector. The plasmids pNLCΔMEK1 (ΔN3, S218E, S222D):ER, pBabe-puro-BRAF:ER (21) and pBabe-puro-H-RASV12 (5) were used when indicated. PRKACB and PRKACG obtained from Addgene (Plasmid 20596 and 20597) have been described previously (22). The retroviral vectors pMSCV-IRES-GFP expressing PRKAR2A or R1A were described previously (23).

Immunoblotting and immunofluorescence

Immunoblot analyses were conducted as described previously (24). For immunofluorescence, cells were fixed either with 4% paraformaldehyde (PFA) to detect protein at the membrane or with methanol at −20°C for 10 minutes to detect protein at all locations. Immunofluoresence staining was conducted as described previously (24). Stainings were superimposed using ImageJ software. Primary antibodies used were: anti-KCNA1 (75-105, external; NeuroMab) used throughout the study, anti-KCNA1 (75-007, internal; NeuroMab) used when mentioned, anti-phosphoERK (9101; Cell Signaling Technology), anti-flag (200472; Stratagene), anti-phospho-histone3Ser10 (ab14955; Abcam), anti-cyclinA (sc-751; Santa Cruz Biotechnology), anti-RAS (610001, BD), and anti-tubulin (T6199, Sigma).

SA-β-Gal analysis, colony-formation assays, and soft agar experiments

Cells were seeded into 6-well plates (at 5×10^4 cells/well). One day later, the various treatments began. Six to 10 days after the initial treatment, the cells were fixed with 4% PFA and processed as described previously (25).

Stastistical analysis

Graphs are presented with SD as errors bars, and Student *t* test was used to determine the *P* value. *, $P < 0.05$; **, $P < 0.01$; and ***, $P < 0.001$, unless specified otherwise in the figure legends.

See the Supplementary Materials and Methods for details.

Results

KCNA1 downregulation induces an OIS escape

To study OIS in human epithelial cells, we used poststasis (which does not express p16INK4a; ref. 19) HMECs. Early passage cells (<3 passages) were immortalized by retroviral transduction of hTert and of 4-hydroxy tamoxifen (4-OHT) inducible oncogene *MEK:ER* (HMEC-TM cells) and subsequently used for the different experiments for no more than 10 passages. To identify new senescence regulators, we carried out a loss-of-function genetic screen. The library was composed of seven pools of shRNA, each pool containing 10,000 shRNA Our strategy was to infect HMEC-TM cells with an shRNA library, treat them with 4-OHT every 2 days for 30 days to activate MEK to completely block cell growth, as seen with control GFP-expressing cells. shRNA in cells that escaped senescence were identified (Fig. 1A; Supplementary Fig. S1A). Among the genes that are targeted by shRNA, KCNA1, a potassium channel, was particularly selected because its shRNA were isolated in several clones (Supplementary Fig S1B), and its expression was shown to be decreased in breast cancer (26) and nothing much was reported about its potential function in cancer.

To validate a role of KCNA1, HMEC-TM were treated with 4-OHT for 3 days, and this resulted in phosphorylation of ERK (the MEK substrate), downregulation of the late mitosis marker P-S10-H3 (Supplementary Fig. S1C), decreased cell growth (Supplementary Fig. S1D and 1E), the appearance of SA-β-Gal activity (Supplementary Fig. S1F), and increased levels of a known set of senescence markers including interleukin (IL)-8 (27), Sprouty2 (28), Dec1, and DcR (Supplementary Fig. S1G; (ref. 29). Nevertheless 10 days after oncogenic stress induction by the 4-OHT treatment, the cells were able to regrow (data not shown), suggesting that, in these experimental settings, the senescent phenotype is not stable; this may be due to p16 inactivation and/or immortalization by the hTert. Therefore, we used these cells as a model presenting the OIS hallmarks and also used nonimmortalized HMEC that are known to display an irreversible senescence upon oncogenic stress induction to confirm a role of KCNA1 in OIS escape (17). Two independent KCNA1-targeting shRNAs were created and confirmed by quantitative reverse transcription (qRT)-PCR and immunofluorescence their ability to downregulate KCNA1 (Fig. 1B and C). KCNA1 knockdown with these new shRNAs enabled cells to escape MEK-induced growth arrest according

Downloaded from cancerres.aacrjournals.org on May 19, 2014. © 2013 American Association for Cancer Research.

Published OnlineFirst June 17, 2013; DOI: 10.1158/0008-5472.CAN-12-3690

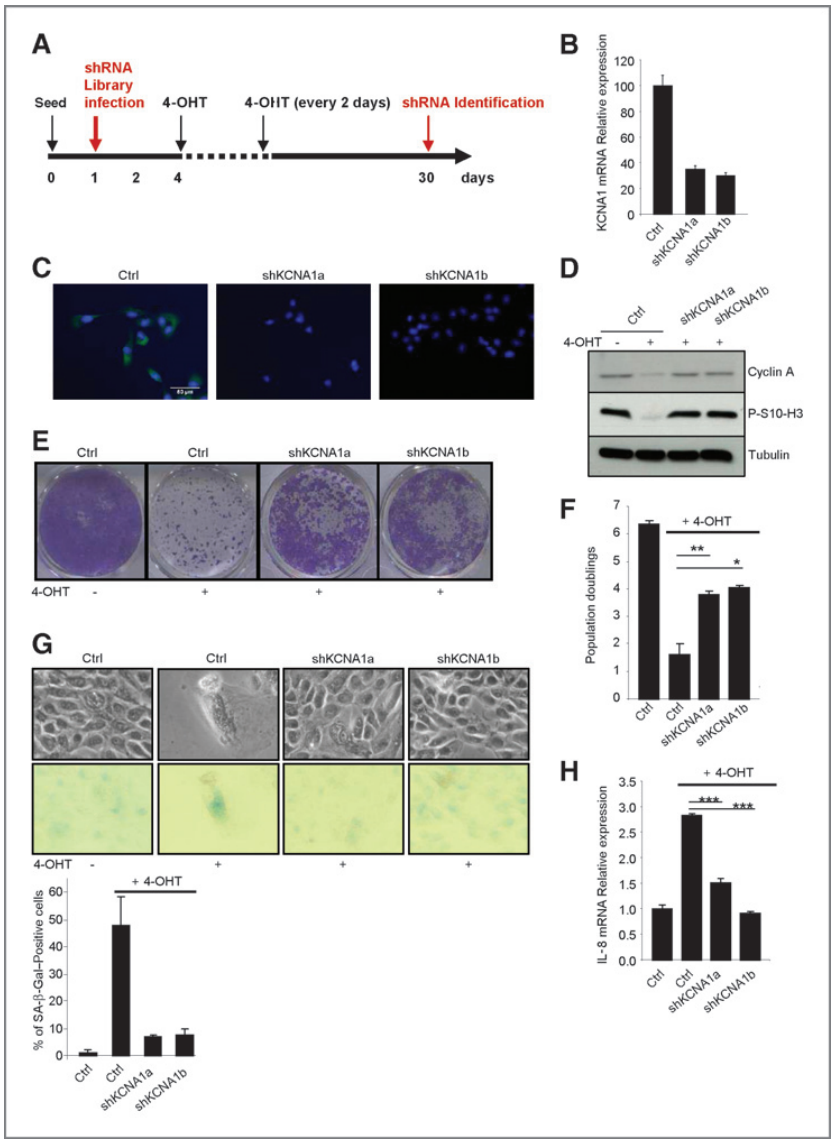

Figure 1. KCNA1 downregulation promotes escape from OIS hallmarks. A, design of the loss-of-function shRNA genetic screen in HMEC-TM cells. B, HMEC-TM cells were infected with a control or with two independent KCNA1-targeting shRNA vectors. After selection, RNAs were prepared and KCNA1 expression was measured by qRT-PCR. Relative KCNA1 mRNA expression was normalized to actin mRNA expression. The experiments shown are representative of three repeats. C, cells were treated with 4-OHT for 3 days, fixed by methanol, and knockdown of KCNA1 protein checked by immunofluorescence. The experiments shown are representative of two repeats. D, infected and selected HMEC-TM cells were seeded and treated 3 times with 4-OHT (400 nmol/L). Six to 10 days after the first 4-OHT treatment, the following assays were conducted. Cell extracts were prepared and analyzed by immunoblotting with antibodies detecting 2 proliferation markers, cyclin A and P-S10-H3. Tubulin was monitored to check the protein loading. The experiments shown are representative of two repeats. E, cells were PFA-fixed and cell growth was monitored with crystal violet staining. The experiments shown are representative of four repeats. F, 8 days after 4-OHT treatment, the cells were counted and number of population doublings calculated. The experiments shown are representative of two repeats. G, after fixation, SA-β-Gal activity assays were conducted. The experiments shown are representative of two repeats. H, RNA were prepared and IL-8 expression analyzed by qRT-PCR. Expression of IL-8 mRNA was normalized against actin mRNA. *, $P < 0.05$; **, $P < 0.01$ and ***, $P < 0.001$.

to the maintenance of cyclin A (accumulated in S, G_2, and early M phases), of P-S10-H3 (accumulated in late M phase; Fig. 1D), the ability to proliferate and form colonies (Fig. 1E and F), and to escape MEK-induced expression of the SA-β-Gal senescence marker (Fig. 1G) or MEK-induced IL-8 expression (Fig. 1H). It also favored an escape from RAF-induced OIS hallmarks

Downloaded from cancerres.aacrjournals.org on May 19, 2014. © 2013 American Association for Cancer Research.

Published OnlineFirst June 17, 2013; DOI: 10.1158/0008-5472.CAN-12-3690

(Supplementary Fig. S2A and B). The ability of KCNA1 knockdown to escape OIS in nonimmortalized HMEC-MEK:ER (HMEC-M) was confirmed by checking cell proliferation (Supplementary Fig. S3A), SA-β-Gal staining (Supplementary Fig. S3B), and IL-8 expression (Supplementary Fig. S3C).

KCNA1 is relocated to the membrane by the oncogenic stress

To verify KCNA1 expression is regulated by oncogenic stress, KCNA1 expression levels were monitored. Both KCNA1 transcripts (Fig. 2A) and KCNA1 protein (Fig. 2B and C and Supplementary Fig. S3D) were found to increase in response to oncogenic stress in immortalized and nonimmortalized HMEC. KCNA1 being a potassium channel involved in potassium efflux from the cell, we next investigated its subcellular localization by confocal microscopy during OIS. Interestingly, KCNA1 was found to localize at the cell membrane (Fig. 2C). To confirm its localization at the membrane during OIS, further immunofluorescence studies were conducted using antibodies recognizing the extracellular and intracellular part of KCNA1 on nonpermeabilized cells. Only the antibody that recognizes the extracellular KCNA1 labeled the cells, confirming the membrane localization of KCNA1 (Fig. 2D and Supplementary Fig. S3D). Both antibodies labeled the cells in a similar fashion in permeabilized cells confirming the specificity of the antibodies for KCNA1. Importantly, we also observed higher apical membrane KCNA1 levels in human prostatic–intraepithelial neoplasias, known to display OIS (7, 30), than in the adjacent normal tissue (Fig. 2E). This is consistent with our *in vitro* observations. Taken together, these results show that KCNA1 expression and localization are regulated by oncogenic stress and are involved in OIS. Interestingly, HMEC in replicative senescence also displayed an increased and membrane-localized KCNA1 (Supplementary Fig. S3E and 3F), suggesting it might have a role in senescence beyond oncogenic–stress-induced senescence.

Having shown that KCNA1 downregulation favors escape from oncogene-induced senescence, we next examined the effect of its constitutive expression. Surprisingly, constitutive expression of KCNA1 (Supplementary Fig. S4A and 4B) did not significantly reduce cell growth (Supplementary Fig. S4C) or induce the appearance of the SA-β-Gal senescence marker (Supplementary Fig. S4D). In addition, ectopically expressed KCNA1 failed to locate at the membrane according to the

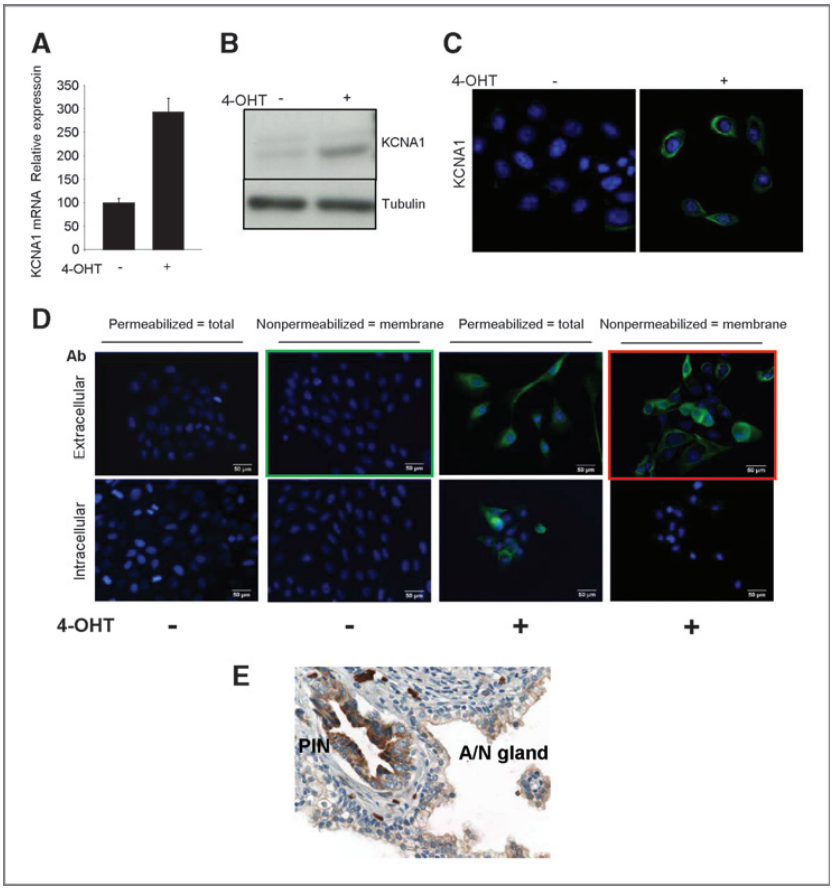

Figure 2. KCNA1 expression is upregulated and membrane-localized by the oncogenic stress. A, after 3 days of treatment with 4-OHT (400 nmol/L), RNAs were prepared and analyzed for KCNA1 expression by qRT-PCR. Expression of KCNA1 mRNA was normalized against actin mRNA. The experiments shown are representative of three repeats. B, after 4-OHT treatment, cell extracts were prepared and analyzed by immunoblotting with antibodies recognizing KCNA1 or tubulin to check loading. C, after 4-OHT treatment, HMEC-TM cells were fixed with methanol and KCNA1 was detected by immunofluorescence. Nuclei are counterstained by Hoechst. Cells were analyzed by confocal microscopy. The experiments shown are representative of three repeats. D, after 4-OHT treatment, HMEC-TM cells were fixed with methanol or PFA and total or membrane-bound KCNA1 were respectively detected by immunofluorescence using an antibody directed against the extracellular or the intracellular part of KCNA1 as indicated. The experiments shown are representative of three repeats. E, KCNA1 expression was analyzed in normal human prostatic gland and prostatic intraepithelial neoplasia.

Downloaded from cancerres.aacrjournals.org on May 19, 2014. © 2013 American Association for Cancer Research.

Published OnlineFirst June 17, 2013; DOI: 10.1158/0008-5472.CAN-12-3690

absence of labeling by immunofluorescence using the antibody recognizing the extracellular part of KCNA1 (Supplementary Fig. S4E, green panel). However, inducing the oncogenic stress allowed the overexpressed KCNA1 to relocate at the membrane (Supplementary Fig. S4E, red panel). To further confirm that a mechanism specifically related to oncogenic stress must be involved in triggering KCNA1 relocation to the membrane, we biotinylated the extracellular part of membrane-bound proteins of live cells with or without the induction of the oncogenic stress. Biotinylated KCNA1 was only observed in cells where oncogenic stress was induced. As expected, KCNA1 was biotinylated and, thus, membrane located upon oncogenic stress (Supplementary Fig. S4F). Accordingly, a low level of oncogenic stress, induced with a low dose of 4-OHT, was sufficient to trigger senescence hallmarks in cells ectopically expressing KCNA1 (Supplementary Fig. S4G–S4J). The same treatment when applied to control cells caused a growth slowdown but no senescence (Supplementary Fig. S4G–S4J). In addition, we observed the translocation of KCNA1 to occur as early as 8 hours after oncogenic stress induction (Supplementary Fig. S4K). Our data show that oncogenic stress induces KCNA1 relocation to the membrane, participating in oncogene-induced senescence. This translocation of KCNA1 to the membrane, probably, is an early event.

Phosphorylation of KCNA1 at Ser446 by PKA is involved on its cytoplasmic retention

We, next, wanted to discover the mechanism controlling the KCNA1 membrane relocation upon oncogenic stress. Electrophysiologic studies have shown that the function of KCNA1 is regulated by its phosphorylation at Ser446 by the protein kinase PKA (31). As phosphorylation is well known to affect subcellular localization, we examined whether phosphorylation by PKA might influence KCNA1 relocation. To this end, we used a pharmacologic inhibitor (H-89) and a PKA activator cocktail (forskolin + IBMx, F/I). Inhibition of PKA by H-89 resulted in endogenous KCNA1 relocation to the membrane even in the absence of oncogenic stress (Fig. 3A), whereas activation of PKA by F/I inhibited KCNA1 relocation in response to oncogenic stress (Fig. 3A). Ectopically expressed active PKA subunits (Supplementary Fig. S5A and 5B) also blocked endogenous KCNA1 membrane localization upon oncogenic stress (Supplementary Fig. S5C), whereas PKA inhibition by constitutively expressing PKA regulatory subunits resulted in KCNA1 increased expression and membrane localization (Supplementary Fig. S5D). Inhibition of PKA by H-89 also resulted in membrane localization of ectopically expressed KCNA1 (Fig. 3B), whereas PKA activation by F/I blocked ectopically expressed KCNA1 relocalization upon oncogenic stress, according to the result of membrane proteins biotinylation experiments (Fig. 3C).

In vitro, we found the purified KCNA1 protein to be phosphorylated by recombinant PKA, and this phosphorylation was abolished by the Ser446Ala mutation (Fig. 3D). In addition, by using a phosphoS/T PKA substrate-specific antibody on immunoprecipitated KCAN1, we observed a loss of KCNA1 phosphorylation after oncogenic stress induction (Fig. 3E). Accordingly, the KCNA1 S446A-mutant expressed in cells could localize to the membrane in the absence of oncogenic stress, in contrast to wild-type (WT) KCNA1 (Fig. 3F and G) present at a similar level (Supplementary Fig. S5E). Conversely, a phosphorylation-mimetic KCNA1-mutant (S446E) failed to relocate to the membrane in response to oncogenic stress, unlike WT KCNA1 (Fig. 3H and I), both proteins being expressed at similar levels (Supplementary Fig. S5F). In summary, KCNA1 relocation to the membrane is repressed by PKA phosphorylation at Ser-446, and this repression might be lost upon oncogenic stress.

Sustaining PKA activity and retaining KCNA1 in the cytoplasm allow OIS bypass

The effect of PKA-mediated phosphorylation on KCNA1 relocation in response to oncogenic stress suggests that PKA activity must be regulated by oncogenic stress. Accordingly, we found oncogenic stress to cause a strong decrease in PKA activity, as estimated by measuring total phosphorylation of PKA substrates. This decrease was countered by F/I PKA activator treatment or by expressing PKA catalytic subunits (Fig. 4A and Supplementary Fig. S6A) and mimicked by H-89 PKA inhibitor treatment (Fig. 4A). Functionally, maintaining PKA activity by ectopically expressing constitutively active PKA subunits or by treating cells with F/I resulted in escape from senescence in immortalized (Fig. 4B–E and Supplementary Fig. S6B) or nonimmortalized HMEC (Supplementary Fig. S7). H-89 PKA inhibitor treatment, which induced KCNA1 plasma membrane localization (Fig. 3A and B), induced a premature senescence (Fig. S6C and D).

We next took advantage of the KCNA1 S446E phosphomimetic mutant, which failed membrane localization upon oncogenic stress, and hypothesized that this mutant may act as a dominant negative form as this channel forms an homotetramer to allow potassium exit. If so, we expected this mutant to induce an OIS bypass as KCNA1 knockdown did. Indeed, ectopic expression of KCNA1 S446E allowed the cells to escape the growth arrest (Fig. 5A and B, for immortalized HMECs, and Supplementary Fig. S3A, for nonimmortalized HMECs), the appearance of the SA-β-Gal senescence marker (Fig. 5C, for immortalized HMECs, and Supplementary Fig. S3B, for nonimmortalized HMECs), and the increase of IL-8 mRNA expression (Fig. 5D, for immortalized HMECs, and Supplementary Fig. S3C, for nonimmortalized HMECs) induced by the oncogenic stress. Further confirming a dominant negative role of KCNA1 S446E mutant, we observed its expression inhibited endogenous (Supplementary Fig. S3D) or constitutively expressed WT KCNA1 (Fig. 5E) to relocate at the membrane upon oncogenic stress induction.

These results support the view that, by inhibiting PKA-induced KCNA1 S446 phosphorylation, oncogenic stress triggers relocation of KCNA1 to the membrane, a mechanism participating in senescence induction.

PKA–KCNA1-membrane potential pathway impacts OIS

As KCNA1 is a channel regulating potassium efflux through the plasma membrane (32) and, as it has relocated to the membrane in response to oncogenic stress, we next investigated whether directly adding potassium to the media might

Downloaded from cancerres.aacrjournals.org on May 19, 2014. © 2013 American Association for Cancer Research.

Published OnlineFirst June 17, 2013; DOI: 10.1158/0008-5472.CAN-12-3690

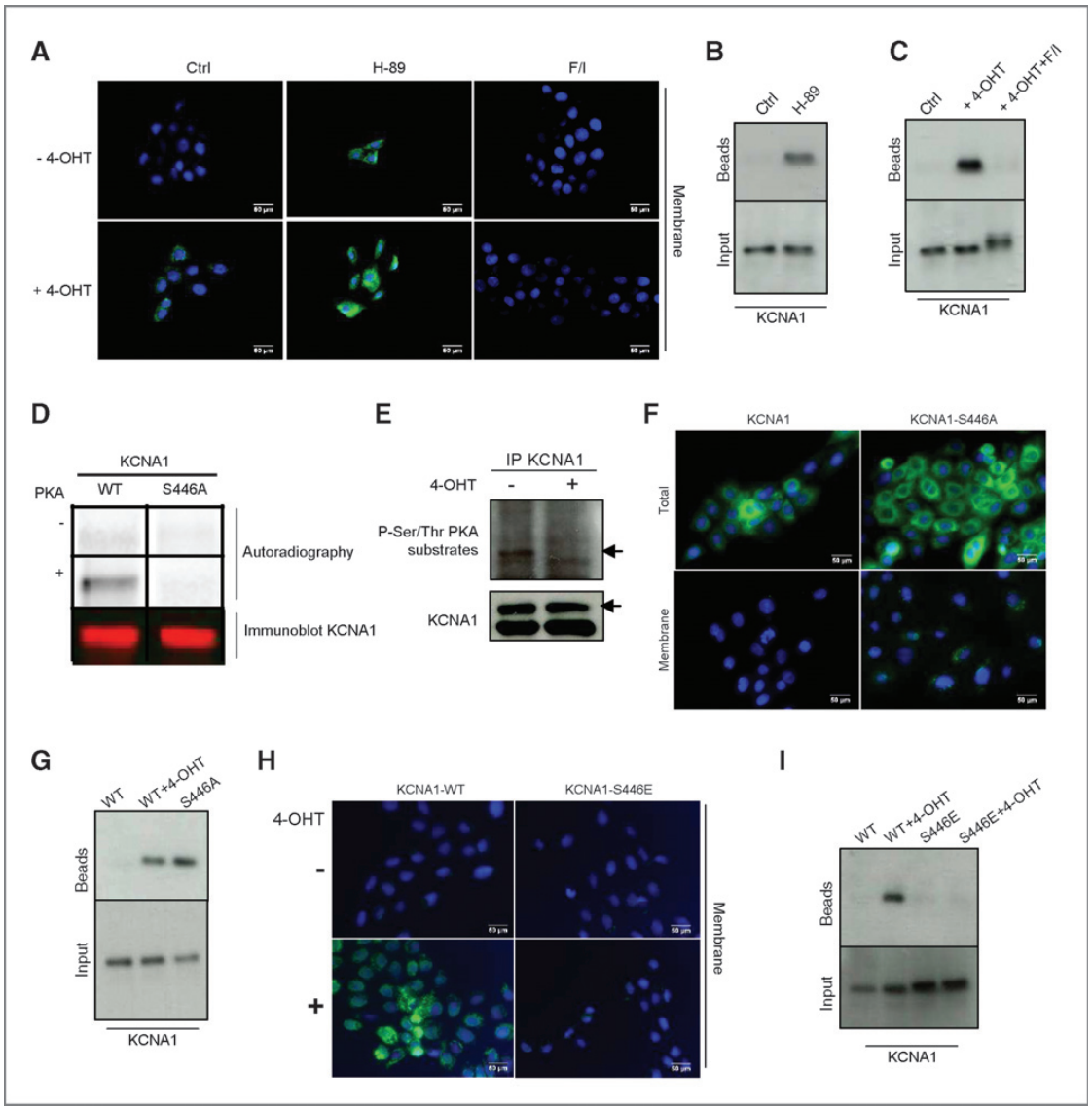

Figure 3. PKA phosphorylates S446 of KCNA1 and has an impact on KCNA1 localization. A, HMEC-TM cells were seeded and left untreated or treated with H-89 PKA inhibitor, with or without 4-OHT, or with the F/I PKA activator, with or without 4-OHT. After 3 daily treatments, the cells were fixed with PFA and subjected to KCNA1 immunofluorescence staining. The experiments shown are representative of two repeats. B and C, HMEC-TM cells expressing KCNA1 were treated with the indicated compounds, and membrane-bound proteins were biotinylated and purified by avidin beads. An immunoblot against total (input) and bound (beads) KCNA1 was next conducted. The experiments shown are representative of two repeats. D, HEK 293T cells were transfected with His-tagged WT- or S446A-mutant KCNA1. The WT and mutant KCNA1 proteins were affinity purified. Eluted KCNA1 protein was phosphorylated alone or with PKA and separated by SDS–PAGE. WT and S446A-mutant KCNA1 phosphorylation by PKA (phosphoimage) and the protein levels (immunoblot) are shown. The experiments shown are representative of two repeats. E, HMEC-TM constitutively expressing KCNA1 were left untreated or were treated three times by 4-OHT at 400 nmol/L. KCNA1 was then immunoprecipitated and an immunoblot was conducted against KCNA1 and against the phosphoS/T PKA substrates. F, HMEC-TM cells were infected with a vector encoding WT or S446A KCNA1, puromycin selected, and seeded. Immunfluorescence analysis against total or membrane KCNA1 were conducted. The experiments shown are representative of three repeats. G, HMEC-TM cells expressing the indicated KCNA1 proteins were biotinylated and the membrane-bound proteins purified. Total (input) and membrane bound (beads) KCNA1 were analyzed by immunoblot. The experiments shown are representative of two repeats. H, HMEC-TM cells were infected with a vector encoding WT or S446E KCNA1, puromycin selected, seeded, and treated with 4-OHT. Membrane-located KCNA1 was visualized by immunofluorescence. The experiments shown are representative of three repeats. I, HMEC-TM cells expressing WT or S446E mutant were treated with or without 4-OHT. Membrane-bound proteins were purified by avidin beads after biotinylation of proteins located at the membrane. Total and membrane-located KCNA1 were then analyzed by immunoblot. The experiments shown are representative of two repeats.

Downloaded from cancerres.aacrjournals.org on May 19, 2014. © 2013 American Association for Cancer Research.

Published OnlineFirst June 17, 2013; DOI: 10.1158/0008-5472.CAN-12-3690

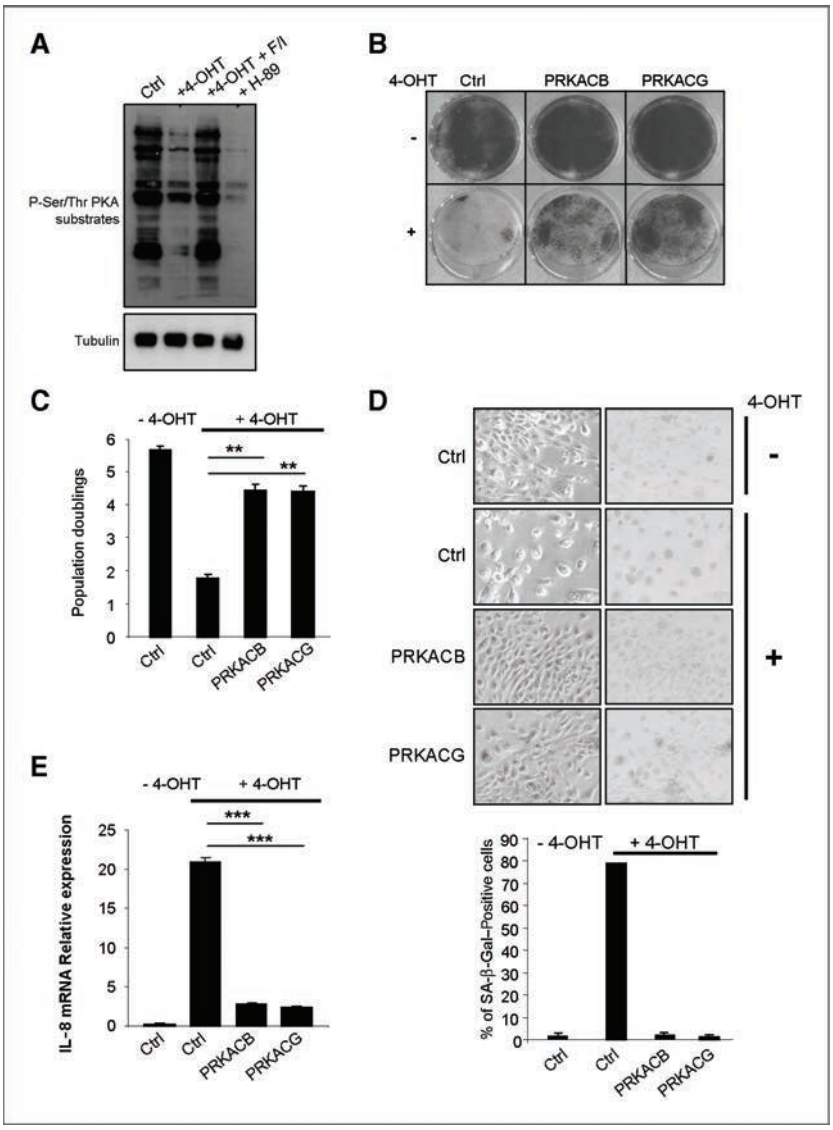

Figure 4. PKA phosphorylation of KCNA1 S446 impact OIS hallmarks escape. A, HMEC-TM cells were treated for 3 days with 4-OHT, 4-OHT + forskolin/IBMx, or H89. Cell extracts were prepared and analyzed by immunoblotting with antibodies directed against P-Ser/Thr PKA substrates and against tubulin for normalization. The experiments shown are representative of two repeats. B, HMEC-TR (RAF:ER) cells were infected with vectors driving expression of the PRKACB or PRKACG PKA catalytic subunit, selected, and seeded. The next day, the cells were left untreated or were treated 3 times and daily with 4-OHT. Eight days after the first treatment, cells were PFA-fixed. Colony assays were conducted by crystal violet staining. C, 7 days after 4-OHT treatment, cells were counted and the number of population doublings calculated. The experiment is representative of two independent repeats. D, the SA-β-Gal assay was conducted. The experiments shown are representative of three repeats. E, RNA were prepared and IL-8 expression analyzed by qRT-PCR. Expression of IL-8 mRNA was normalized against actin mRNA. **, $P < 0.01$ and ***, $P < 0.001$.

impact senescence. Interestingly, this treatment massively induced cellular senescence hallmarks as it resulted in a growth arrest (Fig. 6A and B) and the appearance of SA-β-Gal–positive cells (Fig. 6C) or increased IL-8 mRNA expression (Fig. 6D). Further suggesting a role of the extracellular potassium, an inhibitor of the sodium/potassium ATPase pump known to block potassium entry blocked cell growth (Fig. 6E and F), increased the proportion of SA-β-Gal–positive cells (Fig. 6G), and increased IL-8 mRNA expression (Fig. 6H).

Interestingly, the oncogenic stress was found to cause a variation in membrane potential (ΔV(m); Fig. 6I). This oncogenic–stress-induced variation was largely suppressed in KCNA1-knockdown cells, indicating that KCNA1 mediates it (Fig. 6I). Accordingly, the F/I PKA activator cocktail, which inhibits KCNA1 relocation to the membrane, suppressed the oncogenic–stress-induced membrane potential change, whereas the PKA inhibitor H-89, which induces KCNA1 membrane relocation in the absence of oncogenic stress, induced a membrane potential change (Fig. 6J). The phosphomimetic KCNA1 S446E mutant, in which membrane location by the oncogenic stress was prevented, did not display oncogenic–stress-induced membrane potential change (Fig. 6K). Accordingly, directly adding potassium (Fig. 6L) or blocking the sodium/potassium ATPase pump (Fig. 6M) provoked membrane potential changes. Together, these results support the view that KCNA1 membrane localization upon oncogenic stress results in membrane potential changes. These changes can be prevented by KCNA1 knockdown, by its retention to the

Downloaded from cancerres.aacrjournals.org on May 19, 2014. © 2013 American Association for Cancer Research.

Published OnlineFirst June 17, 2013; DOI: 10.1158/0008-5472.CAN-12-3690

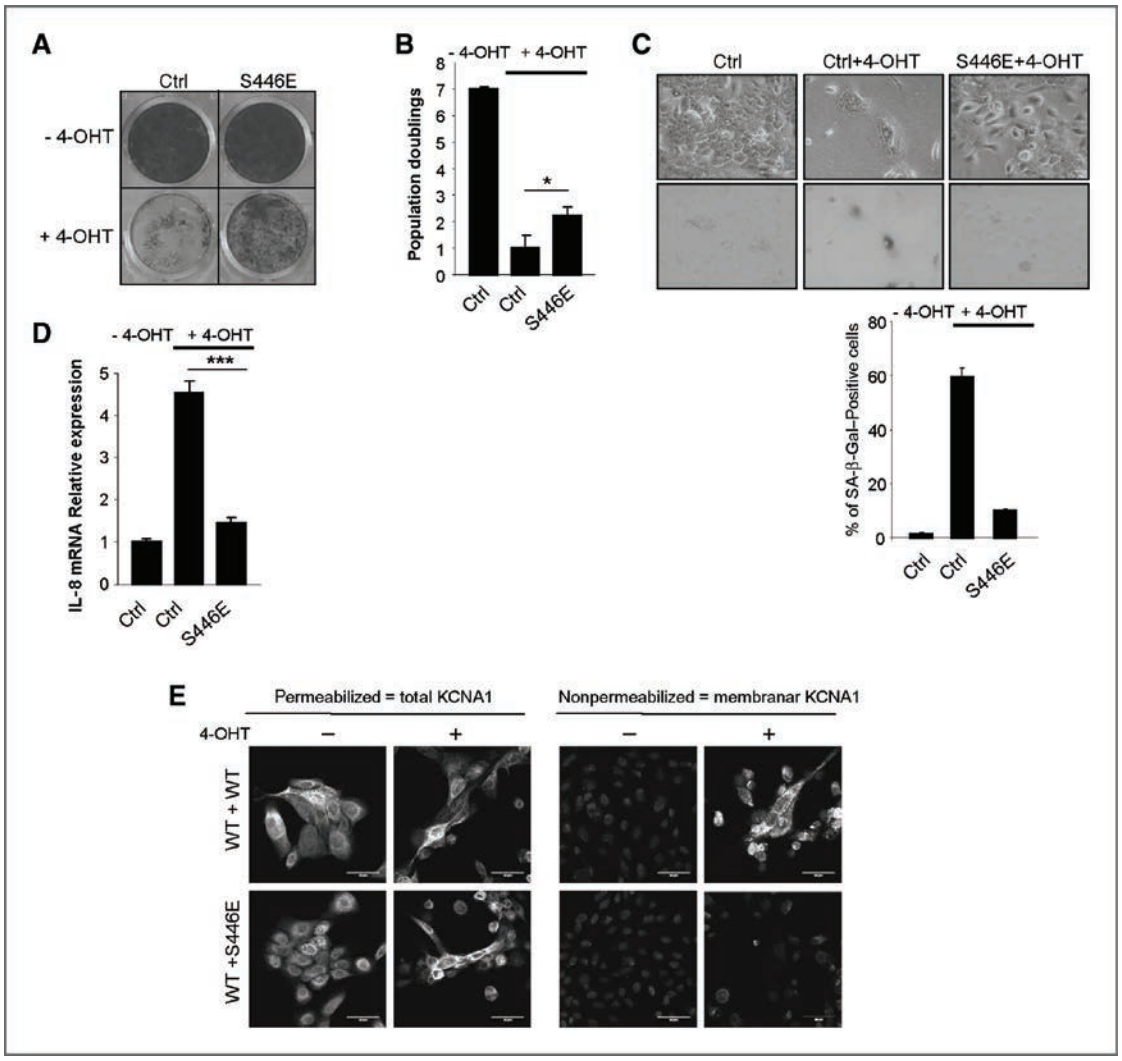

Figure 5. KCNA1 phosphomimetic mutant allows to bypass OIS hallmarks. A–D, HMEC-TM cells were infected with an empty or S446E KCNA1 vector, puromycin selected, seeded, and treated with or without 4-OHT for 3 days. A, 4 days later, cells were PFA-fixed and crystal violet-stained. The experiment is representative of three repeats. B, 4 days later, cells were counted and the number of population doublings calculated. The experiment is representative of two independent repeats. C, 4 days later, cells were analyzed for an SA-β-Gal activity test. The experiments shown are representative of two repeats. D, RNA were prepared and IL-8 expression analyzed by qRT-PCR. Expression of IL-8 mRNA was normalized against actin mRNA. E, HMEC-TM were infected with KCNA1 WT or with KCNA1 WT + S446E mutant. After 4-OHT treatment, HMEC-TM cells were fixed with methanol or PFA and total- or membrane-bound KCNA1 were respectively detected by immunofluorescence. The experiments shown are representative of two repeats. *, $P < 0.05$ and ***, $P < 0.001$.

cytoplasm through PKA activation, and by adding the phosphomimetic KCNA1 mutant. Conversely, these changes are mimicked by adding potassium or blocking potassium entry by the sodium/potassium ATPase pump inhibitor.

PKA–KCNA1 pathway impacts oncogene-induced transformation

Our results, thus far, show that the PKA–KCNA1 pathway regulates oncogenic-stress-induced senescence through a membrane potential change. We, next, investigated whether this pathway might regulate the transformation process. For this we used NIH3T3 cells, spontaneously immortalized cells derived from mouse embryonic fibroblasts. These cells can be transformed by oncogenic RAS (33). When expressed alone in NIH3T3 cells, KCNA1 failed to localize to the membrane, but when coexpressed with oncogenic RAS, it was found at the membrane (Fig. 7A and B). The ability of oncogenic RAS to promote KCNA1 relocation to the membrane was inhibited by

Downloaded from cancerres.aacrjournals.org on May 19, 2014. © 2013 American Association for Cancer Research.

Published OnlineFirst June 17, 2013; DOI: 10.1158/0008-5472.CAN-12-3690

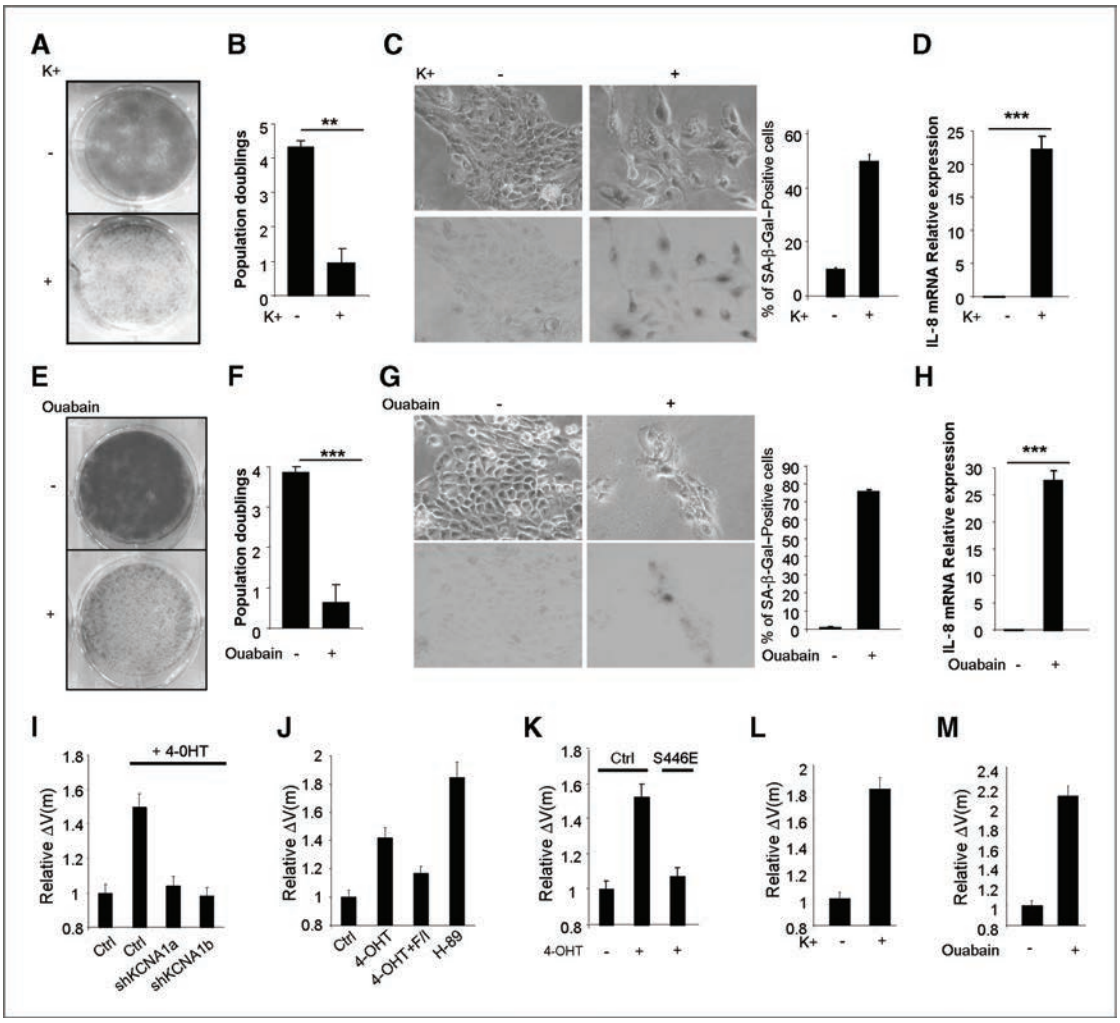

Figure 6. The PKA–KCNA1 pathway affects the membrane potential (Vm). A–D, HMEC-TM cells were incubated for 3 days in normal medium ($[K]^+$ extracellular 5 mmol/L) or in a medium containing 50 mmol/L KCl. A, cells were fixed and crystal violet-stained to measure cell growth. B, cells were counted and the number of population doublings calculated. C, cells were fixed and assayed for their SA-β-Gal activity. D, RNA were prepared and the level of IL-8 mRNA analyzed by qRT-PCR. The experiments shown are representative of at least two repeats. E–H, HMEC-TM cells were incubated twice or not at all with ouabain (50 nmol/L), an inhibitor of the Na^+/K^+ ATPase pump. E, cell growth was measured with crystal violet-staining. F, cells were counted and the number of population doublings calculated. G, cells were fixed and assayed for their SA-β-Gal activity. H, RNA were prepared and the level of IL-8 mRNA analyzed by qRT-PCR. The experiments shown are representative of at least two repeats. I, HMEC-TM cells infected with control or KCNA1–shRNA-encoding vector, selected, and treated with or without 4-OHT for 3 days. They were, next, incubated with DiBAC4 dye to measure their membrane potential [ΔV(m)] by cytometry. The experiments shown are representative of three repeats. J, HMEC-TM cells were treated for 3 days with 4-OHT, with or without the F/I PKA activator or the PKA inhibitor H89. Variation of membrane potential [ΔV(m)] of these cells were determined with DiBAC4 by cytometry. The experiments shown are representative of two repeats. K, HMEC-TM cells infected with control or S446E KCNA1 vectors were selected and treated with or without 4-OHT for 3 days. They were next incubated with DiBAC4 dye to measure their membrane potential [ΔV(m)]. The experiments shown are representative of two repeats. L, HMEC-TM cells were incubated for 3 days in a medium with or without 50 mmol/L KCl. The membrane potential was determined by flow cytometry as described earlier. The experiments shown are representative of two repeats. M, HMEC-TM cells were incubated twice or not at all with ouabain (50 nmol/L). The membrane potential was determined by flow cytometry as described earlier. The experiments shown are representative of two repeats. **, $P < 0.01$ and ***, $P < 0.001$.

constitutive PKA subunit expression (Fig. 7A and B) or PKA induction by F/I (Supplementary Fig. S8A) as on human epithelial cells. As expected, RAS-induced relocation of KCNA1 to the membrane resulted in membrane potential alteration (Fig. 7C), while its sequestration in the cytoplasm caused by F/I-triggered PKA induction maintained the membrane potential (Fig. 7C). Importantly, RAS-induced transformation was blocked when KCNA1 and oncogenic RAS were coexpressed,

Downloaded from cancerres.aacrjournals.org on May 19, 2014. © 2013 American Association for Cancer Research.

Published OnlineFirst June 17, 2013; DOI: 10.1158/0008-5472.CAN-12-3690

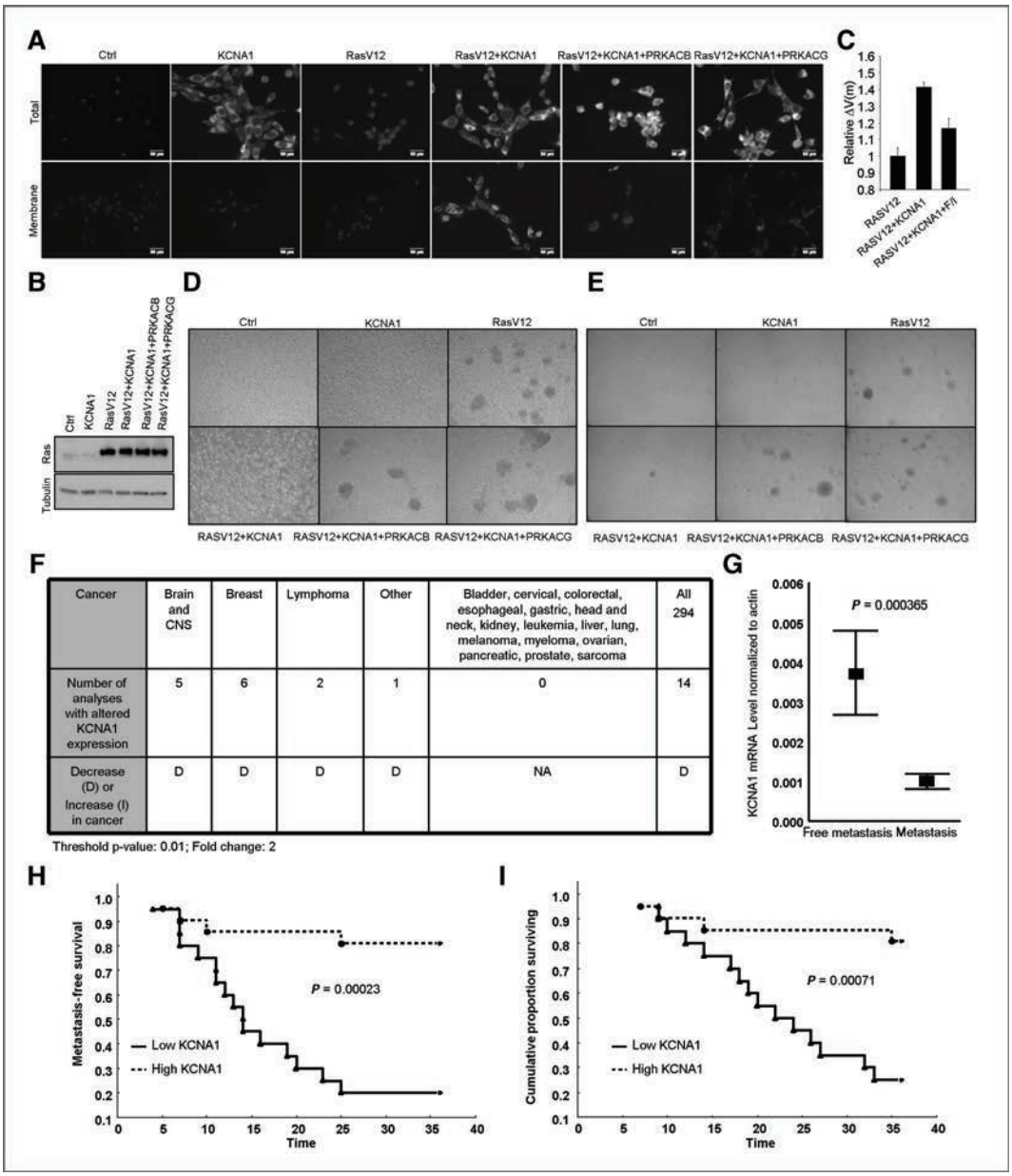

Cancer	Brain and CNS	Breast	Lymphoma	Other	Bladder, cervical, colorectal, esophageal, gastric, head and neck, kidney, leukemia, liver, lung, melanoma, myeloma, ovarian, pancreatic, prostate, sarcoma	All 294
Number of analyses with altered KCNA1 expression	5	6	2	1	0	14
Decrease (D) or Increase (I) in cancer	D	D	D	D	NA	D

Figure 7. The KCNA1 pathway regulates RAS-induced transformation and predicts the risk of developing breast metastases. A, NIH3T3 cells were infected with indicated vectors and selected. Total or membrane-associated KCNA1 was detected by immunofluorescence. The experiments shown are representative of two repeats. B, cell extracts were prepared and analyzed by immunoblot using an antibody directed against RAS. C, NIH3T3 cells expressing the indicated proteins were untreated or treated with F/I for 3 days. The membrane potential was measured with DiBAC4. The experiments shown are representative of two repeats. D, NIH3T3 cells expressing indicated proteins were seeded at the same density. Five days later, representative images were taken and presented. The experiments shown are representative of two repeats. E, 25,000 NIH3T3 cells were seeded in agar. Eleven days later, representative images were taken and presented. The experiments shown are representative of three repeats. F, summary of the KCNA1 mRNA expression found in various cancers as compared with normal counterparts using the oncomine database. G–I, RNA from human primary breast cancer samples were analyzed for KCNA1 mRNA expression by qRT-PCR and normalized against actin mRNA. PCRs were conducted in triplicates. G, relative KCNA1 mRNA expression in samples coming from patient displaying or not a metastasis in 3 years was represented. Means ± SEM are represented. *P* values were determined using the Mann–Whitney U test. H–I, cancer samples were, next, split in 2 groups (high and low KCNA1 levels) and Kaplan–Meier analyses of the probability to live without metastases (H) and to survive (I) were conducted. *P* values were calculated using a log-rank test.

Downloaded from cancerres.aacrjournals.org on May 19, 2014. © 2013 American Association for Cancer Research.

Published OnlineFirst June 17, 2013; DOI: 10.1158/0008-5472.CAN-12-3690

and restored by expression of constitutively active PKA catalytic subunits (Fig. 7D and E) and by F/I treatment (Supplementary Fig. S8B). Interestingly, the phosphomimetic S446E KCNA1 mutant was unable to localize at the membrane (Supplementary Fig. S8D), to induce a membrane potential change (Supplementary Fig. S8C), and to block transformation (Supplementary Fig. S8D) upon RAS expression. This confirms the inhibitory function of PKA-mediated S446 phosphorylation.

A search in the Oncomine database, a cancer microarray database allowing to conduct differential expression analyses comparing most major types of cancer with respective normal tissues, showed that some cancers were found to display an unusually low KCNA1 mRNA level (Fig. 7F). For example, six analyses showed a lower KCNA1 transcript level in breast cancer samples than in normal counterparts (Fig. 7F), and this finding was confirmed at protein level in an independent study (26). We, next, analyzed KCNA1 mRNA expression levels of nontreated breast primary tumors of 41 patients. Twenty displayed metastasis and died before 36 months and 21 showed no metastasis and survived beyond 36 months. Interestingly, KCNA1 mRNA expression was found to be significantly higher in the group displaying no metastasis (Fig. 7G). In order to examine whether low levels of KCNA1 might correlate with an increased risk of developing metastasis and of dying, we conducted a Kaplan–Meier analysis. Tumors displaying higher KCNA1 expression than the median value (≥ 0.00137; including this tumor) was included in the group "high", whereas tumors expressing lower levels than the median value (<0.00137) were included in the group "low". Interestingly, low levels of KCNA1 were associated with an increased risk of developing metastasis and of dying (Fig. 7H and I). Among these 41 primary tumors, 34 were fully characterized for HER-2, ER, and PR expression. We cannot observe any correlation between KCNA1 mRNA levels and luminal A or triple-negative breast cancer subgroups (Supplementary Fig. S9A). The number of samples for luminal B or HER-2$^+$ subtypes was too low to draw any conclusion; nevertheless, our results might suggest that KCNA1 mRNA levels are lower in Her-2$^+$ breast tumors (Supplementary Fig. S9A). As expected, triple-negative subgroups displayed higher risk of metastasis and of dying than the luminal A group (Supplementary Fig. S9B and 9C), showing that KCNA1 was an independent variable for metastasis and survival. Taken together, these data support a functional role of KCNA1 in cancer.

Discussion

Our results show that a downregulation of KCNA1, a voltage-gated delayed potassium channel that is phylogenetically related to the *Drosophila* Shaker channel, leads to an OIS escape. Interestingly, KCNA1 localization is tightly regulated during OIS by PKA activity. Indeed, we show that an inhibition of PKA activity results in a loss of S446 KCNA1 phosphorylation and a subsequent localization of KCNA1 to the membrane. The KCNA1–PKA pathway regulates the membrane potential and directly impacting the membrane potential induces senescence in nontransformed cells. Interestingly, restoring KCNA1 at the membrane inhibits oncogene-induced cellular transformation in NIHT3T3 cells. In those cells, KCNA1 blocks oncogene-induced transformation without inducing cellular senescence, suggesting a more general tumor-suppressive function of KCNA1.

These data strongly support that the function of KCNA1 as a regulator of the extracellular concentration of potassium is required for its antioncogenic effects. However, to definitively prove it, it would be interesting to generate a KCNA1 point mutant able to translocate to the plasma membrane in response to the oncogenic stress, but unable to open and to allow potassium exit.

Evidence for the tumor-suppressive activity for KCNA1 is also provided by the decreased expression of KCNA1 observed in breast cancers (26) and also our observation that low level of KCNA1 correlates with increase aggressiveness of primary breast tumors. Furthermore, the *KCNA1* gene is known to be repressed by the polycomb repressive complexes and by DNA methyl transferases (34, 35), two systems that are involved in the repression of tumor-suppressive genes (36, 37), and this supports a possible tumor-suppressive role for KCNA1.

We observed that oncogenic stress as well as a direct PKA inhibition results in an increased KCNA1 expression. Interestingly, cAMP and PKA activity has been associated with KCNA1 mRNA destabilization (38). However, we show that the membrane localization of KCNA1 is not due to its increase in RNA or protein expression, because overexpression of KCNA1 by ectopic expression does not result in increased membrane localization. The membrane localization occurs only after the induction of oncogenic stress, by PKA inhibition or by expressing a mutated the S446A, a nonphosphorylable amino acid. We then end up with a model where PKA controls the level and the localization of KCNA1. Regulation of the tumor-suppressive function of KCNA1 in this study by the PKA, which is considered to be a possible target for cancer therapy due to its involvement in tumor initiation and progression in numerous cancers (39), suggests that targeting PKA in cancer may activate the KCNA1 tumor-suppressive pathway.

Our data also indicate that in nontransformed cells, the oncogenic stress results in an inhibition of the PKA activity. It has been reported that OIS induces feedback loops aiming to switch off the oncogenic signal (28). As PKA activity positively regulates the Raf–MEK pathway (40, 41), we speculate that the decrease in the PKA activity during OIS that we observed can be due to activation of such loops.

The use of KCNA1 S446E phosphomimetic mutant seems to behave as a dominant negative form as it favors OIS escape and inhibits membrane potential changes during the oncogenic stress. KCNA1 exerts its potassium channel function under an homotetramer form, and our results support the view that, in the tetramer, the phosphorylated form is dominant over the nonphosphorylated one.

Interestingly, the OIS in the HMECs, the cellular model we used, does not involve p16 as it is not expressed because of its hypermethylation (19), and does not required p53 as previously shown (17) and confirmed by us (data not shown). A major future challenge will, thus, be to find out how the exit of potassium and membrane potential changes regulate senescence outcome.

Downloaded from cancerres.aacrjournals.org on May 19, 2014. © 2013 American Association for Cancer Research.

Published OnlineFirst June 17, 2013; DOI: 10.1158/0008-5472.CAN-12-3690

Thus, overall, our data support the view that the PKA-controlled KCNA1 membrane localization switch regulates the response to oncogenic stress. When functional, this pathway should contribute to sensing the aberrant oncogenic signal by responding to senescence induction and blocking of transformation. When the pathway is nonfunctional, this could favor disabling of the senescence program and increase the oncogene-induced transformation.

Disclosure of Potential Conflicts of Interest

No potential conflicts of interest were disclosed.

Authors' Contributions

Conception and design: H. Lallet—Daher, C. Wiel, A. Augert, D. Bernard
Development of methodology: H. Lallet–Daher, C. Wiel, D. Gitenay, N. Navaratnam, D. Bernard
Acquisition of data (provided animals, acquired and managed patients, provided facilities, etc.): N. Navaratnam, S. Verbeke, D. Carling. D. Vindrieux
Analysis and interpretation of data (e.g., statistical analysis, biostatistics, computational analysis): H. Lallet–Daher, C. Wiel, D. Gitenay, B. Le Calve, S. Aubert, D. Vindrieux, D. Bernard
Writing, review, and/or revision of the manuscript: H. Lallet–Daher, N. Navaratnam, A. Augert, S. Aubert, D. Bernard
Administrative, technical, or material support (i.e., reporting or organizing data, constructing databases): C. Wiel, D. Bernard
Study supervision: D. Bernard

Acknowledgments

The authors thank Richard Iggo, Mylène Ferrand, Marc Samyn, and Hélène Simonnet and other laboratory members for their help, suggestions, and discussions.

Grant Support

This work was carried out with the financial support of the "Fondation de France", "Association pour la Recherche sur le Cancer", "Ligue nationale contre le Cancer, comité de Savoie", "Institut National du Cancer", and "RTRS Fondation Synergie Lyon Cancer". H. Lallet–Daher is supported by the Fondation des Treilles.

The costs of publication of this article were defrayed in part by the payment of page charges. This article must therefore be hereby marked *advertisement* in accordance with 18 U.S.C. Section 1734 solely to indicate this fact.

Received September 20, 2012; revised May 24, 2013; accepted June 1, 2013; published OnlineFirst June 17, 2013.

References

1. Bodnar AG, Ouellette M, Frolkis M, Holt SE, Chiu CP, Morin GB, et al. Extension of life-span by introduction of telomerase into normal human cells. Science 1998;279:349–52.
2. Vaziri H, Benchimol S. Reconstitution of telomerase activity in normal human cells leads to elongation of telomeres and extended replicative life span. Curr Biol 1998;8:279–82.
3. Adams PD. Healing and hurting: molecular mechanisms, functions, and pathologies of cellular senescence. Mol Cell 2009;36:2–14.
4. Collado M, Serrano M. Senescence in tumours: evidence from mice and humans. Nat Rev Cancer 2010;10:51–7.
5. Serrano M, Lin AW, McCurrach ME, Beach D, Lowe SW. Oncogenic ras provokes premature cell senescence associated with accumulation of p53 and p16INK4a. Cell 1997;88:593–602.
6. Ben Porath I, Weinberg RA. The signals and pathways activating cellular senescence. Int J Biochem Cell Biol 2005;37:961–76.
7. Acosta JC, O'Loghlen A, Banito A, Guijarro MV, Augert A, Raguz S, et al. Chemokine signaling via the CXCR2 receptor reinforces senescence. Cell 2008;133:1006–18.
8. d'Adda di Fagagna F. Living on a break: cellular senescence as a DNA-damage response. Nat Rev Cancer 2008;8:512–22,.
9. Kuilman T, Michaloglou C, Vredeveld LCW, Douma S, van Doorn R, Desmet C J, et al. Oncogene-induced senescence relayed by an interleukin-dependent inflammatory network. Cell 2008;133: 1019–31.
10. Young AR, Narita M, Ferreira M, Kirschner K, Sadaie M, Darot JF, et al. Autophagy mediates the mitotic senescence transition. Genes Dev 2009;23:798–803.
11. Itahana K, Campisi J, Dimri G. Mechanisms of cellular senescence in human and mouse cells. Biogerontology 2004;5:1–10.
12. Christoffersen NR, Shalgi R, Frankel LB, Leucci E, Lees M, Klausen M, et al. p53-independent upregulation of miR-34a during oncogene-induced senescence represses MYC. Cell Death Differ 2010;17: 236–45.
13. Ewald JA, Desotelle JA, Wilding G, Jarrard DF. Therapy-induced senescence in cancer. J Natl Cancer Inst 2010;102:1536–46.
14. Humbert N, Navaratnam N, Augert A, Da Costa M, Martien S, Wang J, et al. Regulation of ploidy and senescence by the AMPK-related kinase NUAK1. EMBO J 2010;29:376–86.
15. Lin HK, Chen Z, Wang G, Nardella C, Lee SW, Chan CH, et al. Skp2 targeting suppresses tumorigenesis by Arf-p53-independent cellular senescence. Nature 2010;464:374–9.
16. Scurr LL, Pupo GM, Becker TM, Lai K, Schrama D, Haferkamp S, et al. IGFBP7 is not required for B-RAF-induced melanocyte senescence. Cell 2010;141:717–27.
17. Cipriano R, Kan CE, Graham J, Danielpour D, Stampfer M, Jackson MW. TGF-beta signaling engages an ATM-CHK2-p53-independent RAS-induced senescence and prevents malignant transformation in human mammary epithelial cells. Proc Natl Acad Sci USA 2011;108: 8668–73.
18. Bianchi-Smiraglia A, Nikiforov MA. Controversial aspects of oncogene-induced senescence. Cell Cycle 2012;11:4147–51.
19. Kiyono T, Foster SA, Koop JI, McDougall JK, Galloway DA, Klingelhutz AJ. Both Rb/p16INK4a inactivation and telomerase activity are required to immortalize human epithelial cells. Nature 1998;396:84–8.
20. Morita S, Kojima T, Kitamura T. Plat-E: an efficient and stable system for transient packaging of retroviruses. Gene Ther 2000;7:1063–6.
21. Woods D, Parry D, Cherwinski H, Bosch E, Lees E, McMahon M. Raf-induced proliferation or cell cycle arrest is determined by the level of Raf activity with arrest mediated by p21Cip1. Mol Cell Biol 1997;17: 5598–611.
22. Boehm JS, Zhao JJ, Yao J, Kim SY, Firestein R, Dunn IF, et al. Integrative genomic approaches identify IKBKE as a breast cancer oncogene. Cell 2007;129:1065–79.
23. Vuong BQ, Lee M, Kabir S, Irimia C, Macchiarulo S, McKnight GS, et al. Specific recruitment of protein kinase A to the immunoglobulin locus regulates class-switch recombination. Nat Immunol 2009;10:420–6.
24. Bernard D, Quatannens B, Begue A, Vandenbunder B, Abbadie C. Antiproliferative and antiapoptotic effects of crel may occur within the same cells via the up-regulation of manganese superoxide dismutase. Cancer Res 2001;61:2656–64.
25. Augert A, Payre C, de Launoit Y, Gil J, Lambeau G, Bernard D. The M-type receptor PLA2R regulates senescence through the p53 pathway. EMBO Rep 2009;10:271–7.
26. Brevet M, Ahidouch A, Sevestre H, Merviel P, El Hiani Y, Robbe M, et al. Expression of K+ channels in normal and cancerous human breast. Histol Histopathol 2008;23:965–72.
27. Acosta JC, O'Loghlen A, Banito A, Raguz S, Gil J. Control of senescence by CXCR2 and its ligands. Cell Cycle 2008;7:2956–9.
28. Courtois-Cox S, Genther Williams SM, Reczek EE, Johnson BW, McGillicuddy LT, Johannessen CM, et al. A negative feedback signaling network underlies oncogene-induced senescence. Cancer Cell 2006;10:459–72.
29. Collado M, Gil J, Efeyan A, Guerra C, Schuhmacher AJ, Barradas M, et al. Tumour biology: Senescence in premalignant tumours. Nature 2005;436:642.
30. Chen Z, Trotman LC, Shaffer D, Lin HK, Dotan ZA, Niki M, et al. Crucial role of p53-dependent cellular senescence in suppression of Pten-deficient tumorigenesis. Nature 2005;436:725–30.

Downloaded from cancerres.aacrjournals.org on May 19, 2014. © 2013 American Association for Cancer Research.

Published OnlineFirst June 17, 2013; DOI: 10.1158/0008-5472.CAN-12-3690

31. Levin G, Chikvashvili D, Singer-Lahat D, Peretz T, Thornhill WB, Lotan I. Phosphorylation of a K +channel alpha subunit modulates the inactivation conferred by a beta subunit. Involvement of cytoskeleton. J Biol Chem 1996;271:29321–8.
32. Chandy KG, Williams CB, Spencer RH, Aguilar BA, Ghanshani S, Tempel BL, et al. A family of three mouse potassium channel genes with intronless coding regions. Science 1990;247:973–5.
33. McCoy MS, Toole JJ, Cunningham JM, Chang EH, Lowy DR, Weinberg RA. Characterization of a human colon/lung carcinoma oncogene. Nature 1983;302:79–81.
34. Vire E, Brenner C, Deplus R, Blanchon L, Fraga M, Didelot C, et al. The Polycomb group protein EZH2 directly controls DNA methylation. Nature 2005;439:871–4.
35. Kirmizis A, Bartley SM, Kuzmichev A, Margueron R, Reinberg D, Green R, et al. Silencing of human polycomb target genes is associated with methylation of histone H3 Lys 27. Genes Dev 2004;18:1592–605.
36. Ballestar E, Esteller M. Epigenetic gene regulation in cancer. Adv Genet 2008;61:247–67.
37. Tsai HC, Baylin SB. Cancer epigenetics: linking basic biology to clinical medicine. Cell Res 2011;21:502–17.
38. Allen ML, Koh DS, Tempel BL. Cyclic AMP regulates potassium channel expression in C6 glioma by destabilizing Kv1.1 mRNA. Proc Natl Acad Sci U S A 1998;95:7693–8.
39. Naviglio S, Caraglia M, Abbruzzese A, Chiosi E, Di Gesto D, Marra M, et al. Protein kinase A as a biological target in cancer therapy. Expert Opin Ther Targets 2009;13:83–92.
40. Francis H, Glaser S, Ueno Y, Lesage G, Marucci L, Benedetti A, et al. cAMP stimulates the secretory and proliferative capacity of the rat intrahepatic biliary epithelium through changes in the PKA/Src/MEK/ERK1/2 pathway. J Hepatol 2004;41:528–37.
41. Gomes E, Papa L, Hao T, Rockwell P. The VEGFR2 and PKA pathways converge at MEK/ERK1/2 to promote survival in serum deprived neuronal cells. Mol Cell Biochem 2007;305:179–90.

Downloaded from cancerres.aacrjournals.org on May 19, 2014. © 2013 American Association for Cancer Research.

Supplemental Figure Legends

Figure S1. Screening and cellular model of oncogenic stress induce senescence hallmarks. A, HMEC-TM were infected with a control GFP encoding vector or with the 7 pools of shRNA-encoding vectors and treated as explained in the figure 1A. After 30 days, cells were divided into two; half for preparation of gDNA and half stained by crystal violet. Representative dishes are displayed. B, List of the shRNA identified in the cells that have escaped oncogenic-stress induced growth arrest. C-H**,** HMEC-TM were treated daily during three days by 400 nM 4-OHT. Two to 5 days later the various analyses were performed. C, Cell extracts were prepared and expression of the indicated proteins was analyzed by immunoblot. D, Cells were PFA-fixed and crystal violet-stained. E, Population doublings were counted for each condition. F, Cells were PFA-fixed and processed for SA-β-Gal staining. G, RNAs were prepared and retro-transcribed. Quantitative PCR were performed against the indicated senescence markers and normalized to mRNA actin levels.

Figure S2. KCNA1 impacts RAF-induced hallmarks of OIS**.** HMEC-TR (RAF:ER) cells were infected with control or KCNA1-shRNA encoding vectors and selected. Cells were seeded at the same density and when indicated were treated with daily 4-OHT treatment during 3 days. Three days later the various assays were performed. A, Cells were PFA-fixed and crystal-violet stained or B, assayed for their SA-β-Gal activity.

Figure S3. KCNA1 knockdown and KCNA1 mutant S446E promote OIS escape**.** Non-immortalized HMEC were infected with the MEK:ER encoding vector, along with the indicated vectors (ctrl, shKCNA1 or KCNA1S446E). After selection, cells were seeded and treated twice with 4OHT at 100 nM. Twenty days post-seeding cells were analyzed. A, Cells were counted and population doublings were calculated. B, Cells were PFA-fixed, and a SA-β-gal activity test was performed. C, Total RNA were extracted, and level of IL8 mRNA was assessed by RT-QPCR. D, The day after the second 4-OHT treatment, cells were fixed with PFA (membrane) or methanol

(total), and immunofluorescence against KCNA1 was performed. E, Fifty thousand young or senescing HMEC were seeded in a well of 12-cell plate. Four days later, cells were fixed and stained by crystal violet. F, Young and senescing HMEC were fixed and analyzed for KCNA1 localization by immunofluorescence (scale bar: 50 μM).

Figure S4. Membrane-associated KCNA1 favors OIS hallmarks. HMEC-TM cells were infected by a control or KCNA1 encoding vector and selected. A, Cell extracts were prepared and KCNA1 overexpression checked by immunoblot. B, Total KCNA1 levels were detected by immunofluorescence. C, Six days after seeding, the cells were PFA-fixed and crystal violet-stained to monitor growth or D, cells were fixed and an SA-b-Gal assay was performed. E, After seeding, HMEC-TM cells expressing KCNA1 were treated 3 times with or without low doses of 4-OHT (100 nM). The day after the last 4-OHT treatment, the KCNA1-overexpressing cells were fixed with methanol or PFA and total or membrane bound KCNA1 were respectively detected by immunofluorescence. Nuclei are counterstained by Hoechst. F, After seeding, cells were treated with or without 4-OHT. Membrane bound proteins were biotinylated and purified by avidin beads. An immunoblot against total and bound KCNA1 was next performed. G, Seven days after the first 4-OHT treatment, cell growth was monitored with crystal violet-staining. H, seven days after the first 4-OHT treatment cells were counted and the number of population doublings calculated or I, RNA prepared and analyzed by RTqPCR for relative IL8 mRNA expression. J, Five days after the first 4-OHT treatment, senescence was monitored by SA-β-Gal staining. K, HMEC-TM cells were left untreated or were treated with 400 nM 4-OHT. Eight hours later, cells were PFA-fixed and membrane-associated KCNA1 examined after an immunofluorescence labeling.

Figure S5. KCNA1 localization is regulated by PKA. A, HMEC-TR (RAF:ER) cells were infected with control or flagged-PKA catalytic subunits (ctrl, PRKACB or PRKACG) and selected. Cells were next methanol-fixed and analyzed for PRKA expression using an anti-flag antibody by

immunofluorescence. B, Alternatively, cell extracts were prepared and PRKACB/G constitutive expression checked by immunoblot using an Ab directed against the flag tag. C, Cells were treated with or without 4-OHT for 3 days. Cells were then fixed by methanol or PFA and an immunofluorescence against KCNA1 performed. D, HMEC-TM cells were infected with control or PKA regulatory subunits (PRKAR1A or PRKAR2A) and analyzed for KCNA1 expression (in red as the encoding vectors co-expressed the GFP). E-F, HMEC-TM cells were infected with the indicated vectors and puromycin selected. Cell extracts were prepared and analyzed for the expression KCNA1.

Figure S6. PKA activation favors escape from OIS hallmarks. A, HMEC-TM were treated with or without 4-OHT for 3 days. Proteins were extracted and PKA-dependent phosphorylation was analyzed by immunoblot using a specific antibody. B, HMEC-TM cells were treated everyday during 3 days with the indicated chemicals. Next cells were fixed and assayed for their SA-β-Gal activity. C, One day after seeding, HMEC-TM were treated with or without H-89 for 3 days, fixed by PFA and crystal violet stained or D, assayed for SA-β-Gal activity.

Figure S7. PKA activation favors OIS escape. Non-immortalized HMEC were infected with the RAF:ER encoding vector, along with the PKA catalytic subunits (PRKACB/G). After selection, cells were seeded and treated twice with 4-OHT at 100 nM. Twenty days post-seeding cells were analyzed. A, The day after the second 4-OHT treatment, cells were fixed with PFA (membrane) or methanol (total), and immunofluorescence against kCNA1 was performed. B, Cells were counted and population doublings were calculated. C, Cells were PFA-fixed, and a SA-β-gal activity test was performed. D, Total RNA were extracted, and level of IL8 mRNA was assessed by RT-QPCR.

Figure S8. PKA activation reverses the transformation blockage induced by KCNA1. NIH3T3 cells infected with the indicated vectors and selected. A, NIH3T3 cells RASV12+KCNA1 were treated

with forskolin/IBMx for 3 days, fixed with PFA 3% (membrane) or with methanol (total), and analyzed by immunofluorescence using a specific KCNA1 antibody. B, Representatives are shown to illustrate the transformation ability of the NIH3T3 cells. C, Membrane potential of NIH3T3 expressing the indicated proteins were analyzed by flow cytometry. D, NIH3T3 cells were methanol (total) or PFA (membranar) fixed and analyzed by immunofluorescence for KCNA1 and representatives to illustrate the transformation of the NIH3T3 cells are shown.

Figure S9. KCNA1 expression in different breast cancer subgroups. A, KCNA1 mRNA levels were analyzed in 34 breast tumors fully characterized for HER-2, ER and PR status. B and C, Kaplan Meier analyses of the probability to live without metastases (B) and to survive (C) were performed in Luminal A vs Triple negative breast tumors. P values were calculated using a log rank test.

Supplemental Figure 1, Lallet-Daher *et al*

A

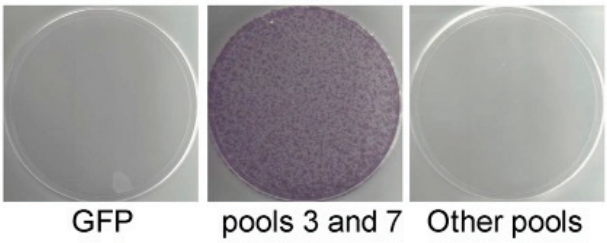

B

shRNA identified more than once over 100 sequences	KCNA1, CASP2
shRNA identified once over 100 sequences	BNIP3L; ESSRB; IL17; AMYADML; PLXND1; SNORB2; ACACB; BRAP; FBXO9; ITPR2; MYOM3; POLM; TRAT1; ACVR2A; FSHR; NDRG3; PPP1R8; UBQLN1; ACSBG2; CNIH4; G6PC; ABCC3; KCTD7; NRK; RAB9A; WASL; ADAM12; COPS2; GHRH; KIF11; OSBPL2; RAB14; ZBTB9; ADAM15; DAD1; GLT8D3; LHX8; PBX3; RNF111; ZCWPW2; ALX1; DDX10; GNRHR; LRRTM1; PDXP; RNF150; ZNF133; AP4M1; EGLN1; HAT1; MAP4; PDXDC2; SDF2L1; ARMCX2; ELF5; IGF1; MCU; PFTK1; SNORA65

C

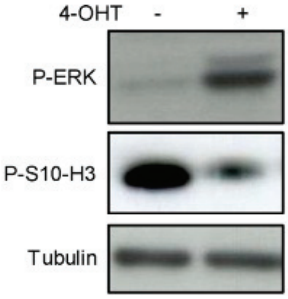

D

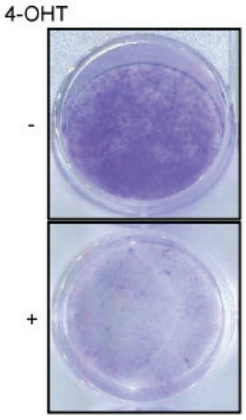

E

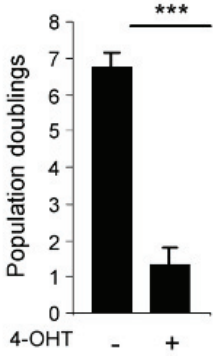

F

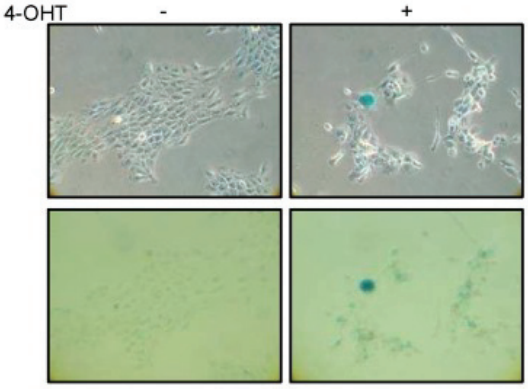

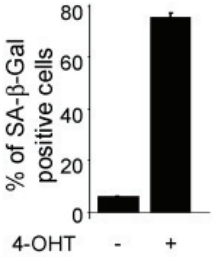

G

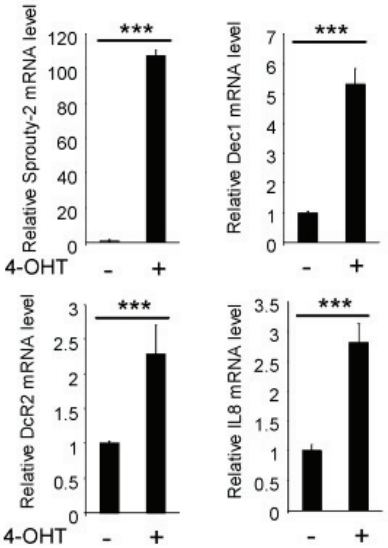

Supplemental Figure 2, Lallet-Daher *et al*

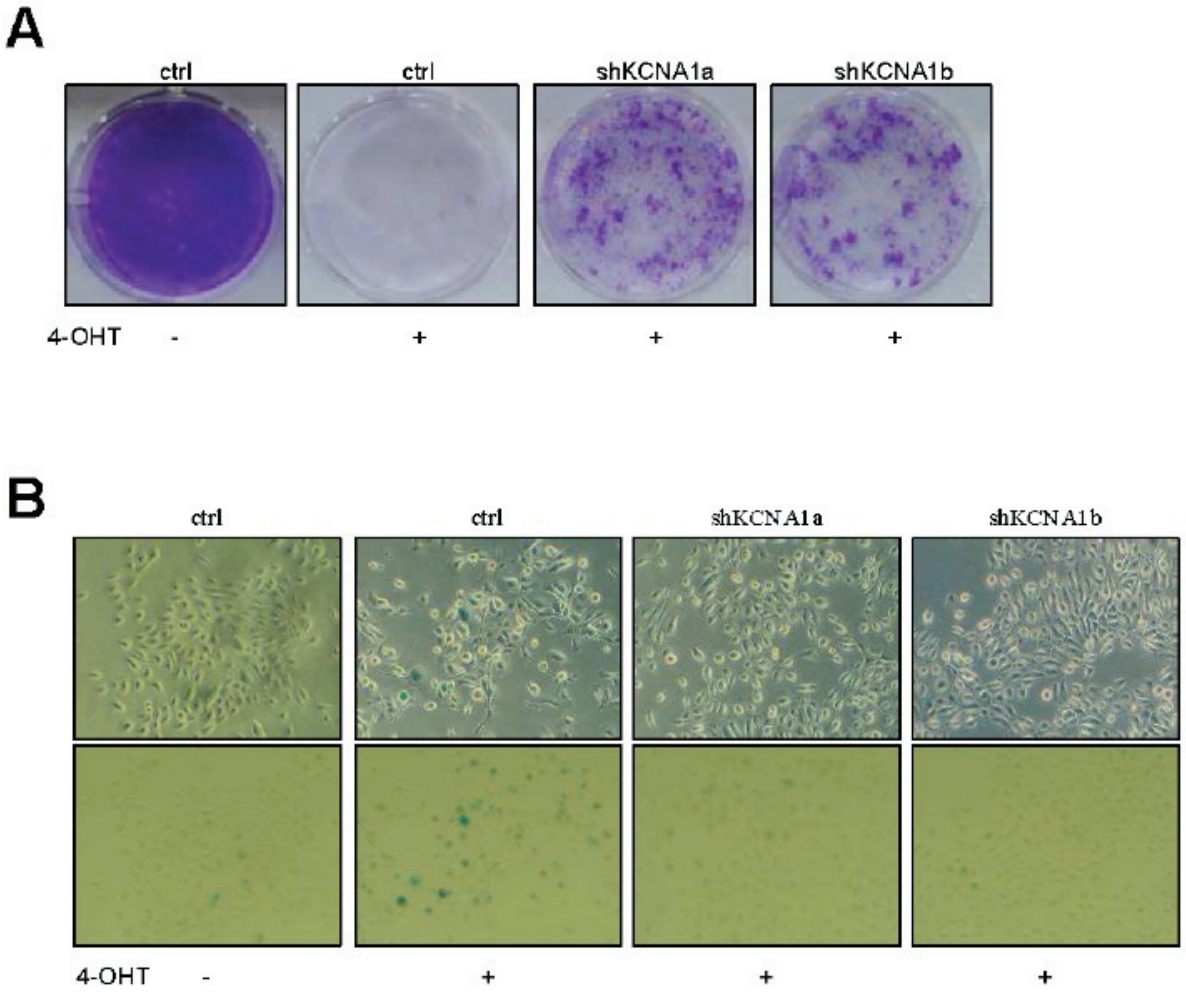

Supplemental Figure 3, Lallet-Daher *et al*

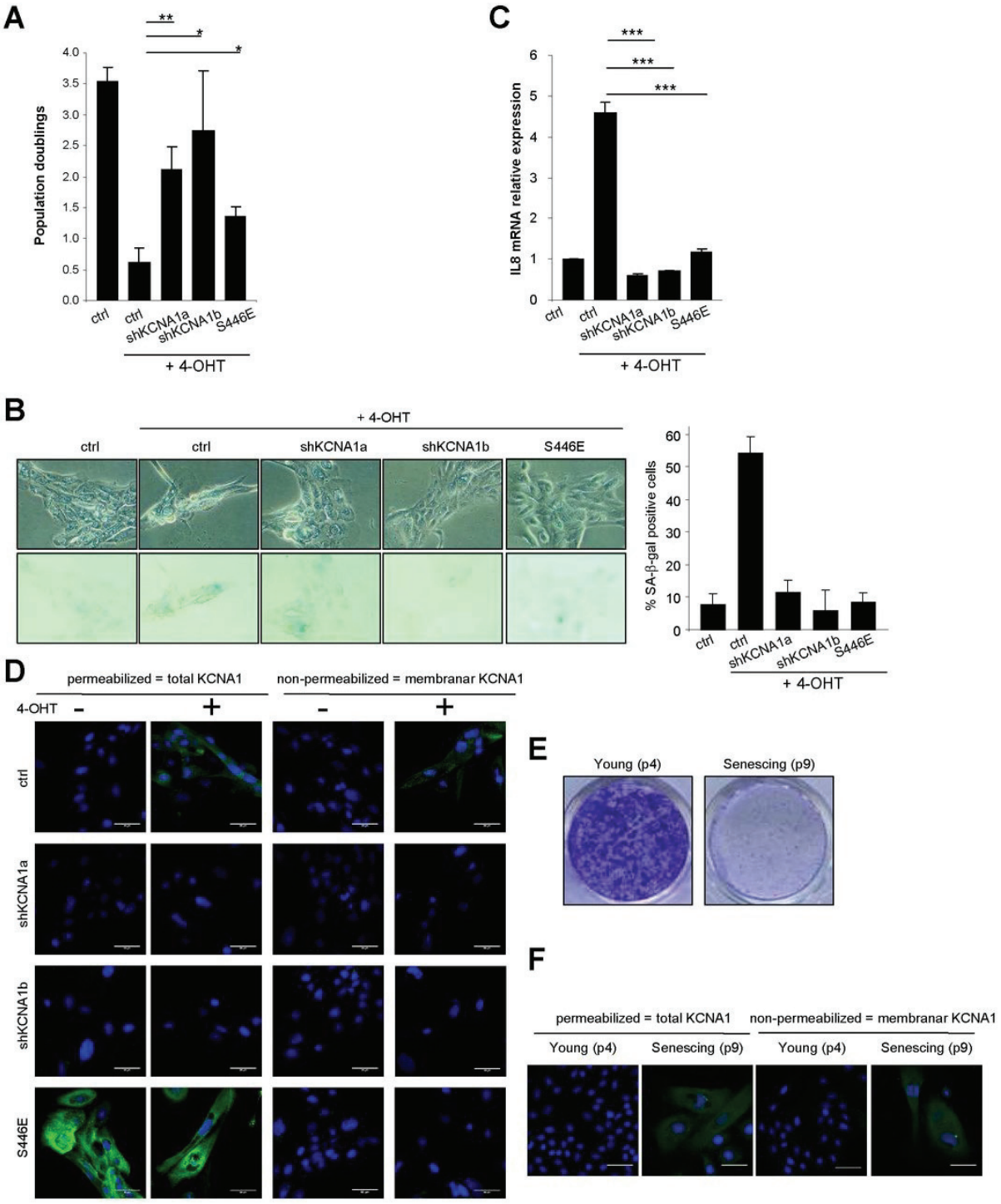

Supplemental Figure 4, Lallet-Daher *et al*

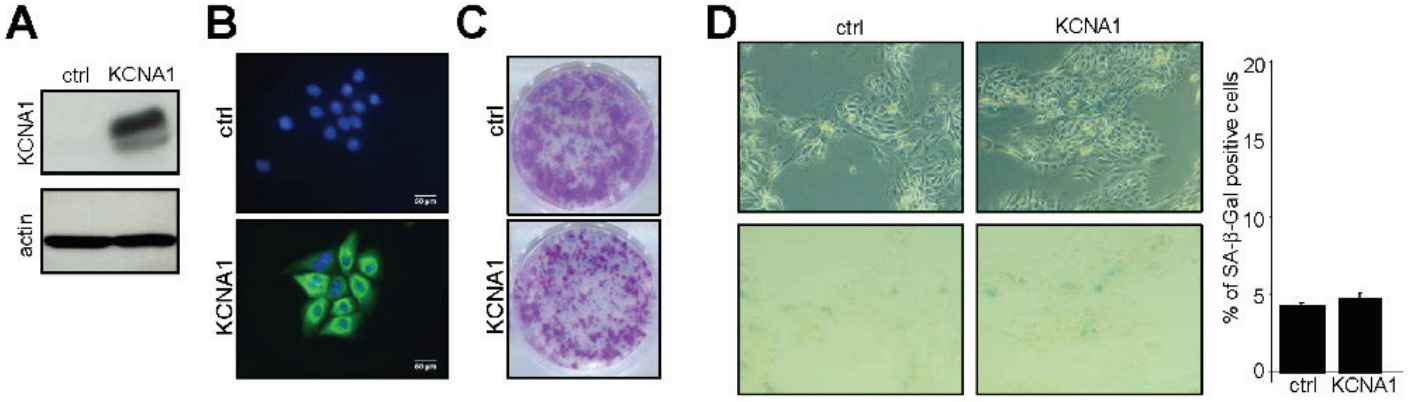

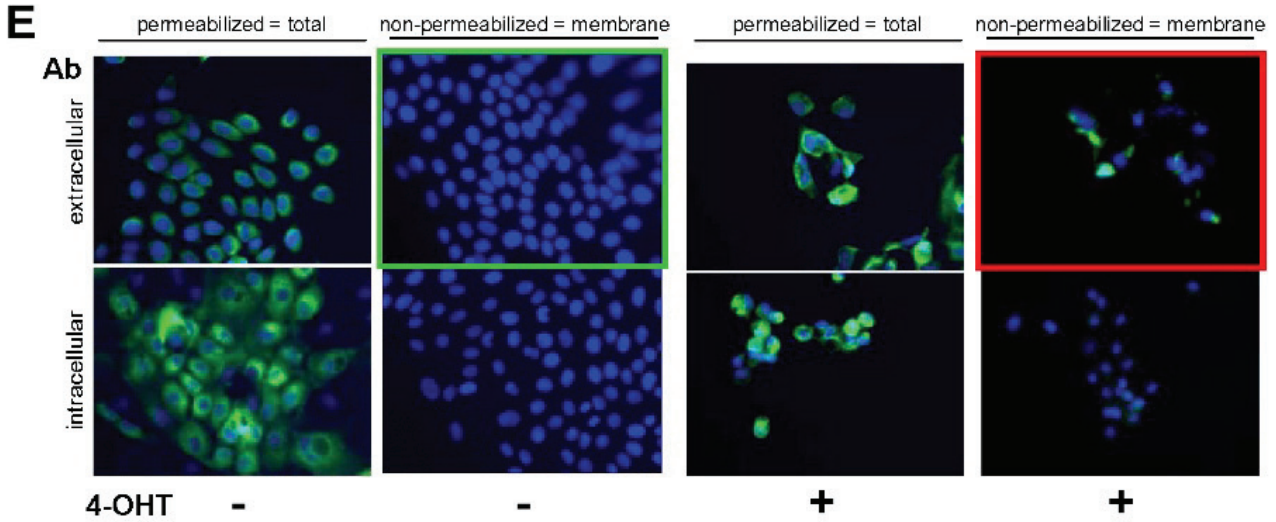

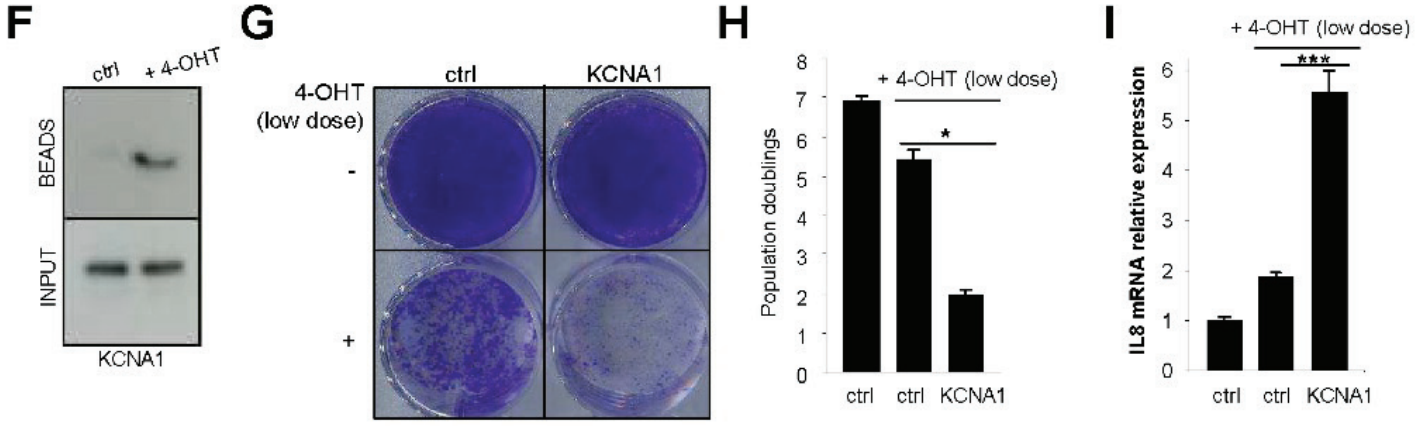

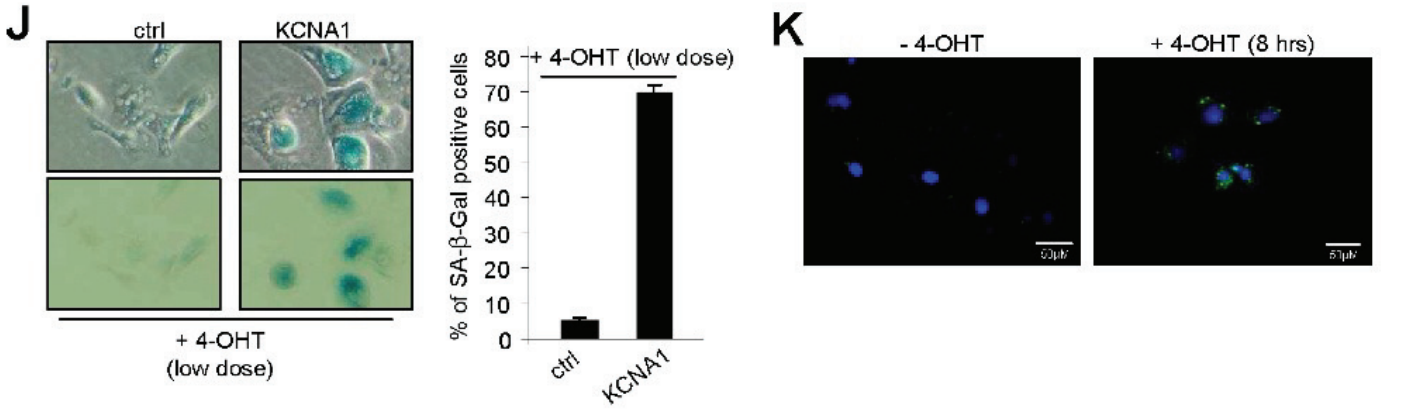

Supplemental Figure 5, Lallet-Daher *et al*

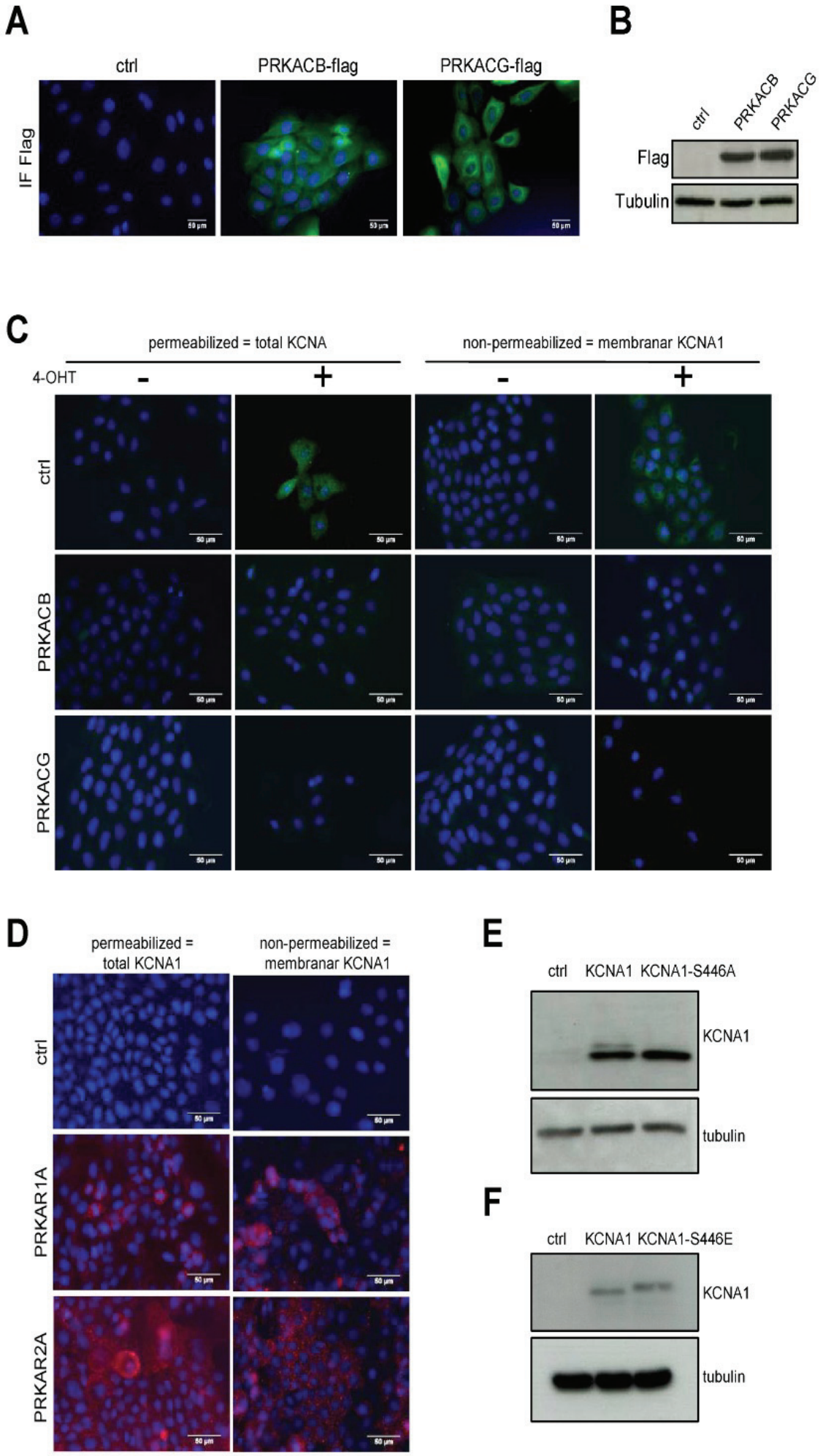

Supplemental Figure 6, Lallet-Daher *et al*

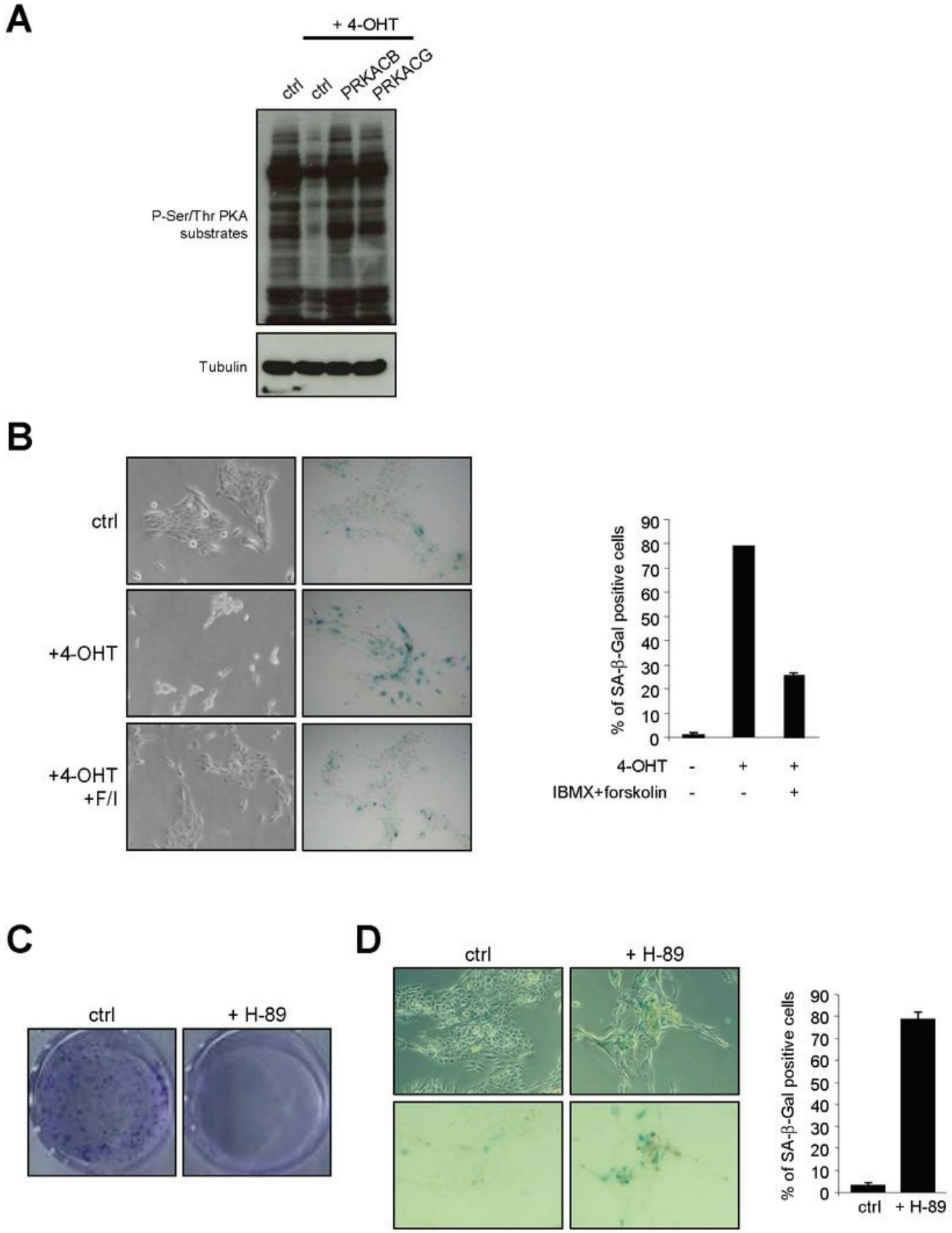

Supplemental Figure 7, Lallet-Daher *et al*

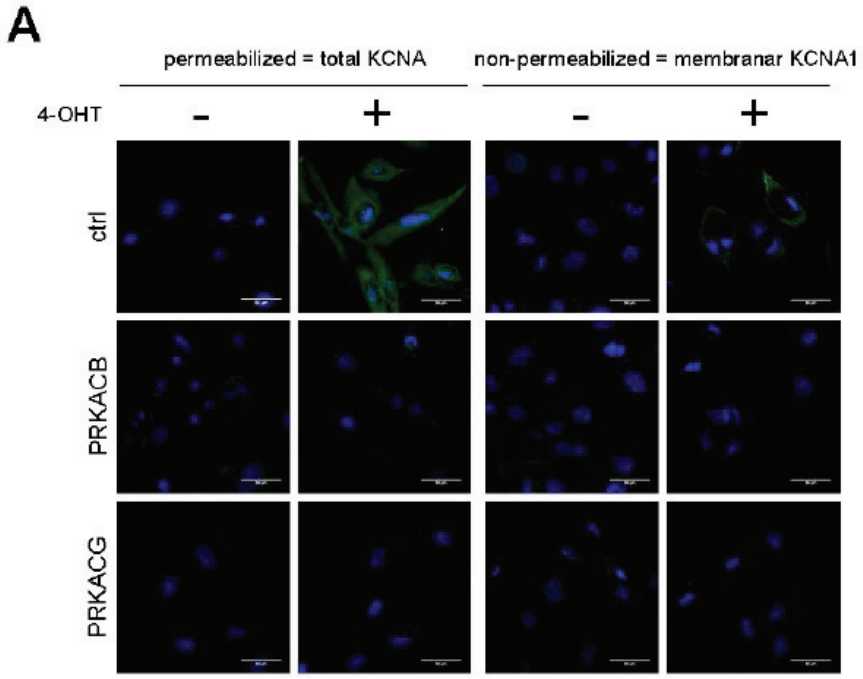

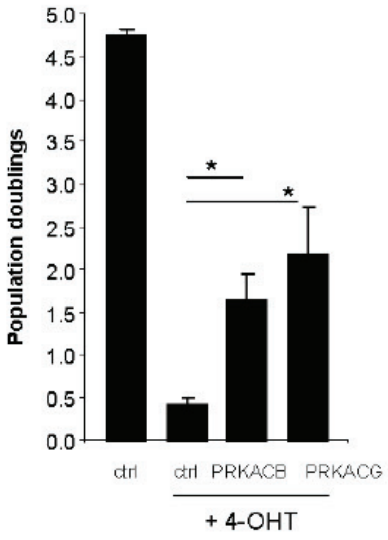

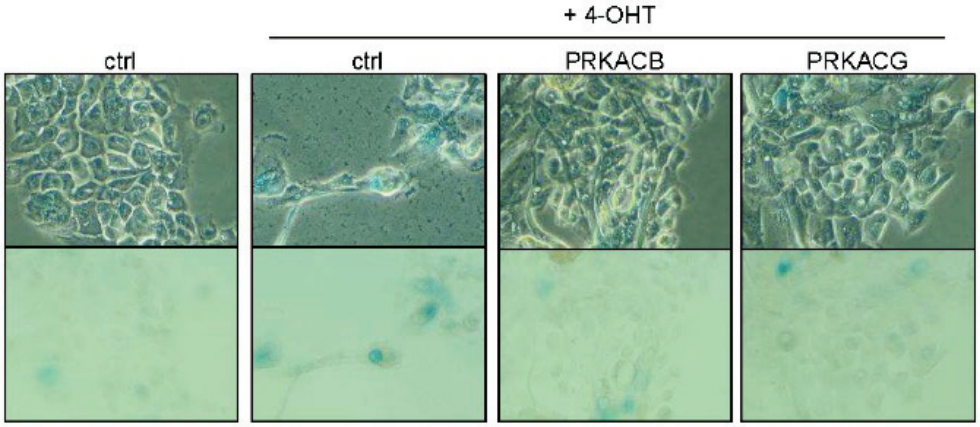

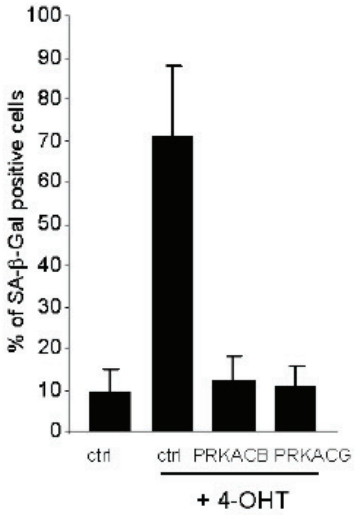

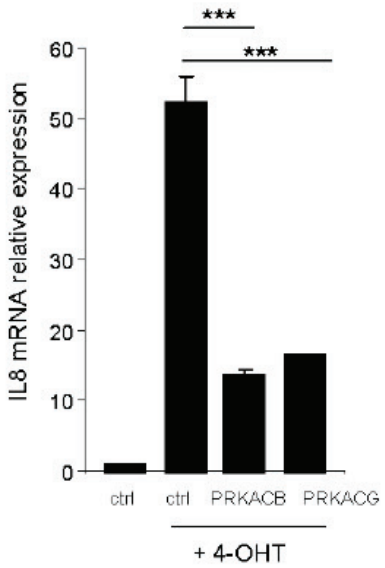

Supplemental Figure 8, Lallet-Daher *et al*

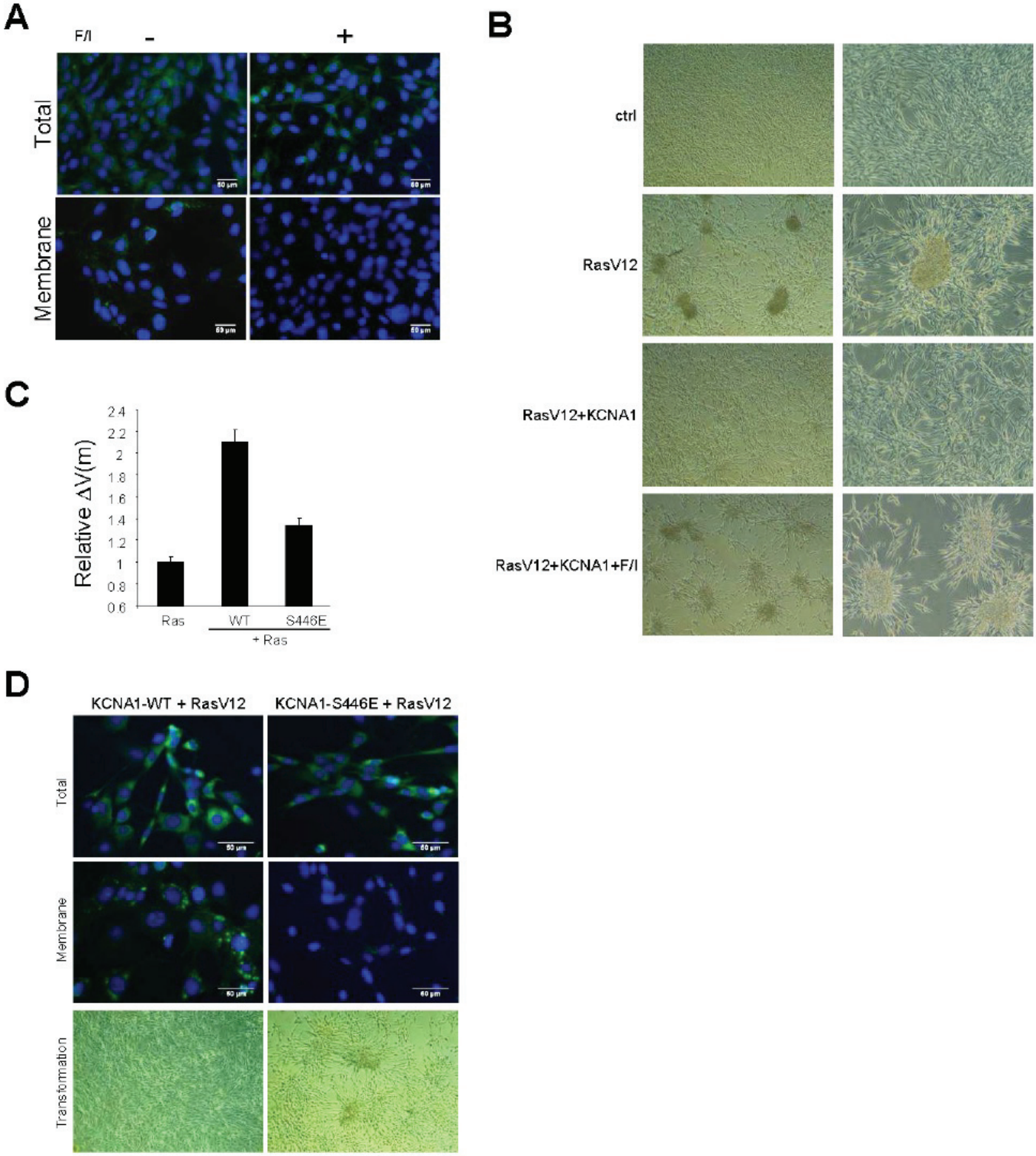

Supplemental Figure 9, Lallet-Daher *et al*

A

Type	Number of samples	% of cohort	Relative level of mRNA KCNA1 expression
Luminal A (ER+ or PR+, Her-)	19	55.88	1
Luminal B (ER or PR+/HER-2+)	2	5.88	0.593119725
HER-2 + (ER-, PR-)	2	5.88	0.226623278
Triple negative	11	32.35	0.995097856

B

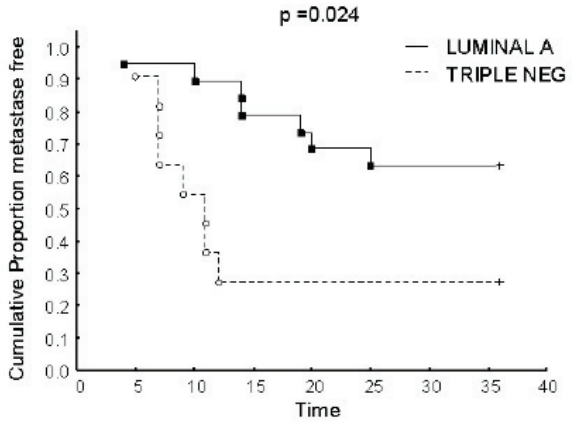

C

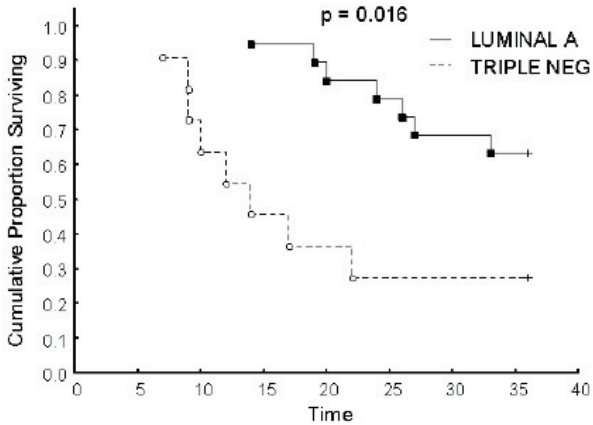

Supplemental Materials and Methods

Cell culture

Upon receipt, cells were thawed, amplified and aliquots frozen. Experiments were performed from these aliquots for no more than 4 months. The cells were maintained at 37°C under a 5% CO2 atmosphere.

Mutagenesis

Mutagenesis was performed with the QuikChange® Lightning Site-directed Mutagenesis Kit (210518, Agilent Technologies) according to the manufacturer's recommendations. The following primers were used KCNA1-S446A 5'-tcgccgcagtgcctctactatgag-3' and revert to generate pLPCX/KCNA1-S446A vector; KCNA1-S446E 5'-tcgccgcagtg*aa*tctactatgag-3' and revert to generate pLPCX/KCNA1-S446E.

Retroviral infection

PEI reagent (Euromedex) was used according to the manufacturer's recommendations to transfect GP293 cells (an amphotropic system) or PlatE cells (an ecotropic system) with the indicated vector. Two days after transfection, the virus-containing supernatant was mixed with fresh medium (1/2) and hexadimethrine bromide at 8 µg/ml (Sigma) and was used to infect target cells. Infected HMECs were selected with G418 (Invitrogen) at 100 µg/ml or/and puromycin (InvivoGen) at 500 ng/ml and infected NIH3T3 cells were selected with puromycin at 1 µg/ml and hygromycin (InvivoGen) at 100 µg/ml.

Reagents

4-Hydroxytamoxifen (4-OHT) (H-7904, Sigma) was used daily for 3 days at different concentrations (100 nM for low dose or 400 nM for normal dose). H-89 (B-1427, Sigma), an

inhibitor of PKA protein, was used daily at 10 µM. Forskolin (1099, TOCRIS Bioscience) and IBMx (2845, TOCRIS Bioscience), activators of PKA protein, were used together daily at the following respective final concentrations: 25 µM and 50 µM.

Biotinylation of membrane bound proteins

The biotinylation experiments were performed according to the manufacturer's recommendations (89881, Perbio) and total and biotinylated KCNA1 were examined by immunoblot.

Immunohistochemistry

Formalin-fixed, paraffin-embedded human prostate samples with prostatic intra-epithelial high-grade neoplasia were selected. Slides were subjected to heat-induced antigen retrieval in EDTA buffer pH 9 at 60°C for 16 h. Primary antibody against KCNA1 (1/100) (APC-009; Alomone Labs) was incubated for 1 h at room temperature. A biotin-free detection system (*ultra*VIEW Universal DAB Detection Kit, Ventana) was used according to a standard protocol, with diaminobenzidine as the chromogen.

Reverse transcription and real-time quantitative PCR

TriReagent (Sigma-Aldrich) was used for phenol-chloroform extraction of total RNA. PhaseLockGel tubes (Eppendorf) were used for phase separation. The First-Strand cDNA Synthesis Kit (GE Healthcare, Chalfont St Giles, UK) was used to synthesize cDNA from 2 µg total RNA. The RT reaction mixture was diluted 1/60 and used as cDNA template for qPCR. TaqMan quantitative PCR was carried out on a LightCycler 2.0 System (Roche Applied Science). The PCR mixture contained 1.33 µl LightCycler TaqMan mix (Roche), 0.201 µl of a pre-mix of primers, and the UPL probe for the KCNA1 gene (TaqMan® Gene Expression Assays (primers/probe) for KCNA1, Invitrogen) and 1.67 µl cDNA template in a 6.67 µl reaction volume. All reactions were

performed in triplicate. The relative amount of mRNA was calculated by the comparative Cp method after normalization with respect to β-actin (ACTB-1 FWD 5'-ATTGGCAATGAGCGGTTC-3' and ACTB-1 REV 5'-GGATGCCACAGGACTCCAT-3').

Membrane potential

The anionic membrane voltage-reporting dye $DiBAC_4$ (Molecular Probes, stock solution at 10 mg/ml in dimethyl sulfoxide (DMSO)) was used at 200 nM to study membrane potential (Vm) variation. The cells were washed 3 times with PBS 1X and the cell pellet was suspended in PBS 1X containing DiBAC4 dye. The cells were loaded by incubation with 1 ml DiBAC4 dye at 37°C for 1 h. The fluorescence intensity was measured with a FACSCalibur flow cytometer (BD Bioscience) at 525 nm, after excitation at 488 nm, and the fluorescence data were analyzed with FlowJo software.

Expression, purification and phosphorylation of KCNA1

PEI was used to transfect HEK 293T cells with a plasmid encoding flag-tagged KCNA1 or S446A mutant of KCNA1. After 36–48 h, the transfected cells were washed three times with ice-cold PBS and collected by scraping into 0.7 ml lysis buffer containing 25 mM HEPES pH 7.5, 1% Triton X-100, protease inhibitors (Roche; 1 tablet/50 ml), phosphatase inhibitors (50 mM sodium fluoride and 5 mM sodium pyrophosphate), 100 mM NaCl, and 1 mM DTT and kept on ice. Harvested cells were dispersed by four passages through a 21-G needle and the lysate was clarified by centrifuging at 14 000 r.p.m. for 20 min. Supernatants were incubated with M2-flag resin (50 µl/500 µl lysate) overnight at 4°C. The protein-bound resin was washed three times for 30 min with lysis buffer containing 150 mM NaCl and once with lysis buffer. Flag-resin-bound KCNA1 and S446A KCNA1 were eluted with 150 µl elution buffer (25 mM HEPES pH 7.5, 1% Triton X-100, protease and phosphatase inhibitors, 10% glycerol, 300 ng/µl flag peptide) by shaking at 4°C for 3–6 h. PKA (0.1-2 µg, Promega) was incubated alone or with flag-eluted wild-type or S446A-mutant KCNA1 at for 20 min at 37°C in 30 µl reaction mixture containing 25 mM HEPES pH 7.5, 1%

Triton X-100, protease and phosphatase inhibitors, 10% glycerol, and 0.25 µl [^{32}P]ATP (6000 Ci/mmol, Perkin-Elmer). As a control, KCNA1 or S446A alone was phosphorylated also in the absence of PKA. The phosphorylation reactions were stopped with SDS–PAGE sample buffer and separated on 10% polyacrylamide gels in Tris-glycine buffer. The gels were fixed and stained with Simply Blue stain (Invitrogen) and destained with water, dried, and phosphorimaged. Gels identical to those just described above were subjected to immunoblotting with anti-flag antibody so as to monitor protein levels.

KCNA1 expression in human samples

The Oncomine database (http://www.oncomine.org/) was used to examine KCNA1 expression in multiple cancer samples as compared to their normal counterparts. RNA human breast tumor samples were provided by the centre Léon Bérard biobank. Kaplan Meier analysis was performed using Statistica software.

Population Doublings

Ten thousand cells were seeded in 12-well plates. At the indicated times, cells were trypsinized, and counted. Population doublings were calculated using this formula: [Ln (final number of cells / initial number of cells)] / Ln 2. Each condition was performed in triplicate.

Article 4 : Glucose metabolism and hexosamine pathway regulate oncogene-induced senescence

OPEN

Citation: Cell Death and Disease (2014) 5, e1089; doi:10.1038/cddis.2014.63
© 2014 Macmillan Publishers Limited All rights reserved 2041-4889/14
www.nature.com/cddis

Glucose metabolism and hexosamine pathway regulate oncogene-induced senescence

D Gitenay[1,2,3,4], C Wiel[1,2,3,4], H Lallet-Daher[1,2,3,4], D Vindrieux[1,2,3,4], S Aubert[5,6], L Payen[1,2,3,4,7], H Simonnet[1,2,3,4] and D Bernard*[,1,2,3,4]

Oncogenic stress-induced senescence (OIS) prevents the ability of oncogenic signals to induce tumorigenesis. It is now largely admitted that the mitogenic effect of oncogenes requires metabolic adaptations to respond to new energetic and bio constituent needs. Yet, whether glucose metabolism affects OIS response is largely unknown. This is largely because of the fact that most of the OIS cellular models are cultivated in glucose excess. In this study, we used human epithelial cells, cultivated without glucose excess, to study alteration and functional role of glucose metabolism during OIS. We report a slowdown of glucose uptake and metabolism during OIS. Increasing glucose metabolism by expressing hexokinase2 (HK2), which converts glucose to glucose-6-phosphate (G6P), favors escape from OIS. Inversely, expressing a G6P, pharmacological inhibition of HK2, or adding nonmetabolizable glucose induced a premature senescence. Manipulations of various metabolites covering G6P downstream pathways (hexosamine, glycolysis, and pentose phosphate pathways) suggest an unexpected role of the hexosamine pathway in controlling OIS. Altogether, our results show that decreased glucose metabolism occurs during and participates to OIS.
Cell Death and Disease (2014) **5,** e1089; doi:10.1038/cddis.2014.63; published online 27 February 2014
Subject Category: Cancer

Otto Warburg was the first to describe a metabolic switch occurring in cancer tissues. In the presence of oxygen, instead of producing adenosine triphosphate (ATP) through oxidative phosphorylation, cancer cells exhibit high rates of glycolysis. Cancer cells divide rapidly and need favorable energy production rates. In these cells, glucose is rendered more bioavailable and metabolizable through upregulation of glucose transporters and metabolic enzymes. Tumor imaging exploits this fact to detect the presence of tumors throughout the body: cancer cells are labeled with the glucose analog ^{18}fluorine-fluorodeoxyglucose. Mechanistically, oncogenes products such as MYC, NF-κB, AKT, HIF, and E2F, and the tumor-suppressor genes products such as p53 and PTEN, which are respectively activated or inhibited in cancer, can act on either glucose transporters, glycolytic enzymes, or both, and this suggests that in cancer cells, the regulation of growth is coupled with that of metabolism.[1–8]

Mounting evidence suggesting that increased glycolysis plays a role in maintaining the malignant behavior of tumor cells has raised interest in targeting the metabolism of cancer cells in cancer therapy,[9–11] but the importance of glucose metabolism alterations early in tumorigenesis is poorly known. Failsafe programs can protect cells from transformation, and escape from them is necessary to allow early tumorigenesis. Senescence, because it involves stable cell cycle arrest and activates immune surveillance,[12] constitutes such a program. Various studies have demonstrated that activation of oncogenes such as RAS, RAF, MEK, and others induces senescence *in vitro*. More recently, work on *in vivo* models has shown that premalignant lesions exhibit high senescence levels, whereas senescence is absent from malignant tumors, thus confirming a tumor-suppressor role for oncogene-induced senescence (OIS).[13]

Little is known about the features of glucose metabolism in cells undergoing OIS. It is also not known whether the features described in malignant tumors are acquired early or late in tumorigenesis. As far as we know, most of the papers studies senescence response in a context of glucose excess (25 mM). Nevertheless, it is difficult to get a precise idea of glucose concentrations used as in most of the papers they are not mentioned, although they influence cell growth and senescence.[14,15]

Alterations in enzyme activities, especially in glycolytic and in tricarboxylic acid pathways, have been reported to modulate senescence response. Indeed, increased glycolytic enzyme activities favor senescence escape in mouse embryonic fiblroblasts.[5] Decreased tricarboxylic acid malic enzymes seem to participate in p53-induced senescence,[16] whereas the use of pyruvate dehydrogenase to fuel tricarboxylic acid cycle promotes senescence,[17] provoking a debate on the role of tricarboxylic acid cycle on senescence. Here, we used human epithelial cells cultivated at 8 mM glucose, rather close to its physiological level, to examine the role, if any, of glucose metabolism during OIS. Surprisingly,

[1]Inserm U1052, Centre de Recherche en Cancérologie de Lyon, Lyon, France; [2]CNRS UMR5286, Lyon, France; [3]Centre Léon Bérard, Lyon, France; [4]Université de Lyon, Lyon, France; [5]Institut de Pathologie, CHRU, Faculté de Médecine, Université de Lille, Lille, France; [6]Inserm U837, Jean-Pierre Aubert Research Center, Team 5, Lille, France and [7]Biochemistry Laboratory of Lyon Sud, Hospices civils de Lyon, Lyon, France
*Corresponding author: D Bernard, Centre de Recherche en Cancérologie de Lyon, 28, rue Laënnec, 69373 Lyon, France. Tel: +33 4 26 55 67 92; Fax: +33 4 78 78 27 20; E-mail: david.bernard@lyon.unicancer.fr
Keywords: oncogene-induced senescence; glucose metabolism; metabolites
Abbreviations: 2DG, 2-deoxy-D-glucose; 4-OHT, 4-hydroxytamoxifen; ATP, adenosine triphosphate; HK2, hexokinase-2; G6P, glucose-6-phosphate OIS, oncogene-induced senescence; PPP, pentose phosphate pathway; SA-β-Gal, senescence-associated β-galactosidase
Received 17.9.13; revised 27.1.14; accepted 28.1.14; Edited by M Federici

we found that glucose uptake and metabolization is altered after oncogenic stress and this alteration participates in senescence.

Results

OIS impairs glucose metabolism. To study glucose metabolism during OIS, we focused on human epithelial cells cultivated without glucose excess. We first immortalized human epithelial cells by expressing hTert to overcome replicative senescence.[18] Next, cells were infected with a retroviral vector coding a fusion protein (MEK/ER or RAF/ER) between a constitutively activated form of MEK1 or delta-BRAF and the hormone-binding domain of the human estrogen receptor (hbER).[19,20] In response to 4-hydroxytamoxifen (4-OHT) and, as expected, MEK/ER-expressing cells showed phosphorylation of the MEK substrate ERK. The MEK induction resulted in a strong decrease of the Phospho-S10-Histone3 mitotic marker (Figure 1a). Accordingly, MEK activation blocked cell growth (Figure 1b), induced the appearance of senescence-associated β-galactosidase activity (SA-β-Gal) (Figure 1c), and increased expression of a set of senescence markers: Sprouty homolog 2 (SPRY2),[21] the interleukin-8 (IL-8),[22] and the Deleted In Esophageal Cancer 1 (DEC1)[23] (Figure 1d). Similar results were obtained using the RAF/ER-expressing cells, RAF being the upstream kinase of MEK (Supplementary Figure 1), showing that RAF or MEK are equivalent systems to induce OIS.

To see whether glucose metabolism was altered during OIS, we first compared glucose consumption by MEK/ER-activated and -inactivated human epithelial cells. Uptake of extracellular glucose measurement revealed markedly decreased glucose consumption by senescent cells (Figure 1e). In agreement with decreased glucose consumption, senescent cells displayed a decreased lactate production (Figure 1f) as well as lower ATP levels (Figure 1g). Adding 4-OHT on immortalized cells (without MEK/ER) did not induce any senescence and glucose metabolism changes excluding a MEK-independent effect of the 4-OHT (Supplementary Figure 2). Altogether, these results show a decrease in glucose metabolism during OIS in human epithelial cells.

Inhibition of the first step of glucose metabolism results in premature senescence. Glucose metabolism is thus regulated during OIS. We next wanted to examine whether cellular glucose metabolization shortage is involved in oncogenic stress-mediated senescence. We then blocked glucose-6-phosphate (G6P) accumulation to see if this would have an impact on senescence of human epithelial cells. This was done by constitutively expressing glucose-6-phosphatase (G6PC3) that catalyzes the conversion of G6P into glucose (Figures 2a and b). As expected, G6PC3 constitutive expression correlated with the decrease of glucose consumption (Figure 2c), lactate production (Figure 2d), and ATP level (Figure 2e). Interestingly, this glucose metabolism drop induced by constitutive G6PC3 expression blocked cell growth (Figure 2f), decreased levels of proliferation markers (Figure 2g), and induced both SA-β-Gal activity (Figure 2h) and the expression of various senescence markers (Figure 2i). Pharmacological inhibition of hexokinases with Lonidamine[24,25] (Supplementary Figure 3) or the use of 2-deoxy-D-glucose (2DG), a non-metabolizable form of glucose (Supplementary Figure 4), also blocked glucose metabolism and induced a premature senescence. Blocking glucose metabolism in human epithelial cells thus results in premature senescence supporting its functional role in OIS.

Hexokinase expression sustains glucose metabolism and favors OIS escape. We next wanted to examine whether increasing glucose metabolism might promote escape of human epithelial cells from OIS by sustaining glucose metabolism. Hexokinases play a major role in this metabolism, catalyzing its first step (conversion of glucose to G6P; Figure 2a) and thus determining both the glucose content of the cell and the level of glucose metabolization.[11,26] We therefore investigated OIS escape and glucose metabolism in human epithelial cells constitutively expressing hexokinase 2 (HK2), the main hexokinase involved in increasing glycolysis in cancer cells.[6,11] After retroviral transduction of HK2, we checked its constitutive expression by immunofluorescence (Figure 3a). As expected, constitutive HK2 expression sustained glucose consumption (Figure 3b), lactate production (Figure 3c), and ATP production (Figure 3d) during oncogenic stress. The sustained glucose metabolism induced by HK2 expression favors escape from OIS, as measured by the ability to grow (Figure 3e), to maintain proliferation markers expression (Figure 3f), and by the absence of SA-β-Gal activity (Figure 3g) and various senescence markers (as determined by RT-qPCR, Figure 3h). Altogether, these results support the view that sustaining glucose metabolism by expressing HK2 allows escape from OIS.

Hexosamine pathway is a major pathway controlling OIS. In order to confirm the above described results, we next investigated the ability of glucose metabolites to allow an OIS bypass. We first began by treating the cells with G6P, the upstream glucose metabolite (Figure 4a). Interestingly, daily treatment with G6P permits the cells to escape oncogenic stress-induced growth arrest (Figure 4b) as well as the appearance of SA-β-Gal marker (Figure 4d). Thus, genetic (HK2 and G6PC ectopic expression), pharmacological (HK inhibition or 2DG), as well as metabolite manipulation through G6P all support the view that sustaining glucose metabolization favors OIS escape.

The upstream glucose metabolite, the G6P, fuels three main pathways: the glycolytic pathway, the hexosamine pathway, and the pentose phosphate pathway (PPP) (Figure 4a). These pathways participate in producing basic cell components, energy, and in controlling the cell redox state. We then decided to investigate these three pathways. A decreased glycolytic pathway has already been proposed to participate in senescence[5] and is thus an obvious candidate pathway. As expected, blocking the glycolysis by the bromopyruvate, a GAPDH inhibitor, induced premature senescence and resulted in strong activation of the energy sensor AMPK (Supplementary Figure 5). Nevertheless, pyruvate glycolysis metabolite was unable to induce an OIS escape (Figures 4c and d) and AMPK was found only slightly activated during OIS (Supplementary Figure 5), suggesting

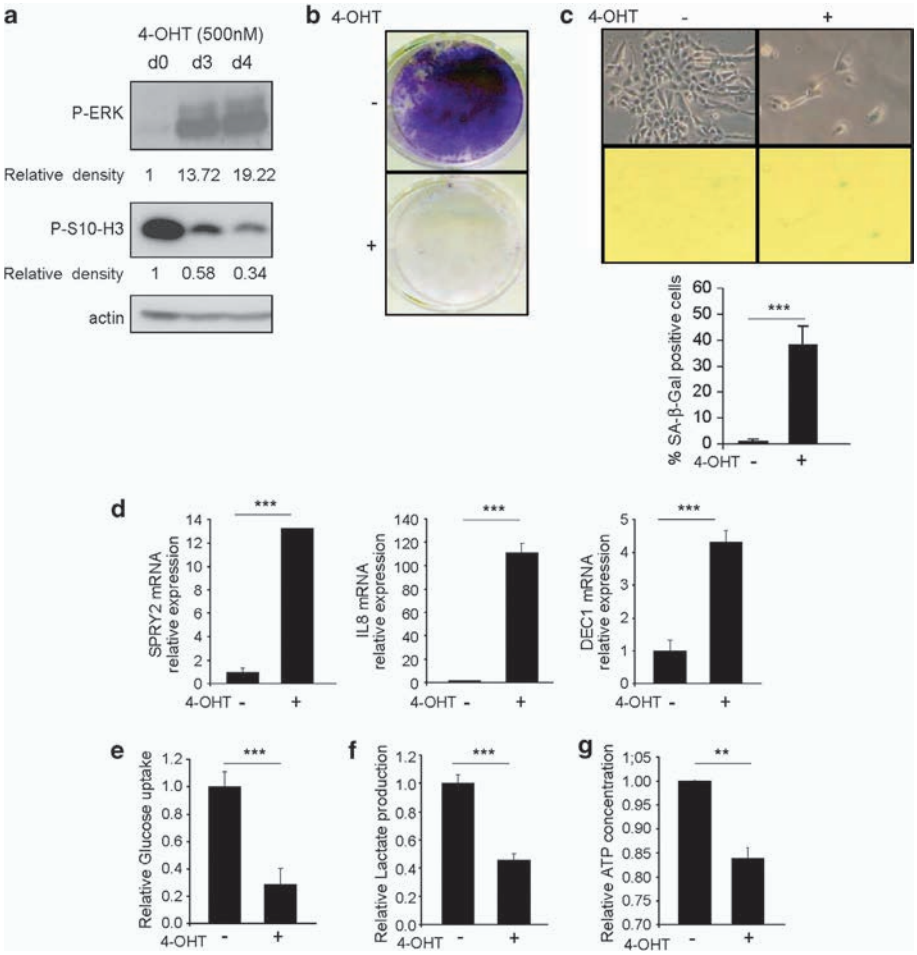

Figure 1 Glucose metabolism decreases during oncogenic stress-induced senescence. Immortalized human epithelial cells expressing the inducible MEK/ER oncogene were treated or not with 4-OHT. (**a**) Cell extracts were prepared after 0, 3, or 4 days of 4-OHT treatment and analyzed by immunoblotting with the indicated antibodies. (**b**) Cells were seeded at the same density and treated or not for 3 days with 4-OHT. After 5 days, they were PFA fixed and crystal violet stained. (**c**) After 3 days with or without 4-OHT treatment, cells were fixed and stained for detection of SA-β-Gal activity. Percentages of stained cells were calculated and representative pictures are shown. (**d**) After 3 days with or without 4-OHT treatment, RNA was prepared and the expression of the indicated senescence markers was analyzed by RT-qPCR and normalized with respect to actin expression. (**e** and **f**) Cells were treated or not for 2 days with 4-OHT, counted, seeded back, and subjected or not to 4-OHT treatment. After 24 h, glucose uptake (**e**) and lactate production (**f**) were determined. (**g**) Cells were treated with or without 4-OHT for 3 days. ATP concentration was determined and normalized with respect to the protein content

that the glycolysis, even if directly inhibited can induce a premature senescence, was not directly involved in the OIS we observed.

We next investigated a putative role of the PPP in OIS. The knockdown of the G6P dehydrogenase (G6PDH), the rate-limiting enzyme of the PPP, did not modify cell growth (Supplementary Figure 5) and the NADPH PPP metabolite was unable to induce an OIS escape (Figures 4c and d), suggesting that PPP was not involved in OIS in our model.

In conclusion, we investigated the potential role of the hexosamine pathway in OIS. Inhibition by azaserine of the glutamine fructose-6-phosphate amidotransferase (GFAT), the first enzyme of the hexosamine pathway, induced a premature senescence (Supplementary Figure 5). Importantly, N-acetylGlucosamine (NAcGluc) was found to allow cells to bypass growth arrest and SA-β-Gal senescence marker appearance (Figures 4c and d) without modifying glucose consumption or lactate production (Supplementary Figure 6). In addition and as during OIS, and by contrast to the effect of the glycolysis pathway inhibition, inhibition of the hexosamine pathway only slightly activated AMPK (Supplementary Figure 5). Together, these results point out the importance of the hexosamine pathway in the OIS response.

Discussion

The interest in glucose metabolism in cancer research field has recently raised and it is now largely recognized that metabolic alterations are part of the oncogenic program.[1–8,16,17] Oncogenic signal, in normal cells, provokes senescence in order to avoid tumorigenesis;[13] the role of glucose metabolism in this process is rather unknown. Although it has been reported that glucose levels affect

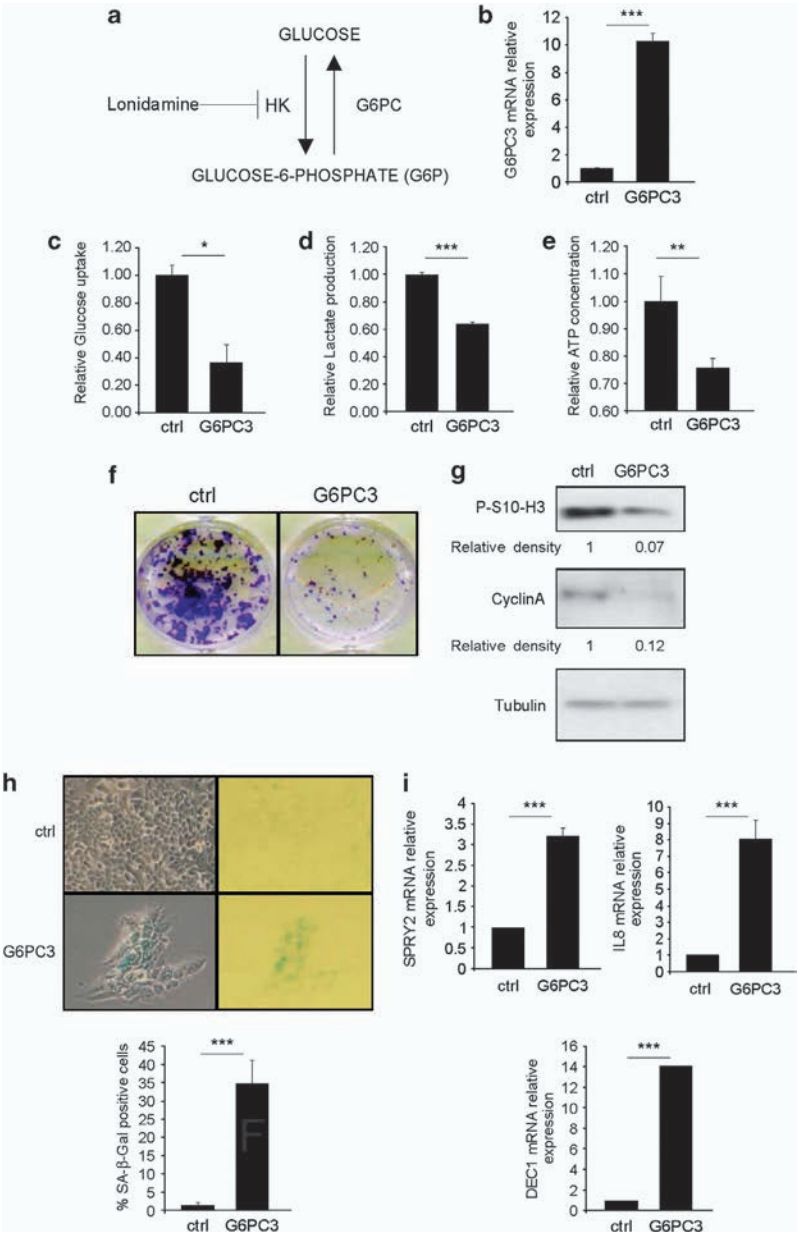

Figure 2 Glucose-6-phosphatase blocks glucose metabolism and causes premature senescence. (**a**) Schematic representation of actors involved in the first glucose metabolism step. (**b**–**i**) Immortalized human epithelial cells were infected with a control or G6PC3-encoding vector and puromycin selected. (**b**) RNAs were extracted and analyzed by RT-qPCR to check for constitutive G6PC3 expression. (**c**–**e**) Equal numbers of cells were seeded and glucose uptake (**c**) or lactate production (**d**) was analyzed after 24 h. (**e**) ATP concentrations were determined and normalized with respect to protein content. (**f**) Cells were seeded at the same density. At 6 days after seeding, they were fixed with PFA and stained with crystal violet. (**g**) Cell lysates were prepared and protein expression analyzed by immunoblotting with the indicated antibodies. (**h**) Cells were PFA fixed and tested for SA-β-Gal activity. (**i**) RNAs were extracted and analyzed by RT-qPCR for expression of the indicated senescence markers

senescence, most of the experiments performed to decipher the events involved in OIS are performed with excess glucose (generally 25 mM). The major problem is that most of the cellular model used (IMR-90, WI38, MEF cells, and so on) are adapted to grow with this high level of glucose, and decreasing this level can affect cell growth.[14] Here, we take advantage of primary human epithelial cells that grow at 8 mM glucose, nearly the normal level of glucose, to investigate the function of glucose metabolism during OIS. Our results show that glucose metabolism is impaired during OIS, in part due to a decreased glucose uptake. This decrease in glucose uptake did not seem to be due to a decrease in Glut1 or Glut3 expression, the expressed Glut in our cells (Supplementary Figure 7). Further work looking at glucose transporter activity and glucose metabolism enzyme activity will be necessary to understand the molecular mechanisms inducing these

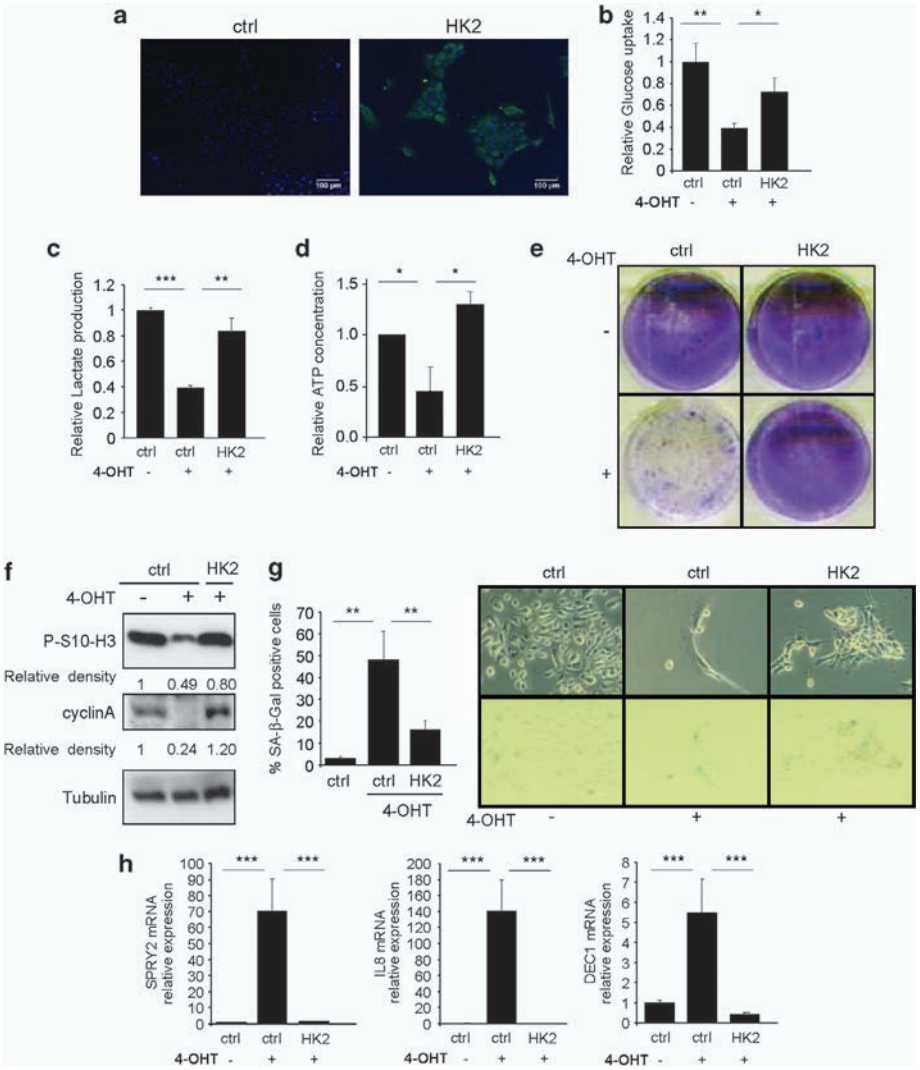

Figure 3 HK2 expression restores glucose metabolism and allows escape from OIS. (**a**–**h**) Immortalized human epithelial cells expressing the inducible RAF/ER oncogene were infected with a control or HK2-encoding retroviral vector and neomycin selected. (**a**) Immunofluorescence against the Flag tag was performed. Nuclei were counterstained with Hoechst. (**b**–**d**) Cells were treated or not for 2 days with 4-OHT, counted, and seeded back with or without 4-OHT. After 24 h, glucose uptake (**b**) and lactate production (**c**) were determined. (**d**) Cells were treated with or without 4-OHT for 3 days as indicated. ATP concentrations were determined and normalized with respect to the protein content. (**e**) Cells were seeded and treated or not for 3 days with 4-OHT. After 5 days, they were PFA fixed and crystal violet stained. (**f**) Cells were seeded and treated or not for 3 days with 4-OHT. After 2 days, cell extracts were prepared and analyzed by immunoblotting with the indicated antibodies. (**g**) Cells were PFA fixed and stained for SA-β-Gal detection. Percentages of stained cells were calculated and representative photographs are displayed. (**h**) RNAs corresponding to the indicated genes were prepared and analyzed by RT-qPCR. Expression levels were normalized with respect to actin expression

glucose metabolism changes during OIS. Restoring glucose metabolism by constitutively expressing the HK2 and by treating the cells with G6P allows to bypass OIS, whereas inhibiting glucose metabolization by blocking the HK activity, by constitutively expressing the glucose-6-phsphatase, or by treating cells with 2DG induces a premature senescence. At first sight, a recent paper from Dorr *et al.*,[27] showing that human and mouse fibroblasts upon RAS-induced senescence display increased glucose consumption and lactate production, might appear opposite to our results. Nevertheless, we indeed observed that MEF cells (in classical culture condition, and hence in 25 mM glucose) upon constitutive RAS expression enter senescence with increased glucose consumption and lactate production (Supplementary Figure 8). This apparently opposite results might be because of the high glucose concentration used in MEF and/or intrinsic differences between fibroblasts and epithelial cells and/or intrinsic differences between RAS and RAF/MEK. Indeed, RAS activates the RAF/MEK pathway and also activates the PI3K pathway that can activate glucose transport and metabolism,[28] eventually explaining the differences between glucose metabolism observed in these different models of OIS. Interestingly, the PI3K pathway has been reported in some models to inhibit RAS/RAF/MEK pathway-induced

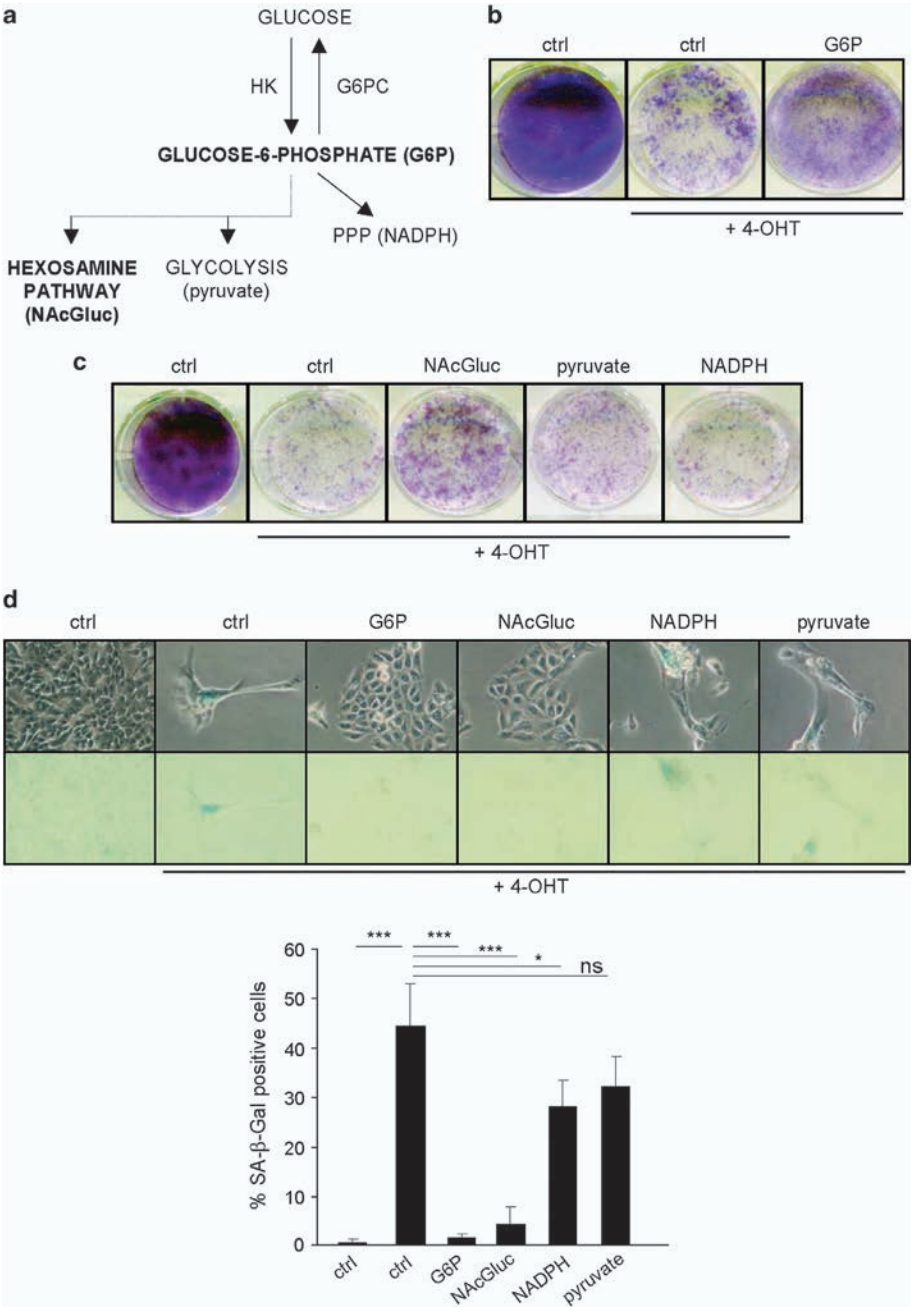

Figure 4 The hexosamine pathway favors OIS escape. (**a**) Schematic representation of key pathways and metabolites involved in glucose metabolism. (**b**) Human epithelial cells expressing MEK/ER were seeded at the same density and treated or not for 3 days with 4-OHT, and every 2 days by G6P at 5 mM. After 5 days, they were PFA fixed and crystal violet stained. (**c**) Human epithelial cells expressing MEK/ER were seeded at the same density and treated every day as indicated with or without NAcGluc at 40 mM, pyruvate at 5 mM, and NADPH at 100 μM, and with 4-OHT for the first 3 days. (**d**) After treatment as indicated in (**b**) and (**c**), cells were PFA fixed and stained for SA-β-Gal detection. Percentages of stained cells were calculated and representative photographs are displayed

senescence,[29,30] suggesting, with our results, that the anti-OIS effect of the PI3K pathway might, in part, be mediated by its ability to increase glucose uptake and metabolism.

Examining the pathways downstream of G6P involved in OIS surprisingly suggest that the hexosamine pathway is a key pathway in the response to oncogenic stress. This pathway controls the *N*- and *O*-glycosylation of the proteins and is involved in numerous biological processes such as ER stress, gene expression, signaling, and trafficking, and thus perturbation in that pathway may have pathophysiological

consequences.[31–34] This does not exclude that for other inducers of senescence other pathways might be involved. For example, ectopic expression of some glycolytic enzymes has been shown to enable MEFs to bypass senescence by enhancing the glycolytic flux, whereas inhibition of these enzymes results in senescence induction.[5]

Enhancement of glucose metabolism, extensively studied in malignant cells, has been shown to participate in malignant behavior.[2] HK2, the most upstream glucose-metabolizing kinase, seems to play an important role in malignant cell growth, as the oncogenic transcription factors Myc and HIF can increase HK2 transcription, and as HK2 expression seems necessary to elicit a malignant cell phenotype.[6,11,35,36] The increased glucose uptake and metabolism observed in malignant cells might thus be, at least in part, acquired during evasion to the oncogenic stress-induced senescence. It might not be surprising taking into account the fact that OIS escape is often considered as a step participating in the malignant conversion of benign tumor.[13,37] Supporting this assumption, HK2 expression is significantly increased in 32% (15.9-fold, $P = 0.00018$) of the malignant melanomas tested as compared with melanocytic nevi, their benign, senescent counterparts (Supplementary Figure 9).[38] In addition and in agreement with our results, a recent paper showed that HK2 is required for tumor initiation induced by KRas or ErbB2.[39]

Altogether, our results support the view that the level of glucose metabolization and the hexosamine pathway are key determinants of the OIS response in human cells. This study naturally opens new avenues of research into relationships between OIS and glucose metabolism.

Materials and Methods

Cell culture. Human mammary epithelial cells (Lonza, Barcelona, Spain) were cultured in mammary epithelial cell growth medium containing 8 mM glucose (Promocell, Heidelberg, Germany) and 100 U/ml penicillin/streptomycin (Life Technologies, Saint Aubin, France). Virus-packaging GP293 cells (Clontech, Saint-Germain-en-Laye, France) were cultured in Dulbecco's modified Eagle's medium (DMEM, Life Technologies) with 10% FBS (Life Technologies) and penicillin/streptomycin. The cells were maintained at 37°C under a 5% CO_2 atmosphere.

Retroviral infection. GP293 cells were transfected with PEI reagent (Euromedex, Souffelweyersheim, France) according to the manufacturer's recommendations. At 2 days after transfection, the viral supernatant was mixed with fresh medium (1/2) and polybrene at 8 μg/ml (Sigma, Lyon, France) to infect target cells. Human epithelial cells were selected with G418 (Life Technologies) at 100 μg/ml or/and puromycin (InvivoGen, Toulouse, France) at 500 ng/ml.

Plasmids and reagents. The plasmids were pNLCΔMEK1 (ΔN3, S218E, S222D)/ER (Neo R) and pBabe-puro-BRAF/ER.[20] pWZL Neo Myr Flag HK2 was obtained from Addgene (Cambridge, MA, USA) (Plasmid 20501).[40] Human G6PC3 cDNA (Human MGC Verified FL cDNA, Clone ID 3050476; Thermo Scientific, Waltham, MA, USA) was excised with *Eco*RI–*Xho*I and inserted into the pLPC-puro vector.

The 4-OHT (H7904, Sigma) was used daily for 3 days at 500 nM. The hexokinase inhibitor Lonidamine (L4900, Sigma) was used daily at 25 μM. G6P (G7772, Sigma) was used every other day at 5 mM, NADPH (N5130, Sigma) was used daily at 100 μM, sodium pyruvate (11360039, Life Technologies) was used at 5 mM daily, and NAcGluc (A3286, Sigma) was used daily at 40 mM.

Immunoblotting and immunofluorescence. Immunoblot and immunofluorescence analyses were performed as described in Bernard *et al.*[41] The primary antibodies used were: anti-phospho-ERK (9101, Cell Signaling, Danvers, MA, USA), anti-Flag (200472, Stratagene, Agilent Technologies, Les Ulis, France), anti-phospho-histone3Ser10 (ab14955, Abcam, Paris, France), anti-cyclin A (H432, sc-751, Santa Cruz Technology, Heidelberg, Germany), and anti-tubulin (T6199, Sigma). Quantification of immunoblots signals were performed using ImageJ software (National Institute of Health, Bethesda, MD, USA) and normalized to normalizator signal (tubulin or actin).

Reverse transcription and real-time quantitative PCR. TriReagent (Sigma-Aldrich) and PhaseLockGel tubes (Eppendorf, Hamburg, Germany) were used for total RNA preparation. The First-Strand cDNA Synthesis Kit (GE Healthcare, Chalfont St. Giles, UK) was used to synthesize cDNA from 2 μg total RNA. The RT reaction mixture was diluted 1/60 and used as cDNA template for quantitative PCR. TaqMan quantitative PCR was carried out on a LightCycler 2.0 System (Roche Applied Science, Meylan, France). The PCR mixture contained 1.33 μl LightCycler TaqMan mix (Roche Applied Science), 0.201 μl of a pre-mix of primers and the UPL probe, and 1.67 μl cDNA template in a 6.67-μl reaction volume. The relative amount of mRNA was calculated by the comparative Cp method after normalization against β-actin. The primers used were: actin (UPL probe #11) forward 5′-ATTGGCAATGAGCGGTTC-3′ and reverse 5′-GGATGCC ACAGGACTCCAT-3′, IL8 (UPL probe #72) forward 5′-ATGGTTCCTT CCGGTGGT-3′ and reverse 5′-AGACAGCAGAGCACACAAGC-3′, Sprouty2 (UPL probe #40) forward 5′- TCAGGTCTTGGAAGTGTGGTC-3′ and reverse 5′-TTTGCACATCGCAGAAAGAA-3′, DEC-1 (UPL probe #84) forward 5′-TTTCT CCCTGACAGCTCACC-3′ and reverse 5′-TGAAAGCACTAACAAACCTAATT GA-3′, and G6PC3 (UPL probe #19) forward 5′-TGGCTCAACCTCATCTTCAA and reverse 5′-AGAAGAGGGGAACTGGTGAAC-3′.

SA-β-Gal analysis. At 6–10 days after initial treatment, the cells were fixed with 4% PFA and processed as described in Augert *et al.*[42]

ATP-level measurement. Human epithelial cells were seeded into 10-cm dishes at 2.10^5 cells/dish and treated with 500 nM 4-OHT daily for 3 days. ATP levels were measured 1 day after the third 4-OHT treatment for human epithelial cells. The cells were washed with iced-cold 1 × PBS and extracted in an ATP-releasing buffer containing 100 nM potassium phosphate buffer at pH 7.8, 2 mM EDTA, 1 mM dithiothreitol, and 1% Triton X-100.[43] Then, 2 μl of lysate was used for protein determination by the Bio-Rad protein assay (Bio-Rad Laboratories, Hercules, CA, USA). This involves adding an acidic dye to the protein-containing lysate and measuring the absorbance at 595 nm with a spectrophotometer. Comparison with a standard curve of bovine serum albumin (BSA, Sigma) provides a relative measurement of protein concentration. Samples were diluted in order to assess the ATP content per 10 μg protein in each condition. ATP was determined according to the manufacturer's instructions (ATP determination kit, Life Technologies). ATP levels were first expressed in nM ATP per 10 μg protein and then normalized with respect to the level in control samples.

Glucose and lactate assays. After senescence induction by 2 days of 500 nM 4-OHT treatment, 9.10^4 cells were seeded into six-well plates and treated or not with 4-OHT. After 24 h, the supernatants were collected and filtered and then glucose and acid lactic were assayed. Assays for glucose and lactic acid were performed with an automated analyzer, Architect C16000 (Abbott Laboratories, Abbott Park, IL, USA).

Lactic acid was quantified on the basis of its lactate oxidase-catalyzed conversion to pyruvate and hydrogen peroxide (H_2O_2), followed by peroxidase-catalyzed conversion of the chromogen precursor ABTS (2,2′-azino-di-(3-ethylbenzthiazoline sulfonate)) to its chromogen in the presence of H_2O_2. The chromogen was quantified spectrophotometrically at 548 nm, and its appearance was strictly proportional to the lactic acid concentration. This assay is linear between 0.020 and 13.32 mmol/l. Manual dilution was performed before quantification in the case of the highest concentrations. Lactate production was calculated as the lactate concentration measured in the cell supernatants minus the lactate concentration measured in the cell medium.

Glucose was quantified enzymatically by coupling of the actions of hexokinase (HK) and G6P dehydrogenase. In the presence of ATP and $Mg2+$, glucose is phosphorylated to G6P by hexokinase, and ADP is produced. The G6P is converted to 6-phosphogluconate by G6P dehydrogenase. This reaction requires conversion nicotinamide adenine dinucleotide from its oxidized form ($NAD+$) to its reduced form (NADH). The glucose concentration is directly proportional to the generated NADH concentration that is spectrophotometrically measured at 340 nm. This assay is linear between 0.28 and 44.40 mmol/l. Samples containing higher concentrations were diluted manually before quantification. Glucose uptake was calculated as the glucose concentration of the medium minus the glucose concentration measured in the cell supernatant.

Statistical analysis. The values are presented as mean ± S.D. unless stated otherwise. Statistical analyses were performed using Student's-*t*-test (mean $^{*}P<0.05$, mean $^{**}P<0.01$, mean $^{***}P<0.001$). Each experience was at least replicated.

Conflict of Interest

The authors declare no conflict of interest.

Acknowledgements. We thank M Ferrand, M Samyn, M Manchon, and D Collin Chavagnac for help and materials, and other laboratory members for helpful suggestions and discussions. This work was carried out with the support of the 'Fondation de France', the 'Comités de l'Ardèche et de la Drome de la Ligue nationale contre le Cancer', the 'Institut National du Cancer', and the 'RTRS Fondation Synergie Lyon Cancer'. CW is supported by the 'Ligue contre le Cancer' and the 'Fondation pour la Recherche Médicale'.

1. Garcia-Cao I, Song MS, Hobbs RM, Laurent G, Giorgi C, de Boer VC *et al.* Systemic elevation of PTEN induces a tumor-suppressive metabolic state. *Cell* 2012; **149**: 49–62.
2. Ward PS, Thompson CB. Metabolic reprogramming: a cancer hallmark even Warburg did not anticipate. *Cancer Cell* 2012; **21**: 297–308.
3. Blanchet E, Annicotte JS, Lagarrigue S, Aguilar V, Clape C, Chavey C *et al.* E2F transcription factor-1 regulates oxidative metabolism. *Nat Cell Biol* 2011; **13**: 1146–1152.
4. Jones RG, Thompson CB. Tumor suppressors and cell metabolism: a recipe for cancer growth. *Genes Dev* 2009; **23**: 537–548.
5. Kondoh H, Lleonart ME, Gil J, Wang J, Degan P, Peters G *et al.* Glycolytic enzymes can modulate cellular life span. *Cancer Res* 2005; **65**: 177–185.
6. Mathupala SP, Rempel A, Pedersen PL. Glucose catabolism in cancer cells: identification and characterization of a marked activation response of the type II hexokinase gene to hypoxic conditions. *J Biol Chem* 2001; **276**: 43407–43412.
7. Suzuki S, Tanaka T, Poyurovsky MV, Nagano H, Mayama T, Ohkubo S *et al.* Phosphate-activated glutaminase (GLS2), a p53-inducible regulator of glutamine metabolism and reactive oxygen species. *Proc Natl Acad Sci USA* 2010; **107**: 7461–7466.
8. Kim JW, Gao P, Liu YC, Semenza GL, Dang CV. Hypoxia-inducible factor 1 and dysregulated c-Myc cooperatively induce vascular endothelial growth factor and metabolic switches hexokinase 2 and pyruvate dehydrogenase kinase 1. *Mol Cell Biol* 2007; **27**: 7381–7393.
9. Levine AJ, Puzio-Kuter AM. The control of the metabolic switch in cancers by oncogenes and tumor suppressor genes. *Science* 2010; **330**: 1340–1344.
10. Zhao Y, Liu H, Riker AI, Fodstad O, Ledoux SP, Wilson GL *et al.* Emerging metabolic targets in cancer therapy. *Front Biosci* 2011; **16**: 1844–1860.
11. Mathupala SP, Ko YH, Pedersen PL. Hexokinase-2 bound to mitochondria: cancer's stygian link to the 'Warburg Effect' and a pivotal target for effective therapy. *Semin Cancer Biol* 2009; **19**: 17–24.
12. Kang TW, Yevsa T, Woller N, Hoenicke L, Wuestefeld T, Dauch D *et al.* Senescence surveillance of pre-malignant hepatocytes limits liver cancer development. *Nature* 2011; **479**: 547–551.
13. Collado M, Serrano M. Senescence in tumours: evidence from mice and humans. *Nat Rev Cancer* 2010; **10**: 51–57.
14. Jones RG, Plas DR, Kubek S, Buzzai M, Mu J, Xu Y *et al.* AMP-activated protein kinase induces a p53-dependent metabolic checkpoint. *Mol Cell* 2005; **18**: 283–293.
15. Zwerschke W, Mazurek S, Stockl P, Hutter E, Eigenbrodt E, Jansen-Durr P. Metabolic analysis of senescent human fibroblasts reveals a role for AMP in cellular senescence. *Biochem J* 2003; **376**: 403–411.
16. Jiang P, Du W, Mancuso A, Wellen KE, Yang X. Reciprocal regulation of p53 and malic enzymes modulates metabolism and senescence. *Nature* 2013; **493**: 689–693.
17. Kaplon J, Zheng L, Meissl K, Chaneton B, Selivanov VA, Mackay G *et al.* A key role for mitochondrial gatekeeper pyruvate dehydrogenase in oncogene-induced senescence. *Nature* 2013; **498**: 109–112.
18. Kiyono T, Foster SA, Koop JI, McDougall JK, Galloway DA, Klingelhutz AJ. Both Rb/p16INK4a inactivation and telomerase activity are required to immortalize human epithelial cells. *Nature* 1998; **396**: 84–88.
19. Blalock WL, Pearce M, Steelman LS, Franklin RA, McCarthy SA, Cherwinski H *et al.* A conditionally-active form of MEK1 results in autocrine tranformation of human and mouse hematopoietic cells. *Oncogene* 2000; **19**: 526–536.
20. Woods D, Parry D, Cherwinski H, Bosch E, Lees E, McMahon M. Raf-induced proliferation or cell cycle arrest is determined by the level of Raf activity with arrest mediated by p21Cip1. *Mol Cell Biol* 1997; **17**: 5598–5611.
21. Courtois-Cox S, Genther Williams SM, Reczek EE, Johnson BW, McGillicuddy LT, Johannessen CM *et al.* A negative feedback signaling network underlies oncogene-induced senescence. *Cancer Cell* 2006; **10**: 459–472.
22. Acosta JC, O'Loghlen A, Banito A, Raguz S, Gil J. Control of senescence by CXCR2 and its ligands. *Cell Cycle* 2008; **7**: 2956–2959.
23. Collado M, Gil J, Efeyan A, Guerra C, Schuhmacher AJ, Barradas M *et al.* Tumour biology: senescence in premalignant tumours. *Nature* 2005; **436**: 642.
24. Floridi A, Paggi MG, Marcante ML, Silvestrini B, Caputo A, C De Martino. Lonidamine, a selective inhibitor of aerobic glycolysis of murine tumor cells. *J Natl Cancer Inst* 1981; **66**: 497–499.
25. Floridi A, Paggi MG, D'Atri S, De Martino C, Marcante ML, Silvestrini B *et al.* Effect of lonidamine on the energy metabolism of Ehrlich ascites tumor cells. *Cancer Res* 1981; **41**: 4661–4666.
26. Wilson JE. Isozymes of mammalian hexokinase: structure, subcellular localization and metabolic function. *J Exp Biol* 2003; **206**: 2049–2057.
27. Dorr JR, Yu Y, Milanovic M, Beuster G, Zasada C, Dabritz JH *et al.* Synthetic lethal metabolic targeting of cellular senescence in cancer therapy. *Nature* 2013; **501**: 421–425.
28. Riley JK, Carayannopoulos MO, Wyman AH, Chi M, Moley KH. Phosphatidylinositol 3-kinase activity is critical for glucose metabolism and embryo survival in murine blastocysts. *J Biol Chem* 2006; **281**: 6010–6019.
29. Kennedy AL, Morton JP, Manoharan I, Nelson DM, Jamieson NB, Pawlikowski JS *et al.* Activation of the PIK3CA/AKT pathway suppresses senescence induced by an activated RAS oncogene to promote tumorigenesis. *Mol Cell* 2011; **42**: 36–49.
30. Vredeveld LC, Possik PA, Smit MA, Meissl K, Michaloglou C, Horlings HM *et al.* Abrogation of BRAFV600E-induced senescence by PI3K pathway activation contributes to melanomagenesis. *Genes Dev* 2012; **26**: 1055–1069.
31. Dennis JW, Lau KS, Demetriou M, Nabi IR. Adaptive regulation at the cell surface by N-glycosylation. *Traffic* 2009; **10**: 1569–1578.
32. Love DC, Krause MW, Hanover JA. O-GlcNAc cycling: emerging roles in development and epigenetics. *Semin Cell Dev Biol* 2010; **21**: 646–654.
33. Wellen KE, Lu C, Mancuso A, Lemons JM, Ryczko M, Dennis JW *et al.* The hexosamine biosynthetic pathway couples growth factor-induced glutamine uptake to glucose metabolism. *Genes Dev* 2010; **24**: 2784–2799.
34. Huber AL, Lebeau J, Guillaumot P, Petrilli V, Malek M, Chilloux J *et al.* p58(IPK)-mediated attenuation of the proapoptotic PERK-CHOP pathway allows malignant progression upon low glucose. *Mol Cell* 2013; **49**: 1049–1059.
35. Smith TA. Mammalian hexokinases and their abnormal expression in cancer. *Br J Biomed Sci* 2000; **57**: 170–178.
36. Wolf A, Agnihotri S, Micallef J, Mukherjee J, Sabha N, Cairns R *et al.* Hexokinase 2 is a key mediator of aerobic glycolysis and promotes tumor growth in human glioblastoma multiforme. *J Exp Med* 2011; **208**: 313–326.
37. Braig M, Schmitt CA. Oncogene-induced senescence: putting the brakes on tumor development. *Cancer Res* 2006; **66**: 2881–2884.
38. Michaloglou C, Vredeveld LC, Soengas MS, Denoyelle C, Kuilman T, van der Horst CM *et al.* BRAFE600-associated senescence-like cell cycle arrest of human naevi. *Nature* 2005; **436**: 720–724.
39. Patra KC, Wang Q, Bhaskar PT, Miller L, Wang Z, Wheaton W *et al.* Hexokinase 2 is required for tumor initiation and maintenance and its systemic deletion is therapeutic in mouse models of cancer. *Cancer Cell* 2013; **24**: 213–228.
40. Boehm JS, Zhao JJ, Yao J, Kim SY, Firestein R, Dunn IF *et al.* Integrative genomic approaches identify IKBKE as a breast cancer oncogene. *Cell* 2007; **129**: 1065–1079.
41. Bernard D, Quatannens B, Begue A, Vandenbunder B, Abbadie C. Antiproliferative and antiapoptotic effects of crel may occur within the same cells *via* the up-regulation of manganese superoxide dismutase. *Cancer Res* 2001; **61**: 2656–2664.
42. Augert A, Payre C, de Launoit Y, Gil J, Lambeau G, Bernard D. The M-type receptor PLA2R regulates senescence through the p53 pathway. *EMBO Rep* 2009; **10**: 271–277.
43. Yang SH, Sarkar SN, Liu R, Perez EJ, Wang X, Wen Y *et al.* Estrogen receptor beta as a mitochondrial vulnerability factor. *J Biol Chem* 2009; **284**: 9540–9548.

Cell Death and Disease **is an open-access journal published by** ***Nature Publishing Group*****. This work is licensed under a Creative Commons Attribution-NonCommercial-ShareAlike 3.0 Unported License. To view a copy of this license, visit http://creativecommons.org/licenses/by-nc-sa/3.0/**

Supplementary Information accompanies this paper on Cell Death and Disease website (http://www.nature.com/cddis)

Supplementary Figure 1

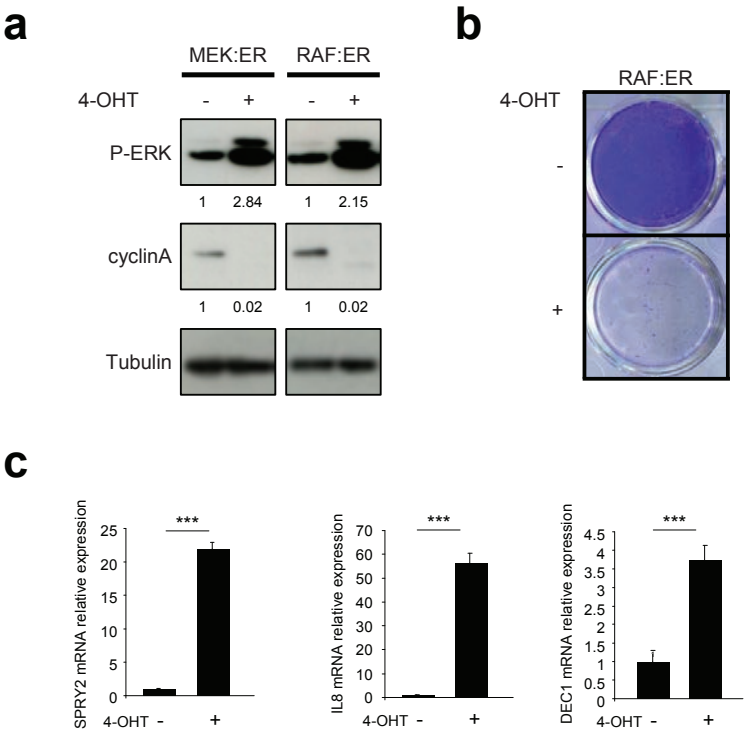

Supplementary Figure 1 Model of RAF:ER induced senescence. (**a**) Immortalized human mammary epithelial cells expressing the inducible MEK:ER or RAF:ER oncogene were treated or not with 4-OHT for 3 days. On day 4 cell extracts were prepared and expression of the indicated proteins were analyzed by immunoblotting. (**b**) RAF:ER-expressing cells were treated or not with 4-OHT for 3 days. After 3 additional days, the cells were PFA-fixed and crystal-violet-stained. (**c**) RAF:ER cells were treated for 3 days with 4-OHT. The next day, RNAs were prepared, reverse-transcribed, and those corresponding to the indicated genes were quantified. Expression was normalized with respect to actin expression.

Supplementary Figure 2

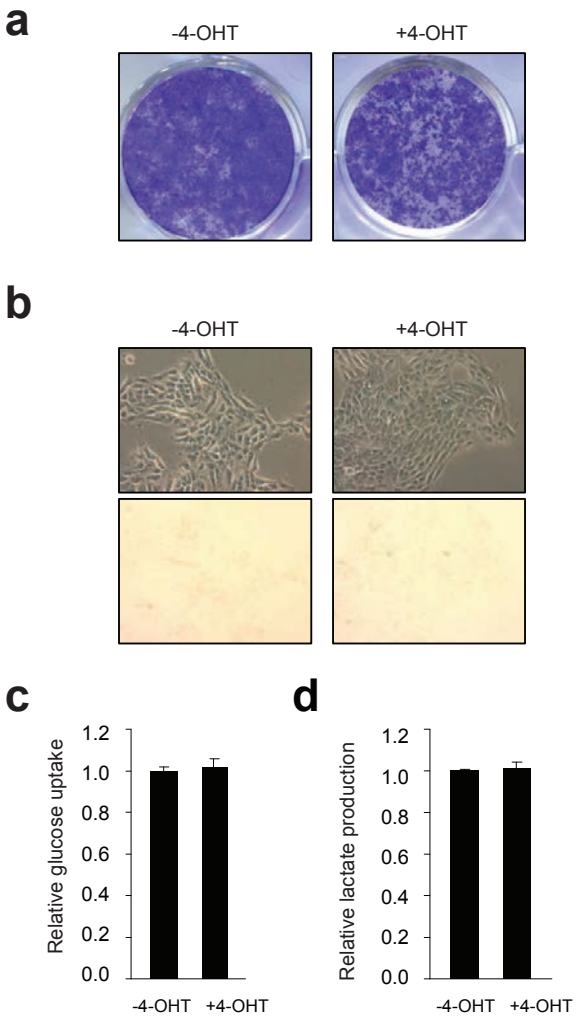

Supplementary Figure 2 4-OHT treatment does not impact senescence and metabolism. (**a-c**) HMECs hTERT without MEK:ER were seeded at the same density and treated with 4-OHT for 3 days. (**a**) Proliferation was assessed by crystal violet staining. (**b**) 4-OHT treatment did not induce any SA-β-gal activity. (**c**) Glucose uptake and (**d**) lactate production remained unchanged under 4-OHT treatment.

Supplementary Figure 3

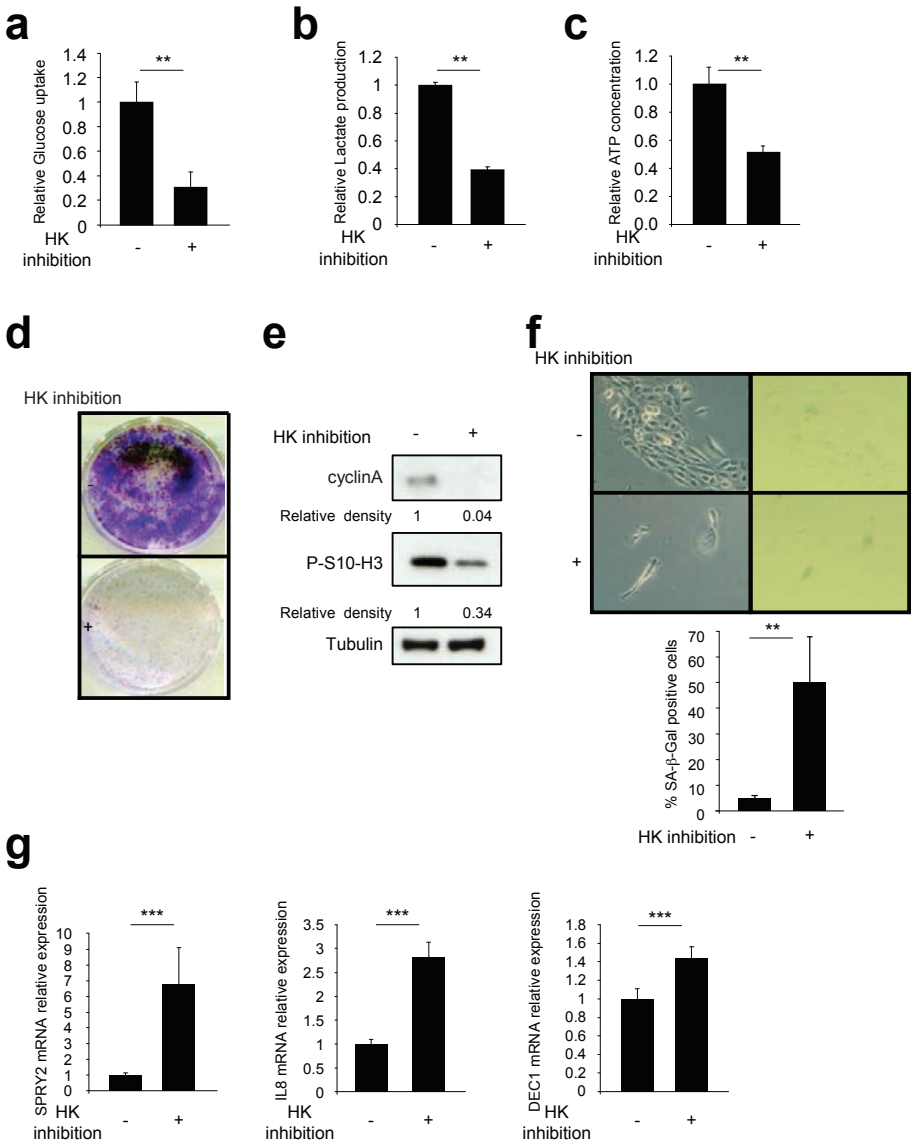

Supplementary Figure 3 Hexokinase inhibition by Lonidamine induces premature senescence. (**a-c**) Cells treated twice with Lonidamine or not treated were seeded at the same density. After 24 h, glucose uptake (**a**), lactate production (**b**) and the ATP concentration (**c**) were determined. (**d**) Immortalized cells were seeded and treated or not with Lonidamine for 3 days. Four days later, the cells were fixed and stained with crystal violet. (**e**) Cells were treated once with or without Lonidamine. The next day, cell extracts were prepared and analyzed by immunoblotting with antibodies targeting the indicated proteins. (**f**) Cells were treated or not with Lonidamine for 3 days. Two days later, an SA-β-Gal assay was performed. (**g**) Cells were grown with or without Lonidamine for 1 day. The following day, RNAs were prepared and expression of the indicated genes was measured by RTqPCR.

Supplementary Figure 4

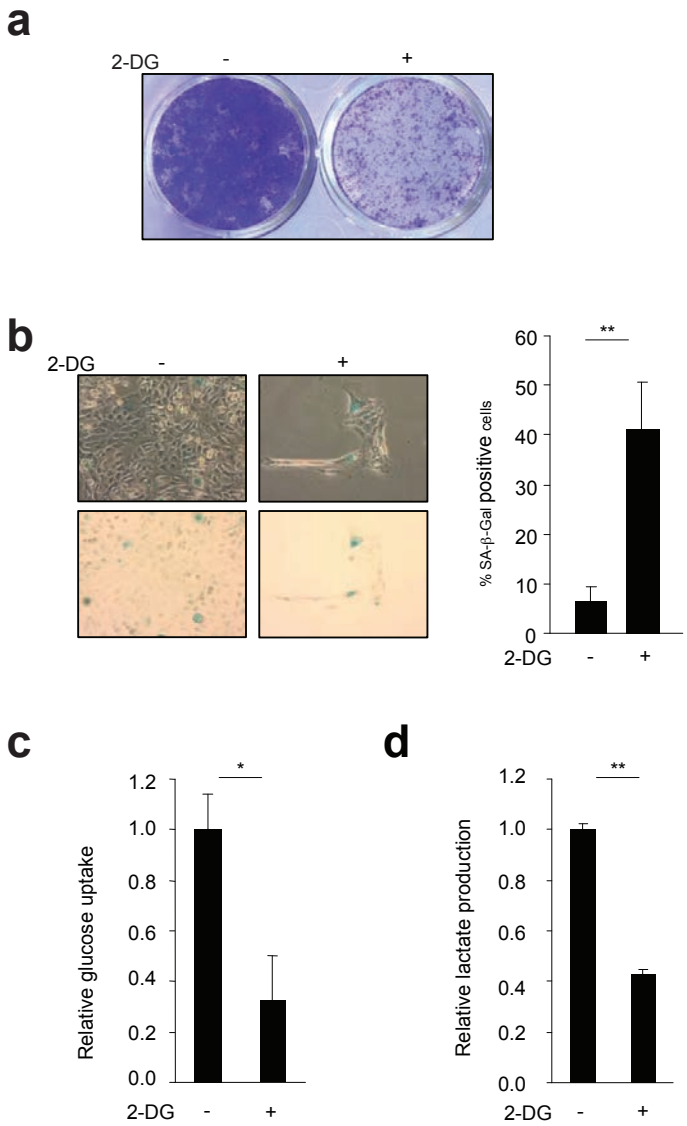

Supplementary Figure 4 Glycolysis inhibition favors senescence. Cells were seeded at the same density and treated with the glycolytic inhibitor 2-deoxy-D-glucose (2-DG) 1 mM for 4 days. (**a**) Proliferation was assessed by crystal violet staining. (**b**) SA-β-gal activity was analyzed after 2-DG treatment or not. (**c**) Treated or non-treated cells were seeded at the same density and glucose uptake and lactate production were determined after 24h.

Supplementary Figure 5

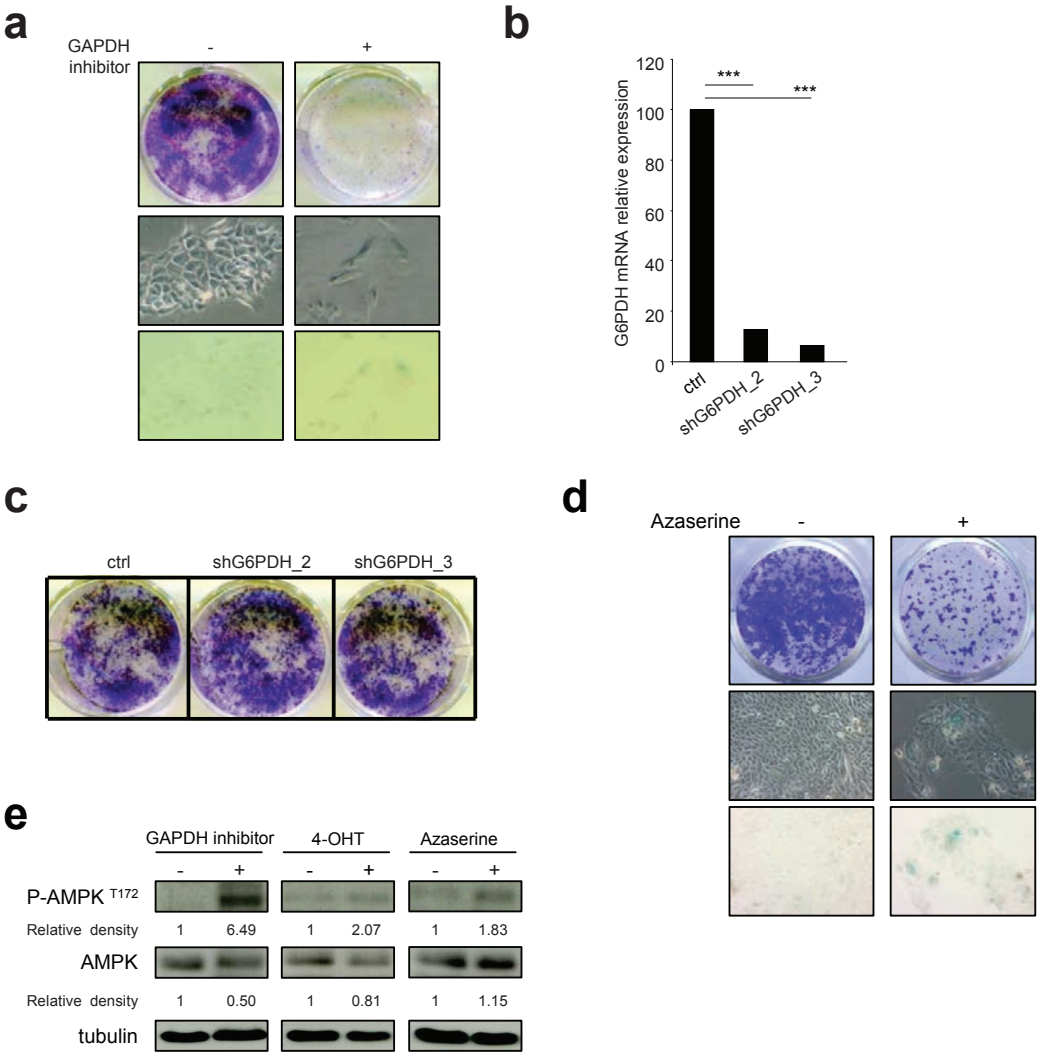

Supplementary Figure 5 Glycolysis and hexosamine pathway inhibition favors premature senescence. (**a**) Cells were seeded at the same density and treated with the GAPDH inhibitor bromopyruvate (20μM) for 4 days. Proliferation was assessed by crystal violet staining and senescence by SA-β-gal activity. (**b**) Cells were infected with 2 shRNA targeting G6PDH enzyme, selected and RNA prepared. RTqPCR was next performed to analyze G6PDH knockdown. (**c**) Proliferation was analyzed by crystal violet staining. (**d**) Cells were seeded and treated for 3 days with 25μM Azaserine, a Glutamine fructose-6-phosphate amidotransferase (GFAT) inhibitor. Cells were fixed and crytal violet stained (upper panel) or assayed for their SA-β-gal activity. (**e**) Cell extracts were prepared and analyzed for the expression of the indicated proteins (anti-AMPK, 2532 Cell Signaling; anti-p-AMPK(Thr172), 2535 Cell Signaling).

Supplementary Figure 6

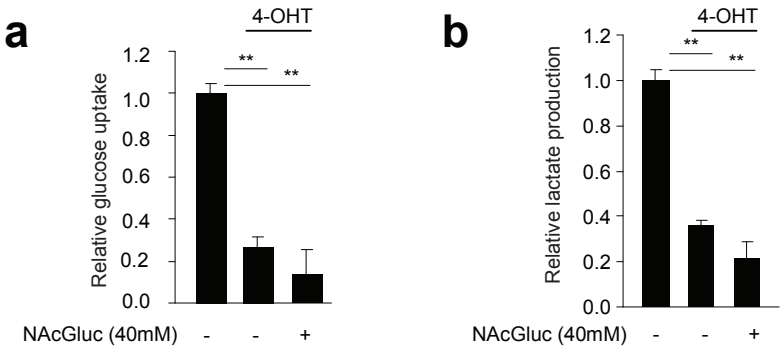

Supplementary Figure 6 N-Acetyl Glucosamine treatment does not modify glucose consumption and lactate production. Treated or non-treated cells as indicated were seeded as for senescence experiments and seeded at the same density the day prior (**a**) glucose uptake and (**b**) lactate production measurement.

Supplementary Figure 7

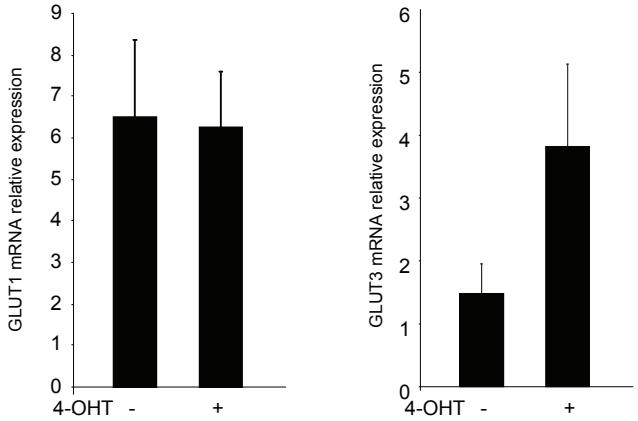

Supplementary Figure 7 Decrease in glucose uptake during OIS is not due to GLUT1/GLUT3 expression donwnregulation. RNA was extracted from treated or non-treated cells with 4-OHT and reverse-transcribed. GLUT1 and GLUT3 expression was assayed by quantitative PCR and normalized with respect to actin expression.

Supplementary Figure 8

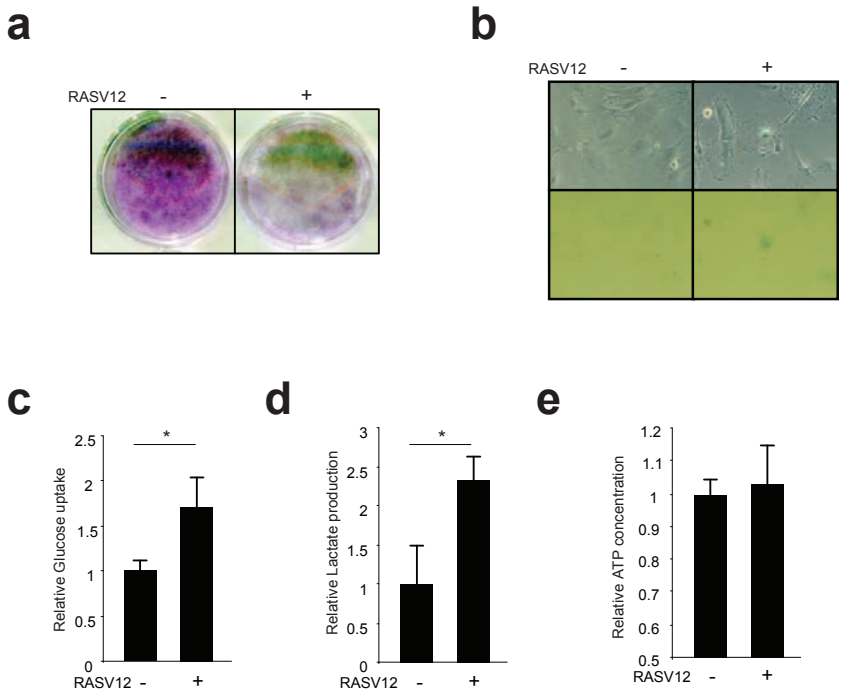

Supplementary Figure 8 OIS does not slow down glucose metabolism in mouse embryonic fibroblasts. MEFs were infected with a control or an RASV12 retroviral vector and puromycin selected. After selection, the various assays were performed. (**a**) Cells were seeded at the same density. After 5 days, they were fixed and crystal-violet-stained. (**b**) Three days after seeding, an SA-β-Gal assay was performed. (**c-e**) The day after cell seeding, glucose uptake (**c**), lactate production (**d**), and the ATP concentration (**e**) were assayed.

Supplementary Figure 9

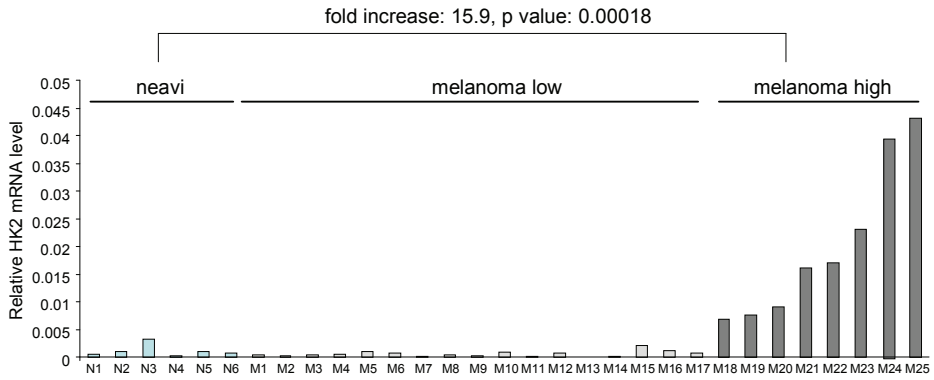

Supplementary Figure 9 HK2 is amplified in vivo during OIS escape in human samples. RNA was extracted from melanocytic naevi and melanomas and reverse-transcribed. HK2 expression was assayed by quantitative PCR and normalized with respect to actin expression.

Article 5 : PLA2R1 mediates tumor suppression by activating JAK2

Published OnlineFirst September 5, 2013; DOI: 10.1158/0008-5472.CAN-13-0318

Tumor and Stem Cell Biology

Cancer Research

PLA2R1 Mediates Tumor Suppression by Activating JAK2

David Vindrieux[1,2,3,4], Arnaud Augert[1,2,3,4,5], Christophe A. Girard[6], Delphine Gitenay[1,2,3,4], Helene Lallet-Daher[1,2,3,4], Clotilde Wiel[1,2,3,4], Benjamin Le Calvé[1,2,3,4], Baptiste Gras[1,2,3,4], Mylène Ferrand[1,2,3,4], Stéphanie Verbeke[7], Yvan de Launoit[5], Xavier Leroy[8,9], Alain Puisieux[1,2,3,4], Sébastien Aubert[8,9], Michael Perrais[9], Michael Gelb[10], Hélène Simonnet[1,2,3,4], Gérard Lambeau[6], and David Bernard[1,2,3,4]

Abstract

Little is known about the physiological role of the phospholipase A2 receptor (PLA2R1). PLA2R1 has been described as regulating the replicative senescence, a telomerase-dependent proliferation arrest. The downstream PLA2R1 signaling and its role in cancer are currently unknown. Senescence induction in response to activated oncogenes is a failsafe program of tumor suppression that must be bypassed for tumorigenesis. We now present evidence that PLA2R1 functions *in vitro* as a tumor suppressor, the depletion of which is sufficient to escape oncogene-induced senescence (OIS), thereby facilitating oncogenic cell transformation. Furthermore, mice that are genetically deficient in PLA2R1 display increased sensitivity to RAS-induced tumorigenesis by facilitating OIS escape, highlighting its physiological role as a tumor suppressor. Unexpectedly, PLA2R1 activated JAK2 and its effector signaling, with PLA2R1-mediated inhibition of cell transformation largely reverted in JAK2-depleted cells. This finding was unexpected as the JAK2 pathway has been associated mainly with protumoral functions and several inhibitors are currently in clinical trials. Taken together, our findings uncover an unanticipated tumor suppressive role for PLA2R1 that is mediated by targeting downstream JAK2 effector signaling. *Cancer Res; 73(20); 6334–45. ©2013 AACR.*

Introduction

During tumorigenesis, dysregulation of oncogenes and tumor suppressor genes interferes with normal cell homeostasis, causing aberrant cell growth (1, 2). Cellular senescence is a crucial barrier against aberrant cell growth, acting as a tumor-suppressive mechanism by inhibiting cell immortalization (3, 4), preventing tumoral progression (5–7), and contributing to the antitumor response of clinical drugs (8, 9).

The identification and characterization of tumor suppressor genes controlling failsafe mechanisms including senescence may reveal new insights into normal cell homeostasis and related defects in tumors. A better understanding of the basic processes involved in tumor development may lead to the discovery of novel biomarkers and new clinically relevant targets and pathways. By conducting loss-of-function genetic screening, we have previously shown that cellular knockdown of the phospholipase A2 receptor (PLA2R1) extends the population-doubling capacity of normal human fibroblasts and thus delays replicative senescence (10). PLA2R1 is a transmembrane receptor of approximately 180 to 200 kDa possessing a large extracellular domain composed of a cysteine-rich domain (Cys-R), a fibronectin-like type II domain (FN-II), and 8 C-type lectin-like domains (CTLD). It contains a single-pass transmembrane domain and a short intracellular cytoplasmic tail. It belongs to the mannose receptor family and binds several secreted phospholipases A2 (sPLA2s), different types of collagens, and carbohydrates. Some secreted phospholipase A2 has also been shown to induce a premature senescence in normal human fibroblasts (11). Nevertheless, the physiological consequences of these ligands and their binding to receptors remain unclear. Overall, the functions of PLA2R1 are, to date, still unclear and unknown in the context of tumorigenesis (12, 13). Given the ability of PLA2R1 to regulate the occurrence of replicative senescence in normal human fibroblasts (10) and the intimate relationship between senescence and cancer, we have investigated its potential role in tumorigenesis.

Materials and Methods

Cell culture

Cell lines were cultured in DMEM (Invitrogen) for MDAMB-231 (ATCC), MDAMB-436 (ATCC), Cama-1 (ATCC), MDA-MB-453 (ATCC), Hs-578T (ATCC), WI38 (ATCC), and

Authors' Affiliations: [1]Inserm U1052, Centre de Recherche en Cancérologie de Lyon; [2]CNRS UMR5286; [3]Centre Léon Bérard; [4]Université de Lyon, Lyon; [5]UMR8161, CNRS/Universités de Lille 1 et 2; [6]Institut de Pharmacologie Moléculaire et Cellulaire, UMR7275, CNRS and Université de Nice-Sophia Antipolis, Valbonne; [7]INSERM U916, Bergonié Cancer Institute, Université Bordeaux, Bordeaux; and [8]Institut de Pathologie, CHRU, Faculté de Médecine, Université de Lille; [9]INSERM U837, Jean-Pierre Aubert Research Center, Team 5, Lille; [10]Department of Medicine, University of Washington, Seattle, Washington

Note: Supplementary data for this article are available at Cancer Research Online (http://cancerres.aacrjournals.org/).

D. Vindrieux and A. Augert contributed equally to this article.

Corresponding Author: David Bernard, CRCL, UMR INSERM U1052/CNRS 5286, Centre Léon Bérard, 28, rue Laënnec, 69373 Lyon, Cedex 08, France. Phone: 33-4-26-55-67-92; Fax: 33-4-78-78-27-20; E-mail: david.bernard@lyon.unicancer.fr

doi: 10.1158/0008-5472.CAN-13-0318

©2013 American Association for Cancer Research.

Downloaded from cancerres.aacrjournals.org on May 19, 2014. © 2013 American Association for Cancer Research.

Published OnlineFirst September 5, 2013; DOI: 10.1158/0008-5472.CAN-13-0318

JAK2- or wild-type (WT)-derived NIH3T3 (14). Virus producing GP293 cells (Clontech) were cultured in DMEM. All medium were supplemented with 10% FBS (Lonza) and 1% penicillin/streptomycin (Invitrogen). Human mammary epithelial cells (HMEC; Clonetics) were cultured in Mammary Epithelial Cell Growth Medium (Promocell) in the presence of 1% penicillin/streptomycin. Normal human keratinocytes (Lonza) were cultured in Keratinocyte Growth Medium 2 (Promocell) in the presence of 1% penicillin/streptomycin. Upon receipt, cells were thawed, amplified, and aliquots frozen. Experiments were conducted from these aliquots within a 4 months period without further authentication of the cell lines. The cells were maintained at 37°C under a 5% CO_2 atmosphere.

Immunohistochemistry

Paraffin-embedded murine tissues were used. Slides were serially sectioned at 4-μm thickness. After deparaffinization and rehydration, the slides were incubated in 5% hydrogen peroxide in sterile water to block endogenous peroxidases. For heat-induced antigen retrieval, tissue sections were boiled in 10 mmol/L citrate buffer pH 6 in a microwave oven for 20 minutes. The slides were then incubated at 4°C overnight with the primary antibody diluted in "low-background" antibody diluent (DAKO Real). After rinsing in PBS, the slides were incubated with a biotinylated secondary antibody bound to a streptavidin peroxidase conjugate (Dako E0468) for 1 hour at room temperature. Bound antibody was revealed and sections were finally counterstained with hematoxylin. The antibodies used are: anti-p16 (sc-1207; Santa Cruz Biotechnology), anti-Ki67 (clone Tec-3, M7249; DAKO), anti-phospho-JAK2 (Tyr 1007; sc-101717; Santa Cruz Biotechnology), anti-DEC1 (XS2130; Novus Biological), anti-DcR2 (ADI-AAP-371-E; Enzo Life Sciences). Immunohistochemistry (IHC) were conducted in parallel with the different samples for a given Ab to achieve comparable staining allowing quantification. Counts were made on the IHC staining conducted from samples obtained from 2 independent mice. At least 1,000 cells taken from 6 to 10 independent fields for p16 or Ki67 staining, or on 15 to 45 independent fields (magnification, ×40) for P-JAK2 were analyzed.

Immunofluorescence

Cell were fixed with methanol, incubated with the various primary antibodies and with secondary antibodies coupled to fluorescent dyes (Invitrogen). Nuclei were stained with Hoechst (Sigma). The primary antibodies used were: anti-phospho-Jak2 (Tyr1007/1008; 3771; Cell Signaling) and anti-PLA2R1 (15). Fluorescence was analyzed by normal or confocal microscopy.

Ligation proximity assay

The first steps (fixation and primary antibodies) were conducted as for the immunofluorescence experiments. For the following next steps, we followed the manufacturer's recommendations (Duolink In Situ; Olink Bioscience).

Transfection and infection

Virus producing GP293 cells were transfected by means of PEI reagent according to the manufacturer's recommendations (Euromedex). Cells were transfected with the VSVg (1 of 6) and the retroviral vector of interest (5 of 6). Two days after transfection, the viral supernatant mixed with fresh medium (1 of 2) and polybrene (final concentration: 8 μg/mL) was used to infect target cells. Cells were infected for a period of 12 to 24 hours depending on the cell type. Importantly, the infection protocols were designed so that practically all cells were infected, as judged by the GFP positive cells. One day postinfection, cells were selected with puromycin at the final concentration of 0.5 to 1 μg/mL depending on the cell type and/or with geneticin at the final concentration of 100 μg/mL.

Transformation assays

To measure anchorage-independent growth, cells were detached with trypsin and resuspended in growth medium. Base agar was prepared with 0.75% low-melting agarose (Lonza) in growth medium. The top agar contained the suspension of cells in 0.45% low-melting agarose ($1.5–3.0 \times 10^4$ cells/well in 6-well plates, depending on the cell type). Plates were incubated for 2 to 3 weeks at 37°C and colonies were counted under a bright light microscope. The mean surface for MDA-MB-436 was quantified with Image J software.

Immunoblot

Cell lysates were prepared in ice-cold Giordano buffer (50 mmol/L Tris-HCl, pH 7.4, 250 mmol/L NaCl, 0.2% Triton X-100, 5 mmol/L EDTA) supplemented with protease and phosphatase inhibitors (Roche). Lysates were clarified by centrifugation at 14,000 rpm for 30 minutes at 4°C. Protein concentrations were measured by means of the Bradford protein assay (Bio-Rad #500-0006). Cell extracts were resolved by SDS-PAGE under nonreducing conditions for PLA2R1 detection or reducing conditions for detection of other proteins and transferred onto nitrocellulose membranes. For detection, the following primary antibodies were used: anti-PLA2R1 (HPA012657; Atlas), antitubulin (T6199; Sigma), anti-Ras (sc-520; Santa Cruz Biotechnology), anti-phosphoERK (9101; Cell Signaling), anti-myc tag (sc-789; Santa Cruz Biotechnology), anti-H3-pSer10 (ab14955; Abcam), anti-phospho-STAT3 Tyr 705 (9145; Cell Signaling), and anti-STAT3 (sc-483; Santa Cruz Biotechnology). After overnight incubation at 4°C with primary antibodies, blots were washed with PBS containing 0.05% Tween, incubated with a peroxidase-coupled secondary antibody, and washed again in PBS containing 0.05% Tween. Antigen–antibody complexes were detected by ECL (Amersham).

Colony formation assays

Colony formation assays were carried out in 12-well plates. Five to ten days after seeding, the cells were washed with PBS, fixed with 4% paraformaldehyde, and stained with 0.05% crystal violet (Sigma-Aldrich).

EdU staining

Infected and selected HMEC were treated with 4OHT. Two weeks later, EdU staining was conducted with EdU Alexa Fluor kit (Invitrogen) according to the manufacturer's recommendations. A total of 10,000 cells were analyzed by flow cytometry and the number of EdU positive cells determined.

Downloaded from cancerres.aacrjournals.org on May 19, 2014. © 2013 American Association for Cancer Research.

Published OnlineFirst September 5, 2013; DOI: 10.1158/0008-5472.CAN-13-0318

RNA extraction, retro-transcription, and PCR

RNA extractions were conducted using a phenol–chloroform method using TriReagent (Sigma-Aldrich). PhaseLockGel tubes (Eppendorf) were used for phase separation. The synthesis of cDNA was conducted from 3 μg of total RNA using the First-Strand cDNA Synthesis Kit (GE Healthcare). The RT reaction was diluted 1 of 60 and used as cDNA template for quantitative PCR (qPCR) analysis. TaqMan qPCR analysis was carried out on a LightCycler 2.0 System (Roche Applied Science). PCR mixtures were made up of the LightCycler TaqMan mix, 200 nmol/L primers and 1.67 μL of cDNA template. Housekeeping gene ACTB was used for normalization. Real-time PCR intron-spanning assays were designed using the ProbeFinder software (Roche Applied Science).

Vectors

Human PLA2R1 (GenBank NM 007366) was amplified by PCR from the PLA2R1-encoding pSupF vector and ligated into the pGEMTeasy vector (Promega), sequenced and subsequently subcloned in the pLPCX retroviral vector (Clontech) using *Xho*I/*Not*I restriction sites. The primers used for the PCR were: Fwd: 5′-TACTCGAGCCACCATGCTGCTGTCGCCGTCGCTG-3′ and Rev WT: 5′-TAGCGGCCGCTTATTGGTCACTCTTCT-CAAGATC-3′. For the PLA2R1 mutant, the same Fwd primer was used and the Rev MUT sequence was: 5′-TAGCGGCCGCT-TATCTCCTGAAGAAGCCACCGTTATG-3′. pMX-IRES-EGFP ctrl or containing SOCS3*myc* was provided by Akihiko Yoshimura (16). The plasmids pLNCX2Neo/H-Ras(G12V)-ER (17) and pBabe-puro-H-RASV12 (18) were used as indicated in the various experiments. Retroviral expressing short hairpin RNA (shRNA) targeting JAK2 were ordered from Source Bioscience Lifesciences (NKI_p3205L241Q). The retroviral vectors expressing shRNAs targeting PLA2R1 were described in ref. 10.

***In vivo* skin carcinogenesis**

PLA2R1 knockout mice were described and genotyped as in ref. 19. Six-week-old PLA2R1 knockout or WT littermate C57BL/6 mice were treated with a single application of 25 μg DMBA (Sigma-Aldrich) in 200 μL acetone, followed by applications twice a week of 200 μL of TPA (Sigma-Aldrich) of a 10^{-4}M solution in acetone. Mice were shaved every 2 to 3 weeks to allow better exposure to TPA. The experiments were conducted in accordance with the animal care guidelines of the European Union and French laws and were validated by the local Animal Ethic Evaluation Committee (CECCAPP).

Promoter activity

Two hundred thousand GP293 cells were plated in 12 well plate, coated with poly-lysine. HO-1 promoter luciferase vector plasmid (20) was transfected with ctrl or with PLA2R1 encoding vector in GP293 using PEI reagent according to the manufacturer's recommendations (Euromedex). Forty-eight hours after transfection, cells were scraped on ice with 100 μL of cold PBS and the luminescence was measured and normalized to the one of actin promoter according to the manufacturer's recommendations (MISSION LightSwitch Luciferase Assay Reagent; Sigma).

SA-β-Gal analysis

SA-β-Gal analyses were conducted as in ref. 21. At least 5 different fields were counted for each condition representing at least 500 events.

Statistical analysis

The values are presented as mean ± SEM. The statistical analysis was conducted using the Student *t* test (*, $P < 0.05$; **, $P < 0.01$; ***, $P < 0.005$). The number of independent replicates for each experiment was indicated in the figure legends.

Results

PLA2R1 decrease favors oncogene-induced senescence escape

Senescence is activated in normal cells in response to telomere shortening (replicative senescence) and to oncogenic signals (oncogene-induced senescence). By blocking cell growth, senescence prevents outgrowth of abnormal cells. We examined the effect of PLA2R1 depletion on oncogene-induced senescence (OIS), a key step in tumoral progression (5, 6). According to the Oncomine database (Compendia Bioscience), a database that allowed us to examine the variation of PLA2R1 expression in several cancers versus normal tissues, PLA2R1 mRNA levels were found to be generally decreased in cancer and especially in breast cancer, we then choose to investigate a putative role of PLA2R1 on OIS using human mammary epithelial cells (Supplementary Table). Young HMECs were infected with a retroviral vector encoding an inducible (ER-coupled) form of a constitutively active RAS gene (H-RASG12V) together with a control shRNA or an shRNA targeting PLA2R1 retroviral vectors. Cells were next selected to stably express the 2 transgenes (RASG12V:ER + control or RASG12V:ER + PLA2R1 shRNA). As expected, shRNA directed against PLA2R1 was able to decrease PLA2R1 messengers as well as endogenous or exogenous PLA2R1 proteins (Supplementary Fig. S1A–S1C). We next checked that control or shRNA-PLA2R1 expressing cells displayed similar RAS activation after 4-OHT treatment according to its stabilization and to ERK phosphorylation, a substrate of MEK, a downstream RAS effecter (Fig. 1A). As expected, the oncogenic stress induced by RAS resulted in a major decrease of the mitotic marker H3-pSer10 (Fig. 1A), blocked cell growth (Fig. 1B), decreased EdU, an analogs of the T, DNA-incorporation (Fig. 1C), increased the average cell size, a mark of senescent cells (Fig. 1D) and resulted in an increase in SA-β-Gal activity (Fig. 1E). In contrast, resistant clones emerged in the PLA2R1 knockdown cells (Fig. 1B). As expected, these cells maintained H3-pSer10 expression (Fig. 1A), displayed higher EdU incorporation (Fig. 1C), were smaller in size (Fig. 1D) and displayed lower levels SA-β-Gal activity (Fig. 1E) than control senescing cells. Knockdown of PLA2R1 with a second shRNA (PLA2R1-2) also favored OIS escape (Supplementary Fig. S1D), suggesting that these effects were not due to off targets effects. These data support the view that PLA2R1 expression decreased improves the ability of HMEC to overcome oncogenic-stress–induced senescence.

Downloaded from cancerres.aacrjournals.org on May 19, 2014. © 2013 American Association for Cancer Research.

Published OnlineFirst September 5, 2013; DOI: 10.1158/0008-5472.CAN-13-0318

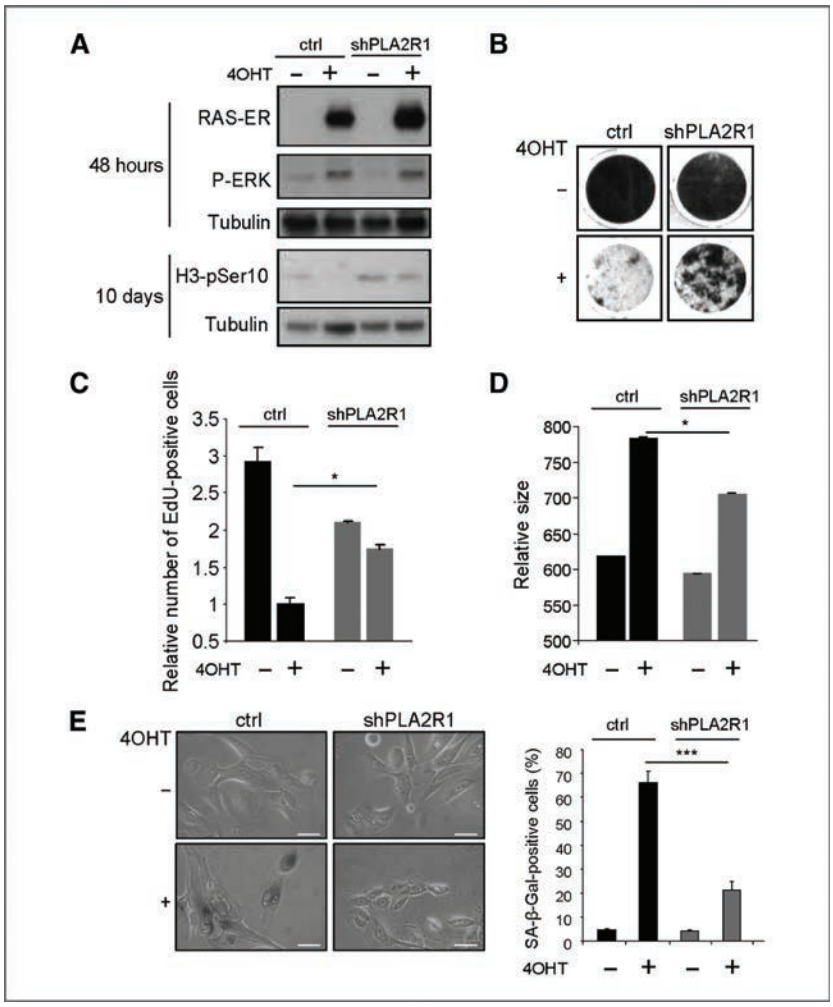

Figure 1. PLA2R1 regulates oncogene-induced senescence. HMEC were coinfected with H-RAS^{G12V}ER encoding retroviral vector (neomycin resistance) with retroviral vectors expressing a control or PLA2R1-targeting shRNA (shPLA2R1; puromycin resistance). They were next selected for a week with puromycin and geneticin. The cells were then counted and plated for the different experiments. Treatment with 4-hydroxytamoxifen (4OHT) was conducted at 100 nmol/L for 48 hours. A, Western blot analysis was conducted at the indicated times after 4OHT treatment with antibodies targeting the indicated proteins. Tubulin was used as loading control. The experiments shown are representative of 3 repeats. B, the colony formation assay was assessed with crystal violet 15 days after 4OHT treatment. The experiments shown are representative of 2 repeats. C, EdU staining was conducted 2 weeks after 4OHT treatment. The relative number of EdU-positive cells was measured by flow cytometry. The experiments shown are representative of 2 repeats. D, Ten days after the 4OHT treatment, relative cell size was measured by flow cytometry gating the FSC (forward scattered light) parameter. The experiments shown are representative of 2 repeats. E, SA-β-Gal analysis was conducted 15 days after 4OHT treatment. Representative pictures are shown (scale bar, 50 μm). SA-β-Gal-positive cells were quantified as indicated in Materials and Methods. The experiments shown are representative of 2 repeats. *, $P < 0.05$; ***, $P < 0.005$.

Ectopic PLA2R1 expression inhibits cancer cell transformation

Cellular transformation requires alterations of failsafe programs such as senescence (2). We therefore wanted to examine whether altering PLA2R1 expression in cancer cells might impact their ability to form clones in soft agar, a hallmark of transformed cells. To this end, the indicated cancer cells were infected with a control or a PLA2R1-encoding vector and selected to stably express PLA2R1. As expected, PLA2R1 was constitutively expressed in these cells according to immunoblot analyses (Fig. 2A and B). PLA2R1 constitutive expression was found to block the growth in soft agar (Fig. 2C and D), supporting a tumor suppressive role of PLA2R1 in cancer cells.

Next, cancer cells were transduced with retroviral vectors expressing a control or an shRNA directed against PLA2R1 and selected to stably inhibit PLA2R1 expression, as validated by

Downloaded from cancerres.aacrjournals.org on May 19, 2014. © 2013 American Association for Cancer Research.

Published OnlineFirst September 5, 2013; DOI: 10.1158/0008-5472.CAN-13-0318

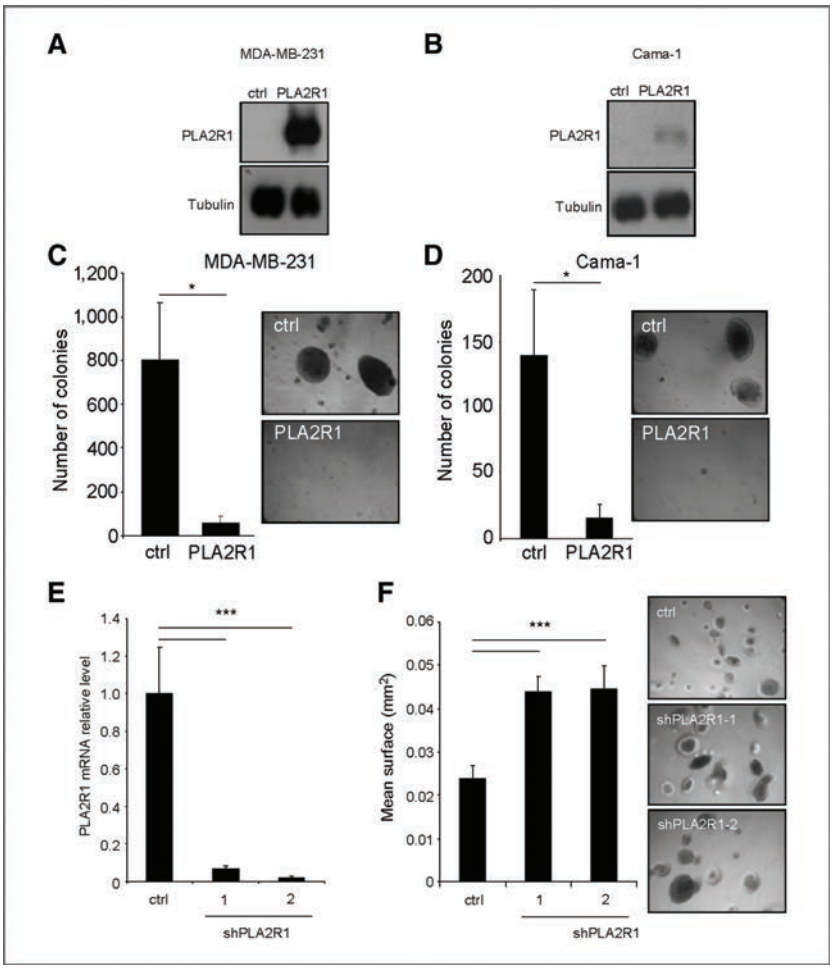

Figure 2. PLA2R1 impacts cancer cell transformation. A and B, the indicated cancer cell lines were infected with a control or a PLA2R1-encoding retroviral vector and puromycin selected. Protein extracts were prepared and PLA2R1 expression verified by Western blot. Tubulin was used as a loading control. The experiments shown are representative of 3 repeats. C and D, the indicated cancer cells were seeded in soft agar and grown for 2 weeks. The number of clones was counted. The experiments shown are representative of 3 repeats. E, MDA-MB-436 cancer cells were infected with retroviral vectors expressing a control or an shRNA directed against PLA2R1 and puromycin selected. After selection, RNAs were prepared and an qRT-PCR conducted against PLA2R1 and normalized to actin levels. The experiments shown are representative of 3 repeats. F, MDA-MB-436 cells were seeded in soft agar and images were taken 3 weeks after seeding. Mean size of the clones were calculated using image J software. The experiments shown are representative of 2 repeats. *, $P < 0.05$; ***, $P < 0.005$.

quantitative reverse transcription (qRT)-PCR (Fig. 2E and Supplementary Fig. S2A). PLA2R1 knockdown was found to increase the transformed phenotype of the MDA-MB-436 cells as measured by the increase size of the soft agar clones (Fig. 2F) and of the slightly transformed Hs-578T cells as measured by the increased ability of these cells to form soft agar clones (Supplementary Fig. S2B). Overall, these results show that the decrease of PLA2R1 expression favors transformation whereas its constitutive expression blocks cancer cell transformation.

PLA2R1 knockout mice display increased sensitivity to RAS-induced carcinogenesis

The above results support the view that PLA2R1 loss might favor senescence escape and transformation. To confirm a tumor suppressive role of PLA2R1, we investigated the *in vivo* cooperation between RAS and PLA2R1 loss using a RAS-dependent skin carcinogenesis protocol. Before doing these experiments targeting the keratinocytes *in vivo*, we wanted to see whether the knockdown of PLA2R1 also favors OIS escape in human normal keratinocytes. As previously described for the HMEC, we stably coexpressed RASG12V:ER and, control or PLA2R1 shRNA in the keratinocytes. As expected, we observed PLA2R1 mRNA decreased in the knockdown cells (Supplementary Fig. 3A). We found that activation of RAS by adding 4-OHT (Supplementary Fig. S3A) resulted, as expected, in a growth arrest (Supplementary Fig. S3B and S3C) and in accumulation of SA-β-Gal positive cells (Supplementary Fig. S3D). By contrast, the PLA2R1 knockdown favors the emergence of OIS resistant cells as judged by their growth and their decreased SA-β-Gal activity (Supplementary Fig. S3B–S3D).

RAS-dependent skin carcinogenesis protocol, 7,12-dimethylbenz(a)anthracene (DMBA) as an initiator and 12-O-tetradecanoylphorbol 13-acetate (TPA) as a promoter (22, 23), was used to induce papillomas in WT and PLA2R1 knockout littermate mice (19). As expected, 6 weeks of treatment (before the appearance of the papillomas) triggered an increase expression of senescence markers such as p16, DEC1, or DcR2

Downloaded from cancerres.aacrjournals.org on May 19, 2014. © 2013 American Association for Cancer Research.

Published OnlineFirst September 5, 2013; DOI: 10.1158/0008-5472.CAN-13-0318

(Supplementary Fig. S4A) in the hyperplasic epidermis. The proliferation marker Ki67 showed that the basal epidermis displayed increase proliferation (Supplementary Fig. S4B). Interestingly, papillomas (observed after 10 weeks of treatment in WT mice) had decreased SA-β-Gal activity (Supplementary Fig. S4C) and displayed a strong decrease in nuclear p16 when compared to adjacent treated skin (Fig. 3A). Of note, the p16 staining was mainly nuclear in the adjacent skin between 6

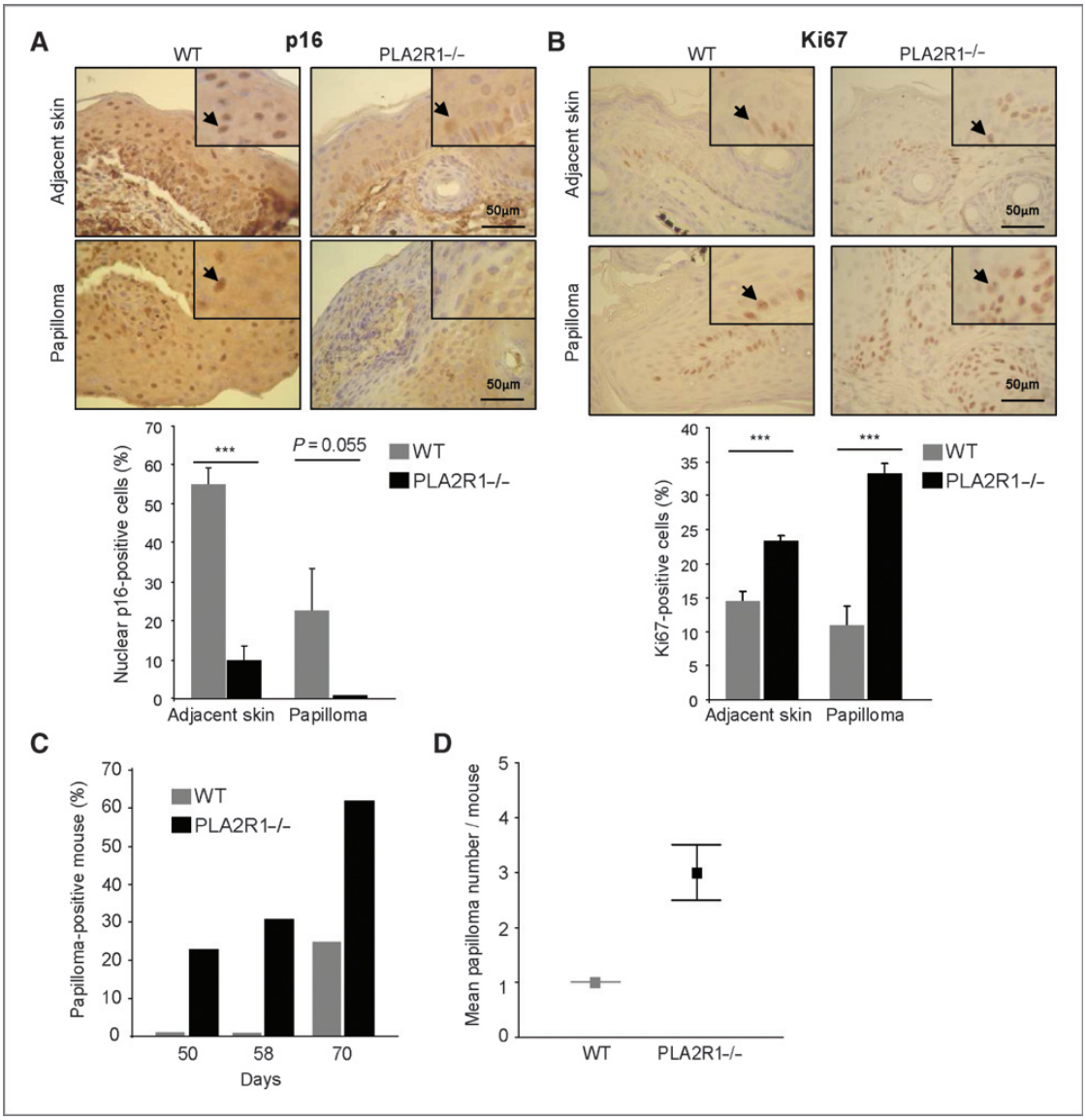

Figure 3. PLA2R1 knockout mice display increased susceptibility to skin carcinogenesis. A, six-weeks-old mice were treated once by the carcinogen DMBA and then daily, twice a week, by the promoter TPA. Ten weeks after beginning the treatment, mice were sacrificed; skins containing papilloma and adjacent tissues, from 2 independent mice per condition, were then fixed and paraffin-embedded. Tissues slides were hematoxylin stained (blue nuclei) and stained by IHC against the p16 senescent marker (brown). p16 nuclear cell counts were conducted on at least 1,000 cells in between 6 and 10 independent fields in tissues from 2 mice per condition. Representative pictures are shown (arrows indicate staining scored as positive). B, mice and skin were processed as described in A, but IHC was conducted against Ki67 proliferation marker. At least 1,000 cells were counted representing at least 6 independent fields of tissues from 2 independent mice per conditions. Representative pictures are shown (arrows indicate staining scored as positive). C, at the indicated time points after the beginning of the treatment, macroscopic analysis on the skin mice were conducted to calculate the percentage of mice displaying at least 1 papilloma (WT, $n = 8$; knockout, $n = 13$). D, in the papilloma-positive mice at day 70 posttreatment, the number of papilloma per mice was counted (WT, $n = 2$; knockout, $n = 8$; ***, $P < 0.005$).

Downloaded from cancerres.aacrjournals.org on May 19, 2014. © 2013 American Association for Cancer Research.

Published OnlineFirst September 5, 2013; DOI: 10.1158/0008-5472.CAN-13-0318

and 10 weeks of treatment (Supplementary Figs. S3A vs. 3A, top). These first observations support the idea that papillomas appear when the senescence response is counteracted; carcinoma might require a complete switch off of all the senescence markers and additional mutations (Supplementary Fig. S4D). As expected (22, 23) both WT- or PLA2R1 knockout–derived papilloma displayed mutations in the 61st codon of H-ras in contrast to nontreated skin (Supplementary Fig. S5).

Importantly, PLA2R1 knockout mice displayed a decreased p16 nuclear staining in adjacent skin as well as in the papilloma when compared to WT mice (Fig. 3A). Accordingly, the percentage of Ki67 positive cells was higher in the adjacent skin as well as in the papillomas, of PLA2R1 knockout mice when compared to the WT counterpart (Fig. 3B). The first papillomas occurred earlier on PLA2R1 knockout mice than on WT mice from the same littermates (50 vs. 70 days; Fig. 3C). Seventy days after the beginning of the treatment, PLA2R1 knockout mice skin displayed on average 3 times more papillomas than WT mice (Fig. 3D). Our *in vivo* data confirms our *in vitro* observations and show that loss of PLA2R1 favors OIS escape and transformation.

PLA2R1 activates JAK2 signaling

To gain insight into signaling pathways mediating PLA2R1 cellular effects, we assayed the ability of chemical inhibitors of some major signaling pathways to inhibit PLA2R1 effects. We observed that constitutive expression of PLA2R1-induced rapid cell death in some cancer cells such as the MDA-MB-453 (unpublished data and Supplementary Fig. S6). We took advantage of this strong apoptotic response to screen for pathway inhibition and reversion of PLA2R1-induced cell death. Among the inhibitors tested, only the JAK2 Z3 inhibitor was able to block PLA2R1-induced cell death (Supplementary Fig. S6). Accordingly, we observed that cancer cells as well as normal cells expressing PLA2R1 displayed an activated JAK2 as confirmed by the appearance of its phosphorylated form (Fig. 4A and Supplementary Figs. S7A and S7B). Activation of JAK2 by PLA2R1 was further supported by subsequent phosphorylation of STAT3, a JAK2 kinase target (Fig. 4B), activation of a JAK-STAT reporter (Fig. 4C; ref. 20), by the transcriptional activation of several JAK2 signaling targets (Fig. 4D; ref. 24), and by the transcriptional decrease of JAK2 signaling targets in PLA2R1-knockdown cells (Fig. S7C). In agreement with these *in vitro* results, DMBA/TPA-treated adjacent skin and papilloma samples from PLA2R1 knockout mice displayed a decrease in JAK2 activation, which correlates to accelerated senescence escape and papillomas formation (Fig. 4E). These results show the ability of PLA2R1 to activate JAK2 and its signaling.

To investigate whether or not PLA2R1 might mediate JAK2 activation through its cytoplasmic tail, we generated a PLA2R1 mutant depleted in its cytoplasmic tail (PLA2R1ΔCyT). Cells were infected with control-, PLA2R1- or PLA2R1ΔCyT-encoding retroviral vectors and selected. PLA2R1 WT and ΔCyT were found to be expressed at similar levels, ΔCyT displaying a small shift corresponding to the loss of the short CyT (Fig. 5A). WT and ΔCyT PLA2R1 forms were both able to induce JAK2 phosphorylation (Fig. 5B) and to activate the JAK2–STAT reporter (Fig. 5C). Finally, they both inhibited the ability of MDA-MB-231 cancer cells to form soft agar clones (Fig. 5D). Together these data indicate that PLA2R1 does not activate JAK2 through its cytoplasmic tail. Nevertheless, they seemed to belong to the same complex as PLA2R1 and P-JAK2 colocalized (Fig. 5E) and were positive to the ligation proximity assay (Fig. 5F). These data support the view that PLA2R1 activates JAK2 indirectly through binding to another membrane protein that remains to identify.

JAK2 mediates PLA2R1 tumor suppressive effect

We next wanted to assess whether the activation of JAK2 participates in PLA2R1 tumor suppressive effects, which may seem at the first sight unexpected given the described oncogenic functions of JAK2 (25, 26). To this end, we compared the ability of PLA2R1 to block cell transformation depending on JAK2 level. Interestingly, JAK2 knockdown (Fig. 6A and Supplementary Fig. S8A) rendered cancer cells resistant to PLA2R1-mediated transformation inhibition (Fig. 6B). To confirm these data, JAK2 knockout- and WT-derived NIH3T3 were transformed by an oncogenic Ras and the ability of constitutive PLA2R1 expression to inhibit transformation was assessed (Fig. 6C). As expected, constitutive PLA2R1 expression decreased the ability of WT NIH3T3 to form colonies in soft agar (Fig. 6D). By contrast, its expression in JAK2 knockout NIH3T3 did not reduce the number of colonies (Fig. 6D). Finally, blocking the JAK–STAT pathway by constitutively expressing SOCS3 (27) reverted transformation inhibition induced by PLA2R1 in cancer cells (Supplementary Fig. S8B and S8C). Taken together, these results show the involvement of JAK2 kinase in mediating the tumor suppressive function of PLA2R1.

Discussion

Our results show that a downregulation of PLA2R1 favors an escape from oncogenic-stress induced senescence in human epithelial cells *in vitro* or in mice epidermis *in vivo*. In addition, the knockdown of PLA2R1 increases the transformation potential of cancer cells whereas its ectopic expression inhibits cancer cells transformation. Together these data support a tumor suppressive role of PLA2R1. Further supporting a tumor suppressive role of PLA2R1, is the fact that PLA2R1 mRNA levels generally decrease in cancers where its expression is significantly altered (Supplementary Table). This bioinformatic analysis corroborates the functional data we have obtained in this study and supports a tumor suppressive role of PLA2R1.

Our data identifies JAK2 as a downstream effecter of PLA2R1 tumor suppressive function. Even if our results constitute the first functional link between PLA2R1 and JAK2, PLA2R1 knockout mice and JAK2 knockout mice present a least one common phenotype. Indeed, PLAR1 knockout mice have been described to be less sensitive to LPS treatment (19). LPS treatment is known to activate JAK2 and JAK2 knockout mice, as PLA2R1 knockout mice are also resistant to LPS-induced endotoxic shock (28, 29). This observation

Downloaded from cancerres.aacrjournals.org on May 19, 2014. © 2013 American Association for Cancer Research.

Published OnlineFirst September 5, 2013; DOI: 10.1158/0008-5472.CAN-13-0318

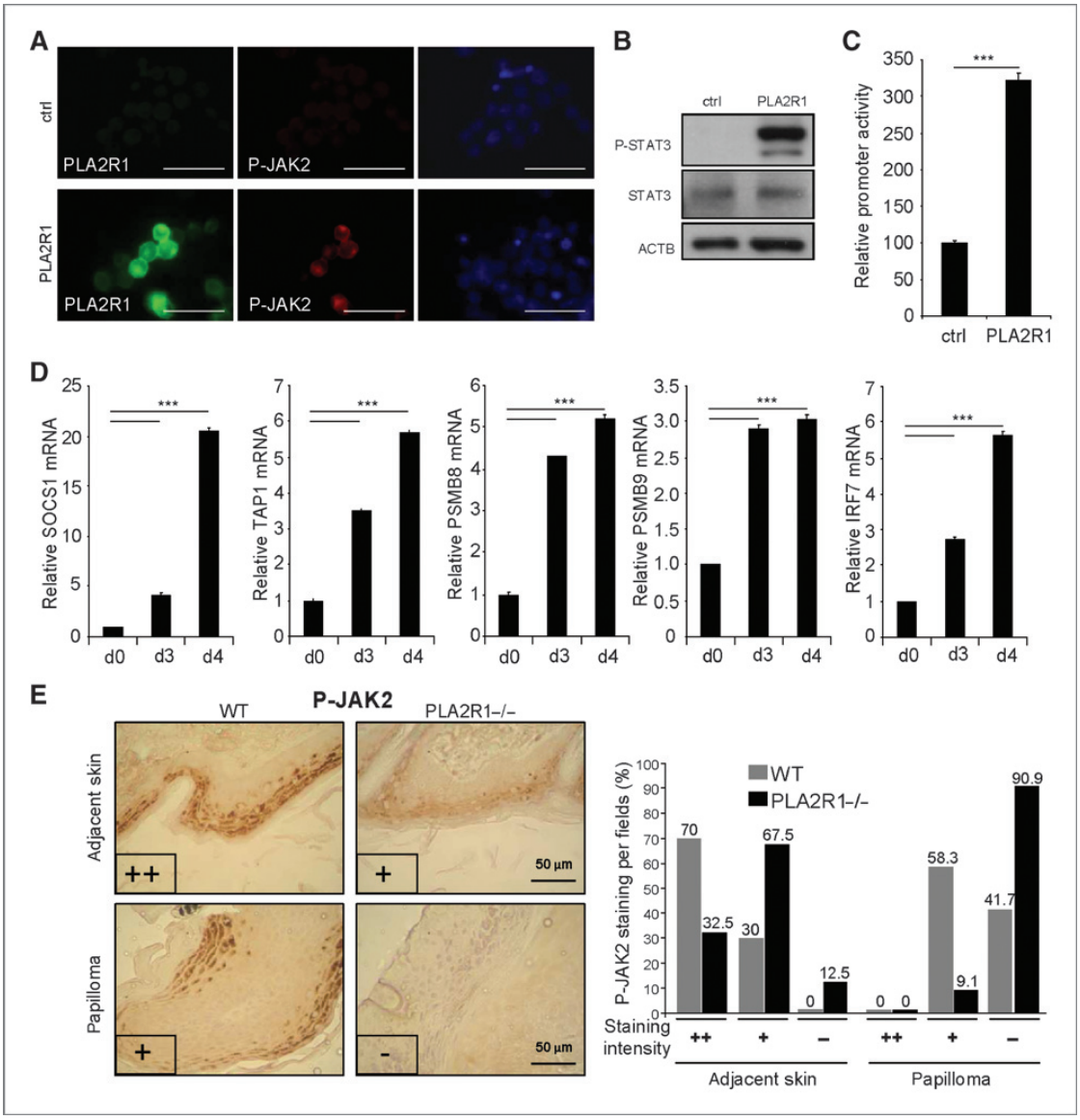

Figure 4. PLA2R1 activates JAK2. A, Cama-1 cancer cells were transfected with a control or a PLA2R1 encoding vector. Two days later, immunofluorecences against PLA2R1 and phospho-JAK2 were conducted. Nuclei were stained by Hoechst dye. Representative pictures are displayed (scale bar, 50 μm). The experiments shown are representative of at least 3 repeats. B, the MDA-MB-231 were infected with a control or a PLA2R1 encoding vector and puromycin selected. Cell extracts were prepared and analyzed by immunoblot for STAT3 phosphorylation and total STAT3. ACTB was used as loading control. The experiments shown are representative of 2 repeats. C, 293 cells were cotranfected with a control or a PLA2R1 encoding vector and a JAK2-promoter activity reporter. Two days later, luciferase activities were measured and normalized to luciferase activity for the actin promoter. The experiments shown are representative of 3 repeats. D, cancer cells were infected with a control or a PLA2R1-encoding retroviral vector and puromycin selected. RNAs were prepared 3 or 4 days later, retro-transcribed, and qPCR was conducted against the indicated genes and normalized against the mRNA expression of ACTB. The experiments shown are representative of 2 repeats. E, IHC against phospho-JAK2 were conducted on skin samples from WT or PLA2R1 knockout mice after 10 weeks of treatment. Fifteen to 45 independent fields (magnification, ×40) from 2 independent mice per condition were analyzed and classified as strongly positive (++), positive (+), or negative (–). Representative fields and how they were scored are also shown. ***, $P < 0.005$.

is in agreement with our observation that PLA2R1 and JAK2 might be actors of the same pathway. In addition, our results suggest that PLA2R1 might belong to a complex containing JAK2 and that PLA2R1 does not require its cytoplasmic tail to activate JAK2. Interestingly, mannose receptor, C type 2 (MRC2), which belongs to the same family of receptors

Downloaded from cancerres.aacrjournals.org on May 19, 2014. © 2013 American Association for Cancer Research.

Published OnlineFirst September 5, 2013; DOI: 10.1158/0008-5472.CAN-13-0318

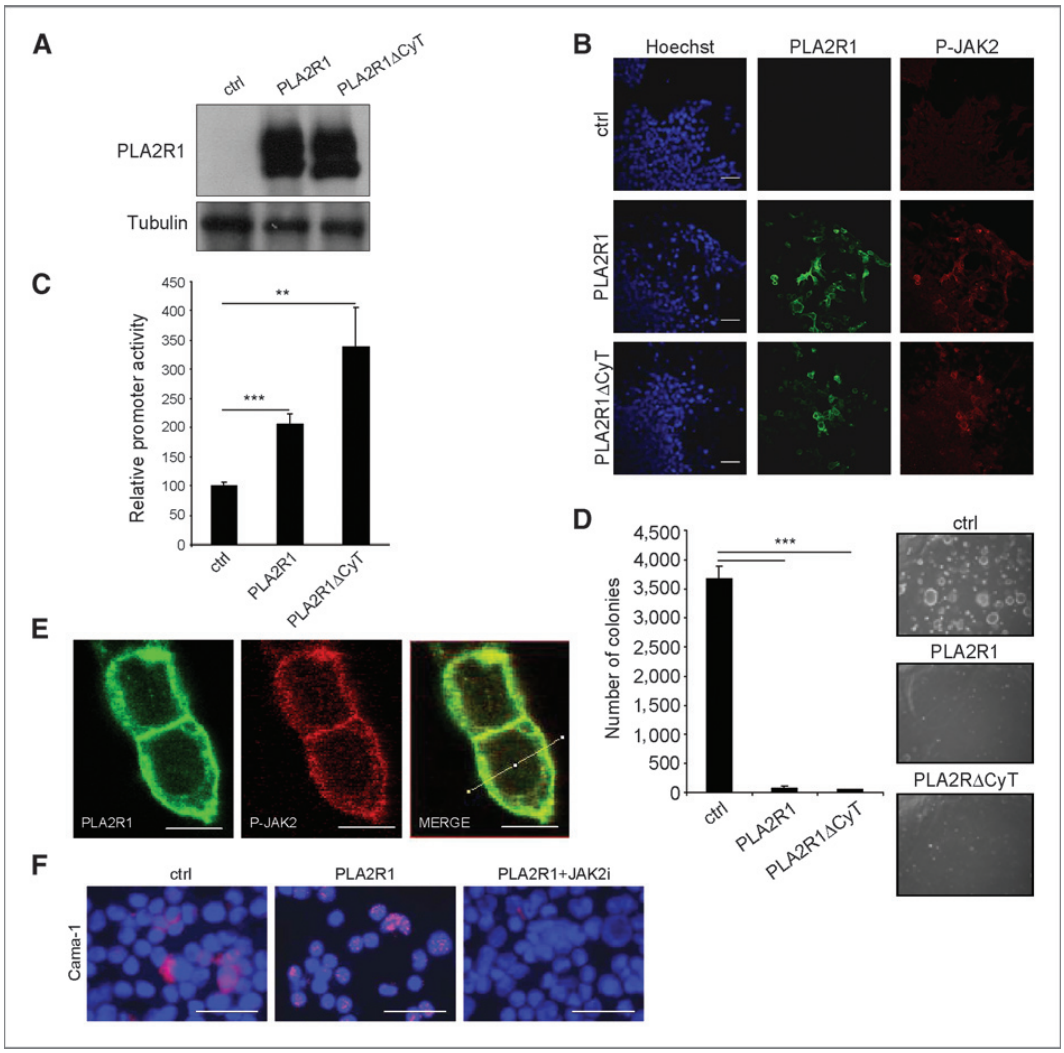

Figure 5. PLA2R1 cytoplasmic tail is not involved in JAK2 activation. A, MDA-MB-231 cells were infected with a control, WT PLA2R1, or mutant PLA2R1ΔCyT encoding retroviral vector and puromycin selected. Cell extracts were prepared and analyzed by immunoblot for PLA2R1 expression. Tubulin was used as a loading control. The experiments shown are representative of 2 repeats. B, 293 cells were transfected with a control, a WT PLA2R1, or a mutant PLA2R1ΔCyT encoding vector. Two days later, immunofluorecences against PLA2R1 and phospho-JAK2 were conducted. Nuclei were stained by Hoechst dye. Representative pictures are shown (scale bar, 50 μm). The experiments shown are representative of 2 repeats. C, 293 cells were cotransfected with a control, a WT PLA2R1, or a mutant PLA2R1ΔCyT encoding vector and a JAK2-promoter activity reporter. Two days later, luciferase activities were measured and normalized to luciferase activity for the actin promoter. The experiments shown are representative of 3 repeats. D, MDA-MB-231 cells were infected with a control, a WT PLA2R1, or a mutant PLA2R1ΔCyT encoding retroviral vector and puromycin selected. Cells were next seeded in soft agar, grown for 2 weeks and the number of clones counted. The experiments shown are representative of 3 repeats. E, 293 cells were transfected with a PLA2R1 encoding vector. Two days later immunofluorecence against PLA2R1 and P-JAK2 conducted. Staining was analyzed using confocal microscopy and fluorescence intensity analyzed using Image J software (scale bar, 10 μm). The experiments shown are representative of 3 repeats. F, cells were transfected by a control or a PLA2R1 encoding vector, treated or not with the Z3 JAK2 inhibitor to check staining specificity, and 2 days later ligation proximity assays were conducted using Ab directed against PLA2R1 and against phospho-JAK2. Red dots show positivity between these 2 proteins (scale bar, 50 μm). The experiments shown are representative of 2 repeats. **, $P < 0.01$; ***, $P < 0.005$.

as PLA2R1, because they share similar domains and organization (30), was found to act as a coreceptor by trimerizing with urokinase receptor and pro-urokinase (31). It is tempting to speculate that PLA2R1 acts as a coreceptor and binds a nonidentified receptor, resulting in the activation of JAK2.

Downloaded from cancerres.aacrjournals.org on May 19, 2014. © 2013 American Association for Cancer Research.

Published OnlineFirst September 5, 2013; DOI: 10.1158/0008-5472.CAN-13-0318

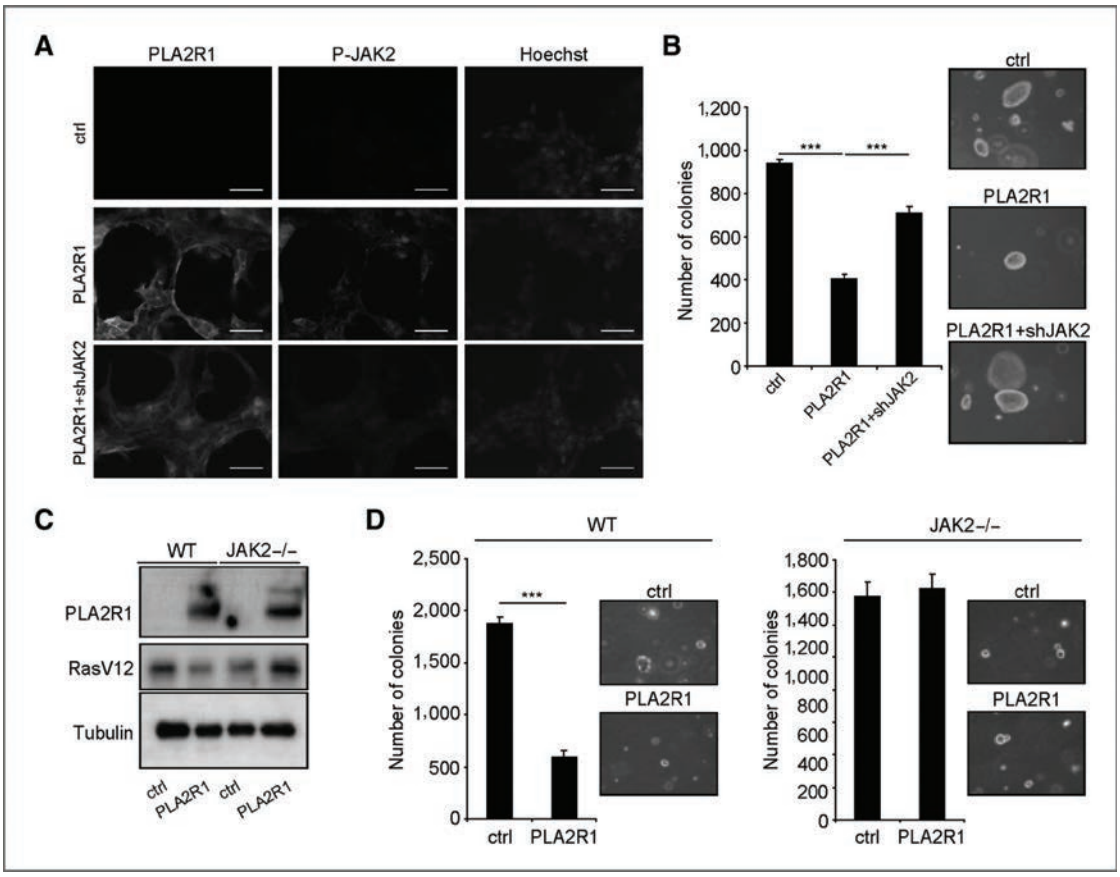

Figure 6. PLA2R1 exerts its antitumoral effect through JAK2. A, MDA-MB-231 cancer cells were infected with or without a PLA2R1 encoding vector and with or without retroviral vectors expressing a shRNA directed against JAK2 and selected. Cells were seeded and fixed the following day. Immunofluorescence against PLA2R1 and phospho-JAK2 was conducted and nuclei were stained using Hoechst dye. Representative pictures are shown (scale bar, 25 μm). The experiments shown are representative of 3 repeats. B, thirty-thousand MDA-MB-231 cancer cells were seeded in agar 2 weeks after seeding, colonies were counted for each indicated condition, and representative photographs are shown. The experiments shown are representative of at least 3 repeats. C, MEF-derived cells NIH3T3 were transduced to express RASV12 and PLA2R1. An immunoblot was conducted to check PLA2R1 and RASV12 expression. Tubulin was used as a loading control. The experiments shown are representative of 3 repeats. D, fifty-thousand cells were seeded in agar. Four weeks later, the number of colonies were counted for each condition and representative pictures are shown. The experiments shown are representative of at least 3 repeats. ***, $P < 0.005$.

JAK2 is activated by numerous ligands, most of them associated to inflammatory and immune responses (32, 33) and is thought, in some cancer types, to be a good target to inhibit (34, 35). Nevertheless, our results point out that JAK2 activation by PLA2R1 contributes to PLA2R1-mediating growth defects. The fact that JAK2 might inhibit tumor initiation is not that surprising taking into account for example its activation by interferon, a well known antitumor factor with prosenescence activity (36–40) or its activation by other known regulator of senescence such as IL6 (41, 42). In addition, some components of the JAK signaling, such as JAK1, STAT1, STAT3, and STAT5A, are induced and involved during the senescence program (43–46). JAK2 signaling might thus exert a dual role on cell growth and cancer.

In conclusion, these exciting new findings on the role of PLA2R1 and its link to JAK2 signaling in the regulation of tumor initiation open prospects for new avenues of research in cancer biology.

Disclosure of Potential Conflicts of Interest

No potential conflicts of interest were disclosed.

Authors' Contributions

Conception and design: D. Vindrieux, A. Augert, D. Gitenay, H. Lallet-Daher, Y. De Launoit, M. Gelb, G. Lambeau, D. Bernard
Development of methodology: D. Vindrieux, A. Augert, D. Gitenay, C. Wiel, B.L. Calve, M. Ferrand, S. Verbeke, M. Gelb
Acquisition of data (provided animals, acquired and managed patients, provided facilities, etc.): D. Vindrieux, A. Augert, B. Gras, X. Leroy, S. Aubert, M. Perrais, M. Gelb, G. Lambeau

Downloaded from cancerres.aacrjournals.org on May 19, 2014. © 2013 American Association for Cancer Research.

Published OnlineFirst September 5, 2013; DOI: 10.1158/0008-5472.CAN-13-0318

Analysis and interpretation of data (e.g., statistical analysis, biostatistics, computational analysis): D. Vindrieux, A. Augert, D. Gitenay, M. Gelb, G. Lambeau
Writing, review, and/or revision of the manuscript: D. Vindrieux, A. Augert, C.A. Girard, Y. De Launoit, S. Aubert, M. Gelb, H. Simonnet, D. Bernard
Administrative, technical, or material support (i.e., reporting or organizing data, constructing databases): C.A. Girard, C. Wiel, B.L. Calve, A. Puisieux, M. Gelb, D. Bernard
Study supervision: M. Gelb, D. Bernard

Acknowledgments

The authors thank the laboratory members for helpful discussions. The authors thank S. Courtois-Cox, H. Mertani, P. Mehlen, C. Abbadie, R. Iggo, S. Léon, I. Treilleux, I. Plo, and LMT facility for helpful discussions and reagents.

Grant Support

This work was carried out with the support of the Association pour la Recherche sur le Cancer, the Association for International Cancer Research for D. Bernard and G. Lambeau; the Institut National du Cancer, the "RTRS Fondation Synergie Lyon Cancer" for D. Bernard; and of the ANR (ANR-09-JCJC-0002) for M. Perrais.

The costs of publication of this article were defrayed in part by the payment of page charges. This article must therefore be hereby marked *advertisement* in accordance with 18 U.S.C. Section 1734 solely to indicate this fact.

Received February 4, 2013; revised July 31, 2013; accepted August 18, 2013; published OnlineFirst September 5, 2013.

References

1. Hahn WC, Counter CM, Lundberg AS, Beijersbergen RL, Brooks MW, Weinberg RA. Creation of human tumour cells with defined genetic elements. Nature 1999;400:464–8.
2. Hanahan D, Weinberg RA. The hallmarks of cancer. Cell 2000;100: 57–70.
3. Bodnar AG, Ouellette M, Frolkis M, Holt SE, Chiu CP, Morin GB, et al. Extension of life-span by introduction of telomerase into normal human cells. Science 1998;279:349–52.
4. Vaziri H, Benchimol S. Reconstitution of telomerase activity in normal human cells leads to elongation of telomeres and extended replicative life span. Curr Biol 1998;8:279–82.
5. Collado M, Serrano M. Senescence in tumours: evidence from mice and humans. Nat Rev Cancer 2010;10:51–7.
6. Kuilman T, Michaloglou C, Mooi WJ, Peeper DS. The essence of senescence. Genes Dev 2010;24:2463–79.
7. Adams PD. Healing and hurting: molecular mechanisms, functions, and pathologies of cellular senescence. Mol Cell 2009;36:2–14.
8. Ewald JA, Desotelle JA, Wilding G, Jarrard DF. Therapy-induced senescence in cancer. J Natl Cancer Inst 2010;102:1536–46.
9. Nardella C, Clohessy JG, Alimonti A, Pandolfi PP. Pro-senescence therapy for cancer treatment. Nat Rev Cancer 2011;11:503–11.
10. Augert A, Payre C, de Launoit Y, Gil J, Lambeau G, Bernard D. The M-type receptor PLA2R regulates senescence through the p53 pathway. EMBO Rep 2009;10:271–7.
11. Kim HJ, Kim KS, Kim SH, Baek SH, Kim HY, Lee C, et al. Induction of cellular senescence by secretory phospholipase A2 in human dermal fibroblasts through an ROS-mediated p53 pathway. J Gerontol A Biol Sci Med Sci 2009;64:351–62.
12. Murakami M, Taketomi Y, Girard C, Yamamoto K, Lambeau G. Emerging roles of secreted phospholipase A2 enzymes: lessons from transgenic and knockout mice. Biochimie 2010;92:561–82.
13. Llorca O. Extended and bent conformations of the mannose receptor family. Cell Mol Life Sci 2008;65:1302–10.
14. Parganas E, Wang D, Stravopodis D, Topham DJ, Marine JC, Teglund S, et al. Jak2 is essential for signaling through a variety of cytokine receptors. Cell 1998;93:385–95.
15. Beck LHjr, Bonegio RG, Lambeau G, Beck DM, Powell DW, Cummins TD, et al. M-type phospholipase A2 receptor as target antigen in idiopathic membranous nephropathy. N Engl J Med 2009;361:11–21.
16. Sasaki A, Inagaki-Ohara K, Yoshida T, Yamanaka A, Sasaki M, Yasukawa H, et al. The N-terminal truncated isoform of SOCS3 translated from an alternative initiation AUG codon under stress conditions is stable due to the lack of a major ubiquitination site, Lys-6. J Biol Chem 2003;278:2432–6.
17. Young AR, Narita M, Ferreira M, Kirschner K, Sadaie M, Darot JF, et al. Autophagy mediates the mitotic senescence transition. Genes Dev 2009;23:798–803.
18. Serrano M, Lin AW, McCurrach ME, Beach D, Lowe SW. Oncogenic ras provokes premature cell senescence associated with accumulation of p53 and p16INK4a. Cell 1997;88:593–602.
19. Hanasaki K, Yokota Y, Ishizaki J, Itoh T, Arita H. Resistance to endotoxic shock in phospholipase A2 receptor-deficient mice. J Biol Chem 1997;272:32792–7.
20. Tron K, Samoylenko A, Musikowski G, Kobe F, Immenschuh S, Schaper F, et al. Regulation of rat heme oxygenase-1 expression by interleukin-6 via the Jak/STAT pathway in hepatocytes. J Hepatol 2006;45:72–80.
21. Debacq-Chainiaux F, Erusalimsky JD, Campisi J, Toussaint O. Protocols to detect senescence-associated beta-galactosidase (SA-betagal) activity, a biomarker of senescent cells in culture and *in vivo*. Nat Protoc 2009;4:1798–806.
22. Abel EL, Angel JM, Kiguchi K, DiGiovanni J. Multi-stage chemical carcinogenesis in mouse skin: fundamentals and applications. Nat Protoc 2009;4:1350–62.
23. Bizub D, Wood AW, Skalka AM. Mutagenesis of the Ha-ras oncogene in mouse skin tumors induced by polycyclic aromatic hydrocarbons. Proc Natl Acad Sci USA 1986;83:6048–52.
24. Rebouissou S, Amessou M, Couchy G, Poussin K, Imbeaud S, Pilati C, et al. Frequent in-frame somatic deletions activate gp130 in inflammatory hepatocellular tumours. Nature 2009;457:200–4.
25. Constantinescu SN, Girardot M, Pecquet C. Mining for JAK-STAT mutations in cancer. Trends Biochem Sci 2008;33:122–31.
26. Hexner EO. JAK2 V617F: implications for thrombosis in myeloproliferative diseases. Curr Opin Hematol 2007;14:450–4.
27. Starr R, Willson TA, Viney EM, Murray LJ, Rayner JR, Jenkins BJ, et al. A family of cytokine-inducible inhibitors of signalling. Nature 1997;387:917–21.
28. Okugawa S, Ota Y, Kitazawa T, Nakayama K, Yanagimoto S, Tsukada K, et al. Janus kinase 2 is involved in lipopolysaccharide-induced activation of macrophages. Am J Physiol Cell Physiol 2003;285: C399–C408.
29. Zhong J, Yang P, Muta K, Dong R, Marrero M, Gong F, et al. Loss of Jak2 selectively suppresses DC-mediated innate immune response and protects mice from lethal dose of LPS-induced septic shock. PLoS One 2010;5:e9593.
30. Stahl PD, Ezekowitz RA. The mannose receptor is a pattern recognition receptor involved in host defense. Curr Opin Immunol 1998;10:50–5.
31. Behrendt N, Jensen ON, Engelholm LH, Mortz E, Mann M, Dano K. A urokinase receptor-associated protein with specific collagen binding properties. J Biol Chem 2000;275:1993–2002.
32. Heinrich PC, Behrmann I, Muller-Newen G, Schaper F, Graeve L. Interleukin-6-type cytokine signalling through the gp130/Jak/STAT pathway. Biochem J 1998;334(Pt 2):297–314.
33. Taga T, Kishimoto T. Signaling mechanisms through cytokine receptors that share signal transducing receptor components. Curr Opin Immunol 1995;7:17–23.
34. Ferrajoli A, Faderl S, Ravandi F, Estrov Z. The JAK-STAT pathway: a therapeutic target in hematological malignancies. Curr Cancer Drug Targets 2006;6:671–9.
35. Quintas-Cardama A, Kantarjian H, Cortes J, Verstovsek S. Janus kinase inhibitors for the treatment of myeloproliferative neoplasias and beyond. Nat Rev Drug Discov 2011;10:127–40.
36. Borden EC, Sen GC, Uze G, Silverman RH, Ransohoff RM, Foster GR, et al. Interferons at age 50: past, current and future impact on biomedicine. Nat Rev Drug Discov 2007;6:975–90.

Downloaded from cancerres.aacrjournals.org on May 19, 2014. © 2013 American Association for Cancer Research.

Published OnlineFirst September 5, 2013; DOI: 10.1158/0008-5472.CAN-13-0318

37. Moiseeva O, Mallette FA, Mukhopadhyay UK, Moores A, Ferbeyre G. DNA damage signaling and p53-dependent senescence after prolonged beta-interferon stimulation. Mol Biol Cell 2006;17: 1583–92.
38. Chawla-Sarkar M, Lindner DJ, Liu YF, Williams BR, Sen GC, Silverman RH, et al. Apoptosis and interferons: role of interferon-stimulated genes as mediators of apoptosis. Apoptosis 2003; 8:237–49.
39. Gresser I. Antitumor effects of interferon. Adv Cancer Res 1972;16: 97–140.
40. Verma A, Kambhampati S, Parmar S, Platanias LC. Jak family of kinases in cancer. Cancer Metastasis Rev 2003;22:423–34.
41. Kuilman T, Michaloglou C, Vredeveld LCW, Douma S, van Doorn R, Desmet CJ, et al. Oncogene-induced senescence relayed by an interleukin-dependent inflammatory network. Cell 2008;133: 1019–31.
42. Kuilman T, Peeper DS. Senescence-messaging secretome: SMS-ing cellular stress. Nat Rev Cancer 2009;9:81–94.
43. Hubackova S, Novakova Z, Krejcikova K, Kosar M, Dobrovolna J, Duskova P, et al. Regulation of the PML tumor suppressor in drug-induced senescence of human normal and cancer cells by JAK/STAT-mediated signaling. Cell Cycle 2010;9:3085–99.
44. Kojima H, Kunimoto H, Inoue T, Nakajima K. The STAT3-IGFBP5 axis is critical for IL-6/gp130-induced premature senescence in human fibroblasts. Cell Cycle 2012;11:730–9.
45. Novakova Z, Hubackova S, Kosar M, Janderova-Rossmeislova L, Dobrovolna J, Vasicova P, et al. Cytokine expression and signaling in drug-induced cellular senescence. Oncogene 2010;29: 273–84.
46. Mallette FA, Gaumont-Leclerc MF, Ferbeyre G. The DNA damage signaling pathway is a critical mediator of oncogene-induced senescence. Genes Dev 2007;21:43–8.

Downloaded from cancerres.aacrjournals.org on May 19, 2014. © 2013 American Association for Cancer Research.

Supplementary Table Legends

Table. PLA2R1 expression decreases in various cancer types. The Oncomine database was interrogated for PLA2R1 expression in cancer with the following threshold; p-value <0.01, fold change >1.5, gene rank all.

Supplementary Figure Legends

Figure S1. The knockdown of PLA2R1 favors OIS escape. A, RNA from HMEC expressing two different shRNA sequences targeting PLA2R1 or a control were prepared. RT-qPCR were performed against PLA2R1 and normalized to actin levels. The experiments shown are representative of two repeats. B, 293 cells were co-transfected with control or a PLA2R1 encoding vector together with a control or independent shRNA sequence targeting PLA2R1. Two days later, cell extracts were prepared and analyzed by immunoblot for expression of PLA2R1. ACTB was used as a loading control. The experiments shown are representative of three repeats. C, Protein extracts from HMEC expressing two different shRNA sequences targeting PLA2R1 or a control were prepared. PLA2R1 expression was checked by immunoblot and ACTB was used as a loading control. The experiments shown are representative of two repeats. D, The same number of HMEC co-expressing H-RAS^{G12V}ER and control, shPLA2R1, or shPLAR1-2 were treated with 4OHT. Fifteen days later cells were fixed and crystal violet stained. The experiments shown are representative of two repeats.

Figure S2. The knockdown of PLA2R1 favors transformation. Hs-578T cells were infected with retroviral vectors expressing a control or shRNA directed against PLA2R1 and puromycin selected. A, After selection, RNAs were prepared, retro-transcribed and a qPCR

was performed against PLA2R1 and normalized to actin levels. The experiments shown are representative of three repeats. The experiments shown are representative of three repeats. B, Hs-578T cells were seeded in soft agar and images were taken 3 weeks after. The number of clones were counted. The experiments shown are representative of three repeats.

Figure S3. The knockdown of PLA2R1 favors OIS escape in human normal keratinocytes. Keratinocytes were co-infected with H-RASG12VER encoding retroviral vector (neomycin resistance) with retroviral vectors expressing a ctrl or 2 independent PLA2R1-targeting shRNA (shPLA2R1) (puromycin resistance). They were next selected for a week with puromycin and geneticin. The cells were then counted and plated for the different experiments. Treatment with 4-hydroxytamoxifen (4OHT) was performed at 100nM for 48 h. A, RNA from keratinocytes expressing two different shRNA sequences targeting PLA2R1 or a control were prepared. RT-qPCR were performed against PLA2R1 and normalized to actin levels. The experiments shown are representative of two repeats. B, Western blot analysis was performed at the indicated times after 4OHT treatment with antibodies targeting the indicated proteins. Tubulin or ACTB was used as loading control. The experiments shown are representative of two repeats. C, The colony formation assay was assessed with crystal violet 10 days after 4OHT treatment. The experiments shown are representative of two repeats. D, SA-β-Gal analysis was performed 7 days after 4OHT treatment. SA-β-Gal-positive cells were quantified as indicated in the methods section. The experiments shown are representative of two repeats.

Figure S4. DMBA/TPA treatment induces senescence and its escape correlates with papillomas formation. A, After six weeks of treatment, WT mice were sacrificed and the expression of p16, DEC1 and DcR2 senescence markers was analyzed by IHC.

Representative pictures are shown. B, Expression of proliferation marker Ki67 was analyzed by IHC. C, Skin samples from DMBA/TPA treated mice containing or not papillomas were extracted, fixed and assessed for the presence of the senescence associated-β-galactosidase activity. D, Schematic representation of the senescence response in function of the alterations we have observed in the mice skin during the DMBA-TPA treatment.

Figure S5. Validation of H-Ras mutation in papilloma. A, Primers used to distinguish between WT H-Ras and H-Ras mutated in the 61st codon are displayed. B, WT or PLA2R1 -/- mice were euthanized. Non-treated or papilloma samples were extracted and frozen. gDNA were prepared using QIAamp DNA kit (Qiagen) according to manufacturer's recommendations. PCR was performed using the indicated primers using GoTaq Flexi kit (Promega) according to manufacturer's recommendations.

Figure S6. JAK2 is involved in PLA2R1-mediated cell growth regulation. A, The table contains the list of chemical used, their targets, concentrations and their effect on the inhibition of PLA2R1-induced MDA-MB-453 cancer cell death. B, MDA-MB-453 cancer cells were infected with a control or PLA2R1-encoding retroviral vectors and puromycin selected. At day 3 post infection, cells were treated with a JAK2 inhibitor at 50 μM. Pictures were taken 2 days later. The experiments shown are representative of three repeats.

Figure S7. PLA2R1 regulates JAK2 activity. A, WI38 cells were infected with a ctrl or a PLA2R1-encoding vector and puromycin selected. After fixation, immunofluorescence against PLA2R1 and phospho-JAK2 was performed and nuclei were stained by Hoechst (scale bar represents 50μm). The experiments shown are representative of two repeats. B, 293 cells were transfected with a ctrl or a PLA2R1-encoding vector. Two days post transfection,

cells were fixed and processed for immunofluorescence (scale bar represents 50μm). The experiments shown are representative of two repeats. C, MDA-MB-436 cells were infected with a ctrl or 2 independent shRNA encoding retroviral vectors targeting PLA2R1 and puromycin selected. RNA were extracted, retro-transcribed and qPCR performed against the indicated genes. The mRNA expressions were normalized to ACTB. The experiments shown are representative of two repeats.

Figure S8. JAK2 mediates PLA2R1 tumor suppressive effects. A, Cancer cells were infected with a ctrl or a shRNA against JAK2 encoding retroviral vectors and selected. RNA were extracted, retro-transcriptions were performed, and qPCR were performed on JAK2 and actin for normalization. The experiments shown are representative of two repeats. B, MDA-MB-231 cancer cells were infected with or without a PLA2R1-encoding retroviral vector, and with or without a SOCS3 encoding vector. Cell extracts were prepared and analyzed by immunoblot against PLA2R1, myc tag for SOCS3 and tubulin as a protein loading control. The experiments shown are representative of two repeats. C, Thirty thousand cells were seeded in agar and grown for 3 weeks. The number of colonies was counted for each indicated condition and representative photographs are shown. The experiments shown are representative of three repeats.

Supplemental Table , Vindrieux et *al*

Analysis Type by Cancer	Cancer versus Normal	
Bladder		2
Brain and CNS	3	3
Breast	1	13
Cervical		2
Colorectal		8
Esophageal	1	3
Gastric	4	
Head and Neck		5
Kidney		12
Leukemia	2	4
Liver		1
Lung	1	1
Lymphoma		1
Melanoma		3
Myeloma		
Other	1	4
Ovarian		
Pancreatic	4	1
Prostate		1
Sarcoma	2	1
Significant unique analysis	19	64
Total unique analysis	386	

Cell color is determined by the best gene rank percentile for the analyses within the cell.

Supplemental Figure 1, Vindrieux et *al*

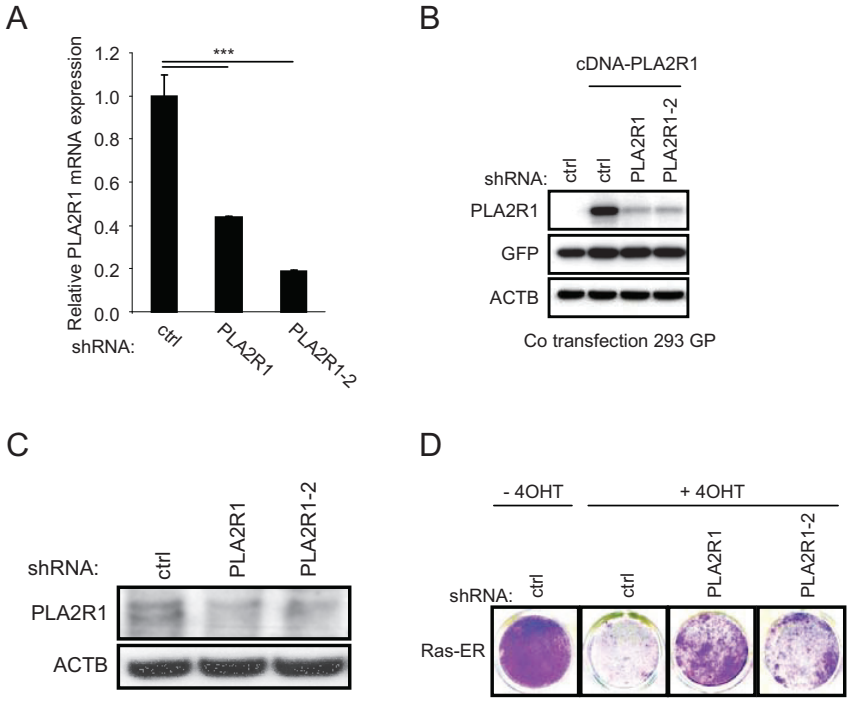

Supplemental Figure 2, Vindrieux et *al*

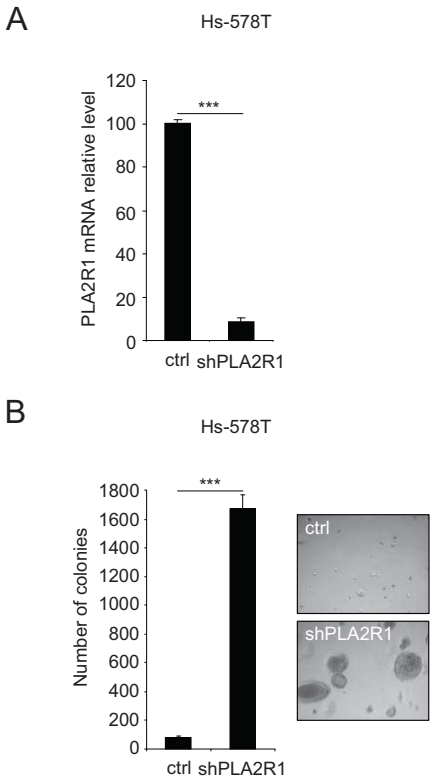

Supplemental Figure 3, Vindrieux et *al*

A

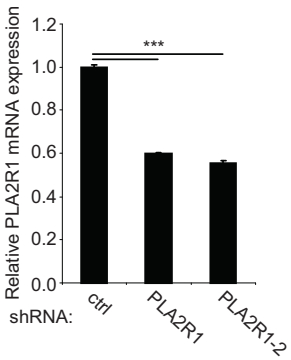

B

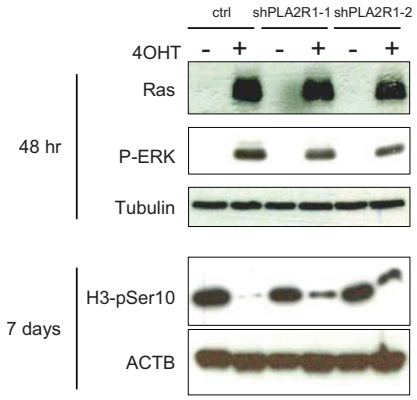

C

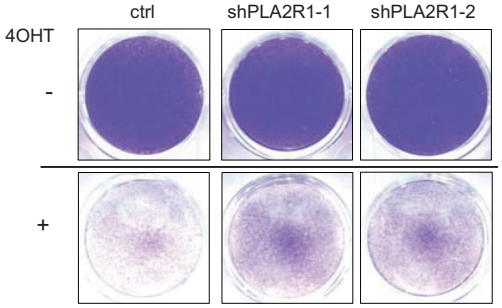

D

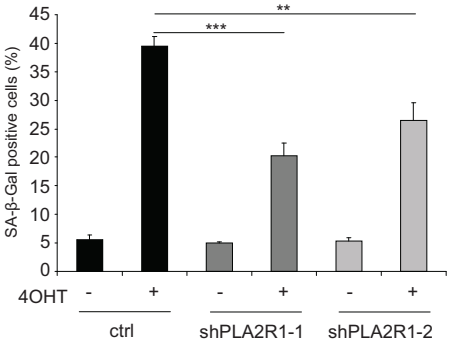

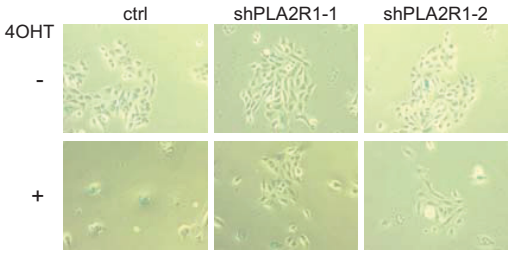

Supplemental Figure 4, Vindrieux et *al*

A

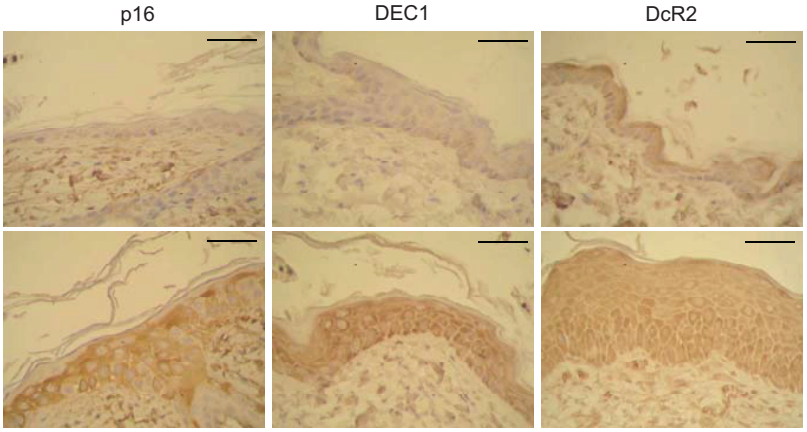

B

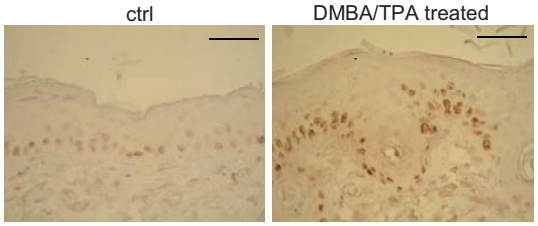

C

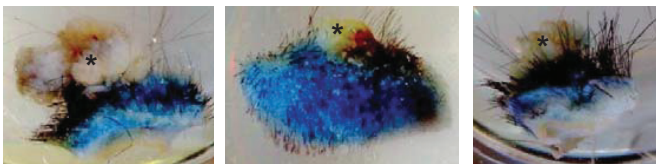

*papilloma

DMBA/TPA treated	SA-β-Gal positivity
skin (n=12)	12/12
papilloma (n=9)	0/9

D

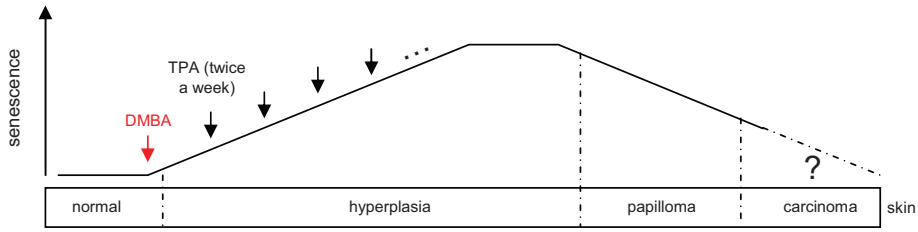

Supplemental Figure 5, Vindrieux et *al*

A

Upstream primer		5'-CTAAGCCTGTTGTTTTGCAGGAC-3'	Amplicon 110bp
Downstream primer	wt	5'-CATGGCACTATACTCTTCTT-3'	
	Mutation 1	5'-CATGGCACTATACTCTTCTA-3'	
	Mutation 2	5'-CATGGCACTATACTCTTCTC-3'	
	Mutation 3	5'-CATGGCACTATACTCTTCTG-3'	

B

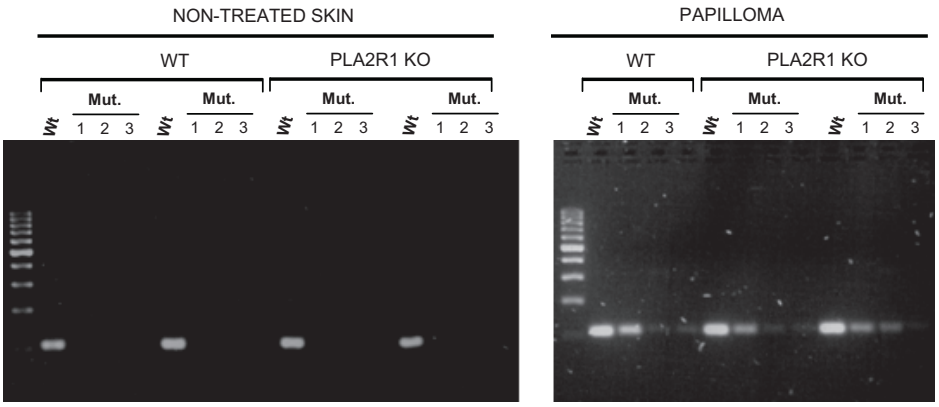

Supplemental Figure 6, Vindrieux et *al*

A

Signaling Pathways targeted

Chemical	Dose	target	Phenotype reversion
NSC 23766	1-100uM	Rac 1	-
SP 600125	5-50uM	JNK 1-2-3	-
PD98059	10-50uM	MEK-1	-
LY294002	10-50uM	PI3K	-
SB202190	1-50uM	p38 MAPK	-
JAKi	1-30nM	JAK	-
JAK2i (Z3)	**10-100uM**	**JAK2**	**++**
JAK3i (I and VI)	25-150uM/2-150nM	JAK3	-

B

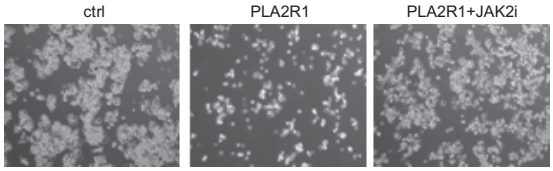

Supplemental Figure 7, Vindrieux et *al*

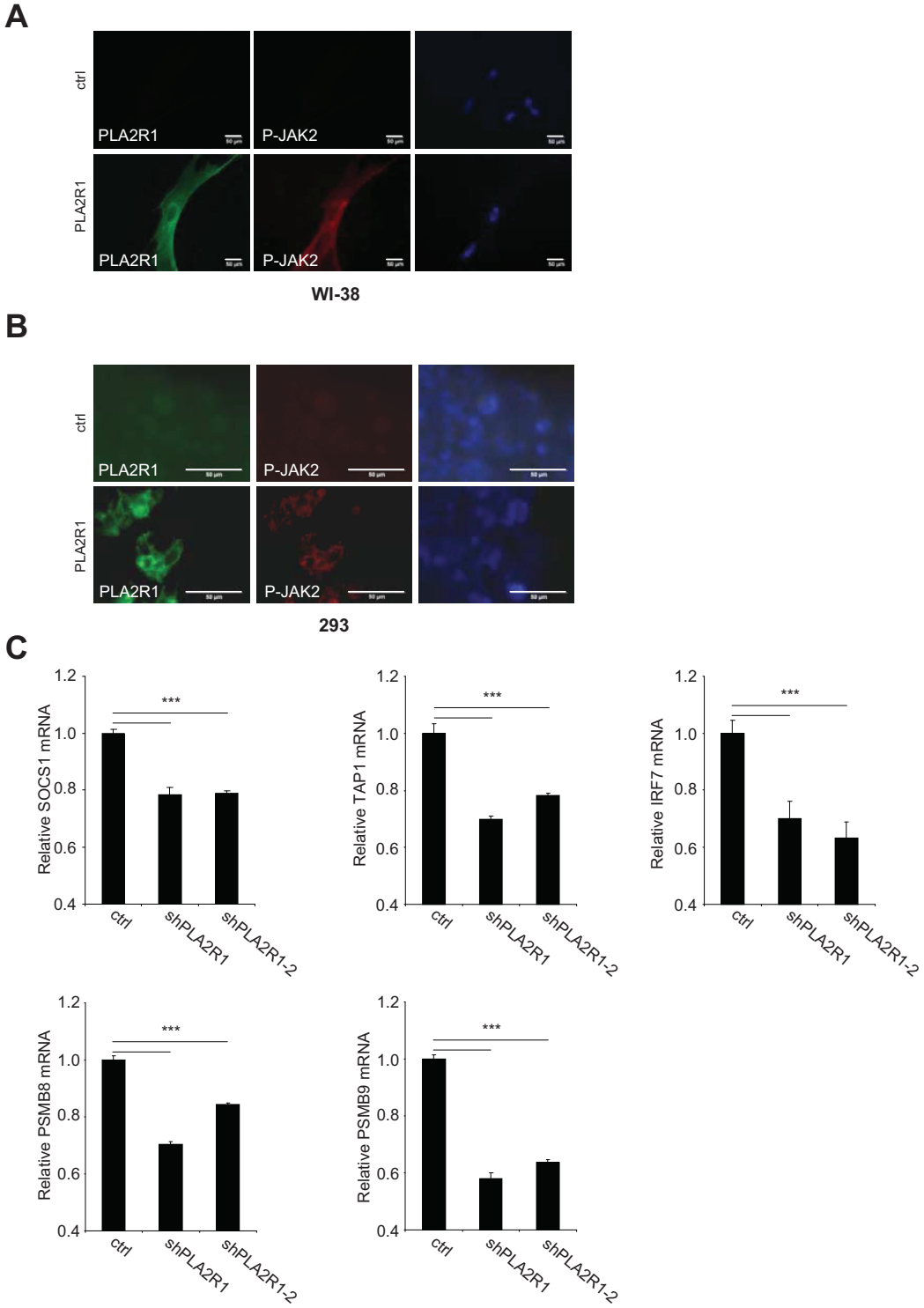
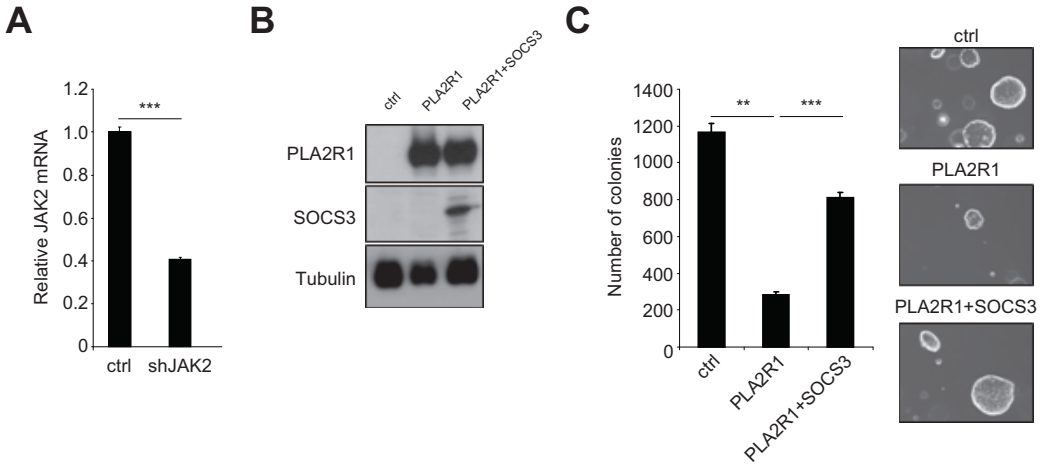
Supplemental Figure 8, Vindrieux et *al*